

ACTA CHIMICA

ACADEMIAE SCIENTIARUM
HUNGARICAE

ADIVVANTIBUS

M. T. BECK, R. BOGNÁR, V. BRUCKNER,
GY. HARDY, K. LEMPET, F. MÁRTA,
K. POLINSZKY, E. PUNGOR,
G. SCHAY, Z. G. SZABÓ, P. TÉTÉNYI

REDIGUNT

B. LENGVEL, et GY. DEÁK

TOMUS 101

FASCICULI 1—2



AKADÉMIAI KIADÓ, BUDAPEST

1979

ACTA CHIM. ACAD. SCI. HUNG.

ACASA2 101 (1—2) 1—214 (1979)

ACTA CHIMICA

A MAGYAR TUDOMÁNYOS AKADÉMIA
KÉMIAI TUDOMÁNYOK OSZTÁLYÁNAK
IDEGEN NYELVŰ KÖZLEMÉNYEI

FŐSZERKESZTŐ
LENGYEL BÉLA

SZERKESZTŐ
DEÁK GYULA

TECHNIKAI SZERKESZTŐ
HAZAI LÁSZLÓ

SZERKESZTŐ BIZOTTSÁG
BECK T. MIHÁLY, BOGNÁR REZSŐ, BRUCKNER GYŐZŐ,
HARDY GYULA, LEMPERT KÁROLY, MÁRTA FERENC,
POLINSZKY KÁROLY, PUNGOR ERNŐ, SCHAY GÉZA,
SZABÓ ZOLTÁN, TÉTÉNYI PÁL

Acta Chimica is a journal for the publication of papers on all aspects of chemistry in English, German, French and Russian.

Acta Chimica is published in 4 volumes per year. Each volume consists of 4 issues of varying size.

Manuscripts should be sent to

Acta Chimica
Budapest, P.O. Box 67, H-1450, Hungary

Correspondence with the editors should be sent to the same address. Manuscripts are not returned to the authors.

Subscription: \$ 36.00 per volume.

Hungarian subscribers should order from Akadémiai Kiadó, 1363 Budapest, P.O. Box 24. Account No. 215 11488.

Orders from other countries are to be sent to "Kultura" Foreign Trading Company H-1389 Budapest 62, P.O. Box 149. Account No. 218 10990) or its representatives abroad.

ACTA CHIMICA

ACADEMIAE SCIENTIARUM
HUNGARICAE

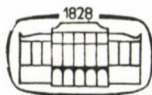
ADIUVANTIBUS

M. T. BECK, R. BOGNÁR, V. BRUCKNER,
GY. HARDY, K. LEMPERT, F. MÁRTA,
K. POLINSZKY, E. PUNGOR,
G. SCHAY, Z. G. SZABÓ, P. TÉTÉNYI

REDIGUNT

B. LENGYEL, et GY. DEÁK

TOMUS 101



AKADÉMIAI KIADÓ, BUDAPEST

1979

ACTA CHIM. ACAD. SCI. HUNG.

ACTA CHIMICA

TOMUS 101

Fasciculi 1—2

Fasciculus 3

Fasciculus 4

INDEX

BÁNFY, D. s. ZÓLYOMI, G.	
BÁNKY-ELŐD, E. s. SZEJTLI, J.	
BÁNYAI, É. s. GIMESI, O.	
BARTHA, L., GYARMATI, GY., KISS, B. A., NÉMETH, T., SALAMON, A., SZALAY, T.: Complex Studies on Intermediary Decomposition Products of Ammonium Paratungstate ...	127
BÉKÉS, F. s. LÁSZTITY, R.	
BERNÁTH, G., FÜLÖP, F., JERKOVICH, GY., SOHÁR, P.: Stereochemical Studies, XXXV. Saturated Heterocycles, XII. Synthesis and Spectroscopical Study of <i>cis</i> -Trimethylene-, <i>cis</i> - and <i>trans</i> -Tetra- and Pentamethylene-2,3,5,6-tetrahydro-1,3-oxazin-4-ones	61
BOGNÁR, R. s. LITKEI, GY.	
BOTÁR, L. s. GÁL, D.	
BURCAT, A., KUDCHADKER, S.: Ideal Gas Thermodynamic Properties for $\text{CH}_3\text{O}\cdot$ and $\cdot\text{CH}_2\text{OH}$ Radicals	249
CSÁNYI, L. J. s. PÉTER, A.	
DANÓCZY, É. s. GÁL, D.	
ESZTERLE, M. s. GUCZI, L.	
FÓTI, G. s. NAGY, L. G.	
FÜLÖP, F. s. BERNÁTH, G.	
GÁL, D., BOTÁR, L., DANÓCZY, É., HAJDU, P. I., LUKÁCS, J., NEMES, I., VIDÓCZY, T.: Modeling of Liquid Phase Hydrocarbon Oxidation Processes	189
GÉCZY, I.: Synthetic Linear Polymers, XXXIV. Change of Specific Properties of Dimethylsiloxane Co-Oligomers as a Function of the Chemical Composition and Size of the Molecule	327
GEGUS, E., KREITER, J., MÉRAY, L., INCZÉDY, J.: Spectrochemical Investigation of Volatile Components Released in Thermochemical Processes, II. Cadmium and Mercuric Salts	347
GIMESI, O., BÁNYAI, É.: Separation and Determination of Radioactive Iodine Isotopes Based on Isotope- and Ion-Exchange	309
GUCZI, L., MATUSEK, K., MARGITFALVI, J., ESZTERLE, M., TILL, F.: Correlation between the Preparation and Catalytic Properties of $\text{PtFe}_2\text{SiO}_2$ Catalysts	107
GYARMATI, GY. s. BARTHA, L.	
GYÓRY, P. s. KALAUS, GY.	
HAJDU, P. I. s. GÁL, D.	
HARSÁNYI, E. G., PÓLOS, L., PUNGOR, E.: Investigation of the Atomization Processes of Tin in Various Atomizers and of the Interference by Copper	139
HENCSEI, P., NAGY, J.: Investigation of the Molecular Structure of Phenol Ethers by Quantum Chemical Methods, I. Experimental Data and Calculation Methods ...	359
HENCSEI, P., PONGOR, G., NAGY, J.: Investigation of the Molecular Structure of Phenol Ethers by Quantum Chemical Methods, II. Results and Discussion	367
HORÁNYI, GY. s. INZELT, GY.	
HORÁNYI, GY. s. INZELT, GY.	
ILLÉS, V., SZALAI, O.: Modelling of the Thermal Decomposition of Hydrocarbons	267
IMRE, J. s. LIPTÁK, A.	
INCZÉDY, J. s. GEGUS, E.	

INZELT, GY., HORÁNYI, GY.: Elektrochemical Behaviour of Ethylene Glycol and its Oxidation Products on a Platinum Electrode, V. Experimental Study of Electro-Oxidation and Oxidation Products of Glycolaldehyde and Glycolic Acid	215
INZELT, GY., HORÁNYI, GY.: Electrochemical Behaviour of Ethylene Glycol and its Oxidation Derivatives on a Platinum Electrode, VI. Oxidation of Ethylene Glycol.....	229
ISLAMUDDIN s. SHAFIULLAH	
JÁNOSSY, L. s. LIPTÁK, A.	
JERKOVICH, GY. s. BERNÁTH, G.	
KALAUS, GY., SZABÓ, L., GYÖRY, P., SZENTIRMAI, É., SZÁNTAY, Cs.: Synthesis of Vinca Alkaloids and Related Compounds, XI. Acrylonitrile Adducts as Intermediates	387
KISS, A. s. ZSUGA, M.	
KISS, B. A. s. BARTHA, L.	
KÓRÓDI, F. s. ZSUGA, M.	
KOVÁCS, J., PINTÉR, I., SZEGŐ, F., TÓTH, G., MESSMER, A.: Phosphinimine Derivatives of Aldopyranoses from Azido Sugars	7
KREITER, J. s. GEGUS, E.	
KUDCHADKER, S. s. BURCAT, A.	
KUSZMANN, J. s. ZÓLYOMI, G.	
LÁSZTITY, R., BÉKÉS, F., NEDELKOVITS, J., VARGA, J.: Investigation of the Complex Proteins of Wheat	281
LÁZÁR, J., VINKLER, E.: Recent Studies on the Reaction of Thiolsulfonates with Alkali Halides	175
LIPTÁK, A., JÁNOSSY, L., IMRE, J., NÁNÁSI, P.: Stereoselective Hydrogenolysis of Dioxolane-Type Benzylidene Acetals. Synthesis of Partially Substituted Galactopyranoside Derivatives	81
LITKEI, GY., MESTER, T., PATONAY, T., BOGNÁR, R.: Flavonoids, XXXIII. Reaction of 2'-OR-Chalcone Dibromides with Cyclohexylamine. Synthesis and Transformations of Chalcone Aziridines	53
LUKÁCS, J. s. GÁL, D.	
MARGITFALVI, J. s. GUCZI, L.	
MATUSEK, K. s. GUCZI, L.	
MÁZOR, L.: A New Method for the Reductive Decomposition of Organic Compounds	3
MEISEL, T., SEYBOLD, K., RÓTH, J.: Application of the Thermoelectric Method in the Study of Phase Transitions of Fatty Acid Salts	179
MÉRAY, L. s. GEGUS, E.	
MESSMER, A. s. KOVÁCS, J.	
MESTER, T. s. LITKEI, GY.	
MINK, J. s. SZILÁGYI, T.	
MOLNÁR, I. s. PAJKOSSY, T.	
NAGY, J. s. HENCSEI, P.	
NAGY, J. s. HENCSEI, P.	
NAGY, L. G., TÖRÖK, G., FÓTI, G.: Structure and Selective Sodium Sorption of Hydrated Antimony Pentoxide	17
NÁNÁSI, P. s. LIPTÁK, A.	
NEDELKOVITS, J. s. LÁSZTITY, R.	
NEMES, I. s. GÁL, D.	
NÉMETH, T. s. BARTHA, L.	
OSZBACH, GY., SZABÓ, D., VITAI, M. E.: Dihydropyran Cycloadducts, III. Reactions of Cyclopentanone Enamines with Benzylidene Ketones	119
PAJKOSSY, T., MOLNÁR, I., PÁLFI, M., SCHILLER, R.: Photoassisted Electrolysis of Water by Semiconductor Electrodes	93
PÁLFI, M. s. PAJKOSSY, T.	
PATONAY, T. s. LITKEI, GY.	
PÉTER, A., CSÁNYI, L. J.: Photocatalytic Methods, II. Photo-Oxidation of Safranin T in the Presence of Iron (III)	379
PINTÉR, I. s. KOVÁCS, J.	
PÓLOS, L. s. HARSÁNYI, E. G.	
PONGOR, G. s. HENCSEI, P.	
PÓSA, V. s. TÓTH, G.	
PUNGOR, E. s. HARSÁNYI, E. G.	
RANA, V. B., SAHNI, S. K., SANGAL, S. K.: Penta and Hexa-coordinated Complexes of Platinum Metals of Potential Pentadentate Ligands	405

RATKOVICS, F., SALAMON, T.: Investigations on the Association of Pentanol Isomers in Liquid Phase	241
REHOREK, D.: Photocatalytic Systems, XVII. Spin-trapping of Radicals in the Photolysis of Cer(IV) in Alcohols (in German)	395
RÓTH, J. s. MEISEL, T.	
SAHNI, S. K. s. RANA, V. B.	
SALAMON, A. s. BARTHA, L.	
SALAMON, T. s. RATKOVICS, F.	
SANGAL, S. K. s. RANA, V. B.	
SÁRKÁNY, A. s. SZILÁGYI, T.	
SCHILLER, R. s. PAJKOSSY, T.	
SEYBOLD, K. s. MEISEL, T.	
SHAFIULLAH, ISLAMUDDIN: Synthesis of 6-Aza-B-homo-19-norcholesta-1,3,5(10)-trien-7-one and its 1-Methyl Derivative	319
SOHÁR, P. s. BERNÁTH, G.	
SOMOGYI-WERNER, K. s. TÖKE, L.	
SZABÓ, D. s. OSZBACH, GY.	
SZABÓ, G. T. s. TÖKE, L.	
SZABÓ, L. s. KALAUS, GY.	
SZABÓ, V. s. ZSUGA, M.	
SZALAI, O. s. ILLÉS, V.	
SZALAY, T. s. BARTHA, L.	
SZÁNTAY, CS. s. KALAUS, GY.	
SZEGŐ, F. s. KOVÁCS, J.	
SZEJTLI, J., SZENTE, L., BÁNKY-ELŐD, E.: Molecular Encapsulation of Volatile, Easily Oxidizable Labile Flavour Substances by Cyclodextrins	27
SZENTE, L. s. SZEJTLI, J.	
SZENTIRMAY, É. s. KALAUS, GY.	
SZILÁGYI, T., SÁRKÁNY, A., MINK, J., TÉTÉNYI, P.: IR Spectra of Hydrocarbons Chemisorbed on Transition Metals, I. The Infrared Cell and Chemisorption of Ethylene on Ni/SiO ₂ Catalyst	259
TÉTÉNYI, P. s. SZILÁGYI, T.	
TILL, F. s. GUCZY, L.	
TÓTH, G. s. KOVÁCS, J.	
TÓTH, G., VAJDA, J., PÓSA, V.: New Control-methods in the Leatherchemistry, I. (in German)	157
TÖKE, L., SZABÓ, G. T., SOMOGYI-WERNER, K.: Polyethylene Glycol Derivatives as Complexing Agents and Phase-Transfer Catalysts, III. Behaviour of Polyoxyethylene Derivatives in Liquid-Liquid Phase Equilibria	47
TÖRÖK, G. s. NAGY, L. G.	
VAJDA, J. s. TÓTH, G.	
VARGA, J. s. LÁSZTITY, R.	
VIDÓCZY, T. s. GÁL, D.	
VINKLER, E. s. LÁZÁR, J.	
VITAI, M. E. s. OSZBACH, GY.	
ZÓLYOMI, G., BÁNFI, D., KUSZMANN, J.: Synthesis of ³ H-Labelled 2-Deoxy-D-ribose and its Derivatives (Short Communication)	323
ZSUGA, M., SZABÓ, V., KÓRÓDI, F., KISS, A.: Reaction of Chromonoids with Nucleophilic Reagents, I. Cleavage of the Pyrone Ring of Chromone Derivatives in Aqueous Alkali	73

THE PRESENT ISSUE OF THIS JOURNAL CONTAINS
PAPERS WHICH HAD BEEN INTENDED FOR
PUBLICATION IN THE JUBILEE VOLUME 100
OF ACTA CHIMICA, BUT HAD TO BE
DELAYED OWING TO LACK OF SPACE

A NEW METHOD FOR THE REDUCTIVE DECOMPOSITION OF ORGANIC COMPOUNDS

L. MÁZOR

*(Institute of General and Analytical Chemistry, Technical University,
Budapest)*

Received May 28, 1978

Accepted for publication July 25, 1978

If organic compounds containing heteroelements are heated with metallic potassium in vacuum, the reaction is not violent and the heteroelements can be converted into the corresponding potassium compounds. After reaction of the melt with alcohol and water, the ions can be determined by suitable microanalytical methods. This method has been used for the microdetermination of halogens, sulfur, phosphorus, arsenic and metals in organic compounds.

In the most cases organic compounds must be decomposed totally before the determination of heteroelements (halogens, sulfur, phosphorus, arsenic, metals, *etc.*) in order to transform the heteroatoms to ionic compounds which are readily available for analytical determination. The decomposition can be carried out by oxidation or reduction. Reduction methods mostly give products more suitable for the determination on the microscale. For example, in the case of sulfur the quantitative microdetermination of sulfide ions is simpler and more accurate than the determination of sulfate ions after oxidative decomposition.

The reductive decomposition can be carried out by heating the compound in hydrogen or ammonia gas stream, or by heating and melting with an alkali or alkali earth metal. Heating with sodium or potassium is well known in organic qualitative analysis as decomposition according to Lassaigne.

Halogen in compounds where it is not strongly bound can be transformed to the corresponding ion by heating with a solution of alkali or sodium methoxide. A more energetic method of decomposition consist of heating in an indifferent solvent containing an alkali metal in finely dispersed or dissolved form [1]. An even more vigorous method is the shaking of the compound with a reagent which contains the alkali metal in an active organic bond, such as disodium biphenyl in ether or tetraethylene glycol dimethyl ether [2, 3]. Some authors [4, 5] were able to decompose even organic fluorine compounds with a solution of disodium-dimethoxyethane complex.

Melting with an alkali metal to achieve the decomposition of organic compounds was first proposed by BÜRGER [6]. ZIMMERMANN's method of determining sulfur in organic compounds starts similarly [7]. Later KAINZ dealt with this method in several papers [8, 9, 10], carrying out the determina-

tion of iodine and bromine, or iodine and chlorine after heating the compounds in a sealed glass ampoule until appearance of potassium metal vapours. The method of BELCHER *et al.* [11] for the determination of iodine and bromine was similar, but done on the submicroscale. Organic fluorine compounds were heated with potassium in a closed metal bomb for more than an hour at 600–650 °C to achieve complete decomposition [12]. A comprehensive survey was given by MACDONALD [13] on the decomposition with alkali metals. Some authors [14] tried to effect the decomposition before sulfur determination in an open tube under a layer of glass beads but they had success only with some non-volatile compounds. The decomposition with alkali metals in an open tube is dangerous because the metal will ignite in the air further the decomposition will not be complete, since if the temperature is not high enough, the high surface tension and viscosity of the molten metal will hinder effective contact with the organic compound.

We have found experimentally that the danger of burning of the hot and molten alkali metal as well as the violent reaction with the organic compound can be avoided if the heating is done at 300–500 °C in vacuum.

Under such conditions only polynitro compounds react violently, yet do not explode. If the boiling point of the compound is below 100 °C, the decomposition is not complete because of the early evaporation of the compound. Elementary sulfur (which was used as standard in the determination of sulfur) cannot be decomposed with potassium only, as not only potassium sulfide but also sulfur compounds of higher oxidation number are formed (*e.g.* polysulfide, thiosulfate). However, if some (3–5 mg) metallic zinc powder is also added, the decomposition is complete yielding only sulfide.

Procedure

The decomposition of the organic compound to be analyzed is carried out in the glass apparatus shown in Fig. 1. Fifty to one hundred mg of potassium is placed and pressed with a flat ended glass rod to the bottom of a small glass test tube. The potassium is prepared by cutting a 10 mm thick slice from the metal and from this small round cakes, of slightly smaller diameter than that of the test tube are cut by means of a cork driller or a glass tube with sharpened edge. The cutting tool is smeared with paraffin oil. The 10 mm long and 5 mm thick cylinders thus prepared can be stored under paraffin oil. When used, a cylinder is cut in half and one piece is placed at the bottom of the test tube, it is covered by 5–10 mg of the organic compound added by means of a weighing handle: the other piece of the potassium is then placed into the tube and compressed. Finally a hole is bored in the center of the potassium filling with a 0.5 mm thick needle, extending to the bottom of the test tube. This hole makes way for the air trapped under the potassium layer.

About 5 ml of water is poured into the outer vessel and the packed test tube is placed inside the platinum heating spiral attached to the stopper and finally the latter is inserted into the vessel. The ground glass joint is lubricated with pure vaseline. Then some water is poured into the collar of the vessel. The apparatus is evacuated through the side arm and connected to a power supply such as a battery of 4–6 V, or same a.c. source of 5–10 V and 10–20 A.

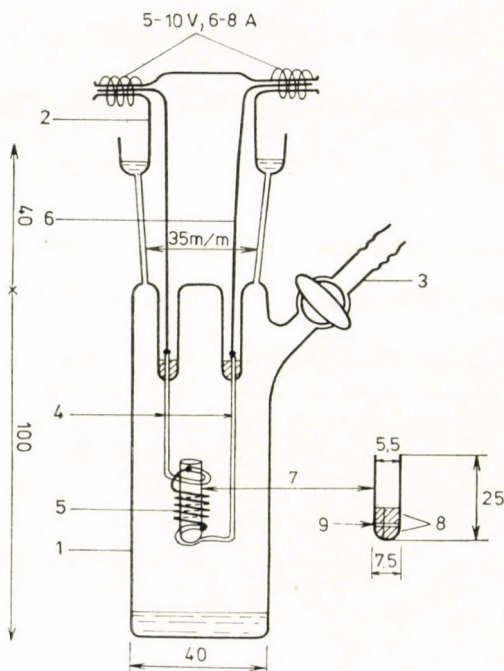


Fig. 1. 1 — Outer vessel, 2 — glass stopper with heating accessories, 3 — suction tube with stopcock, 4 — platinum holder wire of about 1.5 mm diameter, 5 — platinum heating spiral of about 0.5 mm diameter, 6 — copper wire of about 2 mm diameter, 7 — small test tube, 8 — potassium layers, 9 — organic compound between two potassium layers; sizes are given in mm

The intensity of the current is regulated by a toroid transformer or a sliding resistor. The intensity of current is slowly increased at a rate such as to heat the platinum spiral to red hot (about 500 °C) in 20–30 minutes.

For safety it is advisable to cover the apparatus during the heating period with a wire basket.

After having completed the heating period, the current is switched off and the apparatus allowed to cool. The stopcock is opened and after atmospheric pressure has been re-established in the apparatus the stopper is removed and the test tube lifted from inside of the platinum spiral by means of forceps

and placed into a little (about 25 ml, high form) beaker. Ethanol is then poured into the beaker to cover the tube (about 3–5 ml) and allowed to stand until the reaction of the residual potassium with the ethanol is over. If the reaction is slowed down, some water may be poured into the beaker. In the meantime the stopper of the apparatus is replaced and the vessel is rinsed with some water by shaking vigorously: this washing liquid is added to the contents of the beaker. The procedure should be done three times with 2–3 ml of water in each case. The last portion of water is used also to rinse the test tube. About 20–30 ml of alkaline solution (0.2–0.5 N) is thus obtained which can be used as such or after acidification for the determination of the various elements (ions).

Not very volatile organic liquids can also be decomposed by the method described after measuring them in a capillary tube. The drawn end of the capillary is inserted into the hole which has been bored with a needle through the potassium layer. In this case the test tube must be heated slowly with precaution to prevent escape of the liquid from the capillary before the potassium has melted.

Up to now the procedure has been used for the determination of fluorine, chlorine, bromine, iodine, sulfur, phosphorus, arsenic and metals in organic compounds. The method seems to be promising for the determination of the nitrogen content of organic compounds if the organically bound nitrogen is transformed to cyanide ion during the decomposition.

Methods found to be the best for the microdetermination of the various elements (ions) in the solutions obtained after decomposition will be reported in forthcoming papers.

REFERENCES

- [1] ENGO, K., NOMURA, K.: Ann. Rep. Takamina Lab., **4**, 170 (1952); Chem. Abstr., **49**, 7448 (1955)
- [2] PACHERER, B., GAMBRILL, C. M., WILCOX, G. W.: Anal. Chem., **22**, 311 (1950)
- [3] LIGGETT, L. M.: Anal. Chem., **26**, 748 (1951)
- [4] BENNETT, C. E., DEBRECHT, E.: Am. Chem. Soc., 311. Nat. Meeting Miami (1957)
- [5] JOHNCOCK, P., MUSGRAVE, W. K. R., WIPER, A.: Analyst, **84**, 245 (1959)
- [6] BÜRGER, K.: Z. angew. Chem., **54**, 479 (1941), Die Chemie **55**, 245 (1942)
- [7] ZIMMERMANN, W.: Mikrochemie, **31**, 15 (1944), **33**, 122 (1947), **35**, 80 (1950), **40**, 162 (1952)
- [8] KAINZ, G.: Mikrochim. Acta, **35**, 466 (1950)
- [9] KAINZ, G.: Mikrochim. Acta, **38**, 124 (1951)
- [10] KAINZ, G., RESCH, A.: Mikrochim. Acta, **39**, 1 (1952)
- [11] BELCHER, R., SHAH, R. A., WEST, T. S.: J. Chem. Soc., **1958**, 2298, Z. f. anal. Chem., **167**, 289 (1959)
- [12] BELCHER, R., TATLOW, J. C.: Analyst, **76**, 593 (1951)
- [13] MACDONALD, A. M. G.: Ind. Chemie, **31**, 198 (1955)
- [14] MÁZOR, L., ERDEY, L., MEISEL, T.: Mikrochim. Acta, **1960**, 412

László MÁZOR H-1111 Budapest, Gellért tér 4

PHOSPHINIMINE DERIVATIVES OF ALDOPYRANOSES FROM AZIDO SUGARS

J. KOVÁCS, I. PINTÉR*, F. SZEGŐ, G. TÓTH¹ and A. MESSMER*

(Central Research Institute for Chemistry of the Hungarian Academy
of Sciences, Budapest,¹ SOTE Institute for Organic Chemistry,
Budapest)

Received July 17, 1978

Accepted for publication August 1, 1978

The Staudinger reaction of acetylaldosyl azides was extended to other azido sugars affording sugar phosphinimines. The chemical and conformational behaviour of the phosphinimines was studied by their characteristic reactions and ¹H-NMR spectroscopy.

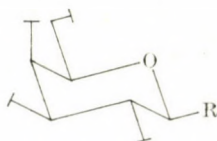
In an earlier short communication [1] we reported the application of the Staudinger reaction [2] to acetylated alderyl azides [3], resulting in the formation of sugar phosphinimines, a new family of carbohydrate compounds. Thus, the reaction of the corresponding azido sugars and triphenylphosphine yielded tetra-*O*-acetyl-β-D-glucosyl-, tetra-*O*-acetyl-β-D-galactosyl-, tri-*O*-acetyl-β-D-xylosyl-, and hepta-*O*-acetyl-β-D-cellobiosyl phosphinimines (**1**, **2**, **3** and **4**, respectively) which proved to be advantageous precursors of *N*-glycosides.



1 R = N=P(O)₃

16 R = N(Me)P[⊖](O)₃ I[⊖]

23 R = N=CHC₆H₄NO₂ (*p*)



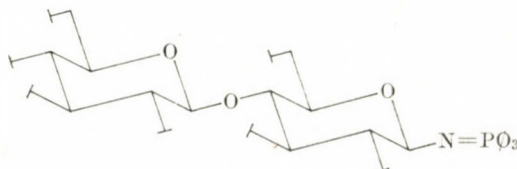
2 R = N=P(O)₃

17 R = N(Me)P[⊖](O)₃ I[⊖]



3 R = N=P(O)₃

18 R = N(Me)P[⊖](O)₃ I[⊖]

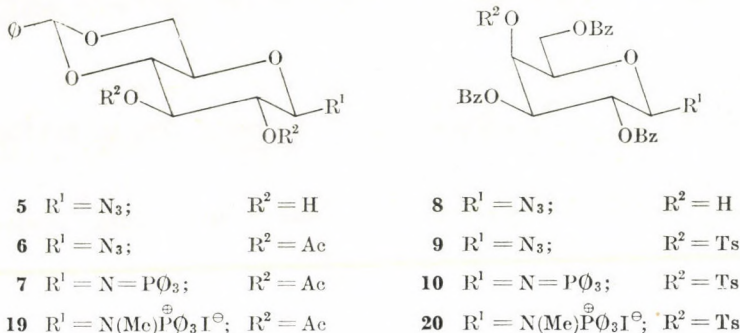


4

Scheme 1

*To whom correspondence should be addressed

Aldosyl phosphinimines were formed not only from fully acetylated alderyl azides but, as was expected, also from derivatives protected otherwise, e.g. 4,6-*O*-benzylidene-2,3-di-*O*-acetyl- β -D-glucopyranosyl azide (6), synthesized from 1- β -azido-D-glucose by standard methods [4], led to phosphinimine 7.

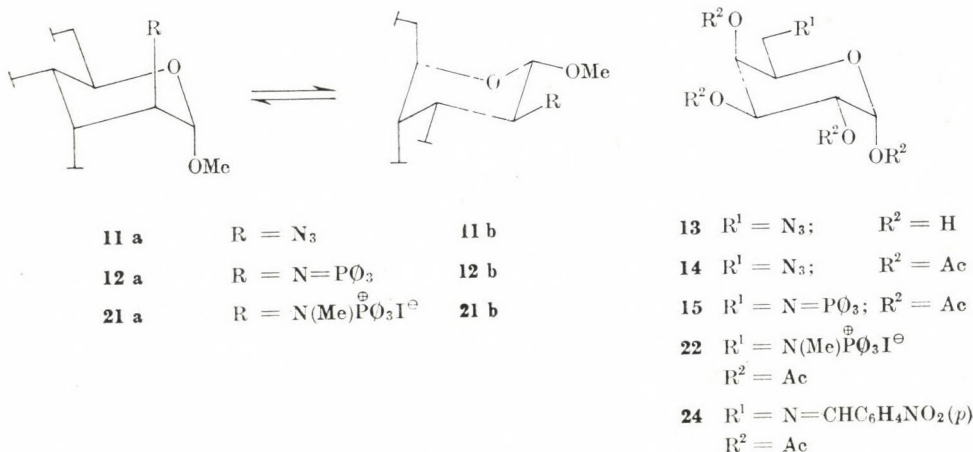


Scheme 2

Similarly, the reaction of triphenylphosphine and 2,3,6-tri-*O*-benzoyl-4-*O*-toluene-*p*-sulfonyl- β -D-galactopyranosyl azide (9), prepared by the method of REIST and coworkers [5], resulted in the corresponding phosphinimine 10.

We have recently shown [6, 7] that the triphenylphosphoranylideneamino group can be attached not only to the anomeric but also to the other carbons of the pyranose ring.

On the basis of this experience a new sugar phosphinimine (12) was obtained from the acetylated derivative (11) [8] of methyl-2-azido-2-deoxy- α -D-altroside [9], having the functional group in axial position on C-2 of the pyranose ring.



Scheme 3

In a similar way the Staudinger reaction of **14** obtained with deacetonation and subsequent acetylation of 6-azido-6-deoxy-1,2;3,4-di-*O*-isopropylidene- α -D-galactopyranose [10] led to 1,2,3,4-tetra-*O*-acetyl-6-deoxy-6-triphenylphosphoranylideneamino- α -D-galactopyranose (**15**).

The different reactivities of the phosphinimino group enabled us to transform these compounds to different sugar derivatives. All phosphinimines were characterized by ready addition with methyl iodide to furnish the corresponding *N*-methylaminophosphonium salts (**16**–**22**). This reaction can be used for the identification of phosphinimines because the methiodide salts are usually easily isolable and more stable than the corresponding phosphinimines.

A characteristic property of the sugar phosphinimines is their Wittig-type reaction with aldehydes to give azomethine derivatives. Thus, treatment of **1** and **15** with *p*-nitrobenzaldehyde afforded Schiff bases (**23**, **24**) of the corresponding amino sugars, which supports the structure of the sugar moiety of phosphinimines. This reaction provides a simple method to produce azomethine derivatives of carbohydrates.

Attempts to deacetylate sugar phosphinimines by Zemplén's method gave no free sugar phosphinimines but glycosylamines as a consequence of decomposition of the phosphinimine moiety. Thus, treatment of **1** and **2** with methanolic sodium methoxide afforded the well known D-glucosylamine [11] and D-galactosylamine [11], respectively. This reaction offers a new convenient synthetic possibility to reduce azides to amines.

Structures of the new sugar phosphinimine derivatives were supported by their ¹H-NMR spectra listed in Table I; the latter contains also the data of some starting azides.

Conformational studies by PAULSEN and coworkers [12] on *N*-substituted-*N*-pentopyranosides have shown that the triphenylphosphoranylideneamino group has a large anomeric effect forcing this group into axial position in the case of the β -anomers. On the other hand, the steric compression of the bulky phosphinimino group counteracts the anomeric effect and may afford conformational equilibria between the *CI* and *IC* conformers.

The *CI* conformation of phosphinimine **7** is considered to be fixed by the fused 1,3-dioxane ring. In the ¹H-NMR spectrum of this compound the anomeric proton appears at δ 4.59 ppm as a doublet of doublets. The splitting of the expected doublet is due to coupling with the phosphorus atom in the β -position ($J_{P,H-1} = 20.5$ Hz). The large coupling constants of $J_{1,2} = 8.0$ Hz and $J_{4,5} = 9.0$ Hz are in good agreement with a *CI* conformation. Comparison of these coupling constants with those for **1** ($J_{1,2} = 7.6$ Hz; $J_{4,5} \sim 8$ Hz) shows that also in the latter case the equilibrium is predominantly shifted towards the *CI* conformer.

Table I

¹H-NMR data of ring protons for compounds 1, 2, 3, 6, 7, 11, 12, 21 and 14

Compound	Chemical shift (δ) in CDCl ₃ (first order couplings, Hz, in parentheses)							
	H-1 (J _{1,2})	H-2 (J _{2,3})	H-3 (J _{3,4})	H-4 (J _{4,5})	H-5	H-6a (J _{5,6})	H-6b (J _{P,C-H})	
1	4.46dd (7.6)	←	5.0—5.3m	→ (~8)	3.61m	← 4.15m →	(20.0)	
2	4.47dd (7.9)	5.46dd (10.1)	4.99dd (3.3)	5.39d (~0)	3.83t	← 4.18d (6.7) →	(21.9)	
3	4.33dd	←	4.9—5.2m	→ (8.3) ^a (4.9) ^b	3.17t ^a 4.03dd ^b		(20.2)	
6 ^c	4.72d (8.3)	4.96t (8.4)	5.34t (8.8)	←	3.6—3.9m	→	4.42dd ^d	
7 ^e	4.59dd (8.0)	← 5.23m →	(9.4)	← (9.0)	3.42—3.83m	→	4.24dd ^f (20.5)	
11	4.70d (3.5)	3.88dd (6.0)	← 5.1—5.3m →		← 4.15—4.55m →			
12	4.56d (2.8)	3.44dd (5.1)	5.03dd (3.2)	5.68dd (7.8)	← 4.2—4.5m →		(22.8)	
21	5.57d (6.6)	3.57m (10.4)	5.53dd (3.7)	5.34t (3.0)	4.06m	4.25 ^g	4.45 ^g (10.0)	
14	6.41d (~1.5)	← 5.37m →	(~2.5)	5.51dd (1.2)	4.31td	3.29dd (5.5)	3.54dd (7.0)	

^a δ_{H-5a}; J_{4,5a}^b δ_{H-5e}; J_{4,5e}^c δ_{H-7} 5.50s^d H-6b = H-6e; J_{5,6e} = 3.6 Hz^e δ_{H-7} 5.48s^f H-6b = H-6e; J_{5,6e} = 4.7 Hz^g AB part of ABX

The large coupling constants of $J_{1,2} = 7.9$ Hz and $J_{2,3} = 10.1$ Hz found for **2** also point to a *C1* conformation, i.e. to the equatorial position of the phosphinimino group. The very small coupling constant $J_{4,5} \sim 0$ Hz is in good agreement with the empirical rule of DE BRUYN and ANTEUNIS [13] concerning the gauche couplings of ring protons in pyranoses.

The $^1\text{H-NMR}$ spectrum of triphenyl-*N*-(2,3,4-tri-*O*-acetyl- β -D-xylopyranosyl)phosphinimine (**3**) in deuterochloroform furnished the coupling constant $J_{4,5a} = 8.3$ Hz. On the other hand, PAULSEN *et al.* [12] found for the same coupling 10.0 Hz in dimethyl sulfoxide- d_6 and suggested that in this solvent **3** exists almost completely in the *C1* conformation. On the basis of these data, the chloroform solution of **3** contains about 70% of the *C1* conformer.

As for 2-substituted derivatives, azide **11** and phosphinimine **12** retain the *C1* conformation (**11a** and **12a**), which is shown by the small values of their coupling constants $J_{1,2}$ (3.5 and 2.8 Hz, respectively). This is surprising, especially in the case of **12** because it shows the bulky triphenylphosphinimino group to be in an axial position. On the contrary, when methoiodide derivative **21** was prepared from **12**, the conformation of the pyranose ring did change to *1C* as was indicated by the increase of $J_{1,2}$ from 2.8 Hz to 6.6 Hz and the decrease of $J_{4,5}$ from 7.8 Hz to 3.0 Hz. The fact that, in this case, the bulky *N*-methylaminotriphenylphosphonio moiety moves to the favourable equatorial position is very probably due not only to the additional steric effect of the small methyl group but also to the positive charge.

According to our results, the Staudinger reaction is generally applicable to all azido sugars and may afford sugar phosphinimines. These readily available derivatives are suitable intermediates in the syntheses of *N*-containing carbohydrates (carbodiimides, heterocyclic derivatives) [14].

Experimental

IR spectra were recorded with a Unicam SP 200 spectrophotometer and the $^1\text{H-NMR}$ spectra were obtained with a JEOL PS-100 instrument in deuterochloroform with tetramethylsilane as internal standard. Optical rotations were measured with an Opton polarimeter.

Triphenyl-*N*-(2,3,4,6-tetra-*O*-acetyl- β -D-glucopyranosyl) phosphinimine (**1**)

To a suspension of tetra-*O*-acetyl- β -D-glucopyranosyl azide [3] (18.5 g, 50 mmol) in dry ether (200 ml) a solution of triphenylphosphine (13.0 g, 50 mmol) in dry ether (50 ml) was added, and the mixture, protected from moisture, was allowed to stand for 1 h. After the azido compound had been dissolved with a strong evolution of nitrogen, crystals of **1** started to separate. After standing overnight in a refrigerator, the crystals were filtered, washed with dry ether and dried over potassium hydroxide in a vacuum desiccator to obtain the crude product (25.8 g, 85%), m.p. 134–35 °C. Recrystallization from dry ether gave pure **1** (16.6 g, 55%) as long, colourless needles, m.p. 135–36 °C, $[\alpha]_D -18.2^\circ$ ($c = 2$, dioxane).

$\text{C}_{32}\text{H}_{34}\text{NO}_9\text{P}$ (607.607). Calcd. P 5.09; CH_3CO 28.34. Found P 5.03; CH_3CO 27.95%. Repeated crystallization of the residue obtained by the evaporation of the mother liquors afforded a further crop of **1** (5.7 g), m.p. 134–35 °C (total yield 22.3 g, 73%).

D-Glucosylamine (Zemplén deacetylation of 1)

To a solution of **1** (1.8 g, 3 mmol) in anhydrous methanol (9 ml) 2 *M* methanolic sodium methoxide (0.1 ml) was added and the solution was left to stand at room temperature for 72 h. The resulting colourless needles were filtered to obtain β -D-glucosylamine (0.4 g, 74%), m.p. 125–30 °C, which, after recrystallization from ethanol, melts at 127–29 °C, $[\alpha]_D + 22.9^\circ$ ($c = 1$, water). LING and NANJI [15] reported m.p. 127–28 °C and $[\alpha]_D + 20.3^\circ$ (water) for D-glucosylamine.

From the methanolic mother liquor triphenylphosphine oxide was obtained (0.4 g, 48%), m.p. 152–53 °C (from benzene-petroleum ether) alone or in admixture with an authentic sample.

Triphenyl-N-(2,3,4,6-tetra-O-acetyl- β -D-galactopyranosyl) phosphinimine (2)

To a suspension of tetra-O-acetyl- β -D-galactopyranosyl azide [3] (7.4 g, 20 mmol) in dry ether (80 ml) a solution of triphenylphosphine (5.2 g, 20 mmol) in dry ether (20 ml) was added and the mixture was allowed to stand at room temperature under protection from moisture. After dissolution of the starting compound, the mixture was refrigerated to obtain the crude product (10.0 g, 82%), which was recrystallized from dioxane-petroleum ether to give pure **2** as fine needles (6.2 g, 51%), m.p. 129–30 °C, $[\alpha]_D - 4.1^\circ$ ($c = 5$, dioxane).

$C_{32}H_{34}NO_9P$ (607.607). Calcd. P 5.09; CH_3CO 28.34. Found P 5.14; CH_3CO 28.25%.

D-Galactosylamine (Zemplén deacetylation of 2)

The solution of **2** (4.86 g, 8 mmol) in anhydrous methanol (20 ml) was treated with 1 *M* methanolic sodium methoxide (0.8 ml) at room temperature for 1 h. After standing overnight in a refrigerator, the separated crystals were filtered, yielding crude D-galactosylamine (1.10 g, 77%), m.p. 132–34 °C. A sample of this compound was crystallized from 80% ethanol to obtain colourless prisms, m.p. 135–36 °C, $[\alpha]_D + 58^\circ \rightarrow +69^\circ$ ($c = 1$, water).

A conventional acetylation of the crude product (0.5 g) with acetic anhydride (1.5 ml) and pyridine (5 ml) gave colourless crystals (0.23 g) of 2,3,4,6-tetra-O-acetyl-N-acetyl- β -D-galactopyranosylamine, m.p. 172–73 °C (from ethanol), $[\alpha]_D + 36^\circ$ ($c = 1$, chloroform); *lit.* [11] m.p., 173 °C, $[\alpha]_D + 34.7^\circ$ (chloroform).

Evaporation of the methanolic mother liquor and treatment with water afforded triphenylphosphine oxide (1.97 g, 89%), m.p. 155–56 °C (from benzene-petroleum ether) alone or in admixture with an authentic sample.

Triphenyl-N-(2,3,4-tri-O-acetyl- β -D-xylopyranosyl)phosphinimine (3)

To a suspension of tri-O-acetyl- β -D-xylopyranosyl azide [3] (12.6 g, 42 mmol) in anhydrous ether, triphenylphosphine (11.2 g, 43 mmol) was added and the mixture was left to stand for 1 h while protected from moisture. After cooling in a refrigerator, the separated white solid was filtered and washed with ether yielding the crude product (20 g, 89%), m.p. 118–19 °C, which was recrystallized from dioxane-petroleum ether to obtain pure **3** as colourless needles (13.4 g, 60%), m.p. 126–28 °C, $[\alpha]_D - 23.8^\circ$ ($c = 2$, dioxane).

$C_{29}H_{30}NO_7P$ (535.542). Calcd. N 2.62; P 5.78. Found N 2.80; P 5.87%.

Triphenyl-N-(2,3,6,2',3',4',6'-hepta-O-acetyl- β -D-cellobiosyl)phosphinimine (4)

To a solution of 2,3,6,2',3',4',6'-hepta-O-acetyl- β -D-cellobiosyl azide [3] (2.6 g, 4 mmol) in anhydrous dioxane (8 ml) triphenylphosphine (1.2 g, 5 mmol) in dioxane (4 ml) was added and the mixture, protected from moisture, was left to stand for 24 h. The solution was added dropwise to petroleum ether (500 ml) to obtain the crude product which was precipitated with petroleum ether from a chloroform solution yielding pure **4** as a white powder (2.5 g, 70%), m.p. 90–95 °C, $[\alpha]_D + 15.7^\circ$ ($c = 2$, dioxane).

$C_{44}H_{50}NO_{17}P$ (895.867). Calcd. P 3.46; CH_3CO 33.63. Found P 3.53; CH_3CO 33.75%.

4,6-O-Benzylidene- β -D-glucopyranosyl azide (5)

A mixture of β -D-glucopyranosyl azide [3] (4.10 g, 20 mmol), finely powdered zinc chloride (2.9 g) and benzaldehyde (10 ml) was shaken for 4 h, then poured into cold water. After successive treating and washing with water, ether, and petroleum ether, the mass solidified (3.90 g, 67%). Recrystallization from ethanol afforded pure **5** (3.05 g, 52%), m.p. 157–58 °C, $[\alpha]_D -53^\circ$ ($c = 2.5$, acetone).

$C_{13}H_{15}N_3O_5$ (293.287). Calcd. C 53.24; H 5.16; N 14.33. Found C 53.90; H 4.82; N 14.12%.

IR (KBr): 3300 cm^{-1} (OH); 2140 cm^{-1} (N_3).

2,3-Di-O-acetyl-4,6-O-benzylidene- β -D-glucopyranosyl azide (6)

Conventional acetylation of **5** (2.50 g, 8.5 mmol) with acetic anhydride and pyridine gave the crude product (3.12 g, 97%) which was twice recrystallized from ethanol to obtain **6** as colourless needles (2.51 g, 78%), m.p. 177 °C, $[\alpha]_D -93^\circ$ ($c = 1.5$, chloroform).

$C_{17}H_{19}N_3O_7$ (377.363). Calcd. C 54.11; H 5.08; N 11.14. Found C 54.33; H 5.58; N 11.10%.

IR (KBr): 2100 cm^{-1} (N_3); 1740 cm^{-1} (AcO).

Triphenyl-N-(2,3-di-O-acetyl-4,6-O-benzylidene- β -D-glucopyranosyl)phosphinimine (7)

To a suspension of **6** (0.94 g, 2.5 mmol) in anhydrous ether (10 ml), a solution of triphenylphosphine (0.67 g, 2.55 mmol) in ether (10 ml) was added and allowed to stand for 4 h under protection from moisture. The solution was evaporated and the resulting glassy product was precipitated with petroleum ether from a benzene solution to give **7** (1.3 g, 85%) as a white amorphous material, $[\alpha]_D +29^\circ$ ($c = 2$, dichloromethane). The completion of the reaction was indicated by the absence of the azide band in the IR spectrum.

$C_{35}H_{34}NO_7P$ (611.640). Calcd. N 2.29; P 5.06. Found N 2.11; P 5.22%.

2,3,5-Tri-O-benzoyl- β -D-galactopyranosyl azide (8)

A solution of β -D-galactosyl azide [3] (2.05 g, 10 mmol) in dry pyridine (20 ml) was cooled to 0 °C, then benzoyl chloride (4.85 g, 34.5 mmol) was added dropwise with stirring. After standing at room temperature for 3 days 70 ml of a cold saturated aqueous solution of sodium bicarbonate was added with stirring to the reaction mixture and was extracted with chloroform (75 ml), washed with water, dried and evaporated to yield the crude product (6 g). Recrystallization from chloroform-petroleum ether gave pure **8** (2.35 g, 45%) as colourless needles, m.p. 147–48 °C, $[\alpha]_D +26.5^\circ$ ($c = 2$, chloroform).

$C_{27}H_{23}N_3O_8$ (517.505). Calcd. C 62.67; H 4.48; N 8.12. Found C 62.42; H 4.77; N 8.45%.

2,3,6-Tri-O-benzoyl-4-O-toluene-p-sulfonyl- β -D-galactopyranosyl azide (9)

To a solution of **8** (2.59 g, 5 mmol) in dry pyridine (10 ml) toluene-p-sulfonyl chloride (3.24 g, 17 mmol) was added with stirring at 0 °C then allowed to stand at room temperature for 3 days. The reaction mixture was poured into ice-water and the precipitate was recrystallized from ethanol to give **9** as colourless needles (2.80 g, 83%), m.p. 180–81 °C, $[\alpha]_D +34^\circ$ ($c = 2$, chloroform).

$C_{34}H_{29}N_3O_{10}S$ (671.969). Calcd. N 6.26; S 4.77. Found N 6.25; S 4.97%.

Triphenyl-N-(2,3,6-tri-O-benzoyl-4-O-toluene-p-sulfonyl- β -D-galactopyranosyl)-phosphinimine (10)

To a solution of **9** (0.67 g, 1 mmol) in dry dichloromethane (20 ml), triphenylphosphine (0.27 g, 1.03 mmol) was added, when a strong nitrogen evolution could be observed. The solution, protected from moisture, was kept for 24 h and then evaporated to obtain **10** (0.90 g) as an amorphous, glassy product, sufficiently pure for further reactions, $[\alpha]_D +92^\circ$ ($c = 2$, dichloromethane).

$C_{52}H_{44}NO_{10}PS$ (905.973). Calcd. N 1.55; P 3.42. Found N 1.76; P 3.29%.

Methyl 3,4,6-tri-*O*-acetyl-2-deoxy-2-(triphenylphosphoranylideneamino- α -D-altroside (12)

To a solution of **11** [8] (3.30 g, 9.56 mmol) in dry ether (20 ml) a solution of triphenylphosphine (2.56 g, 9.75 mmol) in dry ether (15 ml) was added. Nitrogen evolution ceased within 3 h. The mixture was stored overnight under protection from moisture then evaporated. The resulting glassy product was precipitated with petroleum ether from a dichloromethane solution to give **12** as an amorphous material (4.48 g, 81%), $[\alpha]_D +40^\circ$ ($c = 2$, dichloromethane).

$C_{31}H_{34}NO_5P$ (579.596). Calcd. N 2.42; P 5.34. Found N 2.64; P 5.44%.

6-Azido-6-deoxy- α -D-galactose (13)

6-Azido-6-deoxy-1,2,3,4-di-*O*-isopropylidene- α -D-galactopyranose [10] (49.6 g, 0.174 mol) dissolved in a mixture of glacial acetic acid (680 ml) and water (226 ml) was heated for 2 h under reflux on a water bath at 96–97 °C. The solution was then evaporated keeping the temperature below 30 °C and the resulting thick syrup was triturated with ether and with acetonitrile when the material began to crystallize. After standing in a refrigerator for 2 days the white solid was filtered and washed with acetonitrile to obtain the crude product (25.6 g, 72%). Recrystallization from ethanol gave **13** as colourless crystals (20.2 g, 57%), m.p. 133–34 °C, $[\alpha]_D +110^\circ \rightarrow +55^\circ$ ($c = 1$, water).

$C_6H_{11}N_3O_5$ (205.178). Calcd. C 35.12; H 5.40; N 20.48. Found C 35.05; H 4.96; N 20.96%. IR (KBr): 2110 cm^{-1} (N_3).

1,2,3,4-Tetra-*O*-acetyl-6-azido-6-deoxy- α -D-galactopyranose (14)

To a solution of **13** (2.05 g, 10 mmol) in acetic anhydride (20 ml) 5 drops of *cc.* sulfuric acid was added at 0 °C. After 10 min the cooling bath was removed and the mixture was kept at room temperature for 3 h then poured into ice-water. The resulting white precipitate was filtered and washed with water to give the crude product (2.75 g, 74%), m.p. 90–91 °C. Recrystallization from ethanol afforded **14** as colourless plates (1.9 g, 51%), m.p. 92–93 °C, $[\alpha]_D +110^\circ$ ($c = 1$, chloroform).

$C_{14}H_{19}N_3O_9$ (373.330). Calcd. C 45.04; H 5.13; N 11.26. Found C 44.91; H 5.76; N 11.59%.

IR (KBr): 2110 cm^{-1} (N_3); 1745 cm^{-1} (AcO).

1,2,3,4-Tetra-*O*-acetyl-6-deoxy-6-(triphenylphosphoranylideneamino)- α -D-galactopyranose (15)

To a suspension of **14** (4.85 g, 13 mmol) in dry ether (40 ml), triphenylphosphine (3.41 g, 13 mmol) in dry ether (30 ml) was added and the mixture, protected from moisture, was stored for 2 h at room temperature while the evolution of nitrogen ceased. Evaporation of the solution gave **15** as a glassy product (7.88 g, 100%), $[\alpha]_D +53^\circ$ ($c = 1$, dichloromethane).

$C_{32}H_{34}NO_9P$ (607.607). Calcd. P 5.10; CH_3CO 28.34. Found P 4.96; CH_3CO 28.18%. IR ($CHCl_3$): 1745 cm^{-1} (AcO); 1440, 1110 and 700 cm^{-1} (*P*-phenyl).

Triphenyl-(*N*-methyl-2,3,4,6-tetra-*O*-acetyl- β -D-glucopyranosylamino)phosphonium iodide (16)

A solution of **1** (2.00 g, 3.29 mmol) in methyl iodide (8 ml) was kept at room temperature for 2 h. The separated crystals were filtered and washed with ether yielding the crude product (2.45 g, 99%), m.p. 203–204 °C. Two recrystallizations from dichloromethane-ether gave pure **16** (2.05 g, 83%), m.p. 208–209 °C, $[\alpha]_D +25^\circ$ ($c = 2$, chloroform).

$C_{33}H_{37}INO_9P$ (749.552). Calcd. I 16.93; P 4.13. Found I 17.12; P 4.18%.

Triphenyl-(*N*-methyl-2,3,4,6-tetra-*O*-acetyl- β -D-galactopyranosylamino)phosphonium iodide (17)

A solution of **2** (1.00 g, 1.65 mmol) in methyl iodide (5 ml) was allowed to stand for 3 h then saturated with ether. The resulting precipitate (1.11 g, 90%) was recrystallized from dichloromethane-ether to give pure **17** (0.98 g, 79%), m.p. 221 °C, $[\alpha]_D +30^\circ$ ($c = 2$, chloroform).

$C_{33}H_{37}INO_9P$ (749.552). Calcd. I 16.93; P 4.13. Found I 17.31; P 4.07%.

Triphenyl-(*N*-methyl-2,3,4-tri-*O*-acetyl- β -D-xylopyranosylamino)phosphonium iodide (18)

A solution of **3** (3.30 g, 6.16 mmol) in methyl iodide (10 ml) was kept at room temperature for 3 h then mixed with ether to precipitate the crude salt (**18**) (4.03 g, 97%), m.p. 223–24 °C. Recrystallization from ethanol afforded the pure product as a colourless crystalline compound (3.35 g, 80%), m.p. 229–30 °C, $[\alpha]_D +14.5^\circ$ ($c = 2.5$, chloroform).

$C_{30}H_{33}INO_7P$ (677.487). Calcd. I 18.73; P 19.06. Found I 18.75; P 19.24%.

Triphenyl-(*N*-methyl-2,3-di-*O*-acetyl-4,6-*O*-benzylidene- β -D-glucopyranosylamino)phosphonium iodide (19)

A solution of **7** (0.39 g, 0.64 mmol) in methyl iodide (1.5 ml) was allowed to stand overnight, then mixed with an excess of ether to precipitate the crude product (0.42 g, 87%). Recrystallization from ethanol gave pure **19** as pale yellow cubes (0.29 g, 60%), m.p. 240–41 °C, $[\alpha]_D -7^\circ$ ($c = 2$, chloroform).

$C_{36}H_{37}INO_7P$ (753.585). Calcd. N 16.84; P 4.11. Found N 16.87; P 4.16%.

Triphenyl-(*N*-methyl-2,3,6-tri-*O*-benzoyl-4-*O*-toluene-*p*-sulfonyl- β -D-galactopyranosylamino)phosphonium iodide (20)

A solution of **10** (0.60 g, 0.66 mmol) in methyl iodide (2 ml), after standing overnight, was saturated with ether to obtain the crude salt (0.28 g, 40%). Precipitation with ether from dichloromethane solution gave **20** as yellow powder (0.20 g, 29%), m.p. 145–50 °C (dec.), $[\alpha]_D +75.5^\circ$ ($c = 1$, chloroform).

$C_{53}H_{47}INO_{10}PS$ (1047.918). Calcd. I 12.11; P 2.96. Found I 12.30; P 3.09%.

Methyl 3,4,6-tri-*O*-acetyl-2-deoxy-*N*-methyl-2-(triphenylphosphonioamino)- α -D-altroside iodide (21)

A solution of **12** (0.58 g, 1 mmol) in methyl iodide (3 ml), after standing for 2 h, was mixed with ether to precipitate the crude product (0.63 g, 88%). Recrystallization from acetonitrile-ether gave pure **21** as pale yellow crystals (0.55 g, 76%), m.p. 213–14 °C, $[\alpha]_D +25^\circ$ ($c = 2$, chloroform).

$C_{32}H_{37}INO_8P$ (721.541). Calcd. I 17.59; P 4.29. Found I 18.09; P 4.39%.

1,2,3,4-Tetra-*O*-acetyl-6-deoxy-*N*-methyl-6-(triphenylphosphonioamino)- α -D-galactopyranose iodide (22)

A solution of **15** (3.00 g, 4.94 mmol), in methyl iodide (10 ml) was left to stand at room temperature for 2 h then mixed with ether to obtain the crude product (3.60 g, 97%). Recrystallization from dichloromethane-ether gave crystals of **22** (2.88 g, 78%), m.p. 215–16 °C, $[\alpha]_D +63^\circ$ ($c = 2$, chloroform).

$C_{33}H_{37}INO_9P$ (749.552). Calcd. I 16.93; P 4.13. Found I 16.88; P 3.90%.

2,3,4,6-Tetra-*O*-acetyl-*N*-*p*-nitrobenzylidene- β -D-glucopyranosylamine (23)

(A) 2,3,4,6-Tetra-*O*-acetyl- β -D-glucopyranosylamine [**11a**] (0.40 g, 1.15 mmol) and *p*-nitrobenzaldehyde (0.20 g, 1.32 mmol) in methanol (3 ml) were refluxed for 10 min. The mixture was concentrated to dryness and the residue crystallized from chloroform-petroleum ether to give the crude product (0.40 g, 72%). Recrystallization from ethanol gave pure **23** as colourless needles, m.p. 148–49 °C, $[\alpha]_D -22.3^\circ$ ($c = 1$, chloroform).

$C_{21}H_{24}O_{11}N_2$ (480.439). Calcd. C 52.50; H 5.04; N 5.83. Found C 51.89; H 4.91; N 5.95%.

(B) A solution of **1** (1.82 g, 3 mmol) and *p*-nitrobenzaldehyde (0.50 g, 3.3 mmol) in anhydrous dioxane (5 ml) was refluxed for 20 h. The solvent was then removed in vacuum and the residue crystallized from chloroform-petroleum ether yielding the crude product (0.80 g, 56%). Recrystallization from benzene-petroleum ether gave pure **23**, m.p. 148–49 °C alone or in admixture with the sample from (A).

From the chloroform-petroleum ether filtrate, triphenylphosphine oxide (0.61 g, 73%g was isolated, m.p. 153–55 °C (from cyclohexane) which gave no depression on mixture melting point with an authentic sample.

1,2,3,4-Tetra-*O*-acetyl-6-deoxy-6-(*p*-nitrobenzylideneamino)- α -D-galactopyranose (24)

A solution of **15** (1.21 g, 2 mmol) and *p*-nitrobenzaldehyde (0.32 g, 2.1 mmol) in anhydrous ethyleneglycol dimethyl ether was heated under reflux for 15 h, then the solvent was removed in vacuum. The residue was treated with ether to obtain triphenylphosphine oxide (0.35 g, 63%), m.p. 151–52 °C, which gave no depression on mixture melting point with an authentic sample.

Evaporation of the mother liquor gave, after repeated recrystallization from ethanol, Schiff base **24** (0.58 g, 57%), m.p. 151 °C, $[\alpha]_D^{25} + 71.5^\circ$ ($c = 1$, chloroform).

$C_{21}H_{24}N_2O_{11}$ (480.439). Calcd. N 5.83; CH_3CO 35.83. Found N 5.63; CH_3CO 35.58% IR (KBr): 1750 cm^{-1} (AcO); 1645 cm^{-1} (C=N).

REFERENCES

- [1] MESSMER, A., PINTÉR, I., SZEGŐ, F.: *Angew. Chem.*, **76**, 227 (1964)
- [2] STAUDINGER, H., HAUSER, E.: *Helv. Chim. Acta*, **4**, 861 (1921)
- [3] MICHEEL, F., KLEMER, A.: *Advances in Carbohydrate Chemistry*, Vol. **16**, p. 85. Academic Press, New York 1961
- [4a] WHISTLER, R. L., WOLFROM, M. L.: *Methods in Carbohydrate Chemistry*, Vol. **I**, p. 351. Academic Press, New York 1962
- [4b] FREUDENBERG, K., TOEPFFER, H., ANDERSEN, C. C.: *Ber.*, **61**, 1750 (1928)
- [5] REIST, E. J., SPENCER, R. R., CALKINS, D. F., BAKER, B. R., GOODMAN, J.: *J. Org. Chem.*, **30**, 2312 (1965)
- [6] PINTÉR, I., KOVÁCS, J., MESSMER, A.: *Carbohydr. Res.*, **53**, 117 (1977)
- [7] PINTÉR, I., KOVÁCS, J., MESSMER, A., TÓTH, G., LINDBERG, K. B., KÁLMÁN, A.: *Carbohydr. Res.* **72**, 289 (1979)
- [8] CLÖDE, D. M., HORTON, D.: *Carbohydr. Res.*, **14**, 405 (1970)
- [9] GUTHRIE, R. D., MURPHY, D.: *J. Chem. Soc.*, **1963**, 5288
- [10] SZAREK, W. A., JONES, J. K. N.: *Can. J. Chem.*, **43**, 2345 (1965)
- [11a] ELLIS, G. P., HONEYMAN, J.: *Advances in Carbohydrate Chemistry*, Vol. **10**, p. Academic Press, New York 1955
- [11b] FRUSH, H. L., ISBELL, H. S.: *J. Research Natl. Bur. Standards*, **47**, 239 (1951) 95
- [12] PAULSEN, H., GYÖRGYDEÁK, Z., FRIEDMANN, M.: *Chem. Ber.*, **107**, 1590 (1974)
- [13] DE BRUYN, A., ANTEUNIS, M.: *Org. Magn. Res.*, **8**, 228 (1976)
- [14] PINTÉR, I., KOVÁCS, J., MESSMER, A., TÓTH, G.: *Acta Chim. Acad. Sci. Hung.* (to be published)
- [15] LING, A. R., NANJ, D. R.: *J. Chem. Soc.*, **121**, 1682 (1922)

József KOVÁCS

István PINTÉR

András MESSMER

Ferenc SZEGŐ

H-1025 Budapest, Pusztaszeri út 59–67

Gábor TÓTH

Present address: Institute for General and Analytical Chemistry Technical University: H-1521 Budapest, Műgyetem

STRUCTURE AND SELECTIVE SODIUM SORPTION OF HYDRATED ANTIMONY PENTOXIDE

L. G. NAGY, G. TÖRÖK and G. FÓTI

(Department of Applied Chemistry, Technical University,
Budapest)

Received July 11, 1978

Accepted for publication August 3, 1978

A method has been developed for the reproducible preparation of hydrated antimony pentoxide (HAP) of optimal quality, and for its complex qualification. This sorbent separates sodium from multicomponent, neutron-activated samples with maximal selectivity and efficiency. The likely mechanism of sodium sorption has been found to be equivalent sorption on the basis of derivatographic, IR spectroscopic, X-ray diffraction and immersion calorimetric measurements.

Introduction

Neutron activation investigations on biological samples were started by us about ten years ago [1-9]. In addition to the steady increase in the number of essential and toxic trace elements, this choice was also justified by the well-known advantages of neutron activation analysis. We were also influenced by the observation that the intrinsic sensitivity limit of today's trace analytical methods cannot be exploited due to technical or economical reasons and therefore, the selection of the method to be used is determined mainly by the requirements, *viz.* the number of elements to be determined, contamination, concentration range, number of samples, *etc.*

It seems expedient to consider the fast spreading of mechanized and automated analyzing systems, and the fact that owing to matrix effects, nondestructive methods do not always ensure the sensitivity required.

When planning the necessary separation process, we considered that due to the nearly identical elemental composition of biological samples, the same separation technique should be used for every matrix. Consequently, for general purpose trace element survey an automatic or automatable analytical process should be developed.

In order to preserve the advantages of the nondestructive method as much as possible, we endeavoured to develop a flexible and open radiochemical separation process, by which the chemical separation can be carried out in correspondence with the actual requirements (Fig. 1).

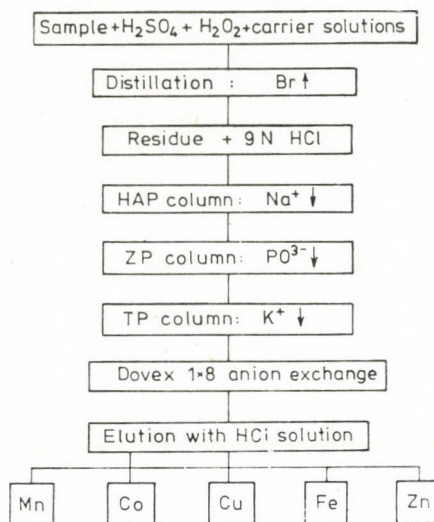


Fig. 1. Separation scheme

These requirements can be most appropriately fulfilled if

1) the inevitable digestion of the sample is combined with a reactive distillation procedure (by this way, *e.g.* the ^{82}Br , a component of the matrix activity can also be removed);

2) the high activity components in the distillation residue (^{24}Na , ^{42}K and ^{32}P) are removed by a selective procedure, *i.e.* a radiochemical separation is performed. By this method, the requirements concerning the selectivity of the further separation steps may be significantly reduced, moreover, in many cases the sample can already be measured;

3) the further separation steps consist of individual separations based on group separations, thus every smaller group of elements can be measured either directly or after individual separation.

For practical use, in addition to the radiochemical process, the whole trace element analysis had to be elaborated and standardized, from sampling and experiment planning to data presentation.

In the following, one of the most important fields is summarized. Hydrated antimony pentoxide (HAP) and the investigations with this material as a sorbent for the removal of ^{24}Na , which is a component of the matrix activity, are presented.

Properties of hydrated antimony pentoxide

Hydrated antimony pentoxide was introduced into radioanalysis for the separation of ^{24}Na by GIRARDI and coworkers because, according to their experiments, it makes possible separations of high selectivity in strongly acidic media [10, 11].

Their results are, however, not always reproducible, and on the basis of their data it is not possible to decide whether this uncertainty is due to the inhomogeneity of the material, the unknown mechanism of sorption or the ill-defined experimental conditions.

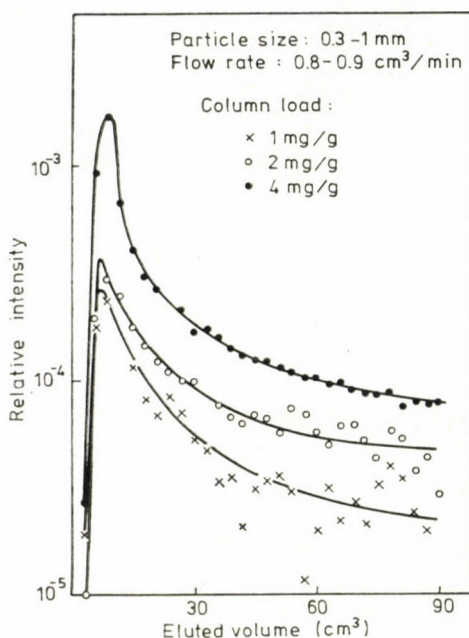


Fig. 2. Differential elution curves

Thus the method is only applicable if the suitable preparation technique and qualification method are previously elaborated, and the industrial parameters are determined. An investigation of the sorption mechanism seems to be necessary too. In the first step, this was considered from the point of view of the solid phase only, the parameters of the liquid being kept unchanged.

For primary qualification of the product a method has been worked out which models the practical application and provides immediately usable data. For this purpose a tracer elution chromatographic technique has been developed.

The relative intensities are calculated from the measured intensities of the eluted fractions in the knowledge of the total intensity on the column. If these values are plotted against the eluted volume or fraction number, a so-called differential elution curve is obtained (Fig. 2). The integrated elution curve is produced by the summation or integration of the differential one (Fig. 3).

The value corresponding to the asymptote of the integrated elution curves can be interpreted as the intensity proportional to the total eluted volume. By plotting the logarithm of this limiting value against the column load, adsorption isotherm data can be obtained. The sorption isotherms, being sensitive indicators of the quality of the preparations, can be used for the

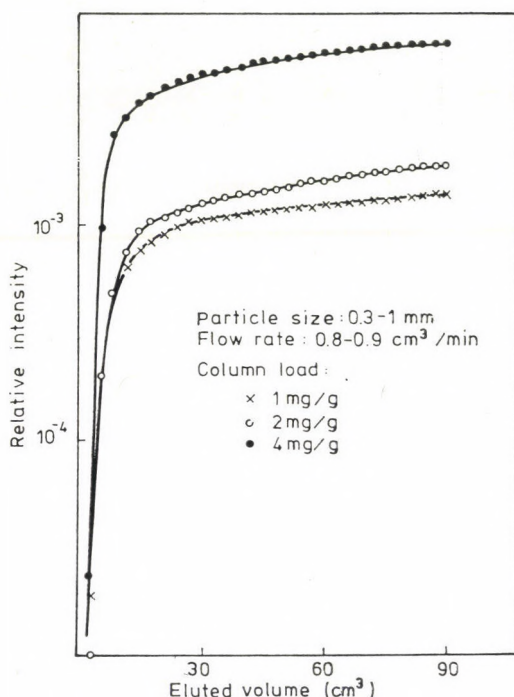


Fig. 3. Integrated elution curves

qualification and optimization of both products and sorption processes (Fig. 4). In Fig. 4 sorption isotherms determined under various experimental conditions are shown. Apparently, the separation factor depends strongly on the flow rate. An increase of 0.8 cm³/min in the flow rate in the interval of 0.8–2.5 cm³/min impairs the separation factors by about one order of magnitude. Consequently, the flow rate should be kept as low as possible.

However, by applying concentrated solutions, the efficiency of the sorption can be improved. A decrease in the dead volume from 1 cm³ to 0.2 cm³ improves the partition coefficient by 0.5–2 orders of magnitude, depending on the column load.

Thus, optimal sorption parameters can be achieved by using the possible least dead volumes and concentrated solutions.

From this concentration dependence it follows that the rate-determining step is a concentration-dependent process.

For the manufacturing process, however, fast and simple qualification methods should be found. For this purpose the simultaneous application of the following two procedures proved to be the most suitable.

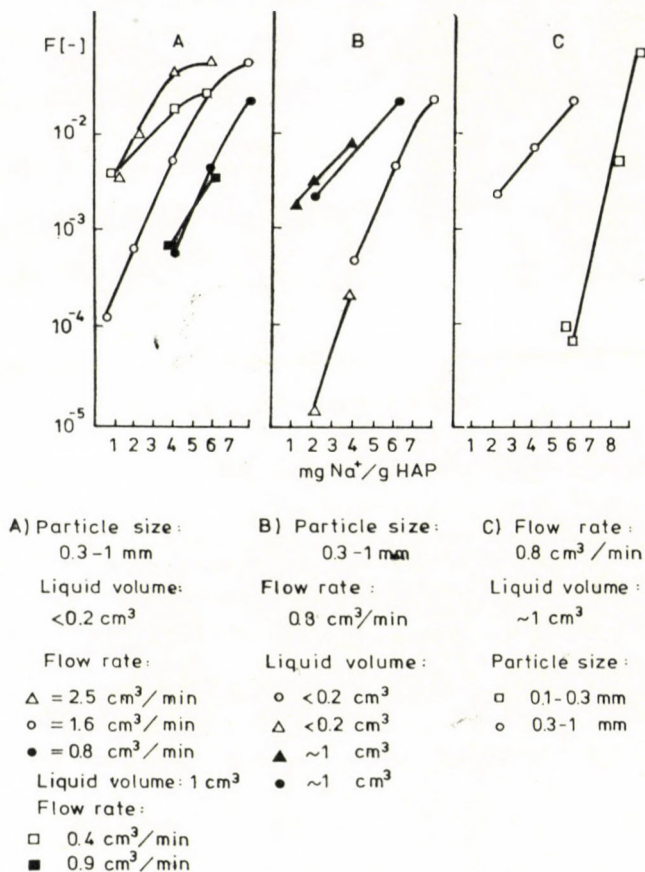


Fig. 4. Sorption isotherms of a "good" HAP preparation

1. Colour test by reflection colorimetry. The materials with the appropriate sorption properties are to be found in the spectral region of the colour ratio 0.15–0.3. The colour-identical wave length is practically 571–574 nm. The procedure is significantly faster, simpler and more accurate than the evaluation of the slopes of reflection spectra in the visible region.

2. The gross of weight loss at 270 °C is determined, which amounts to about 10–15% in case of good preparations.

On the basis of elution measurements, which were completed by ion-exchange and isotopic exchange investigations, it could be concluded that

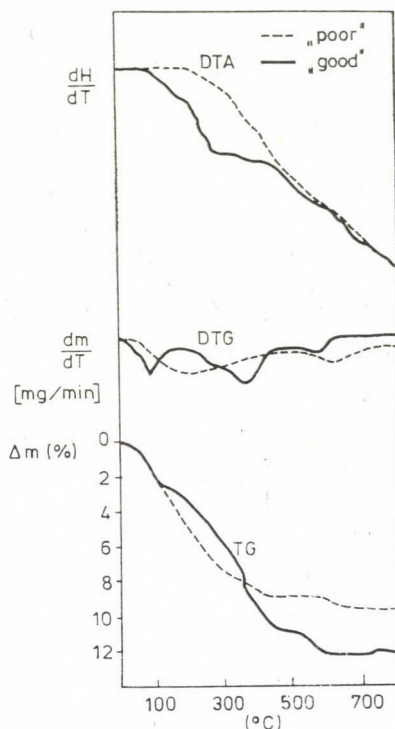


Fig. 5. Derivatograms of the HAP samples

- HAP is a polyfunctional inorganic sorbent, on which ion-exchange or specific irreversible sorption process predominates, depending on the experimental parameters:
- sorption is a fast surface process.

The main results of measurements concerning the structure and sorption mechanism of HAP are presented in Table I. Representative results are illustrated in Figs 5—9. Derivatograms for the good preparations differ significantly from those for the poor ones.

On the TG curves of the good samples three steps can be distinguished: the first one lying between 20 and 150 °C, the second one between 250 and 450 °C and the third one between 550 and 650 °C. The first process is to be assigned to the removal of physically adsorbed water, the second and third ones can be interpreted as structural changes (removal of structural water and oxygen). It should be emphasized that the product treated at 270 °C shows a weight loss already above 20—40 °C, which indicates the mobility of the water content (Fig. 5).

The most characteristic part of the infrared spectrum is the broad absorption maximum between 2500 and 3600 cm^{-1} , which, due to its large band-

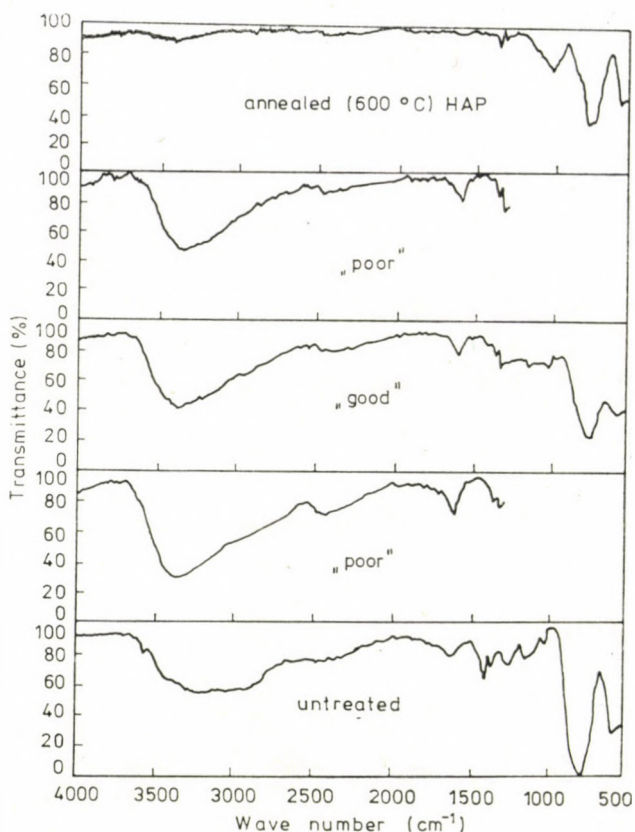


Fig. 6. IR spectra of some HAP samples

Table I

Property	Data	Method
Chemical composition	$\text{Sb}_2^{5+} \cdot \text{Sb}^{3+} \cdot \text{O}_6 \cdot \text{OH} + (\text{H}_2\text{O} \cdot \text{O})_m$ $10 < m < 12$	thermal and activation analysis
Crystal structure	pyrochlor structure $d = 10.3 \text{ \AA}$	X-ray diffraction
Specific surface area	$20 - 30 \text{ m}^2/\text{g}$	sorptometry
Heat of hydration	$6 - 10 \text{ cal/g} \approx 0.3 \text{ cal/m}^2$	microcalorimetry
Fine and hyperfine structure	heteroenergetic and mobile $\text{OH}(\text{H}_2\text{O})$ groups	IR-spectroscopy, colour tests
Porosity	non-porous	Hg-porosimetry
Sorption properties	$c' < 1 \text{ mg/g}$: irreversible sorption $c' > 10 \text{ mg/g}$: ion-exchange model	elution chromatography combined with tracer techniques

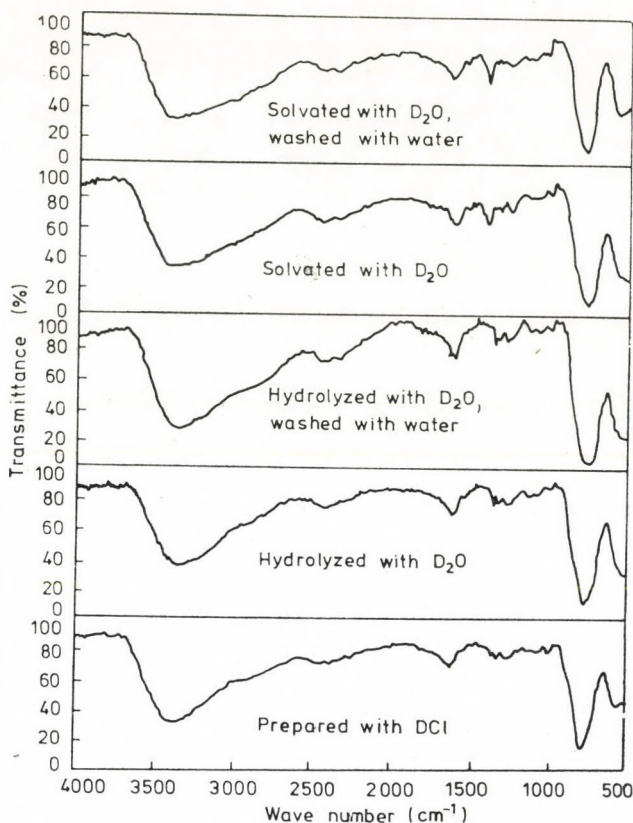


Fig. 7. IR spectra of some HAP samples

width, can be assigned to the stretching mode of heteroenergetically bound water. The mobility of the water content is also proved by the fact that the IR spectra of products deuterated at various stages of the preparation procedure are identical.

According to X-ray diffraction investigations, good samples are all unambiguously crystalline, with a pyrochlor structure. It could be established that the essential condition of sodium sorption is the nearly total occupation of the 48 (f) and 8 (b) positions by oxygen ions and water molecules. Due to structural reasons, the average oxidation state of the good preparations is $5\frac{1}{2}$, because those 16 (d) positions would be occupied by Sb^{3+} ions onto which the desolvated sodium ions can be incorporated (Fig. 8).

The heat of wetting was measured with a quasi-adiabatic microcalorimeter. The hydration of good preparations is a fast process, the shape of the curve is practically determined by the time constant of the apparatus. The heat effect is 22–26 J/g. On the contrary, the hydration of the poor samples is very slow, and the heat of wetting per unit mass is also higher (Fig. 9).

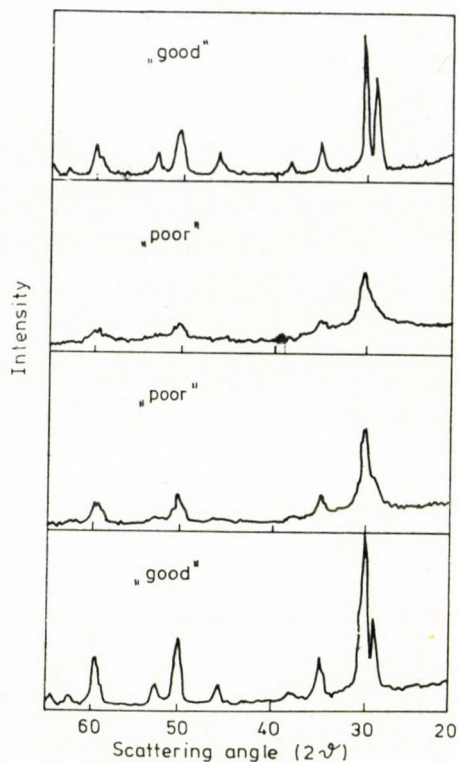


Fig. 8. X-ray diffraction curves of some HAP samples

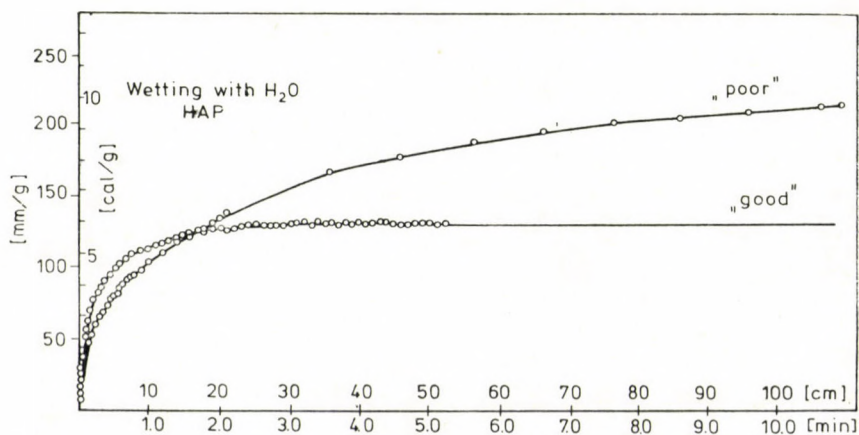


Fig. 9. "Thermal kinetics" of the hydration of HAP

The heats of wetting per unit BET surface are identical within the experimental error: about $1-1.5 \text{ J/m}^2$. This value is an order of magnitude higher than the heat effects measured on charcoals, a fact confirming chemisorption.

Mechanism of sodium sorption on HAP

1. Sorption is a fast surface process.

2. In strongly acidic and complex-forming media, the process is selective for sodium. The disturbing ions are masked presumably *via* the formation of anionic complexes, which is supported *e.g.* by the extremely high selectivity in HCl. The high acid concentration excludes simple ion-exchange processes. It is assumed that in the hydrochloric acid phase the ions are desolvated.

3. Selective sorption with an appropriate partition coefficient (capacity) can be measured on crystalline HAP-s with a well-defined amount and bending of water.

4. According to our sorption capacity measurements, 1–2 sodium ions can be sorbed on each unit cell.

The assumed mechanism is *equivalent sorption*. The sodium ions will occupy empty surface (d) positions and remain partly solvated.

The corresponding counter-ion is bound to the surface by electrostatic forces.

Thus, the process can be regarded as surface sorption in which the empty surface (d) positions act as active centers. Ions with unsuitable geometrical dimensions cannot occupy the vacancies. Ions whose heats of hydration on the active center are smaller than the sum of the binding energies of the ion in the liquid phase cannot be introduced either.

REFERENCES

- [1] TÖRÖK, G., DIEHL, J. F.: *Radiochim. Acta*, **15**, 96 (1971)
- [2] TÖRÖK, G., DIEHL, J. F.: *Radiochim. Acta*, **16**, 106 (1971)
- [3] TÖRÖK, G., FÓTI, G., NAGY, L. G., TÓTH, T., FEUER, L.: *Magy. Kém. Folyóirat*, **78**, 277 (1972)
- [4] TÖRÖK, G., SCHELENZ, R., FISCHER, E.: *Berichte der Bundesforschungsanstalt für Lebensmittelfrischhaltung, Karlsruhe*, Vol. **1**, p. 22 (1972)
- [5] TÖRÖK, G., SCHELENZ, R., FISCHER, E., DIEHL, J. F.: *Z. Anal. Chem.*, **263**, 110 (1973)
- [6] TÖRÖK, G., SCHELENZ, R., FISCHER, E.: *Berichte der Bundesforschungsanstalt für Lebensmittelfrischhaltung*, Vol. **2**, p. 164 (1973)
- [7] NAGY, L. G., TÖRÖK, G., FÓTI, G., TÓTH, F., FEUER, L.: *J. Radioanal. Chem.*, **16**, 245 (1973)
- [8] NAGY, L. G., TÖRÖK, G., FÓTI, G.: *Proc. Internat. Conf. Colloid and Surface Science*, p. 33, Budapest, 1975
- [9] NAGY, L. G., TÖRÖK, G., FEUER, L.: *Proc. Internat. Conf. Modern Trends in Activation Analysis*, p. 626, München, 1976
- [10] GIRARDI, F., SABBIONI, E.: *J. Radioanal. Chem.*, **1**, 169 (1968)
- [11] GIRARDI, F., PIETRA, R., SABBIONI, E.: *Report EUR*, 4287 (1969)

Lajos György NAGY	}	H-1521 Budapest, Egri József u. 20/22.
Gábor TÖRÖK		
György FÓTI		

MOLECULAR ENCAPSULATION OF VOLATILE, EASILY OXIDIZABLE LABILE FLAVOUR SUBSTANCES BY CYCLODEXTRINS

J. SZEJTLI, L. SZENTE and E. BÁNKY-ELŐD

*(Chinoïn Pharmaceutical and Chemical Works, Biochemical
Research Laboratory, Budapest)*

Received June 13, 1978

Accepted for publication August 22, 1978

β -Cyclodextrin inclusion complexes of 25 various flavour substances (spice aromatics and essential oils of vegetable origin) have been prepared. The crystalline complexes contained 8–13% included substance, determined by gas-liquid chromatography. All major components of the original substances were present in the complexes, with a practically unchanged composition. The fact of complex formation was proved by X-ray diffraction and stability tests. The oxygen uptake of the flavour substances — measured by Warburg's method — was reduced to about one tenth by complexation. Volatile components are released from the complexes only above 160 °C, thus under habitual storage conditions the volatility, oxidation and heat-decomposition are reduced to such an extent that the product can be stored for a long time without lessening its utility. These complexes can be used in the food industry as microbiologically noncontaminated, stable aromatic preparations of standardized composition.

Introduction

The various vegetable parts (seed, flower, tuber, leaf, stem, root) containing flavour substances (mainly vegetal essential oils) of natural origin are widely used in nutrition. There are, however, several drawbacks to their use ;

- their preparation and processing in food technology is labourious,
- the composition of the raw substances of vegetable origin is not constant,
- they may contain microbiological and parasitic contaminations,
- the amount of the contained flavour substances and fragrances decreases during storage, and the ratio of their constituents may change disadvantageously.

Liquid aroma extracts, and concentrates have been known for a long time, but in this form (extracted from the cellular structure) they are even less stable. Thus their use is only limited (*e.g.* in canned food industry).

The majority of natural flavour substances and fragrances are monoterpene hydrocarbons, or their oxygenated derivatives. When exposed to the oxygen of air, light and heat they are oxidized, decomposed, become resinous, or they evaporate.

One of the new possibilities to stabilize these substances is the formation of inclusion complexes with cyclodextrins, which process can actually be considered as a molecular encapsulation [1, 2].

Cyclodextrins are cyclic oligomers built up from glucopyranose units. The diameter of the internal cavity of α -cyclodextrin comprising 6 glucopyranose units is about 6 Å, that of the 7 membered β -cyclodextrin is about 8 Å (Fig. 1), and that of 8 membered γ -cyclodextrin is about 10 Å. The primary and secondary hydroxyl groups are to be found on the opposite edges of the torus-like molecules, the "lining" of the ring cavity is formed by oxygen bridge atoms; therefore the external surface of cyclodextrins is of hydrophilic, while the interior of the cavity is of hydrophobic character. The consequence of this

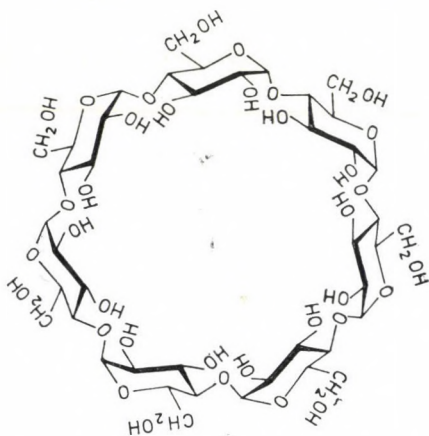


Fig. 1. Structure of β -cyclodextrin

is that cyclodextrins are able to form inclusion complexes with such substances which are less polar than water and their geometrical dimensions correspond to the diameter of the cyclodextrin cavity (Fig. 2).

The interior of the cavity of cyclodextrin molecule dissolved in water is less hydrophilic than the outer surface of the ring, therefore the presence of water molecules in the hollow is energetically unfavoured (Fig. 3); the apolar parts of the organic molecules, dissolved in water, are poorly hydrated, thus energetically unfavoured, too. The poorly hydrated organic guest molecule penetrates into the cyclodextrin cavity, expulsing from there the water molecules of higher enthalpy, resulting in a lower free energy of the system; this seems to be the main driving force of the complex formation. In addition, the ring tension may also decrease, hydrogen bonds are formed *etc.* which factors all contribute to the stabilization of the complex [3].

From the practical point of view, the majority of the components of important essential oils and flavour substances are of a size which can fit tightly into the cavity of the β -cyclodextrin molecule to form inclusion complexes [2].

This phenomenon constitutes the basis of molecular encapsulation of components of aroma substances by means of the formation of cyclodextrin inclusion complexes.

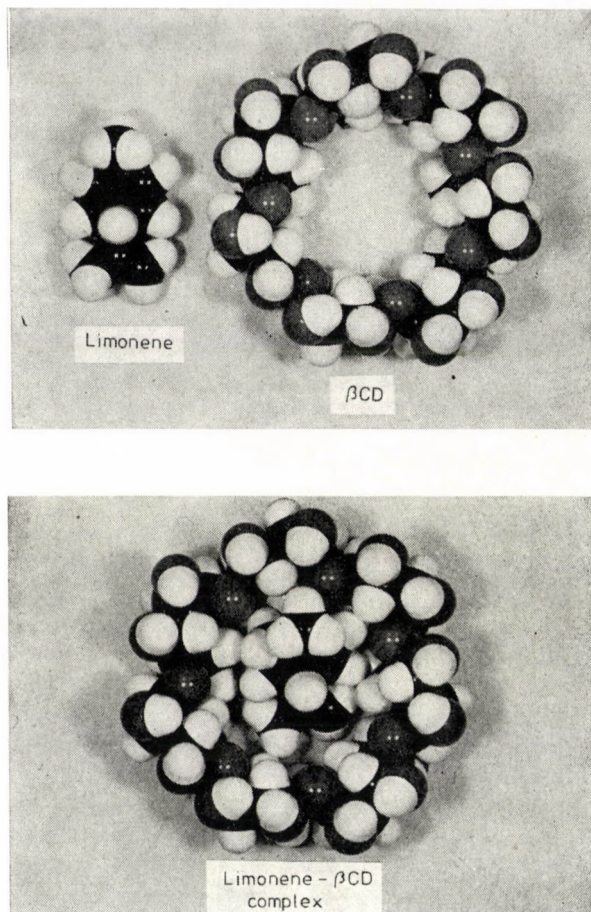


Fig. 2. Scale-model of β -cyclodextrin, limonene and their inclusion complex. All terpene components possessing similar shape and size are suitable to fit tightly into the cyclodextrin cavity

Cyclodextrin inclusion complexes in solution are of stoichiometric composition, for which it is characteristic that the "guest molecule" is to be found in the cavity of the "host molecule", i.e. in the cyclodextrin cavity, and the whole complex is surrounded by a hydrate envelope [4]. In the case of solid, crystalline complexes, the strict stoichiometric composition (guest: host molecular ratio 1 : 1 or 1 : 2) is rare, since cyclodextrin molecules which contain only water molecules incorporated into the cyclodextrin cavity represent spots

of deficiency within the crystal structure. Such a structure is actually a mixture of inclusion complex, cyclodextrin, moreover guest molecules entrapped within the crystals or adsorbed on the crystal surface.

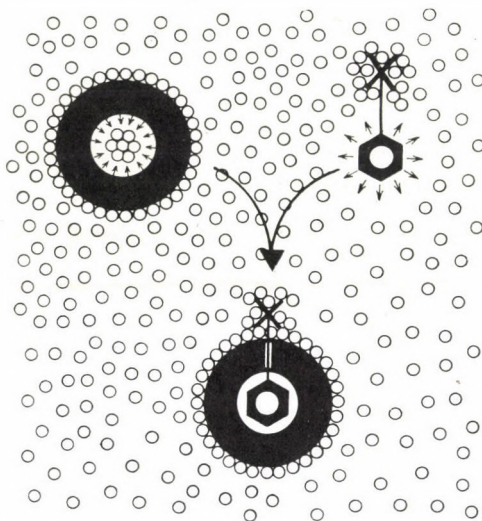


Fig. 3. Schematic representation of the complex formation; \circ = water molecule, \times = hydrophilic substituent of the guest molecule. The interior of the cyclodextrin cavity is poorly hydrated on account of its hydrophobic character, similarly acts the apolar part of the guest molecule; the consequence of complex formation is that the apolar surface of the CD-cavity gets into contact with the apolar surface of the guest molecule

Preparation of inclusion complexes

The method used for the study of the crystallization of cyclodextrin inclusion complexes was described in a previous paper [5]. Aroma complexes have been prepared by adding the aroma substance dissolved in ethanol or diethyl ether under vigorous stirring to an aqueous solution of β -cyclodextrin saturated at 50 °C. It is important to add the solution of the flavour substances only dropwise in order to avoid the formation of an emulsion. With aroma substances which produced immediately an emulsion when added to the aqueous cyclodextrin solution, the complex was prepared in a 30% aqueous ethanol solution. In this solvent mixture cyclodextrin has maximum solubility. After the termination of the addition, the temperature should be maintained for further 15 minutes; thereafter the reaction mixture is cooled to room temperature under steady stirring for 4 and a half hours.

The mixture is stored for 12 hours at about 0 °C, then filtered and dried. In certain cases the solvent is removed by freeze-drying, in which case an amorphous white powder is obtained.

Analysis by gas chromatography

Gas-liquid chromatography is the most suitable method for determining the composition of the original, as well as of the complexed essential oils or flavour substances. Since the taste and aroma properties are decisively influenced not only by the presence of the various components but also by their ratio, it was essential to study whether the components incorporated into the complex are present with the same compositions as found in the original aroma

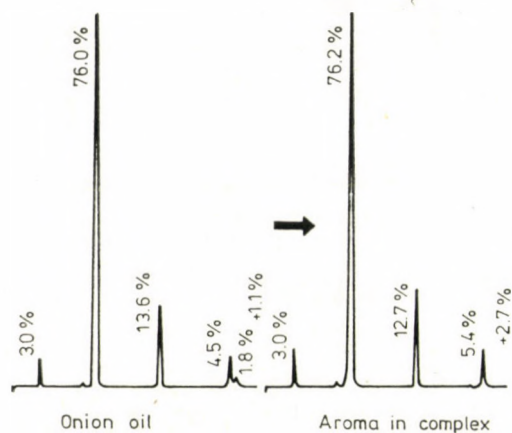


Fig. 4. Gas-liquid chromatogram of free and β -cyclodextrin-complexed onion oil. Column: 4 ft, packed with 10% UCW 982 on Carbowack, t_{inj} : 250 °C, t_{FID} : 300 °C, t_{column} : programmed from 80–250 °C at 10 °C/min, carrier gas: N₂ at 20 ml/min

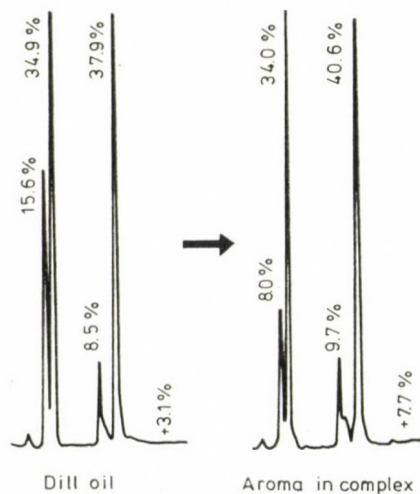


Fig. 5. Gas-liquid chromatogram of free and β -cyclodextrin-complexed dill oil. Parameters: as in Fig. 4

substances. The practical use of these complexes is decisively influenced by this circumstance.

The analyses have been carried out on Hewlett-Packard 5830-A type apparatus. Figures 4 and 5 show the chromatograms obtained. Since no reference substances of adequate purity were available for all components, the retention times observed at the respective chromatographic parameters were used to characterize the individual components. The results for some aroma substances and their complexes are shown in Table I. As seen, all the major components are found nearly in the same relative amount in the complex as in the original oil; thus they are expected to elicit the same effect in the organs of sense.

Table I
Lemon oil

Retention time (min)		Area, %	
Original oil	Complex	Original oil	Complex
2.47	2.47	1.881	1.715
3.79	3.82	0.405	0.641
4.15	4.19	75.782	75.905
4.60	4.63	6.001 (citral)	6.936
5.75	5.75	3.706	3.812
6.71	6.77	4.670 (citronellol)	4.593
7.29	7.31	4.321	4.433
7.89	8.01	0.846	1.007
11.99	12.00	0.723	0.750
13.40	13.52	1.865	0.208

Garlic oil

Retention time (min)		Area, %	
Original oil	Complex	Original oil	Complex
1.13	1.06	0.179	0.097
1.31	1.29 (diallyl disulfide)	81.292	78.986
3.06	3.10	0.086	0.138
3.21	3.20	0.180	0.219
3.48	3.51	17.212	18.715
4.17	4.12	0.011	0.312
6.25	6.25	0.780	0.812
9.82	9.80	0.031	0.186
13.63	13.60	0.026	0.120
17.35	17.39	0.111	0.208
18.10	18.07	0.092	0.172

Allyl mustard oil

Retention time (min)		Area, %	
Original oil	Complex	Original oil	Complex
1.13	1.25	0.079	0.009
1.39	1.38	0.080	0.350
1.61	1.60 (allyl isothiocyanate)	97.157	94.438
3.61	3.40	0.020	0.013
8.36	8.39	0.086	0.375
8.70	8.69	0.065	0.174
9.33	9.31	0.038	0.657
9.55	9.52	1.706	0.033
13.22	13.66	0.770	1.592

Marjoram oil

Retention time (min)		Area, %	
Original oil	Complex	Original oil	Complex
1.95	2.00	1.637	1.539
2.37	2.41	5.959	5.833
2.86	2.90	25.997	26.038
3.31	3.33	14.753	15.011
3.67	3.67	3.156	3.237
4.09	4.12	1.277	0.993
4.71	4.69	20.254	21.037
5.74	5.70	3.774	3.700
6.25	6.26	2.350	2.407
7.88	7.91	3.685	3.557
8.74	8.80	1.877	1.902
9.57	9.61	3.625	3.790
10.22	10.22	4.791	5.007
12.64	12.90	2.903	7.903

Peppermint oil

Retention time (min)			Area, %	
Original oil	Complex		Original oil	Complex
4.68	4.66	(α -pinene)	0.480	0.412
5.24	5.24	(β -pinene)	1.023	1.091
5.93	5.98	(limonene)	6.174	6.170
6.60	6.66	(1,8-cineole)	1.569	1.069
7.29	7.30		0.555	0.496
7.59	7.61	(menthofuran)	18.868	19.000
7.91	7.90	(menthol)	59.490	67.102
9.59	9.59		9.318	4.006
11.05	11.12		0.595	0.020
11.43	11.46	(isomenthone)	1.748	0.608
12.70	12.67		0.126	0.057
14.56	14.50		0.056	0.020

Tarragon oil

Retention time (min)			Area, %	
Original oil	Complex		Original oil	Complex
2.83	2.83		1.853	1.801
3.53	3.30		0.276	0.328
3.79	3.81		0.093	0.090
4.09	4.12		22.829	(phellandrene) 23.000
6.17	6.17		0.016	0.012
6.45	6.43		74.714	(methyl- chavicol) 74.542
10.47	10.49		0.031	0.031
11.65	11.63		0.031	0.052
12.90	13.01		0.143	0.122

Dill oil

Retention time (min)		Area, %	
Original oil	Complex	Original oil	Complex
2.29	2.35	0.862	0.902
2.97	3.00	(limonene) 15.578	15.731
3.21	3.21	34.934	34.957
3.79	3.75	0.143	0.156
4.84	4.87	6.455	6.720
5.01	5.09	2.073	2.130
5.43	5.51	(carvone) 37.880	38.439
8.56	8.59	0.628	0.697
11.02	11.14	0.920	0.831
16.73	16.69	0.577	0.437

Study of the crystalline complexes

No connection is recognized between the stability of the complex in solution and its crystallizability — *i.e.* its solubility. A complex of low stability in solution may be readily separated in crystalline form if it is poorly soluble, and a complex of high stability in dissolved state occasionally cannot be separated in crystalline form: *e.g.* only a mixture of cyclodextrin and guest molecule is recovered instead of the complex on freeze-drying. Therefore, after the isolation of a crystalline product it is always questionable, whether it is only a simple mixture of cyclodextrin and the guest molecule, or it can be regarded more or less as a complex. The complexes possess most rarely a strictly stoichiometric composition thus the determination of the guest molecule contents of the product indicates the formation of a complex only when the guest molecule was an easily volatile fluid [6]. During the drying of the crystalline product the volatile guest molecules vanish if they are not enclosed in a complex. The formation of a simple crystal inclusion is of course also possible, but in such cases considerably less guest molecules can be entrapped than in a complex.

The cyclodextrin inclusion complexes form usually so tiny crystals that one cannot decide even by microscope whether their structure is crystalline or amorphous. A decisive proof for the crystalline structure is supplied by the X-ray diffraction pattern. Cyclodextrin gives a well defined X-ray diffraction powder diagram with sharp peaks; oils have no crystalline structure, therefore they show no X-ray diffraction. Should the registered pattern of the product obtained significantly differ from the X-ray diffraction pattern of cyclodextrin, this is considered a piece of evidence for the formation of a crystalline complex.

The crystalline structures of complexes formed by guest molecules of the same size are similar (*e.g.* monoterpene-containing essential oil complexes). On the diffractograms of several similar complexes the individual peaks appear

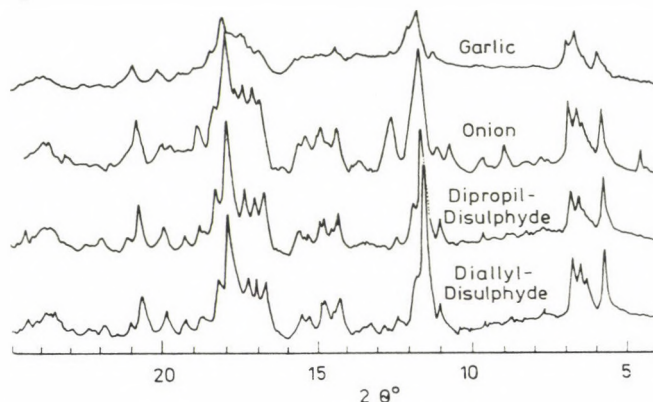


Fig. 6. X-ray diffraction powder pattern (registered on a Philips PW 1060 diffractometer) of β -cyclodextrin inclusion complexes of sulfur-containing aromatics

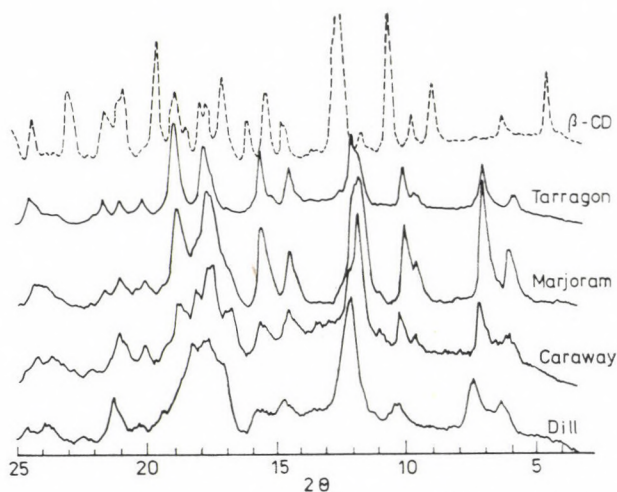


Fig. 7. X-ray diffraction powder pattern (registered on a Philips PW 1060 diffractometer) of β -cyclodextrin complexes of flavour substances containing mainly terpene components

more or less at the same angle values. In the complexes of sulfur-containing oils (garlic and onion oil) related crystal structures can be observed too, but the diffractograms differ significantly from those of the complexes containing terpene-type guest molecules (Figs 6 and 7). In the case of relatively small guest molecules examined so far (with the guest molecule being located entirely inside the cyclodextrin cavity), diffractograms of similar type have been ob-

served. Fatty acids, however, give a completely different type of diffractogram [7]; it may be assumed that the small guest molecules form a "cage" type and the long fatty acid molecules a "channel" type lattice [8].

The crystalline complexes are characterized by a water content of about 7% (the crystal water content of β -cyclodextrin is about 13%). The complexes with a water content below 2% produced by freeze-drying are amorphous, also their diffraction powder pattern consists only of diffuse bands [9].

Such obvious methods as, e.g., infrared spectroscopy are not suitable to prove cyclodextrin complex formation in solid products. The characteristic bands of cyclodextrin, constituting 80 to 95% of the complex, do not change significantly on inclusion complex formation. In the characteristic bands of the guest molecule (5–20% of the complex) usually there is a change, but this remains in most cases unperceivable, because the bands are superimposed by those of cyclodextrin.

As a matter of fact, complex formation can most appropriately be proved by those methods which supply information about the stability of the complexed molecules.

Thermostability of the complexes

For investigating the thermal stability of the complexes the TAS technique (Thermomikro-Abtrenn- und Applikationsverfahren), elaborated by STAHL [10], proved to be the most suitable. This method provides a well appreciable qualitative pattern about the stability of the inclusion complexes of volatile substances.

The substance to be tested is heated in a glass tube, the only outlet of which ends in a capillary. Some substance supplying water vapour (starch, silica gel, etc.) has to be present beside the material to be tested as the procedure is essentially a steam distillation. The crystal water content of cyclodextrin inclusion complexes is sufficient for this purpose, no extra water source is needed.

The studies have been carried out with an apparatus constructed in our laboratory at temperatures from 60 °C to 300 °C; the rate of heating up was 10 ± 2 °C per minute. The evaporated products streaming out through the capillary form deposits on a thin-layer chromatographic plate placed directly to the end of the capillary. By periodical moving of the plate the components released and evaporated are collected on different spots for every 20 °C interval. The components released at various temperatures are developed on Kieselgel G plates with solvent benzene: ethylacetate 90 + 10. Visualization; SbCl_5 in chloroform, heating at 110 °C.

Practically all components of marjoram oil appear in the vapour phase already at 100 °C; the chromatograms are completely homogeneous between

120 and 300 °C, no particular decomposition occurs under the effect of heat (Fig. 8). At 100 °C the simple mixture supplies four components, and at 120 °C the spectra of the oil is complete; at this temperature all components get into the vapour phase. At 240 °C, however, the volatile oil suffers a change (most likely it decomposes), because a substance — otherwise absent from the oil — appears in a considerable quantity next to the starting point; simultaneously, certain components disappear in the domains of R_f 0.6 to 0.8. During the heating of the β -cyclodextrin complex of marjoram oil, volatile components ap-

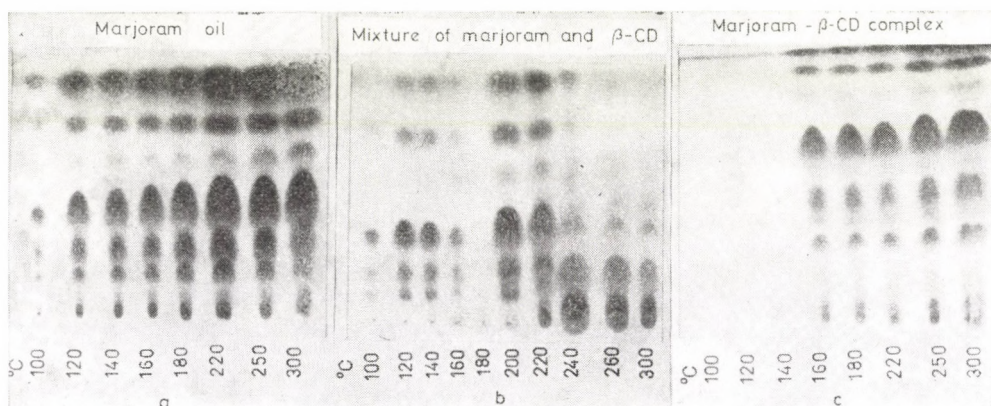


Fig. 8. TAS chromatogram of marjoram oil (8a), of a mixture of marjoram oil and β -cyclodextrin (8b) and marjoram- β -cyclodextrin inclusion complex (8c)

peared first at 160 °C, *i.e.* up to this temperature no loss of the complexed ingredients is probable. Up to 300 °C no considerable decomposition was observed either, only a loss in hydrocarbons (α - and β -pinene R_f 0.97) was conspicuous.

During the heating of tarragon oil at 100 °C all components appear in the chromatogram; a notable thermal decomposition cannot be observed as compared with the original oil. A simple mixture of the oil and β -cyclodextrin gives practically all components at 120 °C, but a slight relative enrichment of methylchavicol (R_f 0.40) and phellandrene (R_f 0.93) can be observed on the chromatographic plate. A perceivable decomposition occurred at 250 °C as shown by the presence of a new component appearing around the starting point. The complexed tarragon oil delivers only a small amount of phellandrene at 120 °C, and further two components are released at 140 °C. All major components appear only at 160 °C. At a higher temperature (250 °C) the chromatogram can no longer be evaluated because of marked decomposition (Fig. 9).

Similar results have been obtained in the thermofractionation studies of other flavour substance complexes. It can be stated that there is a considerable difference between the thermostability of the inclusion complexes and the

simple mixtures, which proves the fact of complex formation; on the other hand, essential oils stabilized by inclusion complex formation are considerably more resistant to thermal effects than the non-complexed oils.

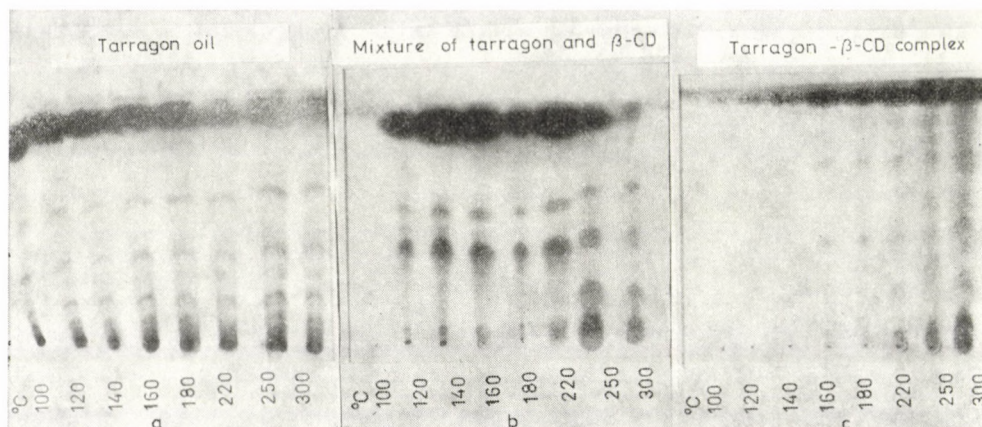


Fig. 9. TAS chromatogram of tarragon oil (9a), of a mixture of tarragon oil and β -cyclodextrin (9b) and tarragon- β -cyclodextrin inclusion complex (9c)

Study of the protection against oxygen

The oxidative transformations characteristic of essential oils bring about a considerable "ageing" effect also in oils cut off from the oxygen of air, through the oxidation-reduction processes disproportionation occurring between the individual components of the oil. This is, however, a slow, retarded process. Essential oils decompose much more rapidly, if they get into permanent contact with the oxygen of air.

The protecting effect of complexation against oxygen was studied by comparing the oxygen consumption of complexed and non-complexed essential oils by Warburg's method.

Pure oxygen was perfused for one minute through Warburg's vessels containing the samples to be tested; the system was then closed, put in a thermostat and the oxygen consumption was registered at 37 °C.

The original oils were placed in the vessel adsorbed on a filter paper disc. Brodie's solution was used as the manometer liquid (density at 37 °C 1.033 g/cm³). Figures 10 and 11 show the amount of oxygen consumed by 1 mg of free or complexed oil as a function of time. As seen in the figures, complex formation considerably decreased the oxygen uptake of both the monocomponent benzaldehyde and the multicomponent lemon oil; the oxygen uptake of the complexed substance is generally less than 10% of the value characteristic of the non-complexed substance.

The thin-layer chromatography of oxidized samples obtained after Warburg's oxidation experiments, when using specific reagents, allows to draw conclusions about the character of changes which have occurred under

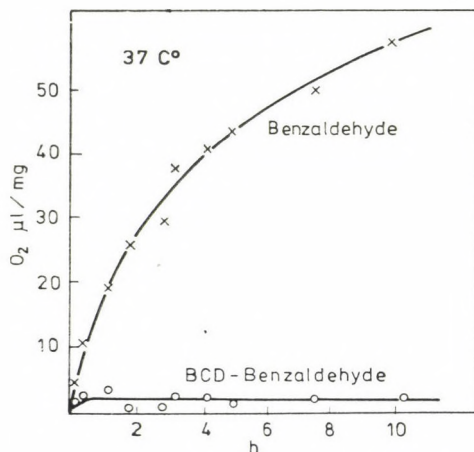


Fig. 10. The oxygen uptake of benzaldehyde and β -cyclodextrin complexed benzaldehyde in pure oxygen atmosphere at 37 °C, measured by Warburg's method

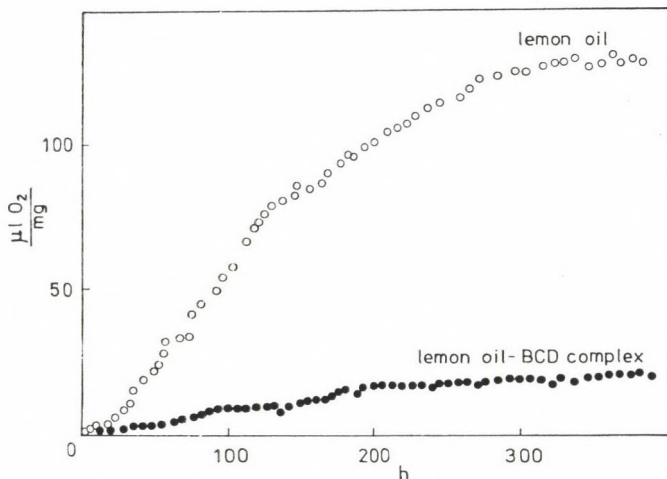


Fig. 11. The oxygen uptake of lemon oil and β -cyclodextrin complexed lemon oil in pure oxygen atmosphere, measured by Warburg's method

the effect of oxygen. For detecting the unsaturated components, a fluorescein-bromine reagent, and for peroxides a ferrous sulfate-rhodanide reagent was used [11].

As seen from Table II, there are no peroxides in the original lemon oil. After oxidation, the complex has one, and the oil four similar components. In

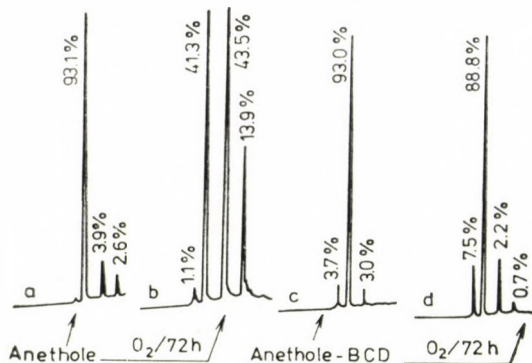


Fig. 12. Gas chromatograms of anethole (12a), of anethole kept in pure oxygen for 72 hours (12b), of anethole- β -cyclodextrin inclusion complex (12c) and the anethole- β -cyclodextrin inclusion complex kept in pure oxygen for 72 hours (12d). Column: 3 m packed with 10% NPS on Chromosorb W sil. 60/80 mesh, t_{inj} : 250 °C, t_{FID} : 220 °C, t_{column} = 100 °C for 4 min, heating to 200 °C at 8 °C/min, 200 °C for 10 min, carrier gas = N₂ at 20 ml/min

Table II

Characterization of the products formed from lemon oil and its cyclodextrin complex under the effect of oxygen
(Solvent mixture : benzol : ethyl acetate (95 : 5)
on silica gel G-60)

R_f	Peroxides (Fe-rhodanide reagent)		
	Lemon oil, original	Re-extracted from the complex after oxidation	Lemon oil, oxidized
0.40		+	+
0.29			+
0.10			+
0.00			+
Unsaturated compounds (fluorescein-bromine reagent)			
0.80—0.82	+	+	+
0.75	+	+	
0.63—0.66	+	+	
0.50—0.55	+	+	+
0.46	+	+	
0.40—0.42	+		
0.35	+	+	
0.28—0.30	+	+	
0.20	+		+
0.0	+	+	

the original oil 10 unsaturated compounds can be distinguished; after oxidation there are eight in the complex, and only three remaining in the uncomplexed oil.

Figure 12 shows the gas chromatograms of anethole and the anethole- β -cyclodextrin complexes, both before and after storing them for 72 hours in oxygen at room temperature.

It is seen that the protection of anethole against oxygen can be accomplished with good efficiency by inclusion complex formation.

Diminution of volatility

The volatility of anethole was studied by thermostating free anethole, anethole adsorbed on glucose, and the anethole- β -cyclodextrin complex at 70, 80 and 90 °C in nitrogen stream. The transferred anethole was absorbed in ice-cool methanol. The time-dependence of volatility established from the anethole concentrations by spectrophotometry is shown in Fig. 13.

While in the case of anethole (A) and anethole adsorbed on glucose (A-Gl) a notable amount of aroma escaped at all the three temperatures, anethole release from the β -cyclodextrin complex was observed only at 90 °C, and even then with a strongly reduced rate.

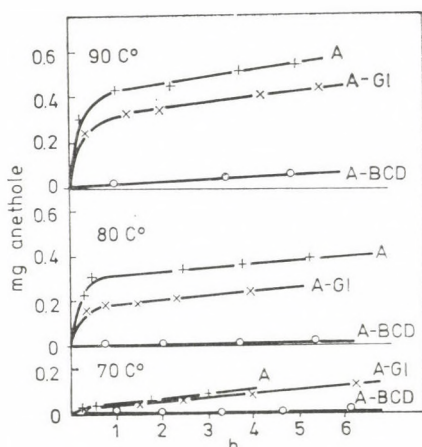


Fig. 13. Volatility of anethole at various temperatures as a function of time (A = anethole; A-Gl = anethole adsorbed on glucose; A-BCD = β -cyclodextrin inclusion complex of anethole).

Reduction of the loss of aroma substances in aqueous solutions

In studying the loss of aroma substances from aqueous solutions, the concentrations of β -cyclodextrin and of anethole were maintained at a level where yet no precipitation of solid complex occurred. Stability was studied with 0.45, 0.9 and 1.8 mole β -CD/mole anethole. (The β -CD concentration of the solution was 0.16, 0.32 and 0.65%.)

The decrease of anethole concentrations in the percentage of the starting value, as a function of time and of the β -CD: anethole molar ratio, is shown in Fig. 14.

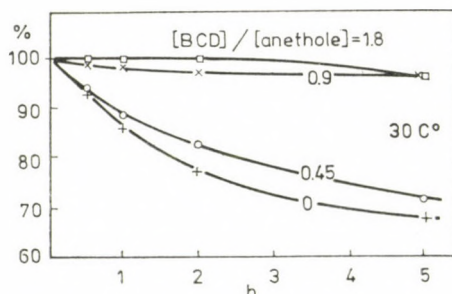


Fig. 14. Loss of anethole on stirring anethole-containing aqueous cyclodextrin solutions of various concentrations at 30 °C in an open beaker

The anethole concentration decreased to 68% of the original value during 5 hours in the β -CD-free solution, whereas in presence of 0.9 and 1.8 mole of β -CD/mole anethole, the decrease was less than 5%.

Plotting the loss of anethole at fixed time intervals *versus* the β -CD concentration, it can be seen that above 0.9 mole β -CD/mole anethole the curves reach a limit value. Thenceforth the anethole loss is very low and remains constant independently from the β -CD concentration.

This is considered as further evidence for the complex formation, with nearly 1 : 1 molar ratio, in solution.

Loss through storage

The loss of aroma during storage conditions was studied as follows. Various flavour substances were stored in open Petri dishes for a longer period at room temperature, either absorbed on glucose, or in the form of β -CD inclusion complexes. Samples were taken from time to time and the content of their aroma substance was determined. The loss of anethole as a function of time is shown in Fig. 15, and that of vanillin in Fig. 16. The amount of adsorbed anethole decreased to 6% of the original value in 14 days, while in the case of the

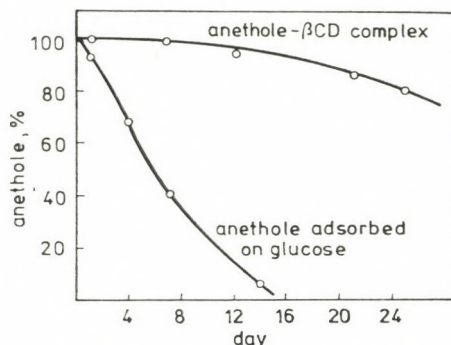


Fig. 15. Loss of anethole as a function of time in the case of anethole adsorbed on glucose, stored at room temperature in an open Petri dish and for the anethole cyclodextrin complex

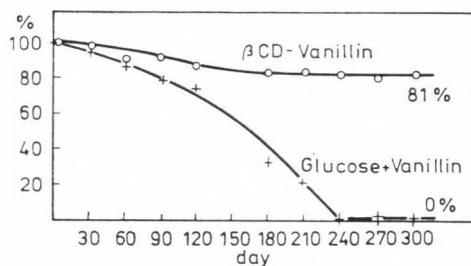


Fig. 16. Loss of vanillin in the case of vanillin-glucose mixture stored at room temperature in an open Petri dish and for the vanillin-cyclodextrin complex

complexed anethole 82% was retained after 25 days. Vanillin — being a crystalline substance — vanished from the mixture completely after about 240 days, whereas in the complex 81% remained unchanged for two years.

Results

The aroma substances whose β -cyclodextrin complexes have been prepared are shown in Table III.

The guest molecule content of the inclusion complexes — determined by gas-liquid chromatography — was between 8 and 13%. All components important for the aromatizing effect have become incorporated in the complex in all cases with practically unaltered composition of the flavour substance; therefore their characteristic taste and practical applicability remained unchanged. The X-ray diffraction powder patterns of the complexes differed significantly from the X-ray diffraction pattern of β -cyclodextrin, proving the formation of a different crystal lattice, thus indirectly the formation of an inclusion complex. Decisive proofs for the complex formation have been supplied by

Table III

Complexed substance	Guest molecule content of the β -CD complex in per cent (determined by GLC)
Bay leaf oil (<i>Laurus nobilis</i>)	10.80
Basil oil (<i>Ocinum basilicum</i>)	10.72
Peppermint oil (<i>Mentha piperita</i>)	9.70
Lemon oil (<i>Citrus medica</i>)	8.75
Anise oil (<i>Illicum verum</i> Hook. fil.)	9.00
Sweet cummin oil (<i>Foeniculum dulce</i>)	10.00
Cinnamon oil (<i>Cinnamomum cassia</i> Blume)	8.76
Garlic oil (<i>Allium sativum</i>)	10.20
Fume aroma (synthetic)	12.20
Thyme oil (<i>Thymus</i> sp.)	9.60
Carrot oil (<i>Daucus carota</i>)	8.82
Caraway oil (<i>Carum carvi</i> L.)	10.50
Coriander oil (<i>Coriandrum sativum</i> L.)	7.72
Dill oil (<i>Anethum graveolens</i>)	6.92
Lovage oil (<i>Levisticum officinale</i>)	4.35
Marjoram oil (<i>Majorana hortensis</i>)	8.00
Raspberry oil (<i>Rubus idaeus</i> L.)	8.66
Mustard oil (<i>Sinapis alba</i>)	10.92
Orange oil (<i>Citrus aurantium</i>)	9.20
Benzaldehyde	8.70
Tarragon oil (<i>Artemisia dracunculus</i>)	10.23
Vanillin (synthetic)	6.20
Onion oil (<i>Allium cepa</i> L.)	10.20
Celery oil (<i>Apium graveolens</i>)	10.00
Sage (<i>Salvia officinalis</i> L.)	8.20

the results of the stability tests of the complexed aroma substances. Stability against oxygen was studied by Warburg's method, and the product after oxygen treatment was further analyzed by gas chromatography and thin-layer chromatography. The oxygen uptake of the complexed flavour substances under similar conditions is only about 10% of that of the non-complexed substances. Stability against heat was studied by the "TAS" technique and pyrolytic gas-liquid chromatography. While the majority of the components of the flavour substances are rather volatile and readily evaporate at about 100 °C, the complexed components start to get released only above 160 °C. When testing the volatility in an inert gas stream, practically no volatility was observed in the case of the complexes up to a temperature of 100 °C.

The β -cyclodextrin inclusion complexes of flavour substances are suitable for the preparation of flavouring compositions in the form of powders or tablets, to be used in households, production units for mass catering, etc. The preparations are stable, their compositions remain unchanged for a long time, and they can be standardized. The results of food processing experiments with cyclodextrin complexes will be reported in another paper. The elaboration of production technologies on industrial scale and toxicological studies required for the registration are in progress.

*

The authors' thanks are due to Dr. K. SIMON (Chinoin, Department of Pharmaceutical Research) for the X-ray diffraction patterns; to J. HARANGI (Biochemical Institute of the University, Debrecen) for the gas-liquid chromatographic studies.

REFERENCES

- [1] ROGERS, W. I., WHALEY, W. M.: U. S. Pat. 3,061,444 (Oct. 30, 1962)
- [2] SZEJTLI, J., SZENTE, L., KOLTA, R., LINDNER, K., ZILAHY, Z., KŐSZEGI, B.: Hung. Pat. Appl. CI-1753 (1977)
- [3] BERGERON, R. J., CHANNING, M. A., GIBELLY, G. J., PILLOR, D. M.: J. Am. Chem. Soc., **99**, 5146 (1977)
- [4] GRIFFITHS, D. W., BENDER, M. L.: J. Am. Chem. Soc., **95**, 1674 (1973)
- [5] SZEJTLI, J., BUDAI, Zs.: Acta Chim. Acad. Sci. Hung. (In the press)
- [6] SZEJTLI, J.: Die Stärke **30**, 427 (1978)
- [7] SZEJTLI, J., STADLER-SZŐKE, Á.: Acta Chim. Acad. Sci. Hung. (In the press)
- [8] SAENGER, W.: Jerusalem Symp. Quantum Chem. Biochem., 1975
- [9] TAKEO, K., KUGE, T.: Agric. Biol. Chem. Tokyo, **34**, 1784 (1970)
- [10] STAHL, E.: J. Chromatog., **37**, 99 (1968)
- [11] FRYKLÖF, L. E.: Farmaceutisk Revy, **56**, 733 (1957)

József SZEJTLI

Lajos SZENTE

Erzsébet BÁNKY-ELŐD

H-1026 Budapest, Endrődi Sándor u. 38—40.

POLYETHYLENE GLYCOL DERIVATIVES AS COMPLEXING AGENTS AND PHASE-TRANSFER CATALYSTS, III.

BEHAVIOUR OF POLYOXYETHYLENE DERIVATIVES IN
LIQUID-LIQUID PHASE EQUILIBRIA

L. TÓKE, G. T. SZABÓ and K. SOMOGYI-WERNER

(*Department of Organic Chemical Technology, Technical
University, Budapest*)

Received July 5, 1978

Accepted for publication August 22, 1978

To characterize the efficiency of polyethers as salt-extracting catalyst, liquid-liquid equilibrium measurements were carried out. The nature of the end groups and the average molecular weight are shown to decide the power of a linear polyether as phase-transfer catalyst.

Compounds complexing alkali ions like crown ethers can serve as phase-transfer catalysts [1]. It is known that non-cyclic polyethers may be used just as well as macrocyclic ones [5-10].

Though the theoretical foundation of phase-transfer catalysis was laid more than 10 years ago [2-4], a monograph [17] in 1977 qualified the factors affecting phase-transfer catalysis as undeveloped. Researches on this subject have been started just in the recent years [11-16].

Experimental

Materials

Polyethylene glycol samples were commercial products supplied by Fluka; the other polyethers were prepared in our laboratory.

Distribution measurements for the sodium salt

In a cell thermostated at $25 \pm 0.5^\circ\text{C}$, 4 cm³ of an aqueous solution of sodium 2,4-dinitrophenolate ($c = 25 \text{ mg/cm}^3$) and 10 cm³ of benzene were stirred for 1 h. The phases were separated, and the extinctions of the solutions, measured at $\lambda = 370 \text{ nm}$, were used to determine the salt concentrations.

Determination of the distribution coefficients of the polyethers

Distilled water (5 cm³), benzene (8 cm³) and the polyether (2 g) were stirred at $25 \pm 0.5^\circ\text{C}$ for 1 h. The phases were separated and sampled.

The samples were weighed, evaporated, and the residue was dried to a constant weight and weighed.

The quotient

$$K_b = \frac{C_B}{C_W}$$

is given as the distribution coefficient [C_B and C_W are the polyether concentrations (%) in the benzene and aqueous phase, respectively].

The complex stability constant values were measured in our laboratory and published previously [6, 7].

Results and Discussion

The purpose of this research was to investigate the efficiency of polyethylene glycols and their derivatives as phase-transfer catalysts. To achieve this end, first we measured the distribution of sodium 2,4-dinitrophenolate in benzene–water systems with and without the addition of polyether.

An increase of the equilibrium salt concentration in benzene was found if polyether was added. For a comparison of the efficiencies, we used the same weight (0.10 g) of different catalysts.

The results thus obtained are plotted in Fig. 1 for three types of polyethers.

The curves of efficiency related to the unit of mass exhibit a maximum. In the cases investigated so far it is at about $n = 13$.

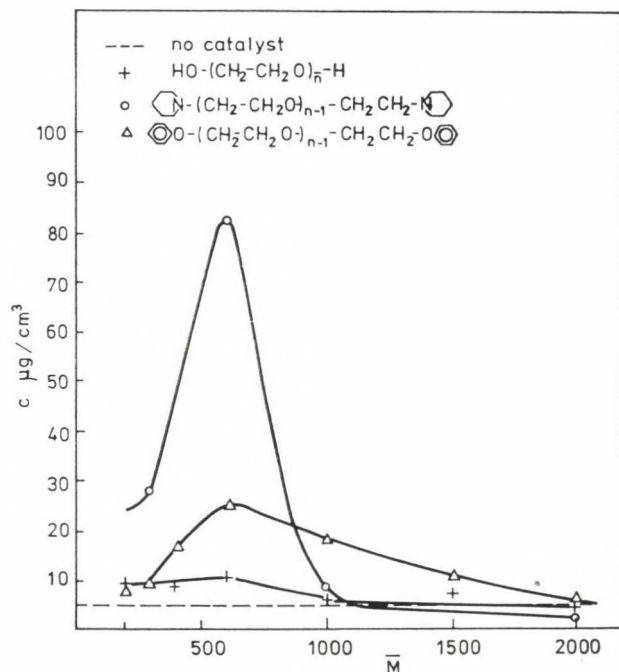


Fig. 1. Concentration of sodium 2,4-dinitrophenolate in the benzene phase vs. average molecular weight

The complexing power of these polyethers shows an increasing tendency with the average molecular weight [6, 7]. Seeking effects leading to the maximum, we compared the distributions of the polyethers between benzene and the aqueous phase with the complexing ability of the polyethers. These data are listed in Table I.

The data in Table I show that the complexing power and the distribution coefficient are affected by the average molecular weight in an opposite way. Obviously, both a high concentration in the organic phase and a good complexing power are advantageous, thus these properties may lead to a maximum salt-extracting efficiency in the range of the medium average molecular weights.

The effect of the catalyst concentration was investigated by varying the weight of the catalysts in the process described above. The results are shown in Fig 2.

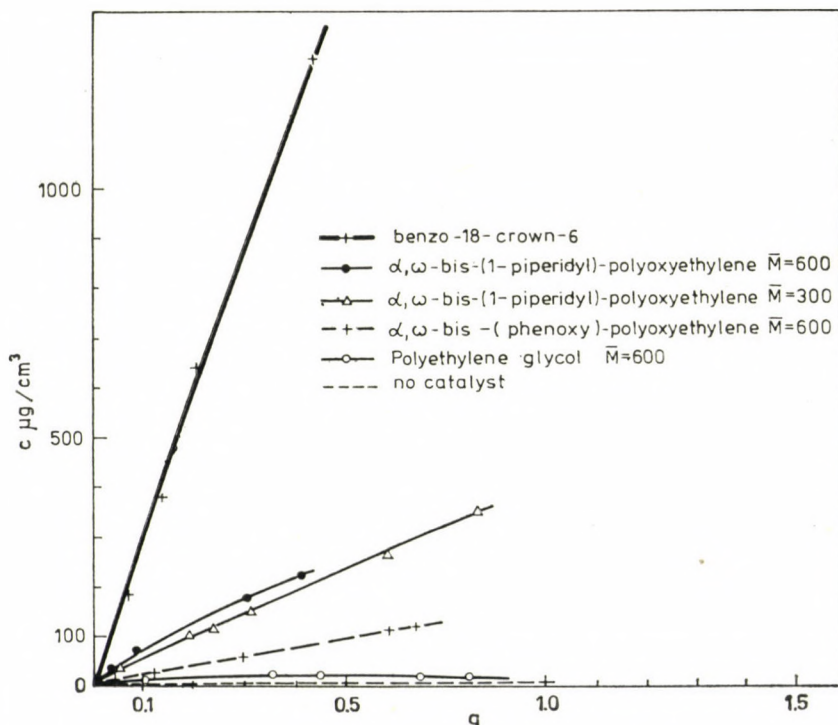
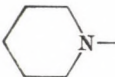
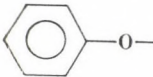


Fig. 2. Concentration of sodium 2,4-dinitrophenolate in the benzene phase vs. quantity of catalyst

Table I
Properties of α , ω -symmetrically disubstituted polyoxyethylenes

End group	\bar{M}	$K_1 \frac{\text{dm}^3}{\text{mole}}$	$K_b \frac{1}{w}$	$C \frac{\text{mg}}{\text{cm}^3}$
HO—	200	44	$3.9 \cdot 10^{-3}$	9.2
	300	100	$3.7 \cdot 10^{-3}$	9.8
	400	180	$2.3 \cdot 10^{-3}$	8.6
	600	360	$< 2 \cdot 10^{-3}$	10.4
	1000	760	$< 2 \cdot 10^{-3}$	6.0
	1500	1230	$< 2 \cdot 10^{-3}$	7.2
	2000	1900	$< 2 \cdot 10^{-3}$	4.4
	4000			4.6
	6000			6.5
	20000			7.3
	300	14	11.4	27.8
	600	71	1.67	82.5
	1000	290	0.32	7.2
	2000	1200	$3.3 \cdot 10^{-2}$	2.4
	200	3	212	8.6
	300	11	126	9.5
	400	31	118	17.0
	600	74	31	25.2
	1000	230	$8.4 \cdot 10^{-1}$	18.4
	1500	480	$2.8 \cdot 10^{-1}$	10.8
	2000	650	$1.5 \cdot 10^{-1}$	64

Other phase-transfer catalysts

Benzo-18-crown-6	$1.6 \cdot 10^4$	7.3	300
Tricaprylmethyl ammonium chloride	—	—	5400
No catalyst			5.5

\bar{M} = average molecular weight of the polyethylene glycol starting material

K_1 = stability constant of the Na^+ complex of the polyether [6, 7]

K_b = distribution coefficient of the polyether between benzene and water

$C \frac{1}{w}$ = concentration of sodium 2,4-dinitrophenolate in the benzene phase under the above-mentioned circumstances, in the presence of 0.10 g of polyether

The stability constants were measured under circumstances different from those of the distribution coefficients, but can be used to show the tendency of the complexing power

A small extinction was found without any catalyst, due to the phenolate. The concentration calculated from this value is shown in Table I marked "no catalyst"

Conclusions

Investigation of the efficiency of polyethers in phase-transfer by measuring their effect on the distribution of a sodium salt between benzene and water, has led us to the following conclusions.

(a) Polyethylene glycols have a rather poor effect as salt-extracting catalysts.

(b) Their salt extracting power can be markedly improved by end group substitution.

(c) End groups suitable for this purpose should shift the distribution to the organic phase while leaving the complexing power as high as possible.

(d) Varying the average chain length of the catalysts containing the same end group, a maximal efficiency is obtained in the range of the medium average molecular weights ($n = 13$ for $-\text{OH}$, N-piperidyl and phenoxy end groups).

Among the linear polyether derivatives investigated so far the best ones have a catalytic power in salt extraction which is comparable with that of benzo-18-crown-6.

*

The authors are indebted to Prof. I. RUSZNÁK for his help in every respect, to Mr. S. Bozsó for technical assistance, to Mr. B. ÁGAI for preparing the benzo-18-crown-6 sample, and to the National Committee for Technical Development for a financial support of this research.

REFERENCES

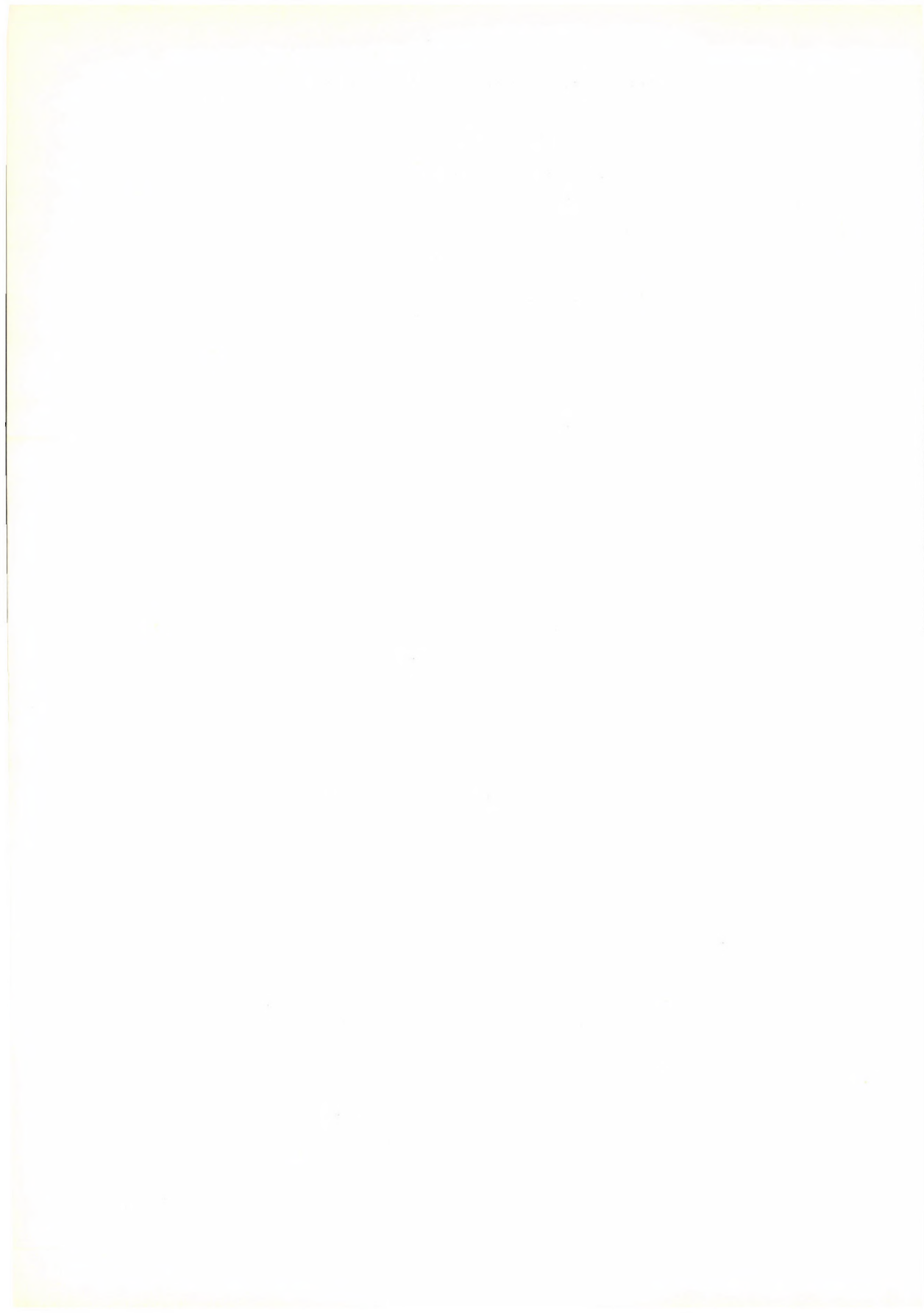
- [1] PEDERSEN, C. I.: *J. Am. Chem. Soc.*, **89**, 7017 (1967)
- [2] MAKOSZA, M., SERAFIN, B.: *Rocz. Chem.*, **39**, 1223 (1965)
- [3] STARKS, C. M., NAPIER, D. R.: *Fr. Demande* 1 573 164 (1970)
- [4] BRANDSTRÖM, A., GUSTAVII, K.: *Acta Chim. Scand.*, **23**, 1215 (1969)
- [5] LEHMKUHL, H., RABET, F., HAUSCHILD, K.: *Synthesis*, **1977**, 184
- [6] TÓKE, L., SZABÓ, G. T.: *Acta Chim. (Budapest)* **93** 421 (1977)
- [7] TÓKE, L., SZABÓ, G. T., ARANYOSI, K.: *Acta Chim. Acad. Sci. Hung.* (To be published)
- [8] EL BASYONY, A., KLIMES, J., KNÖCHEL, A., CEHLER, J., RUDOLPH, C.: *Z. Naturforsch.*, **31b**, 1192 (1976)
- [9] FORNASIER, R., MONTANARI, F.: *Tetrahedron Lett.*, **1976**, 1381
- [10] SHOZO YANAGIDA, KAZUTOMO TAKAHASHI, MITSUO OKAHARA: *Bull. Chem. Soc. Japan*, **50**, 1386 (1977)
- [11] KNÖCHEL, A., OEHLER, J., RUDOLPH, G.: *Z. Naturforsch.*, **32b**, 783 (1977) and other papers of the series
- [12] DOU, H., J.-M., GALLO, R., HASCANALY, P., METZGER, J.: *J. Org. Chem.*, **42**, 4275 (1977)
- [13] DEHMLOW, E., V.: *Angew. Chem.*, **89**, 521 (1977)
- [14] Yoshiaki KOBUE, Katsumi HANJI, Koichi HORIGUCHI, Masahiro ASADA, Yoshinori NAKAYAMA, Junji FURUKAWA: *J. Am. Chem. Soc.*, **98**, 7414 (1976)
- [15] GORDON, J. E., KUTINA, R. E.: *J. Am. Chem. Soc.*, **99**, 3903 (1977)
- [16] FRENSDORFF, H. K.: *J. Am. Chem. Soc.*, **93**, 4684 (1971)
- [17] WEBER, W. P., GOKEL, G. W.: *Phase Transfer Catalysis in Organic Synthesis*. Springer Verlag, Berlin, Heidelberg, New York 1977

László TÓKE

Gábor Tamás SZABÓ

Kornélia SOMOGYI-WERNER

H-1521 Budapest, Műegyetem



FLAVONOIDS, XXXIII*

REACTION OF 2'-OR-CHALCONE DIBROMIDES WITH CYCLOHEXYLAMINE. SYNTHESIS AND TRANSFORMATIONS OF CHALCONE AZIRIDINES**

GY. LITKEI, T. MESTER, T. PATONAY and R. BOGNÁR

(Institute of Organic Chemistry, Kossuth Lajos University,
Debrecen)

Received April 27, 1978

Accepted for publication August 24, 1978

2'-OR-chalcone (**1a**), the chalcone dibromides **2a**, **b**, as well as the α -bromo-chalcone **3a** react with cyclohexylamine to give a mixture of *cis*- (**4a**, **b**) and *trans*-aziridines (**7a**, **b**). Compound **7a** is not stable and is spontaneously transformed into the tautomeric enamine **6a**.

The reaction of **4a** with a base or treatment of **4b** with trifluoroacetic acid gave aurone (**9**), whereas 3-cyclohexylaminoflavanone (**11**) was obtained as the main product when **6a** or **7b** were treated with a base or boron trifluoride etherate, respectively.

The experimental results prove that the earlier assumption concerning the mechanism of the reaction was correct.

Our former studies [1, 2] have shown that 3-cyclohexylaminoflavanone and 2-benzalcoumaranone (aurone) are formed when 2'-OR-chalcones or 2'-OR-chalcone dibromides ($R = H$, $R = COCH_3$) are allowed to react with cyclohexylamine in the presence or in the absence of iodine, respectively. It has been supposed that these reactions proceed *via* isomeric chalcone aziridine intermediates, however, no evidence has been presented for this assumption. Under similar conditions 2'-OR-derivatives ($R = CH_2C_6H_5$ or CH_2OCH_3) gave *cis*- and *trans*-1-cyclohexyl-2-phenyl-3-(2'-OR-benzoyl)-ethyleneimine (**4b**, **7b**) isomers. It has been established that hydrochloric acid in *abs.* ether does not remove the protecting group of the aziridine isomers, thus cyclization to C-3 substituted flavanone cannot occur.

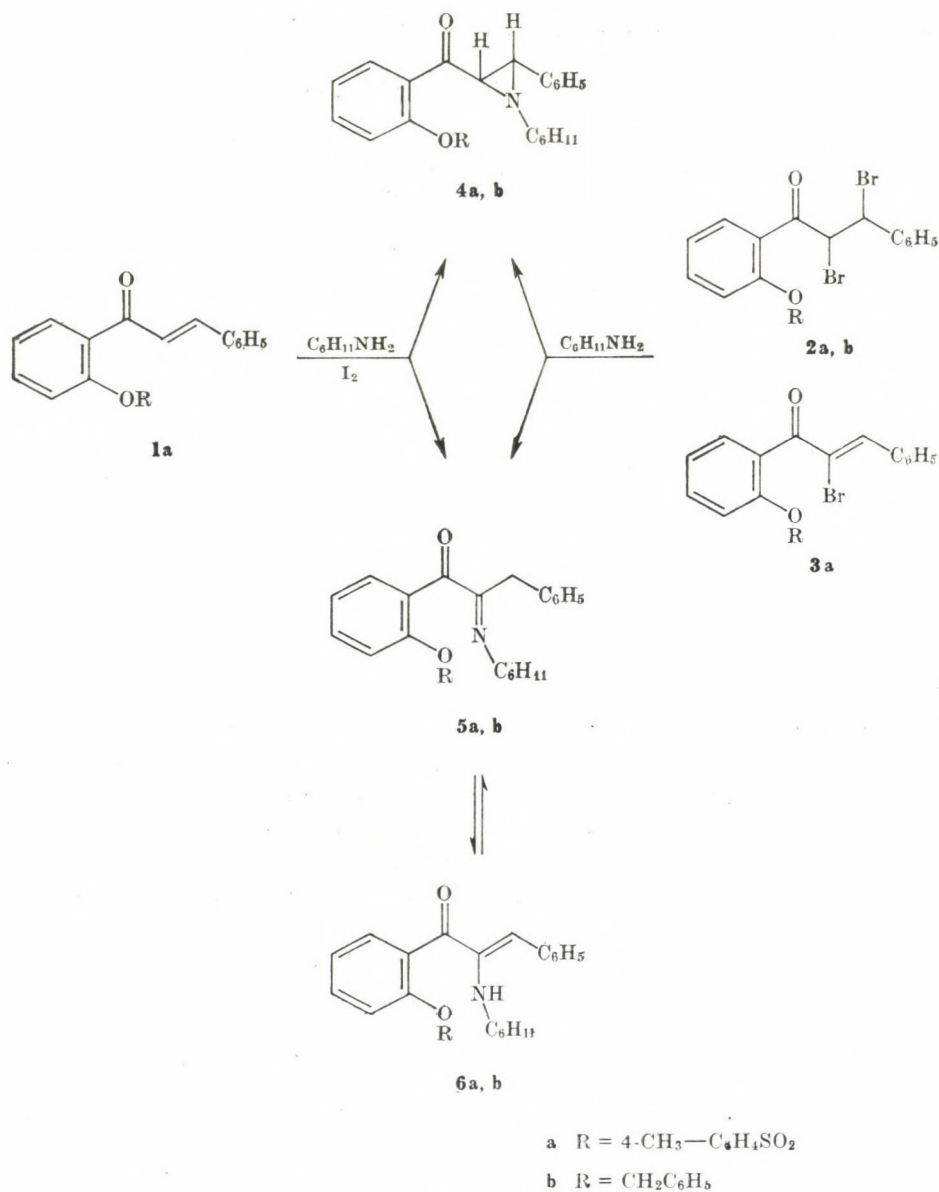
In this paper we report our new results in connection with the synthesis and transformations of 2'-OR-chalcone aziridines.

Synthesis of 2'-OR-chalcone aziridines

The reactions of 2'-tosyloxychalcone (**1a**) with iodine-cyclohexylamine complex [3] under the conditions described previously [2], as well as the treatment of the chalcone dibromide **2a** or the α -bromo-chalcone **3a** with cyclo-

* Part XXXII: R. BOGNÁR, J. BÁLINT and M. RÁKOSI: Ann. 1977, 1529

** A part of this work was presented at the Conference of the Hungarian Chemical Society, Debrecen, 23-26 August, 1977



Scheme 1

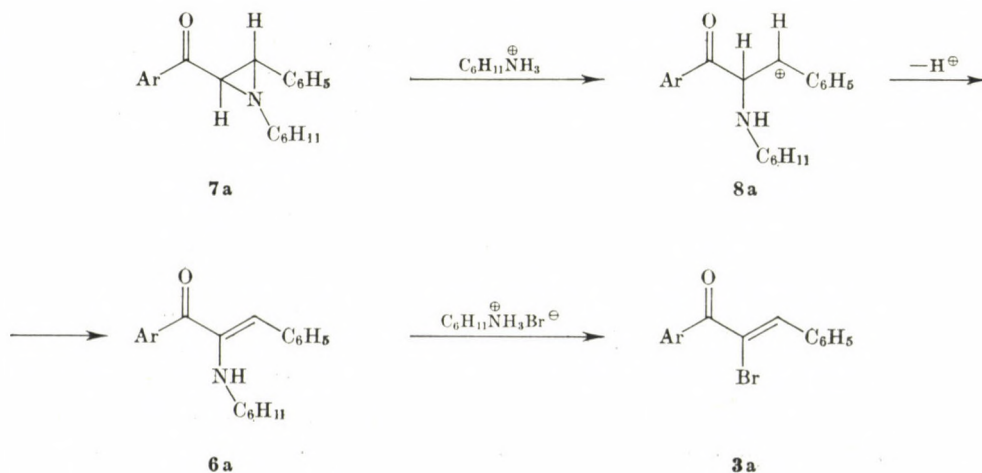
hexylamine in *abs.* benzene resulted in two main products, **4a** and **5a**. According to TLC examinations, the ratio of these two compounds was *cca.* 2 : 8. The main component **5a** could be isolated by fractional crystallization.

In anhydrous methanol the dibromide **2a** gave also a mixture of **4a** and **5a** with cyclohexylamine, however, in this case their ratio was found by TLC to be *cca.* 8 : 2; here **4a** was separated by fractional crystallization. When the

reaction of **2a** was conducted in a more concentrated solution for a longer period of time, the reaction mixture contained **4a** and the α -bromochoalcone **3a**. At the same time the dibromide **2b** with cyclohexylamine in anhydrous methanol gave 90% of **4b**.

In agreement with data in the literature [4] spectroscopic investigations showed that the structure of **4a** and **4b** is *cis*-1-cyclohexyl-2-phenyl-3-(2'-OR-benzoyl)-ethyleneimine. In contradiction with our expectation, spectroscopic examinations revealed that compound **5a** was not a *trans* isomer with structure **7a**. In its IR spectrum the ν C = O frequency was found at 1680 cm^{-1} and, in addition to the complex multiplet of Ar-H and C_6H_{11} and the CH_3 signal, a CH_2 singlet appeared at $\delta = 3.40$ ppm in its NMR spectrum. These results show that compound **5a** has the structure of 2'-tosyloxy- α -(cyclohexylimino) dihydrochalcone. At the same time the broad NH signal at $\delta = 2.65$ ppm suggests an equilibrium mixture containing **5a** together with the tautomeric 2'-tosyloxy- α -(cyclohexylamino)-chalcone (**6a**), the ratio being *cca.* 70 : 20 in deuteriochloroform. Our recent examinations have shown that *trans*-1-cyclohexyl-2-phenyl-3-(2'-benzyloxybenzoyl)ethyleneimine (**7b**) also exists in a tautomeric equilibrium, containing the corresponding enamine **6b**.

Several authors have observed the transformation of *trans*-aziridines into enamines. HEINE *et al.* [5] converted 2,3-dibenzoylaziridine into the corresponding enamine with glacial acetic acid. A similar rearrangement was observed when 2,3-dibromopropionitrile was treated with benzylamine in the presence of triethylamine [6], and it was supposed that the conversion of the intermediary aziridine derivative was facilitated by the quaternary ammonium bromide during the reaction. According to the above-mentioned results it can be supposed that as a result of the attack of cyclohexylammonium bromide on



Scheme 2

the aziridine ring, the *trans*-aziridine **7a** — the presumable intermediate formed from chalcone **1a** — transforms into the enamine **6a** via sequence **7a** → **8a**. Our other experiments have shown that the reaction of the enamine **6a** with cyclohexylammonium bromide gives the α -bromochalcone **3a**, as well.

These experimental facts indicate that the stability of *trans*-aziridines (**7**) is determined by the nature of the protecting group 'R, at position 2'. If it is benzyl or methoxymethyl, only a slight conversion into the enamine **6** occurs, whereas the transformation is complete in the case of the tosyl derivative. The steric properties of the protecting group play no part in the direction of the reaction, thus it is presumably determined by the electronic character of the 2'-OR group. Namely, electron withdrawing groups decrease the electron density at the carbonyl carbon atom, whereas protecting groups of electron releasing character stabilize the *trans*-aziridine ring through a hyperconjugative interaction [7] including the carbonyl group of increased electron density.

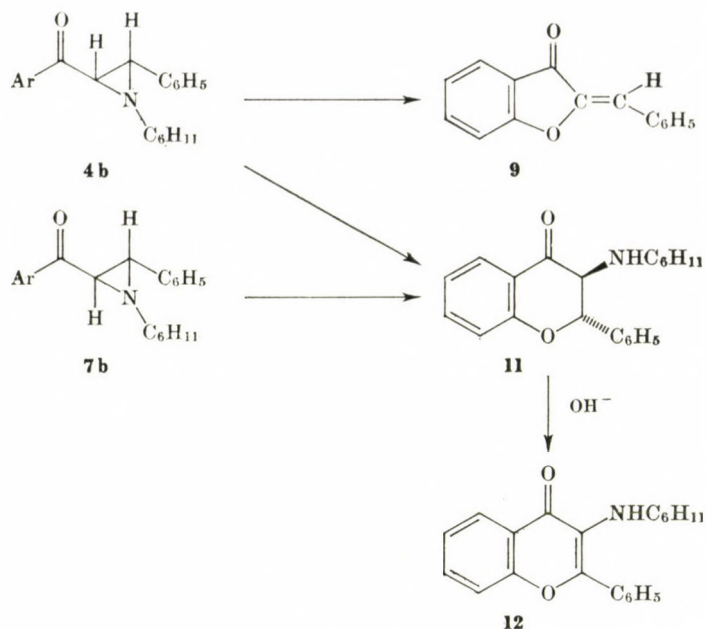
The ratio of the products formed in the reaction of the 2'-OR-chalcone dibromides **2a** and **2b** is also influenced by the nature of the solvent. In dry benzene the main product is the *trans*-aziridine **7b** or the enamine **6a** — formed from **7a** — whereas in *abs.* methanol the main product is the *cis*-aziridine **4a, b**. Several authors [13, 14] have reported on the dependence of the ratio of the formed aziridine isomers on the nature of the solvent, and the mechanism of these reactions has also been discussed.

Transformations of 2'-OR-chalcone aziridines with acidic and alkaline reagents

Italian authors [8] have reported recently that the reaction of both *cis* and *trans*-1-cyclohexyl-2-phenyl-3-(2'-benzyloxybenzoyl)aziridines (**4b** and **7b**) with trifluoroacetic acid (TFA) resulted in the same product, 2,3-*trans*-3-cyclohexylaminoflavanone (**11**). We established that the *cis*-aziridine (**4b**) gave aurone (**9**) as the main product, whereas the reactions of the *trans* isomer (**7b**) resulted mainly in 3-cyclohexylaminoflavanone (**11**).

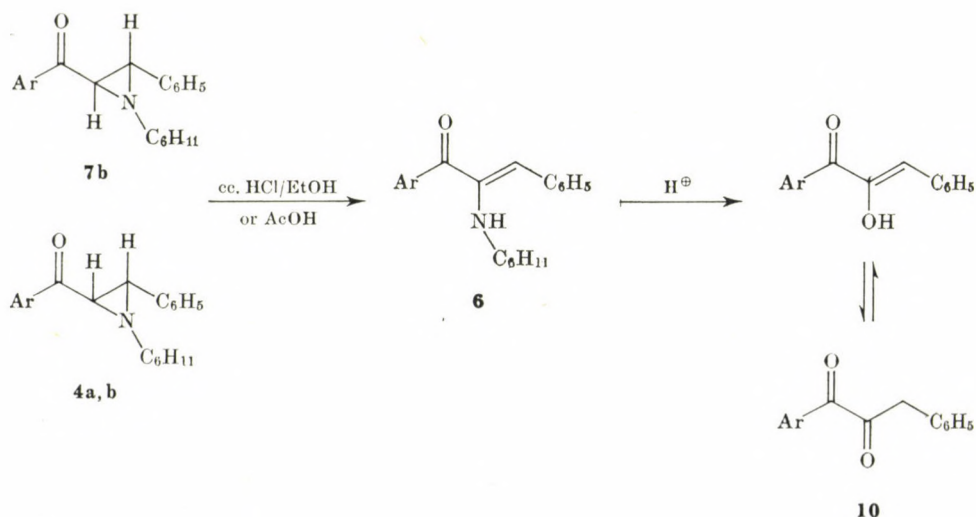
TLC examination showed that a small amount of 3-amino- and 3-hydroxyflavone were also formed in both cases. On the other hand, the reaction of both **4b** and **7b** with boron trifluoride etherate gave mainly compound **11**.

Neither compound **4a** nor the isomeric **5a**—**6a** reacted with TFA or BF₃-etherate under the conditions described above. Ethanol containing concentrated hydrochloric acid did not remove the protecting group and **4a, 4b, 5a** and **7b** transformed into the corresponding diketone **10**. It can be supposed that protonation of both the *cis* (**4a, b**) and *trans* isomers (**7b**) lead to the formation of the enamine **6**, which on hydrolysis gives tautomers of α -hydroxychalcone (**10**). When using glacial acetic acid, similar results were obtained.



Scheme 3

Previously we have reported [2] that the aziridine ring of **4b** and **7b** can be cleaved with hydrochloric acid in dry ether, but formation of the dione **10** could not be observed.



Scheme 4

Compounds **4b** or **7b** do not react with sodium hydroxide. Reaction of **4a** with ethanolic sodium hydroxide results mainly in aurone (**9**) even at room temperature, whereas the equilibrium mixture **5a** \rightleftharpoons **6a** gives **11** as the main product, converting to 3-cyclohexylaminoflavone (**12**) in a secondary reaction.

These experimental facts prove that our earlier assumptions [1, 2] for the mechanism of the reaction were correct. The reaction of 2'-hydroxy- or 2'-acetoxychalcone with cyclohexylamine in the presence of iodine, as well as the reaction of 2'-acetoxychalcone dibromides with cyclohexylamine, give the corresponding *cis*- and *trans*-aziridines, from which aurone and 3-cyclohexylaminoflavanone are formed as the main products in secondary reactions.

Experimental

M.p.'s are uncorrected. The IR spectra were recorded with UNICAM SP 200 G and Perkin-Elmer 283 instruments in KBr pellets. The NMR spectra were recorded with a Jeol MH-100 (100 MHz) instrument with samples in CDCl₃ using TMS as internal standard. TLC investigations were carried out on Kieselgel 60 F 254 (Merck), using toluene-ethyl acetate (8:1) mixture for development.

2'-Tosyloxychalcone dibromide (**2a**)

2'-Tosyloxychalcone (**1a**) [9] (0.053 mole) was dissolved in glacial acetic acid (100 ml) and after the addition of pyridine hydrobromide perbromide [10] (0.063 mole) the reaction mixture was stirred for 2 h. It was then poured into water and the product which precipitated was recrystallized from *abs.* methanol-petroleum ether to yield **2a** (90%), m.p. 113–115 °C.

C₂₂H₁₈Br₂O₄S (538.25). Calcd. Br 29.69. Found Br 29.76%.

Trans-2'-tosyloxy- α -bromochalcone (**3a**)

(a) 2'-Tosyloxychalcone dibromide (**2a**) (0.01 mole) was treated with anhydrous sodium acetate (0.025 mole) in *abs.* *N,N*-dimethylformamide (30 ml) at 90 °C for 3 h. The reaction mixture was diluted with water and the product which precipitated was recrystallized from ethanol to obtain **3a** (85%), m.p. 138–140 °C.

(b) 2'-Tosyloxychalcone dibromide (**2a**) (0.005 mole) was dissolved in anhydrous methanol (50 ml) and treated with methanol saturated with dry ammonia gas. The mixture was allowed to stand in a refrigerator for 24 h. The precipitate was filtered off and recrystallized from methanol to give **3a** (90%) m.p. 138–140 °C.

C₂₂H₁₇BrO₄S (457.38). Calcd. Br 17.47; S 7.01. Found Br 17.53; S 7.05%.

IR: ν C=O 1666 cm⁻¹.

NMR: δ (ppm): 2.23 (s, 3H, CH₃). The signal of H $_{\beta}$ is overlapped by the aromatic protons.

Trans-2'-benzyloxy- α -bromochalcone (**3b**)

Compound **2b** (0.01 mole) was treated with anhydrous sodium acetate (0.025 mole) in 30 ml of *abs.* *N,N*-dimethylformamide at 90 °C for 3 h. The mixture was then poured into water and the syrupy product was extracted with ether. The ethereal layer was washed with water, dried and evaporated and the residue was crystallized from ethanol to afford **3b** (45%), m.p. 70–72 °C.

C₂₂H₁₇BrO₂ (393.27). Calcd. Br 20.31. Found Br 20.40%.

IR: C=O 1665 cm⁻¹.

NMR: δ (ppm): 5.04 (s, 2H, CH₂). The H $_{\beta}$ signal is overlapped by the aromatic protons.

**2'-Tosyloxy- α -(cyclohexylimino)dihydrochalcone
(5a) and *cis*-1-cyclohexyl-2-phenyl-3-(2'-tosyloxybenzoyl)aziridine (4a)**

(a) To a solution of 2'-tosyloxychalcone (**1a**) (0.02 mole) in dry benzene (30 ml) was added by drops a solution of iodine (0.02 mole) and cyclohexylamine (0.06 mole) in benzene (100 ml). After stirring for 24 h the precipitated salts were filtered off and the filtrate was washed with water, dried and evaporated to dryness. TLC examination and NMR investigation showed that the mixture contained *cca.* 20% of **4a**. Repeated recrystallizations of the residue from petroleum ether gave pure **5a**, m.p. 104–106 °C.

$C_{28}H_{29}O_4NS$ (475.57). Calcd. N 2.94. Found N 2.93%.

IR: ν C=O 1680 cm^{-1} .

NMR: δ (ppm): 3.38 (s, 2H, CH_2); 2.66 (broad NH); 2.33 (s, 3H, CH_3); 0.78–2.0 (complex multiplet, C_6H_{11}).

(b) A suspension of **2a** (0.005 mole) in *abs.* methanol (30 ml) was allowed to stand with cyclohexylamine (0.015 mole) in a refrigerator for 4 days. The precipitate was filtered off and the filtrate was washed with water, dried and evaporated to dryness. TLC and NMR examinations showed that the mixture contained mainly the *cis*-isomer **4a** contaminated by **5a**. Recrystallization from petroleum ether yielded **4a** (80%), m.p. 115–117 °C.

$C_{28}H_{29}O_4NS$ (475.57). Calcd. N 2.94. Found N 2.95%.

IR: ν C=O 1692 cm^{-1} .

NMR: δ (ppm): 3.15 (s, 1H, H_α); 3.0 (d, 1H, H_β); 2.32 (s, 3H, CH_3); 0.8–1.9 (m, C_6H_{11}), $J_{H_\alpha, H_\beta} = 8$ Hz).

(c) Reaction of **2a** in *abs.* *N,N*-dimethylformamide as described above resulted in a 1 : 1 mixture of **4a** and **5a**.

(d) 2'-Tosyloxy- α -bromochalcone (**3a**) (0.05 mole) was allowed to react with cyclohexylamine (0.1 mole) in benzene (25 ml) with stirring for 24 h. Work-up of the reaction mixture in the usual manner gave a crude product which contained **4a** and **5a** in a ratio of 9 : 1.

Aurone (9)

(a) The *cis*-aziridine **4b** (0.04 mole) [2] was treated with trifluoroacetic acid (8 ml) under nitrogen atmosphere for 24 h. The reaction mixture was diluted with ether and the ethereal layer was washed with water and aqueous sodium hydrogen carbonate and finally dried. Evaporation gave a yellow syrupy residue which contained mainly the aurone and 3-hydroxyflavone according to TLC. Aurone (**9**) was separated on a Kieselgel 40 column (Merck) using a 8 : 1 benzene-ethyl acetate eluant system. Recrystallization of the crude product from aqueous methanol yielded pure **9**, m.p. 102–104 °C; *lit.* [12] m.p. 108 °C.

3-Cyclohexylaminoflavanone (11)

(a) The *trans*-aziridine **7b** (0.001 mole) [2] was treated with trifluoroacetic acid (2 ml) for 24 h under nitrogen atmosphere. Work-up of the reaction mixture as described above for **9** gave a crude syrupy mixture of 3-cyclohexylaminoflavanone, 3-hydroxyflavone and 3-amino-flavone TLC. This mixture was crystallized from *abs.* ethanol to yield pure **11** (55%), m.p. 103–105 °C; *lit.* [1] m.p. 98–100 °C.

(b) A mixture of the *cis*-aziridine **4b** (0.001 mole) [2] and boron trifluoride etherate (1 ml) in *abs.* benzene (40 ml) was refluxed for 2 h. After cooling, the mixture was washed with water, dried and evaporated. The syrupy residue was then treated with hydrochloric acid in *abs.* ether. The product was found to be identical with the hydrochloride of the flavanone **11** (25%), m.p. 180–181 °C; *lit.* [1] m.p. 180–181 °C.

(c) An analogous reaction of the *trans*-aziridine **7b** resulted in 20% of the hydrochloride of **11**.

The mixed m.p. of the products and the authentic samples showed no depression.

2'-Tosyloxy- α -hydroxychalcone (10)

(a) The *cis*-aziridine **4a** (0.002 mole) was dissolved in *abs.* ethanol (20 ml) and, after the addition of *conc.* HCl (0.1 ml), the mixture was boiled for 2 h. The solvent was then evaporated and the residue dissolved in benzene. The organic solution was washed with water, dried, and evaporated. Crystallization of the residue from methanol yielded 52% of **10**, m.p. 140–142 °C. The product gave positive colour reaction with ethanolic ferric chloride solution.

(b) A mixture of **5a** and **6a** (0.001 mole) was allowed to react with glacial acetic acid at room temperature for 2 days. The residue obtained after evaporation was crystallized from methanol to give **10** (90%), m.p. 141–142 °C.

$C_{22}H_{18}O_5S$ (394.42). Calcd. S 8.12. Found S 7.89%.

IR: ν OH 3380 cm^{-1} ; ν C=O 1660 cm^{-1} .

3-Cyclohexylaminoflavone (12)

A mixture of **5a** and **6a** (0.001 mole) was allowed to react with sodium hydroxide (0.002 mole) in *abs.* ethanol (20 ml) in a refrigerator for 24 h. The mixture was diluted with benzene, the organic layer was washed, dried and evaporated to give a crude product which was recrystallized from *abs.* methanol to yield 58% of **12**, m.p. 119–121 °C; *lit.* [2] m.p. 120–122 °C.

REFERENCES

- [1] BOGNÁR, R., LITKEI, Gy., SZIGETI, P.: Acta Chim. Acad. Sci. Hung., **68**, 421 (1971)
- [2] LITKEI, Gy., BOGNÁR R., SZIGETI, P., TRAPP, V.: Acta Chim. (Budapest) **73**, 95 (1972)
- [3] SOUTHWICH, P. L., CRISTMAN, D. R.: J. Am. Chem. Soc., **74**, 1886 (1952)
- [4] POHLAND, A. E., BADGER, R. C., CROMWELL, N. H.: Tetrahedron Letters, **1965**, 4369
- [5] TURNER, A. B., HEINE, H. W., IRWING, J., BUSH, J. B.: J. Am. Chem. Soc., **87**, 1050 (1965)
- [6] GUNDERMAN, K. D., HOLTZMANN, G., ROSE, H. J., SCHULZE, H.: Chem. Ber., **93**, 1632 (1960)
- [7] CROMWELL, N. H., GRAFF, M. A.: J. Org. Chem., **17**, 414 (1952)
- [8] CACCHI, S., PALMIERI, G., MISITI, D.: J. Chem. Soc. Perkin I, **1976**, 2371
- [9] GORMLEY, T. R., O'SULLIVAN, W. J.: Tetrahedron, **28**, 369 (1973)
- [10] FIESER, L. F.: J. Chem. Ed., **31**, 291 (1954)
- [11] BOGNÁR, R., LITKEI, Gy.: Acta Phys. Chim. Debr., **XVII**, 239 (1971)
- [12] FEUERSTEIN, W., KOSTANECKI, S.: Ber., **31**, 1759 (1898)
- [13] SOUTHWICH, P. L., SHOZDA, R. J.: J. Am. Chem. Soc., **82**, 2888 (1960)
- [14] CROMWELL, N. H.: J. Am. Chem. Soc., **81**, 4702 (1959)

György LITKEI Tamás MESTER Tamás PATONAY Rezső BOGNÁR	}	H-4010 Debrecen, Pf.: 20
--	---	--------------------------

STEREOCHEMICAL STUDIES, XXXV* SATURATED HETEROCYCLES, XII**

SYNTHESIS AND SPECTROSCOPICAL STUDY OF *CIS*-TRIMETHYLENE-,
CIS- AND *TRANS*-TETRA- AND PENTAMETHYLENE-2,3,5,6-
-TETRAHYDRO-1,3-OXAZINE-4-ONES***

G. BERNÁTH, F. FÜLÖP, GY. JERKOVICH¹ and P. SOHÁR¹

(Institute of Organic Chemistry, József Attila University, Szeged,

¹Research Institute for Pharmaceutical Chemistry, Budapest)

Received July 17, 1978

Accepted for publication August 25, 1978

2-(*p*-Chlorophenyl)-*cis*-5,6-trimethylene-, *cis*- and *trans*-5,6-tetra- and pentamethylene-2,3,5,6-tetrahydro-1,3-oxazine-4-ones (**2a-e**) have been prepared from *cis*-2-hydroxy-1-cyclopentanecarboxamide, and from *cis*- and *trans*-2-hydroxy-1-cyclohexane- and 1-cycloheptanecarboxamide (**1a-e**), respectively, by reaction with *p*-chlorobenzaldehyde. Under identical reaction conditions, ring closure did not take place with *trans*-2-hydroxy-1-cyclopentanecarboxamide. From the alicyclic 2-hydroxy-1-carboxamides listed above, some 2-disubstituted tetrahydrooxazine derivatives (**4a, b, 5a-e**) have also been prepared with acetone or alicyclic ketones. The interaction of the 2-hydroxy-1-carboxamides **1a-e** with paraformaldehyde gave the bis-tetrahydrooxazinone derivatives **3a-e** containing a methylene bridge. The favoured conformations of the *cis* isomers of the latter compounds were determined from the PMR spectra; mass spectrametric studies are also discussed.

Introduction

In the course of our earlier work on the synthesis and conformational analysis of bicyclic saturated heterocycles with condensed skeleton containing two hetero atoms, the synthesis and conformational analysis of *cis*-trimethylene- [1], *cis*- and *trans*-tetramethylene- [2] and pentamethylene-2,3,5,6-tetrahydro-4*H*-1,3-oxazines [1], *cis*- and *trans*-4,5-tetramethylene- and pentamethylene-2,3,4,5-tetrahydro-6*H*-1,3-oxazines [1, 2] and the related tetramethylene- and pentamethylene-1,3-oxazine-2-ones [3, 4] have been studied. *Cis*-5,6-trimethylene-, *cis*- and *trans*-5,6-tetramethylene- and pentamethylene-5,6-dihydropyrimidin-4(3*H*)-ones have also been synthesized [5, 6]. The conformation of the former derivatives was investigated by PMR spectroscopy; in the case of some derivatives X-ray diffraction analysis was also used [7-9].

* Part XXXIV: BERNÁTH, G., FÜLÖP, F., MÉSZÁROS, Z., HERMECZ, I., TÓTH, G.: J. Heterocyclic Chem. **16**, 137 (1979)

** Part XI: FÜLÖP, F., HERMECZ, I., MÉSZÁROS, Z., DOMBI, GY., BERNÁTH, G.: J. Heterocyclic Chem. **16**, 457 (1979)

*** Presented in part in the lecture of JERKOVICH, GY., SOHÁR, P., BERNÁTH, G., FÜLÖP, F., at the meeting of the Hungarian Chemical Society in Veszprém, August 8, 1975 (See, Proceedings, p. 133)

In the present paper the syntheses of 2-substituted-*cis*-5,6-trimethylene-, *cis*- and *trans*-5,6-tetramethylene- and pentamethylene-2,3,5,6-tetrahydro-1,3-oxazine-4-ones (**2,4,5**) and of the related symmetric bis-oxazinone derivatives containing a methylene bridge (**3**) are described and studies on the IR, PMR and MS spectra of the latter type of compounds reported. The purpose of the synthesis of these compounds has been not only the conformational analysis of saturated heterocycles being extensively studied stereochemically today [10], but also a pharmacological examination of the synthesized group of compounds. Since there are anti-inflammatory, antipyretic and analgesic agents among the analogous benzoxazinone derivatives [11], it appeared desirable to prepare [12] and examine pharmacologically [12, 13] a series of the corresponding saturated analogues and homologues, larger than that discussed in the present paper. The stereochemogeneous *cis* and *trans* series of homologues made also possible to investigate the relationship between the chemical and stereochemical structure and pharmacological action.

Synthesis

In the synthesis of the model compounds in the course of our earlier studies on *N* → *O* acyl migration, *cis*-2-hydroxy-1-cyclopentanecarboxamide (**1a**) [14] and *cis*- and *trans*-2-hydroxy-1-cyclohexanecarboxamide (**1b**, **1d**) [15] appeared as intermediates. These compounds, as well as *cis*- and *trans*-2-hydroxy-1-cycloheptanecarboxamide (**1c**, **1e**) [4] yielded with *p*-chlorobenzaldehyde the corresponding stereohomogeneous bicyclic tetrahydro-1,3-oxazine-4-ones (**2a-e**) in satisfactory yields, when refluxed in dioxane medium in the presence of catalytic amounts of acid. In accordance with our earlier results on *trans*-1,2-disubstituted-1,3-bifunctional cyclopentane derivatives [14, 16], cyclization could not be achieved under similar conditions when the starting material was *trans*-2-hydroxy-1-cyclopentanecarboxamide.

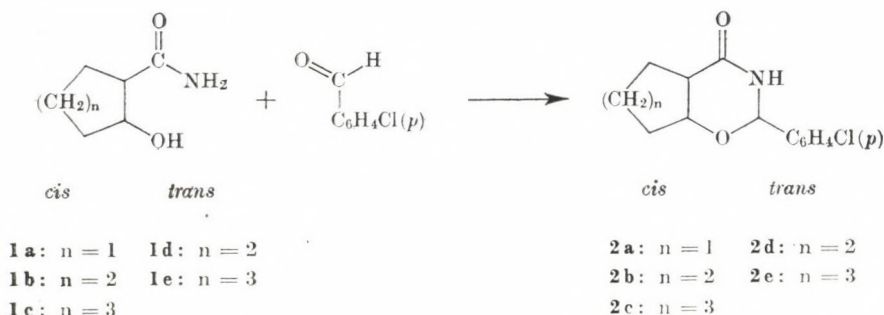


Fig. 1

When *cis*-2-hydroxy-1-cyclohexanecarboxamide (**1b**) was allowed to react with *p*-chlorobenzaldehyde in melt (bath temperature 200 °C), a mixture of the *cis* and *trans* oxazinone (**2b** : **2d** = 70 : 30) was obtained in 1h. With increasing reaction time the decomposition of the product became predominating. No isomerization was observed during the heating of the *cis*-oxazinone **2b** at 200 °C. Isomerization did not occur during the thermal cyclization of *trans*-2-hydroxy-1-cyclohexanecarboxamide (**1d**) either. Thermal cyclization of the homologues with cycloheptane skeleton (**1c**, **1e**) showed results similar to the above mentioned ones.

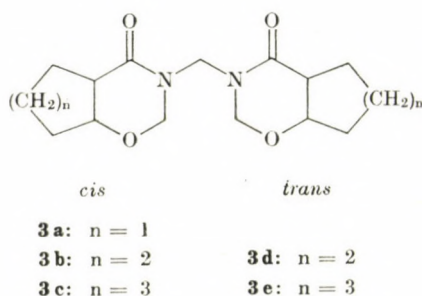


Fig. 2

The formation of a polymeric substance was observed during the reaction of salicylamide and formaldehyde [17, 18]. The reaction of alicyclic 2-hydroxy-1-carboxamides and formaldehyde yielded the *bis* compounds of type **3**. The formation of related compounds with methylene bridges had been reported from 2-hydroxybenzylamine [19] and 4,5-dimethoxy-2-mercaptobenzylamine [20]. In the course of the condensation reaction, first a large excess of paraformaldehyde was employed; however, also after reduction of the amount of paraformaldehyde to even less than the equivalent amount, only products of type **3** could be isolated — in a significantly lower yield. There is a considerable difference in the reactivities of the *cis*- and *trans*-2-hydroxy-1-carboxamide isomers. Under identical conditions, in the reaction of *trans*-2-hydroxy-1-cyclohexanecarboxamide (**1d**) and paraformaldehyde the *trans*-tetramethylene isomer **3d** was formed in a yield more than twice as high as that of the *cis* isomer **3b** obtained from **1b**. The difference in the reactions of the homologous 2-hydroxy-1-cycloheptanecarboxamides and paraformaldehyde was lower, the yield of the *trans* isomer being about 1.5 times higher than that of the *cis* isomer. When the starting material was *trans*-2-hydroxy-1-cyclopentanecarboxamide, no product of cyclization could be obtained with paraformaldehyde either.

Table I

Melting points, analytical data and yields of tetrahydrooxazinones of type 2

Compound	Formula Molecular weight	M.p., °C Solvent	Analysis, % Calculated Found			Yield, %
			C	H	N	
2a	C ₁₃ H ₁₄ ClNO ₂ 251.71	212—213 ethanol	62.03	5.60	5.56	87
			62.04	5.60	5.41	
2b	C ₁₄ H ₁₆ ClNO ₂ 265.73	170 *	63.30	6.07	5.27	78
			63.39	5.99	5.30	
2c	C ₁₅ H ₁₈ ClNO ₂ 279.75	222 *	64.40	6.48	5.00	66
			64.53	6.62	5.01	
2d	C ₁₄ H ₁₆ ClNO ₂ 265.73	191—192 *	63.30	6.07	5.27	76
			63.18	6.02	5.42	
2e	C ₁₅ H ₁₈ ClNO ₂ 279.75	179—181 *	64.40	6.48	5.00	65
			64.46	6.71	5.14	

* Recrystallized from diisopropyl ether : ethanol = 2 : 1

Table II

Melting points, analytical data and yields of bis-oxazinones of type 3

Compound	Formula Molecular weight	M.p., °C Solvent	Analysis, % Calculated Found			Yield, %
			C	H	N	
3a	C ₁₅ H ₂₂ N ₂ O ₄ 294.34	192 ethanol	61.20	7.53	9.52	28
			61.40	7.73	9.88	
3b	C ₁₇ H ₂₆ N ₂ O ₄ 322.39	156—157 ether	63.33	8.13	8.69	30
			63.26	8.35	8.52	
3c	C ₁₈ H ₃₀ N ₂ O ₄ 350.45	137—138.5 ether	65.11	8.63	7.99	31
			65.02	8.82	8.10	
3d	C ₁₇ H ₂₆ N ₂ O ₄ 322.39	192—193 ether	63.33	8.13	8.69	69
			63.25	7.88	8.69	
3e	C ₁₉ H ₃₀ N ₂ O ₄ 350.45	110—111 ether	65.11	8.63	7.99	46
			65.22	8.81	7.87	

FISCHER *et al.* [21] obtained a tetrahydrooxazine derivative with m.p. 162—163 °C in the reaction of acetone with 2-hydroxy-1-cyclohexanecarboxamide of non-declared configuration; the configuration of the product was not given either. When the former reaction was effected using stereohomogeneous **1b** and **1d**, both the *cis* and *trans* products of cyclization had melting points higher than that given above (**4a**: m.p. 169—171 °C; **4b**: m.p. 166—169 °C); the mixed melting point was 160—164 °C. Thus FISCHER *et al.* must have

obtained a tetrahydrooxazinone derivative consisting of a mixture of the *cis* and *trans* isomers (**4a**, **b**).

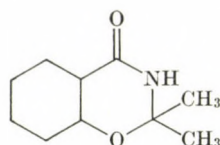
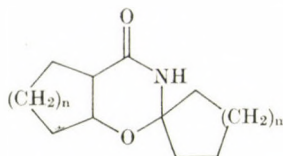
**4a:** *cis***4b:** *trans**cis**trans***5a:** $n = 1, m = 1$ **5b:** $n = 2, m = 1$ **5d:** $n = 2, m = 1$ **5c:** $n = 3, m = 1$ **5e:** $n = 3, m = 1$ **5f:** $n = 1, m = 2$

Fig. 3

In acetone containing 1% HCl, the condensation reaction took place strikingly readily, in 1–2 h at room temperature, or 15–20 min at 40–50 °C. The reactions of the 2-hydroxy-1-carboxamides **1a–e** with alicyclic ketones were similarly fast; in this way the spiro derivatives **5a–f** have been synthesized.

Table III

Melting points, analytical data and yields of spiro-oxazinones of type 5

Com- pound	Formula Molecular weight	M.p., °C	Analysis, %			Yield, %
			Calculated	Found		
			C	H	N	
5a	C ₁₁ H ₁₇ NO ₂ 195.25	167–168	67.66 67.65	8.78 9.00	7.17 7.22	79
5b	C ₁₂ H ₁₉ NO ₂ 209.28	176–177	68.86 69.09	9.15 9.25	6.69 6.76	72
5c	C ₁₃ H ₂₁ NO ₂ 223.31	166	69.92 70.05	9.48 9.62	6.27 6.30	78
5d	C ₁₂ H ₁₉ NO ₂ 209.28	205–206	68.86 69.08	9.15 9.26	6.69 6.54	83
5e	C ₁₃ H ₂₁ NO ₂ 223.31	162–163	69.92 69.92	9.48 9.50	6.27 6.28	77
5f	C ₁₃ H ₂₁ NO ₂ 223.31	169–170	69.92 70.01	9.48 9.57	6.27 6.21	66

* All products were recrystallized from ethyl acetate

IR, PMR and MS data

It has been established earlier that in related saturated heterocycles with condensed skeleton containing two hetero atoms, such as trimethylene-, tetramethylene- and pentamethylenetetrahydro-1,3-oxazines [1, 2], tetramethylene-1,3-oxazine-2-ones [3], trimethylene- and tetramethylenetetrahydropyrimidin-4-ones [5], the favoured conformation of the *cis* isomers is the one in which the hetero atom (nitrogen or oxygen) attached to the annelation point occupies *axial* position, and the methylene group or carbonyl group affixed to the other annelation point is in *equatorial* position. As formerly pointed out [22–24], it could be demonstrated by PMR and X-ray diffraction measurements that the predominating conformation of the *cis* derivatives **2a–c** discussed in the present paper is analogous with the former ones, that is, the oxygen atom and the carbonyl group are in the *axial* and in the *equatorial* position, respectively.

In the present work the spectroscopic data of the derivatives containing methylene bridges (**3a–e**) are reported.

The IR spectra of compounds **3a–e** and **2a–e** (Table IV) are very similar except for the fact that in the former compounds — in accordance with the structures containing methylene bridges — there are no NH bands, thus no absorption is observed at wavenumbers higher than 3000 cm⁻¹. However, there is a very intense amide I band between 1640 and 1660 cm⁻¹, and this is split in the *trans* isomers owing to coupling of the two carbonyl vibrations.

In the PMR spectra (Table IV), the singlet signal of the bridge methylene group appears at high chemical shift values ($\delta \sim 4.9$ ppm), in accordance with the two neighbouring amide nitrogen atoms; its intensity is about half of that

Table IV
IR and PMR data of bis-oxazinones of type 3

Compound	Configuration	IR (KBr), cm ⁻¹ amide-I	¹ H-NMR (CDCl ₃), $\delta_{TMS} = 0$ ppm				
			δ NCH ₂ N	δ OCH ₂ N	$J_{OCH_2N}^{gem}$ Hz	δ OCH	$\Delta\delta$ OCH Hz
3a	<i>cis</i>	1640	4.85 s (2H)	4.90 s (4H)		4.30 m (1H)	15
3b	<i>cis</i>	1660	4.86 s (2H)	4.90 s (4H)		3.95 m (1H)	8
3d	<i>trans</i>	1660, 1640	4.85 s (2H)	5.02, and 4.89 (4H)*	8	3.45 m (1H)	26
3c	<i>cis</i>	1640	4.90 s (6H)			4.00 m (1H)	20
3e	<i>trans</i>	1660, 1650	4.90 s (2H)	4.90, and 4.85 (4H)*	9	3.55 m (1H)	25

* Calculated from the AB-quartet

of the methylene signal in the oxazine ring. The chemical shift of this signal is similarly high, since the vicinity of the amide nitrogen and ether oxygen atoms exert a similar effect on the vicinal methylene protons.

A certainly useful observation in the determination of the configuration of compounds of type **3** with unknown steric structure was that in the *cis* isomers the two methylene protons are isochronous* (they give a singlet signal), while the *trans* isomers produce an AB quartet and the difference in their chemical shifts is higher than 0.1 ppm. Notably, the geminal coupling constant is unusually low (8–9 Hz), owing to the effect of the two neighbouring electron-withdrawing heteroatoms [25a].

This is confirmed by the characteristically different chemical shifts and band widths of the signals of the bridgehead protons geminal with the oxygen atom in the *cis-trans* isomeric pairs. It follows that not only the **3d–e** *trans*, but also the **3a–c** *cis* isomers are conformationally homogeneous systems.

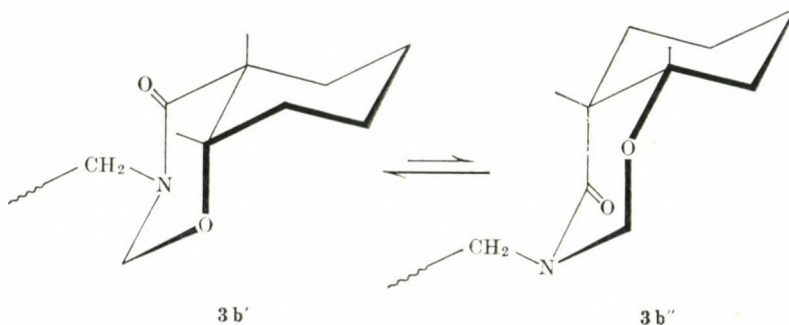


Fig. 4

It can be deduced from the PMR spectra that of the two possible chair-chair conformations of the *cis*-tetramethylene derivative **3b** the predominating one contains the oxygen and carbonyl group attached to the annellation points in *axial* and *equatorial* positions (**3b'**), respectively. Here the signal of the bridgehead methine proton beside the oxygen atom appears at a higher δ value and is much sharper in the *cis* isomer than in the corresponding *trans* one, unambiguously indicating the conformation of the *cis* isomer. In the cyclohexane derivatives and their hetero analogues it is a general rule that the chemical shift of the *equatorial* protons is always higher than that of their *axial* analogues [25b]. Further, from the correlation between the vicinal coupling constants and the magnitude of the dihedral angle [26] the conclusion can be

* The chemical equivalence of the methylene protons in the oxazinone ring of the *cis* isomers **3a–c** is an accidental identity of the resultants of the effects of the neighbouring groups.

drawn that the *equatorial-axial* or *diequatorial* vicinal coupling constants are significantly lower than the *diaxial* coupling constants. In accordance with these facts, the signals of the *equatorial* protons split to a smaller extent and overlapping of the lines result in a smaller band width. The higher δ value and the sharper signals thus equally prove the *equatorial* position of the CHO bridgehead proton. The favoured conformation of the *cis*-trimethylene derivative (**3a**) is analogous with the former case. These favoured conformations are in accordance with the earlier results obtained for related compounds [1–5].

In the PMR spectra of the *cis*- and *trans*-pentamethylene derivatives **3c** and **3e**, the differences in the chemical shifts and band widths of the CHO bridgehead protons are smaller than those observed in the case of the *cis*- and *trans*-tetramethylene isomeric pair **3b** and **3d** (only 0.45 ppm instead of 0.55 ppm and only 5 Hz instead of 18 Hz), which can be explained by the more flexible conformational conditions in 1,2-disubstituted cycloheptane derivatives [27–30]. On the basis of the analogous spectral data of the trimethylene-, tetramethylene- and pentamethylene derivatives, the conformational relationship of the *cis* isomers (**3a–c**) can be deduced, though the conformational equilibrium in case of the pentamethylene derivatives is not so strongly shifted to the favoured conformer than in case of the tetramethylene derivatives. X-ray diffraction analysis of 2-(*p*-chlorophenyl)-*cis*-5,6-pentamethylene-2,3,5,6-tetrahydro-1,3-oxazine-4-one [23, 31], having a structure similar to **3c** in solid state, has revealed that the carbonyl group in the hetero ring is *equatorial*, while the oxygen in CHO is *isoclinal*.

It can be stated from the mass spectra of the *cis* isomers **3a–c** that the character of fragmentation does not depend on the number of members of the alicyclic ring. The base peak in the spectra is due to cleavage of the methylene bridge and the nitrogen atom and the other product of the splitting also appears in the spectrum at a mass higher by 14 units than the base peak.

The molecular ion of the compounds is not stable, its relative intensity being 2–6%. Figure 5 shows the main directions of the mass spectroscopic fragmentation of the trimethylene derivative **3a**. The primary processes leading to the appearance of the fragment ions take place mainly by hydrogen rearrangement. There is an asterisk in the figure where variation of the accelerating voltage results in the appearance of a metastable transition corresponding to the elemental steps given. In general, intense metastable peaks are observed, and this is characteristic of processes involving rearrangement.

The ion formed through release of water is rearranged to yield an ion with a mass number of 154, and one with 137; the latter is also formed by loss of water from the ion with mass number 155 produced from the molecular ion through hydrogen rearrangement. On the basis of these two processes it can be assumed that the hydrogen rearrangement takes place between the two oxazinone rings. The rearranged molecular ion is also responsible for the for-

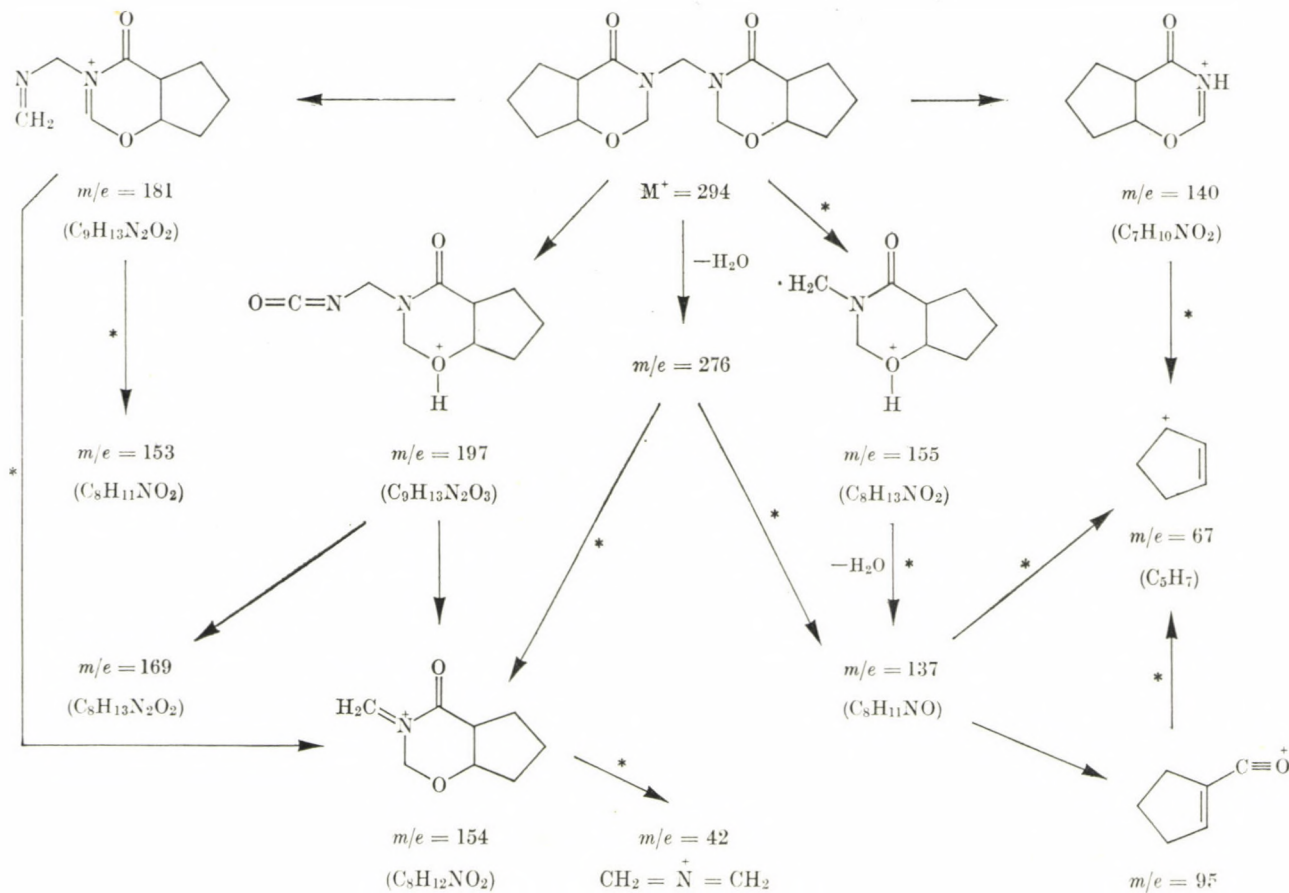


Fig. 5

mation of the ion with mass number 197, which undergoes decomposition with the loss of a neutral CO or HNCO molecule.

The mass spectra of the *cis* derivatives **3b** and **3c** are in good agreement with the mass spectrum of **3a**. The only intense ion not containing a ring appears at the same mass number in all compounds ($m/e = 42$) and, according to the metastable measurements, it is formed almost exclusively from the ion with mass number 154.

The mass spectra of *cis* and *trans* isomers with identical number of ring members differ only in the intensities of the peaks. It can be observed that in the spectra of the *trans* isomers certain ions which can be deduced by rearrangement appear with lower relative intensity than in the spectra of the corresponding *cis* isomers.

Experimental

M.p.'s were measured with a Boetius micro melting point apparatus and were uncorrected. The IR spectra were recorded with a Perkin Elmer 457 instrument in KBr pellets, and the PMR spectra with a Varian A-60D spectrometer in CDCl_3 . The mass spectra were obtained on a Varian MAT-SM-1 instrument. The elemental compositions given were measured with PFK reference at a resolution of $R = 10,000$. The deviation between the measured and calculated masses is less than 0.003 mass units.

The alicyclic 2-hydroxy-1-carboxamides **1a**–**e** used as starting materials were prepared as described in our earlier papers [4, 14, 15].

2-*p*-(Chlorophenyl)-*cis*-5,6-trimethylene-2,3,5,6-tetrahydro-1,3-oxazine-4-one (**2a**)

Compound **1a** (1.29 g; 10 mmoles) and *p*-chlorobenzaldehyde (1.40 g; 10 mmoles) were dissolved in anhydrous dioxan (25 ml) and the solution was acidified with ethanol saturated with hydrochloric acid (2 drops). After refluxing for 20 h, the reaction mixture was concentrated to 1/3 volume whereupon **2a** crystallized (2.19 g; 87%), m.p. 208–211 °C; after recrystallization from ethanol, m.p. 212–213 °C.

Analytical data of compounds of type **2** are summarized in Table I.

Thermal cyclization of **1b** with *p*-chlorobenzaldehyde

Compound **1b** (2.86 g; 20 mmoles) and *p*-chlorobenzaldehyde (2.81 g; 20 mmoles) were acidified with sulfuric acid (1 drop) and kept at 200 °C until the calculated amount of water had distilled (about 1 h). The product was rubbed with some water and filtered off on a glass filter. The PMR spectrum of the crude product (3.9 g; 73%) showed an isomeric ratio *cis* (**2b**): *trans* (**2d**) = 70 : 30.

3,3'-Methylene-di(*cis*-5,6-trimethylene-2,3,5,6-tetrahydro-1,3-oxazine-4-one (**3a**))

Compound **1a** (1.29 g; 10 mmoles), paraformaldehyde (1.2 g; 40 mmole-eq.) and *conc.* sulfuric acid (0.1 ml) were refluxed in anhydrous dioxan (30 h). The solvent was then evaporated and the residual oil dissolved in ether (4×50 ml). The ethereal solution was washed with water, dried (Na_2SO_4) and evaporated to dryness to obtain a white crystalline product (**3a**) (0.41 g; 28%), m.p. 186–189 °C. After two recrystallizations from ethanol, m.p. 192 °C.

Analytical data of compounds of type **3** are shown in Table II.

Spiro *cis*-5,6-tetramethylene-2,3,5,6-tetrahydro-1,3-oxazine-4-one-2,1'-cyclopentane (5b)

Compound **1b** (1.43 g; 10 mmoles) was dissolved in a freshly prepared mixture of cyclopentanone (10 ml) containing 1% HCl. After standing for 24 h, the solution was evaporated to dryness, the residue dissolved in CHCl_3 (50 ml) and this solution was washed with 5% NaHCO_3 and water. After drying (Na_2SO_4) it was evaporated to dryness to obtain the product **5b** (1.5 g; 72%), m.p. 169–173 °C; after recrystallization from ethyl acetate, m.p. 176–177 °C.

Analytical data of compounds of type **5** are shown in Table III.

2,2-Dimethyl-*cis*-5,6-tetramethylene-2,3,5,6-tetrahydro-1,3-oxazine-4-one (4a)

It was prepared from **1b** in acetone containing 1% HCl as described for **5b**. After a reaction time of 5 h the yield was 81%. After crystallization from ether, the product had m.p. 169–171 °C.

$\text{C}_{10}\text{H}_{17}\text{NO}_2$ (183.24). Calcd. C 65.54; H 9.35. Found C 65.45; H 9.46%.

2,2-Dimethyl-*trans*-5,6-tetramethylene-2,3,5,6-tetrahydro-1,3-oxazine-4-one (4b)

This compound was prepared from **1d** in a 5 h reaction, similarly to **4a**; the yield was 79%; recrystallization from ether gave m.p. 166–169 °C.

$\text{C}_{10}\text{H}_{17}\text{NO}_2$ (183.24). Calcd. C 65.54; H 9.35. Found C 65.66; H 9.38%.

*

The authors gratefully acknowledge the financial support of Chemical and Pharmaceutical Works CHINOIN, Budapest, and the supply of some starting materials by REANAL Factory of Laboratory Chemicals, Budapest. They wish to express their sincere thanks to Mrs. G. BOZÓKI-BARTÓK and Mrs. É. GERGELY-GÁCS for the microanalyses and to Miss V. WINDBRECHTINGER, Mr. A. FÜRJES, Miss A. POLYÁK and Mr. M. TOLDI for their technical assistance.

REFERENCES

- [1] BERNÁTH, G., GÖNDÖS, Gy., GERA, L., TÖRÖK, M., KOVÁCS, K., SOHÁR, P.: *Acta Phys. et Chem. Szeged* **19**, 147 (1973)
- [2] BERNÁTH, G., LÁNG, K. L., KOVÁCS, K., RADICS, L.: *Acta Chim. (Budapest)* **73**, 81 (1972)
- [3] SOHÁR, P., BERNÁTH, G.: *Org. Magnetic Resonance* **5**, 169 (1973)
- [4] BERNÁTH, G., GÖNDÖS, Gy., KOVÁCS, K., SOHÁR, P.: *Tetrahedron* **29**, 981 (1973)
- [5] BERNÁTH, G., GÖNDÖS, Gy., GERA, L., FÜLÖP, F., ECSERY, Z., SOHÁR, P.: Lecture presented at the International Symposium on Stereochemistry, Kingston, Ontario, Canada, June 28, 1976
- [6] BERNÁTH, G., GERA, L., GÖNDÖS, Gy., ECSERY, Z., HERMANN, M., SZENTIVÁNYI, M. J., KANYÓ, E.: *Hung. Pat. Appl.*, October 3, 1975, No. CI-1614.
- [7] RIBÁR, B., LAZAR, D., KÁLMÁN, A., SASVÁRI, K., BERNÁTH, G., HACKLER, L.: *Cryst. Struct. Comm.* **6**, 671 (1977)
- [8] BERNÁTH, G., FÜLÖP, F., GERA, L., HACKLER, L., KÁLMÁN, L., ARGAY, Gy., SOHÁR, P.: *Tetrahedron* **35**, 799 (1979)
- [9] LAZAR, D., RIBÁR, B., ARGAY, Gy., KÁLMÁN, A., BERNÁTH, G., FÜLÖP, F.: Lecture at the XIIth Yugoslav Crystallographic Conference, Budva (Yugoslavia), June 8, 1977
- [10] ARMAREGO, W. L. F.: *Stereochemistry of Heterocyclic Compounds*. J. Wiley and Sons, New York 1977
- [11] FINKELSTEIN, J., CHIANG, E.: *J. Med. Chem.* **1968**, 1038
- [12] BERNÁTH, G., MINKER, E., FÜLÖP, F., ECSERY, Z., VIRÁG, S., HERMANN, M., SEBESTYÉN, Gy.: *Hung. Pat. Appl.*, October 25, 1977
- [13] MINKER, E. *et al.*: To be published
- [14] BERNÁTH, G., LÁNG, K. L., GÖNDÖS, Gy., MÁRAI, P., KOVÁCS, K.: *Acta Chim. (Budapest)* **74**, 479 (1972)
- [15] BERNÁTH, G., KOVÁCS, K., LÁNG, K. L.: *Acta Chim. Acad. Sci. Hung.* **64**, 183 (1970)
- [16] FINCH, N., FITT, J. J., HSU, I. H. S.: *J. Org. Chem.* **40**, 206 (1975)
- [17] EINHORT, A., SCHUPP, G.: *Ann.* **343**, 252 (1905)

- [18] HAWORTH, R. D., PEACOCK, D. H., SMITH, W. R., MACGILLIVRAY, R.: J. Chem. Soc. **1952**, 2972
- [19] HOLLY, F. W., COPE, A. C.: J. Am. Chem. Soc. **66**, 1875 (1944)
- [20] SZABÓ, J., VARGA, I., WINKLER, E., BARTHOS, É.: Acta Chim. (Budapest) **72**, 213 (1972)
- [21] FISCHER, H. O. L., DANGSCHAT, G., STETTINER, H.: Ber. **65**, 1032 (1932)
- [22] FÜLÖP, F.: Diploma Thesis, József Attila University, Szeged, Hungary, 1975
- [23] BERNÁTH, G., GÖNDÖS, Gy., FÜLÖP, F., GERA, L.: Lecture at the EUCHEM Conference on Ring Closure Reactions and Related Topics, Castel Gandolfo, Italy, August 28—September 1, 1978
- [24] BERNÁTH, G., FÜLÖP, F.: Lecture at the Conference of the Hungarian Chemical Society, Debrecen, Hungary, August 23—26, 1977: Proceedings, p. 68
- [25] SOHÁR, P.: Mágneses Magrezonancia Spektroszkópia, Vol. **1**, a) p. 76; b) p. 183; Akadémiai Kiadó, Budapest 1976
- [26] KARPLUS, M.: J. Chem. Phys. **30**, 11 (1959)
- [27] HENDRICKSON, J. C., BOECKMAN, R. K., Jr., GLICKSON, J. D.: J. Am. Chem. Soc. **95**, 494 (1973)
- [28] BREDOW, K., FRIEBOLIN, H., KABUSE, S.: Die konformative Beweglichkeit der gesättigten Siebenringverbindungen. In: "Conformational Analysis, Scope and Present Limitations" (Ed.: G. CHIUORDOGLU), p. 51. Academic Press, New York, London 1971
- [29] TOCHTERMANN, W.: Konformative Beweglichkeit von Siebenring-Systemen. In: "Fort-schritte der Chemischen Forschung-Topics in Current Chemistry", Vol. **15**, p. 378. Springer Verlag Berlin, Heidelberg, New York 1970
- [30] BERNÁTH, G., GÖNDÖS, Gy., LÁNG, K. L.: Acta Chim. (Budapest) **81**, 187 (1975)
- [31] To be published

Gábor BERNÁTH Ferenc FÜLÖP Gyula JERKOVICH Pál SOHÁR	{	H-6720 Szeged, Eötvös u. 6. H-1325 Budapest, Újpest 1, POB 82.
---	---	---

REACTION OF CHROMONIDS WITH NUCLEOPHILIC REAGENTS, I.

CLEAVAGE OF THE PYRONE RING OF CHROMONE DERIVATIVES IN AQUEOUS ALKALI

M. ZSUGA, V. SZABÓ, F. KÓRÓDI and A. KISS

(*Institute of Applied Chemistry, Kossuth Lajos University,
Debrecen*)

Received June 22, 1978

Accepted for publication September 1, 1978

The ring cleavage reactions of chromone, flavone, isoflavone, 3-methylchromone and 3-phenoxychromone in aqueous alkali have been studied.

Ring cleavage starts with an isoentropic Ad_N2 -type nucleophilic addition, which is also the rate-determining step. The carbanion (**II**) is then stabilized in accordance with the **III** \rightleftharpoons **IV** equilibrium. The rate constant of the ring cleavage reaction is in a linear correlation with the thermodynamic protonation constant of the carbonyl group of the γ -pyrone ring, which shows that the electron density at C-2 is greatly influenced by the electron distribution of the carbonyl group.

Alkaline hydrolytic degradation is one of the important methods used for the structure elucidation of naturally occurring chromone derivatives [1]. The products of this reaction can be regarded as starting materials for the synthesis of chromone derivatives by ring isomerisation [2]. The compounds formed in the ring opening reaction also influence the composition of the reaction mixture of catalytic hydrogenation [3] or oxidative degradation [4] carried out in alkaline medium. The rate of the ring opening reaction and conversion is influenced by the type and position of the substituents, the state of oxidation of the chromone ring, and the reaction conditions (temperature and alkali concentration) [5, 11].

In our previous papers the ring cleavage of isoflavones with various nucleophilic reagents has been reported [6-9, 11]. We found with all the nucleophiles studied so far that ring cleavage was initiated by a relatively slow, Ad_N2 -type step, followed by fast ring cleavage. Chromone derivatives, treated with hydroxide ion are stabilized — with a few exceptions [11] — by excess alkali as β -dicarbonyl enolates (**IV**) [6, 7]. Hydroxylamine, hydrazine or substituted hydrazines give oximes, hydrazones or substituted hydrazones of a β -ketoaldehyde, which then rapidly rearrange to isoxazole [8] and pyrazole [9] derivatives. With the nucleophiles studied so far attack takes place exclusively at C-2.

The β -dicarbonyl enolates from isoflavones (**IV c**) are stable with a few exceptions [11]; they decompose to 2-hydroxydeoxybenzoin [10] very slowly. This ring opening with hydroxide ions may be regarded, with some limitation,

as a consecutive reversible reaction [7] which can be characterized kinetically by the rate constant k_1 of the rate determining step, *i.e.* of the $\text{Ad}_{\text{N}2}$ addition reaction. The value of k_1 is highly dependent on substitutions in the system and is therefore useful in characterizing the stability and nucleophilic reactivity of the γ -pyrone ring of such compounds [11]. We have found that k_1 not only indicates reactivity towards hydroxide ions, but also shows the relative order of reactivity with other nucleophils.

In this paper we describe an extension of these studies to chromone and certain chromone derivatives.

Experimental

The apparent (pseudo-first order) rate constants k_b were determined by UV spectrophotometry as described previously [6]. The measured and theoretical absorption values — the latter calculated from k_b — were in good agreement ($\bar{\sigma} = 5 \cdot 10^{-3}$ A.u.). The thermodynamic pK_{BH^+} values were determined according to the literature [13], as described in a previous paper [15].

Results and Discussion

The spectra of the chromone derivatives **Ia–d** undergo a change in dilute aqueous alkaline medium. At the kinetic end of the reaction a high intensity, broad maximum appears in the range of 280–292 nm, which is stable for a relatively long period. The λ_{max} (nm) and ($\lg \epsilon$) values are, **Ia**: 280 (4.19); **Ib**: 308 (4.26); **Ic**: 290 (4.30); **Id**: 292 (4.15); **Ie**: 360 (3.90); 320 (4.00). The change of the spectrum of **Ie** differs both in character and in λ_{max} from the spectra of the other chromone derivatives. Ring cleavage is followed by a rather slow decomposition, as shown by a change of the spectrum at the kinetic end towards the superposed spectra of the corresponding decomposition products (*e.g.* salicylic acid, *o*-hydroxyacetophenone derivatives).*

Like with isoflavone derivatives [6], the ring cleavage of chromone derivatives by hydroxide ions, and thus molar absorption at λ_{max} at the kinetic end, is dependent on the hydroxide ion concentration and tends, according to the parameters of the equilibrium $\text{III} \rightleftharpoons \text{IV}$, towards a limit (Fig. 1).

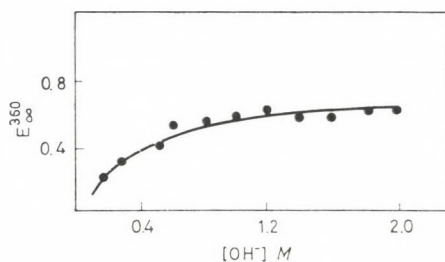
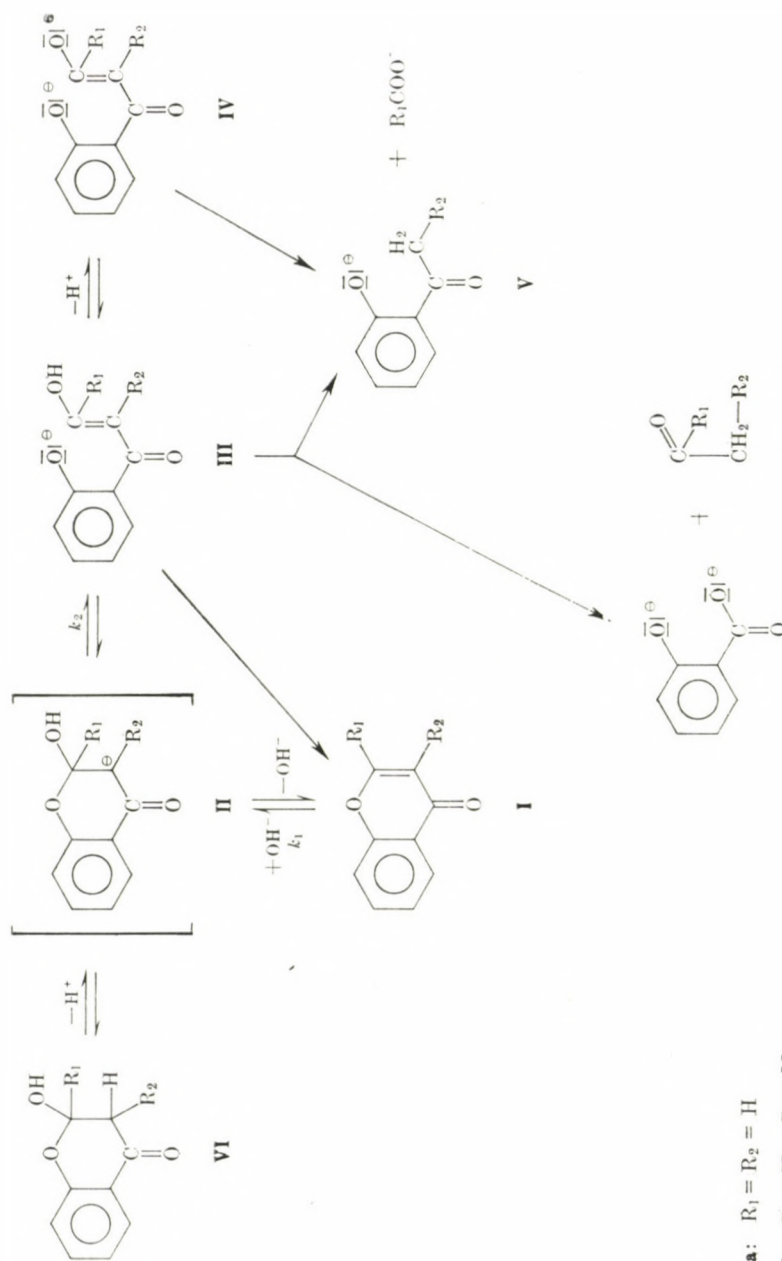


Fig. 1. Change of the absorption of light at the kinetic end of the ring opening reactions of flavone, at 35 °C, as a function of the hydroxide ion concentration ($\lambda = 350$ nm)

* A kinetic study of this decomposition will be reported in a forthcoming publication.



When the reaction mixtures are acidified at the kinetic end, **IIIa–d** give **VIa–d**, whereas **IIIe** gives 2-hydroxybenzoyl benzoylmethane, which then all recyclize slowly to **Ia–e**.

Our measurements thus indicate that the ring cleavage of derivatives **Ia–e** ($\text{I} \rightleftharpoons [\text{II}] \rightleftharpoons \text{III} \rightleftharpoons \text{IV}$) is much slower ($k_1 \ll k_2$) than that of 2-hydroxychromanones (**VI**) ($\text{VI} \rightleftharpoons [\text{II}] \rightleftharpoons \text{III} \rightleftharpoons \text{IV}$).

Therefore, in our opinion, the rate-determining step in the ring cleavage of **I** is the transformation $\text{I} \rightarrow [\text{II}]$. Furthermore, in alkaline solution the derivatives **VI**, at a pH value depending also on the substituents, quickly reach a spectrum, characteristic of the equilibrium $\text{III} \rightleftharpoons \text{IV}$. This spectrum changes towards that of **I** slowly. Thus the transformation $\text{VI} \rightleftharpoons [\text{II}] \rightleftharpoons \text{III} \rightleftharpoons \text{IV}$ must be faster than dehydration $\text{VI} \rightarrow [\text{II}] \rightarrow \text{I}$ ($k_2 \gg k_{-1}$). Accordingly, the kinetics of the ring cleavage of the chromone derivatives studied may be simply formulated as follows:



Applying the BODENSTEIN principle [14], the apparent rate constant in the case of the studied compounds will be:

$$k_b = k_1 [\text{OH}^-], \quad (2)$$

k_b in fact being a linear function of the hydroxide ion concentration (Fig. 2), which proves that the rate-determining step of the ring cleavage reaction is kinetically of second order.

The slopes of the straight lines in Fig. 2 give, in accordance with Eq. 2, the rate constants of ring cleavage (k_1). As expected, the intercepts of the straight lines in Fig. 2 spread around the 0 point. Consequently, the ring cleavage of the chromone derivatives **Ia–e** is analogous to the cleavage of **Ic** [6] or the corresponding C-2-unsubstituted derivatives [11].

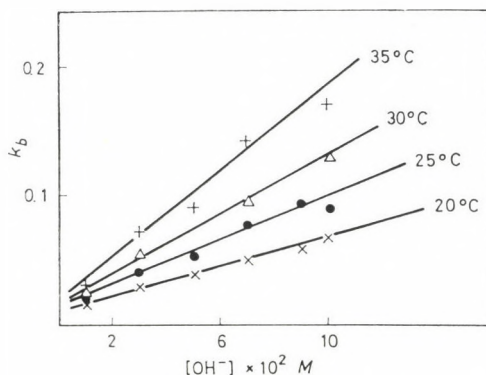


Fig. 2. Dependence of the apparent rate constant of the ring cleavage reaction of chromone (k_b) as a function of the initial hydroxide ion concentration

Table I

Rate constants, activation parameters of cleavage and carbonyl group thermodynamic protonation constants of chromone derivatives

	$t(^{\circ}\text{C})$	$k_1(\text{min}^{-1} \cdot \text{mole}^{-1})$	$E^*(\text{kcal/mole})$	$\Delta S^*(\text{e. u})$	pK_{BH^+}	φ	γ
Ia	20	0.476 ± 0.01	12.9 ± 2.0	-23.9 ± 6.5	2.02	0.37	1
	25	0.864 ± 0.04					
	30	1.108 ± 0.05					
	35	1.448 ± 0.03					
Ib	20	0.512 ± 0.028	12.9 ± 0.5	-23.7 ± 1.7	2.44	0.06	0.91
	25	0.789 ± 0.08					
	30	1.1025 ± 0.13					
	35	1.525 ± 0.08					
Ic	20	3.80 ± 0.18	12.9 ± 0.9	-18.7 ± 4.1	2.77	0.65	6.03
	25	5.21 ± 0.23					
	30	8.67 ± 0.33					
	35	10.99 ± 0.39					
Id	20	11.94 ± 0.98	11.6 ± 0.8	-21.8 ± 2.8	3.13	0.4	21.25
	25	18.36 ± 1.83					
	30	24.40 ± 2.04					
	35	32.05 ± 3.16					
Ie	20	0.021 ± 0.0008	16.1 ± 0.4	-21.3 ± 1.6	1.45	0.01	0.035
	25	0.0314 ± 0.002					
	30	0.0513 ± 0.003					
	35	0.0755 ± 0.0036					

The k_1 constants, determined at different temperatures, and the activation parameters calculated from the $\lg k_1 - 1/T$ equation are summarized in Table I.

The activation energy and activation entropy of ring cleavage of various chromone derivatives indicate bimolecular reaction [12], therefore our earlier observation [6] can be generalized in the case of chromones. Transformation starts with an Ad_N2 type addition being the rate-determining step. Then the carbanion **II** is stabilized in the enol-enolate (**III** \rightleftharpoons **IV**) form.

The rate constant of the nucleophilic addition reaction (k_1) depends on the electron distribution in the ground state, especially on the electron density at C-2. Thus k_1 is useful for the characterization of the stability of chromone

and chromone derivatives toward nucleophiles. Relative stabilities can be defined as follows:

$$\gamma = \frac{k_1^{\text{chr.}}}{k_1^{\text{subst. chr.}}} \quad (3)$$

The numerical values (Table I) are in good agreement with the qualitative observations, and with the well known electronic effects of the substituents.

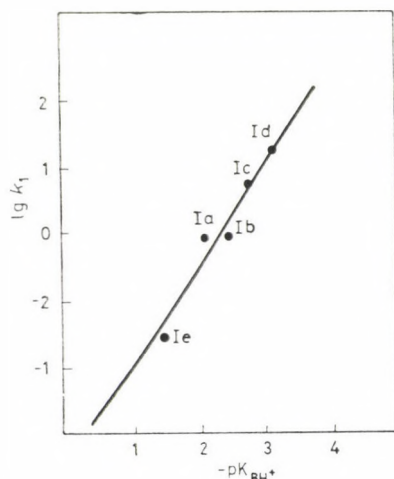


Fig. 3. Dependence of $\log k_1$ of the ring cleavage of various chromone derivatives on pK_{BH^+} at 25 °C

The negative logarithm of the protonation constant of the carbonyl group (pK_{BH^+}) also denotes the electron distribution of the γ -pyrone ring and the chromonoid molecule. If our assumption is correct, there should be an exponential relationship between k_1 and pK_{BH^+} . In the case of the chromone derivatives studied in this work, this correlation is as follows:

$$\log k_1^{25^\circ\text{C}} = -1.55 \text{ pK}_{\text{BH}^+}^{25^\circ\text{C}} - 3.53 \quad (4)$$

(See also Fig. 3.) Equation 4, on the one hand, provides a possibility of studying the electron distribution of these rings and molecules by two methods; on the other hand, it permits a study of the nucleophilic reactivity of molecules where the direct determination of k_1 is not possible because the rate of decomposition ($\text{III} \rightarrow \text{V}$) is higher than the rate of ring cleavage ($\text{I} \rightarrow \text{II} \rightarrow \text{IIs}$). This will be the subject of a forthcoming paper.

Preliminary studies indicate that Eq. 4 may allow to predict the reactivity of chromonoids with other nucleophiles (e.g. nitrogen nucleophiles) by

means of calculating the nucleophilic reactivity. Activation entropy values of the ring cleavage of compounds **Ia**–**e** are very similar (Table I); therefore, the influence of substituents on the structure of the transition state is small. This means that both the point of attack of the hydroxide ions and the stereochemistry of the transition state may be regarded as almost the same.

*

The authors wish to express their thanks to Miss Ilona BODONOVITS for her excellent technical assistance and to Dr. M. RÁKOSI for a gift of the synthetic flavone derivative.

REFERENCES

- [1] COFFEY, S.: *Rodd's Chemistry of Carbon Compounds*, Vol. **IV** E, pp. 144, 164, 211. Elsevier, Amsterdam 1977
- [2] FARKAS, L., MAJOR, Á., STRELISKY, J.: *Ber.*, **96**, 1684 (1963)
FARKAS, L., VÁRADY, J., GOTTSEGEN, Á.: *Tetrahedron Letters*, **1966**, 351
- [3] SZABÓ, V., ANTAL, E.: *Tetrahedron Letters*, **1973**, 1659
- [4] STAMM, O. A., SCHMIDT, H., BÜCHI, J.: *Helv. Chim. Acta*, **41**, 2006 (1958)
- [5] SZABÓ, V.: Thesis, Debrecen, 1958 (In Hungarian);
WALZ, E.: *Ann.*, **489**, 118 (1931);
ELDERFIELD, R. C. editor: *Heterocyclic Compounds*, Vol. **2**, p. 257. Wiley, New York 1951
- [6] SZABÓ, V., ZSUGA, M.: *Acta Chim. (Budapest)* **85**, 179 (1975)
- [7] SZABÓ, V., ZSUGA, M.: *Acta Chim. (Budapest)* **85**, 191 (1975)
- [8] SZABÓ, V., BORDA, J., LOSONCZI, L.: *Magyar Kém. Folyóirat*, **83**, 278 (1977)
- [9] SZABÓ, V., BORDA, J., VÉGH, V.: *Magyar Kém. Folyóirat*, **83**, 393 (1977)
- [10] SZABÓ, V., ZSUGA, M.: *Acta Chim. (Budapest)* **88**, 27 (1976)
- [11] SZABÓ, V., ZSUGA, M.: *Acta Chim. (Budapest)* **97**, 451 (1978)
- [12] BAMFORD, C. H., TIPPER, C. F.: *Comprehensive Chemical Kinetics*, Vol. **8**, p. 16 Elsevier Amsterdam 1976
- [13] BUNETT, J. F., OLSEN, F. P.: *Can. J. Chem.*, **44**, 1899 (1966)
- [14] BODENSTEIN, N.: *Z. Phys. Chem.*, **85**, 329 (1913)
- [15] NAGY, T.: Diplomamunka, Debrecen 1976 (In Hungarian)

Miklós ZSUGA Vince SZABÓ Ferenc KÓRÓDI Anikó KISS	{	H-4010, Debrecen 10.
--	---	----------------------

STEREOSELECTIVE HYDROGENOLYSIS OF DIOXOLANE-TYPE BENZYLIDENE ACETALS

SYNTHESIS OF PARTIALLY SUBSTITUTED GALACTOPYRANOSIDE DERIVATIVES

A. LIPTÁK, L. JÁNOSSY, J. IMRE and P. NÁNÁSI

(Institute of Biochemistry, Kossuth L. University, Debrecen)

Received July 4, 1978

Accepted for publication September 1, 1978

Partially benzylated or partially benzylated and methylated derivatives of α - and β -D-galactopyranosides were prepared by the hydrogenolysis of the *exo*- and *endo*-isomers of 3,4-O-benzylidene- α - and - β -D-galactopyranosides. The *exo* isomers gave the corresponding 3-O-benzyl-4-hydroxy derivatives, whereas the reaction of the *endo* isomers gave the 4-O-benzyl-3-hydroxy analogues in every case. On the hydrogenolysis of acetals containing unsubstituted hydroxyl group, an isomerization of slight degree, dependent on the length of time of the reaction and excess of the reagent, may be supposed. The hydrogenolytic method offers a convenient route for determining the *exo* or *endo* configuration of dioxolane-type benzylidene acetals even if only one of the two isomers is at disposal.

Benzylidene acetals are frequently used intermediates in preparative carbohydrate chemistry due to their stability [1] and ability for crystallization. The new methods, published during the past ten years — first of all the ring cleavage of these derivatives with *N*-bromosuccinimide introduced by HANESSIAN [2] and HULLAR *et al.* [3], the ozonolytic [4] and photochemical [5] oxidation reactions, as well as their reactions with butyllithium elaborated by KLEMER *et al.* [6] — have widened their field of application.

The preparative importance of the hydrogenolytic ring cleavage of benzylidene acetals with the mixed hydride $\text{LiAlH}_4\text{--AlCl}_3$ reagent [7-10] seems to be comparable with the methods mentioned above. The high regiospecificity of this reaction was first observed in our laboratory with 4,6-O-benzylidene acetals of mono- [11-13] and oligosaccharides [14-16]. Recently the regioselective ring cleavage of *p*-methoxybenzylidene acetals — dependent on the steric requirement of the C-3 substituent — has also been reported [17].

In the case of the five-membered dioxolane-type benzylidene acetals the reagent attacks the *axial* oxygen atom of the *exo*-isomers and a product with *equatorial* O-benzyl- and *axial* hydroxyl groups is formed. Owing to the opposite place of attack of the reagent on the *endo* isomers, *i.e.* the *equatorial* oxygen atom of the dioxolane ring, a product with *axial* O-benzyl and *equatorial* hydroxyl groups is formed [18-22].

According to these results, the hydrogenolytic ring cleavage reaction provides a convenient route to partially benzylated carbohydrate derivatives.

In the present study we report on the preparation of some benzyl and methyl ether derivatives of benzyl β -D- and allyl α -D-galactopyranosides.

The preparation of numerous partially benzylated galactopyranoside derivatives has been reported recently. These derivatives served almost exclusively as intermediates in the synthesis of galactose-containing blood group oligosaccharides [23], glycolipids [24–25] and immun-determining oligosaccharides.

During the past ten years the synthesis of the following partially benzylated galactopyranose or galactopyranoside derivatives have been described: 2-*O*-benzyl- [26–28], 3-*O*-benzyl- [26], 4-*O*-benzyl- [29], 2,3-di-*O*-benzyl- [26, 28, 30], 2,4-di-*O*-benzyl- [30–32], 2,6-di-*O*-benzyl- [28, 33, 34], 2,3,4-tri-*O*-benzyl- [12, 27], 2,3,6-tri-*O*-benzyl- [32, 34], 2,4,6-tri-*O*-benzyl- [33, 34] and 3,4,6-tri-*O*-benzyl [35–37] ethers.

The syntheses reported start with the 3,4-*O*-substituted analogues of benzyl β -D- [38] and allyl α -D-galactopyranosides [39]. STOFFYN and STOFFYN [26] reported for the first time that the acid catalyzed acetonation of benzyl β -D-galactopyranoside (1) led to benzyl 3,4-*O*-isopropylidene- β -D-galactopyranoside (2); the unchanged starting material and the corresponding 4,6-*O*-isopropylidene analogue were removed by column chromatography. By modification of this procedure compound 2 was obtained by direct crystallization in 54% yield. Benzylation of 2 using the method of ZEMPLÉN and CSÜRÖS [40] gave 90% of syrupy benzyl 2,6-di-*O*-benzyl-3,4-*O*-isopropylidene- β -D-galactopyranoside (3). The KUHN methylation [41] of 2 yielded benzyl 3,4-*O*-isopropylidene-2,6-di-*O*-methyl- β -D-galactopyranoside (4) in almost quantitative yield. Hydrolysis of 3 and 4 with acetic acid resulted in the hitherto unknown crystalline benzyl 2,6-di-*O*-benzyl- β -D-galactopyranoside (5) and benzyl 2,6-di-*O*-methyl- β -D-galactopyranoside (6), respectively. Methylation of 5 gave the crystalline and hitherto unknown benzyl 2,6-di-*O*-benzyl-3,4-di-*O*-methyl- β -D-galactopyranoside (7). In the $^1\text{H-NMR}$ spectrum of 5 the absorption of six protons corresponding to the three methylene part of benzyl groups was observed at 5.02–4.56 ppm. From among them two appeared as an AB quartet, whereas the C-6 benzyl protons gave a singlet. The doublet of the anomeric proton appeared at 4.44 ppm with a coupling of 9 Hz and the OH group — showing fast proton exchange — was assigned as a broad doublet at 3.14 ppm. The $^1\text{H-NMR}$ spectrum of 6 was consistent with the proposed structure showing the quartet of the methylene part of benzyl group at 4.78 ppm, the $\text{C}_1\text{-H}$ at 4.36 as a doublet, the $\text{C}_2\text{-OCH}_3$ at 3.63 ppm and the $\text{C}_6\text{-OCH}_3$ at 3.42 as sharp singlets. In the case of 7 the two methyl signals appeared close to each other and at lower field (3.60 and 3.56 ppm) indicating the presence of secondary OCH_3 groups.

Catalytic debenylation of 6 and 7 with 10% Pd/C gave the known 2,6-di-*O*-methyl- (8) [42] and 3,4-di-*O*-methyl-D-galactose (9) [43], respectively.

Benzylidenation of **5** using the general procedure (benzaldehyde and zinc chloride) gave a mixture of isomeric 3,4-*O*-benzylidene acetals. The formation of the *exo*- and *endo* isomers were detected both by TLC and $^1\text{H-NMR}$ spectroscopy and their separation was effected by direct fractional crystallization. Benzyl 2,6-di-*O*-benzyl-*exo*-3,4-*O*-benzylidene- β -D-galactopyranoside (**10**) was obtained in 31% yield after crystallization from ethanol, whereas benzyl 2,6-di-*O*-benzyl-*endo*-3,4-*O*-benzylidene- β -D-galactopyranoside (**11**) was crystallized from cyclohexane. Similarly to other isomeric pairs, the two diastereomeric acetals showed different solubility in several solvents and the *endo* isomer was more soluble in all organic solvents than the *exo* analogue.

The steric position of the phenyl group of compounds **10** and **11**, and the configuration of the C-2' atom of their dioxolane rings were determined by their $^1\text{H-NMR}$ data. The acetal hydrogens of the *exo* isomers resonate always at lower field [44] than those of the *endo* isomers. The observed chemical shift was 5.94 and 5.85 ppm for compound **10** and **11**, respectively.

Benzylidenation of **6** according to the procedure of EVANS [45] (benzaldehyde dimethylacetal, *p*-toluene-sulfonic acid, *N,N*-dimethyl-formamide resulted also in a mixture of two diastereomeric compounds. These were detectable by $^1\text{H-NMR}$ investigation or gas [46] and thin-layer chromatographic methods. The *exo* isomers have, in most cases, a higher R_f value than the *endo* isomers, whereas gas chromatographic examination with apolar GLC columns showed a reversed mobility of these compounds, i.e. the retention times of the *exo* isomers were longer than those observed for the *endo* analogues [46].

Both **12** and **13** were obtained in crystalline form after separation by column chromatography.

Hydrogenolysis of **10** with a 20% excess of $\text{LiAlH}_4\text{-AlCl}_3$ (1 : 1) gave benzyl 2,3,6-tri-*O*-benzyl- β -D-galactopyranoside (**14**) as a single product in quantitative yield. The structure of **14** was also proved by converting it into the corresponding 4-*O*-methyl derivative (**15**).

Hydrogenolysis of **11** gave benzyl 2,4,6-tri-*O*-benzyl- β -D-galactopyranoside (**16**), which afforded on methylation the corresponding 3-*O*-methyl derivative (**17**).

The direction of the ring cleavage reaction of **12** and **13** was found to be similar to those mentioned above, i.e. the *exo* isomer (**12**) gave benzyl 3-*O*-benzyl-2,6-di-*O*-methyl- β -D-galactopyranoside (**18**), while the *endo* isomer (**13**) yielded benzyl 4-*O*-benzyl-2,6-di-*O*-methyl- β -D-galactopyranoside (**19**).

The results of these investigations were consistent with those observed earlier i.e. the reagent attacks on the *axial* oxygen atom of the *exo* isomers, whereas the place of attack is on the *equatorial* oxygen in the case of the *endo* isomers. On the other hand, the direction of the reaction is independent of the steric bulk of the neighbouring substituents.

The examinations were extended to some α -D-galactopyranosides as well, in order to determine whether the anomeric configuration of the acetal derivative to be hydrogenolyzed has an effect on the direction of the reaction. On the other hand, the method offered a convenient route to synthesize the hardly available 3,6-O-benzyl-D-galactopyranoside derivatives. It has to be mentioned that the allyl group was used as the aglycone moiety, the selective removal of which [47–49] has recently generated considerable interest. Namely, carbohydrate derivatives concurrently containing allyl and benzyl groups (“temporary” and “persistent” groups) are useful intermediates [50] in complex oligosaccharide syntheses.

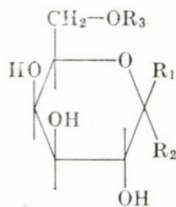
Benzylidenation of allyl 6-O-benzyl- α -D-galactopyranoside (**20**) was carried out according to the method of EVANS and gave, after column chromatography, crystalline allyl 6-O-benzyl-*exo*-3,4-O-benzylidene- α -D-galactopyranoside (**21**), (66%, $\delta_{\text{CH-Ph}}$ 6.16 ppm) and the syrupy *endo* isomer (**22**) (24%, $\delta_{\text{CH-Ph}}$ 5.82 ppm).

Benzylation of **21** and **22** gave the fully protected derivatives allyl 2,6-di-O-benzyl-*exo*-3,4-O-benzylidene- α -D-galactopyranoside (**23**) and allyl 2,6-di-O-benzyl-*endo*-3,4-O-benzylidene- α -D-galactopyranoside (**24**), respectively. The benzylidene protons of these compounds appeared at δ 5.95 and 5.88 ppm, respectively. Hydrogenolysis of **21** at room temperature was complete only in one hour, even if a large excess of the reagent was used, and two products were formed in the ratio of 9 : 1. The application of a large excess of the reagent was necessary due to the consumption of lithium aluminium hydride by the free hydroxyl group of the starting material. It can be expected that the relatively long time necessary for completing the reaction is a consequence of the low solubility of the aluminium alkoxide formed.

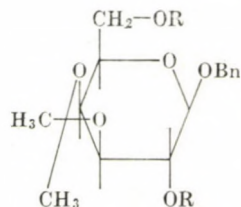
Of the two compounds resulting from the hydrogenolysis of **21** only the main product was isolated, which — according to $^1\text{H-NMR}$ data — contains the aglycone moiety and two benzyl groups. The compound did not consume periodate [51] indicating its allyl 3,6-di-O-benzyl- α -D-galactopyranoside (**25**) structure.

Reductive ring cleavage of the *endo* isomer was effected under the same conditions as described for **21**. Two products were formed in the ratio of 4 : 1 and the by-product was found to be identical with **25**. The main product, containing two benzyl groups ($^1\text{H-NMR}$), could be oxidized with periodate but no formation of formic acid [52] was observed. Thus the product was allyl 4,6-di-O-benzyl- α -D-galactopyranoside (**26**).

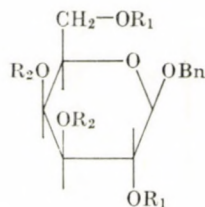
In these cases the lower stereoselectivity can be explained by the prolonged reaction time: the Lewis acid character of chloroaluminate causes the isomerization of the dioxolane ring, and ring cleavage of the resulting *endo* isomer gives a cleaved product unexpected in the case of the *exo*-isomer. It can be generally stated that reaction conditions which do not cause the isomerization



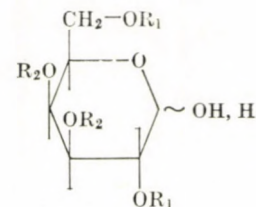
- 1 $R_1 = \text{OBn}, R_2 = R_3 = \text{H}$
 20 $R_1 = \text{H}, R_2 = \text{All}, R_3 = \text{Bn}$



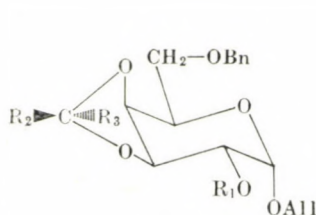
- 2 $R = \text{H}$
 3 $R = \text{Bn}$
 4 $R = \text{CH}_3$



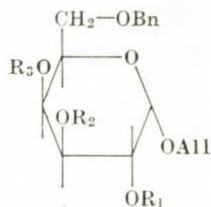
- 5 $R_1 = \text{Bn}, R_2 = \text{H}$
 6 $R_1 = \text{CH}_3, R_2 = \text{H}$
 7 $R_1 = \text{Bn}, R_2 = \text{CH}_3$



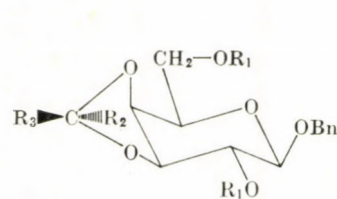
- 8 $R_1 = \text{CH}_3, R_2 = \text{H}$
 9 $R_1 = \text{H}, R_2 = \text{CH}_3$



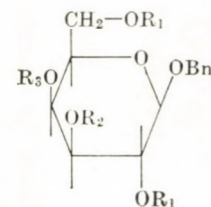
- 21 $R_1 = R_3 = \text{H}, R_2 = \text{Ph}$
 22 $R_1 = R_2 = \text{H}, R_3 = \text{Ph}$
 23 $R_1 = \text{Bn}, R_2 = \text{Ph}, R_3 = \text{H}$
 24 $R_1 = \text{Bn}, R_2 = \text{H}, R_3 = \text{Ph}$



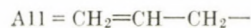
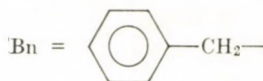
- 25 $R_1 = R_3 = \text{H}, R_2 = \text{Bn}$
 26 $R_1 = R_2 = \text{H}, R_3 = \text{Bn}$
 27 $R_1 = R_2 = \text{Bn}, R_3 = \text{H}$
 28 $R_1 = R_3 = \text{Bn}, R_2 = \text{H}$



- 10 $R_1 = \text{Bn}, R_2 = \text{H}, R_3 = \text{Ph}$
 11 $R_1 = \text{Bn}, R_2 = \text{Ph}, R_3 = \text{H}$
 12 $R_1 = \text{CH}_3, R_2 = \text{H}, R_3 = \text{Ph}$
 13 $R_1 = \text{CH}_3, R_2 = \text{Ph}, R_3 = \text{H}$



- 14 $R_1 = R_2 = \text{Bn}, R_3 = \text{H}$
 15 $R_1 = R_2 = \text{Bn}, R_3 = \text{CH}_3$
 16 $R_1 = R_3 = \text{Bn}, R_2 = \text{H}$
 17 $R_1 = R_3 = \text{Bn}, R_2 = \text{CH}_3$
 18 $R_1 = \text{CH}_3, R_2 = \text{Bn}, R_3 = \text{H}$
 19 $R_1 = \text{CH}_3, R_2 = \text{H}, R_3 = \text{Bn}$



of the dioxolane ring have to be applied for the hydrogenolysis of acetals of such type.

Hydrogenolysis of **23** was completed within 5 minutes at 20°C, and besides **27** a by-product (*max.* 5%) was also detected. The physical data of **27**, isolated by column chromatography, were in good agreement with those reported by NASHED and ANDERSON [53] for allyl 2,3,6-tri-*O*-benzyl- α -D-galactopyranoside.

Ring cleavage of **24** was also fast and resulted exclusively in allyl 2,4,6-tri-*O*-benzyl- α -D-galactopyranoside (**28**) [54], known in the literature.

The results of the present study unequivocally show that the direction of the ring cleavage of dioxolane-type benzylidene acetals in the galactose series is determined also by the steric position of the phenyl group. Thus, the reductive ring cleavage method provides not only a convenient route for synthesizing partially substituted galactopyranosides, but also offers a simple chemical method for the determination of the *exo* or *endo* configuration of dioxolane-type benzylidene acetals, even if only one of the two isomers is at disposal. Namely, *exo* isomers are always transformed into a product containing *equatorial O*-benzyl- and *axial* hydroxyl groups, whereas the *endo* isomers give an analogue with *axial O*-benzyl and *equatorial* hydroxyl group. In determining the configuration of dioxolane-type acetals by ^1H - and ^{13}C -NMR [44, 55] — based on the relative chemical shifts of the acetal protons or carbon atoms — the simultaneous investigation of both isomers was required.

Experimental

M.p.'s were determined on a Kofler hot stage apparatus and are uncorrected. Optical rotations were measured with a Perkin-Elmer 241 automatic polarimeter. NMR spectra were taken on a Jeol MH-100 (100 MHz) instrument using TMS as internal standard. Kieselgel G (E. Merck, Darmstadt) was used for column chromatography and TLC, with the solvent systems given in parentheses. Detection in TLC was effected by charring with sulfuric acid. Gas chromatographic separations were performed with a Hewlett-Packard 5830 A instrument using a 1220 mm long 2.16 mm ID stainless steel column coated with 10% UCW 982 on 80–100 mehs Gas Chrom Q. The operating conditions were: injection port, 250 °C; flame ionization detector, 300 °C; nitrogen flow rate, 20 ml/min; the column temperature was programmed at 2.5 °C/min starting at 250 °C after 1 min isothermal period.

Benzyl 3,4-*O*-isopropylidene- β -D-galactopyranoside (**2**)

A mixture of 20 g benzyl β -D-galactopyranoside (**1**), anhydrous copper sulfate (60 g) and sulfuric acid (1 ml) in acetone (1.2 l) was shaken for 10 h. The mixture was then filtered, the filtrate neutralized with ammonia and the precipitated ammonium sulfate was removed by filtration on a Celite layer. The filtrate was concentrated and the residue dissolved in chloroform, washed with water and dried (Na_2SO_4). The solution was evaporated and the residue crystallized from ethyl acetate–cyclohexane to yield pure **2** (12.5 g; 54.4%), m.p. 124–125 °C; $[\alpha]_{\text{D}} -3.0$ ($c = 2.57$, CHCl_3); R_f 0.24 (ether–chloroform, 19:1). *Lit.* [26] m.p. 123–124 °C; $[\alpha]_{\text{D}} -1.47^\circ$ ($c = 1.12$, chloroform).

Benzyl 2,6-di-*O*-benzyl-3,4-*O*-isopropylidene- β -D-galactopyranoside (3)

Compound **2** (12 g) was benzylated with benzyl chloride (72 ml) and potassium hydroxide (12 g) at 105 °C for 15 h. The reaction mixture was diluted with chloroform and the resulting solution washed with water until neutral. After the addition of a small amount of sodium hydrogen carbonate, the mixture was steam distilled, the residue was extracted with chloroform, the organic layer washed with water and dried (Na_2SO_4). Evaporation gave 17.25 g (90.9%) of syrupy **3**; $[\alpha]_{\text{D}} + 8.0^\circ$ ($c = 0.84$, chloroform), R_f 0.75 (benzene-methanol, 49:1).

NMR (CDCl_3): δ 7.40–7.00 (m, 15H, aromatic protons), 5.05–3.40 (m, 13H, skeleton protons and 3 Ph- CH_2 -), 1.42 (s, 3H, CH_3), 1.37 (s, 3H, CH_3).

$\text{C}_{30}\text{H}_{34}\text{O}_6$ (490.60). Calcd. C 73.44; H 6.98. Found C 73.50; H 7.05%.

Benzyl 3,4-*O*-isopropylidene-2,6-di-*O*-methyl- β -D-galactopyranoside (4)

A mixture of **2** (2 g), methyl iodide (4.1 ml), silver oxide (4.1 g) and *N,N*-dimethylformamide (10 ml) was stirred for 12 h at room temperature. The reaction mixture was diluted with chloroform, filtered and the filtrate was washed with 1% sodium cyanide solution, then with water and dried (Na_2SO_4). Evaporation left syrupy **4** (2.1 g 96.3%); $[\alpha]_{\text{D}} - 12.1^\circ$ ($c = 1.60$, chloroform), R_f 0.50 (benzene-methanol, 49:1).

$\text{C}_{18}\text{H}_{26}\text{O}_6$ (338.40). Calcd. C 63.88; H 5.36. Found C 64.10; H 5.42%.

Benzyl 2,6-di-*O*-benzyl- β -D-galactopyranoside (5)

A suspension of **3** (8.0 g) in 50% (v/v) acetic acid (200 ml) was heated at 80 °C for 6 h. After evaporation of the mixture 6.7 g (91.2%) of syrupy **5** was obtained. Crystallization from ethanol gave 5.42 g (73.3%), m.p. 107–108 °C, $[\alpha]_{\text{D}} - 17.1^\circ$ ($c = 1.22$, chloroform), R_f 0.54 (benzene-methanol, 9:1).

NMR (CDCl_3): δ 7.40–7.05 (m, 15H, aromatic protons), 5.02–4.56 (m, 6H, 3 Ph- CH_2 -), 4.44 (d, 1H, C_1 -H, $J_{1,2} = 9$ Hz), 3.92–3.40 (m, 6H, skeleton protons), 3.14 (b, 2H, 2-OH).

$\text{C}_{27}\text{H}_{30}\text{O}_6$ (450.51). Calcd. C 71.97; H 6.71. Found C 72.10; H 6.80%.

Benzyl 2,6-di-*O*-methyl- β -D-galactopyranoside (6)

Compound **4** (7.3 g) was hydrolyzed as described above for the preparation of **5**. The syrupy product was crystallized from cyclohexane-ethyl acetate to give **6** (5.65 g; 87.8%), m.p. 77–78 °C, $[\alpha]_{\text{D}} - 49.2^\circ$ ($c = 1.4$, chloroform), R_f 0.31 (benzene-methanol, 9:1).

NMR (CDCl_3): δ 7.40–7.05 (m, 5H, aromatic protons), 4.78 (q, 2H, Ph- CH_2 -), 4.36 (d, 1H, C_1 -H, $J_{1,2} = 8$ Hz), 3.94 (b, 1H, -OH), 3.80–3.10 (m, 7H, skeleton protons and -OH), 3.63 (s, 3H, C_2 -OCH₃), 3.42 (s, 3H, C_6 -OCH₃).

$\text{C}_{15}\text{H}_{22}\text{O}_6$ (298.32). Calcd. C 60.38; H 7.44. Found C 61.00; H 7.50%.

Benzyl 2,6-di-*O*-benzyl-3,4-di-*O*-methyl- β -D-galactopyranoside (7)

A mixture of **5** (1.35 g), methyl iodide (2.7 ml) and silver oxide (2.7 g) in *N,N*-dimethylformamide (10 ml) was stirred. After 20 h additional methyl iodide (0.3 ml) was added to the reaction mixture. Stirring for additional 16 h followed and the reaction mixture was then worked up as described above for the preparation of **4**. Recrystallization of the crude product from cyclohexane-petroleum ether yielded **7** (1.31 g; 91.3%), m.p. 102–103 °C, $[\alpha]_{\text{D}} - 52.7^\circ$ ($c = 1.40$, chloroform), R_f 0.85 (benzene-methanol, 9:1).

NMR (CDCl_3): δ 7.40–7.10 (m, 15H, aromatic protons), 5.00–4.20 (m, 7H, C_1 -H and 3 Ph- CH_2 -), 3.92–3.16 (m, 6H, skeleton protons), 3.60 and 3.56 (2s, 6H, 2-OCH₃).

$\text{C}_{29}\text{H}_{34}\text{O}_6$ (478.58). Calcd. C 72.86; H 7.17. Found C 73.05; H 7.25%.

2,6-Di-*O*-methyl-D-galactose (8)

Compound **4** (0.65 g) was dissolved in 1 *M* sulfuric acid (6 ml) and the solution was heated at 100 °C for 4 h. It was then neutralized with barium carbonate, filtered and the filtrate was concentrated to give crystalline **8** (0.2 g; 50%), m.p. 117–120 °C, $[\alpha]_{\text{D}} + 44.3^\circ \rightarrow + 79.5^\circ$ ($c = 0.88$, water). *Lit.* [42] m.p. 119–120 °C, $[\alpha]_{\text{D}} + 48^\circ \rightarrow 87^\circ$ (water).

3,4-Di-*O*-methyl-*D*-galactopyranose (9)

To a solution of **7** (0.7 g) in ethyl acetate (40 ml) a suspension of 10% Pd/C (0.7 g) in ethyl acetate (15 ml) was added. After hydrogenation for 4 h the catalyst was filtered off and the filtrate concentrated to give **9** (0.25 g; 84%), m.p. 165–166 °C, $[\alpha]_D +91^\circ \rightarrow +116^\circ$ ($c = 1.50$, water). Lit. [43] m.p. 164–166 °C, $[\alpha]_D +95^\circ \rightarrow +117^\circ$ (water).

Benzyl 2,6-di-*O*-benzyl-*exo*- (10) and *endo*-3,4-*O*-benzylidene- β -*D*-galactopyranoside (11)

A mixture of **5** (4.9 g), freshly fused zinc chloride (4.9 g) and benzaldehyde (49 ml) was shaken for 36 h. The reaction mixture was then diluted with chloroform, the resulting solution was washed with water and after the addition of a small amount of sodium hydrogen carbonate the mixture was steam distilled. The residue which solidified on cooling was twice recrystallized from ethanol to obtain the pure *exo*-isomer **10** (1.82 g; 31.1%), m.p. 130–132 °C, $[\alpha]_D +5.6^\circ$ ($c = 0.50$, chloroform), R_f 0.69 (benzene-ether, 4:1).

NMR (CDCl₃): δ 7.30–6.90 (m, 20H, aromatic protons), 5.94 (s, 1H, Ph–CH=), 5.00–3.40 (m, 13H, skeleton protons and 3 Ph–CH₂–).

C₃₄H₃₄O₆ (538.64). Calcd. C 75.90; H 6.37. Found C 76.20; H 6.42%.

The mother liquors of the two recrystallizations were evaporated and the residue was recrystallized from cyclohexane to give the pure *endo*-isomer **11** (1.67 g; 28.5%), m.p. 65–66 °C, $[\alpha]_D +15.9^\circ$ ($c = 1.25$, chloroform), R_f 0.63 (benzene-ether, 4:1).

NMR (CDCl₃): δ 7.50–7.10 (m, 20H, aromatic protons), 5.85 (s, 1H, Ph–CH=), 5.10–3.40 (m, 13H, skeleton protons and 3 Ph–CH₂–).

C₃₄H₃₄O₆ (538.64). Calcd. C 75.80; H 6.37. Found C 75.90; H 6.32%.

Benzyl *exo*- (12) and *endo*-3,4-*O*-benzylidene-2,6-di-*O*-methyl- β -*D*-galactopyranoside (13)

A mixture of **6** (2.65 g), benzaldehyde diethylacetal (1.58 g), *N,N*-dimethylformamide (20 ml) and *p*-toluenesulfonic acid (33 mg) was stirred in vacuum at 75 °C for 5 h. The reaction mixture was then poured into ice-water containing sodium hydrogen carbonate and extracted with chloroform. The organic layer was washed with water, dried (Na₂SO₄) and concentrated. Traces of *N,N*-dimethylformamide were removed by vacuum distillation. The residue obtained was purified by column chromatography on Kieselgel G (100 g) using chloroform–acetone (97:3) for elution. The fractions having R_f 0.66 gave on evaporation and recrystallization from ethanol benzyl *exo*-3,4-*O*-benzylidene-2,6-di-*O*-methyl- β -*D*-galactopyranoside (**12**) (0.7 g; 21.1%), m.p. 96 °C, $[\alpha]_D -20.5^\circ$ ($c = 1.27$, chloroform), R_T 2.98 min.

NMR (CDCl₃): δ 7.55–7.10 (m, 10H, aromatic protons), 6.12 (s, 1H, Ph–CH=), 4.80 (q, 2H, Ph–CH₂–), 4.50–3.20 [m, 13H, 7 skeleton protons and δ 3.61 (s, 3H, C₂–OCH₃), 3.39 (s, 3H, C₆–OCH₃)].

C₂₁H₂₆O₆ (374.25). Calcd. C 67.43; H 7.00. Found C 68.10; H 7.11%.

Evaporation of the fractions having R_f 0.54 gave 665 mg (20%) of syrupy benzyl *endo*-3,4-*O*-benzylidene-2,6-di-*O*-methyl- β -*D*-galactopyranoside (**13**), which was crystallized from ethanol; m.p. 58–60 °C, $[\alpha]_D -22.1^\circ$ ($c = 1.34$, chloroform), R_T 2.65 min.

NMR (CDCl₃): δ 7.65–7.10 (m, 10H, aromatic protons), 5.89 (s, 1H, Ph–CH=), 4.80 (q, 2H, Ph–CH₂–), 4.38 (d, 1H, C₁–H, $J_{1,2} = 8$ Hz), 4.20–3.00 [m, 12H, 6 skeleton protons and δ 3.50 (s, 3H, C₂–OCH₃), 3.40 (s, 3H, C₆–OCH₃)].

C₂₁H₂₆O₆ (374.25). Calcd. C 67.43; H 7.00. Found C 67.90; H 6.98%.

Benzyl 2,3,6-tri-*O*-benzyl- β -*D*-galactopyranoside (14)

To a solution of **10** (1.0 g) in 1:1 ether–dichloromethane (60 ml) 0.4 g of LiAlH₄ was added and the solution was heated to boiling. To the hot solution a solution of AlCl₃ (1.0 g) in ether (10 ml) was added within a period of 1–2 min, and refluxing was continued for an additional 15 min. The mixture was then cooled and diluted with ethyl acetate (2 ml) and water (5 ml) and the organic layer was separated. The aqueous layer was washed with dichloromethane (2 × 50 ml) and the combined organic solution was washed with water (5 × 20 ml). After drying (Na₂SO₄) it was concentrated to give syrupy **14** (0.76 g; 76%), $[\alpha]_D -20^\circ$ ($c = 0.53$, chloroform), R_f 0.71 (benzene-methanol, 95:5).

NMR (CDCl₃): δ 7.40–7.07 (m, 20H, aromatic protons), 5.03–4.35 (m, 9H, C₁–H and 4 Ph–CH₂–), 3.97–3.35 (m, 6H, skeleton protons), 2.71 (s, 1H, –OH).

C₃₄H₃₆O₆ (540.66). Calcd. C 75.62; H 6.72. Found C 76.05; H 6.87%.

Benzyl 2,3,6-tri-*O*-benzyl-4-*O*-methyl- β -D-galactopyranoside (15)

A mixture of **14** (0.6 g), methyl iodide (1.0 ml), silver oxide (1.0 g) and *N,N*-dimethylformamide (10 ml) was stirred for 24 h at room temperature. The reaction mixture was worked up as described above for the preparation of **4**. Recrystallization of the crude product from ethanol yielded **15** (0.56 g; 91%), m.p. 89–90 °C, $[\alpha]_D -37.1^\circ$ ($c = 0.96$, chloroform), R_f 0.78 (benzene–methanol, 49 : 1).

NMR (CDCl_3): δ 7.30–7.00 (m, 20H, aromatic protons), 4.95–4.28 (m, 9H, $\text{C}_1\text{—H}$ and 4 Ph— $\text{CH}_2\text{—}$), 3.84–3.30 [m, 9H, 6 skeleton protons and δ 3.50 (s, 3H, — OCH_3)].

Benzyl 2,4,6-tri-*O*-benzyl- β -D-galactopyranoside (16)

To a mixture of **11** (1.0 g), ether (10 ml) and dichloromethane (15 ml) LiAlH_4 (0.33 g) was added, and the solution was heated to reflux temperature. A solution of AlCl_3 (1.0 g) in ether (5 ml) was then dropwise added over a period of 2 min at 40 °C with stirring. Refluxing was continued for an additional 15 min; during this period the starting material disappeared. After cooling, the excess of the reagent was decomposed by the addition of ethyl acetate and $\text{Al}(\text{OH})_3$ was precipitated by dilution with water. The mixture was diluted with dichloromethane, the organic solution was washed with water, dried (Na_2SO_4) and concentrated to give crystalline **16** (0.82 g; 82%), m.p. 60–63 °C, $[\alpha]_D -20.3^\circ$ ($c = 1.31$, chloroform), R_f 0.76 (benzene–methanol, 19 : 1).

NMR (CDCl_3): δ 7.50–7.20 (m, 20H, aromatic protons), 5.08–4.64 (m, 8H, 4 Ph— $\text{CH}_2\text{—}$), 4.57 (d, 1H, $\text{C}_1\text{—H}$, $J_{1,2} = 8$ Hz), 4.50–3.60 (m, 6H, skeleton protons), 2.32 (b, 1H, — OH). $\text{C}_{33}\text{H}_{36}\text{O}_6$ (540.66). Calcd. C 75.62; H 6.72. Found C 75.45; H 6.80%.

Benzyl 2,4,6-tri-*O*-benzyl-3-*O*-methyl- β -D-galactopyranoside (17)

A solution of **16** (0.6 g) was methylated as described above for the preparation of **15**. Recrystallization of the crude product from ethanol yielded **17** (0.54 g; 87%), m.p. 50–52 °C, $[\alpha]_D -15.1^\circ$ ($c = 1.18$, chloroform), R_f 0.82 (benzene–methanol, 49 : 1).

$\text{C}_{35}\text{H}_{38}\text{O}_6$ (554.68). Calcd. C 75.87; H 6.91. Found C 76.10; H 7.01%.

Benzyl 3-*O*-benzyl-2,6-di-*O*-methyl- β -D-galactopyranoside (18)

To a solution of **12** (0.6 g) in ether–dichloromethane (20 ml) 0.2 g of LiAlH_4 and a solution of AlCl_3 (0.6 g) in ether (5 ml) were added. After standing at room temperature for 15 min, the reaction mixture was worked up as described above for the preparation of **14**. The syrupy product was crystallized from ethanol to give **18** (0.48 g; 80%), m.p. 96–98 °C, $[\alpha]_D -28.2^\circ$ ($c = 0.94$, chloroform), R_f 0.48 (benzene–methanol, 97 : 3).

NMR (CDCl_3): δ 7.58–7.20 (m, 10H, aromatic protons), 5.10–4.54 (2q, 4H, 2 Ph— $\text{CH}_2\text{—}$), 4.36 (d, 1H, $\text{C}_1\text{—H}$, $J_{1,2} = 7.9$ Hz), 3.80–3.20 [m, 12H, 6 skeleton protons and 2 — OCH_3], (δ 3.62; $\text{C}_2\text{—OCH}_3$; δ 3.34; $\text{C}_6\text{—OCH}_3$), 2.56 (d, 1H, OH).

$\text{C}_{22}\text{H}_{28}\text{O}_6$ (388.44). Calcd. C 68.02; H 7.27. Found C 68.30; H 7.35%.

Benzyl 4-*O*-benzyl-2,6-di-*O*-methyl- β -D-galactopyranoside (19)

Compound **13** (130 mg) was dissolved in a 1 : 1 mixture of ether and dichloromethane (6 ml) followed by the addition of LiAlH_4 (26 mg). The solution was treated with a solution of AlCl_3 (90 mg) in ether (2 ml). After 5 min the conversion of **13** was complete and the mixture was worked up according to the procedure described above for the preparation of **16**. Recrystallization of the crystalline **19** resulted in 102 mg (75.6%), m.p. 106–108 °C, $[\alpha]_D -52.1^\circ$ ($c = 0.73$, chloroform), R_f 0.50 (benzene–methanol, 97 : 3).

NMR (CDCl_3): δ 7.42–7.20 (m, 10H, aromatic protons), 5.02–4.76 (2q, 4H, 2 Ph— $\text{CH}_2\text{—}$), 4.34 (d, 1H, $\text{C}_1\text{—H}$, $J_{1,2} = 7.2$ Hz), 3.80–3.20 [m, 12H, 6 skeleton protons and 2 — OCH_3], (δ 3.61; $\text{C}_2\text{—OCH}_3$; δ 3.30; $\text{C}_6\text{—OCH}_3$), 2.52 (d, 1H, OH).

$\text{C}_{22}\text{H}_{28}\text{O}_6$ (388.44). Calcd. C 68.02; H 7.27. Found C 67.85; H 7.21%.

Allyl 6-*O*-benzyl-*exo*- (21) and *endo*-3,4-*O*-benzylidene- α -D-galactopyranoside (22)

Allyl 6-*O*-benzyl- α -D-galactopyranoside (**20**) [39] (5.0 g) was dissolved in *N,N*-dimethylformamide (35 ml) and, after the addition of benzaldehyde dimethylacetal (5 ml) and *p*-toluenesulfonic acid (0.1 g), the mixture was stirred in vacuum at 50 °C. After all the starting material **20** had disappeared (60 min), the mixture was worked up as described above for the benzylidenation of **6**. The syrupy product contained two compounds (TLC) in a ratio of 2 : 1. The mixture was chromatographed on a Kieselgel G column (250 g) using benzene-methanol (24 : 1) for elution.

First the syrupy *endo*-isomer (**22**) was isolated (1.55 g; 24.1%), $[\alpha]_D + 38.6^\circ$ ($c = 1.8$, chloroform), R_f 0.50 (benzene-methanol, 24 : 1).

NMR (CDCl_3): δ 7.60–7.10 (m, 10H, aromatic protons), 6.10–5.70 (m, 1H, $-\text{CH}=\text{}$), 5.82 (s, 1H, $\text{Ph}-\text{CH}=\text{}$), 5.36–5.00 (m, 2H, $=\text{CH}_2$), 4.92 (d, 1H, C_1-H , $J_{1,2} = 3.8$ Hz), 4.59 (s, 2H, $\text{Ph}-\text{CH}_2-$), 4.45–3.64 (m, 8H, 6 skeleton protons and $-\text{CH}_2-$), 2.76 (b, 1H, OH). $\text{C}_{23}\text{H}_{26}\text{O}_6$ (398.44). Calcd. C 69.32; H 6.58. Found C 70.05; H 6.65%.

On continuing the elution, the crystalline *exo*-isomer (**21**) was obtained, which was recrystallized from ethanol to yield 4.28 g (66.7%), m.p. 72–73 °C, $[\alpha]_D + 89.1^\circ$ ($c = 0.51$, chloroform), R_f 0.44 (benzene-methanol, 24 : 1).

NMR (CDCl_3): δ 7.50–7.10 (m, 10H, aromatic protons), 6.16 (s, 1H, $\text{Ph}-\text{CH}=\text{}$), 6.10–5.70 (m, 1H, $-\text{CH}=\text{}$), 5.40–5.08 (m, 2H, $=\text{CH}_2$), 4.99 (d, 1H, C_1-H , $J_{1,2} = 4.1$ Hz), 4.59 (d, 2H, $\text{Ph}-\text{CH}_2$), 4.54–3.60 (m, 8H, 6 skeleton protons and $-\text{CH}_2-$), 2.58 (d, 1H, OH). $\text{C}_{23}\text{H}_{26}\text{O}_6$ (398.44). Calcd. C 69.32; H 6.58. Found C 69.18; H 6.61%.

Allyl 2,6-di-*O*-benzyl-*exo*- (23) and *endo*-3,4-*O*-benzylidene- α -D-galactopyranoside (24)

An isomeric mixture of **21** and **22** (5.0 g) — obtained by the benzylidenation of **20** — was stirred overnight with benzyl chloride (50 ml) and potassium hydroxide (7 g) at 105 °C. The reaction mixture was worked up as described for the preparation of **3**. The resulting syrup was chromatographed on a Kieselgel G column (250 g) using benzene-ethyl acetate (9 : 1) for elution to obtain syrupy **23** and **24**.

For **23** (3.29 g; 53.7%), $[\alpha]_D + 56.7^\circ$ ($c = 0.73$, chloroform), R_f 0.60 (benzene-ethyl acetate, 9 : 1).

NMR (CDCl_3): δ 7.50–7.10 (m, 15H, aromatic protons), 6.16–5.76 (m, 1H, $-\text{CH}=\text{}$), 5.95 (s, 1H, $\text{Ph}-\text{CH}=\text{}$), 5.45–5.10 (m, 2H, $=\text{CH}_2$), 4.93 (d, 1H, C_1-H , $J_{1,2} = 3.6$ Hz), 4.84–3.58 (m, 12H, 6 skeleton protons, 2 $\text{Ph}-\text{CH}_2-$ and $-\text{CH}_2-$).

$\text{C}_{30}\text{H}_{32}\text{O}_6$ (488.56). Calcd. C 73.74; H 6.60. Found C 73.56; H 6.71%.

For **24** (0.92 g; 15%), $[\alpha]_D + 38.3^\circ$ ($c = 0.55$, chloroform), R_f 0.50 (benzene-ethyl acetate, 9 : 1).

NMR (CDCl_3): δ 7.50–7.20 (m, 15H, aromatic protons), 6.08–5.68 (m, 1H, $-\text{CH}=\text{}$), 5.88 (s, 1H, $\text{Ph}-\text{CH}=\text{}$), 5.44–5.08 (m, 2H, $=\text{CH}_2$), 4.81 (d, 1H, C_1-H , $J_{1,2} = 3.7$ Hz), 4.72–3.44 (m, 12H, 6 skeleton protons, 2 $\text{Ph}-\text{CH}_2-$ and $-\text{CH}_2-$).

$\text{C}_{30}\text{H}_{32}\text{O}_6$ (488.56). Calcd. C 73.74; H 6.60. Found C 74.05; H 6.68%.

Allyl 3,6-di-*O*-benzyl- α -D-galactopyranoside (25)

To a solution of **21** (0.5 g) in dichloromethane (25 ml) and ether (15 ml) LiAlH_4 (0.29 g) and a solution of AlCl_3 (0.9 g) in ether (10 ml) were added. After stirring for 1 h at room temperature, the reaction was complete and the mixture was worked up as described above for the preparation of **16**. According to TLC two products had been formed in a ratio of 9 : 1. The main product was isolated on a Kieselgel G column (30 g) using benzene-chloroform-acetone-methanol (8 : 10 : 1 : 1) for elution; 410 mg (81.6%) of syrupy **25** was obtained, $[\alpha]_D + 103.6^\circ$ ($c = 1.42$, chloroform), R_f 0.46 (benzene-chloroform-acetone-methanol, 8 : 10 : 1 : 1).

NMR (CDCl_3): δ 7.42–7.20 (m, 10H, aromatic protons), 6.10–5.70 (m, 1H, $-\text{CH}=\text{}$), 5.40–5.08 (m, 2H, $=\text{CH}_2$), 4.96 (d, 1H, C_1-H , $J_{1,2} = 3.8$ Hz), 4.69 (s, 2H, $\text{Ph}-\text{CH}_2-$), 4.56 (s, 2H, $\text{Ph}-\text{CH}_2-$), 4.20–3.52 (m, 8H, 6 skeleton protons and $-\text{CH}_2-$), 2.72 (b, 1H, OH), 2.34 (d, 1H, OH).

$\text{C}_{23}\text{H}_{28}\text{O}_6$ (400.47). Calcd. C 69.06; H 7.06. Found C 70.10; H 7.10%.

Allyl 4,6-di-*O*-benzyl- α -D-galactopyranoside (26)

Ring cleavage of **22** (0.5 g) was carried out according to the procedure given for the preparation of **25**. The ratio of the two products formed was 4:1 TLC. The main product (**26**) was isolated by column chromatography on Kieselgel G (30 g) as a syrup, (360 mg; 71.6%), $[\alpha]_D +79.9^\circ$ ($c = 1.22$, chloroform), R_f 0.35 (benzene-chloroform-acetone-methanol, 8:10:1:1). The by-product was identical with **25**.

NMR (CDCl_3): δ 7.40–7.20 (m, 10H, aromatic protons), 6.04–5.64 (m, 1H, $-\text{CH}=\text{}$), 5.38–5.08 (m, 2H, $=\text{CH}_2$), 4.82 (d, 1H, C_1-H , $J_{1,2} = 4.0$ Hz), 4.72 (q, 2H, $\text{Ph}-\text{CH}_2-$), 4.48 (q, 2H, $\text{Ph}-\text{CH}_2-$), 4.20–3.62 (m, 8H, 6 skeleton protons and $-\text{CH}_2-$), 2.80 (b, 2H, 2-OH).

$\text{C}_{23}\text{H}_{28}\text{O}_6$ (400.47). Calcd. C 69.06; H 7.06. Found C 69.45; H 6.99%.

Allyl 2,3,6-tri-*O*-benzyl- α -D-galactopyranoside (27)

To a solution of **23** (1.0 g) in dichloromethane (25 ml) and ether (15 ml) 154 mg of LiAlH_4 and a solution of AlCl_3 (538 mg) in ether (10 ml) were added. The mixture was stirred at 20°C for 5 min; during this period the reaction was complete. After working up — using the procedure described for **16** — two products were detected by TLC in a ratio of 95:5. The main product was purified on Kieselgel G (30 g) to obtain pure **27** (930 mg; 92.6%), $[\alpha]_D +55.4^\circ$; $[\alpha]_{436} +104.6^\circ$ ($c = 1.60$, chloroform), R_f 0.73 (chloroform-acetone, 19:1). Lit. [53] syrup, $[\alpha]_D +52.8^\circ$, $[\alpha]_{436} +99.7^\circ$ ($c = 1.0$, chloroform).

NMR (CDCl_3): δ 7.42–7.20 (m, 15H, aromatic protons), 6.08–5.68 (m, 1H, $-\text{CH}=\text{}$), 5.40–5.08 (m, 2H, $=\text{CH}_2$), 4.90 (d, 1H, C_1-H), 4.80–4.40 (3q, 6H, 3 $\text{Ph}-\text{CH}_2-$), 4.20–3.48 (m, 8H, 6 skeleton protons and $-\text{CH}_2-$), 2.40 (b, 1H, OH).

$\text{C}_{30}\text{H}_{34}\text{O}_6$ (490.60). Calcd. C 73.53; H 6.99. Found C 74.05; H 7.02%.

Allyl 2,4,6-tri-*O*-benzyl- α -D-galactopyranoside (28)

A solution of **24** (750 mg) in dichloromethane-ether (2:1) was hydrogenolyzed, as described for the preparation of **27**, using LiAlH_4 (116 mg) and 404 mg of AlCl_3 in ether (10 ml). The reaction was complete in 15 min, and besides the main product 5% of **27** was formed (TLC). Purification of the main product was carried out using column chromatography with chloroform-acetone (19:1) for elution to obtain crystalline **28** (680 mg; 90.3%), Recrystallization from ether-hexane gave m.p. 67°C . $[\alpha]_D +61.8^\circ$, $[\alpha]_{436} +117.2^\circ$ ($c = 0.71$, chloroform), R_f 0.55 (chloroform-acetone, 19:1). Lit. [54] m.p. $67-68^\circ\text{C}$, $[\alpha]_D +62.3^\circ$, $[\alpha]_{436} +122.5^\circ$ ($c = 0.81$, chloroform).

NMR (CDCl_3): δ 7.46–7.08 (m, 15H, aromatic protons), 6.02–5.62 (m, 1H, $-\text{CH}=\text{}$), 5.40–5.06 (m, 2H, $=\text{CH}_2$), 4.82 (d, 1H, C_1-H), 4.72–4.52 (3q, 6H, 3 $\text{Ph}-\text{CH}_2-$), 4.20–3.44 (m, 8H, 6 skeleton protons and $-\text{CH}_2-$), 2.60 (b, 1H, OH).

$\text{C}_{30}\text{H}_{34}\text{O}_6$ (490.60). Calcd. C 73.53; H 6.99. Found C 73.48; H 6.78%.

REFERENCES

- [1] McCLOSKEY, C. M.: *Advan. Carbohydr. Chem.*, **12**, 137 (1957)
- [2] HANESSIAN, S.: *Carbohydr. Res.*, **2**, 86 (1966)
- [3] FAJLA, D. L., HULLAR, T. L., SISKIN, S. B.: *Chem. Commun.*, **1966**, 716
- [4] DESLONGCHAMPS, P., MOREAU, C., FREHEL, D., CHENEVERT, R.: *Can. J. Chem.*, **53**, 1204 (1975)
- [5] COLLINS, P. M., OPARAECHÉ, N. N.: *Carbohydr. Res.*, **33**, 35 (1974)
- [6] KLEMER, A., RODEMEYER, G.: *Chem. Ber.*, **107**, 2612 (1974)
- [7] BHATTACHARJEE, S. S., GORIN, P. A. J.: *Can. J. Chem.*, **47**, 1195 (1969)
- [8] BHATTACHARJEE, S. S., GORIN, P. A. J.: *Can. J. Chem.*, **47**, 1207 (1969)
- [9] GORIN, P. A. J., FINLAYSON, A. J.: *Carbohydr. Res.*, **18**, 269 (1971)
- [10] GORIN, P. A. J.: *Carbohydr. Res.*, **18**, 281 (1971)
- [11] NÁNÁSI, P., LIPTÁK, A.: *Magyar Kém. Folyóirat*, **80**, 217 (1974)
- [12] LIPTÁK, A., JODÁL, I., NÁNÁSI, P.: *Carbohydr. Res.*, **44**, 1 (1975)
- [13] LIPTÁK, A., PEKÁR, F., JÁNOSY, L., JODÁL, I., FÜGEDI, P., HARANGI, J., NÁNÁSI, P., SZEJTLI, J.: *Acta Chim. Acad. Sci. Hung.* (In the press)

- [14] NÁNÁSI, P., LIPTÁK, A., JÁNOSY, L.: *Acta Chim. (Budapest)* **88**, 155 (1976)
- [15] LIPTÁK, A., JODÁL, I., NÁNÁSI, P.: *Carbohydr. Res.*, **52**, 17 (1976)
- [16] LIPTÁK, A., NÁNÁSI, P.: *Tetrahedron Letters*, **1977**, 921
- [17] JONIÁK, D., KOSIKOVÁ, B., KOSÁKOVÁ, L.: *Coll. Czech. Chem. Commun.*, **43**, 769 (1978)
- [18] LIPTÁK, A.: *Tetrahedron Letters*, **1976**, 3551
- [19] LIPTÁK, A., FÜGEDI, P., NÁNÁSI, P.: *Carbohydr. Res. (In the press)*
- [20] LIPTÁK, A.: *Carbohydr. Res. (In the press)*
- [21] LIPTÁK, A., BOBÁK, A., NÁNÁSI, P.: *Acta Chim. (Budapest)* **94**, 261 (1977)
- [22] LIPTÁK, A., CZÉGÉNY, I., HARANGI, J., NÁNÁSI, P.: *Carbohydr. Res. (In the press)*
- [23] KABAT, E. A. in *Blood and Tissue Antigens* (Ed. D. AMINOFF), p. 187. Academic Press, Inc., New York 1970
- [24] HAINES, T. H.: *Progr. Chem. Fats and Lipids*, **11**, 297 (1971)
- [25] WIEGANDT, H.: *Angew. Chem. Internat. Edn.*, **7**, 87 (1968)
- [26] STOFFYN, A., STOFFYN, P.: *J. Org. Chem.*, **32**, 4001 (1967)
- [27] GENT, P. A., GIGG, R.: *J. Chem. Soc. Perkin I*, **1974**, 1446
- [28] SCHNEIDER, J., LEE, Y. C., FLOWERS, H. M.: *Carbohydr. Res.*, **36**, 159 (1974)
- [29] LIPTÁK, A., FÜGEDI, P., NÁNÁSI, P.: *Carbohydr. Res. (In the press)*
- [30] ROLLIN, P., SINAY, P.: *C. R. Acad. Sci. Paris, Ser. C*, **284**, 65 (1977)
- [31] DAVID, S., JOHNSON, C. A., VEYRIERES, A.: *Carbohydr. Res.*, **28**, 121 (1973)
- [32] LUBINEAU, A., THIEFFRY, A., VEYRIERES, A.: *Carbohydr. Res.*, **46**, 143 (1976)
- [33] GENT, P. A., GIGG, R., CONANT, J. *Chem. Soc. Perkin I*, **1972**, 1535
- [34] FLOWERS, H. M.: *Carbohydr. Res.*, **39**, 245 (1975)
- [35] GENT, P. A., GIGG, R.: *J. Chem. Soc. Perkin I*, **1975**, 361
- [36] JACQUINET, J. C., SINAY, P.: *Tetrahedron*, **32**, 1693 (1976)
- [37] STANEK, J., SELE, A., JAQUES, R., ROSSI, A.: *Helv. Chim. Acta*, **55**, 434 (1972)
- [38] HELFERICH, B., PORCK, A.: *Ann.*, **586**, 239 (1954)
- [39] GIGG, J., GIGG, R.: *J. Chem. Soc. C*, **1966**, 82
- [40] ZEMPLÉN, G., CSÜRÖS, Z., ANGYAL, S.: *Ber.*, **70**, 1848 (1937)
- [41] KUHN, R., TRISCHMANN, H., LÖW, I.: *Angew. Chem.*, **67**, 32 (1955)
- [42] DEWAR, E. T., PERCIVAL, E. G. V.: *J. Chem. Soc.*, **1947**, 1622
- [43] BACON, J. S., BELL, D. J.: *J. Chem. Soc.*, **1939**, 1869
- [44] BAGGETT, N., BUCK, K. W., FOSTER, A. B., WEBBER, J. M.: *J. Chem. Soc.*, **1965**, 3401
- [45] EVANS, H. E.: *Carbohydr. Res.*, **21**, 473 (1972)
- [46] HARANGI, J., LIPTÁK, A.: *J. Chromatogr.*, **147**, 401 (1978)
- [47] CUNNINGHAM, J., GIGG, R., WARREN, C. D.: *Tetrahedron Letters*, **1964**, 1191
- [48] GENT, P. A., GIGG, R.: *J. C. S. Chem. Commun.*, **1974**, 277
- [49] BOSS, R., SCHEFFOLD, R.: *Angew. Chem. Internat. Edn.*, **15**, 558 (1976)
- [50] GENT, P. A., GIGG, R.: *J. Chem. Soc. Perkin I*, **1974**, 1835
- [51] RANKIN, J. C., JEANES, A.: *J. Am. Chem. Soc.*, **76**, 4435 (1954)
- [52] HALSALL, T. G., HIRST, E. L., JONES, J. K. N.: *J. Chem. Soc.*, **1947**, 1427
- [53] NASHED, M. A., ANDERSON, L.: *Carbohydr. Res.*, **56**, 325 (1977)
- [54] NASHED, M. A., ANDERSON, L.: *Carbohydr. Res.*, **51**, 65 (1976)
- [55] NESZMÉLYI, A., LIPTÁK, A., NÁNÁSI, P.: *Carbohydr. Res.*, **58**, C7 (1977)

András LIPTÁK

Loránt JÁNOSY

János IMRE

Pál NÁNÁSI

H-4010 Debrecen, POB 55.

PHOTOASSISTED ELECTROLYSIS OF WATER BY SEMICONDUCTOR ELECTRODES

T. PAJKOSSY,¹ I. MOLNÁR,² M. PÁLFI,² and R. SCHILLER¹

(¹Central Research Institute for Physics, Budapest,

²Research Institute for Electric Industry, Budapest)

Received July 11, 1978

Accepted for publication September 1, 1978

The effect of illumination of semiconductor electrodes in water electrolysis was studied. Semiconducting substances *n*-type CdS, *n*- and *p*-type CdTe and *n*-type iron oxide were investigated as potential photoactive electrodes. On measuring their voltammetric behaviour as a function of electrolyte composition, both illuminated and in the dark, an increase in current and a shift in the current-voltage curve due to incident light was observed. The effects of intensity and wave length of light and the stability of electrodes were determined. CdS and CdTe became rapidly corroded whereas iron oxide proved to be a stable photoanode in water electrolysis. Its efficiency of transforming white light into electricity is about 1%.

Introduction

The electrochemistry of semiconductors was fathered by semiconductor technology. The electrochemical treatment of semiconducting substances used to be an integral part of device-making processes. It was only in the early seventies that a new phenomenon in semiconductor electrochemistry was observed which might be of practical importance outside the realm of the semiconductor industry.

The observation made by FUJISHIMA and HONDA [1] was the following. An *n*-type semiconducting wafer of crystalline TiO₂ was immersed in an aqueous solution and was shorted to a platinized platinum electrode through a resistor. Upon illumination of the TiO₂ surface, evolution of oxygen and simultaneous evolution of hydrogen at the platinum electrode were observed. The process was accompanied by electric current in the external circuit. Apparently the importance of this process was realized only around 1975. The research started then was greatly stimulated by the practical prospect of producing hydrogen from water using the radiant energy of the sun.

It would be far beyond the scope of this paper to summarize the advantages of hydrogen as a substance for storage and transportation on energy. Excellent, detailed reviews are at the disposal of the interested reader [2]. It should be stated only that hydrogen, produced either thermally or electrolytically, seems to be the most economical medium for storing the energy of highly concentrated primary sources, be it a high temperature nuclear reactor or the sun. Gaseous or liquefied hydrogen or metal hydrides may all qualify

to this end. The unlimited reserves of water and the ecological advantage of burning pure hydrogen which, instead of poisonous pollutants, produces potable water are strong arguments in favour of using this substance.

The light-assisted electrolysis of water, discovered by FUJISHIMA and HONDA, is obviously not the only alternative of solar energy conversion. Heat collecting systems utilize radiant energy as thermal energy. Semiconductor solar cells convert light directly into electricity. Limiting this Introduction to electrochemical means of solar energy conversion, one has to deal with two separate classes of methods [3]. *Photogalvanic cells* are constructed in such a

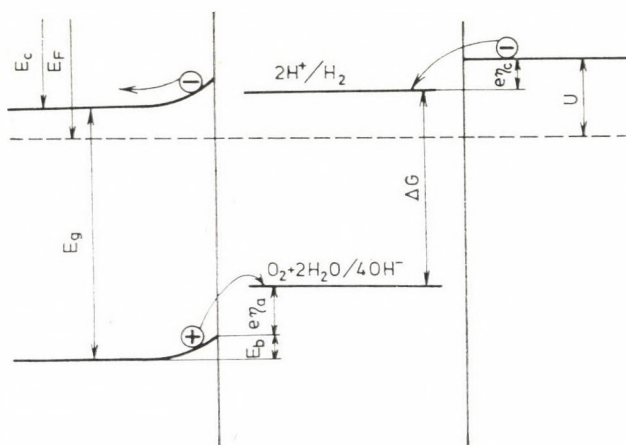


Fig. 1. Energy level scheme of a semiconductor-electrolyte-metal system (see text)

way that light, absorbed in a homogeneous electrolyte solution, brings about energetic products which in turn lose their energy to electrodes immersed in the solution. As a result of this, electricity flows in the external circuit, while the products of the photochemical transformation return to their initial state. The drawback of this method is the inherently low efficiency [4]. Reverse reactions cannot be impeded in a homogeneous solution thus energetic products might easily re-form without producing electric current.

Photovoltaic cells, the archetype of which is the above-mentioned TiO_2 cell, eliminate this disadvantage since light absorption and primary energy conversion proceeds in the electrode near the solid/liquid interface. The working principle of such a cell is rather similar to that of the widely used semiconductor solar cells. When a semiconducting substance is immersed in an electrolyte, a rectifying space-charge zone immediately forms along the interface. In other words, the energy bands of the semiconductor are distorted near the surface, the phenomenon of band bending takes place (Fig. 1). Incident light is absorbed by the semiconductor only if $h\nu$ is larger than the bandgap, E_g .

In this case an electron-hole pair is created which, experiencing the electric field of the space-charge layer, becomes separated. With *n*-type semiconductors, the electron moves toward the bulk of the solid, whereas the hole enters the liquid phase. Hence, oxidation takes place around the the semiconductor and the electron, having travelled to the counter-electrode *via* the external circuit, brings about reduction.

Using a *p*-type semiconductor, the reverse process takes place; electrons are injected from the semiconductor surface into water, thus reduction proceeds around the semiconductor, whereas the site of compensating oxidation processes is the surface of the counter-electrode.

Photovoltaic cells are essentially free of the reverse processes mentioned in connection with photogalvanic cells. Their construction is much simpler than that of the solid state solar cells since the rectifying barrier forms spontaneously upon immersion of the semiconductor into the solution. The desired energy carrier, hydrogen, develops directly without further transformation of electricity into chemical energy.

Photovoltaic cells may be of even more general use than water electrolysis. A number of oxidation—reduction processes can take place at the illuminated semiconductor electrode. Some workers are of the opinion that for example couples like $\text{Fe}^{2+}/\text{Fe}^{3+}$, S/S^{2-} or Cl_2/Cl^- might also be used for the practical purpose of energy transformation [5].

The relationship between the bandgap of the semiconductor E_g , the applied external voltage U , and the Gibbs free energy change of the oxidation—reduction process ΔG , is the following [6]

$$\Delta G = E_g + eU - E_b - e(IR + \eta_c + \eta_a) - (E_c - E_F)$$

where e is the elementary charge: IR the ohmic loss of the cell: η_c and η_a are the cathodic and anodic overvoltages, respectively: E_c is the bottom of the conductivity band: E_F the Fermi energy and E_b the electron energy difference between the bulk and the surface of the semiconductor, *i.e.* the extent of band bending (*cf.* Fig. 1).

An estimate can be made on the basis of this energy scheme for the relationship between bandgap and photovoltage U_p . Taking realistic values, one finds approximately [6b]

$$E_g \cong eU_p + 1 \text{ eV}$$

This means that the photovoltage is about 1 V less than the bandgap of the semiconductor. A photoelectrochemical cell for water electrolysis working without any external voltage must exhibit a voltage due to illumination $U_p \geq 1.23 \text{ V}$, thus the bandgap must be at least 2.23 eV, hence the wavelength of the light absorbed is $\lambda \leq 550 \text{ nm}$. This situation can be improved,

i.e. higher wave length light can also be utilized if the cell is made of an *n*-type photoanode and a *p*-type photocathode [7]. The photovoltages of the two electrodes add up with such an arrangement.

Hence only large bandgap semiconductors are worth considering as potential electrodes for the photoassisted electrolysis of water. This is, however, only a necessary but not sufficient condition a substance must fulfil. It must also be of considerable stability in aqueous solutions, corrosion must be as slow as possible under the conditions of photoelectrolysis. The two requirements are rather difficult to meet simultaneously and this seems to be one of the main obstacles to the practical application of the method for the time being [6h].

A number of compound semiconductors have been investigated in the last few years. TiO_2 was the first and most thoroughly studied substance [8]. The illumination of an *n*-type TiO_2 anode decreases the equilibrium potential of water decomposition by about one volt. The effect is marked, the substance stable but only UV light, $\lambda \leq 350$ nm, produces a photoeffect. This shows that TiO_2 has a bandgap too wide for a good solar energy economy. Substances of narrower bandgap, *i.e.* with an optical absorption in the visible region need to be sought. CdS exhibits rather attractive optical properties: it is known to behave as a good hole-injector [9] but its drawback is low stability — particularly under illumination [10]. To overcome this difficulty, so-called regenerative cells were suggested [11] in which the species oxidized at the anode is reduced at the cathode. Bi_2S_3 and particularly MoS_2 have good optical properties and considerable stability against corrosion [12].

Substances like SnO_2 [13], SrTiO_3 [14], KTaO_3 [15], GaP [16], ZnTe, CdTe, GaAs, InP, SiC, Si [17], Nb_2O_3 , Al_2O_3 , Si_3N_4 [18], Fe_2O_3 [19], WO_3 [20], have also been studied and found to exhibit photoelectrochemical activity. The equilibrium voltage of water decomposition decreased on illumination but an external voltage was always needed to decompose water. Photovoltage alone has never been found to be sufficient to cause water electrolysis.

In the present paper we summarize our preliminary results on photoassisted water electrolysis and some related phenomena. Three substances were chosen: *n*-type CdS produced by evaporation, *n*-type and *p*-type crystalline CdTe and *n*-type iron oxide grown by thermal oxidation. CdS, a comparatively well-described substance, served rather the standardization of our methods. CdTe being available in the form of crystalline samples with dopings of different extent promised the possibility to describe the effect of semiconductor properties in some detail. Iron oxide as a comparatively stable and extremely cheap substance was selected with a view to practical application.

Experimental

Equipment. High pressure Xe lamps of 150 W and 1600 W produced by Tungsram were used. Light was monochromatized either by Zeiss metal interference filters of 5 nm bandwidth or by a SPEX Minimate monochromator, its intensity was controlled by grey filters, measured by a GEandG photometer. Voltammetric curves were taken by a Radelkis OH 404 laboratory potentiostat using saturated calomel electrodes. Some recordings were made by a Hewlett-Packard 70058 type X-Y recorder.

Solutions. Solutions of different acidity were made of a 1/15 molar phosphate buffer. By altering the H^+/K^+ cation ratio, all pH values between 1.5 and 12.5 could be attained, keeping the ionic strength constant. The solutions were usually electrolyzed prior to measurements and bubbled with purified nitrogen gas.

Electrodes. CdS: The semiconducting material was made by vacuum deposition. A thin glass plate was first covered with titanium then with silver. CdS, deposited on top of the silver layer, was of orange-red colour and of a thickness of about 50 μm . A window was opened on the CdS layer near the rim of the plate in order to make an ohmic contact by soldering a piece of copper wire to the bare silver surface. All the metal parts were insulated with varnish. The apparent area of the free CdS surface was 0.5 cm^2 .

CdTe: Both *p*- and *n*-type crystalline materials were available with low and high specific resistivities, viz. for *p*-type samples 1.5×10^4 and 0.3–0.7 Ωcm ; for *n*-type samples 7.4×10^5 and 20 Ωcm . The ingots were cut into slices of about $4 \times 5 \times 1$ mm. Ohmic contacts were made as follows [21]. The slices were immersed in hot concentrated NaOH solution for 30 sec, in dilute NaOH solution for another 30 sec and were then rinsed with hot distilled water and dried. The contact to the *p*-type sample was made by dropping a concentrated $HAuCl_4$ solution on the desired spot, drying and keeping the sample at 200 $^\circ C$ for 10 min. A copper wire was fixed to the gold spot formed using a silver epoxy resin. For making contacts to *n*-type samples a small droplet of 0.1 M $LiNO_3$ solution was brought on to the surface, the water evaporated and the sample heated in hydrogen stream until the $LiNO_3$ melted (≈ 300 $^\circ C$) and it was then kept for 30 min at the final temperature. After cooling the wafer, was rinsed with distilled water and the contact was formed using $HAuCl_4$ as described above. Before measurement all metal parts and the rear of the wafer were insulated with epoxy resin.

Iron oxide: Spectral grade iron and carbon steel was used. The surface was polished, washed with distilled water and dried. The sample was then put into an oven and heated in air at 300 $^\circ C$ for 10 min, at 650 $^\circ C$ for 20 to 120 min, and again at 300 $^\circ C$ for 10 min. At the end of the process a dark grey, compact oxide layer formed. Carbon steel was usually oxidized for not longer than 30 min, spectral grade iron required longer treatment. Etching with hydrochloric acid prior to oxidation had an unsatisfactory effect. The heating at lower temperatures before and after the oxidation proved to be essential for the oxide layer to be compact and adherent. One side of the sample was freed of the oxide in order to make a metallic contact. This side was insulated with varnish. The illuminated apparent surface was 0.5 cm^2 .

Results and Discussion

The direct method of studying photoelectrochemical processes is the determination of the voltammetric behaviour of the electrodes as a function of illumination.

CdS

A characteristic voltammetric curve is given in Fig. 2. Being *n*-type semiconductors, all our CdS samples produced only anodic photoeffect in accordance with expectations. The dark current is rather low in the region where the photocurrent reaches already the range of 1 mA. The photocurrent corrected for the dark current j' , is a linear function of light intensity I , the double logarithmic plot yieldings a straight line of unit slope (Fig. 3).

The photocurrent is influenced by the presence of neutral salts (Fig. 4). If the KCl or KNO_3 concentration is increased, it gradually increases, the highest rate of change being in the 10^{-3} – 10^{-2} M range. Acidity has a rather marked effect, the photocurrent increases with decreasing pH (Fig. 5).

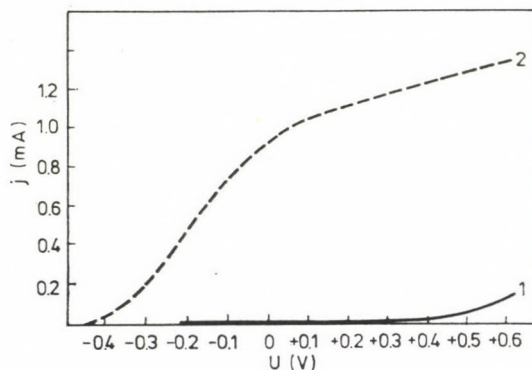


Fig. 2. Voltammetric curves (S.C.E.) of evaporated CdS; (1): dark, (2): illuminated, pH 8.4

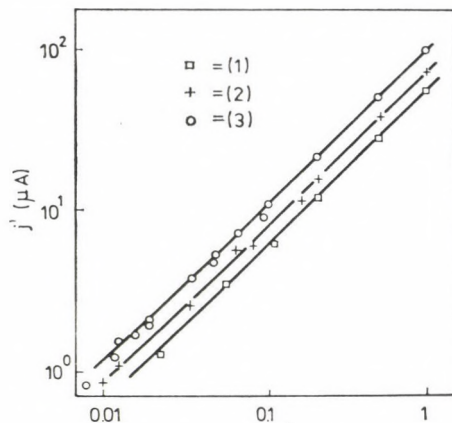


Fig. 3. Photocurrent as a function of light intensity (arbitrary units) measured on CdS, pH 8.4; (1): -0.3 V, (2): 0.0 V, (3): $+0.3$ V (S.C.E.)

The spectral response is advantageous since a good part of the visible spectrum causes a measurable photocurrent (Fig. 6). This fact, in accordance with literature data [9], lends some hope to the practical application of CdS. The efficiency of transformation of light to electric energy is about 0.5% relative to the white light of the Xe lamp. This value is somewhat lower than that obtained with CdS single crystals.

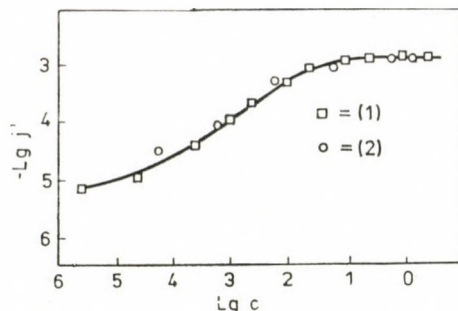


Fig. 4. Photocurrent as a function of total ion concentration measured on CdS, pH 8.4, $U = +0.3$ V (S.C.E.); (1): KNO_3 , (2): KCl

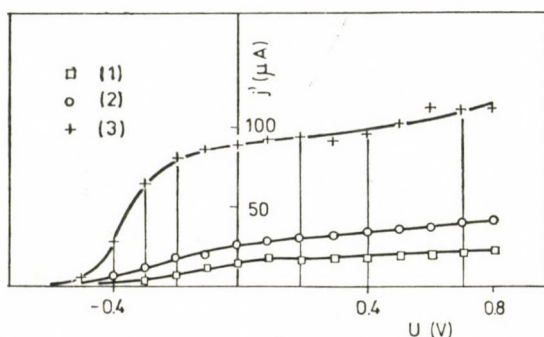


Fig. 5. Voltammetric curves (S.C.E.) of illuminated CdS at different acidities; (1): pH 11.8, (2): pH 7.2, (3): pH 2.1

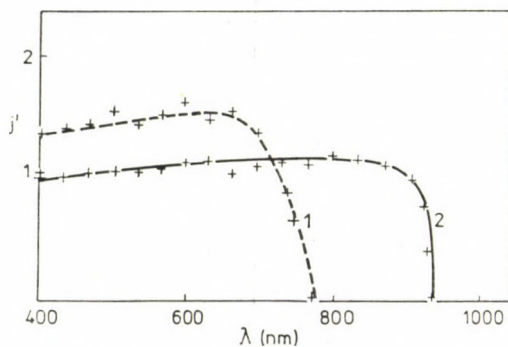


Fig. 6. Spectral distribution of photocurrent normalized to lamp spectrum measured on CdS (1) and CdTe (2), current in arbitrary units

Unfortunately the low stability of this substance particularly under illumination and anodic polarization is a strong argument against practical use. Figure 7 shows the rapid decrease of the photoeffect. Soaking of the electrodes in carbon disulphide after use restores the photoactivity almost completely.

This fact, however, together with a visually observable sulphur layer over illuminated surfaces proves that the photocurrent is due to CdS corrosion (*cf.* Ref. 10). Sulphur precipitation can be prevented by dissolving Na_2S but the increasingly brownish colour of the solution indicates the formation of polysulphide ions. Hence one has to state that despite its attractive optical properties CdS cannot serve as a stable photoanode in photoelectrolysis.

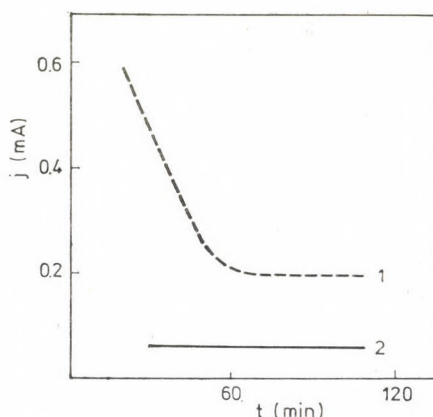


Fig. 7. Ageing of a CdS electrode, pH 8.4, $U = +0.3$ V (S.C.E.); (1): illuminated, (2): dark

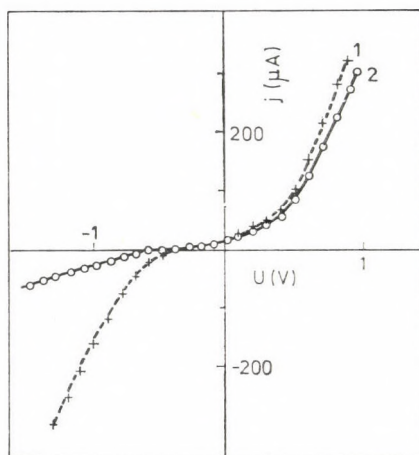


Fig. 8. Voltammetric curves (S.C.E.) of high conductivity *p*-type CdTe, pH 7.2; (1): illuminated, (2): dark

CdTe

Typical voltammetric curves are given in Figs 8–10. A new effect can be observed here. Contrary to expectations, both the *n*- and *p*-type material exhibit anodic as well as cathodic photoeffect. In the case of the high conduc-

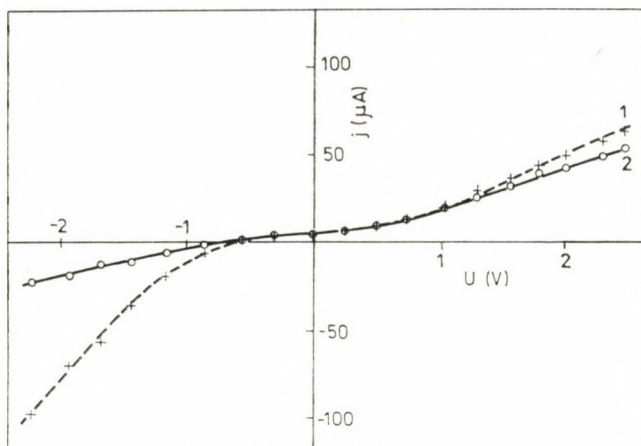


Fig. 9. Voltammetric curves (S.C.E.) of low conductivity *p*-type CdTe, pH 7.2; (1): illuminated, (2): dark

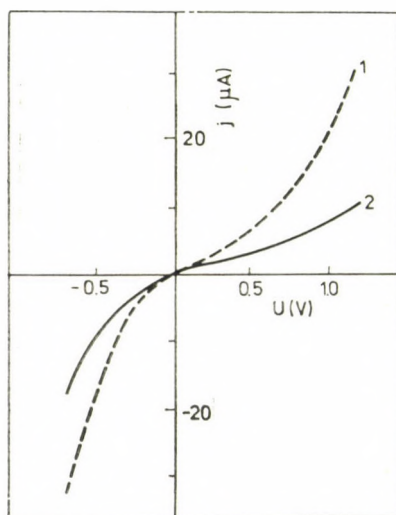


Fig. 10. Photocurrent against potential (S.C.E.) of high conductivity *n*-type CdTe, pH 7.2; (1): illuminated, (2): dark

tivity *n*-type sample, even the extents of the photocurrents of opposite polarity are commensurate. The reason for this phenomenon, which has not been described previously, is not yet clear. Such a behaviour is likely to be expected on the surface of intrinsic semiconductors, where the sign of band bending can easily be altered by changing electrode polarization (See Fig. 1 and Ref. 6a). The anodic and cathodic curves are, however, most symmetric with a highly doped electrode. The understanding of this observation requires further

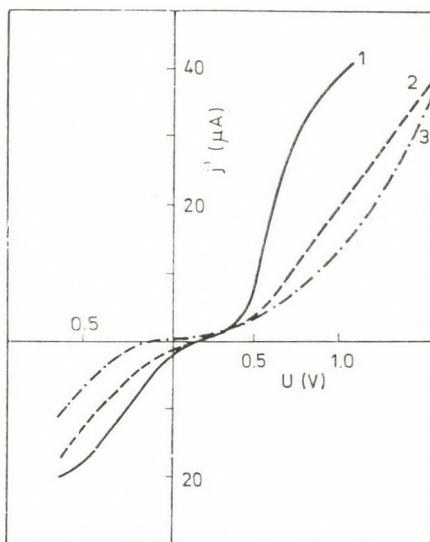


Fig. 11. Photocurrent against potential of illuminated high conductivity *n*-type CdTe at different acidities, pH 2.1 (1), pH 7.2 (2), pH 11.8 (3)

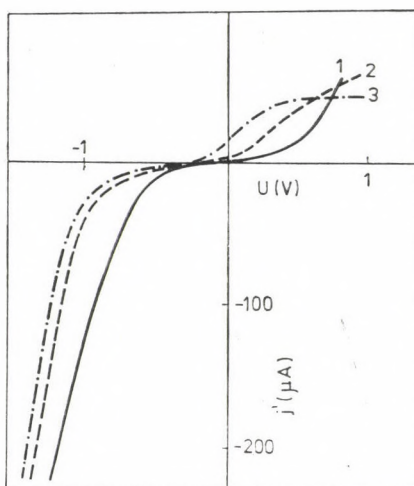


Fig. 12. Voltammetric curves (S.C.E.) of illuminated, high conductivity *p*-type CdTe at different acidities, pH 2.1 (1), pH 7.2 (2), pH 11.8 (3)

studies particularly regarding band bending (*i.e.* measurement of flat band potentials).

The pH effect for *n*-type CdTe is similar to that for *n*-type CdS, increasing acidity increases the photocurrent (Fig. 11). With *p*-type CdTe, the opposite rule is found; an increase in hydrogen ion concentration decreases the photo-effect (Fig. 12).

The spectral distribution of photocurrent extends over an even wider range than that of CdS (Fig. 6). The stability of CdTe is somewhat higher than was found with CdS. The possibility of constructing an electrolyzing cell comprising an *n*-type CdTe anode and a *p*-type cathode is a possibility. Here, however, other factors must also be taken into account. Beyond their photoactivity, electrodes must also exhibit high exchange currents in order to become compatible with traditional electrode materials.

Iron oxide

Our attention has been attracted to iron oxide as stable photoelectrode by the work of YEH and HACKERMAN [19]. Iron oxide shows only an anodic photoeffect regardless of the composition of the iron sheet to be oxidized or to

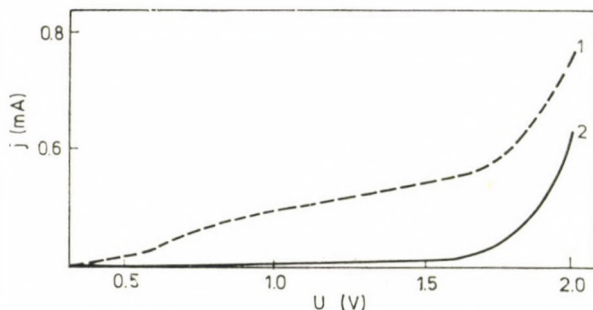


Fig. 13. Voltammetric curves (S.C.E.) of iron oxide (spectral grade iron, 105-min oxidation), pH 8.4; (1): illuminated, (2): dark

the duration of oxidation. A typical current-voltage curve is given in Fig. 13. The low dark current, which changes only slightly with voltage, shows the oxide coating to be compact and of high resistivity. The photocurrent corrected for dark current is proportional to the light intensity (Fig. 14).

The spectral response is given in Fig. 15. The $(\text{photocurrent})^{1/2}$ vs. frequency plot was chosen with reference to FOWLER theory of photoemission [22]. Although we are not convinced that this theory, developed for pure metal surfaces, is strictly valid for the present case, the plot proves to be a good practical implement for the determination of the limiting wave length. As computed from the intercept of the curve with the frequency axis, the highest wave length which produces a photoeffect is about 680 nm. Photoresponse covers a good part of the visible spectrum.

Photocurrent is not accompanied by the dissolution of the anode: at voltages where photocurrents are considerable, oxygen evolution at the photoanode and hydrogen evolution at the platinum counter-electrode can be observed. When illumination ceases, the gas evolution stops.

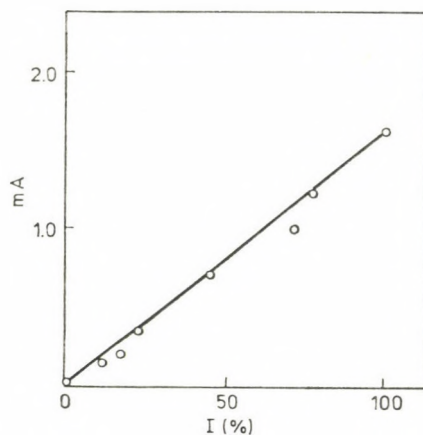


Fig. 14. Dependence of photocurrent on the relative light intensity measured on iron oxide (carbon steel, 20-min oxidation), pH 8.4, $U = 1.6$ V (S.C.E.)

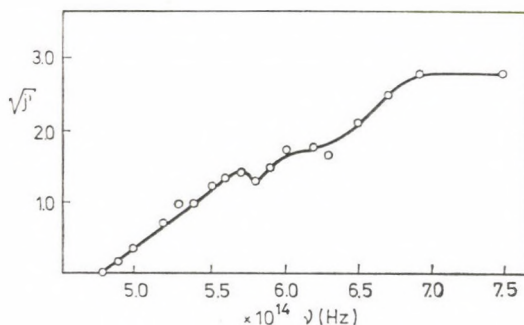


Fig. 15. Square root of photocurrent normalized to lamp spectrum measured on iron oxide (spectral grade iron, 45-min oxidation) as a function of frequency, pH 8.4, $U = 1.2$ V (S.C.E.)

The efficiency of light energy conversion relative to the white light of the Xe lamp is about 1%. This value does not change too markedly with experimental conditions.

Conclusions

The compound semiconductors CdS, CdTe and iron oxide exhibit a photoactivity in electrochemical processes absorbing light and producing photocurrent in a broad region of the visible spectrum. Being rather unstable, CdS effects hydrogen evolution at the expense of its anodic oxidation. CdTe is of anomalous behaviour since both *n*- and *p*-type materials show anodic and cathodic photoeffects. Iron oxide grown by thermal oxidation can serve as a

stable photoanode suitable for the true photoelectrolysis of water. The efficiency of this last process is about 1%.

*

The authors express their gratitude to Mr. G. PALOTAY, Dr. A. LUTTER and Mr. J. MANDICS for their help in producing the electrodes, to Dr. E. LENDVAI for a loan of CdTe ingots and to Mrs. Á. HORVÁTH for her assistance in the measurements.

REFERENCES

- [1] FUJISHIMA, A., HONDA, K.: *Nature*, **238**, 37 (1972)
- [2] a) BOCKRIS, J. O'M.: *Energy: The Solar-Hydrogen Alternative*. Architecture Press, London 1975, b) LEGASOV, V. A., et al.: *Atomno-vodorodnaya energetika*, Kurchatov Institute, Moscow 1976, c) MARCHETTI, C.: *CEER*, p. 7. January 1973, d) MCAULIFFE, C. A.: *Chem. Brit.*, **13**, 559 (1977)
- [3] a) GERISCHER, H.: *Ber. Bunsenges. Phys. Chem.*, **23**, 503 (1975), b) ARCHER, M. D.: *J. Appl. Electrochem.*, **5**, 17 (1975)
- [4] a) LICHTIN, N. N.: *ERDA Abstr.*, **1** (No. 2), 1136 (1976), b) TIEN, H. T., MOUNTZ, J. M.: *Energy Res.*, **2**, 197 (1978)
- [5] GERISCHER, H.: *J. Electroanal. Chem. Interface Electrochem.*, **58**, 236 (1975)
- [6] a) GERISCHER, H.: in EYRING, H., HENDERSON, D., JOST, W.: *Physical Chemistry*, Vol. IXA, p. 463. Academic Press, New York 1970, b) MANASSEN, I., CAHEN, D., HODES, G., SOFER A.: *Nature*, **263**, 97 (1976), c) NOZIK, A. H.: *Nature*, **257**, 383 (1975), d) NOZIK, A. J.: *Proc. Int. World Hydrogen Energy Conf.*, Vol. II, 5B-31. Miami Beach 1976, e) BOLTS, J. M., WRIGHTON, M. S.: *J. Phys. Chem.*, **80**, 2641 (1976), f) PETER, L.: *Nature*, **273**, 490 (1978), g) BOCKRIS, J. O'M., UOSAKI, K.: *J. Electrochem. Soc.*, **125**, 223 (1978), h) BARD, A. J., WRIGHTON, M. S.: *J. Electrochem. Soc.*, **124**, 1706 (1977), i) MEMMING, R.: *J. Electrochem. Soc.*, **125**, 117 (1978)
- [7] YONEYAMA, H., SOKAMOTO, H., TAMURA, H.: *Electrochimica Acta*, **20**, 341 (1975)
- [8] a) KEENEY, J., WEINSTEIN, D. H., HAAS, G. M.: *Nature*, **253**, 719 (1975), b) WRIGHTON, M. S., et al.: *Proc. Natn. Acad. Sci. USA*, **72**, 1518 (1975), c) HARDEE, K. L., BARD, A. J.: *J. Electrochem. Soc.*, **122**, 739 (1975), d) MÖLLERS, F., TOLLE, H. I., MEMMING, R.: *J. Electrochem. Soc.*, **121**, 1160 (1974), e) OHNISHI, T., NAKOTO, Y., TSUBOMURA, H.: *Ber. Bunsenges. Phys. Chem.*, **79**, 253 (1975), f) OHASHI, K., McCANN, J., BOCKRIS, J. O'M.: *Nature*, **266**, 610 (1977), g) DUTOIT, E. C., CARDON, F., GOMES, W. P.: *Ber. Bunsenges. Phys. Chem.*, **80**, 475 (1976), h) MORISAKI, H., HARIGA, M., YAZAWA, K.: *Appl. Phys. Lett.*, **30**, 7 (1977), i) DAVIDSON, R. S., SLATER, R. M.: *J. Chem. Soc. Faraday Trans. I*, **72**, 2416 (1976), j) DUTOIT, E. C., CARDEN, F., GOMES, P.: *Ber. Bunsenges. Phys. Chem.*, **80**, 1285 (1976), k) CAREY, J. H., OLIVER, B. G.: *Nature*, **259**, 554 (1976), l) MOORTHY, P. N., et al.: *Bhabha Inst. Rept. Abst. No. 0240* (1977), m) WILLIAMS, F., NOZIK, A. J.: *Nature*, **271**, 137 (1978), n) SPITLER, M. T., CALVIN, M.: *J. Chem. Phys.*, **66**, 4294 (1977), o) NOUFI, R. N., KOHL, P. A., FRANK, S. N., BARD, A. J.: *J. Electrochem. Soc.*, **125**, 246 (1978), p) FLEISCHHAUER, P. D., ALLEN, J. K.: *J. Phys. Chem.*, **82**, 432 (1978)
- [9] a) van den BERGHE, R. A. L., CARDON, F., GOMES, V. P.: *Ber. Bunsenges. Phys. Chem.*, **78**, 331 (1974), b) PETTINGER, B., SCHÖPPEL, H.-R., GERISCHER, H.: *Ber. Bunsenges. Phys. Chem.*, **80**, 851 (1976)
- [10] ANDERSON, W. W., CHAI, Y. G.: *Energy Conversion*, **15**, 85 (1976)
- [11] a) GERISCHER, H., GOBRECHT, J.: *Ber. Bunsenges. Phys. Chem.*, **80**, 327 (1976), b) cf. part of Ref. 5
- [12] a) TRIBUTSCH, H.: *Ber. Bunsenges. Phys. Chem.*, **81**, 361 (1977), b) TRIBUTSCH, H.: *Z. f. Naturforsch.*, **32a**, 972 (1977), c) TRIBUTSCH, H., BENNETT, J. C.: *J. Electroanal. Chem.*, **81**, 97 (1977)
- [13] a) MÖLLERS, F., MEMMING, R.: *Ber. Bunsenges. Phys. Chem.*, **76**, 469 (1972), b) KIM, H., LAITINEN, H. A.: *J. Electrochem. Soc.*, **122**, 53 (1975), c) TOMKIEWICZ, M., WOODALL, J. M.: *J. Electrochem. Soc.*, **124**, 1436 (1977)
- [14] a) WATANABE, T., FUJISHIMA, A., HONDA, K.: *Bull. Chem. Soc. Japan*, **49**, 355 (1976), b) WRIGHTON, M. S., WOLCZANSKI, P. T., ELLIS, A. B.: *J. Solid State Chem.*, **22**, 17 (1977)

- [15] ELLIS, A. B., KAISER, S. W., WRIGHTON, M. S.: J. Phys. Chem., **80**, 1325 (1976)
- [16] a) NAKATO, Y., ABE, K., TSUBOMURA, H.: Ber. Bunsenges. Phys. Chem., **80**, 1001 (1976),
b) BOCKRIS, J. O'M., UOSAKI, K.: J. Electrochem. Soc., **124**, 1348 (1977), c) MADOU, M. J., CARDON, F., GOMES, P.: Ber. Bunsenges. Phys. Chem., **81**, 1186 (1977),
d) YONEYAMA, H., MAYUMI, S., TAMURA, H.: J. Electrochem. Soc., **125**, 68 (1978)
- [17] a) OHASHI, K., UOSAKI, K., BOCKRIS, J. O'M.: Energy Res., **1**, 25 (1977), b) DANAHER, W. J., LYONS, L. E.: Nature, **271**, 139 (1978)
- [18] cf. Ref. 13c
- [19] YEH, L-S. R., HACKERMAN, N.: J. Electrochem. Soc., **124**, 833 (1977)
- [20] a) GISSLER, W., MEMMING, R.: J. Electrochem. Soc., **124**, 710 (1977), b) HODES, G., CAHEN, S., MANASSEN, J.: Nature, **260**, 312 (1976), c) GERRARD, W. A.: J. Electroanal. Chem., **86**, 421, (1978)
- [21] BAKER, W. D., MILNES, A. G.: J. Electrochem. Soc., **119**, 1269 (1972)
- [22] a) DUBRIDGE, L. A.: New Theories of the Photoelectric Effect. Hermann, Paris 1935,
b) MAURER, R. J.: in Condon, Odishaw, Handbook of Physics, 2nd ed. p. 8-67 Me-Graw-Hill, New York, 1967

Tamás PAJKOSSY	}	H-1525 Budapest, P.O.B. 49
Róbert SCHILLER		
István MOLNÁR	}	H-1158 Budapest, Cservenka Miklós út 86
Miklós PÁLFY		

CORRELATION BETWEEN THE PREPARATION AND CATALYTIC PROPERTIES OF PtFe/SiO₂ CATALYSTS

L. GUCZI, K. MATUSEK, J. MARGITFALVI, M. ESZTERLE and F. TILL¹

(*Institute of Isotopes of the Hungarian Academy of Sciences, Budapest,*

¹*Laboratory for Inorganic Chemistry of the Hungarian Academy of
Sciences, Budapest)*

Received July 14, 1978

Accepted for publication September 1, 1978

Organometallic [Pt(CH₃)₃Cl denoted by *A*] and ionic [Pt(NH₃)₄²⁺ denoted by *B*] platinum complexes were used to prepare highly dispersed, silica supported platinum catalysts. In the case of *A* the amount of alkyl complex is strongly affected by the experimental conditions, such as solvent and support pretreatment. *B* gives a catalyst of higher dispersion and higher total metal loading than does *A*. Using different platinum sources, not only the number of metal atoms can be influenced but the nature of these sites also depends on the Pt complex applied. To prepare bimetallic catalysts, iron was used in different forms and the best way of preparation established. TG-MS, Mössbauer and chemisorption studies provide evidence for metallic interaction between the two metals. A correlation has been found between the concentration of metal atoms on the surface and the rate of hydrogenolysis of ethane and *n*-butane. The intrinsic activity of platinum is influenced by added iron and considerable deviations from this behaviour can be observed only at high iron loads.

Introduction

Of the possible transition metal combinations, only a few attempts have been made at the characterization of the PtFe system. BARTHOLOMEW and BOUDART [1] have used Mössbauer spectroscopy and chemisorption in their exploratory work and established the formation of a PtFe alloy in carbon supported PtFe catalysts; no enrichment in the surface phase for the whole concentration range was observed. GARTEN and OLLIS [2] gave further evidence for the alloy phase by studying PdFe supported on alumina. GARTEN [3] has observed the formation of a PtFe phase on a SiO₂ support and at low iron concentrations found iron enrichment on the surface induced by oxygen at high temperatures, which could be eliminated by repeated hydrogen treatment.

On the other hand, ENGELS and coworkers [4, 5] have observed by X-ray diffraction the formation of a superstructure phase, Pt₃Fe, for non-supported platinum-iron alloys in the concentration range between 10 and 15 atom% iron.

In the present study we wish to avoid strong interactions between the metallic component and the silica gel as catalyst support [6]. In order to achieve a large metallic dispersion, platinum was deposited by an ion exchange method.

Furthermore, we wish to study the preparation of bimetallic catalysts in different ways, to characterize them by TG-MS, Mössbauer spectroscopy and adsorption, and to utilize the hydrogenolysis of simple hydrocarbons, e.g. ethane and *n*-butane, for the elucidation of the interaction between platinum and iron.

Experimental

Catalyst preparation

Pt-silica gel

Pt(NH₃)₄²⁺ ions were exchanged with the surface hydroxyl group of silica gel (SAS specific surface area 560 m²/g) by the method of BENESI *et al.* [7]. Pt(NH₃)₄²⁺/SiO₂ was dried at 383 K overnight (VI), followed by a 1-hour treatment in oxygen at 573 K and a 3-hour reduction in a stream of hydrogen at 773 K. This procedure is considered as standard treatment [8].

[Pt(CH₃)₃Cl]₄ an organometallic compound in tetrameric form, was also applied as follows [9]:

(I): SiO₂ was evacuated at 773 K for 1 h and impregnated by a solution containing Pt(CH₃)₃Cl. (II): Same as (I) but treated with a nitric acid solution of pH = 1. (III): Same SiO₂ treatment as for catalyst (I) but Pt(CH₃)₃Cl was dissolved in benzene. (IV): SiO₂ was evacuated at 423 K for 30 min and impregnated with a solution containing Pt(CH₃)₃Cl dissolved in benzene. (V): SiO₂ treatment identical with (IV), but Pt(CH₃)₃Cl was dissolved in *n*-heptane. In all cases the nominal concentration of Pt was 1.1 wt. %.

PtFe/SiO₂ bimetallic catalysts

(VII): Sample (I) impregnated with a solution containing 0.2 wt. % Fe in the form of Fe(NO₃)₃ at pH = 1. (VIII): Sample (I) reduced in hydrogen for 3 h at 773 K and impregnated with ferric nitrate as sample (VII). (IX): Sample (I) treated with Fe(CO)₅ dissolved in *n*-hexane. (X): SiO₂ treated as in the case of (I) and co-impregnated with an *n*-hexane solution containing 1.1 wt. % Pt and 0.2 wt. % Fe in form of Pt(CH₃)₃Cl and Fe(CO)₅, respectively.

(XI), (XII): Sample (VI) treated with alcoholic solutions of ferrocene (0.2 wt. % and 1 wt. %, respectively).

(XIII): Sample (VI) treated with nitric acid at pH = 1. (XIV), (XV), (XVI): Sample (VI) impregnated with solution containing Fe(NO₃)₃ with 0.1, 0.2 and 0.7 wt. % iron, respectively, at pH = 1.

(XVII): A physical mixture of Pt(NH₃)₄²⁺/SiO₂ and Fe(NO₃)₃/SiO₂ with the final concentration of 1.1 wt. % Pt and 0.7 wt. % Fe.

(XVIII): Silica gel impregnated with a solution containing 0.5 wt. % Fe(NO₃)₃ at pH = 1.

Catalyst characterization and catalytic apparatus

In some cases the catalyst sample has been studied after exchange by the TG-MS method, using a Mettler microbalance connected to a Balzers QMS-511 quadrupole mass spectrometer by which the product of thermal decomposition could be measured with peak multiplexer. A Mössbauer spectrometer working in the constant acceleration mode was applied to gather information about the different stages during the preparation of the PtFe bimetallic system. The metal content of the catalysts formed was measured by X-ray fluorescence using a ¹⁰⁹Cd source (5 mCi). Since the samples were amorphous by X-ray diffraction, they have been occasionally checked by small angle X-ray diffraction.

The number of surface metal atoms was determined by the chemisorption method described elsewhere [8].

A circulation apparatus was used to measure the catalytic activity of the catalysts prepared in ethane and *n*-butane hydrogenolysis. Reaction products were analyzed by gas chromatography using a column filled with alumina.

Results

Catalyst characterization

The interaction of ionic $\text{Pt}(\text{NH}_3)_4^{2+}$ and covalent $\text{Pt}(\text{CH}_3)_3\text{Cl}$ platinum complexes with the silica gel surface is illustrated in Figs 1 and 2. In Fig. 1, a decrease in the number of surface OH groups of silica gel as a result of the formation of Si-O-Pt bonds in the reaction between silica gel and $\text{Pt}(\text{NH}_3)_4^{2+}$ is obviously indicated by the smaller H_2O peak appearing at high temperatures and the simultaneous NH_3 peaks due to the decomposition of the complex deposited on silica gel. This appears to be a direct proof for the linkage between the surface OH groups and $\text{Pt}(\text{NH}_3)_4^{2+}$.

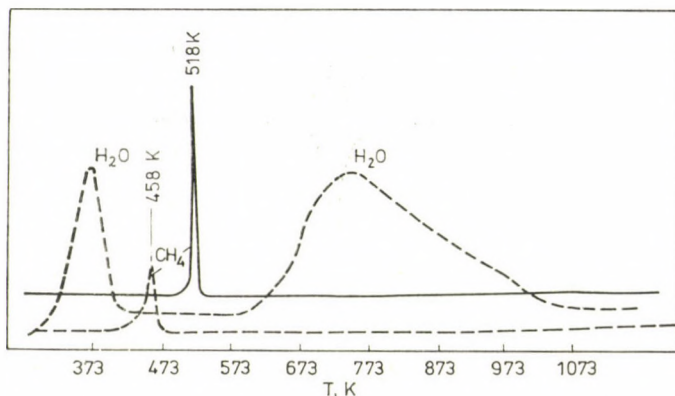


Fig. 1. TG-MS data on pure SiO_2 (solid line) and $\text{Pt}(\text{NH}_3)_4^{2+}$ -silica gel (dotted line) samples

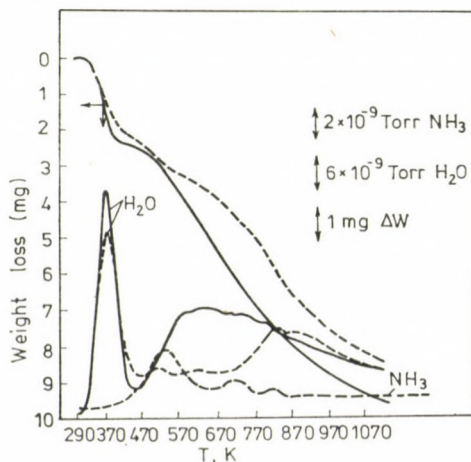


Fig. 2. TG-MS data on the thermal decomposition of silica gel-supported $\text{Pt}(\text{CH}_3)_3\text{Cl}$ (dotted line) and on the solid complex (solid line)

In Fig. 2, methane formation on the thermal decomposition of supported and unsupported Pt(CH₃)₃Cl in nitrogen atmosphere is presented. A considerable decrease of the decomposition temperature of silica-supported Pt(CH₃)₃Cl as well as a shift in product distribution to methane formation point to a strong interaction between Si-OH and the Pt(CH₃)₃Cl complex.

The formation of FePt bimetallic clusters on the silica gel support has already been studied by Mössbauer spectroscopy [10]. However, the way in

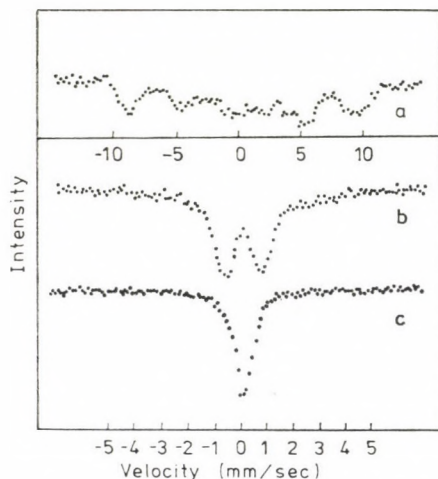


Fig. 3. Mössbauer spectra of the 0.2 wt. % Fe—1.1 wt. % Pt/SiO₂ sample. *a*) Impregnated sample (recorded at 77 K); *b*) Calcined at 573 K in O₂ (recorded at 298 K in O₂ atmosphere); *c*) Reduced at 973 K in H₂ (recorded at 298 K in H₂ atmosphere)

which the metallic phase is formed can also be traced by this technique. Sample (VI) impregnated with an Fe(NO₃)₃ solution containing 0.6 mg ⁵⁷Fe in 88% enrichment in 300 mg sample at pH = 1 shows no Mössbauer signal at room temperature after 2 × 10⁶ counts collected. At 77 K, however, a six-line spectrum is obtained, which is characteristic of spin-spin relaxation, indicating the presence of nearly isolated Fe³⁺ ions on the surface (see Fig. 3, curve *a*). Upon decomposition of the Pt complex—⁵⁷Fe(NO₃)₃ mixture in the calcination process at 573 K, a high-spin Fe³⁺ doublet is formed, *i.e.* the Fe₂O₃ particles are small enough to show a superparamagnetic behaviour. From the spectrum obtained at 77 K, a particle size smaller than about 8.0 nm can be estimated. The interaction at this stage is further confirmed by the TG—MS method, as shown in Fig. 4. Upon the decomposition of the Pt complex — Fe³⁺ salt mixture in an argon atmosphere, the disappearance of the ammonia peak and the simultaneous formation of substantial amounts of nitrogen and H₂O due to the direct oxidation of ammonia by nitrate ions can be observed.

After reduction of the bimetallic sample in a hydrogen atmosphere, the morphology of the catalyst does not change. The superparamagnetism of the reduced sample shown in Fig. 3 (curve c) serves as an excellent indication that further changes in the particle size do not occur.

An earlier study [10] on the oxidation-reduction behaviour of bimetallic catalysts containing 0.2 wt. % Fe has shown that most of the iron in the oxidized sample can be reduced at room temperature. However, this is not so at high iron loads (0.7 wt. % Fe). In Table I the results on the reduction of a previously oxidized sample are summarized.

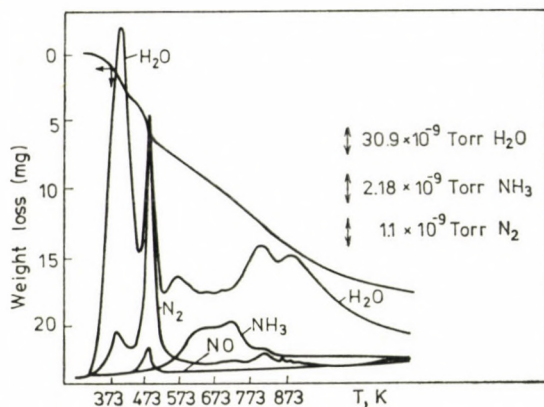


Fig. 4. TG-MS data on the 1.1 wt. % Pt(NH₃)₄ - 0.7 wt. % Fe(NO₃)₃-silica gel sample

Table I

Effect of treatments at different temperatures on the 1.1 wt. % Pt-0.7 wt. % Fe on silica gel sample

	T (K)	IS(Fe ³⁺) (mm s ⁻¹)	QS(Fe ³⁺) (mm s ⁻¹)	IS(Fe ²⁺) (mm s ⁻¹)	QS(Fe ²⁺) (mm s ⁻¹)	IS(Fe) (mm s ⁻¹)	Fe Fe ³⁺ + Fe ²⁺	χ ² /df
Reduction at	873	0.41 ± 0.03	0.89 ± 0.12	1.00 ± 0.12	2.00 ± 0.10	-0.09 ± 0.12	1.17 ± 0.05	3.22
Oxidation at*	298	0.38	1.02	—	—	—	0	1.03
Reduction at	298	0.40	0.92	1.00	2.01	-0.07	0.83	1.32
Reduction at	573	0.40	0.87	1.11	1.97	-0.02	1.01	2.23
Reduction at	723	0.41	0.99	1.00	2.00	0.02	1.15	3.08
Reduction at	873	0.41	0.98	1.10	2.10	0.05	1.12	2.23

* The same quadrupole doublet was obtained upon oxidation at 573 and 773 K after the above procedure.

Here all iron atoms can be found on the surface since upon oxidation these are completely converted into high-spin Fe³⁺ ions and only part of these ions can be found in a low-valent state at room temperature reduction, whereas at high temperatures the Fe/(Fe³⁺ + Fe²⁺) ratio again achieves the original value (compare rows 3, 6 and 1).

In Table II the metal concentrations on the support measured by X-ray fluorescence are presented (columns 2 and 3). Generally it can be established that the amount of platinum deposited by using the covalent Pt complex is smaller than in the case of the platinum tetrammine complex. In the former case the amount of platinum on the surface can be controlled by the pretreatment of the silica gel surface as well as by the solvent used. The higher the pretreatment temperature [see (IV) and (III)], the lower the amount of Pt on SiO₂. The same trend can be observed when a more reactive solvent is used [compare (V) to (IV) and (I) to (III)]. The Pt concentration is also influenced by the acid treatment needed for iron deposition in the form of Fe(NO₃)₃ to a much larger extent in the case of Pt(CH₃)₃Cl than with the platinum tetrammine complex [see (I) and (II) as well as (VI) and (XIII)].

Table II

Metal content, dispersion and rates of ethane and n-butane hydrogenolysis

No. catalyst	Pt (wt.%)	Fe (wt.%)	O ₂ -H ₂ titration (H ₂ /μmol/g _{cat})	D	Surface metal atoms (10 ⁻⁴ mol/g _{metal})	Rate of hydrogenolysis (mol s ⁻¹ g _{metal} ⁻¹)	
						Ethane (573 K)	n-Butane (523 K)
I	0.52	0	7.8	0.18	9.35	2.28 × 10 ⁻⁸	4.48 × 10 ⁻⁸
II	0.42	0	2.6	0.08	3.86	1.68 × 10 ⁻⁹	2.05 × 10 ⁻⁸
III	0.15	0	1.4	0.11	—	—	—
IV	0.20	0	2.6	0.16	—	—	—
V	0.32	0	4.8	0.18	—	—	—
VI	1.15	0	32.3	0.34	18.3	1.78 × 10 ⁻⁵	5.73 × 10 ⁻⁶
VII	0.47	0.20	0.6	0.01	0.79	3.9 × 10 ⁻¹⁰	5.43 × 10 ⁻⁹
VIII	0.39	0.11	5.2	0.08	8.3	1.2 × 10 ⁻⁸	4.71 × 10 ⁻⁸
IX	0.33	0.01	4.9	0.16	9.2	2.45 × 10 ⁻⁹	3.6 × 10 ⁻⁸
X	0.30	0.01	4.3	0.15	8.9	2.12 × 10 ⁻⁹	7.16 × 10 ⁻⁹
XI	0.98	0.20	18.0	0.13	11.4	3.91 × 10 ⁻⁶	9.88 × 10 ⁻⁶
XII	0.98	0.54	5.1	0.06	3.2	3.78 × 10 ⁻⁷	9.19 × 10 ⁻⁷
XIII	1.10	0	21.9	0.27	12.4	5.58 × 10 ⁻⁶	4.54 × 10 ⁻⁶
XIV	1.0	0.1	28.2	0.34	15.9	1.15 × 10 ⁻⁵	1.28 × 10 ⁻⁵
XV	1.0	0.2	18.0	0.27	9.3	9.33 × 10 ⁻⁷	2.72 × 10 ⁻⁶
XVI	1.0	0.7	4.9	0.06	1.8	5.86 × 10 ⁻⁸	1.04 × 10 ⁻⁷
XVIII	0	0.5	—	0.13	—	1.95 × 10 ⁻⁹	1.73 × 10 ⁻⁹

Of the different forms of iron used for the preparation of bimetallic catalysts, only Fe(NO₃)₃ at pH = 1 and ferrocene at pH = 7 appear to be effective, whereas the others do not seem to be suitable compounds for this purpose.

In column 4, the results of hydrogen-oxygen titrations are collected. Apart from catalysts (XVI) and (XVIII), this value is an adequate measure of the amount of metal atoms on the silica gel surface [11]. In these samples, room temperature titration with hydrogen does not remove all the oxygen adsorbed, whereas in the other cases the presence of iron does not affect the

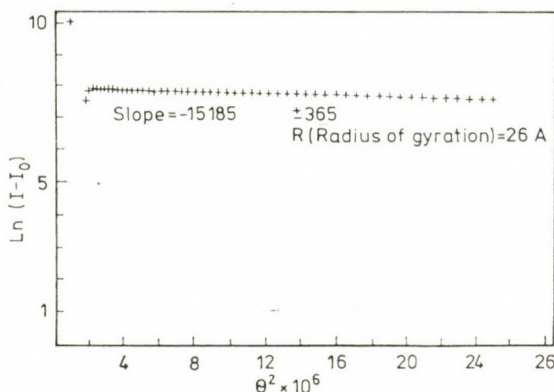


Fig. 5. Guinier plot of the small-angle X-ray diffraction data on a Pt/SiO₂ catalyst

reversibility of O₂—H₂ titration. In column 5 the metal dispersions defined as $D = \frac{N_S}{N_T}$, where N_S and N_T are the number of surface and total metal atoms, respectively, are presented. For the case of catalyst (VI), the particle size has been determined by small angle X-ray diffraction. The Guinier plot is presented in Fig. 5. The straight line of the plot shows that the catalyst is monodisperse with a particle size of 2.6 nm. The particle size determined by hydrogen titration changes in the range of 2.1 and 2.7 nm, depending on the model (spherical, octahedral, etc.) chosen. The agreement seems good, therefore, the results of the chemisorption method are reliable.

Catalytic reactions

Hydrogenolysis of ethane and *n*-butane as test reactions were applied to gain further insight into the PtFe/SiO₂ bimetallic system. All reactions have been studied using a 1 : 10 hydrocarbon to hydrogen mixture.

In Fig. 6 the rate of hydrogenolysis of ethane and butane in mol s⁻¹ g_{metal}⁻¹ units (see columns 6 and 7 in Table II) is plotted on a logarithmic scale

for catalysts prepared from the platinum tetrammine complex and from Pt(CH₃)₃Cl as a function of the surface metal atom concentration expressed in mol metal atom per gram metal (column 5 in Table II).

The plot indicates that the rates of reaction on catalysts prepared from Pt(NH₃)₄²⁺ on silica gel reveal a much higher catalytic activity than those formed from the covalent Pt complex. The experimental points for the former

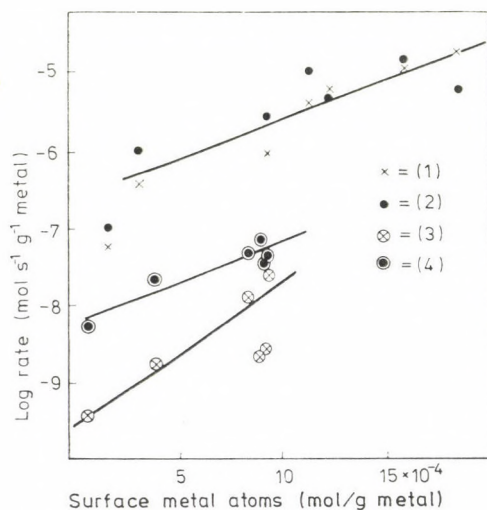


Fig. 6. Log rate vs. surface metal atom concentration in the hydrogenolysis of ethane and *n*-butane. Symbols: (1) ethane on Pt(NH₃)₄²⁺-silica gel, (2) *n*-butane on Pt(NH₃)₄²⁺-silica gel, (3) ethane on Pt(CH₃)₃Cl-silica gel, (4) *n*-butane on Pt(CH₃)₃Cl-silica gel

lie on a straight line except for the catalyst containing 0.7 wt. % iron, regardless of whether the catalyst has been treated at pH = 1 or not. The correlation

Table III

Selectivity values for *n*-butane hydrogenolysis

No. Catalyst	Temp. (K)	S _{C₁}	S _{C₂}	S _{C₃}	S _{i-C₄}
(I)	529	0.3	1	0.34	0.17
(II)	502	0.35	0.56	0.37	0.36
(VI)	497	0.41	1.18	0.37	0.04
(XIII)	513	0.43	0.90	0.35	0.15
(VIII)	537	0.25	0.32	0.24	0.60
(XII)	529	0.75	0.57	0.66	0.04
(XVI)	513	1.00	0.36	0.92	0.02

between the catalytic activity and the concentration of surface metal atoms is rather poor for catalysts from Pt(CH₃)₃Cl/SiO₂.

In Table III some characteristic data on the selectivity changes in *n*-butane hydrogenolysis are presented. It can be established that on catalysts prepared from the platinum tetrammine complex, the selectivity to isobutane formation is low compared with Pt(CH₃)₃Cl/SiO₂. The acid treatment, however, increases the S_{i-C_4} values in both cases. The further enhancement in this value on Pt(CH₃)₃Cl/SiO₂ catalysts is very significant upon iron addition, whereas no effect can be observed with platinum tetrammine catalysts. The physical mixture behaves as if the Pt/SiO₂ catalyst were prepared without added iron.

Discussion

In the present work it is strongly confirmed that the final shape of a supported catalyst is taken already at the very first step of the preparation procedure. Subsequent treatments have only a minor importance. This is proved by the different characters of the Pt/SiO₂ catalysts prepared by using ionic and covalent Pt complexes although in both cases finally metallic platinum is formed. Different treatments afterwards also alter the metal contents, dispersion, the adsorption and catalytic character of the supported metal catalyst but the basic properties are carried by these catalysts from the beginning.

The above statement becomes obvious when the TG-MS data are discussed. In both Pt complexes Si-O-Pt bonds are formed after their solutions are contacted with the surface. However, this bond for the Pt(CH₃)₃Cl complex is weaker, resulting in a smaller metal concentration on SiO₂ and, which is more important, chlorine is retained by the complex and this basically controls the character of the catalyst formed.

These factors are even more important in the preparation of bimetallic catalysts. When the impregnation with Fe(NO₃)₃ occurs in an acidic medium the ions are well distributed on the surface. Even so, in the calcination process they are brought into contact with platinum previously deposited on the silica gel. Indeed, the formation of nitrogen and water upon the decomposition of Pt(NH₃)₄²⁺/SiO₂ impregnated with ferric nitrate indicated in Fig. 2 may be the explanation of why the complex strongly held by Pt-O-Si bonds interacts with iron in the calcination phase. This interaction probably hinders the further migration and agglomeration of iron oxide particles, therefore, no change in the superparamagnetic behaviour can be observed when it is converted into a metallic phase as can be learned from Fig. 3. At the same time, this contact ensures the reduction of ferric ions into PtFe clusters and into finely dispersed iron on the surface. Separate measurements by the Mössbauer technique for iron, by small angle X-ray diffraction for Pt and by chemisorption for both

show that the metallic particles formed are very small. The existence of small PtFe particles on the surface is, therefore, strongly confirmed unless Pt and Fe particles are existing separately on the surface (this is very unlikely because a physical mixture behaves as if it were Pt/SiO₂ alone).

Previously the behaviour of PtFe/SiO₂ catalysts has been thoroughly investigated. Mössbauer measurements have given strong support that at low iron loads, a PtFe cluster is formed which can be reversibly oxidized and reduced at room temperature. At high iron loads, the best fit was obtained when a single peak with zero isomer shift was assumed with a constrained doublet for Fe³⁺ and Fe²⁺ [10].

In the present study it is clearly shown that all iron atoms at high iron load are located at or near to the surface since they are completely converted into Fe³⁺ upon room temperature oxidation. Room temperature reduction does not convert all ferric ions into zerovalent iron, which means that on the surface Fe⁰ atoms are surrounded by iron in a cubic array and by PtFe clusters.

A comparison of catalysts (VI) and (XIII) shows that there is a small drop in the number of surface Pt atoms because the loss in the platinum content of the catalyst subjected to an acid treatment is negligible, as indicated by X-ray fluorescence measurements. The essential identity of catalysts with and without acid treatment is further proved by the fact that the adsorption properties of bimetallic catalysts produced either by Fe(NO₃)₃ impregnation at pH = 1 and/or by impregnation with ferrocene in alcohol at pH = 7 [compare catalysts (XI) and (XV) as well as (XII) and (XVI)] are close to each other.

We have already observed that [9] in some cases a parallelism can be found between the adsorption properties and the catalytic activity. In Fig. 6 this proportionality between the number of surface metal atoms and the rate of hydrogenolysis can be found only in the case of catalysts prepared from Pt(NH₃)₄²⁺ regardless of whether it has been treated at pH = 1 or not.

Although there is no essential change in the concentration of surface metal atoms when the catalysts are prepared from Pt(CH₃)₃Cl, their intrinsic activities are still much lower than with the platinum tetrammine complex. As we have already mentioned, one of the reasons of this unexpected behaviour may be that upon impregnation of the silica gel surface chlorine atoms are retained by the molecule and a Pt-O-Si bond is formed *via* the cleavage of one methyl group. This statement is supported by the experiments carried out with other organometallic complexes [12], in which the hydrocarbon ligand was always cleaved from the metal complex.

As far as the metal concentration on the support is concerned, it is significant that the actual metal content for both Pt and Fe is usually lower than the nominal value.

On comparing the Pt contents of catalysts (I), (III), (IV) and (V), an increasing metal load is apparent with decreasing interaction between solvent

and silica gel (in the benzene-heptane-hexane sequence). The same effect is found with decreasing pretreatment temperature, because the number of hydroxyl groups supplying the hydrogen atoms decreases with increasing temperature. Catalyst treatment with an acid solution partly removes the Pt(CH₃)Cl complex [compare (I) and (II)].

Of the methods used for the preparation of PtFe catalysts, co-impregnation does not seem suitable to achieve high iron loads, similarly to the application of Fe(CO)₅. The highest iron content can be obtained by post-impregnation of catalysts (VI) and (VIII) as well as by impregnation of catalyst (VI) with ferrocene. The same is valid for Pt(NH₃)₄²⁺/SiO₂ impregnated with an Fe(NO₃)₃ solution. Upon hydrogenation HCl is trapped by the support, which becomes acidic and thus the structure of the metallic phase is completely different. Indeed, upon acid treatment, the hydrogenolysis activity of the catalyst decreases [see *e.g.* (I) and (II) as well as (VI) and (XIII)] with a simultaneous increase of the isomerization activity (see Table III). This may be due to the enhancement of the acidic character but a dispersion effect may not be excluded.

The proportionality expressed by Fig. 6, which is equivalent to the increase of the turnover number as a function of metallic dispersion, means that hydrogenolysis can be considered as a demanding reaction [13, 14] similarly to those observed on pure Pt/SiO₂ catalysts [15]. The essential difference is that in the latter case the degree of the change is smaller. In our opinion, this is the consequence of iron influence on platinum, therefore, we believe that not only the dispersion of platinum is enhanced by added iron, as has been stated earlier [4, 5], but the intrinsic activity of the active sites is also influenced by iron. There is one exception, the sample with the highest iron content (XVI), for which not only the rate deviates from that determined by the straight line, but also the selectivity in butane hydrogenolysis resembles that characteristic of non-noble transition metals [16–18].

Conclusions

1) Of Pt(CH₃)₃Cl (A) and Pt(NH₃)₄²⁺ (B) the latter is the better choice to obtain metal particles with the highest number of Pt atoms on the surface. (A) is also suitable to produce catalysts of high dispersion, however, the amount of the alkyl complex bonded to silica gel is strongly affected by the experimental conditions, such as solvent, support pretreatment, *etc.* The total amount of Pt is smaller in the case of (A) than for (B). Upon preparation from different Pt sources, not only the number of surface metal atoms can be influenced, but the nature of these sites also depends on the Pt complex used.

2) TG-MS and Mössbauer data, along with gas adsorption, give evidence for metallic interaction between iron and platinum prior to and after standard

treatment. The catalysts are well dispersed and at least a part of iron can be oxidized and reduced at room temperature, which again points to direct contact between the two metals.

3) A correlation has been found between the concentration of metal atoms on the surface and the rate of hydrogenolysis of ethane and *n*-butane. The intrinsic catalytic activity of platinum is influenced by the iron additive and considerable deviations from this behaviour can only be observed at high iron loads.

*

The authors are indebted to Dr. T. SZÉKELY for valuable discussions, to Dr. G. BODOR for small-angle X-ray measurements, and to Mrs. G. STEFFLER and Mr. I. BOGYAI for technical assistance.

REFERENCES

- [1] BARTHOLOMEW, C. H., BOUDART, M.: *J. Catal.*, **29**, 278 (1973)
- [2] GARTEN, R. L., OLLIS, D. F.: *J. Catal.*, **35**, 232 (1974)
- [3] GARTEN, R. L.: Mössbauer Effect Methodology. Vol. **10**, 1976
- [4] ENGELS, S., MÖRKE, W., SIEDLER, J.: *Z. Anorg. Allgem. Chem.*, **431**, 181 (1977)
- [5] ENGELS, S., MÖRKE, W., SIEDLER, J.: *Z. Anorg. Allgem. Chem.*, **431**, 191 (1977)
- [6] JACONO, La., SCHIAVELLO, M., CIMINO, A.: *J. Phys. Chem.*, **75**, 1044 (1971)
- [7] BENESI, H. A., CURTIS, M. P., STUDER, J.: *J. Catal.*, **10**, 328 (1969)
- [8] GUCZI, L., MATUSEK, K., ESZTERLE, M. *J. Catal.* (In press)
- [9] GUCZI, L., MATUSEK, K., MARGITFALVI, J.: *React. Kinet. Catal. Lett.*, **8**, 309 (1978)
- [10] DÉZSI, I., NAGY, D. L., ESZTERLE, M., GUCZI, L.: *React. Kinet. Catal. Lett.*, **8**, 301 (1978)
- [11] GUCZI, L.: Plenary lecture, Federal Conference on Supported Metal Catalysts in Hydrocarbon Reactions, Novosibirsk, June 29–31, 1978
- [12] YERMAKOV, Yu. I.: *Catal. Rev.*, **13**, 77 (1976)
- [13] BOUDART, M.: *AIChE Journal*, **18**, 465 (1972)
- [14] BRUNELLE, J. P., SUGIER, A., LE PAGE, J. F.: *J. Catal.*, **43**, 273 (1976)
- [15] GUCZI, L., GUDKOV, B. S.: *React. Kinet. Catal. Lett.*, **9**, 343 (1978)
- [16] GUCZI, L., GUDKOV, B. S., TÉTÉNYI, P.: *J. Catal.*, **24**, 187 (1972)
- [17] BABERNICS, L., GUCZI, L., MATUSEK, K., SÁRKÁNY, A., TÉTÉNYI, P.: 6th Int Congr. Catal., Paper A 36, London 1976
- [18] SINFELT, J.: *Adv. Catal.*, **23**, 91 (1973)

László GUCZI

Károly MATUSEK

József MARGITFALVI

Matild ESZTERLE

Ferenc TILL

H-1525 Budapest, P.O.B. 77

DIHYDROPYRAN CYCLOADDUCTS, III*

REACTIONS OF CYCLOPENTANONE ENAMINES WITH BENZYLIDENE KETONES

GY. OSZBACH, D. SZABÓ and M. E. VITAI

(Chemical Department of the Medical University, Pécs)

Received June 23, 1978

Accepted for publication September 4, 1978

Cyclopentanone enamines react with benzylideneacetophenone to yield adducts of the Michael type; with benzylidenecyclohexanones, under very mild conditions, the products are cyclopentapyranes. The steric structure of the latter compounds was investigated by examining the hydrolysis products.

Electrophilic olefins react with enamines in widely different ways, depending on their structures [1, 2]. Enamines of six-membered cyclic ketones can usually be converted with benzylidene ketones into dihydropyrans [3, 4]. There are few data available regarding the analogous reactions of cyclopentanone enamines: the isolation of Michael adducts has been reported [5, 6], but it cannot be excluded that failure in achieving cyclization was due to the rather drastic reaction conditions. Recently, KÖNST *et al.* raised again the possibility of the intermediary formation of dihydropyrans [7]. In seeking experimental evidence for the existence of such intermediates, we allowed some benzylidene ketones to react with cyclopentanone enamines under very mild conditions.

1-Pyrrolidinylcyclopentene (**Ia**, $X = -$) yielded with benzylideneacetophenone (**II**) the well-known diketone **VII** at 0 °C in anhydrous ethanol, in spite of the nominally anhydrous conditions [8]. Under the same conditions, piperidino- (**Ib**, $X = CH_2$) and morpholinocyclopentene (**Ic**, $X = O$) were converted with **II** into the enamino ketones **IVb**, **c**, unknown up to now. In the IR spectra of **IVb** and **c**, the band at 1680 cm^{-1} can be assigned to the phenyl ketone, that at 1630 cm^{-1} to the enamine double bond. The PMR spectra of **IVb** and **c** indicate an interesting tautomerism: although the enamine double bond usually tends to occupy the least substituted site [1], about 40% of the tetrasubstituted tautomer **Vb** and **c** must be assumed to exist in chloroform solution on the basis of the fact that methine signal of the trisubstituted olefin bond represents only 0.6 protons. Compounds **IVb** and **c** can be hydrolyzed with dilute hydrochloric acid to the diketone **VII**. The possible reaction paths are summarized in Fig. 1.

There are two possibilities for the stabilization of the zwitterion **III** formed in the first step [4, 9]: charge equalization may yield **IV**, or compound **VI**

* Part II, see Ref. [4]

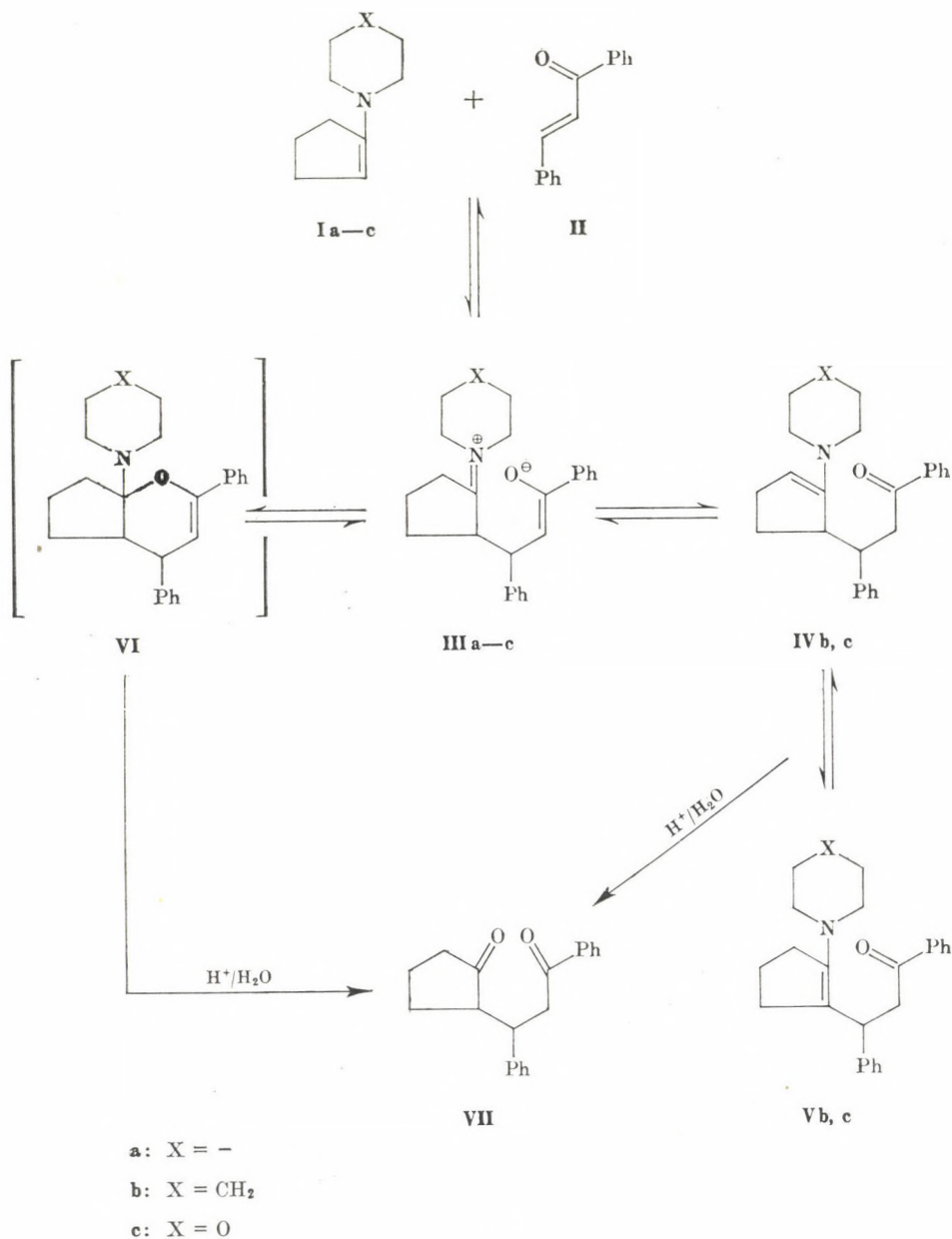


Fig. 1

can be formed in an intramolecular addition step. Actually compounds **IVb, c** were isolated. The transient formation of the cyclopentapyran **VI** cannot be excluded, in view of the fact that the corresponding benzopyrans can be

synthesized [4], although they are liable to ring cleavage. Evidently, there is another effect playing a part here in addition to the electron-withdrawing action of the phenyl group at C-2: this is the strain produced by the overlapping position of the substituents 4a—7a in the five-membered ring, which is obviously absent in the six-membered ring A. We assumed that after the removal of the phenyl group from the immediate vicinity of the oxo group, the overlapping positions alone would not prevent ring closure.

Indeed, all the three enamines (**Ia**, **b**, **c**) yielded the expected cyclopentabenzopyran (**IXa—c**) with 2-benzylidenecyclohexanone (**VIII**). Unambiguous evidence for the occurrence of cyclization is that the IR spectra of the products contain only one double bond: the "enol ether band" at about 1690 cm^{-1} . The PMR spectra can hardly be evaluated; on hydrolysis of **IXa—c** in dilute acid, the ketol **XI** was obtained, and this chemical conversion helped the elucidation of the deeper structure of **IX** by proving the *cis* position of the two hydrogen atoms in the pyrane ring (Fig. 2).

The structure of the ketol (**XI**) was established on the basis of the following considerations: a carbonyl band appeared in the IR spectrum at 1740 cm^{-1} when recorded in the solid state. Such a high frequency can only be expected in the five-membered cyclic ketone, thus the alternative structure **XII** can be dismissed. The steric position of the hydroxyl group at C-4a was also established on the basis of the IR spectrum: in solid state and in 10^{-3} mole/l carbon tetrachloride solutions, vibrations characteristic of intramolecular hydrogen bond appear at 3395 cm^{-1} and at 3410 and 3603 cm^{-1} , respectively. The bond is rather weak: the average distance of the two oxygen atoms measured in the Dreiding model is about 3.1 \AA , and this is responsible for the widening of the free OH band and the carbonyl band observed in dilute solutions. The configuration of the C-9 atom and the *trans* B/C ring anellation can be established from the PMR spectrum: the signal of the C-9 proton (doublet of doublets) (3.18 , $J_{8,9} = 3\text{ Hz}$, $J_{9,9a} = 12\text{ Hz}$) and the absence of the splitting of the phenyl signals is equally consistent with the structure given. (Simultaneous or one by one changes of the configurations of the 9 and 9a carbon atoms also yield dihedral angles of about 60° and nearly the same extent of splitting, and in the presence of an *axial* phenyl group no hydrogen bond could be formed between the oxygen atoms.) Compound **XI** undergoes dehydration strikingly readily, which also supports the *trans* ring anellation.

2,6-Dibenzylidenecyclohexanone (**XIV**) gives a cycloadduct (**XVa—c**) with all the three enamines (**Ia—c**) (Fig. 3). The IR spectra of the compounds are altered as compared with those of **IXa—c**, in accordance with the changes in the structure: the band of the enol ether appears at a frequency lower by about 45 cm^{-1} (conjugation) and the band assigned to the double bond in the benzylidene group is found at about 1620 cm^{-1} . The PMR spectra are rather diffuse but agree with the structure given.

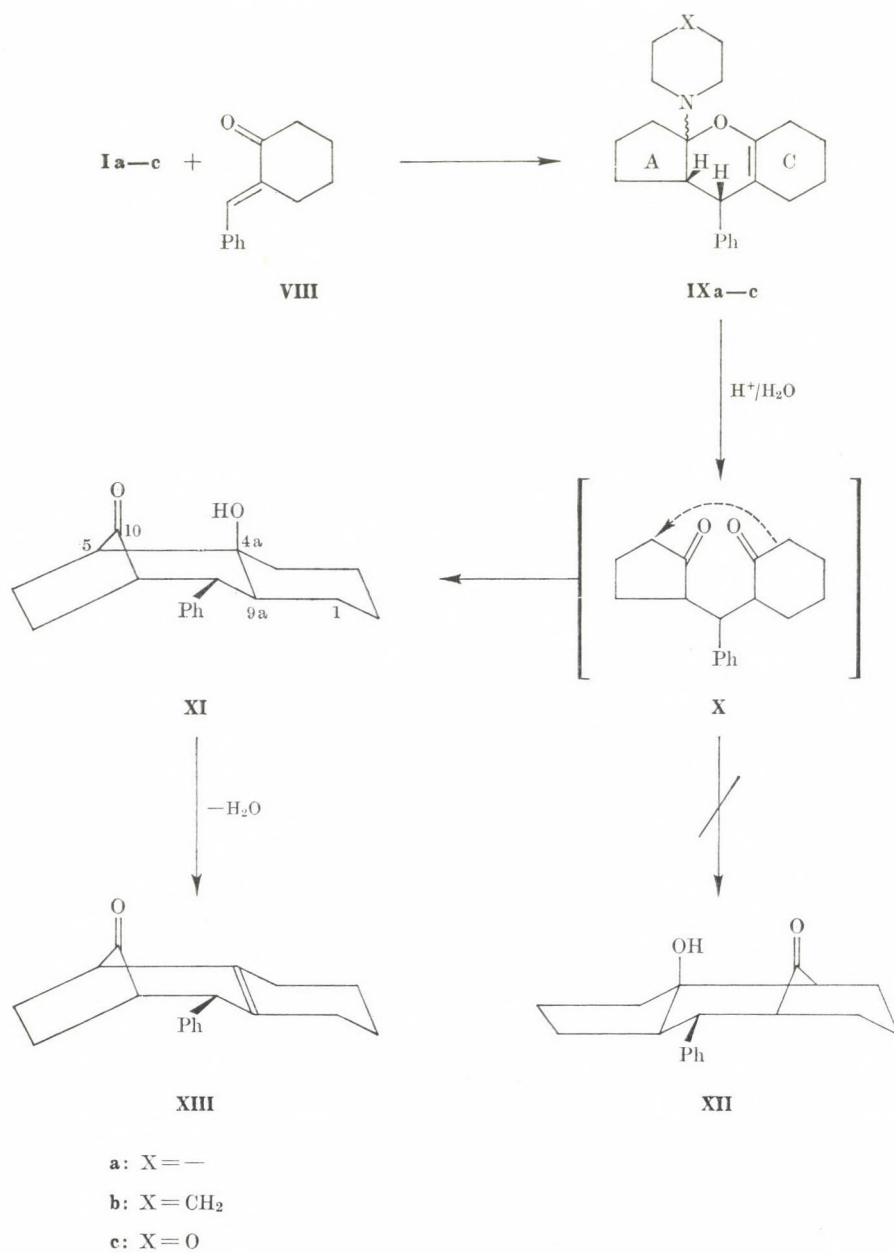
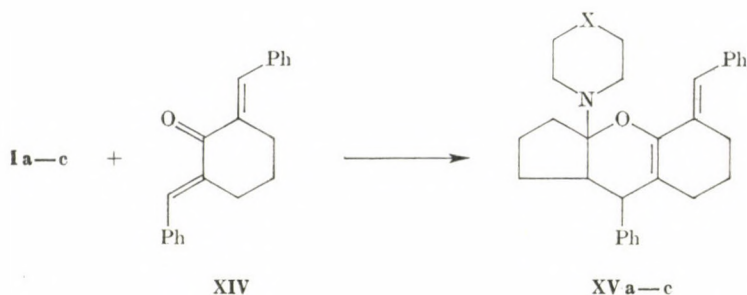


Fig. 2



a: X = —

b: X = CH₂

c: X = O

Fig. 3

Table I

Compound	Method Yield, %	M.p., °C Solvent of crystallization	Molecular formula (M.w.)	Analysis, % Calcd./Found		
				C	H	N
IVb	A 98	124—127 ethyl acetate-ether	C ₂₅ H ₂₉ NO (359.52)	83.52	8.13	3.90
				83.54	8.29	3.79
IVc	A 70	115—117 petroleum ether	C ₂₄ H ₂₇ NO ₂ (361.49)	79.75	7.53	3.87
				79.41	7.74	3.91
VII	A ; B 79 ; 52	78—80* petroleum ether	C ₂₀ H ₂₀ O ₂ (292.38)	82.16	6.89	—
				82.24	6.75	—
IXa	A 60	95—97 petroleum ether	C ₂₂ H ₂₉ NO (323.48)	81.69	9.04	4.33
				81.85	9.31	4.44
IXb	A 79	114—117 petroleum ether	C ₂₃ H ₃₁ NO (337.51)	81.86	9.26	4.15
				81.71	9.19	4.29
IXc	A 78	135—138 petroleum ether	C ₂₂ H ₂₉ NO ₂ (339.48)	77.83	8.61	4.12
				77.49	8.84	4.24
XI	B 76	210 ethanol	C ₁₈ H ₂₂ O ₂ (270.37)	80.00	8.20	—
				79.90	8.23	—
XIII	C 46	syrup	C ₁₈ H ₂₀ O (252.30)	85.67	7.99	—
				85.90	8.21	—
XVa	A 90	138—141 benzene-methanol	C ₂₉ H ₃₃ NO (411.59)	84.63	8.08	3.40
				84.33	8.26	3.37
XVb	A 76	132—135 ethyl acetate	C ₃₀ H ₃₅ NO (425.62)	84.66	8.28	3.29
				84.77	8.15	3.29
XVc	A 90	123—125 ethanol	C ₂₉ H ₃₃ NO ₂ (429.59)	81.46	7.78	3.28
				81.55	7.58	3.40

* Lit. [6, 8] m.p. 78—80 °C.

Table II

Compound	IR, cm ⁻¹	PMR δ (ppm) TMS=O
IVb	1683 phenyl ketone 1624 C=C enamine 1600 C=C aromatic 1582	8.1—7.0 m, 10H, CH aromatic 4.31 br, 0.6H, CH enamine
IVc	1680 C=O phenyl ketone 1620 C=C enamine 1598 C=C aromatic 1582	8.1—7.1 m, 10H, CH aromatic 4.36 br, 0.6H, CH enamine
VII	1738 C=C c-aliphatic 1687 C=C phenyl ketone 1600 C=C aromatic	8.1—7.3 m, 10H, CH aromatic
IXa	1695 C=C enol ether 1600 C=C aromatic	7.25 "s",* 5H, CH aromatic
IXb	1696 C=C enol ether 1602 C=C aromatic	7.28 "s",* 5H, CH aromatic 3.00 br, 1H, >CH-Ph
IXc	1692 C=C enol ether 1603 C=C aromatic	7.28 "s",* 5H, CH aromatic 2.98 br, 1H, >CH-Ph
XI	3395 OH assoc. 1740 C=O c-pentanone 3603** free OH 3410** OH assoc. 1740** C=O c-pentanone	7.25 "s",* 5H, CH aromatic 3.18 dd, 1H, >CH-Ph ($J_{8,9} = 3\text{Hz}$, $J_{9,9a} = 12\text{Hz}$) 1.76 s, 1H, OH
XIII	1740 C=O c-pentanone 1710 (sh) C=C	7.40 "s",* 5H, CH aromatic
XVa	1644 C=C enol ether 1615 C=C-Ph 1600 C=C aromatic	7.50—7.20 m, 10H, CH aromatic 7.03 s, 1H, =CH-Ph 3.14 d, 1H, >CH-Ph ($J = 6\text{Hz}$)
XVb	1648 C=C enol ether 1618 C=C-Ph 1600 C=C aromatic	7.50—7.20 m, 10H, CH aromatic 7.04 s, 1H, =CH-Ph 3.20 d, 1H, >CH-Ph ($J = 5\text{Hz}$) 7.50—7.20 m, 10H, CH aromatic
XVc	1644 C=C enol ether 1613 C=C-Ph 1599 C=C aromatic	7.07 s, 1H, =CH-Ph 3.45 t, 4H, $\text{CH}_2\text{-O-CH}_2$ ($J = 4.5\text{Hz}$) 3.23 br, 1H, >CH-Ph

* "s" = quasi-singlet

** Recorded in CCl₄ solution

Experimental

M.p.'s are uncorrected. The IR spectra were recorded with a Zeiss UR-10 spectrophotometer in KBr pellets, the solution spectra were obtained in 10^{-3} mole/l solutions in CCl_4 . The PMR spectra were recorded with a Perkin-Elmer R-12 instrument in CDCl_3 solutions. Physical data and elemental analyses of the compounds prepared are given in Table I; Table II contains their spectral data.

(A) General method of achieving the addition reactions (IVb, c, VII, IXa—c, XVa—c)

A solution of the unsaturated ketone (II, VIII or XIV) (0.02 mole) and the enamine (Ia, b or c) (0.02 mole) in anhydrous ethanol (40 ml) was stirred at 0°C until a sample taken from the reaction mixture contained no ketone (tested chromatographically on a Kieselgel H_{254} layer in benzene—ethyl acetate 40:1 mixture) (3—12 h). The crystals which separated were filtered off, washed with cold ethanol and crystallized from a suitable solvent (Table I).

(B) Hydrolysis of IVb, c, IXa, b, c

The starting material (0.005 mole) was stirred overnight in 2N HCl solution (20 ml) and chloroform (20 ml). The phases were separated, the aqueous phase was extracted with chloroform, washed with water and evaporated to dryness. The residue was crystallized from petroleum ether (VII) or ethanol (XI).

(C) 9-Phenyl-5,8-methano-1,2,3,4,6,7,8,9-octahydro-5H-benzocyclohepten-10-one (XIII)

Compound XI (1.35 g; 0.005 mole) was boiled for 30 min in anhydrous benzene (25 ml) in the presence of *p*-toluenesulfonic acid (40 mg) under a Dean-Stark trap. After cooling, the solution was washed with NaHCO_3 solution then with water, dried and evaporated to dryness. The syrupy substance obtained could be neither distilled nor crystallized. For analysis, a small amount of the substance was dissolved in benzene, sucked through activated carbon, evaporated to dryness and the almost colourless sample obtained in this way was analyzed.

REFERENCES

- [1] STORK, G., BRIZZOLARA, A., LANDESMAN, H., SZMUSZKOVICZ, J., TERRELL, R.: J. Am. Chem. Soc., **85**, 207 (1963)
- [2] SZMUSZKOVICZ, J.: Adv. Org. Chem., **4**, 1 (1963)
- [3] BALAJI RAO, R., BHIDE, G. V.: Chem. Ind., **1969**, 1095
- [4] OSZBACH, Gy., SZABÓ, D., VITAI, M. E.: Acta Chim. Acad. Sci. Hung., **95**, 273 (1977) and references cited therein
- [5] DE JONGH, H. A. P., GERHARTL, F. J., WYNBERG, H.: J. Org. Chem., **30**, 1409 (1965)
- [6] BIRKOFER, L., SUNG MAN KIM, ENGELS, H. D.: Ber., **95**, 1495 (1962)
- [7] KÖNST, W. M. B., WITTEVEEN, J. G., BOELEN, H.: Tetrahedron, **32**, 1415 (1976)
- [8] STOBBE, J.: J. Pract. Chem., **2** **86**, 209 (1912)
- [9] FLEMING, I., KARGER, M. H.: J. Chem. Soc., C, **1967**, 226

György OSZBACH

Dezső SZABÓ

M. Erzsébet VITAI

H-7643 Pécs, Szigeti út 12.



COMPLEX STUDIES ON INTERMEDIER DECOMPOSITION PRODUCTS OF AMMONIUM PARATUNGSTATE

L. BARTHA,¹ GY. GYARMATI,² B. A. KISS,² T. NEMETH,¹ A. SALAMON,¹ and
T. SZALAY³

¹(Research Institute for Technical Physics of the Hungarian Academy of
Sciences, Budapest, ²Tungsram Research Laboratory, Budapest,

³Institute for Physical Chemistry of the University Debrecen)

Received July 13, 1978

Accepted for publication September 9, 1978

The blue oxide — an intermedier product of the thermal decomposition of the ammonium paratungstate ($\text{APT} \cdot 5\text{H}_2\text{O}$) — has been investigated by means of X-ray diffraction, infrared spectroscopy, pH-metry, ion exchange, and redox potential measurements.

A connection was found between the phase composition and some chemical behaviour.

The presence of the tetragonal hydrogen tungsten bronz and that of a hexagonal mixed ammonium hydrogen tungsten bronz is established and the chemical reactivity of the blue oxide is connected to them.

Introduction

The research of W and of its compounds has been a characteristic activity of Hungarian scientists for the last few decades. Some basic discoveries can be connected to them. HEGEDÜS and MILLNER [1] described the determining role of β -W in the doping mechanism. NEUGEBAUER *et al.* [2] published first the existence of the ammonium W-bronze and mentioned later [3] its ion-exchanging ability. The presence of hydrogen tungsten bronze in blue oxide was already mentioned by HEGEDÜS [23]. GADO [4] gave the explanation for the structural characteristics of the W oxides with oxygen defect.

The present work deals with the study of an intermedier product of the thermal decomposition of the ammonium paratungstate $5\text{H}_2\text{O}$ (APT), the so called blue oxide which has an approximate formula of $\text{WO}_{2.8-2.9}$ and is a multicomponent material. The aqueous reactions of this blue oxide and of the yellow tungsten oxide ($\text{WO}_3 \cdot \text{H}_2\text{O}$), have been investigated in details in the recent years [5-12]. The aim of these studies was the better understanding of the doping mechanism of the tungsten oxide. It was found that not only the parameters of the solution but also those of the solid phase (composition, grain size, *etc.*) might play a determining role in the interaction, all the more that the blue oxide is a mixed phase with components not described satis-

factorily. The earlier measurements were not able to clarify which components are responsible for the reactivity of the material. It was found only that blue oxide samples which were proved to be identical tested by means of usual methods (*e.g.* BET surface measurement, annealing weight loss, *etc.*) show different behaviour (in ion exchange capacity, in redox properties, *etc.*) under the same conditions of the liquid phase.

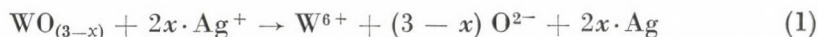
In the present work we are going to describe some properties of the blue oxide and to explain them, first of all in order to understand the connections between the reactivity and the phase composition.

Experiments and Results

For the experiments blue oxide samples were prepared by thermal decomposition of APT in laboratory furnace as follows ;

10 g APT was placed in a Mo-Ni boat and pushed into the furnace the temperature of which was stabilized already at different temperatures between 350 and 600 °C. It was annealed for 45 min either in N₂, Ar or H₂ gas, or in a mixture of them. The gas flow rate was 25–50 l/hour.

The oxygen index (OI) *i.e.* the O/W atomic ratio of the samples was determined according to CHOAIN and MARION [13]. The determination is based on Eq. 1 ;



Ag⁺ ions were added in form of thiocyanide complex in alkaline solution. The reduced silver was filtered on a glass filter, dissolved in HNO₃ and determined by means of the thiocyanide method. The reproducibility of the OI values was ± 0.005 .

Figure 1 shows the dependence of the OI on the decomposition temperature.

The OI decreases very slowly between 350 and 400 °C to about 2.99, then it drops faster to about 2.80 in the range of 400–600 °C. Further reduction takes place only at higher temperatures but the product cannot be considered as a blue oxide any more and will not be the object of our present study.

Investigation of ion exchange properties

a) Radioactive tracer experiments

Blue oxide samples were mixed with aqueous KCl solution labelled with ⁴²K isotope as described earlier [7] and having reached the equilibrium (3 min) the K⁺ ion concentration (activity) of the separated solution was measured.

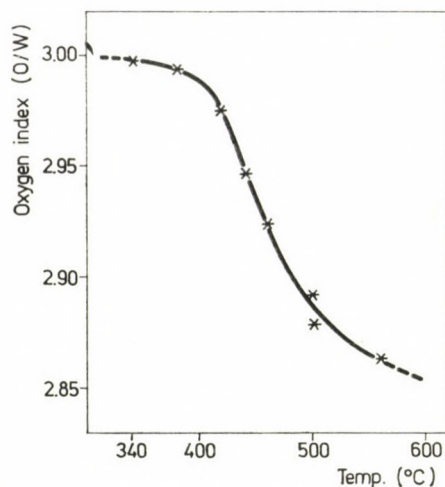


Fig. 1. Dependence of OI on APT decomposition temperature (2 l/h H_2 —30 l/h Ar)

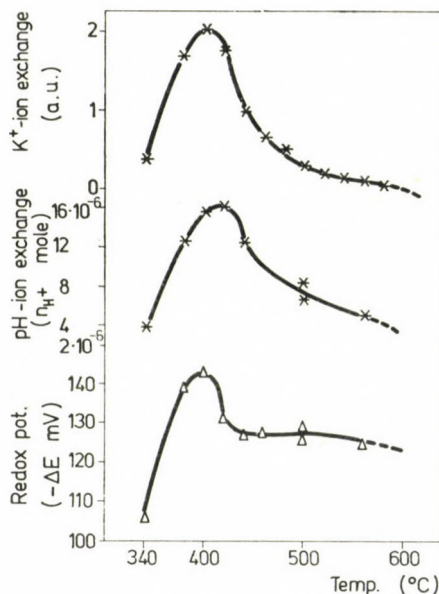


Fig. 2. a) The K^+ ion exchange ability of blue oxide; b) H^+ ion quantity developed due to K^+ exchange in blue oxide in aqueous media (80 cm³ deionized water + 20 cm³ 0.1 *n* KCl, 800 mg blue oxide); c) redox potential of blue oxide $K_3[Fe(CN)_6]$ systems (88 cm³ deionized water + 10 cm³ *n* HCl + 2 cm³ 0.3 *M* $K_3[Fe(CN)_6]$, 200 mg blue oxide)

Fig. 2 shows the dependence of the ion exchange on the decomposition temperature.

The ion exchange capacity increases rapidly till the decomposition temperature of 430 °C ($OI \approx 2.97$). Then it starts to decrease and reaches a nearly constant OI value of about 2.88.

b) pH-metric experiments

The pH value of the liquid phase decreases very fast for a short period in the course of the ion exchange. The number of H^+ ions causing the change of pH agrees well with that of K^+ ions taking place in the ion exchange [10].

After the ion exchange process a further slow change of pH can be observed over a long time.

Rapid reaction occurs only if ionic solutions are present but not in presence of pure water. In this latter case only a slow process is observable which is considered to be the hydrolysis of the blue oxide components (Fig. 3), and which is not the rate determining factor of the ion exchange process.

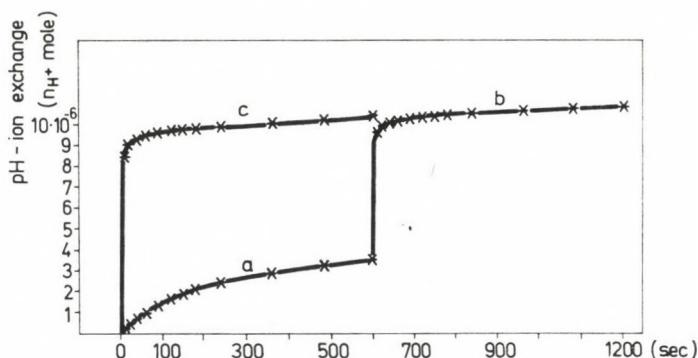


Fig. 3. Hydrolysis and ion exchange of blue oxide in aqueous media: hydrolysis (a) followed by additional K^+ ion exchange (b), hydrolysis and simultaneous K^+ ion exchange (c), (solutions: 100 cm³ deionized water (a); + 20 cm³ 0.1 *n* KCl (b); 80 cm³ deionized water + 20 cm³ 0.1 *n* KCl (c). — 800 mg blue oxide)

Figure 2 shows the change of H^+ ion quantity caused by K^+ ion exchange in blue oxide samples, corrected with the corresponding increment of the hydrolysis. The n_{H^+} curve has also maximum at 420 °C, at the decomposition temperature and fits well to the $^{42}K^+$ ion exchange curve. This proves the relation of the two processes, therefore the more simple pH measurements can be used for the indirect determination of the ion exchange ability of blue oxide samples.

A typical rate curve of the hydrolysis (Fig. 4) has several characteristic breaks, which lead to the conclusion that the blue oxide is a mixture of different solid phases. The number of phases depends on the conditions (temperature, atmosphere) of the thermal decomposition, and can be at least two.

On the bases of hydrolysis, ion exchange and pH measurements we suggest that the ion exchange ability of this multiphase material is connected not only with the oxyhydrate, formed during the hydrolysis, as we supposed earlier [10], but rather with some other components of the solid phase too.

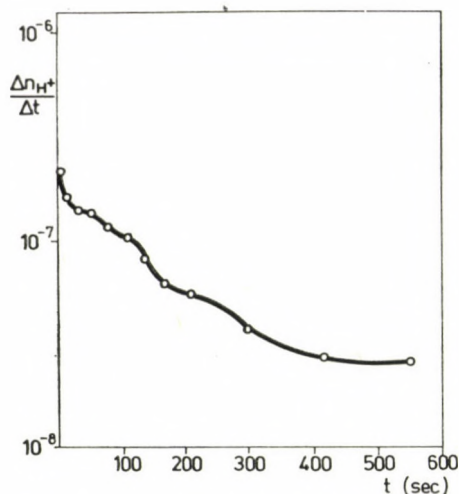


Fig. 4. A typical hydrolysis rate curve

Investigation of redox properties

The OI of the blue oxide samples is always less than 3. We confirmed the earlier perception [6] that blue oxide acts as a strong reducing agent under suitable conditions. The chemical determination of the OI is also based on this property. We have determined the reducing ability of the blue oxide by the following method; blue oxide was mixed to an acidic $K_3[Fe(CN)_6]$ solution and the change of redox potential was measured with Au electrode against *cc.* calomel electrode. Figure 2 shows the dependence of the redox potential on the decomposition temperature of the blue oxide. The curve has a character similar to that for ion exchange and pH values. The main difference observed is that it stabilizes in the high temperature range at a higher relative value, probably because the $W_{20}O_{58}$ phase itself, which is stable in this range, has also a reducing ability comparable to that of the bronze (M_xWO_3) [16].

All the measurements described above prove that the reactivity of the blue oxide increases with the decomposition temperature up till about 400–420 °C and over this temperature it drops rapidly.

Investigation of the phase composition of the blue oxide

a) Infrared absorption spectrometric investigations

The spectra of blue oxide samples were recorded in KBr pellets with an UR 10 IR spectrometer. It was found, that the wave number of the single absorption band, appeared in the frequency range of the W–O–W vibration, moved towards higher frequencies with decreasing OI. Later, the band split

to a higher and a lower frequency maximum, and finally the latter one became dominant. This is in agreement with our earlier observations [14].

The curve of Fig. 5 shows the frequency displacement of the ν_{W-O-W} stretching band vs. OI. Three breaks can be observed which prove the existence

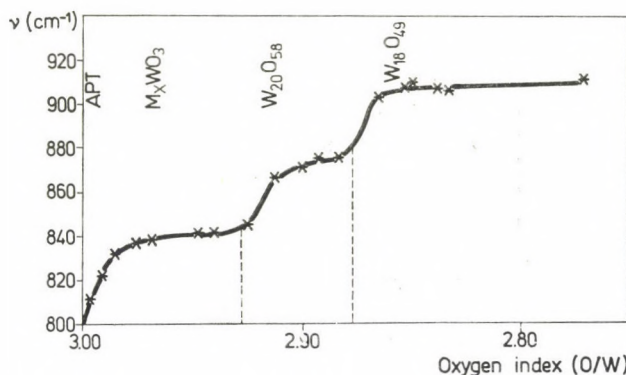


Fig. 5. Frequency displacement of the ν_{W-O-W} stretching band

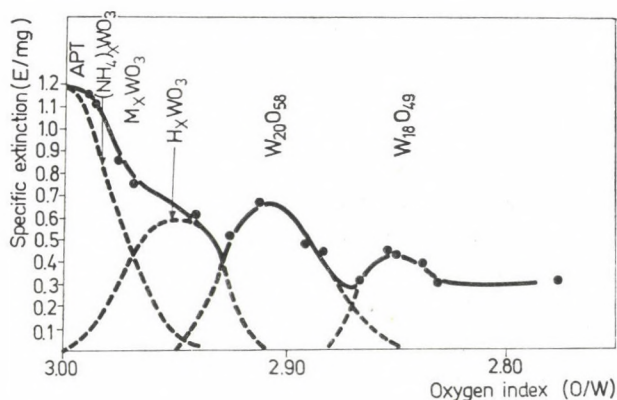


Fig. 6. Dependence of specific intensities of the bands on OI

of at least three independent phases. The knowledge of the characteristic vibration frequencies of the pure phases enabled the identification of the phases in the blue oxide samples [15].

The curve of Fig. 6 where the change of the specific intensities of the bands are given in the dependence of the OI, is even more informative. The curve describes reliably the phase changes and shows the mixed phase regions. In the range of the ATB the existence of two phases can be supposed. It gives no details but encourages us to search for at least two different bronzes with other methods too. It confirms also the assumption, that the ion exchange properties are connected with the bronze phase.

b) X-ray structure investigations

The X-ray diffractometric studies and powder X-ray photographs using a Guinier camera (CuK_α) of our blue oxide proved the presence of the ATB but gave evidences for the existence of the tetragonal hydrogen tungsten bronze (THTB) too (Table I).

Table I

	2θ	$d(\text{\AA}^\circ)$	(hkl)	I/I_0 (%)	ASTM
Hexagonal ATB	39.2	2.296	211	30	5—532
Tetragonal hydrogen tungsten bronze (THTB)	41.78	2.167	201	40	23—1448
$\text{W}_{20}\text{O}_{58}$	40.75	2.211	218, 413	70	5—386
$\text{W}_{18}\text{O}_{49}$	—	—	—	—	5—393

Conclusions on the quantitative relations were drawn on the basis of characteristic lines in the usual manner (see Table II).

Table II

OI	Hexagonal NH_4 -bronze (ATB)	Tetragonal H-bronze (THTB)	$\text{W}_{20}\text{O}_{58}$	$\text{W}_{18}\text{O}_{49}$
2.999	3	8.5	—	—
2.996	2.4	3.5	—	—
2.990	1.5	5.5	—	—
2.986	2.8	6.0	—	—
2.975	3.0	7.0	—	—
2.968	3.2	8.0	—	—
2.947	1.0	7.5	—	—
2.940	2.0	3.5	—	—
2.925	—	7.0	3.5	—
2.912	—	—	7.5	—
2.901	—	—	8.0	—
2.892	—	4.0	10.0	—
2.883	—	—	14.5	—
2.865	—	—	17.0	—
2.853	—	—	9.5	—
2.850	—	—	7.5	strong
2.837	—	—	11.5	medium + weak ph.
2.832	—	—	13.5	weak
2.770	—	—	—	strong

The numbers given for the different phases are the peak height values of the characteristic lines given in Table I.

c) Determination of the nitrogen content by means of activation analysis

The ATB content of the blue oxide can be characterized with its N concentration, though this characterization is not very strict because of the

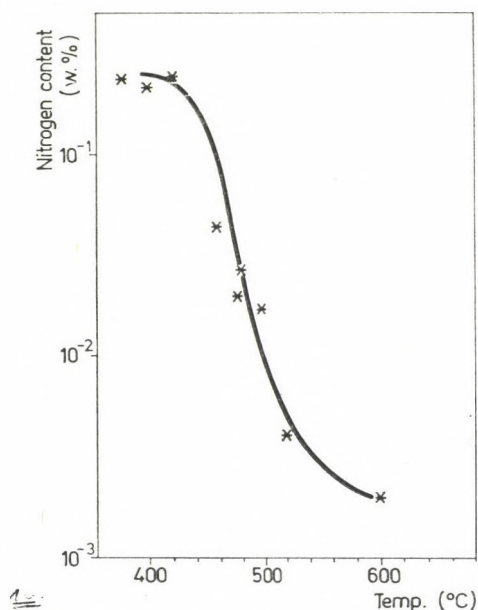


Fig. 7. N-content of the blue oxides as a function of the decomposition temperature

fairly uncertain chemical composition of the ATB [16], similarly to other tungsten bronzes.

The $^{14}\text{N}(\text{d}, \text{p}) \rightarrow ^{15}\text{N}$ reaction has been used and the emitted proton radiation (9 MeV) was selectively measured. Figure 7 shows the dependence of the N content of the blue oxide on the decomposition temperature. After a short, constant region till 400 °C (OI \approx 2.98), the N content drops to 1% of its original value. Mass spectrometry proves the release of NH_3 in the decreasing OI range.

Discussion and Conclusions

The complex study of the blue oxide helps to characterize its composition depending on the temperature of APT decomposition and helps also to understand the role of individual phases in the chemical interaction with aqueous

ionic solutions. As the outer morphology and grain size distribution of blue oxide do not change considerably in the temperature range of its preparation [17], the different properties of blue oxide samples can be well correlated with the components of the solid phase.

On the basis of the experimental results we came to the conclusion that the high chemical activity of blue oxide samples has to be attributed to its bronze phases which are the main components at the reactivity maximum. Some preliminary studies, on the other hand, proved that the pure tungsten oxide compound (WO_3 , $\text{W}_{20}\text{O}_{58}$, $\text{W}_{18}\text{O}_{49}$, WO_2) prepared at high temperatures in closed ampoule [4] showed low chemical reactivity in aqueous ionic solution. The existence of bronze phases is in good agreement with the literature. It has been described by several authors that in the course of thermal decomposition of APT a new, fairly unstable compound, an ammonium tungsten bronze (ATB) can be prepared, and the most probable temperature range of its existence is between 350 and 400 °C [2, 18–20]. Our results proved the existence of the hexagonal ATB but another tetragonal phase also, appeared what we identified as THTB.

The existence range of ATB and THTB agrees well with that of the ion exchange activity. The assumption of the exclusive role of the ATB is contradictory because it gives no explanation to the NH_4^+ ion exchange behaviour of the blue oxide connected with the release of H^+ ions, what was observed earlier [12]. This phenomenon can be understood only by assuming the presence and role of THTB.

The determining role of hydrolysis products in the ion exchange can be excluded because the reaction rate of ion exchange is much higher than that of the hydrolysis and the ion exchange abilities of pure tungsten oxide compounds are much less despite of almost the same degree of their hydrolysis. The components of the blue oxide and not the secondary hydrolysis products are responsible for the chemical interactions.

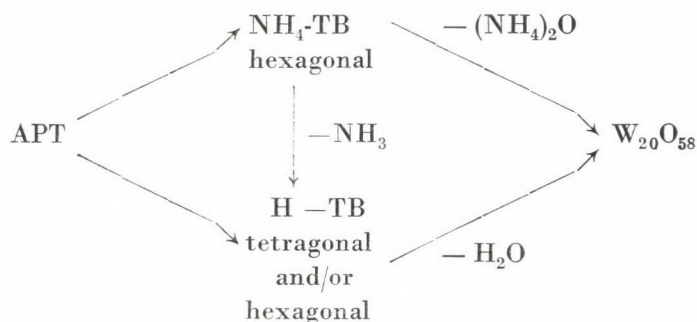
On the other hand, results on vacuum annealed products of blue tungsten oxides produced in different atmospheres showed an increase of their chemical activities (see Table III) preserving basically the hexagonal structure without any change in their THTB contents.

Table III

Vacuum annealing temp. (°C)	original	25 °C	150 °C	250 °C	310 °C 1 hour	310 °C 3 hour
K ⁺ ion exchange (n_{H^+} + mol)	$22.2 \cdot 10^{-6}$	$23.4 \cdot 10^{-6}$	$24.2 \cdot 10^{-6}$	$29.8 \cdot 10^{-6}$	$36.2 \cdot 10^{-6}$	$45.9 \cdot 10^{-6}$

On such indirect basis the existence of a new HTB phase of hexagonal structure can be proposed as a result of "dry" ammonium release (not accompanied by the liberation of equivalent amount of water) — found by means of mass spectrometry during vacuum annealing. The development of this phase may cause only a slight distortion in the hexagonal lattice structure of the ATB as it is the case of HTB and ATB of the same tetragonal structure which is hardly detectable by X-ray methods and it probably seems to be some mixed ATB–HTB phase responsible for the increased chemical activity. NEUGEBAUER *et al.* [2] gave their ATB formula in the form of $(\text{NH}_4)_x \cdot \text{WO}_3 \cdot y\text{H}_2\text{O}$. According to our present knowledge he had probably the same mixed ATB–HTB material, which should have been formulated as $(\text{NH}_4)_x \text{H}_y \cdot \text{WO}_3 \cdot (\text{OH})_y$.

On the basis of our results a question arises about the origin of HTB phases; whether they are decomposition products of APT or they develop directly by the interaction of APT with hydrogen atmosphere. Depending on what is the answer to this question, two mechanisms for the formation of β -tungsten oxide are expected as follows;



To decide what is the real way of decomposition one has to consider that the THTB identified in our samples makes the $\text{APT} \rightarrow \text{THTB}$ route probable, while the proposed new HHTB is an indication in favour of the route shown by dashed line. The ATB–HTB mixed phase of hexagonal structure might decompose either after a certain NH_3 loss to tetragonal HTB or losing all of its NH_3 and or H_2O content to β -tungsten oxide.

This type of explanations seems to be valid despite to some literature indications reporting only ATB [21] or even no bronze phase at all [22] in reduction intermediate products of APT. The mechanism of the development and decomposition of the bronzes has to be clarified also by other methods.

The present model of the blue oxide enables us to explain the variable behaviour of products prepared under industrial conditions and found to be identical tested with usual methods. According to the maximum character of the reactivity curves slight changes in the temperature of the thermal decom-

position may result great changes in the ATB/HTB ratio without having any considerable change of the OI.

We have applied most of our measurements described above for several accidental industrial samples. The results are summarized in Fig. 8. It can definitely be seen that the K^+ ion exchange deviations of these samples can

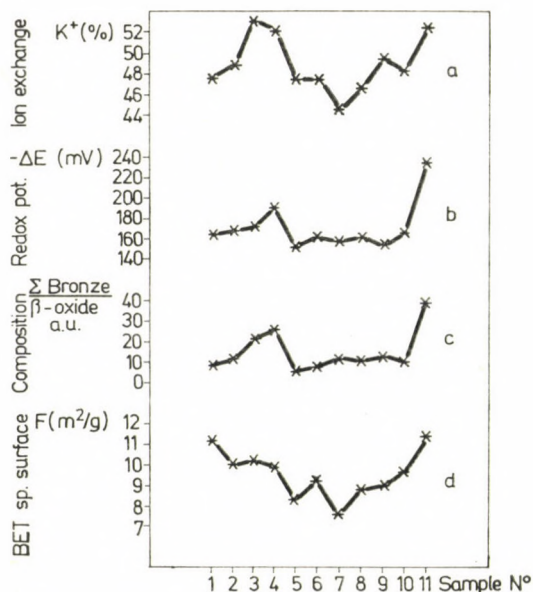


Fig. 8. Characteristic values of industrial samples

be correlated to the ratio; sum of bronze content: β -tungsten oxid, and to the reduction ability (redox potential decrease) too. In comparison to these parameters the differences in specific surface are less determining factors. For characterization of blue oxide samples the phase analysis and the electrochemical behaviour seem to be fundamental, and for a satisfactory production control the combination of several methods should be applied.

*

The authors are indebted to Prof. T. MILLNER, Dr. J. NEUGEBAUER and L. VARGA for fruitful discussions.

REFERENCES

- [1] HEGEDÜS, A. J., MILLNER, T. et al.: Z. anorg. allg. Chem., **281**, 64 (1955)
- [2] NEUGEBAUER, J., HEGEDÜS, A., MILLNER, T.: Z. anorg. allg. Chemie, **302**, 50 (1959)
- [3] NEUGEBAUER, J.: Dissertation 1971, Budapest p. 15
- [4] GADO, P.: Cand. Dissertation 1970, Budapest
- [5] MEEL, F. A. M. M., VERHEIJEN, A. W. J.: Spring Meeting Metallurgical Society of AIME, Boston (1972) Lect. 317

- [6] BARTHA, L., SZALAY, T.: Acta Techn. Acad. Sci. Hung., **78**, 309 (1964)
- [7] SZALAY, T., BARTHA, L.: Z. phys. Chem., **255**, 974 (1974)
- [8] SZALAY, T., BARTHA, L.: Z. phys. Chem., **255**, 981 (1974)
- [9] SZALAY, T., BARTHA, L.: Magyar Kémiai Folyóirat, **81**, 67 (1975)
- [10] SZALAY, T., BARTHA, L., NÉMETH, T.: Magyar Kémiai Folyóirat, **82**, 135 (1976)
- [11] SZALAY, T., BARTHA, L., NÉMETH, T., LENGYEL, J.: React. of Solids, **1977**, 449
- [12] SZALAY, T.: Cand. Thesis (1977) Debrecen
- [13] CHOAIN, C., MARION, F.: Bull. Soc. Chim., **1963**, 212
- [14] KISS, B. A.: TUNGSRAM Techn. Mitt., **35**, 1465 (1977)
- [15] KISS, B. A.: Acta Chim. (Budapest) **84**, 393 (1975)
- [16] KISS, B. A.: Cand. Thesis (1973) Budapest
- [17] KISS, B. A., NÉMETH, T., et al.: J. Materials Science (In press)
- [18] GIER, T. E., PLASE, D. C., et al.: Inorg. Chem., **7**, 1646 (1968)
- [19] DICKENS, P. G., HALLIWELL, A. C., et al.: Trans. Faraday Soc., **67**, 794 (1971)
- [20] HAGENMÜLLER, P.: in Comprehensive Inorganic Chemistry, Vol. **4**, 541 (1973)
- [21] DAHL, M.: Proc. 5th Eur. Symp. on Powder Met. Stockholm, **2**, 143 (1978)
- [22] BASU, A. K., SALE, F. R.: Modern Dev. in Powder Met. Vol. **9**, (1977) 171. Am. Powder Met. Inst. (Ed. HAUSNER, H.).
- [23] HEGEDÜS, A.: Dissertation 1972, Budapest, p. 29.

László BARTHA Tibor NÉMETH András SALAMON	}	H-1325 Budapest, Újpest 1. P.O.B. 76.
Gyula GYARMATI András B. KISS	}	H-1044 Budapest, Váci út 77.
Tibor SZALAY		H-4010 Debrecen, Kossuth Lajos u. 1.

INVESTIGATION OF THE ATOMIZATION PROCESSES OF TIN IN VARIOUS ATOMIZERS AND OF THE INTERFERENCE BY COPPER

E. G. HARSÁNYI, L. PÓLOS and E. PUNGOR

*(Institute for General and Analytical Chemistry,
Technical University, Budapest)*

Received July 10, 1978

Accepted for publication September 10, 1978

The atomization processes of tin were investigated in acetylene-air, acetylene-nitrous oxide, premixed hydrogen-air and diffusion hydrogen-(nitrogen) entrained air flames. It was stated that the chemical reaction with hydrogen radicals plays an important part in the formation of free tin atoms.

The interference by the copper matrix and anions with tin determination was also investigated in flames and in graphite furnace. It could be established that in solutions containing hydrochloric acid copper catalyzes the oxidation of tin.

In recent years several authors paid attention to the interpretation of the special behaviour of tin when it was determined in different flames and electrothermal atomizers. The investigations were directed to the excitation and atomization processes of tin [1, 2, 3, 4, 5], and to the discussion of the numerous interfering effects occurring in atomic absorption determinations [1, 6, 7, 8, 9]. In some other papers the analytical application of AAS methods for the determination of tin [10-18] in various flames and graphite atomizers have been dealt with.

In this work it is intended to add to the earlier experience our results connected with the determination of tin by flame and by flameless AAS methods. Our analytical task was the determination of tin in high purity copper. In connection with this problem we wanted to elucidate and interpret the atomization processes of tin in various flames and in the graphite atomizer.

A special enhancing effect of the copper matrix was observed on the absorbance of tin, therefore the investigation of the interference by copper was also necessary.

The atomization of tin proved to involve different processes in acetylene and hydrogen flames and in the graphite tube. These atomizers will be discussed separately, the interfering effect of copper in all the atomizers will be discussed at the end of the paper.

Experimental

Apparatus

A VARIAN TECHTRON MODEL AA6 atomic absorption spectrometer was used for the absorption and emission measurements. The absorbance of tin was measured at 286.3 nm in order to avoid the nonspecific absorbance occurring at the 224.6 nm line.

The emission of tin monoxide was measured at 348.4 nm, the atomic emission of tin at 284 nm, the emission of tin hydride at 609.5 nm, and the band absorption of tin chloride at 226.9 nm, respectively.

Acetylene-air, acetylene-nitrous oxide, hydrogen-air, and diffusion hydrogen flames were used.

A VARIAN MODEL CRA 63 electrothermal atomizer was used for the flameless AAS determinations with the graphite tube version. 5 μ l portions of solution were pipetted and nitrogen sheath gas was applied with hydrogen added.

Reagents

Tin stock solution was prepared by dissolving metallic tin of high purity in hydrochloric acid. The concentration of the stock solution was 1000 μ g/ml. Working solutions were diluted from the stock solution and contained also 1 w/v% hydrochloric acid.

Emission and band absorption measurements were carried out with tin solutions of 10,000 μ g/ml and 50,000 μ g/ml concentrations in hydrochloric acid.

Results and Discussion

Atomization of tin in acetylene flames

The absorbance of tin was measured by varying the flame composition and the flame height in acetylene-air and acetylene-nitrous oxide flames.

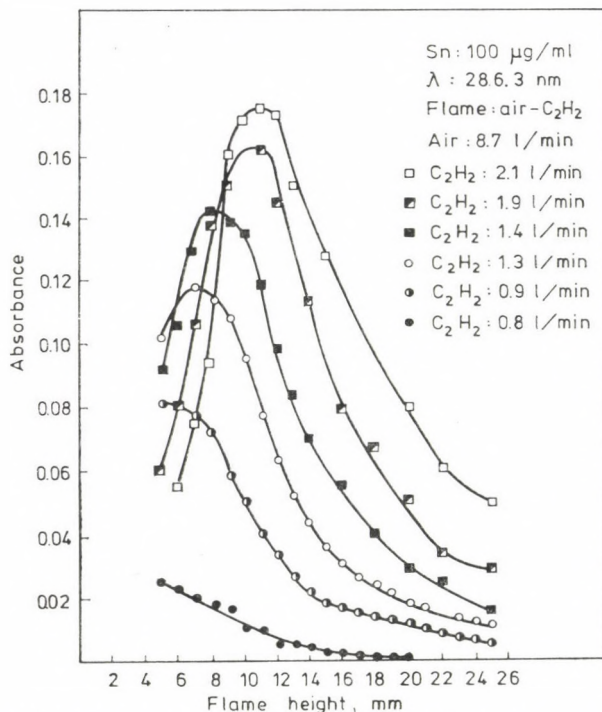


Fig. 1. The change in absorbance of Sn as function of the flame height at various flame compositions in acetylene-air flame

(The flame height is the distance between the burner head and the center of the light beam of the hollow cathode lamp above the burner head. Below 5 mm flame height the burner covers a part of the light beam, therefore determinations can only be done above this height.)

The flame height was varied from 5 to 25 mm. The variation of flame composition was carried out by keeping the flow rate of air constant (8.7 l/min)

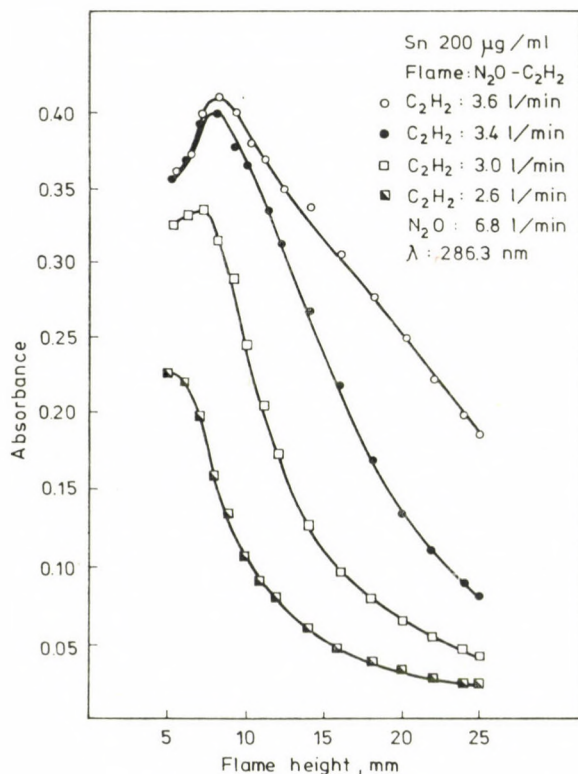


Fig. 2. The change in absorbance of Sn as function of the flame height at various flame compositions in acetylene-nitrous-oxide flame

in order to obtain the same aspirating rate, and varying the flow rate of acetylene. The change in absorbance as function of the flame height (absorbance distribution) measured at various flame compositions in acetylene-air flame is shown in Fig. 1, while that in acetylene-nitrous oxide flame in Fig. 2.

It can be seen from the figures that the more reducing (fuel rich) the flame, the higher absorbance can be achieved at a given flame height above the reaction zone. In oxidizing (fuel lean) flames the absorbances are much lower than in reducing flames. This fact can be attributed to the formation of stable oxides. In order to support this assumption we measured the emission distribution of the SnO species at 248.4 nm.

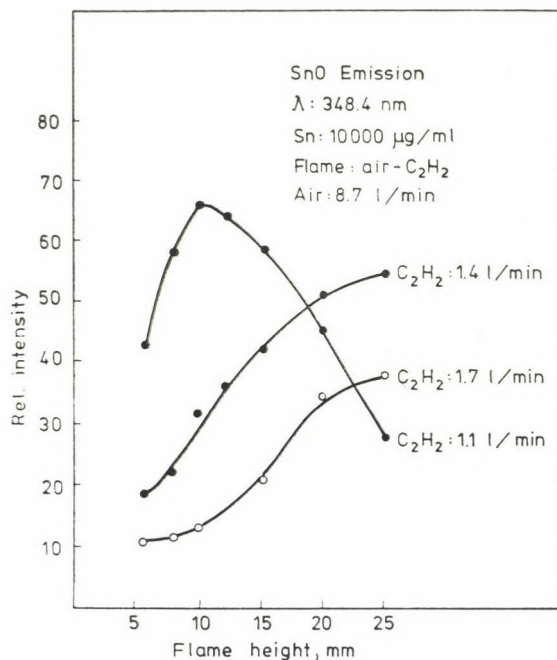


Fig. 3. Emission distribution of SnO in acetylene-air flame

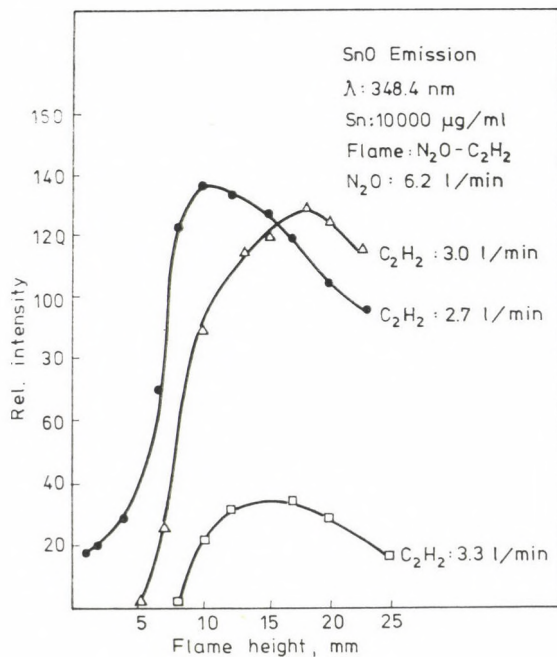


Fig. 4. Emission distribution of SnO in acetylene-nitrous-oxide flame

Figure 3 shows the emission distribution of SnO in acetylene–air flame and Fig. 4 that in acetylene–nitrous oxide flame. In an oxidizing flame significant SnO band emission can be measured even at lower flame heights, in a reducing flame the SnO band emission can be measured only at higher flame heights, where the absorbance of tin decreases. In acetylene–air flame the temperature distribution as the function of the flame height was determined at different flame compositions by the line reversal method (Fig. 5).

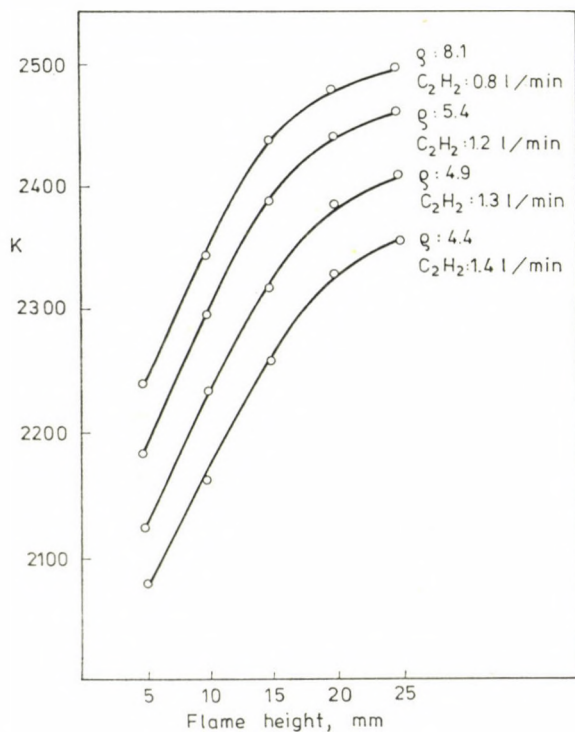


Fig. 5. Temperature distribution as function of the flame height at various flame compositions

$$\left(q = \frac{\text{flow rate of air}}{\text{flow rate of acetylene}} \right)$$

This measurement was necessary in order to find out whether there exists any correlation between free atom concentration and temperature distribution. In reducing flames, where tin can be determined with a higher sensitivity, the temperature is lower than in oxidizing flames. Tin atoms can be formed not only by thermal dissociation of the SnO species, but by chemical reduction due to the reducing components in the flame, e.g. C, CH, H radicals. The dissociation energy of SnO is 5.3 eV. The absorbance does not increase with increasing temperature which indicates that the dissociation does not

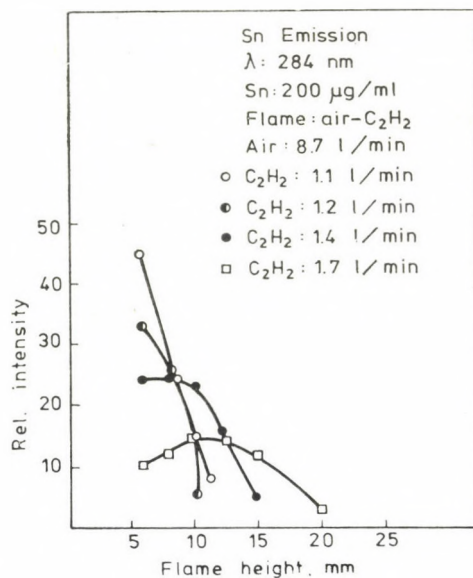


Fig. 6. Emission intensity of Sn as function of the flame height at various flame compositions in acetylene-air flame

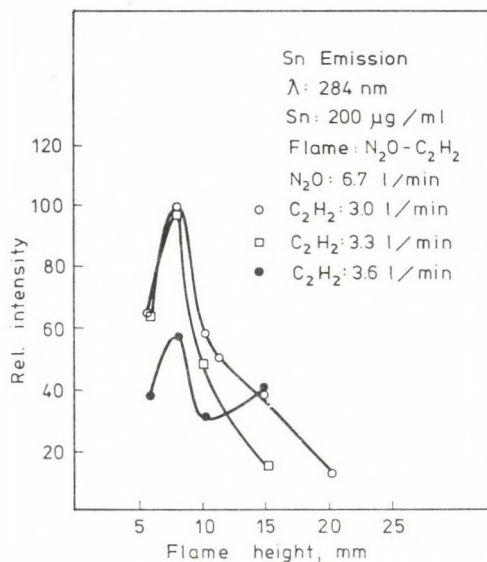


Fig. 7. Emission intensity of Sn as function of the flame height at various flame compositions in acetylene-nitrous oxide flame

take place appreciably. The formation of Sn atoms by chemical reactions has been described in the literature. The supposed reactions are as follows :

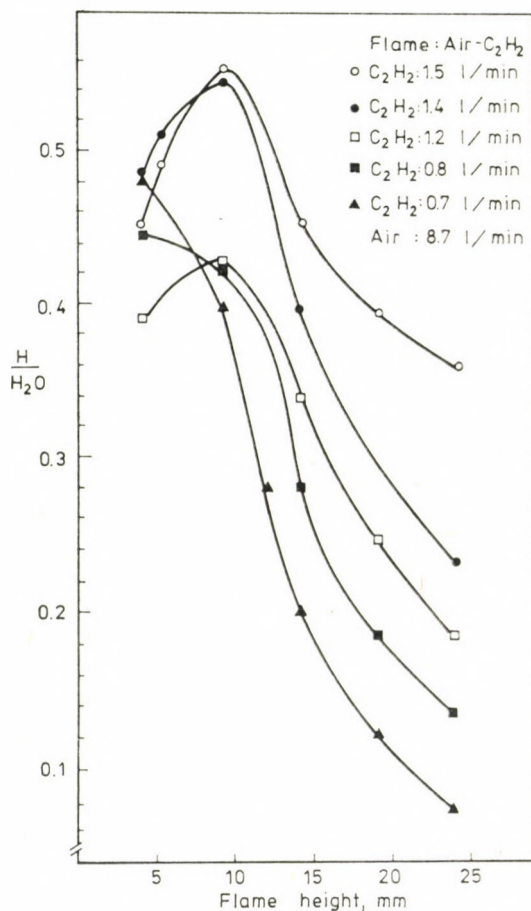
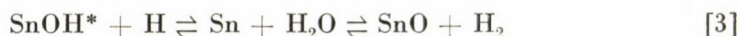
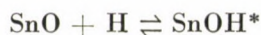


Fig. 8. $\text{H}/\text{H}_2\text{O}$ ratio distribution in acetylene-air flame

The production of the Sn atoms through chemical reaction can be explained by measuring the Sn emission in acetylene flames. The emission of Sn can be measured at the lower flame zones, where chemiluminescence excitation takes place [4]. We determined the emission distribution of Sn at 284 nm as function of the flame height at different flame compositions in C_2H_2 -air (Fig. 6) and C_2H_2 - N_2O (Fig. 7) flames as well. In acetylene flames at the lower flame zones

where the Sn emission is measurable SnO species can not be formed in a great concentration. It is formed only in the higher flame zones where the concentration of the reducing components of the flames is lower.

The reducing character of flames can be characterized by measuring the H radical distribution in the flame. The distribution of the H/H₂O ratio in acetylene–air flame was determined by the lithium hydroxide method [19],

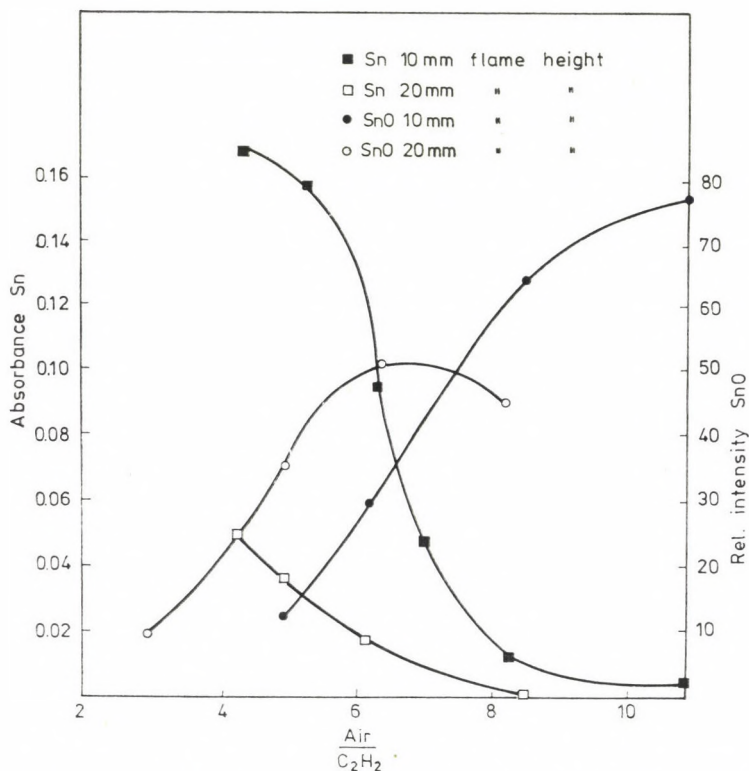


Fig. 9. Sn absorbance and SnO emission intensity as function of the flame composition at two flame height values

as function of the flame height at different flame compositions. The curves describing the H/H₂O distribution can be seen in Fig. 8. Since the H₂O concentration in a flame is much higher than the H radical concentration and its change is negligible, the change in the H/H₂O ratio characterizes the change in the H radical concentration. In acetylene–air flame the H/H₂O distribution and the absorbance distribution show similar character, as can be seen by comparing Figures 1 and 8.

HALLS [20] also reports on the relationship between the H radical concentration and the absorbance distribution in the case of elements forming refractory oxides.

The higher the H radical concentration, the higher is the absorbance of tin. The highest sensitivity can be obtained in a reducing flame. In an oxidizing flame the highest tin absorbance and the highest H radical concentration could be measured at low flame heights (5 mm).

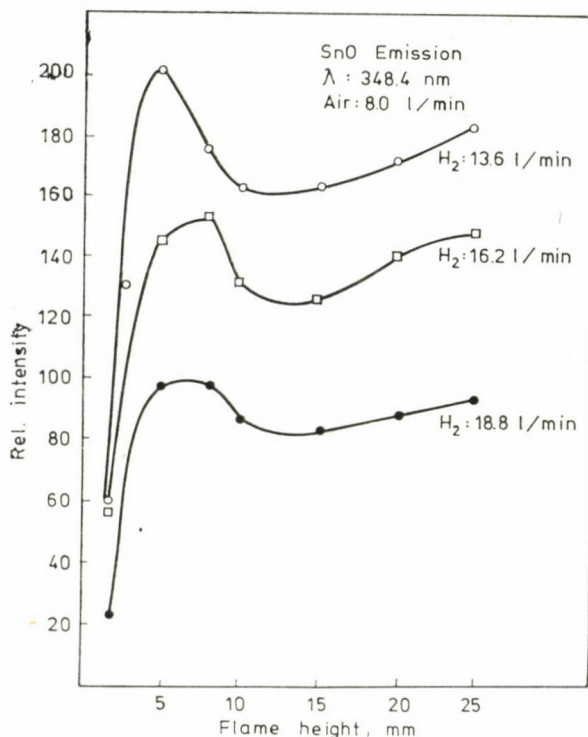


Fig. 10. SnO emission intensity as function of the flame height at different flame composition in hydrogen-air flame

In Fig. 9 the tin absorbance and SnO emission are plotted as function of the flame composition $\left(\varrho = \frac{\text{air flow rate}}{\text{C}_2\text{H}_2 \text{ flow rate}} \right)$ at two flame heights.

In this figure we can follow the reverse tendency of the formation of free Sn atoms and SnO species. Summarizing our results it can be stated that in acetylene flames tin atoms are formed by chemical reactions at the lower flame zones. On increasing the reducing character of the flame, the concentration of the free tin atoms increases. The SnO formation becomes more probable at a flame height where the absorbance of tin decreases. In oxidizing flames the SnO formation takes place already in the lower flame zones.

Atomization of tin in hydrogen flames

In hydrogen flames the highly reducing H radicals might play a significant role in the atom formation. In air-hydrogen and hydrogen diffusion flames the sensitivity of the determination of tin is about five times higher than in acetylene flames. SnO emission could be observed by us only in air-hydrogen flame. The SnO emission intensity is plotted in Fig. 10 as function of the flame

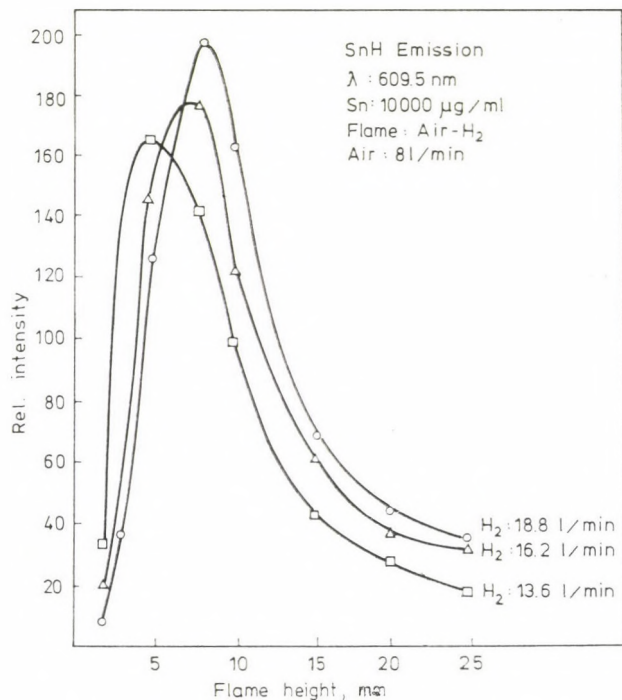


Fig. 11. SnH emission intensity as function of the flame height at various flame compositions in hydrogen-air flame

height at different flame compositions. Our results were similar to those obtained by BULEWICZ [3] who investigated the tin atomization in a flame of similar type but with another burner head. Sample introduction was carried out partly by aspirating a concentrated tin solution and partly by introducing dry SnCl₄ vapour into the flame. The aim of the investigations of BULEWICZ was to study the spectrochemical behaviour of tin and not a chemical analysis. Some authors suppose [6] that there is a relationship between the atom formation of tin and the tin hydride formation in hydrogen flames. Hydrides are readily formed in the presence of high H radical concentration. In both flames investigated the SnH distribution was determined at 609.5 nm as function of the flame height at various flame compositions (Fig. 11, Fig. 12) and compared

with the absorbance distribution measured in these flames. The absorbance values plotted as function of flame height at various flame compositions can be seen in Figures 13 and 14 in hydrogen–air and hydrogen–nitrogen entrained air flames, respectively. Comparing the absorbance distribution in the two hydrogen flames it can be stated that the maxima of the curves in hydrogen–air flame are shifted to the higher flame zones on increasing the reducing character of the flame. In contrast with diffusion hydrogen flame the maxima are at the

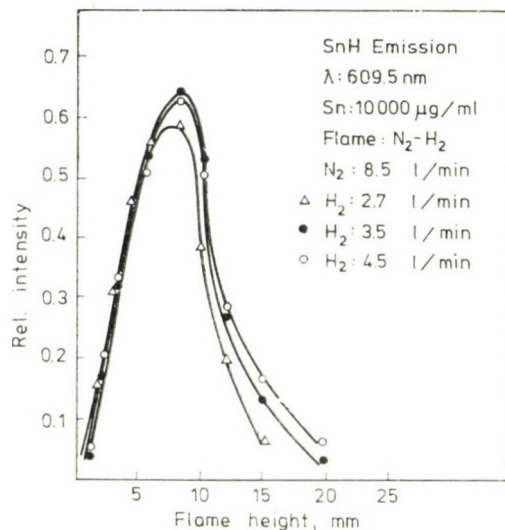
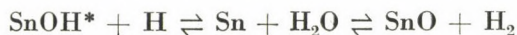


Fig. 12. SnH emission intensity as function of the flame height at various flame compositions in hydrogen- (nitrogen) entrained air flame

same flame height due to the slower recombination reactions of the H radicals.

Tin absorbance and tin hydride distribution curves show similar shapes in the same flame and the maxima can be found at the same flame height and flame composition. It seems possible that tin atoms are formed after the formation and dissociation of the SnH species. The dissociation energy of SnH is 2.7 eV. Because of the low dissociation energy SnH dissociates easily even in cool flames. The maximal temperature of air–hydrogen flame is about 2300 K [24]. The temperature of hydrogen diffusion flame at 10 mm flame height is 280 °C and at the edge at the same flame height 830 °C [25].

These measurements support the assumption of NAKAHARA [6] who supposes the formation of free Sn atoms through SnH production. According to BULEWICZ [3] SnO is reduced in hydrogen–air flame to tin atoms by H radicals in the following reactions;



We could determine SnO species in hydrogen–air flame and the curves obtained seem to be in good agreement with the equations. The SnO species (Fig. 10)

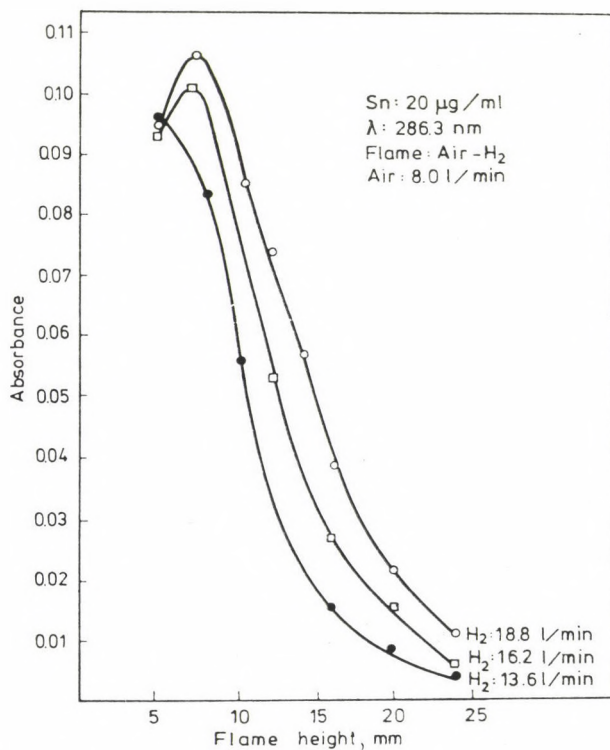


Fig. 13. Absorbance of Sn as function of flame height at various flame compositions in hydrogen–air flame

shows higher emission intensity at lower flame heights indicating the presence of SnO. The SnO emission decreases at flame heights where the absorbance of tin and the emission of SnH increase. Higher flame zones become again more favourable to SnO formation.

According to our experimental results in hydrogen flames the atomization process of tin is connected with the formation and dissociation of SnH. In hydrogen–air flames a more complicated atomization process can take place involving the reduction of the oxide and dissociation of salt.

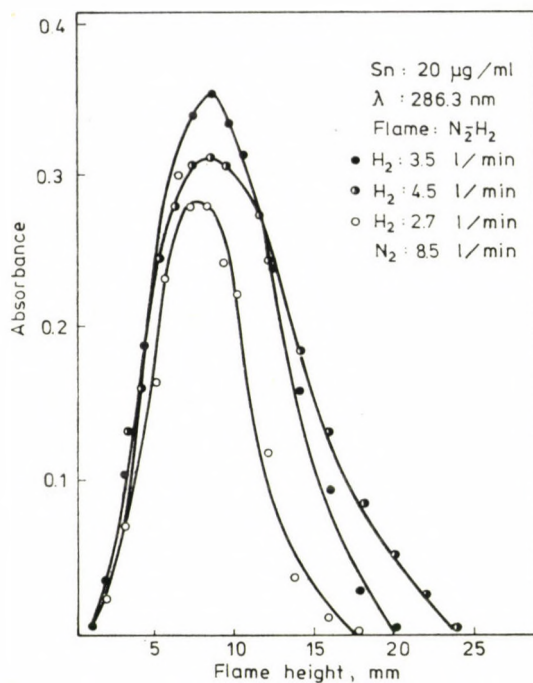


Fig. 14. Absorbance of Sn as function of flame height at various flame compositions in hydrogen-(nitrogen) entrained air flame

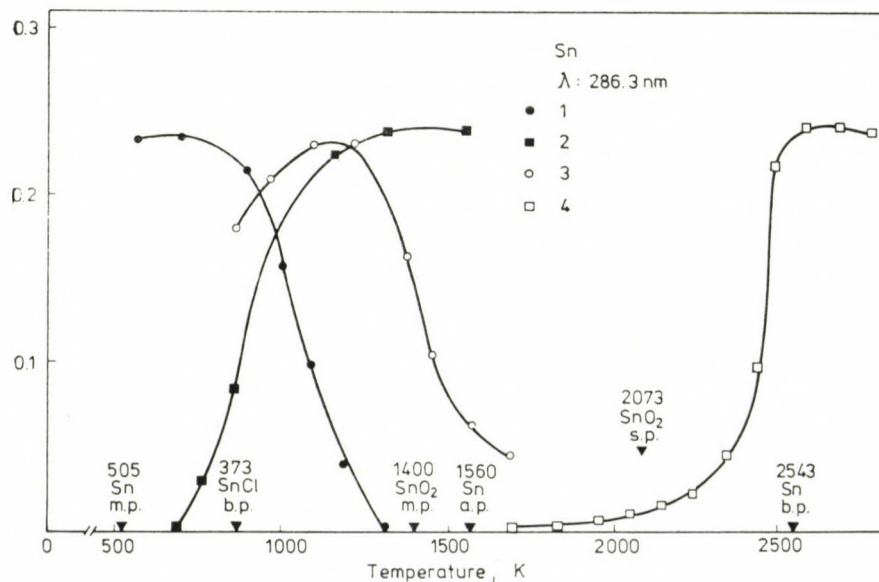
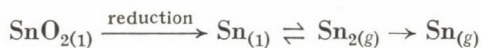


Fig. 15. Double curves of Sn in hydrochloric acid (1: pyrolysis curve, 2: atomization curve) and in sulphuric acid (3: pyrolysis curve, 4: atomization curve)

The atomization of tin in graphite furnace

The most probable reaction for Sn atom formation in the graphite furnace according to STURGEON and coworkers [21] is the reduction of SnO_2 by graphite.



This process can only be assumed for sample solutions containing oxianions (sulphate).

In solutions containing hydrochloric acid chlorides are formed in the condensed phase and tin atoms are resulted by the dissociation of chlorides in the gas phase. The different atomization processes can be experimentally proved by plotting the double curves suggested by WELZ [22] in sulphuric acid and in hydrochloric acid media. The results of our measurements are shown in Fig. 15. In hydrochloric acid medium the appearance temperature of tin is much lower than in sulphuric acid solution because of the evaporation in the form of chloride. The appearance temperature is the temperature at which the first atomization signal appears [23].

The evaporation in chloride form could be experimentally evidenced by measuring the SnCl absorption at a wavelength of 226.9 nm using the VARIAN CRA 63 graphite atomizer in RAMP heating mood. Five μl tin solution of 50,000 $\mu\text{g/ml}$ concentration was introduced into the graphite tube. The absorbance was measured by using the H_2 lamp applied for background correction.

The absorbance signal as function of the heating time can be seen in Fig. 16. The heating temperature correlated with the heating time was not measured thus only qualitative conclusions could be drawn. The SnCl absorbance signal can be obtained already at the beginning of the heating yielding a double peak. This can be explained by the evaporation of Sn in the form of SnCl_4 (boiling point 114 °C) and in the form of SnCl_2 (boiling point 614 °C). It must be mentioned that the two processes: the evaporation in chloride form and the reduction of $\text{SnO}_{2(1)}$ to $\text{Sn}_{(1)}$ may take place simultaneously.

In dilute hydrochloric acid medium also tin oxide is present due to hydrolysis of tin chloride.

Investigation of the interference by copper with tin determination

When tin is determined in copper matrix the absorbance signal of tin shows a significant enhancement depending on copper concentration. We measured the absorbance of tin at various copper concentrations in four different flame types and plotted the relative absorbance change as function of the copper concentration (Fig. 17). Copper was added to the hydrochloric acid-containing tin solution of constant concentration as the chloride. The interference

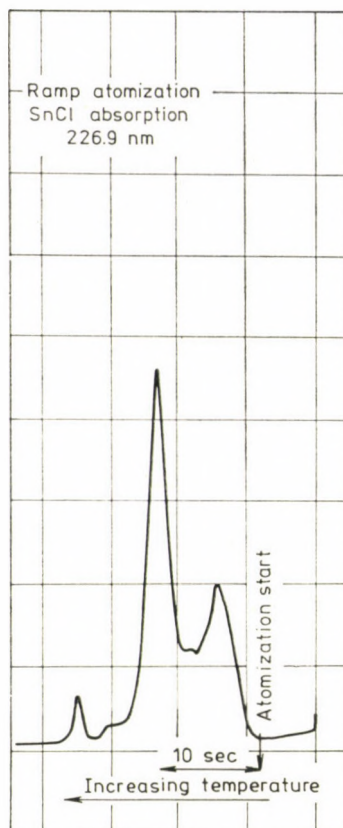


Fig. 16. SnCl absorbance signal shape in the course of the heating period with CRA graphite atomizer. Ramp atomization

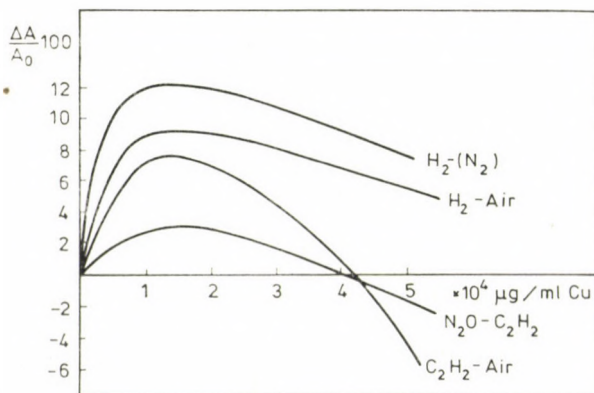


Fig. 17. Effect of copper matrix on the tin signal in different flames

was more significant in hydrogen flames. The same type of interference could be observed with the graphite tube method (Fig. 18). Five μl of tin solution of 5 $\mu\text{g}/\text{ml}$ concentration were pipetted into the graphite tube. Copper chloride was mixed to the tin solution in increasing concentrations. The absorbance increased up to 0.1% copper concentration (1000 $\mu\text{g}/\text{ml}$) and above this concentration a significant decrease in absorbance could be measured. This decrease can be explained by assuming that the dissociation of tin chloride is suppressed by the excess of chlorine originating from the copper chloride.

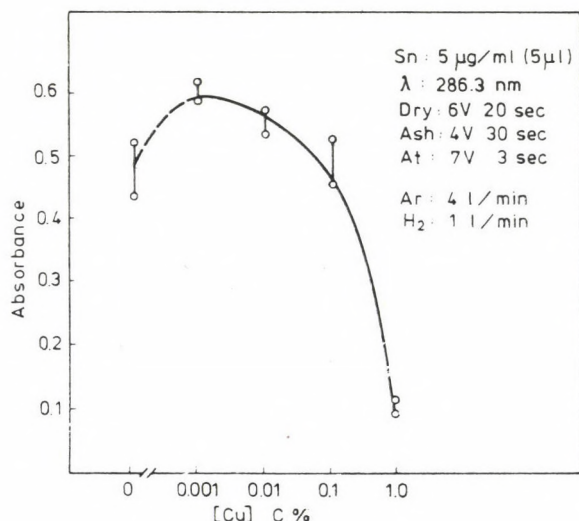


Fig. 18. Effect of copper matrix on the tin signal in graphite atomizer

The increase in absorbance in the presence of copper chloride can be explained by assuming that the vaporization of tin is facilitated in the presence of copper. In condensed phase in the redox reaction;



tin(IV) chloride molecules can be formed, the volatility of which is higher than that of the tin(II) chloride. SnCl_4 formation could also be assumed in the course of the following experiment SnCl absorption was measured at a wavelength of 226.9 nm as function of the heating time in tin(II) chloride solution already demonstrated in Fig. 16. When the solution contained also copper(II) chloride (Fig. 19), the first peak on the absorbance signal increased significantly. The first peak corresponds to a lower vaporization temperature, and it can be attri-

buted to the evaporation of Sn(IV) chloride. The absorbance of the pure Cu(II) chloride solution was also measured in order to detect and separate the signal originating from the copper(II) chloride matrix.

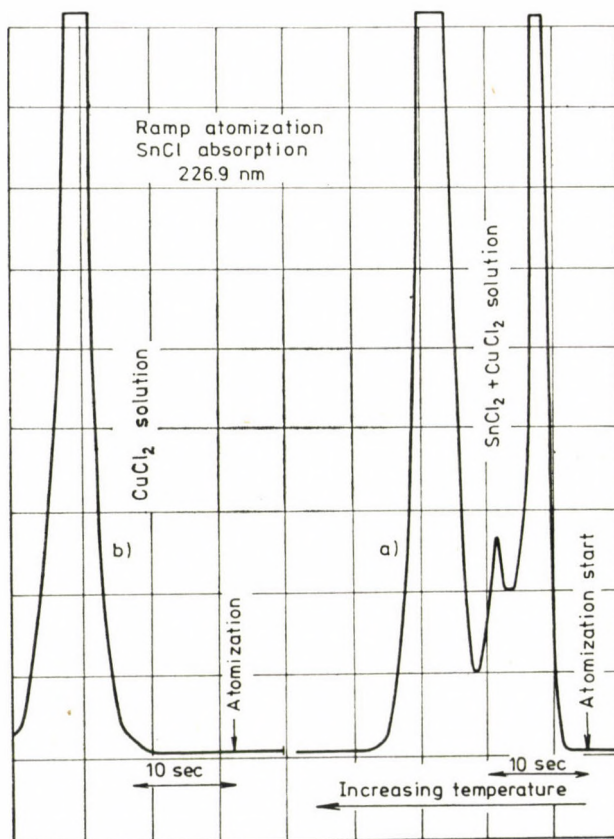


Fig. 19. SnCl absorbance signal shape in the atomization period using the CRA graphite atomizer. Ramp atomization. a) Solution containing SnCl_2 and CuCl_2 pipetted into the tube. b) CuCl_2 solution pipetted into the tube

Conclusions

In our work we tried to explain the atomization processes of tin in four flame types, acetylene-air acetylene-nitrous oxide, hydrogen-air, hydrogen diffusion flame and in graphite tube as well. We determined the flame profiles (*i.e.* the absorbance distribution) in the flames investigated and followed the emission distribution of some species influencing the atomization of Sn in these flames (SnO , SnH , H radical, Sn). The SnO emission measurements in acetylene flames have shown that Sn atoms can not be formed by the thermal dissocia-

tion of SnO, but in a chemical reaction of SnO with reducing flame components in the low flame zones. In higher flame zones the SnO formation is favoured. Sn emission measurements in acetylene flames showed the formation of excited Sn atoms by chemiluminescent excitation too.

In hydrogen flames SnH seems to be a predominating species, however in air-H₂ flame SnO is also formed.

In graphite tube the atomization process of Sn may be different depending on the anions present in the test solution. In a solution containing oxianions Sn atoms are formed by reduction by graphite and in solutions containing hydrochloric acid the main atomization reaction is the evaporation in chloride form and the dissociation of chlorides in the gas phase.

The interfering effect of copper chloride with the tin absorbance can be explained by the production of SnCl₄. This is a more volatile species than SnCl₂.

REFERENCES

- [1] RUBEŠKA, I.: *Spectrochim. Acta*, **29B**, 263 (1977)
- [2] VICKERS, T. J., COTTRELL, C. R., BRAKEY, D. W.: *Spectrochim. Acta*, **25B**, 437 (1970)
- [3] BULEWICZ, E. M., PADLEY, P. J.: *Trans. Faraday Soc.*, **67**, 2337 (1971)
- [4] GIBSON, I. H., GROSSMAN, W. E. L., COOKE, W. D.: *Anal. Chem.*, **35**, 266 (1963)
- [5] L'VOV, B. V., KATZKOV, D. A., KRUGLIKOVA, L. P., ORLOV, N. A., POLZIK, L. K.: *Zsurn. Anal. Chim.*, **XXX**, 1861 (1975)
- [6] NAKAHARA, T., MUNEMORI, M., MUSA, S.: *Anal. Chim. Acta*, **62**, 267 (1972)
- [7] JULIANO, P. O., HARRISON, W. W.: *Anal. Chem.*, **42**, 84 (1970)
- [8] BALLA, K. Z., HARSÁNYI, E. G., PÓLOS, L., PUNGOR, R.: *Microchim. Acta*, **1**, 107 (1975)
- [9] RUBEŠKA, I., MIKŠOVSKY, M.: *Atomic Absorption Newsletter*, **11**, 57 (1972)
- [10] GATEHOUSE, B. M., WILLIS, J. B.: *Spectrochim. Acta*, **17**, 710 (1961)
- [11] ALLAN, J. E.: *Spectrochim. Acta*, **18**, 259 (1962)
- [12] AGAZZI, E. J.: *Anal. Chem.*, **37**, 364 (1965)
- [13] BOWMAN, J. A.: *Anal. Chim. Acta*, **42**, 285 (1968)
- [14] CAPACHO-DELGADO, L., MANNING, D. C.: *Spectrochim. Acta*, **22**, 1505 (1966)
- [15] MCGEE, W. W., WINEFORDNER, J. D.: *Anal. Chim. Acta*, **37**, 429 (1967)
- [16] DAGNALL, R. M., FLEET, B., RISBY, T. H., DEANS, D. R.: *Talanta*, **18**, 155 (1971)
- [17] HEADRIDGE, J. B., SOWERBUTTS, A.: *Analyst*, **97**, 442 (1972)
- [18] TRACHMAN, H. L., TYBERG, A. J., BRANIGAN, D.: *Anal. Chem.*, **49**, 1090 (1977)
- [19] PUNGOR, E.: *Flame Photometry Theory*, Akadémiai Kiadó, Budapest 1967
- [20] HALLS, D. J.: *Anal. Chim. Acta*, **88**, 69 (1977)
- [21] STURGEON, R. E., CHAKRABARTI, C. L., LANGFORD, C. H.: *Anal. Chem.*, **48**, 1792 (1976)
- [22] WELZ, B.: Paper presented at the XVII. CSI (1973)
- [23] CAMPBELL, W. C., OTTAWAY, J. M.: *Talanta*, **21**, 837 (1974)
- [24] KIRKBRIGHT, G. F., SARGENT, M.: *Atomic Absorption and Fluorescence Spectroscopy*, Academic Press London, New York, San Francisco 1974
- [25] DAGNALL, R. M., THOMPSON, K. C., WEST, T. S.: *Analyst*, **92**, 506 (1967)

Etelka GRÁF-HARSÁNYI
László PÓLOS
Ernő PUNGOR

H-1111 Budapest, Gellért tér 4.

NEUERE ÜBERWACHUNGSMETHODEN IN DER GERBERECHEMIE, I

G. TÓTH,¹ J. VAJDA¹ und V. PÓSA²

(¹Pécsér Lederfabrik, Forschungsinstitut f. Leder,² Kunstleder und Schuhe, Budapest)

Eingegangen am 5. Juli 1978

Zur Veröffentlichung angenommen am 15. September 1978

In der ersten Teil werden neuere Überwachungsmethoden behandelt, die in Großgerbereien zur Kontrolle der Wasserwerkstätten anwendbar sind. Es wird nachgewiesen, daß angetrocknete gesalzene Rohhäute bedeutend langsamer aufweichen trotzdem, daß das Herauslösen des Salzes nicht verhindert wird. Zur Kontrolle der Weiche eignet sich die Bestimmung des wasserfreien Hautmaterials besser als das früher angewandte Weichgewicht. Die Wirkung des Äschers geschieht durch die Bestimmungen der Na_2S -Konzentration, $\text{SH} : \text{OH}$ Verhältnis, Prallfestigkeit sowie durch die Kontrolle der haarlösenden Wirkung und Eiweißverlust. Es werden Zusammenhänge zwischen Eiweißverlust und Prallfestigkeit, weiter die Bindung und Auswaschbarkeit von verschiedenen Basen diskutiert. Orientierungsversuche wurden durchgeführt über die Schwächung bzw. totale Zerstörung der Zone der Haarwurzel in *konc.* Na_2S -Lösungen, die wegen der Losnarbigkeit des Fertigleders wichtig sind.

Die Gerbereien haben sich in unserem Lande in den letzten 30 Jahren zu großen Lederwerken entwickelt. Dieser Prozeß hat die Notwendigkeit einer Neuorganisation der Qualitätskontrolle mit sich gebracht, was leicht verständlich ist, wenn man in Betracht zieht, daß die Rohhaut wenigstens 30 Arbeitsphasen bis zum Fertigleder durchläuft [1], und die Qualität in großem Maße von der Betriebsüberwachung abhängt. In den heutigen Großbetrieben sind die technischen Leiter nicht mehr imstande, alles selber zu überwachen, und sind auf ein wirksames Kontrollsystem angewiesen [2].

Die Kontrolle ist bei denjenigen Arbeitsphasen verhältnismäßig leicht, wo die Qualität des Leders gleich nach der Beendigung der Arbeit zu kontrollieren ist. Schwieriger ist aber dies, wenn man die Güte der beendeten Arbeitsphase nur am fertiger Leder beurteilen kann. So kann z.B. nur im fertigen Zustand endgültig entschieden werden, ob die Blößen im Äscher genügend aufgeschlossen waren und infolgedessen das Oberleder weich genug geworden ist.

Die Betriebsüberwachung ist umso wirkungsvoller, je eingehender und bewußter die Beschreibung der Technologie ist. Wir meinen damit, daß die Wirkungen der einzelnen Arbeitsphasen und Chemikalien auf die Qualität des Fertigleders aufgeklärt und bekannt sind. Deswegen befassen wir uns im folgenden mit diesen Problemen.

Während der letzten Jahrzehnte haben wir mehrere Überwachungsmethoden ausgearbeitet, und im vorigen Jahre wurde in der Pécsér Leder-

fabrik die Betriebsüberwachung bei folgenden Arbeitsphasen planmäßig eingeführt ;

Weichen, Äscherung, Entkalkung, Pickel, Chromgerbung, Entfettung, Entsäuerung, Zurichtung sowie Kontrolle der Hautfehler, Deckfilmeigenschaften, Festigkeitseigenschaften der Blöße, Biegungselastizität der Leder im nassen und trockenem Zustand, Abriebfestigkeit von Sohlenleder. Diese Methoden sollen im folgenden vom Standpunkt der Qualitätskontrolle aus besprochen werden.

Kontrolle der Weiche

Zweck der Rohhautweiche ist, daß der Wassergehalt der frisch abgezogenen Haut erreicht wird. Deswegen muß das Konservierungssalz zum größten Teil entfernt werden. Die Entfernung hängt

von der Menge und Temperatur des Wassers,
die Zeitdauer des Waschens,
der mechanischen Bewegung und
vom Feuchtigkeitsgehalt der Rohhaut ab.

Bei frisch gesalzenen Rohhäuten ist die Weiche bei dreimaligem Wasserwechsel meistens in 6—8 Stunden beendet. Angetrocknete Rohhäute weichen langsamer auf.

Die Weiche pflegt man durch das Abwägen des Weichgewichtes zu kontrollieren. Salzreife Rohhäute, die nicht angetrocknet sind, geben kurzhaarig (auf 1 mm abgeschoren) 136% Weichgewicht (Tabelle I). Das Weichgewicht gibt aber nur dann eine richtige Auskunft über die Güte der Weiche, wenn bekannt ist, wie weit die Haut gegenüber dem salzreifen Gewicht eingetrocknet ist. Dies ist aber meistens nicht der Fall. Wie groß solch ein Fehler sein kann ist z.B. aus Tabelle I zu entnehmen: 100 g einer salzreifen an der Luft auf 71 g eingetrockneten Haut geben nach 24 Stunden Weiche bei 25 °C ein Weichgewicht von 115 g. Der auf das Gewicht der angetrockneten Haut bezogene Wert (162%) könnte als fast genügend beurteilt werden. In Wirklichkeit ist aber die Haut noch nicht genügend geweicht (118% bezogen auf salzreifes Gewicht). Das Weichgewicht ist auch wegen des zwischen den Haaren zurückgebliebenen Wassers ungenau.

Der Feuchtigkeitsgehalt der geschorenen und geweichten Häute wurde deshalb bestimmt und in Prozent des wasserfreien Hautmaterials angegeben. Gut geweichte Häute weisen einen auf wasserfreies Hautmaterial bezogenen Feuchtigkeitsgehalt von 200% auf.

Die Versuche wurden mit geschorenen Hautstücken durchgeführt, die aus einem lateinischen Quadrat des Krupons ausgestanzt wurden. Zur Weiche wurde eine Wassermenge angewendet, die dem anderthalbfachen frischen Salzgewicht entspricht. Das beim Antrocknen der Häute abgegebene Wasser

Tabelle I

Weichgewichte salzreifer und angetrockneter Rohhäute

	Salzreif	Angetrocknet			
Gewicht in % des salzreifen Gewichts	100	84		71	
Weichgewicht nach	In Prozent vom				
	salzreifen	salzreifen	angetrock- neten	salzreifen	angetrock- neten
	Gewicht				
1 Stunden	120	99	118	84	118
2 Stunden	129	107	128	90	127
3 Stunden	133	—	—	—	—
4 Stunden	136	120	143	100	141
24 Stunden	136	130	155	115	162

wurde noch zusätzlich zugegeben. Zeitweise wurde das ausgewaschene Salz (NaCl), das wasserfreie Hautmaterial nach Formalinkonzervierung und Trocknen bei 102 °C und das Weichgewicht nach Abtropfen bestimmt. Aus diesen Daten wurde der Wassergehalt der geweichten Haut berechnet.

Das Auswaschen des Salzgehaltes von salzreifen (frisch gesalzenen) und angetrockneten Rohhäuten als Funktion der Zeit wird in Abbildung 1 demonstriert. In Abb. 2 ist der in Prozent des wasserfreien Hautmaterials angegebene Feuchtigkeitsgehalt der Rohhaut in Abhängigkeit von der Weichdauer dargestellt. Tabelle II zeigt die Zusammensetzungen von salzreifen und verschiedenartig angetrockneten Rohhäuten nach 4 und 24-stündiger Weiche in dest. Wasser bei 25 °C.

Aus den Versuchen kann folgendes geschlossen werden ;

1. Das Auswaschen des Salzgehaltes wird durch das Antrocknen nicht verlangsamt, ja sogar erleichtert, weil einerseits die Waschwassermenge auf 150% des salzreifen Gewichts bezogen wurde, anderseits die Fasern langsamer quellen und dadurch die Diffusion schneller wird.

2. Aus Abb. 2 ist ersichtlich, daß die angetrockneten Häute langsamer aufweichen. Deswegen müssen frischgesalzene und angetrocknete Häute separat und nach anderer Technologie geweicht werden. Es ist bekannt, daß das Kollagen sein Hydratwasser nur sehr langsam wieder aufnimmt [3].

3. Das Weichen von angetrockneten Rohhäuten soll unbedingt durch mechanische Operationen (Strecken, Walken) erleichtert werden, da sonst die Weiche zu lang dauert. Walken mit wenig Wasser beschleunigt die Wasseraufnahme [4].

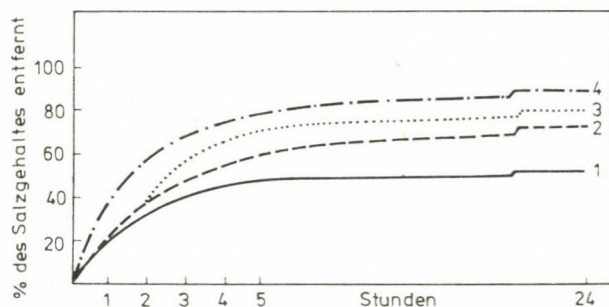


Abb. 1. Entfernung des Salzgehaltes während der Weiche. (1): Salzreife Rohhaut mit 150% Wasser geweicht; (2): Salzreife Rohhaut mit $2 \times 150\%$ Wasser geweicht; (3): Salzreife Rohhaut mit $3 \times 150\%$ Wasser geweicht; (4): Angetrocknete Rohhaut (25% Gewichtsverlust) mit $3 \times 150\%$ Wasser geweicht

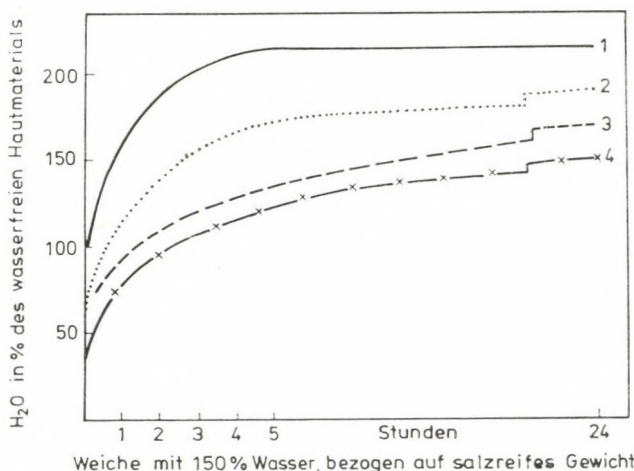


Abb. 2. Feuchtigkeitsgehalt der Rohhaut während der Weiche. (1): Salzreife Rohhaut; (2): Salzreife Rohhaut 16% angetrocknet; (3): Salzreife Rohhaut 22% angetrocknet; (4): Salzreife Rohhaut 29% angetrocknet

Unsere Betriebsüberwachung fand als Monatsdurchschnitt bei der Weiche nach

2 Stunden	bzw. 6 Stunden
3,2%	4,4% Salzgehalt,
3,63	2,23 Quadrat-Streuung,
1,4	1,49 Standardabweichung,
0,49	0,39 Durchschnittlicher Standard-Fehler.

Wir beurteilen diese Durchschnittswerte als übereinstimmend mit unseren Laboruntersuchungen.

Tabelle II

Zusammensetzung von salzreifen und verschiedenartig angetrockneten Rohhäuten vor und nach der Weiche ($3 \times 150\%$ Wasser, 25°C)

Gewichtsverlust %	Salzreife		Wenig angetrocknete		Angetrocknete	
	Rohhäute					
	0		16		29	
	vor	nach	vor	nach	vor	nach
	4 Stunden Weiche					
Wasserfreies Hautmaterial %	43,6	32,0	52,0	36,4	61,3	43,6
Salzgehalt (NaCl %)	12,4	1,0	14,7	1,1	17,5	1,3
Feuchtigkeit %	44,0	67,0	33,3	62,5	21,2	55,1
	24 Stunden Weiche					
Wasserfreies Hautmaterial %	43,6	32,0	52,0	33,5	61,3	38,0
Salzgehalt (NaCl %)	12,4	1,0	14,7	1,0	17,5	1,0
Feuchtigkeit %	44,0	67,0	33,3	65,5	21,2	61,0

Überwachung des Äschers

Die Äscherung wird heute meistens mit $\text{Na}_2\text{S} + \text{Ca}(\text{OH})_2$ unter Zugabe von Hilfsmitteln (NaOH , Na_2SO_3 , Dimethylamin, Zucker, Mercaptan-Produkte usw.) ausgeführt. Bei der täglichen Kontrolle werden S^{--} , $\text{SH} : \text{OH}$, pH, Temperatur sowie die Prallheit der Blöße bestimmt. Die Auswahl der S^{--} -Bestimmung ist wegen der vielen, in verbrauchten Äscherflüssigkeiten vorhandenen Verunreinigungen wichtig. Die jodometrische Methode ist zwar genau, aber nur bei reinen S^{--} -Lösungen brauchbar. Weniger genau ist die Zinksulfatmethode, bei der der Titrationsendpunkt durch Tüpfeln mit Nitroprussidnatrium-Lösung bestimmt wird [5]. Am besten hat sich die Methode von BOOTH bewährt, nach der die Titration mit K_3FeCN_6 vorgenommen wird [6]. Als Indikator dient Ferrodimethylglyoxim. Diese Methode gibt auch bei verbrauchten Äscherflüssigkeiten verlässliche Resultate. Vorteile sind schnelle Ausführung und gute Reproduzierbarkeit. Bei der Bestimmung von S^{--} in Abwässern wird H_2S in saurer Lösung abdestilliert und als CdS gefällt. Mercaptane werden dabei teilweise mitbestimmt.

Haarlösende Wirkung des Äschers

Um eine gute Enthhaarung im Faßäsher zu erreichen, sollen mindestens 50–70% der Haare aufgelöst werden, da sonst Haarwurzeln und Epidermisreste (Grund, Gneiss) im Leder [7], [8] zurückbleiben und Schwierigkeiten bei

Tabelle III

Haarzerstörende Wirkungen verschiedener Äscherflüssigkeiten

Zusammen- setzung	Mol.-Ver- hältnis	Konzentra- tion g/l	Tage	pH	Gelöstes Keratin %
NaHS	—	8,6	3	11,8	3
Na ₂ S	—	6,0	3	12,5	51
NaHS + Na ₂ S	} 2 : 1	8,6	3	12,5	70
Na ₂ S		6,0			
Na ₂ S + CaO	} 2 : 1	3,0	3	12,67	36
CaO		1,07			
Na ₂ S + CaO	} 2 : 1	6,0	3	12,75	76
CaO		2,14			
Na ₂ S + CaO	} 1 : 1	3,0	3	12,60	20
CaO		2,14			
Na ₂ S + CaO	} 1 : 1	6,0	3	12,66	75
CaO		4,28			
Na ₂ S + NaOH	} 10 : 1	5,70	3	12,86	72
NaOH		0,30			
NaOH	—	3,0	3	12,80	0

der Gerbung und Färbung verursachen können. Tabelle III zeigt die haarlösende Wirkung einiger in der Praxis bewährter Äscherflüssigkeiten [9]. Aus den in dieser Tabelle angeführten Daten ist zu entnehmen, daß der pH-Wert über 12 und die minimale Na₂S-Konzentration über 3 g/l sein soll. In der Praxis wendet man sicherheitshalber die 2—3 fache Sulfidmenge an.

Eiweißlösende Wirkung des Äschers

Eine zu hohe Konzentration der Äscherflüssigkeit bringt die Gefahr von Hautverlusten mit sich und kann zu einem zu weitgehenden Aufschluß der Faser führen (Losnarbigkeit). Das Auflösen der Proteine in den Äscherflüssigkeiten wurde eingehend untersucht.

Obwohl sich Kollagen in praxisnahen Äscherflüssigkeiten nur in geringem Maße löst, können doch die Wasserstoffbrücken in den aus Helix-Triplexen bestehenden Kollagen-Fasern so weit geschwächt werden, daß die Narbenschicht des Leders lose wird. Besonders die Verbindung zwischen dem Pars Papillaris und Corium kann leicht geschwächt werden. Die Eiweiße der Narbenschicht bestehen nur zu 70—90% aus Kollagen [10]. Deswegen soll bei

der Bestimmung des Eiweißverlustes nicht nur das gelöste Kollagen, sondern das gesamte gelöste Eiweiß bestimmt werden.

Ein bedeutender Teil des gelösten Eiweißes der nicht zu dem Eiweißverlust der Hautsubstanz gerechnet werden kann, stammt vom Abbau des Keratins. Das Gleiche gilt auch für die Muskelfaser der Unterhautgewebe (Subcutis). Die Bestimmung des Eiweißverlustes wurde deshalb nach Entfernung der Haare sowie des Subcutis vorgenommen. Die in der Haut zurückgebliebenen Epidermis- und Haarwurzel-Reste machten 2% des Rohhaut-Trockengewichtes aus, deren löslicher Teil von dem gelösten Gesamteiweiß abgezogen wurde.

Die bei Anwendung einiger praxisnaher Äscherflüssigkeiten unterschiedlicher Konzentration nach verschiedenen Zeiten in Lösung gegangenen Eiweißmengen sind in Tabelle IV angeführt. Die Konzentration ist in mÄq.Na/l angegeben, der Ca(OH)_2 -Gehalt ist also nicht in die angegebenen Werte einbezogen. Der besseren Anschaulichkeit wegen sollen von den zahlreichen Daten einige graphisch dargestellt werden. Aus Abbildung 3 ist zu ersehen, daß die bei gleicher Na-Konzentration in einem Tag in Lösung gehende Eiweißmenge (ohne Keratin) in der Reihenfolge.

NaHS , Na_2S , $\text{Na}_2\text{S} + \text{Ca(OH)}_2(1:1)$, $\text{Na}_2\text{S} + \text{NaOH}(10:1)$, NaOH zunimmt. Die in Lösung gehende Eiweißmenge nimmt auch in Gegenwart von wenig NaOH stark mit der Zeit zu. Bei NaOH -Konzentrationen von über 300 mÄq/l beginnt das Hautmaterial zu versulzen.

Tabelle IV

In Lösung gegangene Eiweißmengen in % des gewichteten Rohhautmaterials nach Abzug des gelösten Keratins

Zusammensetzung	Natrium-Konzentration*								
	77 mÄq/l			154 mÄq/l			308 mÄq/l		
	1	3	6	1	3	6	1	3	6
	Tage								
NaHS	0,55	0,68	0,96	0,66	0,85	1,10	—	—	—
$2\text{NaHS} + \text{Na}_2\text{S}$	1,02	1,33	1,75	1,41	1,47	2,12	1,98	2,45	2,96
Na_2S	0,97	1,46	1,90	1,42	1,84	2,05	2,30	2,60	3,10
$2\text{Na}_2\text{S} + \text{Ca(OH)}_2^*$	1,13	1,75	2,15	1,55	2,45	3,30	2,60	3,00	3,73
$\text{Na}_2\text{S} + \text{Ca(OH)}_2^*$	1,37	2,02	3,00	1,47	2,45	3,45	2,80	3,23	3,85
$10\text{Na}_2\text{S} + \text{NaOH}$	2,38	2,46	2,54	2,48	2,97	3,47	3,35	4,27	5,20
NaOH	2,70	4,40	6,80	3,60	5,80	8,30	4,60	8,60	13,15
Ca(OH)_2	—	—	—	—	—	—	1,50	—	—

* Ca(OH)_2 ist zusätzlich in Lösung

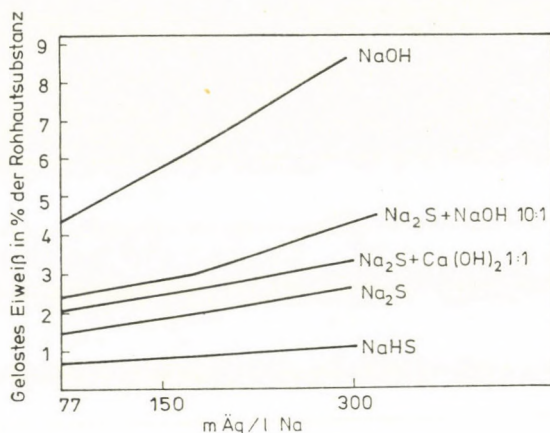


Abb. 3. Eiweißverlust der Rohhaut in 3 Tagen in verschiedenen Äscherflüssigkeiten bei 22 °C (ohne Keratin)

Prallheit der Blöße

Bei der Beurteilung der Blößenqualität wird auch die Prallheit beachtet. Zur genaueren Charakterisierung dieser subjektiven Eigenschaft haben wir einen Parameter aus Zusammendrückbarkeit und Biegeelastizitätsmodul gebildet (Prallfestigkeit) [8]. Die verschiedenen topographischen Teilen der Blöße weisen hinsichtlich der Prallfestigkeit charakteristische Unterschiede auf (siehe Tabelle V).

Gleiche Rohhäute geben mit verschiedenem Äscher verschiedene Prallfestigkeitswerte. Um Oberleder von gleicher Qualität herzustellen soll man deswegen Blößen mit gleicher Prallheit zur Gerbung bringen. Erfahrungsgemäß geben zu pralle Blößen losere Fertigleder als Blößen von mittlerer Prallheit [15].

Tabelle V

Werte der Prallfestigkeit bei verschiedenen Teilen der Blöße

		Krupenteil der Blöße aus einer		Bauchteil der Blöße
		festen	losen	
		Rohhaut		
Biegeelastizitätsmodul auf gleiche Dicke umgerechnet in kg/cm²	a	14,1	5,4	0,2
Reziprokwert der Zusammendrückbarkeit bei 1,5 kg/cm²	b	$\frac{1}{0,11} \cdot 1 \cdot 5 = 13,6$	$\frac{1}{0,18} \cdot 1 \cdot 5 = 8,3$	$\frac{1}{0,55} \cdot 1 \cdot 5 = 2,7$
Prallfestigkeit	a + b	27,7	13,7	2,9

Um den Einfluß verschiedener Äscherflüssigkeiten auf die Prallfestigkeit der Blöße festzustellen, haben wir Versuchsserien mit folgenden Ergebnissen durchgeführt;

1. Die Prallfestigkeit der Blöße hängt — neben anderen Faktoren — vom pH-Endwert ab (siehe Abb. 4).

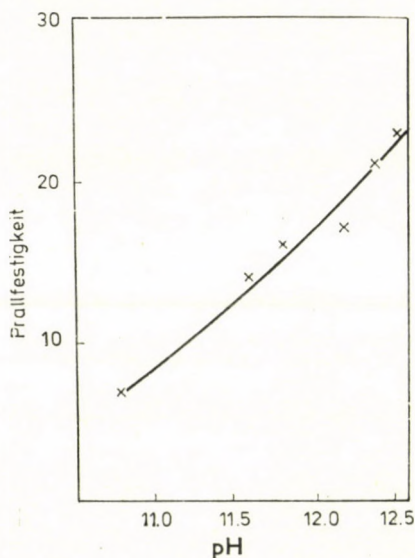


Abb. 4. Abhängigkeit der Prallfestigkeit vom End-pH-Wert in Na_2S -Äschern nach zwei Tagen

2. Bei erhöhten Na_2S -Konzentrationen und längerer Äscherdauer wird die Prallfestigkeit erhöht, wenn genügend OH^- -Ionen nachgebildet werden. Die Rohhaut bindet OH^- -Ionen und eine Nachbildung erfolgt durch Inlösunggehen von Kalk (siehe Abb. 5).

3. In $[\text{Na}_2\text{S} + \text{Ca}(\text{OH})_2]$ -Äscherflüssigkeiten sichert das größere Verhältnis von Flüssigkeit:| Haut leichter den OH^- -Ionen-Nachschub, deswegen werden die Blößen praller.

4. Obwohl zu erwarten wäre, daß mit zunehmendem Herauslösen der Eiweißstoffe die Prallheit der Blöße verringert wird, wurde festgestellt, daß bei Verlängerung der Äscherdauer nicht nur mehr Eiweiße herausgelöst, sondern bei genügender Nachbildung der OH^- -Ionen aus überschüssigem Kalk gleichzeitig auch die Blößen praller werden. Da in pralleren Blößen die Diffusion wegen der Quellung der Faser langsamer ist, lösen sich weniger Eiweißstoffe heraus. Wenn bei längerer Äscherung gleichzeitig auch pH verringernde Zusatzstoffe (Zucker, Dimethylamin-Präparate usw.) zur Anwendung kommen, werden noch mehr Eiweißstoffe herausgelöst, die Blöße wird mehr aufgeschlossen und das Oberleder weicher.

5. Wird die Na_2S -Konzentration [bei $\text{Na}_2\text{S} + \text{Ca}(\text{OH})_2 = 1 : 1$] erhöht, so wird das Lösen des Keratins am meisten beschleunigt. Die Prallheit der Blöße und das Herauslösen der Hautproteine wird weniger stark beeinflusst (siehe Abb. 6).

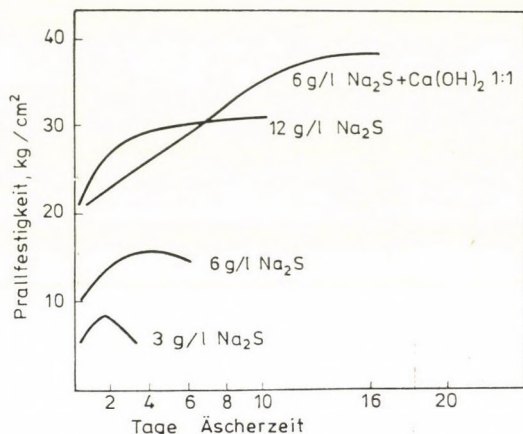


Abb. 5. Veränderung der Prallfestigkeit als Funktion der Äscherzeit in verschiedenen Äscherflüssigkeiten bei 22 °C

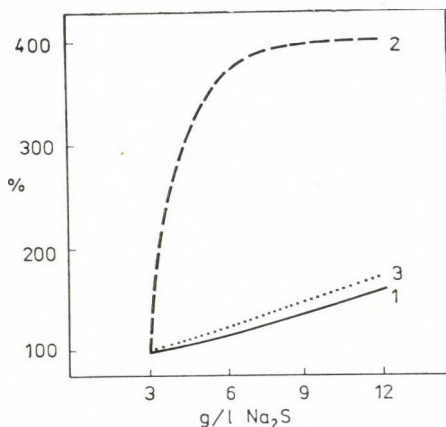


Abb. 6. Zusammenhang zwischen Prallheit, Eiweißverlust der Blöße sowie Keratinabbau als Funktion der Na_2S -Konzentration $\text{Na}_2\text{S} : \text{Ca}(\text{OH})_2 = 1 : 1$ Äscher 3 Tage

(1): Eiweißverlust in Prozenten des Wertes, der bei 3 g/l Na_2S gemessen wurde; (2): Gelöstes Keratin in Prozenten des Wertes, der bei 3 g/l Na_2S gemessen wurde; (3): Prallfestigkeit in Prozenten des Wertes, der bei 3 g/l Na_2S gemessen wurde

6. Die oben erwähnten Feststellungen wurden bei 22 °C beobachtet, bei höheren Temperaturen wird das Aufschließen der Blöße und das Herauslösen der Eiweißstoffe stark beschleunigt. Konzentrierte Na_2S -Lösungen zerstören bei höheren Temperaturen die empfindliche Hautschichten, und die Narbe schei-

det sich vom Corium ab. Schaden wird besonders dann angerichtet, wenn 60%-iges Na_2S in festem Zustand mit der gewechten Haut in Berührung kommt. Nach unseren Messungen wird bei der Lösung von geschmolzenem oder lamelliertem Na_2S eine Wärmemenge von etwa 60 Kal/kg freigesetzt, wodurch die Blöße bei ruhendem Faß stark beschädigt wird [11].

Wir haben schon früher beobachtet, daß z.B. aus dem oberen Teil der Haut auch dann zweimal soviel Eiweiß als aus dem unteren (Corium) Teil heraus-gelöst wird, wenn vorher das Keratin entfernt wurde.

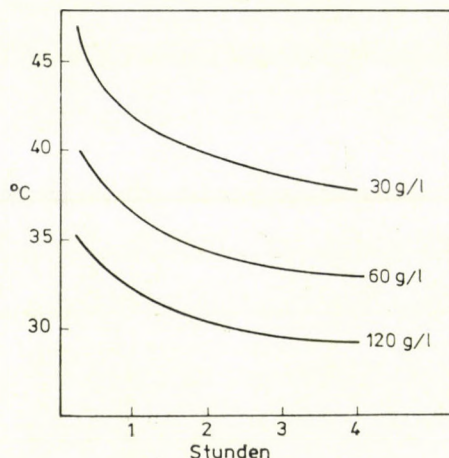


Abb. 7. Ablösung der Narben-Schicht als Funktion der Na_2S -Konzentration, Temperatur und Zeitdauer

Wir haben Orientierungsversuche durchgeführt, unter welchen Umständen die Narben-Schicht zerstört wird. Abb. 7 zeigt die grobe Zerstörung der Narben-Schicht in Abhängigkeit von der Na_2S -Konzentration, der Temperatur und der Zeitdauer. Die Äschertechnologien sollen in der Weise vorgeschrieben werden, daß diese Parameter weit unter den schädlichen Werten bleiben.

Zusammenhang zwischen Prallheit und Eiweißverlust

Der Zusammenhang zwischen der Prallheit der Blöße und dem Herauslösen von Hautmaterial und Keratin wird in den Abbildungen 6 und 8. veranschaulicht. In Abb. 8 sind auf der Ordinate diese Größen in Prozent des Wertes, der nach 1-tägiger Äscherung erreicht wird, aufgetragen. Es ist ersichtlich, daß sich die Äscherungszeit am meisten auf den Eiweißverlust auswirkt.

In Abb 6 sind auf der Ordinate die gleichen Größen in Prozent des Wertes aufgetragen, der bei einer Konzentration von 3 g/l Na_2S nach dreitägiger

Äscherung erreicht wird. Es ist zu ersehen, daß mit steigender Na_2S -Konzentration die Menge an gelöstem Keratin am stärksten ansteigt. Abbildungen 6 und 8 bestätigen gleichermaßen die in der Praxis bewährte technologische Tendenz, daß eine kurze kräftige Äscherung die Herstellung eines festnarbigen, von Haarresten befreiten Oberleder am meisten gewährleistet, weil dadurch eine mäßig pralle Blöße in kurzer Zeit ohne hohen Eiweißverlust herstellbar ist. Die optimale Zeitdauer der Äscherung hängt selbstverständlich auch von der Dicke der Rohhaut ab. Da die Diffusion mit der Quadratwurzel der Dicke abnimmt, dauert die Durchäscherung einer dickeren Haut längere Zeit.

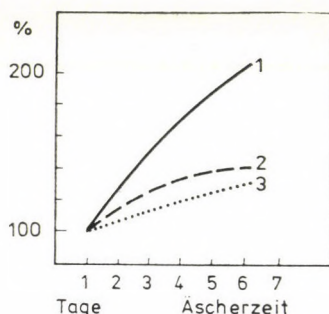


Abb. 8. Zusammenhang zwischen Prallheit, Eiweißverlust der Blöße sowie Keratinabbau als Funktion der Zeit. (1): Eiweißverlust in Prozenten des Wertes, der nach einem Tag gemessen wurde; (2): Gelöstes Keratin in Prozenten des Wertes, der nach einem Tag gemessen wurde; (3): Prallfestigkeit in Prozenten des Wertes, der nach einem Tag gemessen wurde

Die Wirkungen von $\text{Na}_2\text{S} + \text{Ca}(\text{OH})_2$ und $\text{Na}_2\text{S} + \text{NaOH}$ Äschern unterscheiden sich bedeutend. Bei NaOH enthaltenden Äschern ist die gesamte OH^- -Ionen-Menge beim Zeitpunkt der Dosierung schon in Lösung, während bei kalkhaltigen Äschern OH^- -Ionen wegen der Schwerlöslichkeit des Kalkes nur nach und nach in Lösung gehen. NaOH soll deswegen nur vorsichtig zugegeben werden, um eine Überquellung des Narbens zu vermeiden. Bei $\text{Ca}(\text{OH})_2$ enthaltenden Äscherflüssigkeiten ist diese Vorsichtsmaßnahme kaum nötig, weil der pH-Wert sich sozusagen automatisch reguliert.

Bindungsfestigkeit verschiedener Basen

Die OH^- -Konzentration — die die Wirkung der Äscherflüssigkeit entscheidend beeinflusst — hängt einerseits von der chemischen Zusammensetzung, andererseits von der Basenbindungs-Kapazität der Rohhaut ab. Wir haben deswegen diese Frage näher untersucht [12].

Die alkalische Quellung der Kollagenfaser wird mit dem elektrostatischen Abstoßung gleichartig aufgeladener Gruppen erklärt [13]. Die Bindung der Basen hängt hauptsächlich von der Konzentration und Art der Kationen ab. Die zweiwertigen Basen werden stärker als einwertige an Kollagen gebunden.

Tabelle VI enthält Daten über die Bindung von Basen aus einigen verschieden zusammengesetzten Äscherflüssigkeiten durch die Rohhaut. Der Übersichtlichkeit wegen werden Werte von äquivalenten Basenmengen verglichen. Die Rohhaut kann von den bei der Äscherung verwendeten Chemikalien die in Abbildung 9 angegebenen Mengen aufnehmen. Die Fähigkeit der Rohhaut, verschiedene Basen zu binden, zeigt in Abhängigkeit von der Konzentration keine so charakteristische Maxima, wie sie bei der Säurebindung beobachtet wurden. Von den gebräuchlichen Äscherchemikalien ist $\text{Ca}(\text{OH})_2$ die Substanz, aus deren Lösung von der Rohhaut die meisten OH^- -Ionen gebunden werden, und zwar ungefähr dreimal soviel wie aus einer Na_2S -Lösung gleicher Konzentration unter Zugrundelegung der Reaktionsgleichung



Tabelle VI

*Basenbindung von 35 g geweichter Rohhaut als Funktion der Basenkonzentration
Trockengewicht 11,0 g. Flüssigkeit 200 ml*

Angebotene Basenmenge mÄq	Zurücktitrierte Base mÄq	Aufgenommene	Gebundene
		Basenmenge mÄq auf 1 g wasserfreie Hautsub- stanz bezogen	
7,7 NH_4OH	6,5	0,11	0,03
7,7 NaHS	6,2	0,14	0,06
13,1 NaHS	11,5	0,15	0,08
7,7 Na_2S	5,8	0,17	0,13
13,1 Na_2S	9,5	0,31	0,19
7,7 NaOH	5,1	0,23	0,16
13,1 NaOH	8,6	0,41	0,32
10 $\text{Ca}(\text{OH})_2$ Suspension	3,4	0,60	0,55
20 $\text{Ca}(\text{OH})_2$ Suspension	11,6	0,76	0,63
30 $\text{Ca}(\text{OH})_2$ Suspension	20,9	0,83	0,69
50 $\text{Ca}(\text{OH})_2$ Suspension	39,7	0,93	0,80

Es ist zweckmäßig die gebundenen bzw. aufgenommenen Milliäquivalente auf die praxisnähere prozentuale Dosierung umzurechnen. Meistens wird auf Salzgewicht der Rohhaut 1,8% Na_2S im Äscher verwendet ($= 46 \text{ mÄq}/100 \text{ g Rohhaut}$), wovon die Rohhaut maximal nur $13,3 \text{ mÄq}$ aufnimmt. 100 g Rohhaut (Salzgewicht) enthält etwa 43 g wasserfreie Hautsubstanz (Kollagen) mit einem maximalen Basenaufnahmevermögen von $0,92 \times 43 = 39,5 \text{ mÄq}$. Nach den Angaben in Abb. 9 bzw. Tabelle VI ist nämlich das maximale Basenaufnahmevermögen aus $\text{Ca}(\text{OH})_2$ -Lösungen $0,92 \text{ mÄq/g Kollagen}$, das aus Na_2S -Lösungen dagegen $0,31 \times 43 = 13,3 \text{ mÄq}$.

100 g Rohhaut binden also nach dem Weichen bei einer Dosierung von 1,8% Na_2S schnell eine Basenmenge von $13,3 \text{ mÄq}$ — die nur $1/3$ der maximal aufnehmbaren OH^- -Ionen ausmacht — so daß der pH-Wert der Äscherflüssigkeit stark absinken müßte. Die fehlende OH^- Menge wird durch $\text{Ca}(\text{OH})_2$

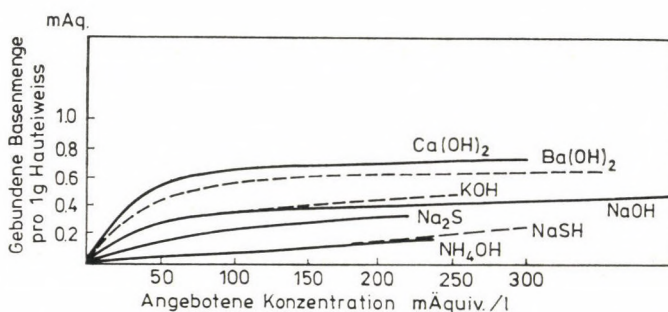


Abb. 9. Basenbindungsvermögen von Hautsubstanz Flüssigkeitsmenge : Hautsubstanz = 20 : 1

ergänzt und das graduelle Inlösungsgehen des Kalkes wird die Konstanz des pH-Wertes gewährleisten. Theoretisch würde etwa 1% $\text{Ca}(\text{OH})_2$ genügen, um die fehlende OH^- Menge zu ersetzen, doch wird in der Praxis die 3–5fache Menge angewendet, weil die entstehenden Kalkseifen die Kalkstückchen umhüllen und auch durch Carbonatbildung die Wirksamkeit vermindert wird.

Allgemein wird die Meinung vertreten, daß zu viel Kalk die Oberleder lose macht [14], [15]. Die haarlösende Wirkung ist bei einem $\text{SH} : \text{OH}^-$ -Verhältnis von 1 am besten. Bei Technologien bei denen die fehlenden OH^- -Ionen durch NaOH ergänzt werden, kann die schnelle Zugabe eine Überquellung, bei einer NaOH -Konzentration von 300 mÄq/l sogar Versulzung des Narbens verursachen. Die Technologien des Äschers müssen so gestaltet werden, daß keine plötzliche pH-Steigerungen eintreten.

Auswaschbarkeit verschiedener Basen

Wegen der Entkalkung ist die Auswaschbarkeit der verschiedenen Basen wichtig. Diesbezügliche Untersuchungen wurden an Rindsblößen vorgenommen, die mit der dreifachen Gewichtsmenge dest. Wassers bei 25 °C gewaschen wurden. Das Washwasser wurde stündlich gewechselt und der Basengehalt der Blößen von Zeit zu Zeit bestimmt. Die Ergebnisse sind in Abb. 10 dargestellt. Am leichtesten läßt sich NH_4OH , am schwersten $\text{Ca}(\text{OH})_2$ auswaschen. Wegen dieser Eigenschaft werden Ammoniumsalze bei der Entkalkung verwendet. Die Entfernung der Äscherchemikalien erfolgt in 3 Stufen.

a) Abspülen der im Überschuß angewandten und von der Blöße nicht gebundenen Chemikalien.

b) Graduelle Dissoziation bzw. Hydrolyse des Kollagensalzes zu Alkali- bzw. Erdalkali-Lauge.

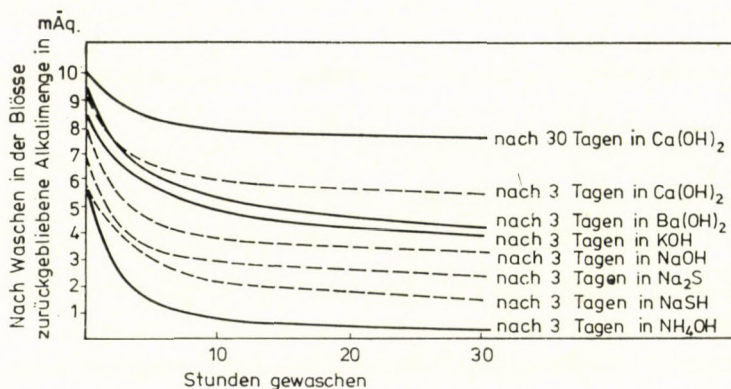
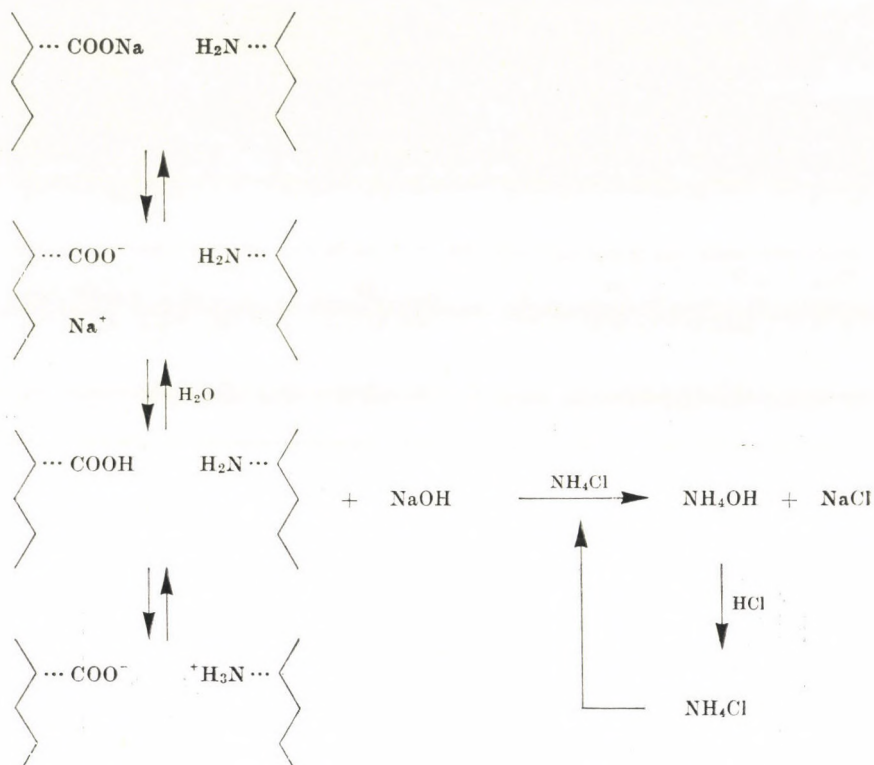


Abb. 10. Entfernung des Basengehaltes der Blöße (11 g wasserfreie Hautsubstanz) durch Waschen mit je 100 ml Wasser

c) Verschiebung des Gleichgewichtes mit Ammoniumsalzen zugunsten der Dissoziation und Rückbildung der Ammoniumsalze bis zum isoelektrischen Zustand mit Entkalkungssäuren.



Die drei Phasen der Entkalkung können, wie Abb. 11 zeigt, durch die Abnahme des Basengehaltes der Blöße mit der Zeit gut verfolgt werden.

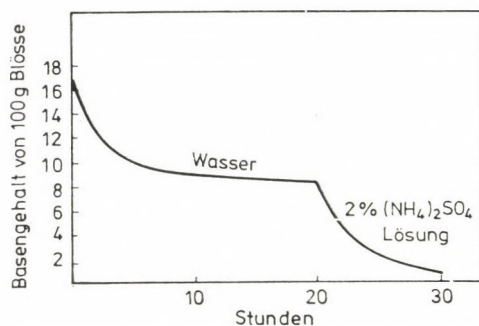


Abb. 11. Verlauf des Auswaschens und der Entkalkung von 100 g Blöße (2% Na₂S, 0,5% CaO) mit je 100 ml Flotte

Bindungsindizes der Säuren

Da weiche Oberleder nur aus entsprechend entkalkten Blößen herzustellen sind, ist es Aufgabe der Betriebsüberwachung, den Basengehalt der Blößen vor der Gerbung kontinuierlich zu messen. Bei der Entkalkung benutzt man als Säure Salz- und Milchsäure. Salzsäure wird wegen der Billigkeit sowie der guten Löslichkeit des CaCl_2 angewandt. Als Nachteil ist zu erwähnen, daß der pH-Wert wegen der Gefahr einer Säurequellung nicht unter 5 sinken darf und somit die Dosierung sehr sorgfältig erfolgen muß. Bei Rohhäuten mit feinen Narben verwendet man die teure Milchsäure.

Wir konnten nachweisen, daß die Gefahr einer Säurequellung durch den Bindungsindex gut nachweisbar ist. Wir definierten den Bindungsindex als den Quotient der Angebots- und Gleichgewichtskonzentration bei einem Verhältnis von 20 für Flotte zu Hautsubstanz [10]. Gibt man z.B. in Gegenwart von Salz 15 mÄq HCl zu 100 g geweihte Haut (Trockengewicht 31,5 g) in 500 ml Wasser, so findet man in der Lösung nach Einstellung des Gleichgewichtes 0,3 mÄq HCl. Der Bindungsindex der Salzsäure ist also $15 : 0,3 = 50$. Bei der Zugabe einer gleichen Menge (15 mÄq) Milchsäure bleiben 3 mÄq in Lösung, der Bindungsindex ist $15 : 3 = 5$. Bei Zugabe äquivalenter Mengen von Salz- und Milchsäure bleibt also 10-mal soviel Milchsäure in Lösung als Salzsäure. Die Gefahr der Säurequellung ist bei Milchsäure kleiner, weil

die gebundene Salzsäure mit 14,7 mÄq 98%,

die gebundene Milchsäure mit 12,0 mÄq 80% der angebotenen Säure entspricht.

Tabelle VII

Bindungsindex = Quotient aus Angebots- und Gleichgewichts-Konzentration

	Bindungsindex bei etwa				
	30	50	80	120	200
	mÄq/l Angebots-Konzentration				
H_2SO_4	87,0	8,0	2,0	1,6	1,4
HCl	50,0	8,6	—	1,8	1,4
Oxalsäure	—	—	—	2,0	—
Naphtalinsulfosäure	—	—	—	2,0	—
Ameisensäure	—	4,1	2,1	1,7	—
Essigsäure	—	2,3	1,6	1,5	1,3
Milchsäure	5,0	3,7	2,8	2,0	1,5
$\text{Ca}(\text{OH})_2$	3,0	2,8	2,0	1,5	1,3
$\text{Ba}(\text{OH})_2$	2,7	2,3	2,1	1,6	—
KOH	1,6	1,5	1,5	—	1,3
NaOH	1,6	1,5	1,5	1,4	1,3
Na_2S	1,5	1,4	1,3	1,3	1,2
NH_4OH	1,2	1,2	1,2	1,2	1,2

Der Bindungsindex der verschiedenen Säuren ist ein besserer Parameter für die Bindungsstärke als die maximal gebundene Säuremenge (Tabelle VII). Bei der Überwachung der Äscherei haben wir folgende Durchschnittswerte registriert ;

	nach 3 Stunden	6 St.
Na ₂ S g/l	10,9	11,25
Quadratstreuung	5,46	5,49
Standardabweichung	2,34	2,14
Durchschnittlicher Standardfehler	0,65	0,59
SH : OH	0,78	0,81
Quadratstreuung	0,04	0,05
Standardabweichung	0,20	0,23
Durchschnittlicher Quadratfehler	0,06	0,06

Basengehalt nach der Entkalkung in mÄq/g Kollagen:

Durchschnitt	0,2
Quadratstreuung	0,01
Standardabweichung	0,12
Durchschnittlicher	
Standardfehler	0,01

Die Streuung des Na₂S-Gehaltes hängt mit dem Antrocknen der Rohhäute zusammen.

Im folgenden Teil werden die Kontrolle des Pickels und der Gerbung behandelt.

LITERATUR

- [1] VAJDA, J.: Vortrag auf dem VI. Kongreß der Lederindustrie, Budapest, 18. 10. (1978)
- [2] TÓTH, G., VAJDA, J.: Kongreß der Jugoslawischen Leder- und Schuhindustrie, Zagreb, 22. 2. (1978)
- [3] MITTON, R. G.: J. Soc. Leather Trade Chem, **1947**, 44 und **1964**, 409
- [4] TÓTH, G.: Int. Kongreß über Rohhäute, Gottwaldov 20. 9. (1967)
- [5] KÜNTZEL, A.: Gerbereichemisches Taschenbuch, Dresden—Leipzig, 6. Auflage (1955)
- [6] BOOTH, A.: J. Soc. Leather Trade Chem., **1956**, 238 und **1959**, 106
- [7] HEIDEMANN, E.: Das Leder, **1968**, 73 und 333
- [8] TÓTH, G., VERES, L.: Das Leder, **1971**, 48
- [9] TÓTH, G.: Bőr és Cipőtechnika, **1969**, 89
- [10] REICH, G.: Kollagen, Dresden, Verlag Theodor Steinkopff, 19 (1966)
- [11] Unveröffentlicht
- [12] TÓTH, G.: Das Leder, **1969**, 9
- [13] KÜNTZEL, A.: In W. Grassmann's Handbuch der Gerbereichemie und Lederfabrikation, Verlag von Julius Springer, Wien, 607 (1944)
- [14] ZISSEL, L.: Das Leder, **1955**, 289
- [15] VERMES, L.: Bőr és Cipőtechnika, **1958**, 12

Géza TÓTH
József VAJDA
Vilmos PÓSA

} H-7621 Pécs, Pécsi Bőrgyár

H-1047 Budapest, IV., Újpest, Paksi J. u. 43.

RECENT STUDIES ON THE REACTION OF THIOLSULFONATES WITH ALKALI HALIDES

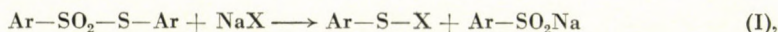
J. LÁZÁR and E. VINKLER

(Pharmaceutical Chemical Department, Medical University, Szeged)

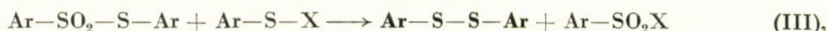
Received June 29, 1978

Accepted for publication October 10, 1978

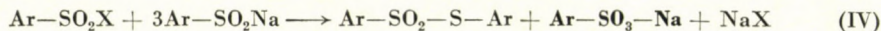
Thiolsulfonates react with sodium halides or sodium thiocyanate in dimethylformamide to give the corresponding disulfide and the sodium salt of the sulfonic acid. Three subsequent or parallel reactions are suggested to explain the reaction mechanism; these have been substantiated by literature data and model experiments. First a nucleophilic cleavage of the thiolsulfonates takes place



followed by the electrophilic reaction of the starting thiolsulfonate with the sulfenyl compound formed:

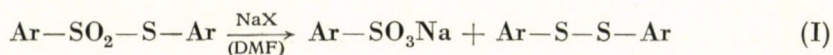


and the third reaction occurs between the sulfinate salt (from Eq. I) and the sulfonyl compound (from Eq. III):



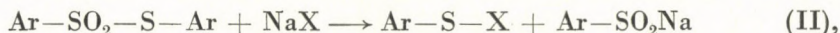
(End-products are shown in bold-face.)

During the nucleophilic splitting of thiolsulfonates in anhydrous media it was observed that, when the reaction was effected in dimethylformamide solution with sodium thiocyanate, disulfide and the sodium salt of the sulfonic acid were formed, instead of the expected cleavage products. The sodium sulfonate was isolated as its *S*-benzylisothiuronium salt. When the reaction was carried out with sodium bromide, sodium chloride, or sodium iodide instead of sodium thiocyanate, the same result was obtained, only the amounts of the reaction products varied (Eq. I).



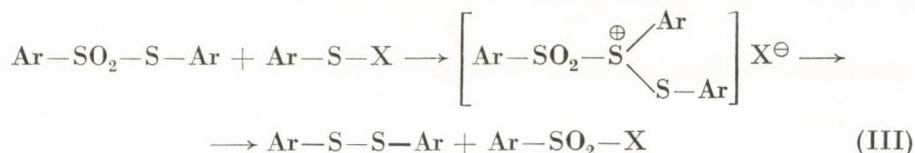
The aim of the present work was to examine the course of this reaction in detail.

KICE and ROGERS [1] studying alkali halides as catalysts in reactions between thiolsulfonates and amines in aqueous dioxan observed the thiolsulfonates converted primarily into sulfenyl halides and sodium sulfinate under such reaction conditions (Eq. II).



We assumed that the reaction in dimethylformamide is initiated by the same process.

Considering the possible further conversions of the reaction products and the starting compound, the electrophilic reaction of the sulfonyl compound formed with the starting thiosulfonate seemed probable (Eq. III).



This reaction between methanesulfonyl chloride and methanethiolsulfonate was described by DOUGLASS [2]. In the case of aromatic thiosulfonates ($\text{Ar-SO}_2\text{-S-Ar}$) the reaction in either polar (glacial acetic acid) [3], or apolar (benzene) [4] solutions was not observed.

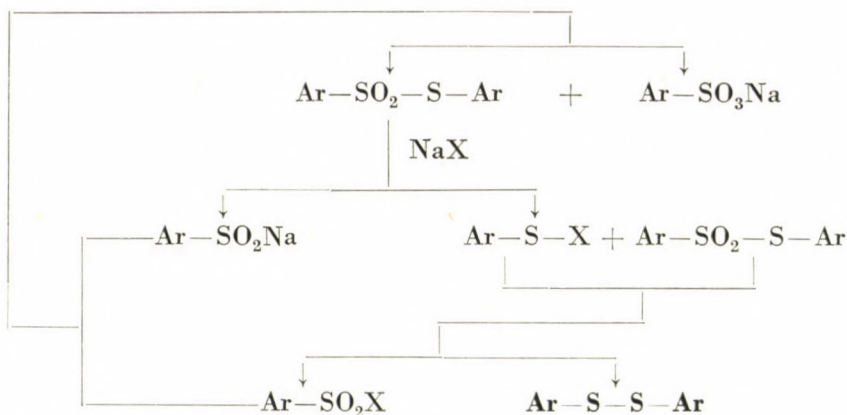
In order to confirm the reaction path of the formation of the end-products and the individual steps of the mechanism assumed, *p*-toluenethiolsulfonate was allowed to react with *p*-toluenesulfonyl chloride in dimethylformamide under identical conditions, whereupon the end-products shown above (Eq. III) were obtained. The reaction was successfully effected also in acetonitrile with *p*-toluenesulfonyl bromide, and the resulting sulfonyl bromide was identified from the reaction mixture after conversion with ammonia into the sulfonamide.

On the basis of a paper by CORSON and PEWS [5] the third step was assumed to be the reaction of sodium *p*-toluenesulfinate (formed in Reaction II) with *p*-toluenesulfonyl chloride (formed in Reaction III);



When CORSON and PEWS [5] allowed *p*-toluenesulfonyl chloride to react a double excess of sodium *p*-toluenesulfinate (molar ratio 1 : 3) in acetonitrile, the products were mainly *p*-toluenethiolsulfonate and sodium *p*-toluenesulfonate, accompanied by a small amount of disulfone. This reaction was repeated in dimethylformamide, *i.e.*, under the reaction conditions employed by us, in order to confirm the mechanism suggested. Work-up of the reaction mixture gave only thiosulfonate and sulfonic acid in a good yield (isolated as the *S*-benzylisothiuronium salt). The course of the reaction was discussed in detail by CORSON and PEWS [5], also considering the researches of KICE and PAWLOWSKI [6].

On the basis of the reactions outlined above (Eqs. II–IV), the conversions of thiosulfonates on the effect of alkali halides in dimethylformamide are summarized in the following Scheme:



X = Cl, Br, I, SCN

(The end-products of the reaction are shown in bold-face.)

Experimental

M.p.'s were determined on a Boetius (Franz Küstner, Dresden) micro-hot-stage and are uncorrected.

Reaction of *p*-toluenethiosulfonate with alkali halides or thiocyanate in dimethylformamide

p-Toluenethiosulfonate (13.5 g; 0.05 mole) was dissolved in dimethylformamide (50 ml) and the appropriate alkali compound (0.05 mole) (sodium chloride, bromide, iodide or thiocyanate) was added. The reaction mixture was heated in an oil bath at 110 °C (± 5 °C), with stirring, for 24 h. Dimethylformamide was evaporated in vacuum (water pump) and the residue poured into water (200 ml) and extracted with benzene. *S*-Benzylisothiuronium chloride (15 g; approx. 0.075 mole) dissolved in water (50 ml) was added to the aqueous phase, which was then refrigerated and the *S*-benzylisothiuronium *p*-toluenesulfonate was filtered off and dried, m.p. 180–182 °C. After evaporation of the benzene the residue was either recrystallized from petroleum ether, or subjected to chromatographic separation on a silicagel column to obtain the disulfide and the thiosulfonate. M.p. of the disulfide was 44–45 °C, that of the thiosulfonate was 76 °C. The results of the experiments are summarized in Table I.

Table I

	NaBr	NaSCN	NaI*	NaCl
<i>S</i> -Benzylisothiuronium <i>p</i> -toluenesulfonate	12.5 g	7.8 g	4.7 g	4.6 g
<i>p</i> -Toluene disulfide	7.3 g	3.0 g	1.5 g	1.0 g
Unchanged <i>p</i> -toluenethiol- sulfonate	traces	1.4 g	7.5 g	8.9 g

* With the precipitation of iodine

Reaction of *p*-toluenethiolsulfonate and *p*-toluenesulfonyl chloride in dimethylformamide

p-Toluenethiolsulfonate (6.95 g; 0.025 mole) was dissolved in dimethylformamide (50 ml) and a solution of *p*-toluenesulfonyl chloride (3.37 g; 0.0125 mole + 10%), prepared from *p*-toluene disulfide with chlorine gas in carbon tetrachloride (30 ml), was added dropwise during 16 h, while stirring the mixture in an oil bath at 110 °C (± 5 °C). The reaction mixture was refluxed further for 8 h. Dimethylformamide was evaporated in vacuum (water pump) and the residue poured into water (200 ml), and extracted with benzene. A solution of *S*-benzylisothiuronium chloride (10 g; about 0.05 mole) in water (50 ml) was added to the aqueous phase which was then refrigerated and the *S*-benzylisothiuronium *p*-toluenesulfonate was filtered off and dried (7.14 g; 85%), m.p. 180–182 °C. The benzene fraction was dried, concentrated and transferred to a silicagel column, eluted with petroleum ether and benzene; thus the disulfide (5.7 g; 94%), m.p. 44–45 °C, and unchanged thiolsulfonate (0.45 g; 6.4%), m.p. 76 °C, were isolated.

Reaction of *p*-toluenethiolsulfonate with *p*-toluenesulfonyl bromide in acetonitrile

p-Toluenethiolsulfonate (6.95 g; 0.025 mole) was dissolved in acetonitrile (50 ml) and a solution of *p*-toluenesulfonyl bromide, prepared from *p*-toluene disulfide (3.37 g; 0.0125 mole + 10%) with bromine (2.2 g; 0.0125 mole + 10%), was added to it dropwise during 1 h, under stirring in an oil bath at 75 °C. The reaction mixture was refluxed further for 2 h, the solvent was evaporated in vacuum (water pump), the residue was dissolved in dry benzene and saturated with ammonia gas. The benzene was then evaporated, petroleum ether was added to the residue and the precipitate was filtered off, washed thoroughly with petroleum ether and dried. Ammonium bromide was removed by washing the precipitate with water on the filter, and the residual *p*-toluenesulfonamide was dried (3.26 g; 75%), m.p. 139 °C. The petroleum ether solution was subjected to chromatographic separation on a silicagel column using petroleum ether and benzene as eluants; thus the disulfide (5.8 g; 96%), m.p. 44–45 °C and unchanged thiolsulfonate (0.35 g; 5%), m.p. 76 °C were isolated.

Reaction of *p*-toluenesulfonyl chloride with sodium *p*-toluenesulfinate in dimethylformamide

p-Toluenesulfonyl chloride (9.53 g; 0.05 mole) was dissolved in DMF (100 ml) and sodium *p*-toluenesulfinate (26.7 g; 0.15 mole) was added. The reaction mixture was then refluxed in an oil bath at 110 °C (± 5 °C) under stirring with a magnetic stirrer for 24 h. The dimethylformamide was evaporated in vacuum (water pump) and the residue was extracted with benzene after pouring it into water (200 ml). A solution of *S*-benzylisothiuronium chloride (40 g; about 0.2 mole) in water (100 ml) was added to the aqueous phase, it was refrigerated and the crystals were filtered off and dried. *S*-Benzylisothiuronium *p*-toluenesulfonate (31 g; 183%, calculated for *p*-toluenesulfonyl chloride) was obtained, m.p. 180–182 °C. The benzene phase was evaporated and the residue recrystallized from petroleum ether to obtain *p*-toluenethiolsulfonate (11 g; 79%, calculated for *p*-toluenesulfonyl chloride), m.p. 76 °C.

The compounds synthesized in the above experiments were identified, after repeated recrystallizations, on the basis of m.p., mixed m.p., TLC (adsorbent: Kieselgel 60 G, Merck; developing mixture: benzene–petroleum ether (5:5); detecting agent: alkaline potassium permanganate) and elemental analysis.

Separation of the disulfide-thiolsulfonate mixture was achieved either by fractional recrystallization from petroleum ether, or by chromatographic separation on a silicagel column ("Kieselgel 40 für die Säulen-Chromatographie", 0.062–0.20 mm, Merck), using petroleum ether and benzene as eluants.

REFERENCES

- [1] KICE, J. L., ROGERS, T. E.: J. Org. Chem., **41**, 225 (1976)
- [2] DOUGLASS, I. B.: J. Org. Chem. **24**, 2004 (1959)
- [3] PINTYE, J., STÁJER, G., VINKLER, E.: Acta Chim. Acad. Sci. Hung., **95**, 307 (1977)
- [4] PINTYE, J.: Private communication
- [5] CORSON, F. P., PEWS, R. G.: J. Org. Chem., **36**, 1654 (1971)
- [6] KICE, J. L., PAWŁOWSKI, N.: J. Am. Chem. Soc., **86**, 4898 (1964)

János LÁZÁR
Elemér VINKLER } H-6701 Szeged, Eötvös u. 6.

APPLICATION OF THE THERMOELECTRIC METHOD IN THE STUDY OF PHASE TRANSITIONS OF FATTY ACID SALTS

T. MEISEL, K. SEYBOLD and J. RÓTH

(*Institute of General and Analytical Chemistry, Technical
University, Budapest*)

Received July 10, 1978

Accepted for publication October 20, 1978

Some examples of the application of the thermoelectric method have been presented. By this method, for compounds in the smectic mesophase, the special anomaly of conductivity, the memory effect, has been determined and qualitatively interpreted.

The temperature dependence of the permittivity or conductance of a given sample may be studied by thermoelectric analysis (TEA). As is known, phase and polymorphic transitions are accompanied by sharp anomalies in electrical conductivity [1]. Equilibrium phase transitions may be induced by the change of temperature, pressure and composition.

This paper summarizes our results obtained in the course of TEA studies on polymorphic and phase transitions of ionic type organic salts as a function of the temperature. Greater changes in the electric conductivity (EC) could be observed generally in the phase transitions of ionic melts than in polymorphic transitions. By the appropriate choice of the experimental parameters, the effect of the latter may be made negligible. In polymorphic transitions the EC signal is generally registered as a peak, while a phase transition is recorded as a jump followed by a steady shift. The temperature dependence of the conductivity of a given phase and the activation energy calculated from by the Arrhenius plot is dependent also on the structure of the phase. A characteristic feature of the compound under investigation was that some possessed a smectic mesophase. This property was also dependent on the number of carbon atoms in the fatty acid molecule and on the nature of the cation. Thermoelectric methods have been widely applied for studying the characteristics of liquid crystals, mainly in the case of nematic and cholesteric phases [2], while relatively few data are available in the literature for the smectic phase. The reported data refer rather to the investigation of the structure of lyotropic systems. The thermotropic amphiphilic phase of alkali and heavy metal soaps have been studied only recently by this method [3-8]. Our earlier investigations performed by the TEA method on non-mesophase fatty acids have also been extended to compounds in the mesophase [9, 10]. Our studies were performed by continuous low frequency a.c. measurements, often with the simultaneous application of TEA and differential thermal analysis (DTA) [11-13].

Experimental

We have studied alkali metal and thallium acetates, propionates and butyrates as well as sodium and thallium salts of open chain fatty acids containing 5–9, 12, 14, 16 and 18 carbon atoms. Data on preparation, purification, analysis and thermal stability have been reported earlier [9–15]. The TEA–DTA device has been described in a previous paper [16], its flow chart being presented in Fig. 1. Capillary cells were used [9, 10] and the microcell with gold electrodes evaporated onto glass surfaces is presented in Fig. 2a. With special regard to the organic substance investigated, the following remarks are pertinent to the measuring technique used.

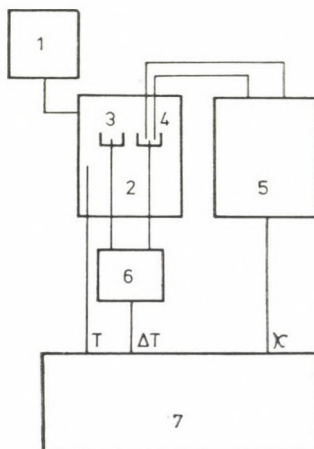


Fig. 1a. General view of simultaneous DTA–TEA apparatus. (1) Temperature program; (2) furnace; (3) reference material; (4) sample; (5) conductometer; (6) amplifier; (7) recorder

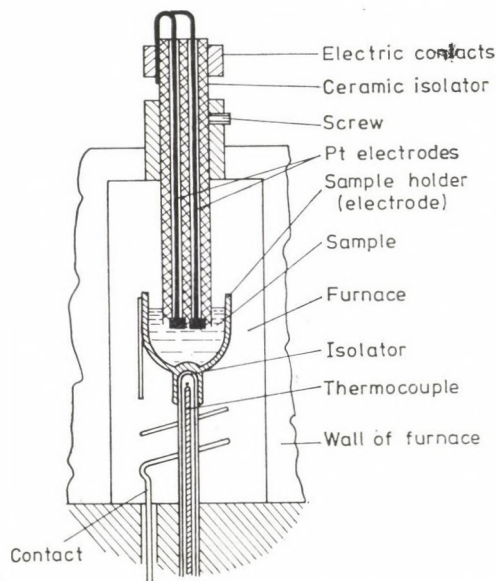


Fig. 1b. Detailed view of the measuring cell

The reliability and reproducibility of the TEA measurements greatly depend on the purity of the samples. The presence of contaminations, the solvent and its water content have dramatic effects on the data measured. Perfect contact between the sample and electrodes must be ensured. The frequency dependence of the data must be studied and the possibility of electrode reactions must also be taken into consideration. We have found that small amounts of the initial substances, free fatty acids, metals, metal oxides do not affect the conductivity values measured. The water content should, however, be reduced to a minimum. The compounds were, therefore, prepared and crystallized in anhydrous solvents. Volatile traces of the solvent were removed in vacuum and measurements were carried out in a dry inert gas atmosphere. In this way the temperature range of thermal stability could also be increased. On reproduction of the measurements, some decomposition reactions could be observed and the samples were mildly decolourized. The measurements ceased to be reproducible, however, only upon thermal decomposition, involving also intensive gas evolution at higher temperatures. Satisfactory contact was ensured by melting the sample prior to the measurements. In some cases, however, this excluded the possibility of observing polymorphic transitions at lower temperatures. When studying the frequency dependence of the EC curve for some of our compounds, we found the effect of frequency change to be negligible in the range between 80 Hz and 20 kHz. By means of the simultaneous system, identification of the phase transition of salts with many polymorphic transitions could be easily carried out. From the DTA signals recorded by the device, no quantitative caloric data could be obtained. EC curves indicated phase transitions unambiguously in a well reproducible way. For derivatives with liquid crystal properties, corresponding to the two phase transitions, two EC jumps have been recorded while the simple solid to isotropic liquid transition was indicated only by a sharp shoulder.

During application of the simultaneous measuring device, using a crucible as sample holder, it could be observed that upon transition from an isotropic liquid to a mesophase, during the cooling cycle, the EC curve of the mesophase was affected by the rate of cooling. Although the phenomenon was found to be partly reproducible, unambiguous investigations could be carried out only by applying a capillary type cell. Results as well as their interpretation are also supported by the data obtained with the cell shown in Figs 2a, b.

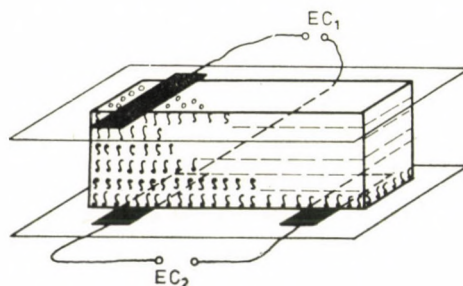


Fig. 2a. Schematic electrode arrangement in the microcell. EC₁ = on opposite slides; EC₂ = on the same slide

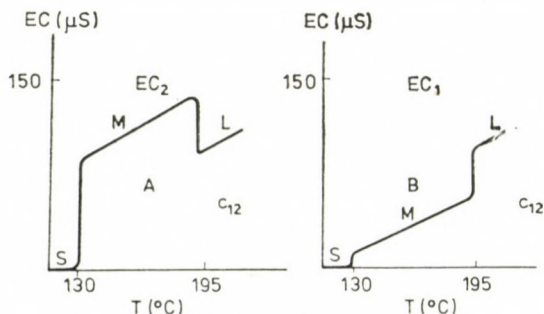


Fig. 2b. Electrical conductivity of Tl(I) laurate measured between two glass slides. A = parallel to the smectic planes; B = perpendicular to the smectic planes

In some instances, cell constants were not taken into account in the evaluation of the results. The routine technique, determination by means of a potassium chloride solution, did not afford reliable data as measurements were carried out at much higher temperatures than during calibration. In addition, as will be seen, the geometry of the cell has a specific effect on the measurements and has an active role in the development of conductivity.

Results and Discussion

The thermoelectric properties of alkali acetates having no mesophases have been described [9,10]. Changes in the EC curve assigned to phase transitions and the activation energy of the conductivity of melts have been deter-

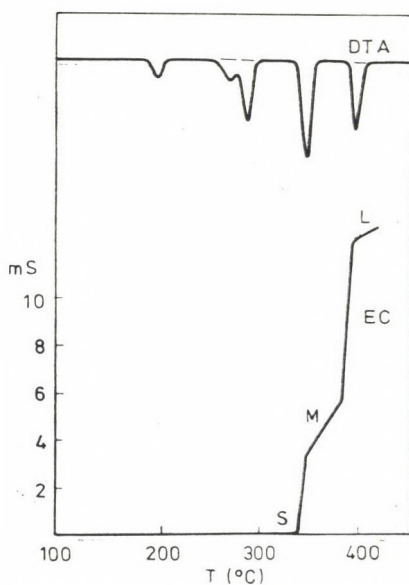


Fig. 3. Simultaneously measured DTA and EC signals of potassium butyrate

mined. The activation energies of viscosities have been similarly identified. From these values correlations have been deduced for the structure and thermal decomposition of the melts as well [9,10].

The thermoelectric investigation of C_3 – C_4 alkali salts pointed to the presence of a mesophase. Literature data on salts with given cations recorded the smectic phase only for those having C_5 or higher carbon numbers [2, 17, 18]. In addition to the not too satisfactory DTA data, thermo-optical studies with polarized light [5] and simultaneous DTA–TEA measurements applied by us gave unambiguous evidence (See e.g., Fig. 3) on these points.

In the following, data obtained in the investigation of sodium and thallium fatty acid salts, containing 5 or more carbon atoms and having a meso-

phase in a relatively wide range of temperature, will be presented and evaluated. For both sodium and thallium(I) salts, the EC curve obtained from data measured in a device equipped with a crucible approximately correspond to the expected values. It can be observed in Figs. 4a, b and 5a, b that the transition to the mesophase as well as its cessation is indicated by a jump in the curve. The conductivity of the mesophase showed a not quite linear change

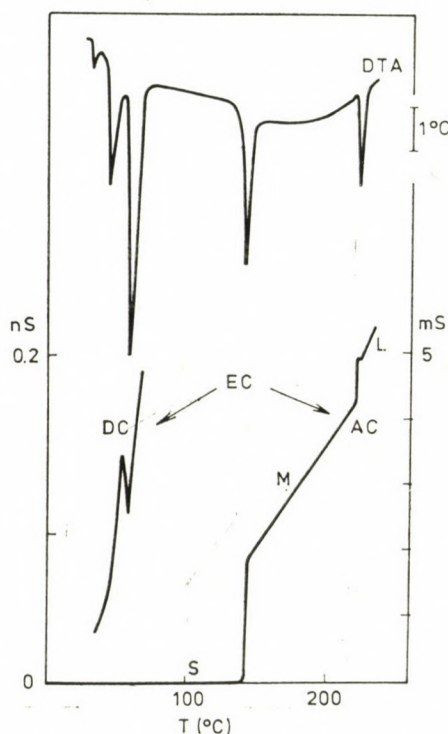


Fig. 4a. DTA—EC curves of sodium valerate

both in the heating and cooling cycles. In the cooling cycle an unusual change could be observed in the conductivity of the mesophase, *viz.* a constant displacement of the curve. These shifts were not reproducible for sodium salts but could be repeated in the case of thallium salts. Based on our hypothesis on the phenomenon, a capillary type measurement cell was applied for the study of this anomalous behaviour. Our findings can be summarized as follows.

The two jumps corresponding to the two phase transitions are unambiguously reproducible whereas their relative size could be reproduced only under strictly identical experimental conditions. During repetition of the measurements, the conductivity was constant for both the isotropic liquid and solid

phase of given compounds. The EC data obtained in the mesophase showed a strong dependence on the cooling rate applied during the transition from the isotropic liquid to the mesophase. This dependence, well reproducible for thallium salts but less reproducible for sodium salts, was modified by the form of the measuring cell used. With a capillary cell the conductivity of the mesophase increased with the increase of the cooling rate (see Fig. 6a, b). The shift of the curve was smaller and less pronounced with the crucible type cell and even an

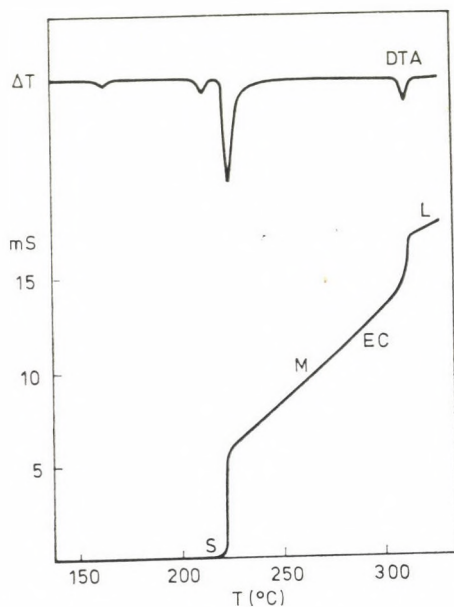


Fig. 4b. DTA—EC curves for thallium(I) pelargonate. DC = direct current; AC = alternating current; S = solid phase; M = mesophase; L = isotropic liquid phase (in all Figures)

opposite trend could be observed. Another difference observed with the two different types of cells was that with the microcell, highest EC values were measured in the isotropic liquid phase, whereas with the capillary cell, the conductivity of the mesophase was found to be higher at cooling rates higher than the given value. This latter phenomenon was observed, however, only for thallium salts. At an arbitrary temperature corresponding to the mesophase, the application of shear force along the length of the capillary resulted in a maximum EC value at a given temperature (Fig. 6b). The EC curve obtained in a cooling cycle at a given rate and up to room temperature could be unambiguously reproduced in the next heating cycle even if the cooling rate was arbitrarily changed after transition from the isotropic liquid phase to the mesomorphic state. From these observations it may be assumed that the structure developed in the phase transition from i. liquid to mesomorphic as a function

of cooling rate, determines the structure affecting also the electric conductivity of the mesophase. In other words, the mesomorphic compounds studied seem to "remember" the cooling rate applied in the previous phase. At the same time, the enthalpy and entropy values belonging to the phase transition in question were well reproducible and independent of the rate of heat treatment. Another important finding is that the electric field of the conductometer does

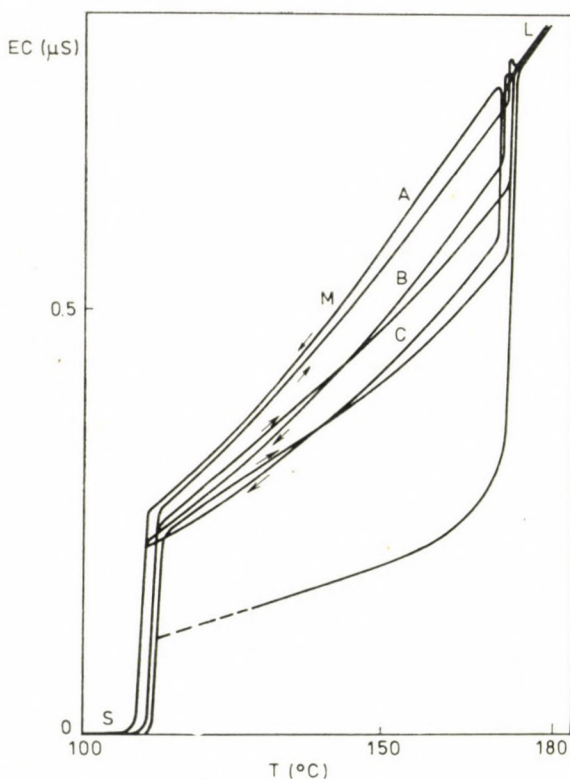


Fig. 5a. EC vs. temperature correlation measured in a crucible type sample holder in the case of thallium(I) stearate as a function of the cooling rate applied during the mesomorphic transition of the isotropic liquid. Cooling rate: A = 0.5 °C/min; B = 10 °C/min; C = 20 °C/min

not alter the results. Application of the microcell provided data corresponding to our earlier observations. The phenomena observed are due to the fact that these salts in the melt phase dissociate also as a function of the temperature and the smaller metal ions with high ion mobilities relative to the anions are responsible for the electric conduction. Another important observation is that in solid mesomorphic transition the crystalline solid system is only "half"-molten and the polar-headed fatty acids carrying an electric charge maintain their structure of ordered arrangement [8, 18]. In the mesophase, the macros-

copic mobility of the metal ions is determined by the different structure of the texture. The discrepancy in the structure may be assigned to the orientation, affected also by the material, surface properties and geometry of the measuring cell as well as by the rate of transition from the statistically disordered state to the mesophase.

If a shear force is applied, the resulting maximum conductivity as well as the measurements presented in Fig. 6b show that the smectic planes are

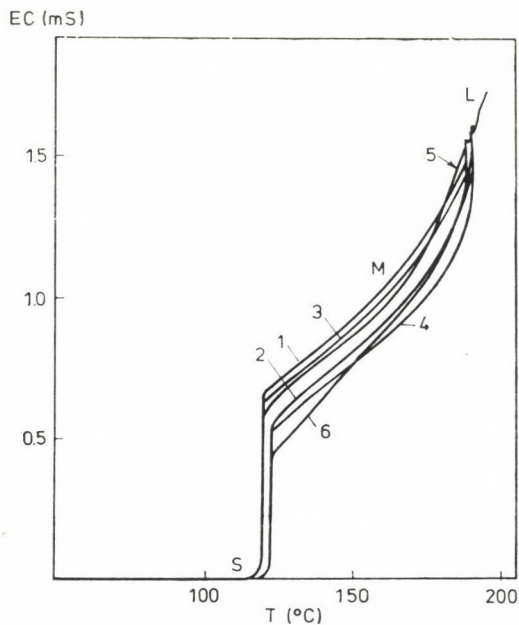


Fig. 5b. Same as 5a. in the case of thallium(I) miristate. 1 = Cooling rate: 5 °C/min; 2 = heating rate: 5 °C/min; 3 = cooling rate: 20 °C/min; 4 = heating rate: 5 °C/min; 5 = cooling rate: 0.5 °C/min; 6 = heating rate: 10 °C/min

nearly parallel to the wall of the capillary and the channels formed between the planes offer a most favourable possibility for cation migration. At lower cooling rates the development of the domain structure is less oriented by the wall than during rapid cooling. The explanation of this is the formation of crystal centers starts at the cell wall due to the relatively high temperature gradients, while at lower cooling rates the process takes place in the bulk of the capillary. These less ordered domains are less favourable for the movement of the conducting ion. With the increase of capillary diameter, the orientation effect of the cell wall becomes much less pronounced; the dependence of EC plotted on the rate of cooling in the mesophase gave much less discrepancy. With measurements in the crucible cell the difference in the geometry and material of the wall and the much less favourable bulk to wall surface ratio,

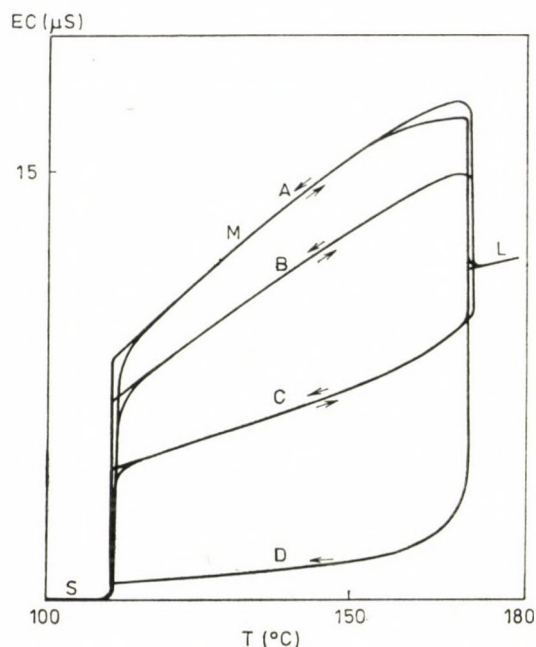


Fig. 6a. Electrical conductivity vs. temperature correlation of thallium(I) stearate, measured in a capillary type cell, as a function of the cooling rate applied during the liquid mesomorphic transition. Cooling rate $A = 10$ °C/min, $B = 1$ °C/min, $C = 0.2$ °C/min, $D = 0.05$ °C/min

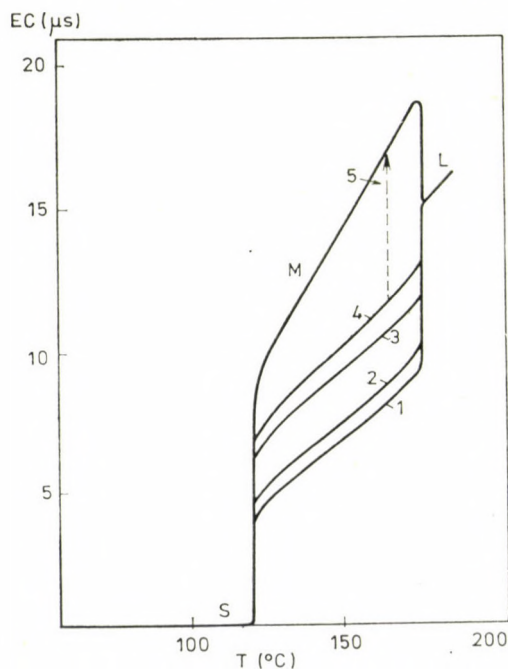


Fig. 6b. Same as in Fig. 6a, for thallium(I) miristate. Cooling rate $1 = 0.5$ °C/min; $2 = 1$ °C/min; $3 = 5$ °C/min; $4 = 8$ °C/min; $5 =$ effect of shear force

these effects could not be unambiguously detected as in the case of the capillary cell. The difference in the thermoelectric behaviour of sodium and thallium salts is due to the different abilities of these salts to crystallization.

The "memory" effect may be attributed to the fact that the transition arrangement determines also the fine structure of the real crystal phase.

REFERENCES

- [1] ADLER, D.: Crit. Phenomena Alloy, Supercond. Battelle Inst. Mater. Sci. Colloq. 5th 1970, 567—591. Ed. by MILLS, R. E., GROW, M. New York 1971
- [2] Liquid Crystals and Plastic Crystals. Eds GRAY, G. W., WINDSOR, P. A., Vol. 2, Chapter 5, Ellis Horwood Ltd. Chichester 1972
- [3] VOLD, R. D., HELDMAN, M. J.: J. Phys. Chem., **52**, 148 (1948)
- [4] FOGG, P. G. T., PINK, R. C.: J. Chem. Soc., **1959**, 1735
- [5] UBBELOHDE, A. R., MICHELS, H. J., DURUZ, J. J.: Nature, **228**, 50 (1970)
- [6] EKWUNIFE, M. E., NWACHUKWU, M. U., REINHART, F. P., SIME, S. J.: J. Chem. Soc. Faraday I, **71**, 1432 (1974)
- [7] EKPE, U. J., SIME, S. J.: J. Chem. Soc. Faraday I, **72**, 1144 (1976)
- [8] DURUZ, J. J., MICHELS, M. J., UBBELOHDE, A. R.: Proc. Roy. Soc. A, **322**, 281 (1971)
- [9] HALMOS, Z., MEISEL, T., SEYBOLD, K., ERDEY, L.: Talanta, **17**, 1191 (1970)
- [10] HALMOS, Z., MEISEL, T.: Periodica Polytechnica, **17**, 90 (1973)
- [11] RÓTH, J.: Dissertation, Technical University of Budapest, 1975
- [12] SEYBOLD, K.: Dissertation, Technical University of Budapest, 1977
- [13] RÓTH, J., MEISEL, T., SEYBOLD, K., HALMOS, Z.: J. Thermal Anal., **10**, 223 (1976)
- [14] MEISEL, T., SEYBOLD, K., HALMOS, Z., RÓTH, J., MÉLYKUTI, Cs.: J. Thermal Anal., **10**, 419 (1976)
- [15] HALMOS, Z., SEYBOLD, K., MEISEL, T.: Thermal Analysis, Proc. Fourth ICTA Budapest, 1974, Ed. I. BUZÁS, Vol. 2, p. 429. Akadémiai Kiadó, Budapest 1975
- [16] HALMOS, Z., WENDLANDT, W. W.: Thermochim. Acta, **7**, 95 (1973)
- [17] PORTER, R. S., BARRALL, E. M., JOHNSON, J. F.: Thermal Analysis, Proc. Second ICTA Worcester 1968, Eds SCHWENKER, R. F., GARN, P. D., Vol. 1, p. 597. Academic Press, New York—London 1969
- [18] SKOULIOS, A., LUZZATI, V.: Nature, **183**, 1310 (1959)

Tibor MEISEL

Károly SEYBOLD

Júlia RÓTH

H-1521 Budapest, Gellér tér 4.

MODELING OF LIQUID PHASE HYDROCARBON OXIDATION PROCESSES

D. GÁL, L. BOTÁR, É. DANÓCZY, I. P. HAJDU, J. LUKÁCS, I. NEMES and
T. VIDÓCZY

*(Central Research Institute for Chemistry, Hungarian Academy of Sciences,
Budapest)*

Received August 11, 1978

Accepted for publication October 30, 1978

In order to optimize the investigation of the liquid phase hydrocarbon oxidation processes, a modeling procedure is suggested. The procedure is arranged along three black boxes the first including the mission oriented information collection of data available from literature sources.

The data collection leads directly to the planning of experimentation, including studies on the overall process as well as on subsystems and elementary processes.

The third box refers to the kinetic-mathematical treatment of data obtained previously.

Oxidation of ethylbenzene served as a prototype for the modeling and results published earlier in different periodicals were summarized.

Essentially, the study of a certain chemical transformation — within the framework of chemical kinetics — means the “exploration” of a “black box” operated by the following factors.

1) Species participating in the transformation and the elementary processes involved in it.

2) Internal interactions (internal conformities) of the system, such as

a) general interactions valid for any chemical system (*e.g.* principle of the independence of elementary processes, principle of charge conservation, *etc.*)

b) isomorphic interactions characterizing “similar” systems *e.g.* cage effect, wall effect, *etc.*

c) special interactions characterized by correlations between the concentrations of the species.

Based on this approach, the kinetic study of any chemical transformation — the aim of which is the elucidation of the kinetics and mechanism of the process under investigation — means the elaboration of an algorithm including questions addressed to the “black box” and methods for the assessment of the answers.

1. Inducement of modeling

The fast evolution of research on degenerate branching chain reactions and among them on hydrocarbon oxidation reactions — started after the appearance of the monograph of SEMENOV [1]. Recently, mainly in the last

decade, a demand arised for a new approach in these studies due basically to three motivations;

- accessibility of up-to-date and highly efficient equipment permitting broad spectra of chemical analysis,
- the spreading of computers and accessibility of computer programs for the treatment of multistep reaction systems,
- expansion of systems theory for treating complex phenomena.

A possible version of the new approach could be the modeling of the processes defined as follows.

Modeling is a general conception expressing scientific approach to a given group of reactions.

Accordingly, modeling can be characterized by the following features; it is not limited to a single overall reaction within the reaction group: its aim is the acquirement of concrete information and discernment of scientific relations: it is attached to a certain group of reactions.

Obviously, with respect to its aims modeling does not differ from the aims of scientific research in general, it is merely an instrument of scientific research and consequently it must correspond adequately to the level of our present theoretical and practical knowledge.

It is the hope of the authors that the modeling to be expounded in the present paper is consonant with the demands for the new approach, that is, (i) it is based on the information accumulated for the reaction group to be studied, (ii) it takes into account the possibilities provided by computers and (iii) it regards the given reaction group as a whole system considering both the classical kinetic (inductive) as well as the deductive approaches based on rational reduction.

Furthermore, modeling as a tool is justified only if it furnishes new information and enables the conscious planning of further experimental and theoretical investigations.

These latter conditions, however, can be resolved only practically: by its application for the study of a "prototype" being an overall process and belonging to the reaction group.

2. The Modeling Scheme

The modeling scheme suggested is represented by Fig. 1. As can be seen from Fig. 1, it can be grouped in three boxes;

1. Mission Oriented Information Collection (MOIC) summarizing operations to be carried out in the first stages.

2. Experimental Procedures (EXPERIMENTAL) containing different types of experimentation.

3. Data Synthesis (SYNTHESIS) represents the kinetic-mathematical treatment of the qualitative and quantitative values obtained "in" boxes MOIC and EXPERIMENT.

Every box contains several suboperations abbreviated accordingly and discussed later.

Boxes are interconnected by information fluxes. It is assumed that between MOIC and SYNTHESIS two types: direct and indirect — the latter *via* EXPERIMENT — information fluxes are realized, while a counter-flux flows from SYNTHESIS to MOIC. (The sole exception is the direct coupling between SNW and SS — explained later — called by analogy a *tunnel effect*.)

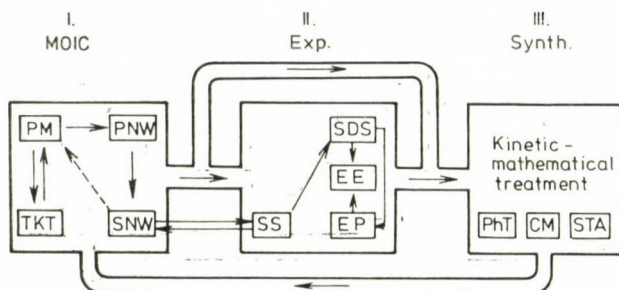


Fig. 1

Although not apparent from the planar representation of the modeling scheme, the information counter-flux always generates a new MOIC which is more abundant.

The internal arrows in the boxes refer to information fluxes between suboperations. Among them, as can be seen from Fig. 1, there exists one reversible arrow pair called by analogy *pre-equilibrium* and indicating that the reversibly coupled suboperations might reversibly and directly modify their sources.

2.1 The Box MOIC

The first partial operation of MOIC is the collection of the Possible Mechanism (PM) defined as the set of all those elementary steps which were suggested according to literature data to participate in the overall process — or in processes analogous to the prototype — in the experimental parameter region independently of their quantitative weight in the overall process. The exclusion criterion for an elementary process is the unambiguous experimental proof that it does not occur.

In principle, the PM can be constructed by combinatorial analysis with a fixed species space. However, this is recommended only if the prototype seems to be a less studied overall process, otherwise the PM would be increased superfluously, affecting harmfully the efficiency of the whole modeling procedure.

The independence of the elementary processes of their weight played in the overall reaction is fundamental. Namely, it is well known that this weight varies with the conversion and modeling should not be limited to the initial stages of the overall process.

The collection of the PM is followed by its Thermochemical Kinetic Treatment (TKT) in order to reduce, eventually to extend the PM. This reduction or extension is denoted by the reversible coupling of PM and TKT.

The PM modified possibly by TKT serves as a basis for the construction of the Possible Reaction Network (PNW). This latter is a well defined system of the chemical processes included in the PM in which system the single processes are interconnected by their reactants.

Operation PNW includes also the construction of reaction subnetworks and partial networks differing from the PNW by correspondence to *reduced* PM's. Reduction might be carried out in the light of chemical evidences or practical requirements.

There is however, a special network construction which is of fundamental importance regarding the planning of experimentation. This is the so-called Sequence-Network (SNW) reflecting the entirety of the precursor — product relations for species included in the PM and eventually reduced arbitrarily. (In the literature, instead of SNW, the analogous expressions of reaction pathways or reaction scheme are used.)

2.2 The Box EXPERIMENT

The completion of operations in box MOIC permits the rational planning of the experimental work.

The first suboperation of this work should be Sequence Studies (SS) with the aim the prove (or disprove) the SNW constructed from literature data (or by combinatorial analysis) with the help of direct experiments including the determination of the concentrations of the main products against conversion.

This task can be solved by rather different methods such as the Kinetic Isotope Method (KIM) [2], Method of Open Systems [3] and in certain — though very limited cases — by the simple kinetic analysis of the accumulation curves of the products.

The reversible coupling between SS and SNW means that the results of the former might correct directly the latter. If this occurs, the PM itself should also be corrected by simple reduction or extension denoted by the dotted arrow leading from SNW to PM.

The left side operation in the box EXPERIMENT refers to the overall reaction, while right side operations represent partial systems. First of them is the study of the Sequence Network Defined Subsystems (SNDS).

The precursor — product relations in the SNW are denoted — as a rule — by arrows. These arrows represent no stoichiometric relations, but sets of parallel and consecutive elementary processes. (Only in very rare and fortunate cases do they represent a single elementary process.) These sets can be easily selected as subsets from the PM with the help of a special algorithm elaborated for this purpose.

The subsystems can be studied creating "artificial" mixtures in which the initial components are the precursors belonging to the "arrow" to be investigated. The experimental conditions (temperature, pressure, etc.) should advisably correspond to those applied for the overall system.

The main aim of the investigations of the SNDS is the extension of the information with respect to the overall system by reducing the species space.

The adequacy of the data obtained by operations SS and SNDS, that is, the mutual applicability of the quantitative results, must be checked permanently, e.g. by the investigation of Environmental Effects (EE).

Namely, it can be assumed that inasmuch as the mutual applicability of the data is not fulfilled, this is due primarily to internal structural changes in the system, such as solvent effects changes in the radical balance, formation of different complexes with hydrogen bridges, etc.

One of the basic aspects of the modeling procedure is the study of Elementary Processes (EP). This can be realized partly within the overall system if a suitable physical method is accessible (e.g. chemiluminescence measurements to follow the combination processes of peroxy radicals, application of CIDNP, etc.).

Partly, however, artificial mixtures must be generated and the species space drastically reduced (inhibitor method, "in situ" generation of radicals by using azocompounds in the absence of substrates, etc.).

Operation EP should also be coupled to EE since the changes in the environment affect strongly the adequacy of the data.

It should be emphasized that operations in box EXPERIMENT exceed the usual classical approaches which limit the considerations to investigation of the parameters of the overall reaction. Research on subsystems or elementary processes, if any, was carried out detached both in time and space from the studies on the overall process, that is, the mutual applicability of the data had rarely been checked.

The approach suggested here is very essential if information is required at high conversions where the interaction of the intermediates and their competition for the radicals become rather complicated and exclusive information with respect to the overall process is insufficient.

2.3 The Box SYNTHESIS

This box contains operations dealing with the kinetic-mathematical treatment of data obtained earlier.

With respect to degenerate branching chain reactions, three different — but in addition supplementary — tendencies can be observed.

a) Phenomenological treatment of the initial stages of the reaction (PhT), elaborated for liquid phase oxidation processes by EMANUEL and coworkers [4]. This procedure starts with a "small" or "minimal" mechanism and kinetic expressions derived from this mechanism should fit the initial stages of the experimental curves. In the case of a "good" fitting, the rate constants or their combination for the starting mechanism can be determined. The choice of the starting mechanism is based on chemical evidences and the application of the Bodenstein-Semenov principle is a precondition of the procedure. The starting mechanism might be improved by increasing the number of elementary processes.

b) Computer simulation of the overall reaction (CS) uses a set of elementary steps, the size of which considerably exceeds that used in the previous treatment, though being smaller, than the PM. Similarly to the previous procedure, the selection of the elementary processes is based on kinetic evidences, and both measured and estimated rate constants and activation parameters are used without the application of the steady state approach.

The kinetic curves of the accumulation of the products are simulated by computer programs. Simulated and measured curves are compared and their conformities serve as criteria for the proper selection of the elementary processes and rate constants [5].

In the case of satisfactory conformity, so-called "sensitivity tests" can be carried out by varying the rate constants of certain types of processes (propagation, termination, *etc.*) and repeating the computer simulation. Thus we obtain information on the products whose accumulation is most sensitive to the actual values of the rate constants.

c) Systems theory approach (STA). It starts from the PM as a whole system and intends to reduce it by mathematical methods (*e.g.* mathematical logical procedures). The reduced PM is used for computer simulation similarly to the previous treatment.

The three above treatments are not controversial, although they differ considerably. Their consistency increases in the given order, because the subjective factors are decreasing and the amount of information increases.

In spite of the differences, all three procedures are justified and the proper selection should be motivated by the aims of the actual research.

Although prospectively the STA seems to become the most suitable for the approximation of the "true mechanism" of the processes, at present ap-

proaches (a) (at low conversions) and (b) (at higher conversions) provide more and useful information.

3. Proper selection of the prototype

Although in principle any of the processes belonging to the reaction group can be chosen, the efficiency of modeling depends strongly on the proper selection of the prototype.

It is suggested that two demands should be primarily fulfilled when choosing a proper prototype.

a) Theoretically the prototype should reflect the characteristic features of the reaction group but should not represent an extremum. For example, when studying the gas phase oxidation of hydrocarbons, the choice of methane oxidation as a prototype would not be very suitable due to its extreme character: the excessive stability of methane toward oxidation, the lack of cool flame phenomena during its slow oxidation, *etc.*

b) Practically it is important that the amount of the literature information should be considerable, which is expedient especially in constructing the PM and the different networks.

A further practical requirement is the suitable experimental treatment including a possibly small species space.

4. Application of the modeling procedure to the liquid phase oxidation of ethylbenzene

The following motivations for choosing the liquid phase oxidation of ethylbenzene as prototype can be mentioned.

For this oxidation process, relatively many data are available in the literature, among them rate constants of elementary processes included in its PM with more or less acceptable accuracy. Its species space is reasonable, contains only 13 species. Several new experimental techniques have been elaborated using this reaction as a model process, among them, sequence studies, chemiluminescence measurements, investigations of homogeneous catalysts in such types of processes, *etc.*

Here we review only very briefly the main results obtained by using the liquid phase oxidation of ethylbenzene in the temperature interval 40–130 °C as prototype for the modeling procedure suggested.

Its PM contains 52 elementary processes [6], which can be divided in four groups; *initiation processes*, that is, interactions between the initial substrates, *chain propagation* represented by radical attack on stable molecules, *degenerate branching* which are decomposition processes of stable intermediates into radicals, and *termination processes*, *i.e.* radical combinations. When col-

lecting the PM, meticulous care was taken that the PM should be appropriate in representing the overall process up to high conversions.

The carbon skeleton sequence network of ethylbenzene oxidation — constructed according to a special algorithm published elsewhere [7, 8] — indicates that the transport of the carbon skeleton proceeds from the substrate to hydroperoxide molecules and also directly to both ketone and alcohol molecules [9, 10]. The transformation of the hydroperoxide yields also ketone and alcohol, while an additional alcohol — ketone carbon skeleton transition should be taken into account if the PM correctly represents the overall reaction.

Operation SS has been carried out by tracer methods, initially labeling the alcohol (phenyl methyl carbinol) [11–14].

It has been established that the alcohol is, indeed, an intermediate formed and consumed simultaneously during the oxidation. Its consumption occurs only in one direction; toward the ketone. Under the experimental conditions the ketone (acetophenone) is the end product of the reaction and the pathways of its formation are *a*) *via* alcohol molecules; *b*) *via* hydroperoxide or peroxy radical combination (direct route). The ratio of the pathways *a/b* varies with the conversion; in the initial stages, the direct route predominates and route *a* becomes important only at later stages.

The rates of these routes were determined quantitatively as a function of conversion.

Experiments carried out in the presence of labeled hydroperoxide molecules [15–18] necessitated the slight modification of the theoretical SNW. It has been established, namely, that alcohol formation and direct ketone formation are realized *via* two different routes; partly by the transformation of hydroperoxide molecules and partly by the interaction of peroxy radicals formed as primary unstable intermediates from the substrate. These different routes have been separated and their rates determined as a function of conversion.

Data obtained by adding both labeled alcohol and hydroperoxide support the increasing role of secondary process: the further transformation of stable intermediates with increasing conversion. This fact motivated our efforts to study the reactivity of the stable intermediates toward radicals accumulated in the system.

According to our values — obtained as a side product of the tracer experiments [19–20] — the reactivity increases in the order ethylbenzene < α -phenyl ethyl hydroperoxide < phenyl methyl carbinol in good conformity with the increased role of the intermediates at higher conversions.

Within the framework of operation SNDS, the kinetics and mechanism of the following systems have been investigated: transformation of alcohol into ketone [21–22]; transformation of hydroperoxide into alcohol and ketone [23–25]; rates of formation of radicals [26–27].

It has been established [22] that the alcohol molecules undergo radical-induced transformation, yielding ketone in a chain processes, presumably with hydrogen peroxy radicals (HO_2^\cdot) as chain carriers. The latter are formed *via* isomerization and decomposition of oxyperoxy radicals derived from alcohol radicals.

The transformation of hydroperoxide molecules [25] was realized both by their homolytic and radical-induced decompositions, where the latter processes are predominant, while the former ones — though their role as initiation reactions is of importance [15] — can be neglected as contributors to the consumption.

Further results of operation SNDS were the determinations of certain elementary rate constants such as those of processes between peroxy radicals and hydroperoxide as well as alcohol molecules. Chemiluminescence studies are under way in order to gain information with respect to the combination reactions of radicals [28–29].

Among operations EE, detailed studies have been carried out and are in progress with respect to the H-bridged complexes of hydroperoxide molecules as well as between hydroperoxide molecules and other stable compounds accumulated in the system. Although the quantitative evaluation of these data is not yet finished, it can be stated already that alcohol and ketone molecules affect strongly the environment of the hydroperoxide complexes interacting with both monomers and dimers as well as in certain cases with the oligomers, too.

In order to complete the kinetic-mathematical treatment of the overall process, an algorithm has been elaborated to select the elementary processes responsible for the different pathways [10]. It has been shown that in the present system, under the conditions chosen, any product can be obtained by no more than two consecutive steps from its precursor though the number of parallel processes is not restricted.

The mathematical-logical treatment of the PM led us to the selection of the minimal mechanisms [30–31] summarizing in a qualitative form steps which describe the consumption of the initial compounds, the formation and consumption of the intermediates and the formation of the end products.

The computer simulation of the overall process has been started [32–33] and by using 40 elementary processes and their kinetic parameters — either determined or estimated — fair agreement has been achieved up to about 20% conversion between experimental and calculated product accumulation curves.

Furthermore the contributions of the different steps with respect to the overall process and the accumulation of the different products have been calculated. It seems interesting to note that at 120 °C for the first 10 hours the minimal mechanism including steps which contribute more than 95% to the

different types of processes (initiation, propagation, branching, termination) is nearly identical with the mechanism used for the phenomenological calculations and obtained from chemical evidences or intuition.

5. Conclusions

The advantages of the modeling procedure suggested in the present paper are the following.

1. It can efficiently use literature information *via* systematizing and synthesis.
2. It yields efficient help in planning experiments to provide maximum information.
3. It contains new evaluation methods.
4. It is opposed to considerations widely used in chemical kinetics which aim to "determine the mechanism" of a given complex process.

REFERENCES

- [1] SEMENOV, N. N.: Chain Reactions. GNTI, Leningrad 1934 (in Russian)
- [2] NEIMAN, M. B., GÁL, D.: The Kinetic Isotope Method and Its Application. Elsevier-Akadémiai Kiadó, Budapest 1972
- [3] SKIBIDA, I. P., MAIZUS, Z. K., EMANUEL, N. M.: Usp. Khim., **38**, 3 (1948)
- [4] EMANUEL, N. M., DENISOV, E. T., MAIZUS, Z. K.: Chain Reactions of Hydrocarbon Oxidation in the Liquid Phase. Nauka, Moscow 1965 (in Russian)
- [5] ALLARA, D. I., EDELSON, D., IRWIN, K. C.: Int. J. Chem. Kin., **4**, 345 (1972)
- [6] GÁL, D., NEMES, I., BOTÁR, L.: Magy. Kém. Folyóirat, **82**, 326 (1976)
- [7] NEMES, I., VIDÓCZY, T., BOTÁR, L., GÁL, D.: Magy. Kém. Folyóirat, **82**, 332 (1976)
- [8] NEMES, I., VIDÓCZY, T., BOTÁR, L., GÁL, D.: Theoret. Chim. Acta, **45**, 215, (1977)
- [9] NEMES, I., VIDÓCZY, T., BOTÁR, L., GÁL, D.: Theoret. Chim. Acta, **45**, 225, (1977)
- [10] NEMES, I., VIDÓCZY, T., GÁL, D.: Theoret. Chim. Acta, **46**, 243 (1977)
- [11] GÁL, D., DANÓCZY, É., NEMES, I., VIDÓCZY, T., HAJDU, P.: Ann. N. Y. Acad. Sci., **213**, 51 (1973)
- [12] DANÓCZY, É., VASVÁRI, G., GÁL, D.: J. Phys. Chem., **76**, 2785 (1972)
- [13] DANÓCZY, É., VASVÁRI, G., GÁL, D.: Magy. Kém. Folyóirat, **77**, 632 (1971)
- [14] DANÓCZY, É., NEMES, I., GÁL, D.: Magy. Kém. Folyóirat, **79**, 73 (1973)
- [15] DANÓCZY, É., NEMES, I., VIDÓCZY, T., GÁL, D.: JCS Faraday Trans. I, **71**, 841 (1975)
- [16] DANÓCZY, É., NEMES, I., GÁL, D.: JCS Faraday Trans. I, **73**, 135 (1977)
- [17] DANÓCZY, É., NEMES, I., VIDÓCZY, T., GÁL, D.: Magy. Kém. Folyóirat, **79**, 545 (1973)
- [18] DANÓCZY, É., GÁL, D.: JCS Faraday Trans. I (In press)
- [19] NEMES, I., DANÓCZY, É., VIDÓCZY, T., GÁL, D.: Magy. Kém. Folyóirat, **81**, 395 (1975)
- [20] NEMES, I., DANÓCZY, É., VIDÓCZY, T., GÁL, D.: Combustion and Flame, **27**, 285 (1976)
- [21] VIDÓCZY, T., DANÓCZY, É., GÁL, D.: Magy. Kém. Folyóirat, **79**, 258 (1973)
- [22] VIDÓCZY, T., DANÓCZY, É., GÁL, D.: J. Phys. Chem., **78**, 828 (1974)
- [23] RUBAJLO, V. A., NEMES, I., EMANUEL, N. M., GÁL, D.: Magy. Kém. Folyóirat, **80**, 465 (1974)
- [24] HAJDU, P., GÁL, D.: Magy. Kém. Folyóirat, **82**, 399 (1976)
- [25] HAJDU, P., NEMES, I., GÁL, D., RUBAYLO, V. I., EMANUEL, N. M.: Can. J. Chem., **55**, 2677 (1977)
- [26] VIDÓCZY, T., GÁL, D.: Z. phys. Chem. NF, **106**, 269 (1977)
- [27] VIDÓCZY, T., GÁL, D.: Z. phys. Chem. NF (In press)

- [28] SIMON, P., VASVÁRI, G., KENDE, I., GÁL, D.: *Magy. Kém. Folyóirat*, **78**, 393 (1972)
[29] SIMON, P., GÁL, D.: *Magy. Kém. Folyóirat*, **78**, 611 (1972)
[30] NEMES, I., BOTÁR, L., GÁL, D.: *Z. phys. Chem.*, **255**, 311 (1974)
[31] NEMES, I., BOTÁR, L., GÁL, D.: *Z. phys. Chem.*, **255**, 378 (1974)
[32] RUBAYLO, V. A., VIDÓCZY, T., NEMES, I., STREHO, M., EMANUEL, N. M., GÁL, D.: *Magy. Kém. Folyóirat*, **81**, 75 (1975)
[33] VIDÓCZY, T., LUKÁCS, J., NEMES, I., GÁL, D.: *Magy. Kém. Folyóirat*, **85**, 97 (1979)

Dezső GÁL

László BOTÁR

Éva DANÓCZY

Péter HAJDU

Júlia LUKÁCS

István NEMES

Tamás VIDÓCZY

H-1025 Budapest, Pusztaszeri út 59—67.

RECENSIONES

Polymerization of Organized Systems

Edited by Hans-Georg ELIAS, Midland Macromolecular
Monographs, Vol. 3. 230 pages

Gordon and Breach Science Publishers, New York, London, Paris 1977

Polymerization processes in organized systems are promising from both the theoretical and practical points of view. Hence, it was quite obvious that this topic was covered by the program of one of the first annual meetings of the Midland Macromolecular Institute. As there are relatively few scientists engaged in this field in the world, it was a good opportunity to assemble the representatives of the most active laboratories to present achievements and unsolved problems. The discussions following the lectures are also included in the book; this enables the reader to enjoy the feeling of active "participation" in the meeting.

The lectures dealt with the relationships of solid state polymerization, liquid crystalline polymerization, polymerizations in mono- and multilayers, polymerization on surfaces, solid phase polycondensation and with polymerization of a monomer in interaction with a polymer matrix. It is unfortunate that merely an abstract of the survey-like first lecture (Herbert MORAWETZ: "Polymerization and Other Organic Reactions in the Crystalline State") can be found in this collection, since the complete text has been published elsewhere. In the lecture of Bernhard WUNDERLICH, entitled "Polymer Crystal Nucleation and Growth from the Gaseous and Liquid Monomer", the role of structure formation and start of crystallization in the polymerization process are treated. The outstanding results of the lecturer in this field are well known. Investigations of polymerization procedures carried out in mono and multilayers, reflect the advantageous effect of the preordered monomer on the rate of polymerization. Not too much can be learned about the structure of the polymers formed in this manner.

The lectures which concern polymerization reactions in mesophase collect the results obtained up to that time, reflecting the knowledge then available. Speed-up of research work in this area during the last one and half year has since resulted in a better understanding of these phenomena. The lectures in question also reveal that the structures of polymers obtained in polymerization processes in liquid crystalline medium were not examined sufficiently. Besides, the term "liquid crystal polymer" became suddenly current in the literature, without an explanation what is to be understood by this concept. When passing over to macromolecular systems from low molecular weight liquid crystalline structures, the former required exact definitions and unambiguous experimental evidence to prove one or other (nematic, smectic or cholesteric) polymeric structure. None of the solid state, liquid crystalline and mono- or multilayer polymerizations have been analyzed by the authors with sufficient attention from the aspect of phase conditions. In all these cases the polymer formed in the ordered medium, and the yet unreacted monomer give rise to a binary system, which changes with the progress of polymerization affecting the kinetics and polymeric structure.

It is a pity that the problems of matrix polymerization are discussed only briefly and those of the channel complex polymerizations not at all.

The book may be very useful for those who are interested in the problems of polymerization processes in organized systems.

GY. HARDY

Proceedings of the Fourth Tihany Symposium on Radiation Chemistry

Edited by P. HEDVIG and R. SCHILLER

Akadémiai Kiadó, Budapest 1977, 1085 pages

At the end of 1977 Akadémiai Kiadó published the volume "Proceedings of the Fourth Tihany Symposium on Radiation Chemistry" edited by Péter HEDVIG and Róbert SCHILLER. The symposium was held in Keszthely, June 1–5, 1976. The Tihany Symposia on Radiation Chemistry are classed in the international world of radiation chemistry among the more important meetings of high scientific level. These symposia are organized every 4–5 years.

The Tihany Symposia have become the traditional meeting place of researchers from different parts of the world, and have achieved fame not only because of the topics of high scientific level, animated discussions and debates, but also on account of the excellent organization, pleasant atmosphere and the splendid entertaining programs. The number of participants increased steadily and at the last, 4th Symposium amounted 173 persons from 22 countries.

Besides the conventionally represented European countries in the geographical vicinity to Hungary and overseas countries (USA, Canada, Japan), Iraqi and Turkish scientists participated for the first time in this meeting.

Papers were read in four different sections, and accordingly, the subject of the recently published volume is divided into four chapters:

1. organic substances — 33 papers,
2. polymers — 41 papers,
3. aqueous solutions — 33 papers,
4. other topics (not to be classed into the above chapters) — 15 papers.

Papers dealing with biochemical and biophysical problems were presented for the first time at the Tihany Symposium.

The volume contains the full text of the papers and the ensuing discussions, which makes more interesting the reading of the subject.

In this brief review it is practically impossible to enumerate and discuss the problems dealt with in the papers and to evaluate the results obtained. It can be established in general that the subjects reflect truly the modern trends of research in the field of radiation chemistry: on the one hand, research on the elucidation of the nature of elementary processes is continued (using more and more advanced techniques) at moments when these processes are just "*in statu nascendi*", the reactions of the excited and ionized molecules and particles with one another, with the matrix and the additives are further studied, while on the other hand, considerable effort is made to realize processes on an industrial scale on the basis of the theoretical results attained so far. This proved to be particularly successful in the radiation chemistry of polymers.

The multitude of results attained in the last twenty years in radiation chemistry makes it possible to attempt on the basis of these data the formulation of general rules. Such attempts in the volume are for example the elucidation of the effect of the state of aggregation, temperature and of molecular structure on radiolysis, or of the similarities and differences between radiation chemical and photochemical processes, etc. The number of chemical models exposed to radiation, as well as that of physical and chemical test methods increases. All these are reflected in the book.

The lecture texts are published with care, in good English, the drawings and diagrams are of excellent quality, and the endeavour of the editors to unify in the volume the units in the drawings is to be particularly praised.

The volume contains the list of participants, arranged according to countries, and the subject index at the end of the book facilitates orientation, a quick search for the theme wanted.

The presentation of the book, its typographical execution reflect befittingly its rich content of value. The book may be recommended to scientific researchers and postgraduate students active in the field of radiation- and photochemistry, to students who wish to specialize in these branches of science, further to researchers studying elementary chemical reactions.

G. PUTIRSKAYA

Siegfried DÄHNE and Siegfried KULPE

Structural Principles of Unsaturated Organic Compounds with Special Reference to X-Ray Structure Analysis of Coloured Substances

Akademie-Verlag, Berlin 1977

This book was published by the Akademie-Verlag, Berlin, as item N-8 in the 1977-series of mathematical, natural science, and technical treatises of the Academy of Sciences of the GDR.

Bond length data of unsaturated compounds determined by X-ray diffraction analyses also prove the existence of polymethine structures, even as they prove the existence of transition states between the polymethinic, polienic, and aromatic, i.e. the three limiting structures. In addition to this, the novel, unexpected results of these analyses allow a deeper insight into the molecular and electron structure of coloured organic compounds.

In cases of steric hindrance, the fundamental principles which govern the structures of such compounds are comparatively easy to interpret. Of independent, energetically stabilized, ideally aromatically structured groups, especially of π -electron sextets, further of independent, energetically stabilized ideal polymethine groups as many as consistently possible may be identified in the compound, both these types at distances of about one and a half bond lengths between the atoms.

When ideal structures are perturbed by a branching of the conjugated system, or by bonding between groups of different structures, or by a growing asymmetry due to the substitution effect of ideal fragments, then — according to Pauling's rule — the sum of bonds originating in one atom is constant. This explains the emergence of polyene bonds, with less or more pronounced single-bond or double-bond character according to the extensiveness of the conjugated π -electron system in the compound. A deviation from Pauling's rule is found in the conjugated polymethines in which the bond distances are modified by coulomb forces engendered by perturbations due to changes of the charge density, characteristic of ideal polymethines.

Progress in the field of X-ray diffraction analysis aims at the construction of more faultless and automated instrumentation and at the application of more sophisticated and up-to-date mathematical and physical techniques in which programming and computerization are also utilized.

A still more accurate elucidation of structures is promised by the use of the neutron diffraction method.

The first and introductory chapter of this 128-page volume deals with the study of chemical structures and X-ray diffraction analysis; the second chapter discusses structural characteristics of coloured organic compounds. Using the cyanines, oxonols, S-terminal and C-terminal polymethine derivatives as examples: the third chapter describes the structures of the nearly ideal polymethine dye-stuffs. The fourth chapter deals with the intermediary products of polymethine-polyene structures. Here the groups with monomethine structure, merocyanines, thia-merocyanines, non-symmetrical monomethine oxonols, tri-, and pentamethine meropolymethines, and derivatives with longer methine chains are reviewed. Substituted benzene derivatives and conjugated heterocycles, as instances of polymethine-aromatic intermediates, form the subject of the fifth chapter. In the sixth the ideal polymethine-polymethine bonding, the bonded meropolymethines, the polyene-polymethine and aromatic-polymethine couplings, the coupling effects of naphthoquinone and anthraquinone, indigo-type dye-stuffs and polymethines linked into cycles are discussed. In the seventh chapter polymethine radicals, radical cations and anions, and complexes formed with radical-like polymethine structures are dealt with. Hydrocarbons of a stable polymethine structure are treated in the eighth chapters. Chapters 9, 10, and 11 contain a summary, addenda and the list of 939 references to the literature.

This book may rightly claim the attention of researchers interested in the theoretical questions of dye-stuff chemistry and the structural aspects of colouring matters.

I. RUSZNÁK

A kémia újabb eredményei (New Results in Chemistry), Vol. 37

Akadémiai Kiadó, Budapest 1977

This volume of the series, edited by Béla CSÁKVÁRI comprises the following two reviews

(1) P. NÁNÁSI and J. SZEJTLI: Stereochemistry of di- and polysaccharides (168 pages, 219 references)

This review covers a much wider field of stereochemistry than indicated in the title. The first chapter (59 pages) deals with the basic principles of conformational analysis, starting from the very definition of conformation and ending with the discussion of the stereochemistry of polysubstituted cyclohexanes. The second chapter (64 pages) is concerned with the different conformational aspects of the pyranose ring, putting special emphasis on the abbreviated printed nomenclature which was suggested first in 1969 by one of the authors (J. SZEJTLI), to be used instead of structural formulas in carbohydrate chemistry.

In the third chapter (24 pages) the authors deal at last with the topic given in the title, i.e. with the conformational analysis of disaccharides, particularly with the conformational energy maps of the most common dipyranosides maltose and cellobiose. This chapter, as well as the last one, dealing with the conformation of polysaccharides (39 pages) gives a very up-to-date review of these topics. Especially in the last chapter the authors are very fair in discussing all the different hypotheses and the underlying experimental facts, independently, whether they are in agreement with or in contradiction to the hypothesis published by one of the authors (J. SZEJTLI) some years ago.

After having read this review, it is a very difficult task to decide whom it should be recommended to. According to the subject-matter and the proportions of the four chapters, it seems to be an introduction into conformational analysis in general, but the reviewer would certainly not recommend it to any chemist, who is not already acquainted with this field of stereochemistry. The opposition is based not so much on the content, but rather on the inaccurate definitions and careless style, by which the reader will be rather confused and disappointed, and surely not encouraged to learn more about conformational analysis in general, and about the stereochemistry of carbohydrates, in particular. In this respect this review is a complete failure.

On the other hand, the last two chapters, amounting to about one third of the whole review, are up to date and give a very useful aid to all chemists dealing with the stereochemistry of di- and polysaccharides. This applies especially to the references, which are carefully selected and enable the reader to get a full view of the rather debated shape (conformation) of the different macromolecules.

(2) T. DÉVÉNYI: Ion-exchange thin-layer chromatography in biochemistry (57 pages, 171 references)

The author is a well known expert in the field of ion-exchange chromatography and played an important role in developing a new ion-exchange TLC system, which is produced and marketed in Hungary under the name Fixion 50 \times 8. The present review is not only an excellent introduction into this rather rapidly developing new field of TLC, but at the same time it gives the historical background, the different practical applications and the necessary know-how of this method. Every reader will be encouraged by the convincing results to apply ion-exchange TLC in his own field of research. The special usefulness of this analytical method is based not only on its accuracy and sensitivity, but also on its potency for using it at different places, where a large number of samples have to be analyzed within relatively short time. For this routine task especially the newly introduced videodensitometry is of great importance, which was developed by the active cooperation of the author with other institutes.

J. KUSZMANN

J. A. MOORE, T. J. BARTON: *Organic Chemistry: An Overview*

W. B. Saunders Company, Philadelphia 1978, 384 pages

Starting from different aspects according to different demands, organic chemistry is taught in the institutions of higher education and at the universities at different levels. The author, writing a textbook for students who do not consider organic chemistry as a major subject (medical students, students of agricultural sciences, biology, physics), seems to be in this respect in an easier position. Actually, however, a task of this kind is very difficult, because the necessary restriction of educational and informative subject, fitted to the sphere of interest, cannot lead to an apodictic or superficial discussion. The up-to-date conception system of the branch of science must be distinctly accentuated in spite of the limited extent, moreover, in addition to foundation of the material and to the communication of information arousing interest, the subject discussed must give rise to thoughts, must stimulate thinking.

J. A. MOORE (University of Delaware) and his co-author T. J. BARTON (Iowa State University) have successfully met this manysided requirement, so that their textbook can be recommended for students who do not consider organic chemistry as a major subject. This book, containing excellent didactic suggestions, will be of value to all concerned with the teaching of organic chemistry.

The handbook of almost 400 pages is divided into 16 chapters. Three chapters deal with general problems (chemical bond, stereochemistry, determination of structure). Eight chapters discuss in the traditional way compound families of fundamental importance, classed according to functional groups. In addition to their correct and modern foundation, these chapters are made particularly interesting by frequent references to compounds playing a part in everyday life, and by sub-chapters, inserted as "Special Topic", which, fitted to the given chapter, deal with natural compounds of more complicated structure. At the same time, five separate chapters are devoted to other groups of natural compounds of prominent importance (carbohydrates, proteins, alkaloids, nucleic acids) and to their *in vivo* reactions.

Easy survey and the grasping of essentials are greatly facilitated by the "Summary and Highlights", to be found at the end of each chapter. In accordance with the requirements of up-to-date teaching, the text is interwoven with almost 300 "Problems", which can be solved on the basis of acquired knowledge, or starting from the same. The miniature encyclopedia, "Glossary of Terms", at the end of the handbook is interesting and useful.

The nice presentation of the book, the red and black printing, motivated didactically, the well constructed figures and the 12 coloured attractive interleaves, a feast to the eye, deserve special mention.

Á. KUCSMAN

T. TÖRÖK, J. MIKA, and E. GEGUS: *Emission Spectrochemical Analysis*

Akadémiai Kiadó, Budapest 1978

This work is the organic sequel of the book: "Emission Spectroscopy Fundamentals" published by Akadémiai Kiadó, in 1973. While the latter deals with the theoretical basis of optical emission spectrometry and with the principles underlying the construction and operation of the instruments, the present book discusses the practical questions of chemical analysis by emission spectra.

The volume comprises 692 pages; it contains seven principal chapters and a part composed of tables. The problems of the preparation of samples for analysis, the various radiation sources used for excitation in various states, the parameters of and how these affect the intensity of the spectrum lines are treated in detail. Further, the general aspects and the methods of qualitative and quantitative analysis are discussed, together with methods severally specified for the most current metals and alloys. Separate chapters deal with instruments and the methodology of spectrometry and spectroscopy. A brief summary of the fundamentals of calculating the error and the mathematics of the statistical evaluation of spectrochemical analyses conclude this work. At the end of the several sub-chapters the most important references to the literature are listed. The book contains about 100 tables and 220 figures, also a detailed subject index.

This book will be of great assistance to those engaged in the practice of analysis or employed in research and development, because it discusses the most up-to-date methods besides the proven and accepted ones and directs attention to questions yet unanswered. The collection of tables at the end of the book enables the user to find all important relevant data in a single volume.

MRS I. KERÉKES

Nicolaos D. EPIOTIS: *Theory of Organic Reactions*

Springer Verlag, Berlin, Heidelberg, New York 1978, 290 pages

The Woodward-Hoffman interpretation of pericyclic reactions has initiated the publication of an enormous amount of papers, reviews, monographs and handbooks since the middle of the sixties.

The language of molecular orbital theory has entered the everyday organic chemical literature. The theory has become more and more sophisticated, which, however, does not necessarily mean that no better, more established aspect can be presented in this field.

The author of the present book has suggested just such a new approach. According to him, the deficiencies of earlier approaches require the development of a new qualitative theory of chemical reactivity which makes possible the construction of potential energy surfaces. His aim is "to suggest ways in which gas phase and solution mechanistic chemistry, synthesis, spectroscopy and theory can be united".

The book is divided into the following chapters: 1. One-Determinantal Theory of Chemical Reactivity; 2. Configuration Interaction Overview of Chemical Reactivity; 3. The Dynamic Linear Combination of Fragment Configurations Method; 4. Even-Even Intermolecular Multicentric Reactions; 5. The Problem of Correlation Imposed Barriers; 6. Reactivity Trends of Thermal Cycloadditions; 7. Reactivity Trends of Singlet Photochemical Cycloadditions; 8. Miscellaneous Intermolecular Multicentric Reactions; 9. Addition Reactions; 10. Even-Odd Multicentric Intermolecular Reactions; 11. Potential Energy Surfaces for Odd-Odd Multicentric Intermolecular Reactions; 12. Even-Even Intermolecular Bicentric Reactions; 13. Even-Odd Intermolecular Bicentric Reactions; 14. Odd-Odd Intermolecular Bicentric Reactions; Potential Energy Surfaces for Geometric Isomerization and Radical Combination; 15. Odd-Odd Intramolecular Multicentric Reactions; 17. Mechanisms of Electrocyclic Reactions; 18. Triplet Reactivity; 19. Photophysical Processes; 20. The Importance of Low Lying Nonvalence Orbitals; 21. Divertissements; 22. A Contrast of "Accepted" Concepts of Organic Reactivity and the Present Work.

Undoubtedly, the book is not simply a re-expression of accepted ideas. Only time can reveal, how will the great majority of organic chemists accept these new approaches, or find them unacceptable.

There is one little thing, which seems to be superfluous in the reviewer's opinion, and this is the word "chorochemistry" introduced in the book; this seems to be a synonym of "stereochemistry".

Reading of the book is undoubtedly a serious intellectual adventure for those who are acquainted, at least in the main, with the literature of pericyclic reactions published in the last 15 years.

Cs. SZÁNTAY

M. L. BENDER and M. KOMIYAMA: *Cyclodextrin Chemistry*

X + 96 pages, 14 figs, 37 tables

Reactivity and Structure
Concepts in Organic Chemistry, Vol. 6.Editors: HAFNER, K., LEHN, J.-M., REES, C. W., SCHLEYER, P.V.R.,
TROST, B. M. and ZAHRADNIK, R.

Springer-Verlag, Berlin—Heidelberg—New York 1978

The first observation on cyclodextrins dates back to 1891. Since then an enormous treasury of experimental material has accumulated on these amazing compounds. Notwithstanding, their practical applications long remained inhibited by their high price and also by the lack of appropriate theoretical fundamentals of cyclodextrin chemistry. It is just very recently that cyclodextrins have acquired high actuality, as their industrial production has been realized at a reasonable price and simultaneously — as shown by BENDER—KOMIYAMA's book — the experimental facts and their theoretical basis have become solid enough to permit these compounds to pass from curiosity to industrial application.

Cyclodextrin research as well as any book written on this topic is therefore of high actuality.

Contents: pp. 1—9: Nomenclature, structure and physical properties of cyclodextrins
pp. 10—27: The formation of inclusion complexes, their structure, determination of the dissociation constants, and the complex-stabilizing forces
pp. 28—32: Some selected practical applications of cyclodextrin complexes
pp. 39—49: Covalent catalysis: hydrolysis of phenyl esters, amides, organophosphates and carbonates catalyzed by cyclodextrins
pp. 50—60: Non-covalent catalysis by cyclodextrins: microsolvent effect and conformational effect
pp. 61—64: Asymmetric catalysis by cyclodextrins, selective complex formation of D,L-stereoisomers, selective hydrolysis of esters and organophosphates, steric orientation of addition and oxidation reactions
pp. 65—78: Covalent and non-covalent modifications of cyclodextrins resulting in increased catalytic effects.

The 307 references cited in the book comprise nearly the half of the papers and patents published up to 1978 on cyclodextrins, their derivatives and complexes. The book is an excellent and compact survey on cyclodextrin catalysis; however, the contents and title of the book are not concordant.

Discussion of the following topics is omitted: the enzymic conversion of starch to cyclodextrins, the purification, analysis, biological and toxicological effects of cyclodextrins, their industrial applications (drugs, aromatics, pesticides, vitamins, etc.), and a great deal of the patent literature is missing.

Considering that a widespread application of cyclodextrin inclusion complexes is expected in the near future in the pharmaceutical and food industries, a contingent second edition of this book would need a thorough completion, considering that this well written book is at present the only one on cyclodextrins.

J. SZEJTLI

*Lecture Notes in Chemistry, Vol. 6.***I. HARGITTAI: *Sulphone Molecular Structures***

Springer Verlag, Berlin—Heidelberg—New York 1978, 175 pages

The author summarizes the electron diffraction (ED) and microwave spectroscopic (MW) studies on sulphone molecules in gaseous phase. The book consists of two parts: Molecular geometries and Structural variations. After a brief introduction to the basic ideas of ED and MW the structure determination of 20 sulphone derivatives is reviewed in the first part. The second part discusses the conformational properties, bond lengths and angles of

these molecules. The geometrical parameters found for the SO_2X group are compared with that of the analogous sulphoxides and sulphides. An attempt to find correlation between geometrical and vibrational parameters concludes the book. References are given at the end.

The importance of combining MW with ED investigations is well documented. The best part of the book is on the characteristic variations in bond lengths and angles where the usefulness of the valence shell electron repulsion (VSEPR) model is illustrated. Unfortunately the geometrical parameters obtained by X-ray diffraction for sulphone derivatives in crystal phase are given in the book without e.s.d.'s and without any discussion. It would have been very useful if a critical comparison of the data for different states had been given by the author.

The book is recommended for theoretical chemists.

K. SIMON

W. CARRUTHERS; *Some Modern Methods of Organic Synthesis*, 2nd edition

Cambridge University Press

Cambridge 1978, 532 pages

The first edition of this book was reviewed on page 122, Volume 78 of this journal, where I expressed the opinion that "the book may be of wide interest to practising scientists in industry and in scientific research institutions whose work involves the synthesis of organic compounds". Nothing proves better the success of the book than a new and partly revised and extended edition seven years after the first edition. In the preface to the new edition the author explains the necessity of revision and extension as follows: "a considerable amount of new material has been included to take account of advances in knowledge and of new synthetic methods which have come into use since publication of the first edition. The increasing application of organic derivatives of sulfur, selenium and silicon in synthesis and improvements in the methods for selective alkylation of ketones and for reversing the polarity of functional groups ("Umpolung") are among the subjects discussed more fully in this edition." In full agreement with the aforesaid, the reader can but greet the publishing of the new edition of this book.

The new edition of this well-known textbook provides a survey of many of the most useful methods and reagents recently introduced into synthetic organic chemistry. The scope and limitations of each method, in relation to the structure and stereochemistry of the products, are fully described and possible reaction mechanisms are discussed.

The first chapter deals with the formation of carbon-carbon single bonds, discussing among others the following problems: alkylation of relatively acidic methylene groups, γ -alkylation of 1,3-dicarbonyl compounds, the enamine and related reactions. Umpolung (dipole inversion), directed aldol condensations, coupling of organonickel and organocopper complexes, synthetic applications of carbenes and carbenoids, and some photocyclization reactions.

The next chapter discusses the formation of carbon-carbon double bonds, and within this β -elimination reactions, the Wittig and related reactions, the decarboxylation of β -lactones, stereospecific synthesis from 1,2-diols and the Claisen rearrangement of allyl vinyl ethers.

In the third chapter an excellent survey of the Diels-Alder reaction is given, the fourth chapter is dedicated to the reactions of unactivated C-H reactions (the Hofman-Loeffler-Freytag reaction, cyclization reactions of nitrenes, the Barton reactions and related processes, reactions of monohydric alcohols with lead tetraacetate). The next chapter discusses exhaustively the synthetic application of organoboranes and organosilanes, the sixth chapter deals with oxidation reactions [oxidation of hydrocarbons, alcohols, ketones, oxidation of olefinic bonds, oxidation with ruthenium tetroxide, nickel peroxide and thallium(III) nitrate]. Of the reductive methods catalytic hydrogenation, reduction by dissolved metals and by hydride transfer reagents are discussed.

In appreciation of the second edition we fully agree with the opinion of the reviewer of the J. Am. Chem. Soc. "... the author has been eminently successful in his aim to prepare a text for advanced undergraduates and beginning graduate students. These and other "students" of synthetic organic chemistry should find this book extremely useful".

GY. DEÁK

Handbook of Analytical Chemistry (Edited by W. FRESSENIUS)Part III, Volume 4 a γ

Tin

by J. W. PRICE and R. SMITH

Springer-Verlag, Berlin—Heidelberg—New York 1978

262 pages with 31 figures

The book is the newest volume of the well-known series: "Handbuch der analytischen Chemie, Dritter Teil, Elemente der vierten Hauptgruppe" written, in English, on the usually high level of these handbooks. But the personality of the authors makes it even more excellent: their remarks, attitudes, personal experiences, *etc.* give the book in several chapters nearly literary worth over the highly scientific and precise reviews.

Of course, not all the chapters are of equal quality. *E.g.* among the 20 main chapters, the first one dealing with the possibilities of the detection of tin and tin compounds does not fit into the profile of the book, and later more and better informations can be found about the qualitative analysis of tin in the special chapters as side notes.

The possibilities of the determination and the separation of tin are discussed in the next 8 chapters: gravimetric, volumetric, photometric and electrochemical methods; solvent extraction; atomic absorption spectroscopy; emission spectroscopy; X-ray fluorescence; radiochemical and Mössbauer methods; that is to say all of the most important and at the same time the most recent methods with several references. The authors do not try to enumerate all of the publications, the data are ordered and emphasized. In chapters mentioned, their effort is most successful in the chapter dealing with volumetric methods and less successful in chapter of "Solvent Extraction". It seems that the authors dislike the "l'art pour l'art" chemistry — and a lot of work done in solvent extraction neglect sometimes the practical background of the possibilities. The best methods which can be used for solving practical problems are less discussed in this chapter but can be read in other chapters connected directly to special tasks.

These special tasks are grouped in the next chapters starting with the "Analysis of tin ores and concentrates." (The other main chapters of this part which can be called the practical part of the handbook are as follow: analysis of secondary materials and intermediates; analysis of tin alloys and solders; analysis of ingot tin; tin in copper-base alloys; tin in ferrous alloys; tinplate.) All of the possibilities are accounted, but the authors' experiences and their attitudes gleam several times. What is more, the problem of sampling is discussed as a central problem since exact determinations can not be performed without precise sampling.

As it follows from the grouping, there are several repetitions but they seem to be unavoidable and make the book supposedly more usable for chemists interested in the concrete problems.

The next chapter of the handbook dealing with the problems of organotin compounds is perhaps its best one. Since the use of these compounds as PVC stabilizers (mono- and dimethyltin and dibutyl- or dioctyltin compounds); as industrial biocides and surface disinfectants in wood preservations; as agricultural fungicides, particularly on potatoes; *etc.* is more and more increased and their analytical chemistry rather differs from that of other tin compounds; the separate summary is well motivated.

Although other chapters mention the tin pollution and the analytical possibilities of its control, but most problems are discussed in this chapter: as the migration of organotin compounds from PVC into foods; residues on crops and in soils; determination in air and water; *etc.* It is worth to mention that at the end of this chapter, which is the longest one in the book, 205, mostly very recent, references can be found.

It seems that the place of the two extremely short last chapters ("Tin and tin-alloy electroplating solutions" and "Tin chemicals") is an editorial error after this excellent chapter both logically and psychologically; they should have been placed earlier and in this case they do not disturb the closed whole of the book — or, at least, this feeling of the reader.

In spite of the mentioned minor objections, this volume on the quantitative analyses of tin is an extremely good survey, which can be used not only by specialists, but can be recommended to libraries collecting books on analytical chemistry.

L. BARCZA

Advances in Polymer Science, Vol. 26. Conformation and Morphology

Springer Verlag, Berlin—Heidelberg—New York 1978, 183 pages

The volume contains four loosely related papers. The first paper (W. HOLZMÜLLER: Molecular Mobility, Deformation and Relaxation Processes in Polymers; 63 pages, 60 references) is a review of the theoretical interpretation of the viscoelastic flow, dielectric behaviour, further on all the time dependent reactions of polymers based on statistical mechanics *viz.* based on the so called concept of molecular displacement. After demonstrating the basic correlations, the probability of the flip-flop motion of the molecular segments is calculated on the basis of the unharmonicity of thermal motion of atomic groups and the Lennard-Jones potential. The differential equations are solved among the limit conditions given by different rheological conditions of the polymer. The equations derived based on this concept gave better approximations of the experimental values than those obtained by other theories (*e.g.* WLF-equation).

The paper is entirely theoretical, demonstrating an apparently comprehensive concept. Experimental data are only occasionally presented, and then to support postulations. As the theory is phenomenologic, the parameters may be chosen to preference, thus the theoretical data generally fit the simple experimental results. Although the theory is considered general, it seems doubtful that it can be applied to rigid chain polymers or polymers with bulky side groups with essential mesomorphic structure.

The second paper (Yu. LIPATOV: The Iso-Free-Volume State and Glass Transition in Amorphous Polymers. New Development of the Theory; 42 pages, 109 references) presents a critical discussion of vitrifying — one of the most disputed properties of amorphous polymers — on the basis of the iso-free-volume state concept. The author points out that the free volume itself is not a well-defined category and different volumes can be obtained from different ways of estimation, but the experimental values obtained in different polymers scattered even more than the theoretical ones. Applying these theoretical considerations to heterogeneous systems (polymer blends, copolymers, filled polymers) the results are even less accurate than those obtained for homogeneous systems. LIPATOV expresses his doubts on the model of free volume. Accordingly T_g can neither be regarded as a temperature of iso-free-volume state nor of iso-viscosity state. The iso-free-volume state concept gives correct qualitative but false quantitative results. The iso-entropy state is proposed as a possible solution of the problems.

LIPATOV's criticism seems even more justified regarding properties of above listed specific polymers: where the specificities of the spontaneously ordered rigid chain polymers in the glassy state are to be described. The mesomorphic polymers in glassy state are considered yet as new materials, however, their number increases daily. Thus the question arises: which structure represents the general properties of polymers (the structure of flexible chain polymers or the structure of polymers with rigid chains or the structure of those with bulky side chains)? Apparently the properties of the latter can not be extrapolated from the theoretical considerations used in the case of flexible chain polymers.

The subject of the third paper (J. E. HERZ, P. REMPP, W. BORCHARD: Model Networks; 31 pages, 67 references) deals with the swelling and deformation of gels prepared from flexible chains with a known length by adding branch points with known functionality and in a well-defined number to them. The mode of the preparation of the model networks is described. The structural changes during the swelling and those caused by mechanical deformation are investigated by small angle X-ray scattering and by neutron diffraction (the Bragg formula on p. 117 is erroneous!) and these are examined as the function of the quality of the swelling solvent and the density of the branch points (molecular weight of the flexible chain). The T_g of the network is inversely proportional to the chain length. The modulus measured in the deformed gels is a linear function of a power of the chain length. The value of the power is determined by the quality of the solvent (θ or good solvent). The properties of the model networks combined with swelling and deformation studies support the concept of high elasticity.

The paper presents a very useful method for the further investigation of rubbers and rubber like behaviour of high molecular weight materials.

The fourth paper (R. KITAMURA, F. HORII: NMR Approach to the Phase Structure of Linear Polyethylene; 42 pages, 80 references) discusses the results obtained by the deconvolution of the measured broad line NMR spectrum of linear (high density) polyethylene. The spectra resolved into three components with different breadth. The parameters of the broad,

the narrow and the medium with line are very similar in polyethylene samples of different molecular weights and temperatures. The relative weight of the three components depends on the molecular weight and the temperature at bulk crystallized samples and fibers is, however, independent of the temperature and the molecular weight of lamellas crystallized from solution, where even the narrow line has a very low weight. The line with medium breadth appears parallel with the appearing of gamma relaxation by increasing temperature. Its relative weight remains constant when beta relaxation as well as the appearance of the narrow line is observed. When alpha relaxation is observed the characters of the lines differ from those observed at lower temperatures. The authors conclude the PE consisted of different phases, their relative amounts depend on the molecular weight and the temperature of bulk crystallized materials, including fibers with different draw ratios. The lamellas crystallized from diluted solution have only one phase which means that the structure of bulk crystallized materials can not be characterized by the folded chain lamellas.

This is in agreement with other papers suggesting that the concept of folded chain model widely accepted in literature needs strict criticism. The folded chain model was the only to explain the observation on very thick lamellas grown from diluted solution, however, it seems inapplicable to bulk crystallized materials and even less to modelling the structure of nonflexible amorphous chain polymers. The presence of a medium breadth NMR line in the spectrum suggests us to identify this phase as the nematic phase of linear polyethylene suggested earlier by many authors.

The papers of this volume present very good review of the structural, the rheological and the relaxation problems of flexible chain polymers in their different states (liquid — HOLZMÜLLER, high elastic — HERZ *et al.*, glassy — LIPATOV, and crystalline — KITAMURA and HORII) to all scientists and engineers interested in this field.

F. CSER

G. DECONNINCK: *Introduction to Radioanalytical Physics*

Joint edition published by Akadémiai Kiadó, Budapest
and Elsevier Scientific Publishing Company, Amsterdam
1978, 242 pages

This book is the first volume of the Nuclear Methods Monograph series of the Journal of Radioanalytical Chemistry and Radiochemical and Radioanalytical Letters. The editors are identical with those of the periodicals mentioned, Drs. T. BRAUN and E. BUDOSÓ.

The main objective of the book is to describe the theoretical principles of nuclear reactions induced by charged particles and high energy photons and to outline their possible uses or chemical analysis, the practical realization of which was brought only by the technological achievements of the last decade. One may only welcome such an attempt to survey all those nuclear methods which have extended the scope of radioanalytical techniques over the classical neutron activation and tracer applications.

The book is divided into six chapters. Chapter 1 (34 pages) deals with kinematics, classification and mechanisms of nuclear reactions in general, and includes also a detailed description of reaction cross sections. Chapter 2 (26 pages) describes phenomena taking place in the atomic shells following charged particle bombardment, that is ionization, X-ray emission, secondary electron emission and related analytical applications (X-ray fluorescence, stopping power, particle range and channeling effect measurements). Chapter 3 (35 pages) covers elastic scattering of charged particles and the application of this technique in depth profile analysis of surface layers and trace analysis. Chapter 4 (47 pages) is concerned with analytical applications of nuclear reaction gamma-ray measurements. Methods, based on measuring both prompt and delayed gamma photons induced by charged particle activation are discussed in detail. A short description of the photon activation method is also given. Chapter 5 comprises 28 pages and describes analytical applications of detecting charged particles produced in (p, α), (d, p), (d, α), (t, p), (t, α) and (p, n) reactions. This technique is particularly sensitive for light elements and also suitable for profile analysis of thin surface layers. Activation analysis using charged particles or photon induced reactions, the subject dealt with in the last (6th) chapter (23 pages) seems to be in the author's center of interest. This is shown by the entirely different way of presentation as compared with the previous chapters, giving more analytically practical points, more recent references, often to own papers, etc.

Some 133 references, mostly from the period 1970–75, help the reader to follow the developments in more detail. "Solved problems" or "examples", indeed, offer numerical figures as illustrations for the nuclear data, parameters and other quantities dealt with in the text. The quality of graphical illustrations is satisfactory.

According to the author, the book "has been designed as a textbook for the use of scientists of diverse scientific background . . .", therefore, "prior knowledge of nuclear sciences is not essential, apart from elementary courses on radioactivity." From the point of view of an analytical chemist, however, the approach adopted (excluding the final chapter) is rather mathematical, and it is questionable whether the numerous complicated formulae given without detailed derivation can be understood without previous or simultaneous quantummechanical and nuclear physical studies.

All in all, the book is supplying a deficiency indeed and contains a good deal of relevant theoretical information, so it can be recommended as a textbook primarily for students of courses on applied nuclear physics and chemistry. From this point of view, it is a pity that the author did not undertake the pioneering work of presenting the material using the S. I. units.

T. BEREZNAI

H. DACHS (Ed.): *Neutron Diffraction (Topics in Current Physics, Vol. 6.)*

Springer-Verlag, Berlin—Heidelberg—New York 1978

An offset printing on 357 pages with 138 pictures

This book, written by an international team clustered around the editor H. DACHS covers almost every relevant field of the practical application of neutron diffraction (*n.d.*) in structural research of condensed matter. Since the pioneering work of WOLLAN and SHULL (1946) *n.d.* has been used more and more frequently whenever the investigation of structures of materials was difficult (*e.g.* localization of hydrogen atoms in crystal structures) or totally impossible (*e.g.* study of solid state magnetism, localization of atomic nuclei, *etc.*) by means of X-rays. This method has thus been developed into an important and powerful supplement to X-ray investigations. The area of chemical binding has received a new impetus from the union of X-ray and neutron diffraction. Neutron small angle scattering and the method based on the deuteration of high polymers open new perspectives in protein research and in the biology of macromolecules. Of equal importance is the application of *n.d.* in metallurgy and liquid structures, as well.

A substantial and clear summary of the principles of *n.d.* is given by the editor in Chapter 1 (pp. 1–40). He makes it clear that the readers are expected to be familiar with X-ray diffraction and the interaction of neutrons with substances. For those who are not, proper sources of knowledge (*e.g.* the known book of G. E. BACON) are recommended. The production and application of polarized neutrons (Chapter 2, pp. 41–69) are followed by the description of "The study of charge density distribution in solids" in Chapter 3 (pp. 71–111). The substance of these very important (N-X and X-X) electron density calculations for theoretical and modern structural chemistry is presented by P. COPPENS with great skill.

In Chapter 4 (pp. 113–149) one can find a fascinating description of how magnetic structures can be revealed by *n.d.* A comprehensive explanation and classification of SHUBNIKOV groups helps to understand their important role in the study of magnetic moments. Topics of solid state physics known as "disordered structures, phase transitions and critical phenomena" are compiled in Chapters 5 and 6 (pp. 151–242).

Chapter 7 (pp. 243–270) introduces the reader to the problems of molecular biology from the aspect of a relatively new diffraction method in the analysis of fairly complicated biological structures (*e.g.* viruses). G. ZACCAI gives a good survey of the progress made so far in this field with some hints at further possibilities.

The investigation of different sorts of liquids by means of neutron scattering is discussed in Chapter 8 (pp. 271–302). Several practical examples help to follow the developments in this area. The last, Chapter 9 (pp. 303–351) deals with the theory of dynamical neutron diffraction and its application (*e.g.* neutron topography, interferometry, *etc.*). Each chapter is accomplished by a list of useful references.

The reviewer is pleased to recommend this practical guide to the neutron diffraction technique to all researchers, teachers and students interested in one or several possibilities of its manifold application.

A. KÁLMÁN

D. I. DAVIES and M. J. PARROTT: *Free Radicals in Organic Synthesis, Reactivity and Structure*

(Concepts in Organic Chemistry, Vol. 7)

(Editors K. HAFNER, C. W. REES, B. M. TROST, J. M. LAHM,
P. von RAGUÉ SCHLEYER and R. ZAHRADNIK)

Springer-Verlag, Berlin, Heidelberg, New York
1978, XII + 169 pages

The present book is a significantly supplemented version of a paper written by the authors in 1975 under the same title, and it consists of 13 chapters. In Chapter 1, a short general survey is given (12 pages) on the preparation of free radicals and their reactions of different types (Radical-Radical Reactions, Addition Reactions, Substitution, Fragmentation, Rearrangement, Oxidation), while in the following 12 chapters the reactions of free radicals suitable for the preparation of members of various compound classes are discussed (Alkanes and Alkenes, Aromatic, Heteroaromatic and Fluoroaromatic Compounds, Halogen Compounds, Alcohols, Ethers and Hydroperoxides, Aldehydes and Ketones, Carboxylic Acids and their Derivatives, Nitrogen-containing Compounds, Stable Free Radicals, Naturally Occurring and Related Compounds). There is a list of references at the end of each chapter; the number of references is 960, the latest dates are from 1976 and 1977. The book is also completed with Author and Subject Indices.

The authors review several very useful data, positive and negative experiences (which reactions of free radicals are used advisably, and which are *not* worth of experimenting in the preparation of members of certain compound classes, or for the introduction of certain functional groups); however, the limited space (on the average, chapters 2–13 consist of less than 12 pages each) did not allow the authors to be comprehensive; rather illustrations of the synthetic value of particular reactions are given.

An undisputed virtue of the book is that it strongly emphasizes and calls attention to the importance of free radical reactions in preparative organic chemistry, which is — in spite of several older monographs and comprehensive papers — a very up-to-date task, in the reviewer's opinion. Therefore, perusal of this book will be useful for many organic chemists. It is another question, however, how many of them will use the volume systematically and regularly. Most probably those who aim at the development of preparative methods based on new reactions involving free radicals. For these chemists the data published and critically evaluated in the present book will afford a good basis for the start, yet, the number of such persons may not be very high. The great majority of synthetic organic chemists usually face the task of finding the most suitable method for the introduction of a functional group into a given skeleton. Whether this is done by free radical or other mechanism is of less importance except when there is some reason, e.g., requirements in selectivity, which automatically excludes the use of ionic reactions.

K. LEMPERT

Philipp GÜTLICH, Rainer LINK and Alfred TRAUTWEIN:
Mössbauer Spectroscopy and Transition Metal Chemistry

(Inorganic Chemistry Concepts, Vol. 3.)

Springer Verlag, Berlin, Heidelberg, New York 1978, 280 pages

The monograph consists of 8 chapters and contains more than 500 references and 160 figures.

The 20th anniversary of the discovery of the Mössbauer effect was celebrated by a workshop organized by one of the authors (P. GÜTLICH) in April, 1977. The spectroscopic method based on this effect has developed at an unparalleled rate and its application is continuously extending in chemistry, physics, metallurgy, biology, geology and other sciences. The number of papers published yearly on topics of Mössbauer spectroscopy is thousands, and probably several dozens of monographs have been published only in the Russian and English

languages, dealing with this method. Most of these books try to illustrate the possibly complete, very wide field of applications of Mössbauer spectroscopy, on the basis of more or less examples and references. This aim can be achieved with more and more difficulties, hence it must be regarded very useful that P. GÜTLICH and his co-authors describe the applicability of the method only in a special, yet rather broad field, the chemistry of transition metals.

In the first five chapters of the book the physical fundamentals of recoil-free nuclear resonance gamma absorption (Mössbauer effect), the most important characteristics of Mössbauer spectroscopy based on it and the techniques of measurement are discussed. The sixth chapter introduces the interpretation possibilities of the Mössbauer parameters of iron compounds by means of several examples. It can clearly be felt when reading this chapter that there is a chemist and a physicist expert in quantum chemistry, too, among the authors. This chapter gives a lucid picture about the nature and importance of the information obtained from the Mössbauer spectra regarding the electron structure, chemical bonds and magnetic properties, and on the quantum chemical apparatus required for the calculations starting from these Mössbauer parameters.

In Chapter 7, the literature dealing with the Mössbauer spectroscopy of Mössbauer-active transition metals other than iron, such as Ni, Zn, Ru, Hf, Ta, W, Os, Ir, Pt, Au, Hg isotopes yielding stronger or weaker effects is given.

In Chapter 8, the authors present a group of Mössbauer spectroscopic investigations on transition metals (primarily on iron), which do not belong closely to the topics of chemical structure investigation (solid-state reactions, frozen solutions, surface examinations, metallurgy, aftereffects and biology). It seems that in this chapter the authors abandoned their original intention to deal with a closer field instead of surveying the full scale of applicability of Mössbauer spectroscopy, and here they tried to show as much of the use of the method as possible. This could, however, hardly be achieved, probably because of the limited volume of the book; therefore, often only reference is made to the various problems. The list of references attached to the subchapters is often longer than the actual text.

This chapter is suitable primarily for finding literature for the various topics.

In summary, it can be stated that the present book represents a monograph useful for experts as well as for researchers engaged in related fields.

A. VÉRTES

INDEX

ANALYTICAL CHEMISTRY

- A New Method for the Reductive Decomposition of Organic Compounds, L. MÁZOR 3
 Investigation of the Atomization Processes of Tin in Various Atomizers and of the Interference by Copper, E. G. HARSÁNYI, L. PÓLOS, E. PUNGOR 139
 Application of the Thermoelectric Method in the Study of Phase Transitions of Fatty Acid Salts, T. MEISEL, K. SEYBOLD, J. RÓTH 179

PHYSICAL AND INORGANIC CHEMISTRY

- Structure and Selective Sodium Sorption of Hydrated Antimony Pentoxide, L. G. NAGY, G. TÖRÖK, G. FÓTI 17
 Photoassisted Electrolysis of Water by Semiconductor Electrodes, T. PAJKOSSY, I. MOLNÁR, M. PÁLFY, R. SCHILLER 93
 Correlation between the Preparation and Catalytic Properties of PtFe/SiO₂ Catalysts, L. GUZZI, K. MATUSEK, J. MARGITFALVI, M. ESZTERLE, F. TILL 107
 Complex Studies on Intermediary Decomposition Products of Ammonium Paratungstate, L. BARTHA, GY. GYARMATI, B. A. KISS, T. NÉMETH, A. SALAMON, T. SZALAY 127
 Modeling of Liquid Phase Hydrocarbon Oxidation Processes, D. GÁL, L. BOTÁR, É. DANÓCZY, I. P. HAJDU, J. LUKÁCS, I. NEMES, T. VIDÓCZY 189

ORGANIC CHEMISTRY

- Phosphinimine Derivatives of Aldopyranoses from Azido Sugars, J. KOVÁCS, I. PINTÉR, F. SZEGŐ, G. TÓTH and A. MESSMER 7
 Molecular Encapsulation of Volatile, Easily Oxidizable Labile Flavour Substances by Cyclodextrins, J. SZEJTLI, L. SZENTE, E. BÁNKY-ELŐD 27
 Polyethylene Glycol Derivatives as Complexing Agents and Phase-Transfer Catalysts. III. Behaviour of Polyoxyethylene Derivatives in Liquid-Liquid Phase Equilibria, L. TÓKE, G. T. SZABÓ, K. SOMOGYI-WERNER 47
 Flavonoids, XXXIII. Reaction of 2'-OR-Chalcone Dibromides with Cyclohexylamine. Synthesis and Transformations of Chalcone Aziridines, GY. LITKEI, T. MESTER, T. PATONAY, R. BOGNÁR 53
 Stereochemical Studies, XXXV. Saturated Heterocycles, XII. Synthesis and Spectroscopical Study of *cis*-Trimethylene-, *cis*- and *trans*-Tetra- and Pentamethylene-2,3,5,6-tetrahydro-1,3-oxazine-4-ones, G. BERNÁTH, F. FÜLÖP, GY. JERKOVICH, P. SOHÁR 61
 Reaction of Chromonoids with Nucleophilic Reagents, I. Cleavage of the Pyrone Ring of Chromone Derivatives in Aqueous Alkali, M. ZSUGA, V. SZABÓ, F. KÓRÓDI, A. KISS 73
 Stereoselective Hydrogenolysis of Dioxolane-Type Benzylidene Acetals. Synthesis of Partially Substituted Galactopyranoside Derivatives, A. LIPTÁK, L. JÁNOSSY, J. IMRE, P. NÁNÁSI 81
 Dihydropyran Cycloadducts, III. Reactions of Cyclopentanone Enamines with Benzylidene Ketones, GY. OSZBACH, D. SZABÓ, M. E. VITAI 119
 Recent Studies on the Reaction of Thiolsulfonates with Alkali Halides, J. LÁZÁR, E. VINKLER 175

CHEMICAL TECHNOLOGY

- New Control-methods in the Leatherchemistry, I, G. TÓTH, J. VAJDA, V. PÓSA (in German) 157
 RECENSIONES 201

Printed in Hungary

A kiadásért felel az Akadémiai Kiadó igazgatója

Műszaki szerkesztő: Zacsik Annamária

A kézirat nyomdába érkezett: 1979. II. 8. — Terjedelem: 18,90 (A/5) ív, 123 ábra

79.6786 Akadémiai Nyomda, Budapest — Felelős vezető: Bernát György

РЕЗЮМЕ

Метод восстановительного разложения органических соединений

Л. МАЗОР

Если органические соединения, содержащие гетероэлемент, подвергать нагреву совместно с металлическим калнем в вакууме, то протекает небурная реакция и гетероэлементы могут быть превращены в соответствующие калиевые соединения. После взаимодействия сплава со спиртом и водой ионы определяются соответствующим микроаналитическим методом. Этот метод может быть использован для микроанализа галогенов, серы, фосфора, мышьяка и металлов в органических соединениях.

Фосфиниминовые производные альдопираноз из азидосахаров

Й. КОВАЧ, И. ПИНТЕР, Г. ТОТ, А. МЕССМЕР и Ф. СЕГЁ

Реакция Штаудингера для ацетиальдозил азидов была распространена на другие азидосахара и приводит к образованию фосфиниминов сахаров. Химическое и конформационное поведение фосфиниминов было изучено с помощью их характерных реакций и ЯМР спектроскопии, соответственно.

Структура гидратированной пятиокиси сурьмы и механизм селективной сорбции натрия

Л. ДЬ. НАДЬ, Г. ТЁРЕК и ДЬ. ФОТИ

Был разработан метод воспроизводимого получения гидратированной пятиокиси сурьмы (НАР), оптимального количества, а также метод контроля качества комплекса, с той целью, чтобы сорбент выделял натрий из многокомпонентных образцов, активированных нейтронами, с максимальной селективностью и эффективностью. На основе данных — среди прочих других — дериватографических, ИК спектроскопических, рентгенодифракционных и погружно-калориметрических измерений было заключено, что механизм связывания иона натрия соответствует эквивалентной сорбции.

Молекулярное капсулирование летучих, легко окисляющихся, нестабильных душистых веществ с циклодекстринами

Й. СЕЙТЛИ, Л. СЕНТЕ и Э. БАНКИ-ЭЛЁД

Были получены комплексы включений 25 различных душистых веществ (пряные вещества растительного происхождения и летучие масла) с β -циклодекстрином. Согласно результатам газовой хроматографической исследований, содержание эффективного ве-

щества в комплексе включений составляло 8—13%. Исходные компоненты все встроились в комплексы, взаимное отношение душистых веществ в комплексе, с точки зрения практического использования, в незначительной мере отклоняется от исходного соотношения душистых веществ. Факт комплексообразования подтверждался рентгенодифракционными исследованиями, а также исследованиями стабильности. Поглощение кислорода полученными комплексами, измеренное с помощью техники Варбурга, составляло около 10% от поглощения кислорода исходными душистыми веществами. Ароматные вещества не испаряются из комплексов вплоть до температуры 160°C, т. е. в обычных условиях хранения летучесть, окисление и разложение под влиянием тепла в значительной степени уменьшаются, и тем самым продукт может быть сохранен и использован в течение продолжительного времени. Комплексы ароматных веществ — это незагрязненные с микробиологической точки зрения, стабильные, со стандартным составом, негабаритные, сохраняемые в течение продолжительного времени, сразу используемые душистые продукты. Благодаря всем этим свойствам они с успехом могут быть использованы в пищевой промышленности.

Производные полиэтиленгликоля как комплексообразующие реагенты и катализ с переносом фазы, III.

Поведение производных полиоксиэтилена в фазовых равновесиях жидкость-жидкость

Л. ТЁКЕ, Г. Т. САБО и К. ШМОДИ-ВЕРНЕР

Для характеристики эффективности полиэфигов в качестве солеэкстрагирующих катализаторов были проведены измерения равновесий жидкость-жидкость. Было доказано что конечные группы и средний молекулярный вес линейных полиэфигов определяют его каталитическую силу в переносе фазы.

Флавоноиды, XXXIII.

Реакция дибромидов 2'-OR-халконов с циклогексиламиноком.

Синтез халконазиридинов и их превращения

ДЬ. ЛИТКЕИ, Т. МЕШТЕР, Т. ПАТОНАИ и Р. БОГНАР

2'-OR-Халкон (1a), дибромиды халкона (2a, b) а также d-бромхалкон (3a) с циклогексиламиноком дают смесь *цис*-(4a, b) и *транс*-азиридинов (7a, b). Соединение 7a не стабильно и спонтанно превращается в таутомерный энамин (6a).

Реакция 4a с основанием или обработка 4b трифторуксусной кислотой приводит к образованию аурана (9), а взаимодействие соединений 6a или 7b с основанием или эфиратом фтористого бора дает в качестве основного продукта 3-циклогексиламинофлаванон (11).

Экспериментальные данные подтвердили правильность механизма, предполагаемого ранее.

Стереохимические исследования, XXXV. Насыщенные гетероциклы, XII.

Синтез и спектроскопическое исследование *цис*-триметилен-, *цис*- и *транс*-тетра- и пентаметилен-2, 3, 5, 6-тетрагидро-1, 3-оксазин-4-онов

Г. БЕРНАТ, Ф. ФЮЛЁП, ДЬ. ЕРКОВИЧ и П. ШОХАР

Из *цис*-2-гидрокси-1-циклопентанкарбоксимида, а также *цис*- и *транс*-2-гидрокси-1-циклогексан- и 1-циклопентанкарбоксамидов (1a—e) с помощью *n*-хлорбензалдегида были получены 2-(*n*-хлорфенил)-*цис*-5,6-триметилен-, *цис*- и *транс*-5,6-тетра- и пентаметилен-2,3,5,6-тетрагидро-1,3-оксазин-4-оны. В тех же самых условиях *транс*-2-гидрокси-1-

циклопентанкарбоксамид не дает циклического продукта. Из предыдущих алициклических 2-гидрокси-1-карбоксамидов с помощью ацетона или алициклических кетонов были получены 2-замещенные тетрагидрооксазиновые производные (4a, b, 5a—e). Реакция 2-гидрокси-1-карбоксамидов (1a—e) с параформальдегидом приводит к образованию производных бис-тетрагидрооксазона с метиленовым мостиком. На основе спектров ЯМР—H¹ были установлены предпочитаемые конформации *цис*-изомеров последних соединений. Обсуждаются результаты масс-спектрографических исследований этих соединений.

Реакция хромоноидов с нуклеофильными реагентами, I.

Разрыв пиринового кольца производных хромона в водной щелочи

М. ЖУГА, В. САБО, Ф. КОРОДИ и А. КИШ

Был исследован разрыв кольца хромона, флавона, изофлавона, 3-метилхромона и 3-феноксихромона в водной щелочи.

Раскрытие кольца начинается изознтропийным нуклеофильным присоединением типа Ad_N², которое, в свою очередь, является ступенью, лимитирующей скорость процесса. Карбоний (II) затем стабилизируется в согласии с равновесием III \rightleftharpoons IV. Константа скорости разрыва кольца находится в линейной корреляции с константой термодинамического протонирования карбонильной группы γ -пиринового кольца, что указывает на то, что электронная плотность на С-2 сильно зависит от электронного распределения в карбонильной группе.

Стереоселективный гидрогенолиз бензилиденовых ацеталей типа диоксала.

Синтез частично замещенных производных галактропиранозида

А. ЛИПТАК, Л. ЯНОШИ, Й. ИМРЕ и П. НАНАШИ

Частично бензилированные или частично бензилированные и метилированные производные α - и β -D-галактопиранозидов были получены гидрогенолизом *экзо*- и *эндо*-изомеров 3,4-O-бензилиден- α - и β -D-галактопиранозидов. *Экзо*-изомеры дают соответствующие 3-O-бензил-4-гидрокси-производные, в то время как для *эндо*-изомеров были получены 4-O-бензил-3-гидрокси-аналоги во всех случаях. Для гидрогенолиза ацеталей, содержащих незамещенную гидроксильную группу, полагалась изомеризация в слабой степени, зависящая от времени протекания реакции и избытка реагента. Метод гидрогенолиза представляет собой удобный путь определения *экзо*- или *эндо*-конфигураций бензилиденовых ацеталей типа диоксала, даже при наличии лишь одного из двух изомеров.

Фотоэлектролиз воды полупроводниковыми электродами

Т. ПАЙКОШИ, И. МОЛЬНАР, М. ПАЛЬФИ и Р. ШИЛЛЕР

Был исследован эффект освещения полупроводниковых электродов в электролизе воды. В качестве возможных фотоактивных электродов были исследованы полупроводниковые вещества CdS — типа-*п*, CdTe — типа-*п* и *р* и окись железа — типа-*п*. Измеряя их вольтамметрическое поведение в зависимости от состава электролита как при освещении, так и в темноте, наблюдалось уменьшение тока и смещение кривой ток-напряжение вследствие падающего света. Были определены эффекты интенсивности и длины волны света на стабильность электродов. CdS и CdTe быстро корродируются, в то время как окись железа оказалась стабильным фотоанодом в электролизе воды. Ее эффективность превращения белого света в электричество равна около 1%.

Корреляция между поличением и каталитическими свойствами катализатора PtFe/SiO_2

Л. ГУЦИ, К. МАТУШЕК, Й. МАРГИТФАЛВИ, М. ЭСТЕРЛЕ и Ф. ТИЛЛ

Органометаллический $[\text{Pt}(\text{C}_2\text{H}_5)_3\text{Cl}]$, обозначаемый *A* и ионный $[\text{Pt}(\text{NH}_3)_4]^{+2}$, обозначаемый *B*] платиновые комплексы были использованы для приготовления высоко диспергированных платиновых катализаторов, нанесенных на окись алюминия. В случае *A* количество алкильного комплекса сильно зависит от экспериментальных условий, таких как растворитель и предварительная обработка носителя. *B* дает катализатор с более высокой дисперсностью и с более высокой металлической загрузкой, чем в случае *A*. Используя различные источники платины, можно оказывать влияние не только на число атомов металла, но и природа этих мест также зависит от используемого комплекса платины. Для приготовления биметаллических катализаторов было использовано железо в различных формах, в результате чего был разработан наилучший способ приготовления. На основе ТГ — МС исследований, спектров Мёссбауэра, а также хемосорбционных исследований были получены доказательства металлического взаимодействия между двумя металлами. Была найдена корреляция между концентрацией атомов металла на поверхности и скоростью гидрогенолиза этана и *n*-бутана. Добавки железа влияют на внутреннюю активность платины, однако, значительные отклонения от этого поведения наблюдались лишь при высоких нагрузках железа.

Циклоаддукты дигидропирана, III

Реакции цикlopentanонэнаминов с бензилиденкетонами

ДЬ. ОСБАХ, Д. САБО и М. Е. ВИТАИ

Цикlopentanонэнамины с бензилиденацетофеноном дают аддукты типа Михаэля, в то время как с бензилиденциклогексанонами — даже в очень мягких условиях — образуются цикlopентапираны. Заключение относительно пространственной структуры могут быть сделаны, исходя из продуктов их гидролиза.

Комплексное исследование промежуточных продуктов разложения паравольфрамата аммония

Л. БАРТА, ДЬ. ДЬАРМАТИ, Б. А. КИШ, Т. НЕМЕТ, А. ШАЛАМОН и Т. САЛАИ

Синяя окись — промежуточный продукт термического разложения паравольфрамата аммония ($\text{APT} \cdot 5\text{H}_2\text{O}$) — была исследована с помощью рентгено-дифракционного анализа, ИК спектроскопии, рН-метрии ионообменных реакций и измерением окислительно-восстановительных потенциалов. Была найдена связь между фазовым состоянием и химическим поведением.

Утверждается присутствие тетрагональной водородной бронзы вольфрама и гексагональной, смешанной с аммонийноводородной бронзы вольфрама; химическая реактивность синей окиси связана с ними.

Исследование процессов атомизации олова в различных атомизаторах и влияние меди

Ф. Г. ХАРШАНИ, Л. ПОЛОШ и Э. ПУНГОР

Изучали процессы атомизации олова в смесях ацетилена с двуокисью азота, водорода с воздухом и водорода с азотом. Было установлено, что химические реакции, с участием водородных радикалов, играют важную роль при образовании свободных атомов олова. Было исследовано влияние медной матрицы и анионов на определение олова в графитной печи. Установили, что, если олово присутствует в виде хлорида, то медь катализирует окисление олова.

Новые методы контроля в химической кожевенной промышленности. I

Г. ТОТ, Й. ВАЙДА и В. ПОША

Рассматриваются такие методы контроля производства, которые могут быть успешно использованы в зольных цехах больших кожевенных заводов.

Понижение содержания гидратной воды сырых кож, консервированных солью, сопровождается более трудной замочкой несмотря на то, что растворение соли ускоряется. Для контроля замочки сырых кож более пригодным является определение содержания сухого материала в коже, нежели ранее используемый, так наз., «мочильный вес».

Контроль отзола ведется на основе определения концентрации Na_2S , отношения $\text{SH} : \text{OH}$, натяжения голяя, а также эффектов деструкции ворса и растворения белков.

Обсуждается присоединение различных зольных веществ, и их вымачивание, а также была получена зависимость между натяжением голяя и потерей белков. Приводятся эксперименты относительно ослабления так наз. «хиалин» слоя, а также его полной деструкции в концентрированных растворах Na_2S , что очень важно с точки зрения тощести лицевой стороны мягкой кожи.

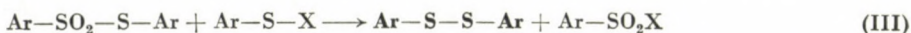
Новейшие данные относительно реакции тиолсульфоновых эфиров со щелочными галогенидами

Я. ЛАЗАР и Э. ВИНКЛЕР

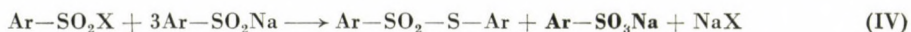
Тиолсульфонаты под влиянием галоидов или роданида натрия в диметилформамидном растворе превращаются в дисульфиды и натриевую соль сульфоновой кислоты. Механизм реакции описывается тремя последовательными и параллельными реакциями подтверждается литературными данными и модельными экспериментами. Первая реакция — это нуклеофильное расщепление тиолсульфонатов:



Вторая реакция — это электрофильная реакция исходного тиолсульфоната с образовавшимся в реакции (I) сульфениловым соединением:



Третья реакция — это взаимодействие сульфидной соли, образующейся в первой реакции, с сульфениловым соединением, образующимся во второй реакции:



Конечные продукты реакции обведены).

Применение термоэлектрического метода в исследовании фазовых переходов солей жирных кислот

Т. МЕЙЗЕЛ, К. ШЕЙБОЛЬД и Й. РОТ

Приводятся некоторые примеры применения термоэлектрического метода. С помощью этого метода для соединений в смектической мезофазе были определены и качественно интерпретированы специальные аномалии проводимости и эффект мемории.

Моделирование процессов жидкофазного окисления углеводородов

Д. ГАЛ, Л. БОТАР, Е. ДАНОЦИ, П. ХАЙДУ, Й. ЛУКАЧ, И. НЕМЕШ и Т. ВИДОЦИ

Для оптимизации исследований процессов жидкофазного окисления углеводородов предлагается модельная процедура. Процедура смонтирована в трех черных коробках. Назначение первой коробки заключается в ориентировочной информации на основе данных, взятых из литературы.

Сбор данных ведет непосредственно к планированию экспериментов, включая исследование суммарного процесса, а также субсистем и элементарных процессов.

Третья коробка относится к кинетически-математической обработке данных, полученных ранее.

Окисление этилбензола служит прототипом моделирования. Результаты, опубликованные ранее в различных журналах, суммированы.

Les Acta Chimica paraissent en français, allemand, anglais et russe et publient des mémoires du domaine des sciences chimiques.

Les Acta Chimica sont publiés sous forme de fascicules. Quatre fascicules seront réunis en un volume (4 volumes par an).

On est prié d'envoyer les manuscrits destinés à la rédaction à l'adresse suivante:

Acta Chimica
Budapest, P.O. Box 67, H-1450, Hongrie

Toute correspondance doit être envoyée à cette même adresse.

La rédaction ne rend pas de manuscrit.

Le prix de l'abonnement: \$ 36,00 par volume.

Abonnement en Hongrie à l'Akadémiiai Kiadó (1363 Budapest, P. O. B. 24, C. C. B. 215 11488), à l'étranger à l'Entreprise du Commerce Extérieur «Kultura» (H-1389 Budapest 62, P. O. B. 149 Compte-courant No. 218 10990) ou chez représentants à l'étranger.

Die Acta Chimica veröffentlichen Abhandlungen aus dem Bereich der chemischen Wissenschaften in deutscher, englischer, französischer und russischer Sprache.

Die Acta Chimica erscheinen in Heften wechselnden Umfanges. Vier Hefte bilden einen Band. Jährlich erscheinen 4 Bände.

Die zur Veröffentlichung bestimmten Manuskripte sind an folgende Adresse zu senden

Acta Chimica
Budapest, Postfach 67, H-1450, Ungarn

An die gleiche Anschrift ist jede für die Redaktion bestimmte Korrespondenz zu richten. Manuskripte werden nicht zurückerstattet.

Abonnementspreis pro Band: \$ 36,00.

Bestellbar für das Inland bei Akadémiiai Kiadó (1363 Budapest, Postfach 24, Bankkonto Nr. 215 11488), für das Ausland bei «Kultura» Außenhandelsunternehmen (H-1389 Budapest 62, P. O. B. 149. Bankkonto Nr. 218 10990) oder seinen Auslandsvertretungen.

«Acta Chimica» издают стихи по химии на русском, английском, французском и немецком языках.

«Acta Chimica» выходит отдельными выпусками разного объема, 4 выпуска составляют один том и за год выйдут 4 тома.

Предназначенные для публикации рукописи следует направлять по адресу:

Acta Chimica
Budapest, P.O. Box 67, H-1450, ВНР

Всякую корреспонденцию в редакцию направляйте по этому же адресу.

Редакция рукописей не возвращает.

Подписная цена — \$ 36,00 за том.

Отечественные подписчики направляйте свои заявки по адресу Издательства Академии Наук (1363 Budapest, P.O.B. 24, Текущий счет 215 11 188), а иностранные подписчики через организацию по внешней торговле «Kultura» (H-1389 Budapest 62, P.O.B. 149. Текущий счет 218 10990) или через ее заграничные представительства и уполномоченных.

Reviews of the Hungarian Academy of Sciences are obtainable
at the following addresses:

AUSTRALIA

C.B.D. LIBRARY AND SUBSCRIPTION SERVICE,
Box 4886, G.P.O., *Sydney N.S.W. 2001*
COSMOS BOOKSHOP, 145 Ackland Street, *St. Kilda (Melbourne), Victoria 3182*

AUSTRIA

GLOBUS, Höchstädtplatz 3. *1200 Wien XX*

BELGIUM

OFFICE INTERNATIONAL DE LIBRAIRIE, 30
Avenue Marnix, *1050 Bruxelles*
LIBRAIRIE DU MONDE ENTIER, 162 Rue du
Midi, *1000 Bruxelles*

BULGARIA

HEMUS, Bulvar Ruszki 6, *Sofia*

CANADA

PANNONIA BOOKS, P.O. Box 1017, Postal Sta-
tion "B", *Toronto, Ontario M5T 2T8*

CHINA

CNPICOR, Periodical Department, P.O. Box 50,
Peking

CZECHOSLOVAKIA

MAĎARSKÁ KULTURA, Národní třída 22,
115 33 Praha

PNS DOVOZ TISKU, Vinohradská 46, *Praha 2*

PNS DOVOZ TLAČE, *Bratislava 2*

DENMARK

EJNAR MUNKSGAARD, Norregade 6, *1165 Copenhagen*

FINLAND

AKATEEMINEN KIRJAKAUPPA, P.O. Box 128,
SF-00101 Helsinki 10

FRANCE

EUROPERIODIQUES S.A., 31 Avenue de Ver-
sailles, *78170 La Celle St.-Cloud*

LIBRAIRIE LAVOISIER, 11 rue Lavoisier, *75008 Paris*

OFFICE INTERNATIONAL DE DOCUMENTA-
TION ET LIBRAIRIE, 48 rue Gay-Lussac, *75240 Paris Cedex 05*

GERMAN DEMOCRATIC REPUBLIC

HAUS DER UNGARISCHEN KULTUR, Karl-
Liebknecht-Strasse 9, *DDR-102 Berlin*

DEUTSCHE POST ZEITUNGSVERTRIEBSAMT,
Strasse der Pariser Kommune 3-4, *DDR-104 Berlin*

GERMAN FEDERAL REPUBLIC

KUNST UND WISSEN ERICH BIEBER, Postfach
46, *7000 Stuttgart 1*

GREAT BRITAIN

BLACKWELL'S PERIODICALS DIVISION, Hythe
Bridge Street, *Oxford OX1 2ET*

BUMPUS, HALDANE AND MAXWELL LTD.,
Cower Works, *Olney, Bucks MK46 4BN*

COLLET'S HOLDINGS LTD., Denington Estate,
Wellingborough, Northants NN8 2QT

WM. DAWSON AND SONS LTD., Cannon House,
Folkestone, Kent CT19 5EE

H. K. LEWIS AND CO., 136 Gower Street, *London WC1E 6BS*

GREECE

KOSTARAKIS BROTHERS, International Book-
sellers, 2 Hippokratous Street, *Athens-143*

HOLLAND

MEULENHOF-BRUNA B.V., Beulingstraat 2,
Amsterdam

MARTINUS NIJHOFF B.V., Lange Voorhout
9-11, *Den Haag*

SWETS SUBSCRIPTION SERVICE, 347b Heere-
weg, *Lisse*

INDIA

ALLIED PUBLISHING PRIVATE LTD., 13/14
Asaf Ali Road, *New Delhi 110001*

150 B-6 Mount Road, *Madras 600002*

INTERNATIONAL BOOK HOUSE PVT. LTD.,
Madame Cama Road, *Bombay 400039*

THE STATE TRADING CORPORATION OF
INDIA LTD., Books Import Division, Chandralok,
36 Janpath, *New Delhi 110001*

ITALY

EUGENIO CARLUCCI, P.O. Box 252, *70100 Bari*

INTERSCIENTIA, Via Mazzé 28, *10149 Torino*

LIBRERIA COMMISSIONARIA SANSONI, Via
Lamarmora 45, *50121 Firenze*

SANTO VANASIA, Via M. Macchi 58, *20124 Milano*

D. E. A., Via Lima 28, *00198 Roma*

JAPAN

KINOKUNIYA BOOK-STORE CO. LTD., 17-7
Shinjuku-ku 3 chome, Shinjuku-ku, *Tokyo 160-91*

MARUZEN COMPANY LTD., Book Department,
P.O. Box 5050 Tokyo International, *Tokyo 100-31*

NAUKA LTD., IMPORT DEPARTMENT, 2-30-19
Minami Ikebukuro, Toshima-ku, *Tokyo 171*

KOREA

CHULPANMUL, *Phenjan*

NORWAY

TANUM-CAMMERMEYER, Karl Johansgatan
41-43, *1000 Oslo*

POLAND

WĘGIERSKI INSTYTUT KULTURY, Marszał-
kowska 80, *Warszawa*

CKP I W ul. Towarowa 28 00-958 *Warsaw*

ROMANIA

D. E. P., *București*

ROMLIBRI, Str. Biserica Amzei 7, *București*

SOVIET UNION

SOJUZPETCHATJ — IMPORT, *Moscow*

and the post offices in each town

MEZHDUNARODNAYA KNIGA, *Moscow G-200*

SPAIN

DIAZ DE SANTOS, Lagasca 95, *Madrid 6*

SWEDEN

ALMQVIST AND WIKSELL, Gamla Brogatan 26,
101 20 Stockholm

GUMPERTS UNIVERSITETSBOKHANDEL AB,
Box 346, *401 25 Göteborg 1*

SWITZERLAND

KARGER LIBRI AG, Petersgraben 31, *4011 Basel*

USA

EBSCO SUBSCRIPTION SERVICES, P.O. Box
1943, *Birmingham, Alabama 35201*

F. W. FAXON COMPANY, INC., 15 Southwest
Park, *Westwood, Mass. 02090*

THE MOORE-COTTRELL SUBSCRIPTION

AGENCIES, North Cohocton, *N. Y. 14868*

READ-MORE PUBLICATIONS, INC., 140 Cedar
Street, *New York, N. Y. 10006*

STECHELT-MACMILLAN, INC., 7250 Westfield
Avenue, *Pennsauken N.J. 08110*

VIETNAM

XUNHASABA, 32, Hai Ba Trung, *Hanoi*

YUGOSLAVIA

JUGOSLAVENSKA KNJIGA, Terazije 27, *Beograd*
FORUM, Vojvode Mišića 1, *21000 Novi Sad*

ACTA CHIMICA

ACADEMIAE SCIENTIARUM HUNGARICAE

ADIUVANTIBUS

M. T. BECK, R. BOGNÁR, V. BRUCKNER,
GY. HARDY, K. LEMPert, F. MÁRTA,
K. POLINSZKY, E. PUNGOR,
G. SCHAY, Z. G. SZABÓ, P. TÉTÉNYI

REDIGUNT

B. LÉNGYEL et GY. DEÁK

TOMUS 101

FASCICULUS 3



AKADÉMIAI KIADÓ, BUDAPEST

1979

ACTA CHIM. ACAD. SCI. HUNG.

ACASA2 101 (3) 215-307 (1979)

ACTA CHIMICA

A MAGYAR TUDOMÁNYOS AKADÉMIA
KÉMIAI TUDOMÁNYOK OSZTÁLYÁNAK
IDEGEN NYELVŰ KÖZLEMÉNYEI

FŐSZERKESZTŐ
LENGYEL BÉLA

SZERKESZTŐ
DEÁK GYULA

TECHNIKAI SZERKESZTŐ
HAZAI LÁSZLÓ

SZERKESZTŐ BIZOTTSÁG
BECK T. MIHÁLY, BOGNÁR REZSŐ, BRUCKNER GYŐZŐ,
HARDY GYULA, LEMPERT KÁROLY, MÁRTA FERENC,
POLINSZKY KÁROLY, PUNGOR ERNŐ, SCHAY GÉZA,
SZABÓ ZOLTÁN, TÉTÉNYI PÁL

Acta Chimica is a journal for the publication of papers on all aspects of chemistry in English, German, French and Russian.

Acta Chimica is published in 4 volumes per year. Each volume consists of 4 issues of varying size.

Manuscripts should be sent to

Acta Chimica
Budapest, P.O. Box 67, H-1450, Hungary

Correspondence with the editors should be sent to the same address. Manuscripts are not returned to the authors.

Subscription: \$ 36.00 per volume.

Hungarian subscribers should order from Akadémiai Kiadó, 1363 Budapest, P.O. Box 24. Account No. 215 11488.

Orders from other countries are to be sent to "Kultura" Foreign Trading Company H-1389 Budapest 62, P.O. Box 149. Account No. 218 10990) or its representatives abroad.

ELECTROCHEMICAL BEHAVIOUR OF ETHYLENE GLYCOL AND ITS OXIDATION PRODUCTS ON A PLATINUM ELECTRODE, V

EXPERIMENTAL STUDY OF ELECTRO-OXIDATION AND OXIDATION PRODUCTS
OF GLYCOLALDEHYDE AND GLYCOLIC ACID

GY. INZELT and GY. HORÁNYI¹

(Department of Physical Chemistry and Radiology, Eötvös Loránd University, Budapest,
¹Central Research Institute for Chemistry of the Hungarian Academy of Sciences, Budapest)

Received April 13, 1978

Accepted for publication August 24, 1978

The electro-oxidations of glycolic acid and glycolaldehyde were studied on a platinized platinum electrode in $M HClO_4$ background electrolyte. Two steps may be observed in the initial section of the steady-state potentiostatic polarization curves. This feature was also displayed in the polarization curves of glyoxal and glyoxalic acid, studied previously. By analogy, in the present case too it is assumed that the occurrence of the steps may be explained in part by the inhibitory effect due to chemisorption, and in part to a change in the depth of oxidation. The results of various analytical methods led to the finding that a process involving a charge transfer of 2F per mol predominates at not too high potentials in the case of glycolaldehyde. Consequently, mainly glyoxal with less glycolic acid is formed. With the increase of the potential, oxalic acid is to be found in ever higher proportions among the products in the solution phase, and at potentials corresponding to the second step carbon dioxide will be the end-product of the reaction.

In the potential interval corresponding to the first step in the case of glycolic acid, glyoxalic acid and oxalic acid are to be found in the solution, while at the potentials corresponding to the second step the formation of carbon dioxide similarly comes into the foreground.

In previous publications we dealt with questions of the oxidation of glyoxal and glyoxalic acid [1–3]. It was assumed of both compounds that they are intermediates of the total electro-oxidation of ethylene glycol, leading to oxalic acid and then carbon dioxide. In the present publication, in an attempt to confirm the assumed oxidation scheme, we deal with a study of the products formed in the electro-oxidation of glycolaldehyde and glycolic acid, and with the polarization properties of these compounds.

The nature of the products, and the ratios of the different products, may vary to a considerable extent with the electrode potential. To elucidate the mechanism of the oxidation process, it appears indispensable to establish the connection between the electrode potential and the change in the product composition. Few data relating to this are available in the literature, and even these cannot be regarded as free of contradictions. The difficulty is primarily caused by the fact that compounds fairly similar in chemical behaviour must be detected and determined in the presence of one another in order that the

steps of the oxidation may be identified. Accordingly, it was regarded as one of our essential tasks to select or elaborate appropriate analytical procedures.

It must additionally be noted that earlier investigations [4–6] were primarily directed towards the establishment of the main regularities characteristic of the strong chemisorption of these compounds. The investigations of such a nature were generally based on the assumption that the strongly (irreversibly) chemisorbed molecules play a key role in the steady-state oxidation processes. An ever increasing number of signs now indicate that the strong chemisorption and the oxidation of the chemisorbed molecules is probably only a parallel reaction pathway to the chemically well distinguishable process resulting in the intermediates. The phenomena observed in the oxidation of glyoxal and glyoxalic acid were interpreted in the previous publication in this way. In the cases of oxalic acid and glycolic acid, experimental evidence too is available with regard to well distinguishable reversible adsorption [7, 8]. Overall, therefore, we tend to place the emphasis not on what transformations the chemisorbed molecules may undergo, but on what components appear in the solution phase. Naturally, it is still necessary to take into account the literature data relating to the composition and transformation of the strongly chemisorbed molecules, so that the reaction pathway proceeding via chemisorption may be differentiated more clearly from the other reactions.

Experimental

A. Electrochemical investigation methods

The polarization measurements were made as reported in earlier publications, in M $HClO_4$ background electrolyte. For purposes of analysis the products were prepared in a cell with a cylindrical platinized platinum main electrode, having a geometrical surface area of 160 cm^2 . The auxiliary electrode placed into the center of the cylinder formed by the main electrode was selected so as to have a surface area about two orders of magnitude lower than that of the main electrode. The main and auxiliary electrode compartments were separated by a glass filter. Because of the low surface area of the auxiliary electrode, the reduction of oxidation products possibly diffusing through the glass filter could not have been appreciable, and hence practically only hydrogen evolved, on the auxiliary electrode during the anodic polarization of the main electrode.

B. Analytical investigation methods

The methods employed for the detection and quantitative determination of the products of the individual reactions are listed below.

(a) Oxalic acid

Oxalic acid was determined by the method reported previously [9].

(b) Glycolaldehyde

Glycolaldehyde was determined by the FEHLING—SCHOORL method modified in accordance with our purposes [10]. This method in effect serves for the determination of sugars. Glycolaldehyde is a compound essentially analogous with sugars, and it is known [11] to give the Fehling reaction. In our case it had to be taken into consideration that ethylene glycol,

glyoxal, and glyoxalic acid are also present in the examined solution, in addition to glycolaldehyde. Ethylene glycol and glyoxal do not give the Fehling reaction. In contrast, if the reaction mixture is boiled in the usual manner, glyoxalic acid reduces the Fehling solution to a slight extent, and its presence may therefore interfere with the determination. To avoid this, boiling must be avoided. In our experience, in the case of glycolaldehyde the reaction proceeds rapidly at 40–50 °C, but glyoxalic acid reacts only very slowly at such temperatures. Similarly as for sugars, a strict stoichiometric correlation cannot be established between the amount of glycolaldehyde and the Cu_2O precipitated, because of the side-reactions (e.g. the Cannizzaro reaction), and it is necessary to prepare a calibration curve or a table. Accordingly, the determination was carried out as follows.

2–15 cm^3 Fehling II solution (346 g potassium sodium tartarate and 100 g NaOH dissolved in distilled water and the solution made up to 1 liter) was added to 2–15 cm^3 Fehling I solution (69.28 g $\text{CuSO}_4 \cdot 5\text{H}_2\text{O}$ dissolved in distilled water and the solution made up to 1 liter). An appropriately selected quantity (2–10 cm^3) of the sample, neutralized with 1 M NaOH, was added to the reagent. The reaction mixture was heated mildly (40–50 °C). As mentioned above, boiling was avoided, as any glyoxalic acid present also consumes the reagent. (Otherwise, conclusions as to the glyoxalic acid content can be drawn from the difference between the results given by the boiled and the mildly heated samples, but the determination of glyoxalic acid is less accurate, since, depending on the concentration, the efficiency of this reaction is 10–36% compared to that for glycolaldehyde.)

The reaction mixture was quickly cooled to 25 °C, 1–5 g KI was added, and the solution was acidified with sulfuric acid. The liberated iodine was titrated with 0.01 or 0.1 N $\text{Na}_2\text{S}_2\text{O}_3$ until the mixture was pale-yellow. After the addition of 2 ml starch solution, the titration was continued until the blue colour had disappeared. By comparison with a calibration diagram similarly prepared, the glycolaldehyde concentration of the sample was obtained with an accuracy of 2–6%. The determination is not disturbed by ethylene glycol, or by its other oxidation products (glyoxal glycolic acid, oxalic acid).

(c) Glycolic acid

Glycolic acid was detected by paper chromatography. With ammonia – water – ethanol (1:3:16) as developing mixture in ascending chromatography on Whatman-1 paper, glycolic acid is well separated from the other components, and can be developed with 1% acidic KMnO_4 solution. A butanone – acetone – water – formic acid (40:2:6:1) mixture can also be employed effectively in a descending chromatography procedure. Details on these procedures are to be found in the literature [12].

(d) Glyoxal

A reaction described in the literature [13] was utilized for the qualitative detection of glyoxal. A little freshly sublimed *o*-aminophenol and CaO were added to a few drops of the solution under examination. The presence of glyoxal was indicated by a red colour. With given reagent and sample proportions, there is a possibility for a rough estimation of the concentration of glyoxal on the basis of the intensity of the colour, with the aid of a suitable comparative series.

(e) Glyoxalic acid

The glyoxalic acid intermediate was isolated from among the oxidation products of glycolic acid, in the form of its dinitrophenylhydrazone. 0.1 g dinitrophenylhydrazine dissolved in 10 ml of 50% sulfuric acid was added to a 10–20 ml sample, with a concentration of at least 10^{-2} mol/dm³ as regards glyoxalic acid. Depending on the glyoxalic acid concentration, a yellow crystalline precipitate separated out after a shorter or a longer time. The melting point determined after filtration, washing and drying was compared with the literature melting point value and with the melting point of the phenylhydrazone precipitated from pure glyoxalic acid. (The melting point of the phenylhydrazone precipitated from among the oxidation products of glycolic acid was 193–195 °C and 192–194 °C for two different samples; that for the phenylhydrazone prepared from pure glyoxalic acid was 192–194 °C; and the literature values [14] were 190–200 °C.) In our experience, the solubility of the dinitrophenylhydrazone of glyoxalic acid is relatively high, and there was therefore no possibility for the quantitative determination of glyoxalic acid in the form of its dinitrophenylhydrazone.

Results

The technique used to record the polarization curves was the same as that employed in the cases of glyoxal and glyoxalic acid [1–3]. Just as in the previous investigations, the variation of the rate of oxidation with the concentration was studied by increasing the concentration by addition of the compound in question at each given potential.

A. Polarization properties of glycolic acid

Curve *a* in Fig. 1 is the polarization curve of glycolic acid, recorded at a given concentration with the stationary potentiostatic method. An appreciable difference is not observed in the natures and forms of the curves recorded at different concentrations. Similarly to the electro-oxidation of other organic substances, the shapes of the potentiostatic polarization curves are not independent of the direction of the recording, *i.e.* a hysteresis can be observed. This is illustrated by curve *b* of Fig. 1. The cause of the hysteresis is the irreversible adsorption of oxygen. It is striking in curve *b* of Fig. 1 that in a wide potential interval the rate of oxidation is practically negligibly small. From this, the conclusion may be drawn that the oxidation of glycolic acid on the already developed surface oxide layer is an inhibited process, and the probability of direct reaction of the surface oxides and glycolic acid is also slight. The increase of the current at potentials more negative than 900 mV can be explained unambiguously by the electrochemical reduction of the oxide layer.

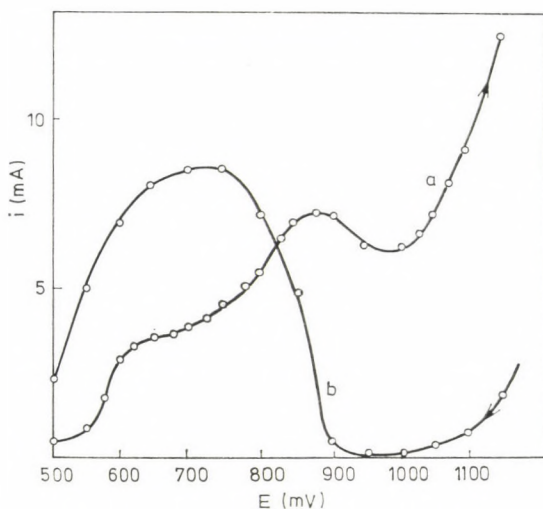


Fig. 1. Polarization curve of glycolic acid (1.25×10^{-1} mol/dm³). Recording in direction of (a) increasing, (b) decreasing potentials

In contrast with the two compounds investigated previously (glyoxal and glyoxalic acid), a maximum can be observed on the polarization curve recorded in the direction of increasing potentials. This phenomenon can always be observed by the increase of the potential in the case of the oxidation of alcohols, because of the inhibitory effect of the ever more significant oxygen adsorption. Accordingly, the appearance of the maximum cannot be regarded as surprising, for in the case of glycolic acid (at least as the first step) there can hardly be any possible alternative to the oxidation of the alcoholic hydroxy group. The further rise in the polarization curve, following the maximum and then the minimum, can be interpreted by the opening of a new reaction path. In the following we shall examine only those phenomena which occur in the potential interval prior to the maximum. In this section, two steps are to be found on the polarization curve, similarly as in the cases of glyoxal and glyoxalic acid. For these compounds, the occurrence of the steps was explained in that the increase of the potential leads to the removal of the chemisorbed molecules exerting the inhibitory effect (step 1), and to a change in the depth of the oxidation (step 2). It may be presumed that this is also the situation in the case of glycolic acid, but this question can be decided only in the knowledge of the change in the composition of the products with the variation of the potential. Our examinations of this nature are reported in the following section. However, the similarity is manifested not only in the shapes of the polarization curves, but also in the concentration-dependence of the oxidation current. Figure 2 presents current (i) vs. concentration (c) curves recorded at different potentials. When the related current and concentration values are plotted in the form $1/i$ vs. $1/c$, as in Fig. 3, straight lines are obtained, i.e. it may be concluded that adsorption conditions of Langmuir type prevail.

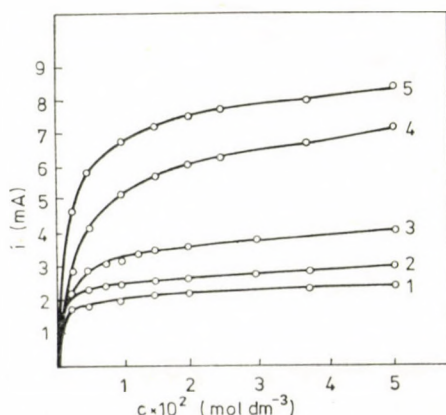


Fig. 2. Variation of the rate of oxidation of glycolic acid with the concentration at different potentials; (1) 600; (2) 700; (3) 800; (4) 900; (5) 1000 mV

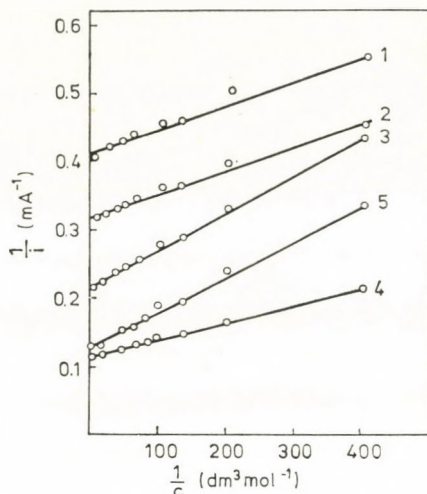


Fig. 3. Data of Fig. 2 plotted as $1/i$ vs. $1/c$. (1) 600; (2) 700; (3) 800; (4) 900; (5) 1000 mV

B. Chemism of the oxidation of glycolic acid

It was earlier demonstrated [1] that, under the same experimental conditions, of all the two carbon atom-containing oxidation products of ethylene glycol (with the exception of oxalic acid) glycolic acid is oxidized the most slowly at potentials more negative than 800 mV. This also emerges from a comparison of the polarization curve given in the preceding section and the polarization curves relating to glyoxal and glyoxalic acid, reported previously [1].

In the course of the oxidation of glycolic acid at 600–800 mV, various amounts of glyoxalic acid and oxalic acid can be detected, depending on the duration of the electrolysis. Above 800 mV, an intensive evolution of carbon dioxide can be observed. The formation of carbon dioxide is also apparent at lower potentials; in this case the phenomenon can presumably be attributed to the total oxidation of the chemisorbed molecules, similarly as observed for glyoxalic acid.

On the above basis, the reaction series



may be assumed for the complete oxidation of glycolic acid. To check this assumption, the current yield referring to oxalic acid was examined at different potentials. The electrolysis was continued for such a time that at most 5–10% of the initial quantity of glycolic acid should undergo transformation. The amount of oxalic acid formed in the solution was determined by the method given in the Experimental section. The current yield referring to oxalic acid is presented as a function of the potential in curve *a* of Fig. 4.

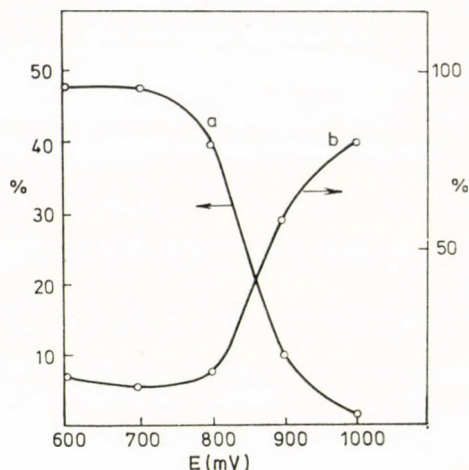


Fig. 4. (a) Current yield referring to oxalic acid in the case of the oxidation of glycolic acid, as a function of the potential. (b) Current yield referring to carbon dioxide during the oxidation of glycolic acid, as a function of the potential

It emerges from the Figure that even at 600 mV oxalic acid is formed to a considerable extent. At the same time, the dinitrophenylhydrazone of glyoxalic acid can also be precipitated from solution with dinitrophenylhydrazine. In essence, therefore, the situation is that a part of the glyoxalic acid formed is converted fairly rapidly to oxalic acid. This is otherwise in agreement with the fact that at the potentials in question the rate of oxidation of glyoxalic acid is higher than that of glycolic acid.

At 800–900 mV, however, the current yield referring to oxalic acid decreases significantly. A similar phenomenon was observed during the study of the oxidation of glyoxalic acid [2, 3]. In the case of glyoxalic acid the current yield referring to oxalic acid at 600 mV was 90–95%; above 750–800 mV this became smaller and smaller with the increase of the potential. The phenomenon can be explained clearly by the oxidation of oxalic acid. It is obvious that this is also the situation in the case of glycolic acid. All this is well illustrated by the potential-dependence of the current yield referring to carbon dioxide, shown in curve *b* of Fig. 4.

C. Polarization properties of glycolaldehyde

Figure 5 presents a polarization curve recorded at relatively high glycolaldehyde concentration. Here too the phenomenon of hysteresis is exhibited. Two steps are again to be found before the maximum in the polarization curve recorded in the direction of increasing potentials. The existence of the maximum at the same time permits the conclusion that the oxidation of the

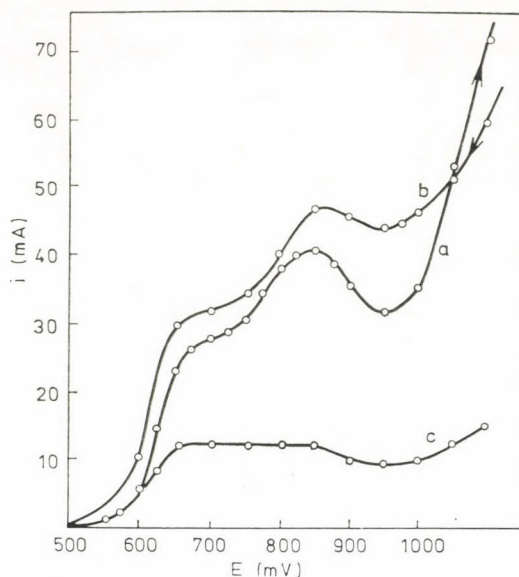
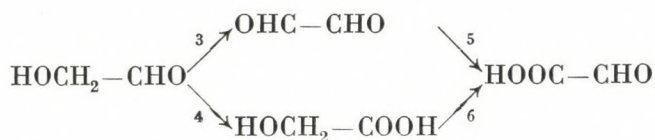


Fig. 5. Polarization curve of glycolaldehyde (2×10^{-1} mol/dm³) recorded in the direction of (a) increasing, (b) decreasing potentials, (c) polarization curve at a concentration of 2×10^{-2} mol/dm³

—CH₂OH group too plays a role in the reaction, *i.e.* it is not probable that the oxidation is restricted exclusively or primarily to the aldehyde group. In the case of glycolaldehyde the shapes of the polarization curves are by no means independent of the concentration. This follows from a comparison of curves *a* and *c* in Fig. 5. The definite appearance of the two steps can be observed only at concentrations much higher than 10^{-2} mol/dm³. At lower concentrations a comparatively long plateau is obtained instead of the second step in a wide potential interval. *i* vs. *c* and $1/i$ vs. $1/c$ curves recorded in this concentration range are presented in Figs 6 and 7. These curves do not differ as regards their natures from those presented for glycolic acid, and the $1/i$ vs. $1/c$ plot is again linear to a good approximation.

D. Chemism of the oxidation of glycolaldehyde

In the oxidation of glycolaldehyde we are primarily faced with the problem that the first step of the oxidation may occur in two ways, as illustrated in the following reaction scheme:



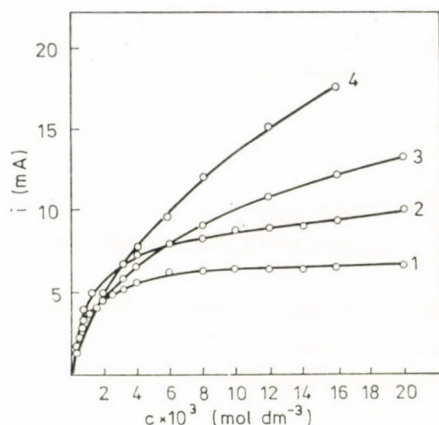


Fig. 6. Variation of the rate of oxidation of glycolaldehyde with the concentration at different potentials; (1) 600; (2) 700; (3) 800; (4) 1000 mV

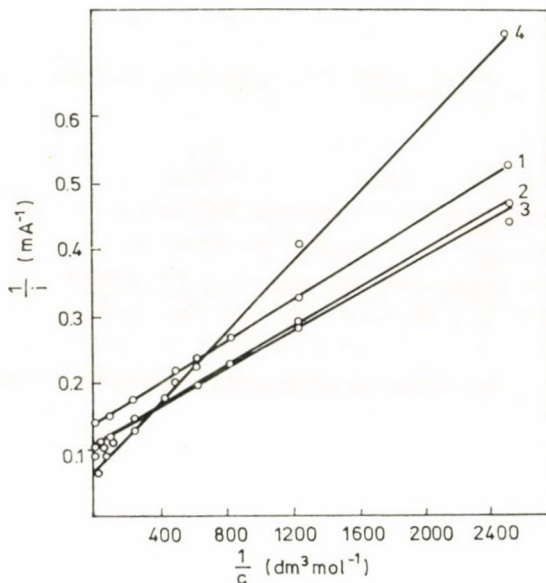


Fig. 7. Data of Fig. 6 plotted as $1/i$ vs. $1/c$; (1) 600; (2) 700; (3) 800; (4) 1000 mV

Reaction steps 5 and 6 have already been examined in the present and previous publications, and there is no doubt as to their reality. We also know that the rate of transformation *via* reaction 5 is higher in general than that *via* reaction 6. We were unable to develop a suitable procedure for quantitative examination of the products, *i.e.* for quantitative determination of glyoxal and glycolic acid. By the tests described in the Methods section, however, it

was established that both glyoxal and glycolic acid are formed in the course of the reaction. As already mentioned, with the aid of an appropriate calibration series there is a possibility for the estimation of the amount of glyoxal formed, on the basis of the intensity of the colour produced in the *o*-aminophenol test. Conclusions may also be drawn as to the quantity of glycolic acid, on the basis of the paper chromatographic analysis. Overall, it could be established that step 3 plays a substantially greater role than reaction 4 in the transformation. A comparison of the polarization curves reveals that the currents measured in the oxidation of glycolaldehyde are generally larger than those found in the case of glyoxal, and substantially larger than those determined for glycolic acid. Clearly, this can only be explained in that the sum of the rates of steps 3 and 4 (*i.e.* predominantly the rate of step 3) is larger than the rates of the subsequent reactions, *i.e.* the initial section of the polarization curve of glycolaldehyde reflects the rates corresponding to reaction steps 3 and 4. To prove this, we made a study of the variation (decrease) of the glycolaldehyde concentration as a function of the charge passing through the system. The average charge necessary for the transformation of 1 mol glycolaldehyde can be determined from the experimental data. It emerged that in the potential interval of 600–700 mV the consumption of an average charge of only 2.2–2.4F per mol must be reckoned with, even if some 30–50% of the initial quantity of glycolaldehyde undergoes transformation.

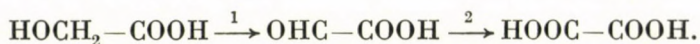
In these experiments the variation of the concentration of oxalic acid was also examined. It was found that with the increase of the potential an increasing, but relatively slight extent of oxalic acid formation too may be observed. Naturally, it is also necessary to take into account the formation of the other intermediates between glycolaldehyde and oxalic acid. (As already mentioned, glyoxal and glycolic acid can be detected in the liquid phase.) In addition, the total oxidation of the strongly chemisorbing glycolaldehyde also plays a role, as indicated by the similarly slight evolution of CO₂. When all this is taken into consideration, the utilization of a charge of 2.2–2.4F per mol clearly points to the decisive role being played by a reaction involving a charge transfer of 2F, and this can only be the formation of glyoxal or glycolic acid. It was mentioned previously that the proportion of glycolic acid formation is subordinate to that of glyoxal. These results were obtained at comparatively low initial glycolaldehyde concentration (a few times 10⁻² mol/dm³), *i.e.* when the second step has not yet appeared on the polarization curve.

Discussion

The experimental results permit the statement that the reactions examined proceed in a stepwise manner, and that all of the chemically well defined intermediates containing two carbon atoms appear in the solution phase.

At all events, it may be concluded from this observation that the desorption of the individual compounds (at least in the instants immediately following their formation) is not a greatly hindered process. It is also known that these compounds (with the exception of oxalic acid and glycolic acid) may be strongly chemisorbed on the surface of platinum, and both their chemisorption and the oxidation of the chemisorbed molecules result in a much more extensive conversion than might justify the appearance of the products with lower degrees of oxidation in the solution phase.

This contradiction can only be resolved if the chemisorption and the chemical transformation are conceived of as parallel processes; both reactions can be regarded as taking place *via* a common, weak adsorption state, similarly as in the interpretation of the oxidation of methanol and its oxidation products [15]. The two steps appearing on the polarization curve in the oxidation of glycolic acid may be explained in essentially the same way as was done in the case of glyoxalic acid. It was found above that in the potential interval corresponding to the first step the reaction sequence predominantly occurring is



The fact that the rate of oxidation of glycolic acid is lower than that of glyoxalic acid indicates that the rate constant characterizing step 1 in this scheme is smaller than that for step 2. It also follows from this that even in the case of relatively low glycolic acid conversions an appreciable amount of oxalic acid is formed. One part of the glyoxalic acid formed from glycolic acid passes into the solution by means of desorption and diffusion, while another part is further oxidized to oxalic acid. As the steady state is approached, the glyoxalic acid concentration must increase (assuming that the concentration of glycolic acid may be regarded as practically constant), and it then becomes constant in the steady state. It is probable that the steady state was still fairly distant during the investigations relating to the current yield, for in the opposite case higher values should have been obtained for the current yield referring to oxalic acid. At any event, it emerged that the current yield referring to oxalic acid does not depend on the potential in the potential interval of 600–800 mV, *i.e.* the ratio of the rates of steps 1 and 3 did not vary with the potential either. The appearance of the first step in the oxidation of glyoxalic acid was explained in that the rate of removal of the strongly chemisorbed molecules which are formed in side-reactions from glyoxalic acid and which inhibit the main reaction depends on the potential. On the other hand, the rate of the glyoxalic acid — oxalic acid transformation was regarded as practically independent of the potential. Since primarily glyoxalic acid is formed from glycolic acid, the inhibitory effect of chemisorption must be displayed even if glycolic acid were otherwise to have only a slight tendency to undergo strong chemisorption.

The reason why this must be emphasized is that, as already mentioned, tracer adsorption measurements relating to glycolic acid, carried out at low concentrations, indicate that reversibility can be observed in its adsorption, at potentials at which the oxidation of glycolic acid does not occur [8].

Similarly as for glyoxalic acid, the appearance of the second step here too is connected with the fact that carbon dioxide will increasingly be the end-product of the oxidation at the potentials corresponding to the second step, *i.e.* the oxidation of oxalic acid plays an ever more important role.

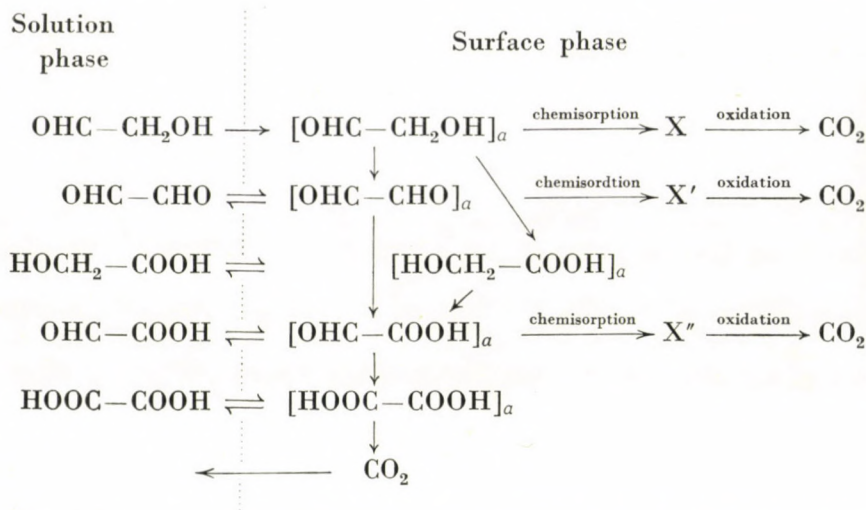
Reference is made to earlier publications [2, 3] with regard to how the main tendencies observed in the occurrence and shapes of the steps can be interpreted on the basis of the above considerations.

In the case of glycolaldehyde, it must primarily be taken into account that in a wide potential interval, particularly at low glycolaldehyde concentrations, the rate of the first step of the reaction, resulting in glyoxal (or glycolic acid), is substantially higher than that of any of the subsequent reaction steps. The experimental data showed that even in the case of comparatively prolonged polarization the charge passing through the system per mol of reacted glycolaldehyde does not differ greatly from $2F$. Accordingly, the second step does not appear on the polarization curve at low concentrations, for the participation of the oxalic acid — carbon dioxide transformation in the measured current is then not too significant, even above 750–800 mV. The appearance of the second step with the increase of the glycolaldehyde concentration can be explained in that the increase of the rate of the first reaction step automatically results in an increase in the surface concentrations of the intermediates, and at the same time in the rates of conversion of the intermediates. Naturally, this also refers to oxalic acid and to the oxalic acid — carbon dioxide transformation. On the basis of this consideration, it must also be assumed that the rates of conversion of the intermediates increase to a greater extent than that of the first reaction step.

In agreement with the earlier findings, the first step to be observed in the polarization curve of glycolaldehyde may be explained by irreversible chemisorption [2, 3]. Overall, the scheme on page 227 may be given for the full oxidation sequence starting from glycolaldehyde.

For the reasons already mentioned, chemisorbed forms were not assumed in the cases of oxalic acid and glycolic acid. Because of the linearity of the $1/i$ vs. $1/c$ curves, it may be assumed that one adsorbing molecule does indeed take part in the reaction, and that (similarly as previously) conditions of Langmuir type hold for the adsorption.

It can be seen that for both glycolaldehyde and glycolic acid kinetic relations may be given which are in principle of the same type as those written for glyoxalic acid in our earlier publications. Attention must be drawn to the difficulty that the adsorption displacement effects of the different components



on one another cannot be taken into account, while the possible variation in the adsorption of the individual components with the potential can no longer be neglected completely. The clarification of the roles of all these factors may form the subject of further investigations.

REFERENCES

- [1] HORÁNYI, Gy., INZELT, Gy., SZETÉY, Z.: *Acta Chim. Acad. Sci. Hung.* **98**, 49 (1978)
- [2] INZELT, Gy., HORÁNYI, Gy.: *Acta Chim. Acad. Sci. Hung.* **98**, 403 (1978)
- [3] INZELT, Gy., HORÁNYI, Gy.: *Acta Chim. Acad. Sci. Hung.* **99**, 393 (1979)
- [4] TRASATTI, S., FORMARO, L.: *J. Electroanal. Chem.*, **17**, 343 (1968); FORMARO, L., CASTELLI, G.: *J. Electroanal. Chem.*, **28**, 363 (1970)
- [5] WEBER, J., VASILEV, Yu. B., BAGOTSKII, V. S.: *Elektrokhimiya*, **2**, 515, 522 (1966); BAGOTSKII, V. S., VASILEV, Yu. B.: *Electrochim. Acta*, **9**, 869 (1964)
- [6] SIDHESWARAN, P.: *J. Electrochem. Soc. India*, **24**, 81 (1975); **26**, 35 (1977); INDIRA, C. J., SIDHESWARAN, P.: *Trans. SAEST*, **8**, 103 (1973); *Ind. J. Chem.*, **12**, 1077 (1974)
- [7] HORÁNYI, Gy., HEGEDÜS, D., RIZMAYER, E. M.: *J. Electroanal. Chem.*, **40**, 393 (1972)
- [8] HORÁNYI, Gy., VÉRTES, Gy., RIZMAYER, E. M.: *J. Electroanal. Chem.*, **48**, 207 (1973)
- [9] SZETÉY, Z., INZELT, Gy., HORÁNYI, Gy.: *Acta Chim. Acad. Sci. Hung.* (In press)
- [10] SCHULEK, E., SZABÓ, Z. L.: *Theoretical principles and methods of quantitative analytical chemistry* (In Hungarian), pp. 243–244. Tankönyvkiadó, Budapest 1973
- [11] Beilsteins *Handbuch der Organischen Chemie*, H 817, E IV, Springer, Berlin, Heidelberg, New York 1975
- [12] *Spravochnik khimika. IV. Khimiya*, p. 137. Moscow, Leningrad 1965; HÁIS, J. M., MACEK, K.: *Handbook of paper chromatography* (In Hungarian). Akadémiai Kiadó, Budapest 1961
- [13] FEIGL, F.: *Spot Tests in Organic Analysis*, p. 468. Elsevier, Amsterdam, London, New York, Princeton 1960
- [14] Beilsteins *Handbuch der Organischen Chemie*, H 594, E III, Berlin, Göttingen, Heidelberg 1962
- [15] VASILEV, Yu. B., BAGOTSKII, V. S., CHAZOVA, O. A.: *Elektrokhimiya*, **11**, 1505 (1975)

György INZELT H-1088 Budapest, Puskin u. 11–13.

György HORÁNYI H-1025 Budapest, Püsztaszeri út 59–67.

ELECTROCHEMICAL BEHAVIOUR OF ETHYLENE GLYCOL AND ITS OXIDATION DERIVATIVES ON A PLATINUM ELECTRODE, VI

OXIDATION OF ETHYLENE GLYCOL

GY. INZELT and GY. HORÁNYI¹

(Department of Physical Chemistry and Radiology, Eötvös Loránd University, Budapest, ¹Central Research Institute for Chemistry of the Hungarian Academy of Sciences, Budapest)

Received June 7, 1978

Accepted for publication July 26, 1978

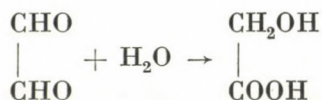
The electro-oxidation of ethylene glycol was investigated in acidic medium on a platinized platinum electrode. In contrast with the earlier literature reports, it was established that glycolaldehyde is formed in the first step of the oxidation reaction, and the current yield relating to glycolaldehyde can attain even 70–80% at not too high positive potentials. The further oxidation of glycolaldehyde results in glyoxal, glyoxalic acid and oxalic acid. On the basis of these findings, it is necessary to modify the earlier conceptions regarding the mechanism of oxidation of ethylene glycol. With the utilization of the earlier results relating to the oxidation of the oxidation derivatives of ethylene glycol, the shapes of these potentiostatic polarization curves were explained in that the dehydrogenation reaction resulting in glycolaldehyde does not depend on the potential of the electrode, whereas the coverage referring to the chemisorbed molecules formed in the side-reaction, *i.e.* the magnitude of the surface area available for the reaction, does depend on the electrode potential.

Experimental results were reported earlier [1–5] in connection with the electro-oxidation and electro-reduction of two carbon atom-containing oxidation derivatives of ethylene glycol (glyoxal, glyoxalic acid, glycolic acid, glycolaldehyde) in acidic medium on a platinized platinum electrode. An experiment was also performed in an attempt to interpret the phenomena observed. It was assumed that the compounds examined feature among the intermediates of the oxidation of ethylene glycol resulting in carbon dioxide. In the earlier work we succeeded in confirming that every compound with a higher degree of oxidation appears in the course of oxidation of a compound with a lower degree of oxidation, *i.e.* the oxidation proceeds stepwise, in a series of elementary steps.

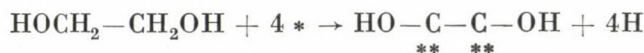
On this basis, therefore, it would be expected that glycolaldehyde should be formed as the first step in the electro-oxidation of ethylene glycol, and that it should also appear in the solution phase. However, this expectation can by no means be reconciled with the view widespread in the literature.

The literature relating to the oxidation of ethylene glycol can automatically be divided into two parts, depending on whether the investigations were

carried out in acidic or in alkaline medium [6–11]. We are interested in the examinations performed in acidic medium. In connection with the application of an alkaline medium, it should be mentioned here only that the liquid-phase transformations of the intermediates of the electro-oxidation may disturb to a considerable extent study of the process occurring on the electrode. Such a transformation, for instance, is the intramolecular Cannizzaro reaction of glyoxal



which proceeds even at room temperature. We must discuss primarily the investigations by BAGOTSKY *et al.* [6] and VIJH [7] relating to the oxidation of ethylene glycol in acidic medium on a platinum electrode. BAGOTSKY *et al.* state that the first step in the oxidation of ethylene glycol is a chemisorption process accompanied by the splitting-off of four hydrogen atoms, which they described with the equation



in which * denotes the surface sites. Glyoxal was detected in the solution phase in the course of the oxidation, and this was considered to be in accordance with the above chemisorption mechanism. VIJH too is of the view that glyoxal is the lowest oxidation state that can be detected in the solution phase, and he therefore regards it is probable that ethylene glycol is bound to the surface of the platinum by both of its carbon atoms simultaneously, and that the formation of glycolaldehyde does not occur. As regards the higher oxidation states, only the presence of oxalic acid was demonstrated with absolute certainty in the solution phase.

VIJH examines the possibility of various mechanisms, but comes to the conclusion that occurrence of the chemisorption reaction proposed by BAGOTSKY can not be excluded in any of the cases. In our view this finding is by no means a sound one, for it is difficult to justify the appearance of glyoxal in the solution phase of the chemisorption proceeding as the first step of the reaction even is accompanied by a degree of oxidation equivalent to the formation of glyoxal. The appearance of glyoxal could only be explained in that the strongly chemisorbed molecule is nevertheless capable of desorbing from the surface. VIJH gives a scheme which he considers to be in agreement with the results of both his own kinetic studies and those of BAGOTSKY *et al.* He assumes the following steps for the actual oxidation:



The notation PtC means the chemisorbed surface complex produced by the loss of four hydrogen atoms. It is obvious that the oxidation of a complex from which four hydrogen atoms have already split off cannot result in glyoxal. Hence, we do not know what the expression "products" in the right-hand side of the equation actually means.

In addition to the above objections, attention must also be drawn to the fact that we cannot be certain that glycolaldehyde was actually not formed in the experiments of BAGOTSKY *et al.* and VIJH. Their publications do not contain sufficient information as to the methods they used to be sure of this. As they employed a bright electrode with a low surface area, the quantity of products could not have been too high even in the event of comparatively long electrolysis times, *i.e.* there must have been appreciable difficulties in the detection of the individual components. From the fact that the concentration of some assumed intermediate in the solution phase does not achieve the lower limit of detectability attainable with a given analytical method, it can certainly not be concluded that the reaction does not take place *via* this intermediate.

It is clear to see that the possibility of formation of glycolaldehyde must of necessity be excluded if it is assumed that the first step of the oxidation reaction is chemisorption accompanied by the splitting-off of several hydrogen atoms. Detection of the various intermediates in the solution phase is therefore the key question from the aspect of the investigation of the mechanism of the oxidation. In an earlier publication we have already discussed the main questions connected with the oxidation of glycolaldehyde. Accordingly, in the present paper attention must primarily be devoted to the detection of glycolaldehyde among the oxidation products of ethylene glycol, or to demonstrating convincingly that it is not formed.

Results

The electrochemical methods employed were the same as described in our previous publications. Reference is made to these too with regard to the methods used to determine glycolaldehyde and oxalic acid, and to detect glycolic acid and glyoxal [2–5].

Figure 1 presents polarization curves of ethylene glycol, recorded at various concentrations. The Figure reveals that at not too low concentrations a definite maximum appears in the polarization curves; this is generally characteristic of the curves observed in the case of alcohols, and its appearance can be explained by the inhibitory effect of oxygen adsorption. Similarly in the case of high concentrations, a break too may be observed well before the maximum in the polarization curve. The two steps occurring for the compounds examined previously [2–5], therefore, can be observed only in this distorted

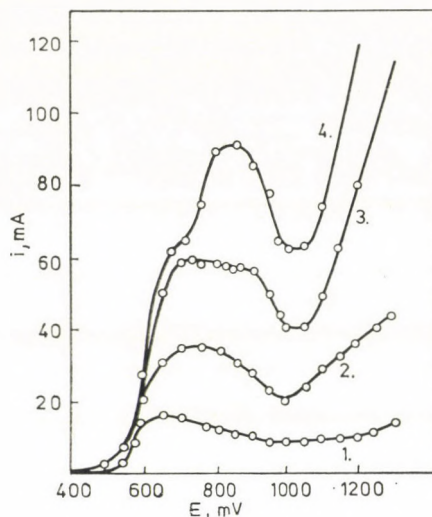


Fig. 1. Polarization curve of ethylene glycol in $M \text{HClO}_4$ base electrolyte at various concentrations. (1) 5×10^{-3} ; (2) 2.5×10^{-2} ; (3) 10^{-1} ; (4) $3.6 \times 10^{-1} \text{ mol/dm}^3$.

form in the case of ethylene glycol. At low concentrations the maximum can already be observed only very diffusely, and there is no trace at all of the appearance of the step. Observations of such a nature were also made in the case of the oxidation of glycolaldehyde [5].

Before we turn to further considerations connected with the polarization curves, an answer must be given above all to the question touched on above: Just what oxidation products are formed, and is glycolaldehyde obtained or not?

Even the first qualitative results led to the finding that the formation of a significant amount of glycolaldehyde must be reckoned with in oxidations in the potential interval 550–700 mV. On this basis, the quantity of glycolaldehyde formed in the course of the electrolysis was determined at various potentials, care being taken that conversions higher than the transformation of 5–10% of the ethylene glycol in the solution should not be reached, and that the concentration of the intermediate formed should not be too high. The current yield values referring to the glycolaldehyde are given in Table I. As these tabulated data show, at low potentials (575, 625 mV) the charge passed through the system is largely devoted to the transformation of ethylene glycol to glycolaldehyde. At higher potentials glyoxal and oxalic acid too are obtained in ever greater amounts, and the appearance of glycolic acid can also be observed. The situation is the same in the event of prolonged electrolysis. All this indicates, however, that primarily glycolaldehyde is formed on the oxidation of ethylene glycol, and the glyoxal appears only as a result of the further oxidation of the glycolaldehyde. In principle, of course, it

Table I

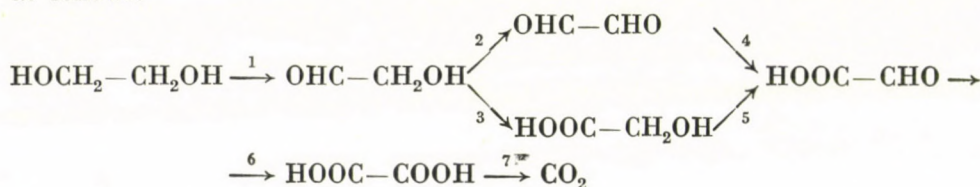
Current yield referring to glycolaldehyde as a function of the potential in the oxidation of ethylene glycol

Potential (mV)	Current yield (%)
575	85
625	75
675	63

cannot be excluded that the reaction path assumed in the literature exists, in the course of which four hydrogen atoms split off simultaneously from the ethylene glycol adsorbing and chemisorbing on the surface, with the formation of glyoxal; however, because of the experimentally found high current yield referring to the glycolaldehyde, the role of this can only be a subordinate one.

At any event, it may be stated that in the case of the oxidation of ethylene glycol primarily only one of the $-\text{CH}_2\text{OH}$ groups reacts, and following this reaction, depending on the potential and the experimental conditions, the glycolaldehyde formed either diffuses into the solution or is further oxidized to various extents on the surface of the electrode. As a result, all of the intermediates up to and including oxalic acid which have previously been dealt with [2–5] appear in the solution.

From the experimental results presented above and in our earlier publications, the conclusion must be reached that all those intermediates postulated to occur [1] are formed in the oxidation of ethylene glycol. This scheme was as follows:



It is characteristic of this scheme that the intermediates are formed stepwise. In a stationary state the following equalities must hold for the individual part-currents (i):

$$i_1 = i_2 + i_3 = i_4 + i_5 = i_6 = i_7.$$

The experimental observations permit the conclusions that

$$i_2 > i_3 \text{ and } i_4 > i_5.$$

The stationary state naturally means that the concentration is constant as regards every component featuring in the series of reactions. $dc_i/dt \sim 0$, where c_i is the concentration of the i -th component. Since this state is very

difficult to attain, and different stationary concentration ratios should hold at each different potential, strictly speaking a true stationary polarization curve cannot be obtained, for the concentrations of the intermediates (or some of them) in the solution increase because of the diffusion from the surface of the electrode.

To return to the polarization characteristics of ethylene glycol, it may be stated that essentially the same type of regularities are observed as for the compounds studied earlier. Thus, the concentration-dependence of the polarization current (Fig. 2) can be linearized in the plotting $1/i$ vs. $1/c$, just

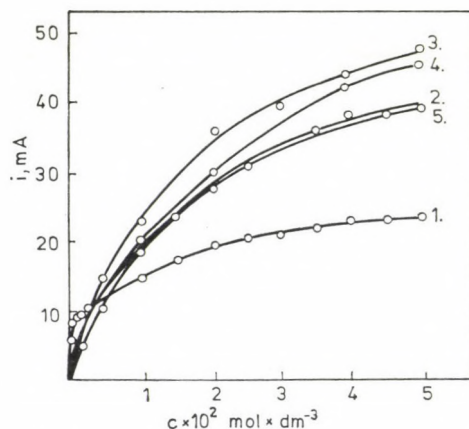


Fig. 2. Concentration-dependence of the current at various potentials. (1) 600; (2) 700; (3) 800; (4) 900; (5) 1000 mV

as in the previous cases, as can be seen in Fig. 3. It emerges from the foregoing that, particularly at potentials more negative than 750 mV, the polarization curve essentially reflects the transformation of ethylene glycol to glycolaldehyde. At low concentrations and thus at low reaction rates, *i.e.* even at higher potentials in the case of low rates of formation of the intermediates, the formation of glycolaldehyde is faster than the rates of further oxidation of the intermediates, and primarily oxalic acid. This is presumably the explanation for the plateau-like section in polarization curves recorded at low concentrations.

As already mentioned, such sections can also be observed in the polarization curve of glycolaldehyde. It was seen in the previous cases that the rate of the dehydrogenation reaction does not depend on the electrode potential. The rise occurring in the polarization curves at above 750 mV in the cases of glyoxalic acid, glyoxal, glycolic acid and glycolaldehyde oxidations could be explained in that the rate of oxidation of the oxalic acid formed in the series of reactions depends strongly on the potential. A step therefore appears only

if oxalic acid is formed at an appreciable rate, and its further oxidation also takes place. This can only be reckoned with if the first reaction steps too proceed at high rate, *i.e.* in the case of relatively high ethylene glycol concentrations. Since the oxalic acid \rightarrow carbon dioxide transition forms only a small part of the overall oxidation transformation (a charge of 2F compared to a charge of 10F for the total oxidation), if a step-type increase appears at all it will be a fairly diffuse one.

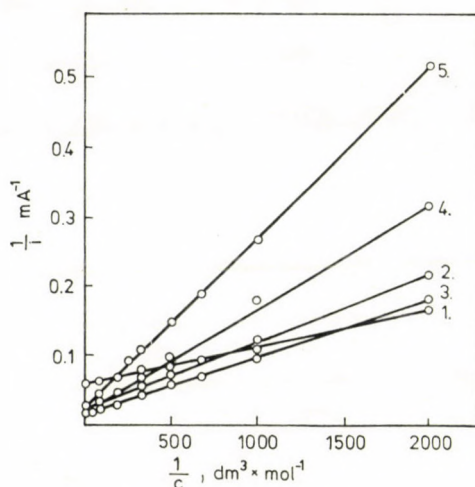
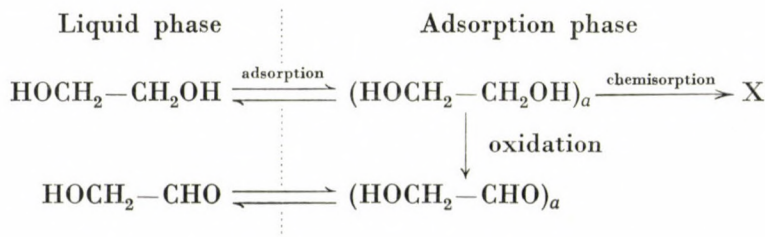


Fig. 3. Relation between $1/i$ and $1/c$ at various potentials. (1) 600; (2) 700; (3) 800; (4) 900; (5) 1000 mV

The section of the polarization curve preceding 750–800 mV is naturally to be interpreted in the same way as for the compounds investigated previously, *i.e.* in this range it is the rate of chemisorption or of oxidation of the chemisorbed molecules which, by regulating the number of free surface sites available, governs the rate of the ethylene glycol \rightarrow glycolaldehyde transformation not dependent on the electrode potential. If the train of thoughts employed in the earlier publications is followed [3–5], with the assumption that only the ethylene glycol \rightarrow glycolaldehyde transformation need be reckoned with, the following reactions may be taken into consideration:



From consideration of this reaction scheme, if the coverage relating to the product may be neglected (a condition that the concentration of glycolaldehyde in the solution should be low), the rate of adsorption of ethylene glycol is

$$w_a^e = k_a^e c (1 - \Theta_k - \Theta_e), \quad (1)$$

where Θ_k and Θ_e are the coverages relating to the chemisorbed and weakly-bound molecules, respectively, and c is the concentration of ethylene glycol in the solution.

The desorption rate is

$$w_d^e = k_d^e \Theta_e. \quad (2)$$

The rate of formation of the chemisorbed molecule from the weakly-bound one is

$$w_k = k_r \Theta_e. \quad (3)$$

The rate of oxidation of the chemisorbed molecule at a given potential is

$$w_0^k = k_0^k \Theta_k. \quad (4)$$

The rate of oxidation of the weakly-bound molecule is

$$w_0^e = k_0^e \Theta_e. \quad (5)$$

If the considerations employed in [3] are applied, we obtain the relation

$$w_0^e = \frac{k_0^e k_a^e c}{k_d^e + (1 + p) k_a^e c} = A \frac{BC}{1 + BC}, \quad (6)$$

in which

$$A = \frac{k_0^e}{1 + p} \quad \text{and} \quad B = \frac{(1 + p) k_a^e}{k_d^e} \quad (7)$$

and

$$p = \frac{\Theta_k}{\Theta_e} = \frac{k_r}{k_0^k}. \quad (8)$$

It follows from eq. (6) that, in the plotting $1/w$ vs. $1/c$, a linear correlation exists between the rate of oxidation and the concentration, *i.e.* a correlation in accordance with the experimental results is obtained. Similarly, if the train of thoughts outlined in [3] is applied to the potential-dependence of the rate, we obtain a relation of the type

$$w_0^e = \frac{Qc}{1 + Kc} \frac{\exp [b_p^e(E - E_0^x)]}{1 + \exp [b_p^e(E - E_0^x)]}, \quad (9)$$

where Q and b_p^e are constant, and $E_0^x = \frac{1}{b_p^e} \ln \frac{Yc}{1 + Kc}$ ($Y = \text{constant}$). At low ethylene glycol concentrations, the shape of the polarization curve can indeed be described approximately by a curve of the above type.

Figure 4 depicts the data of the experimental i vs. E curves in the plotting $\log(i_m^1/i - 1)$ vs. E (similarly as in the earlier publications, i_m^1 is twice the current value relating to the inflexion point in the initial section of the polarization curve). In the case of a reaction rate which can be given by eq. (9), a straight line must be obtained in this plotting. Figure 4 demonstrates that this condition holds just as in the cases examined previously [3, 4].

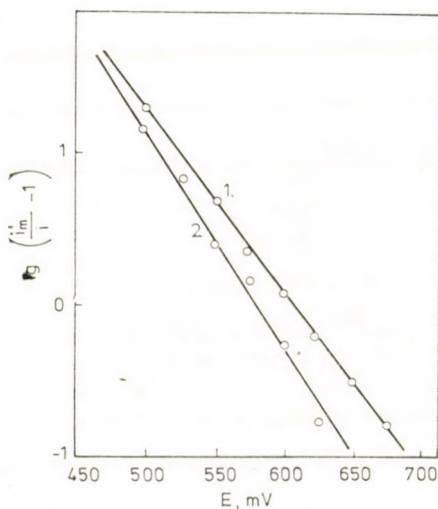
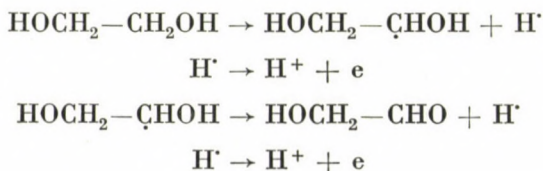


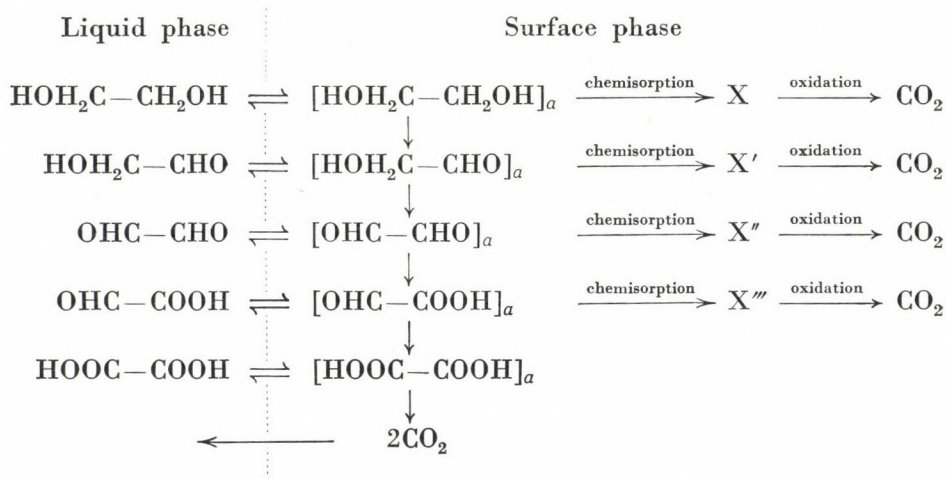
Fig. 4. Potential-dependence of $\log(i_m^1/i - 1)$. (1) 3.6×10^{-1} ; (2) 3.25×10^{-2} mol/dm³

Discussion

On the basis of the experimental results presented in this paper and the deductions drawn from the earlier publications, the conclusion must be reached that the main part of the electro-oxidation process is the oxidation of ethylene glycol via glycolaldehyde. This latter reaction is in essence a dehydrogenation process:



It is known from the literature that the dehydrogenation occurring on the chemisorption of ethylene glycol is of a greater extent than that observed in the reaction resulting in glycolaldehyde. From a chemisorbed molecule of such a type, therefore, glycolaldehyde can not be formed in any way. Two possibilities suggest themselves for resolution of the contradiction. One is to assume a weak adsorption interaction too, independent of the chemisorption, between the ethylene glycol and the surface, and to explain the oxidation reaction by the transformation of these weakly-adsorbed molecules. The other possibility is to regard the weakly-adsorbed molecule as a primary formation, and to regard the chemisorption and the oxidation as parallel reactions of the weakly-bound molecules. In this latter case, the complete reaction scheme can be given as follows:



One of the possible schemes for oxidation of ethylene glycol, adsorption and desorption being taken into consideration

For the sake of simplicity, the pathway proceeding via glycolic acid has not been shown in the scheme. We can not speak of irreversible chemisorption in the case of oxalic acid, and hence such a reaction cannot be included in the scheme either.

The arrows pointing in both directions across the phase boundary do not mean, of course, that an adsorption equilibrium is unconditionally established when the reactions occur. These arrows merely indicate that, in the course of their formation, the individual components definitely come into such a state, when their desorption from the surface is not irreversibly hindered. The extents to which the individual intermediates accumulate in the solution depend on the ratios of the reaction rates, the desorption rates and the transport rates. The essence of the mechanistic picture described here is that the chemisorption

and the oxidation of the chemisorbed molecules act only as side-reactions. At any event, the experimental results prove fairly conclusively that this is indeed the situation, and the profound chemisorption changes play only a subordinate role in the oxidation of ethylene glycol and its oxidation intermediates.

REFERENCES

- [1] HORÁNYI, Gy., INZELT, Gy., SZETÉY, Z.: *Acta Chim. Acad. Sci. Hung.*, **97**, 313 (1978)
- [2] HORÁNYI, Gy., INZELT, Gy., SZETÉY, Z.: *Acta Chim. Acad. Sci. Hung.*, **98**, 49 (1978)
- [3] INZELT, Gy., HORÁNYI, Gy.: *Acta Chim. Acad. Sci. Hung.* **98**, 403 (1978)
- [4] INZELT, Gy., HORÁNYI, Gy.: *Acta Chim. Acad. Sci. Hung.* **99**, 393 (1979)
- [5] INZELT, Gy., HORÁNYI, Gy.: *Acta Chim. Acad. Sci. Hung.* **101**, 215 (1979)
- [6] WEBER, J., VASILYEV, J. B., BAGOTSKY, V. S.: *Elektrokhimiya*, **2**, 515, 522 (1966); BAGOTSKY, V. S., VASILYEV, Yu. B.: *Electrochim. Acta*, **9**, 869 (1964)
- [7] VIJH, A. K.: *Can. J. Chem.*, **48**, 197 (1970); **49**, 78 (1971)
- [8] DANIEL-BEK, V. S., VITVITSKAYA, G. V.: *Zhur. Prikl. Khim.*, **37**, 1724 (1964); DANIEL-BEK, V. S., VITVITSKAYA, G. V., DANILENKO, I. F.: *Zhur. Prikl. Khim.*, **38**, 806 (1965)
- [9] DANIEL-BEK, V. S., GLAZATOVA, T. N.: *Zhur. Prikl. Khim.*, **39**, 2510 (1966)
- [10] *Brit. Pat.* 1,051,614 (1966)
- [11] HAUFFE, W., HEITBAUM, J., VIELSTICH, W.: 27th Meeting of ISE, Várna 1977, Extended Abstract, p. 210; HAUFFE, W., HEITBAUM, J.: *Electrochimica Acta*, **23**, 299 (1978)

György INZELT H-1088 Budapest, Puskin u. 11–13.

György HORÁNYI H-1025 Budapest, Pusztaszeri út 59–67.

INVESTIGATIONS ON THE ASSOCIATION OF PENTANOL ISOMERS IN LIQUID PHASE

F. RATKOVICS and T. SALAMON

(Department of Physical Chemistry, Veszprém University of Chemical Technology,
Veszprém)

Received May 26, 1978

Accepted for publication August 24, 1978

The viscosity of seven pentanol isomers has been studied in the temperature range of 20–70 °C. The activation enthalpy of viscous flow was calculated, and it was found to increase with the number of branchings from *n*-pentanol (20.4 kJ/mol) to 2,2-dimethylpropane(1)-ol (30.3 kJ/mol). From the study of the mixtures of 1-methylbutane(1)-ol and 1,1-dimethylpropane(1)-ol with *n*-hexane, the conclusion can be drawn that the activation enthalpy of viscous flow is related to the mean degree of association of the alcohol also for the branched alcohols in the same way as it was found for normal alcohols. The results show that the more branched isomers have a higher degree of association. This can be explained by the fact that the formation of cyclic multimers is sterically hindered by the hydrocarbon branchings, thus promoting the formation of longer chain like multimers.

In spite of the great number of works concerning the liquid phase association of alcohols, even the basic question of the cyclic or chain character of polymerization at room temperature could not be clarified satisfactorily. One main reason of the contradictory views is that only few authors have investigated pure alcohols and, on the other hand, no methods are available by means of which it would be possible to prove unambiguously the cyclic or chain character of the liquid phase association of alcohols. The experimental results, in general, could be interpreted in both ways, as it occurred for example in the case of dielectric relaxation, where from the same data certain authors concluded on chain [1] and others on cyclic [2] structures. Opinions differ in the same way when interpreting the results of infrared spectroscopic measurements; according to one interpretation, the OH absorption band of the monomer (near to 3650 cm⁻¹) falls together with, or is to be found in the immediate neighbourhood of the absorption bands of the terminal OH groups [3], consequently, the pure alcohols are associated cyclically, because in these alcohols that band is practically undetectable.

According to an other interpretation, however the band of the terminal OH group is shifted to much lower wavenumbers, and pure alcohols are characterized by chain-type association [4].

Our own investigations, by which we sought an answer to the question exposed in the introduction, were based upon the recognition that the viscosity and the enthalpy of viscous flow depend on the mass of the kinetic units tak-

ing part in the molecular movement, that is on the number of the CH_2 , CH_3 , OH , NH , NH_2 , etc. atom groups in the flow unit [5].

From our investigations it became clear that in alcohols the associated molecules represent independent kinetic units during viscous flow. In homologous alcohols higher than ethanol, the flow can be considered as following the so-called segment motion mechanism, which has already been successfully applied for hydrocarbons, and the mean life-time of the associates is several orders of magnitude greater than the time needed for the jump of atom groups from one lattice point into another in the case of a quasi-crystalline liquid model. As the associated molecules flow together, the mean relative molecular mass of the multimers can be calculated from the activation enthalpy of viscous flow. Similar results have been obtained by the study of primary, secondary and tertiary aliphatic amines and carboxylic acids, as well.

In this paper we report of investigations aimed at the study of the association of various pentanol isomers in the pure state and in their mixtures with *n*-hexane. The viscosity coefficients (η) of pure alcohols at 20 °C, activation enthalpies of viscous flow (ΔH_v) and the mean degree of association calculated from ΔH_v (α) are summarized in Table I. Data concerning the dependence of the viscosity coefficient on the temperature for 2,2-dimethylpropane-(1)-ol are given in Table II.

Table I
Mean degree of association of pentanol isomers in liquid phase

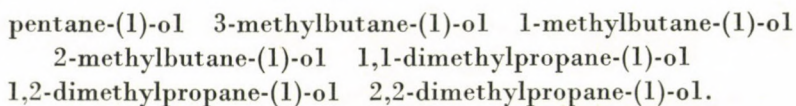
Component	Temperature range studied (°C)	ΔH_v [J/mol]	$10^4 \cdot \eta_{20^\circ}$ [Pas]	α
Pentane(1)-ol	20–60 [6]	$20\,371 \pm 628$	35.8	3.46
3-Methylbutane-(1)-ol	20–60 [7]	$22\,242 \pm 134$	43.6	3.82
1-Methylbutane-(1)-ol	20–60	$23\,405 \pm 167$	37.5	4.04
2-Methylbutane-(1)-ol	19.3–70 [6, 8]	$25\,854 \pm 293$	54.0	4.50
1,1-Dimethyl-propane-(1)-ol	20–60	$28\,562 \pm 753$	35.3	5.02
1,2-Dimethyl-propane-(1)-ol	18.2–76.5 [8]	$29\,349 \pm 1046$	52.6	5.16
2,2-Dimethyl-propane-(1)-ol	55–70	$30\,353 \pm 753$	solid	5.35

Table II
Viscosity coefficient of 2,2-dimethylpropane-(1)-ol as a function of the temperature

t (°C)	$10^4 \eta$ [Pas]
55.0	20.2
60.0	17.0
65.0	14.6
70.0	12.5

Upon evaluation of the results, it is immediately apparent that the activation enthalpy of viscous flow is significantly influenced by the molecular structure. From the most flexible *i*-pentanol to the more rigid 2,2-dimethylpropane-(1)-ol this value nearly doubles with the decrease in flexibility.

When applying the method worked out for the investigation of *n*-alcohols, this result means that the average degree of association of the alcohols studied increases in parallel to the increase of the activation enthalpy of viscous flow in the following sequence:



From these results it can be concluded that upon increasing the number of chain branchings in the molecule, the formation of cyclic alcohol multimers is suppressed due to steric hindrance. Instead, chain like multimers are formed, and in these the mean degree of association is greater than in cyclic multimers of 1-pentanol. The question may arise whether it is allowed to conclude from the activation enthalpy of viscous flow on the degree of association in cases when the flexibility of the molecule is considerably restricted by chain branchings. For it can also be supposed that the higher activation enthalpies found in the case of pentanol isomers containing chain branching can simply be explained by the more rigid molecular structure. In order to clarify this problem, we have also investigated the activation enthalpy of viscous flow in the mixtures of 1-methylbutane-(1)-ol and 1,1-dimethylpropane-(1)-ol with *n*-hexane. These results are presented in Tables III–VI and Figs 1–3.

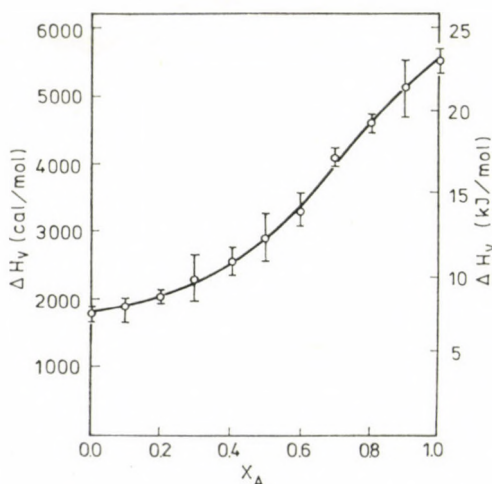


Fig. 1. Activation enthalpy of viscous flow for the 1-methylbutane-(1)-ol (A) — *n*-hexane (B) mixture as a function of the composition

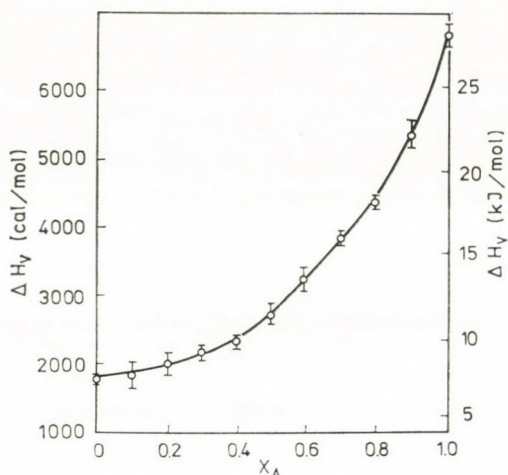


Fig. 2. Activation enthalpy of viscous flow for the 1-1-dimethylpropane-(1)-ol (A) — *n*-hexane (B) mixture as a function of the composition

It can be seen that the higher activation enthalpy of viscous flow is not a characteristic of the molecule, but can be attributed to the properties of the liquid structure, because the activation enthalpy of viscous flow for the mixtures of the two, significantly different alcohols with *n*-hexane becomes identical at an alcohol mole fraction of 0.88 (X_a). At lower alcohol concentra-

Table III

Viscosity coefficient of the mixture methylbutane-(1)-ol (A) — *n*-hexane (B) as a function of the temperature

x_A	$\eta \cdot 10^4$ [Pas]				
	T (K)				
	293	303	313	323	333
0.00	3.02	2.73	2.47	2.26	2.07
0.10	3.04	2.80	2.49	2.28	2.20
0.20	3.51	3.10	2.77	2.54	2.29
0.30	4.28	3.82	3.60	3.10	2.61
0.40	6.33	5.37	4.40	3.85	3.30
0.50	7.93	6.82	5.44	4.72	4.54
0.60	10.92	8.78	8.02	6.34	5.48
0.70	15.63	12.28	9.67	8.05	6.66
0.80	20.82	15.88	12.10	9.81	8.44
0.90	28.43	19.65	14.84	11.38	9.91
1.00	37.42	26.77	20.14	14.66	11.96

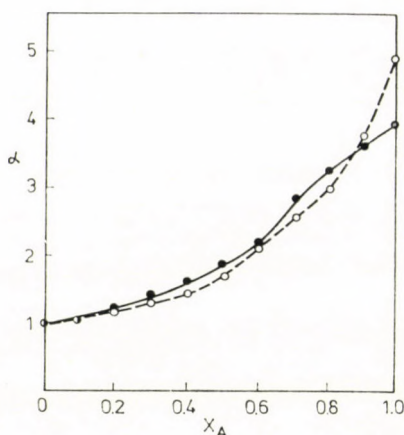


Fig. 3. Mean degree of association of the mixtures of 1-methylbutane-(1)-ol — *n*-hexane and 1,1-dimethylpropane-(1)-ol — *n*-hexane vs. the mole fraction of the alcohol

tions the shape of the curves is similar, and the starting slopes are also practically identical. If the higher activation enthalpy were characteristic for the molecule, then (considering that this quantity has been found to be non-additive for non-associated mixtures) this could not be possible. Thus, our statement that the mean degree of association can be also calculated from the activation enthalpy for the branched alcohols seems to be correct.

Table IV

Viscosity coefficient of the mixture 1,1-dimethylpropane-(1)-ol — *n*-hexane as a function of the temperature

x_A	$\eta \cdot 10^4$ [Pas]				
	$T(K)$				
	293	303	313	323	333
0.00	3.02	2.93	2.47	2.26	2.16
0.10	3.06	2.80	2.47	2.28	2.20
0.20	3.29	2.94	2.66	2.47	2.38
0.30	3.82	3.37	2.97	2.66	2.47
0.40	4.45	3.96	3.46	3.08	2.77
0.50	5.40	4.57	3.93	3.34	2.97
0.60	7.24	6.07	5.32	4.38	3.69
0.70	9.58	7.76	6.43	5.15	4.36
0.80	14.10	10.90	8.59	6.92	5.74
0.90	21.41	14.93	11.24	8.90	6.97
1.00	35.35	23.55	15.92	11.60	8.64

Table V

Activation enthalpy of viscous flow, mean degree of association for the mixture and the alcohol in the 1-methylbutane-(1)-ol — n-hexane mixture as a function of the composition

X_A	ΔH_v (J/mol)	α	α_A
0.00	7308	1.02	—
0.10	7655	1.08	—
0.20	8496	1.24	—
0.30	9631	1.47	—
0.40	10.765	1.67	—
0.50	12.067	1.92	—
0.60	13.774	2.24	12.92
0.70	17.236	2.90	15.61
0.80	19.391	3.30	7.76
0.90	21.564	3.71	5.31
1.00	23.351	4.04	4.04

Hence our results can be summarized in that the association degree of pentanols increases with the increasing number of branchings and the decrease in the flexibility of the molecule. A reason for this may be that the branching chains suppress the formation of cyclic multimers but do not hinder the formation of chain-like multimers with higher degree of association. As a result, for the structure of pentanol isomers with more branchings the presence of great amounts of chain-like multimers is characteristic.

Table VI

Activation enthalpy of viscous flow, mean degree of association for the mixture and the alcohol in 1,1-dimethylpropane-(1)-ol — n-hexane mixture as a function of the composition

X_A	ΔH_v [J/mol]	α	α_A
0.00	7308	1.02	—
0.10	7701	1.22	—
0.20	8400	1.22	—
0.30	9015	1.43	—
0.40	9739	1.48	5.29
0.50	11.309	1.77	7.70
0.60	13.511	2.19	10.60
0.70	16.035	2.67	9.39
0.80	18.245	3.08	6.42
0.90	22.376	3.86	5.66
1.00	28.562	5.02	5.02

REFERENCES

- [1] RACZY, L., CONSTANT, E., LEBRUN, A.: J. Chem. Phys., **64**, 1180 (1967)
- [2] BORDEWIJK, P., GRANSCH, F., BÖTTCHER, C. J.: J. Phys. Chem. **73**, 3255 (1969)
- [3] BELLAMY, L. J., PACE, R. J.: Spectrochim. Acta, **22**, 525 (1966)
- [4] MECKE, E.: Discuss. Faraday Soc., **9**, 161 (1950)
- [5] RATKOVICS, F., SALAMON, T., DOMONKOS, L.: Acta Chim. Acad. Sci. Hung., **83**, 71 (1974)
- [6] SALAMON, T., LISZI, J., RATKOVICS, F.: Acta Chim. Acad. Sci. Hung., **87**, 137 (1975)
- [7] RAZNEVIC, K.: Hőtechnikai táblázatok, Műszaki Könyvkiadó, Budapest, Zágráb 1964
- [8] THOMAS, L. H., MEATYARD, R.: J. Chem. Soc. I, **1963**, 1986

Ferenc RATKOVICS }
Tamás SALAMON } H-8200 Veszprém, P.O. Box 28.

IDEAL GAS THERMODYNAMIC PROPERTIES FOR $\text{CH}_3\text{O}\cdot$ AND $\cdot\text{CH}_2\text{OH}$ RADICALS

A. BURCAT* and S. KUDCHADKER¹

(Department of Chemical Engineering Louisiana State University, Baton Rouge, Louisiana,
¹Thermodynamic Research Center, Texas A & M University, College Station,
Texas)

Received May 8, 1978

In revised form August 16, 1978

Accepted for publication August 28, 1978

The thermodynamic properties of $\text{CH}_3\text{O}\cdot$ and $\cdot\text{CH}_2\text{OH}$ are calculated from assigned vibrations of methanol. The values are compared with former calculations done following different methods.

Introduction

The science of combustion has an interest in the thermodynamic properties of fuels and radicals of those fuels in order to enable the kinetic calculations of the combustion processes.

In this study we will present the ideal gas thermodynamic functions of two such radicals involved with methanol and methane combustion. Methanol serves recently as a target for extensive investigation as a possible future fuel [1]. Two of its most important degradation radicals are CH_3O and CH_2OH . The thermodynamic properties of both are little known. It is intended here to provide values that can be used in conjunction with the JANAT [7], or API Project 44 tables, for thermodynamic and kinetic calculations.

Calculations

The thermodynamic properties of CH_3O and CH_2OH were calculated following a proposal by FÖRGETEG and BÉRCES [2] to use the vibrational frequencies of methanol and omit the frequencies of OH for CH_3O and of CH_3 for CH_2OH . The proper methanol vibrations were taken from SHIMANOUCHI [3] and are listed in Table I. The calculations were done with PAC2, the last version of GORDON and McBRIDE's [4] thermodynamic programs, by the rigid rotator harmonic oscillator (RRHO) method. The thermodynamic values are presented in Tables II and III for CH_3O and CH_2OH respectively. For the CH_2OH radical the RRHO calculation is corrected for the internal rotation as explained below.

*Permanent address: Department of Aeronautical Engineering, Technion – Israel Institute of Technology, Haifa, Israel. To whom correspondence should be addressed.

In Tables II and III the H_T° column is the absolute enthalpy value expressed in the engineering practice by assuming $H_{298}^\circ = \Delta H_{f298}^\circ$ thus

$$H_T^\circ = \Delta H_{f298}^\circ + (H_T^\circ - H_{298}^\circ)$$

This allows for immediate usage by engineers and easy calculation of the $H_T - H_{298}$ values.

Table I
Selected values of physical and chemical molecular constants

SHIMANOUCHI's [3] Vibration assignment	ν CH ₃ OH	CH ₃ O	CH ₂ OH
OH stretch	1 3681	—	(1) 3681
CH ₃ a-stretch	2 3000	(1) 3000	—
CH ₃ s-stretch	3 2844	(2) 2844	(2) 2844
CH ₃ d-deform	4 1477	(3) 1477	—
CH ₃ s-deform	5 1455	(4) 1455	(3) 1455
OH bend	6 1345	—	(4) 1345
CH ₃ rock	7 1060	(5) 1060	(5) 1060
CO stretch	8 1033	(6) 1033	(6) 1119
CH ₃ d-stretch	9 2960	(7) 2960	(7) 2960
CH ₃ d-deform	10 1477	(8) 1477	—
CH ₃ rock	11 1165	(9) 1165	(8) 1165
ΔH_{f298}° kcal (ref [5])		+3.9	—4.0
$I_a \times 10^{39}$ g cm ²	0.6578	0.511	0.4041
$I_b \times 10^{39}$ g cm ²	3.4004	3.83	3.0848
$I_c \times 10^{39}$ g cm ²	3.5306	3.83	3.1518
$I_r \times 10^{40}$ g cm ²	0.993	—	0.79
Potential barrier parameters			
V_2 kcal	—	—	2.0
V_3 kcal	1.06706	—	—
V_6 kcal	—0.00149	—	—
B cm ⁻¹	28.182	—	35.4411
σ	3	3	1
Ground State			
Statistical Weight	1	2	2

Table II
Ideal Gas Thermodynamic Properties of CH₃O
 Formula Weight, 31.034.

T °K	C_p° cal/mole °K	$H_T^\circ - H_0^\circ$ cal/mole	S_T° cal/mole °K	$-(G_T^\circ - H_0^\circ)$ cal/mole	H_T° cal/mole	$(\Delta H_T^\circ)_f$ cal/mole	Log K_f
0	—	0	—	0	1468.8	5794.3	—
100	7.9490	794.9	45.6909	3774.2	2263.7	5089.7	—13.7018
200	8.1193	1594.0	51.2248	8650.9	3062.9	4558.4	—8.3434
298.15	9.0867	2431.2	54.6174	13853.0	3900.0	3900.0	—6.8048
300	9.1127	2448.0	54.6737	13954.1	3916.8	3886.8	—6.7869
400	10.7314	3437.6	57.5094	19566.2	4906.4	3233.9	—6.1339
500	12.4425	4596.9	60.0893	25447.7	6065.8	2660.3	—5.8102
600	14.0152	5921.3	62.4996	31578.4	7390.1	2179.1	—5.6332
700	15.4045	7393.8	64.7667	37942.9	8862.7	1784.7	—5.5304
800	16.6193	8996.4	66.9048	44527.5	10465.2	1470.2	—5.4666
900	17.6780	10712.5	68.9249	51319.9	12181.3	1224.3	—5.4256
1000	18.5983	12527.4	70.8362	58308.8	13996.2	1042.7	—5.3981
1100	19.3970	14428.1	72.6471	65483.8	15896.9	911.9	—5.3786
1200	20.0896	16403.2	74.3653	72835.2	17872.1	826.1	—5.3645
1300	20.6903	18442.9	75.9976	80354.0	19911.8	772.3	—5.3531
1400	21.2119	20538.7	77.5505	88032.0	22007.5	749.0	—5.3443
1500	21.6657	22683.1	79.0298	95861.6	24151.9	744.9	—5.3367
1600	22.0616	24869.9	80.4410	103835.7	26338.7	756.2	—5.3294
1700	22.4079	27093.7	81.7891	111947.7	28562.6	784.6	—5.3235
1800	22.7119	29350.0	83.0787	120191.6	30818.9	821.9	—5.3176
1900	22.9797	31634.9	84.3140	128561.7	33103.8	868.2	—5.3124
2000	23.2163	33944.9	85.4988	137052.7	35413.8	920.8	—5.3072
2100	23.4261	36277.3	86.6367	145659.9	37746.1	977.6	—5.3024
2200	23.6129	38629.4	87.7309	154378.6	40098.2	1034.8	—5.2974
2300	23.7796	40999.2	88.7843	163204.7	42468.0	1096.0	—5.2930
2400	23.9290	43384.7	89.7995	172134.1	44853.6	1155.1	—5.2887
2500	24.0632	45784.5	90.7792	181163.3	47253.3	1212.3	—5.2839
2600	24.1842	48197.0	91.7253	190288.9	49665.8	1269.8	—5.2801
2700	24.2935	50620.9	92.6402	199507.4	52089.8	1324.3	—5.2759
2800	24.3927	53055.3	93.5255	208815.9	54524.2	1376.7	—5.2719
2900	24.4828	55499.2	94.3830	218211.4	56968.0	1425.5	—5.2685
3000	24.5650	57951.6	95.2144	227691.6	59420.5	1470.5	—5.2646

Table II (contd.)

T °K	C_p° cal/mole °K	$H_T^\circ - H_0^\circ$ cal/mole	S_T° cal/mole °K	$-(G_T^\circ - H_T^\circ)$ cal/mole	H_T° cal/mole	$(\Delta H_T^\circ)_f$ cal/mole	Log K_f
3100	24.6400	60411.9	96.0211	237253.6	61880.8	1514.3	-5.2611
3200	24.7087	62879.4	96.8046	246895.1	64348.3	1551.8	-5.2577
3300	24.7717	65353.5	97.5658	256613.7	66822.3	1584.3	-5.2544
3400	24.8298	67833.6	98.3062	266407.5	69302.4	1613.5	-5.2513
3500	24.8832	70319.2	99.0268	276274.4	71788.1	1635.6	-5.2483
3600	24.9326	72810.1	99.7284	286212.2	74278.9	1654.0	-5.2454
3700	24.9783	75305.7	100.4122	296219.5	76774.5	1664.1	-5.2428
3800	25.0206	77805.6	101.0789	306294.2	79274.5	1671.5	-5.2404
3900	25.0600	80309.7	101.7294	316434.7	81778.5	1670.6	-5.2379
4000	25.0965	82817.6	102.3643	326639.6	84286.4	1664.4	-5.2355
4100	25.1306	85328.9	102.9844	336907.0	86797.7	1652.3	-5.2332
4200	25.1624	87843.6	103.5904	347235.9	89312.4	1633.0	-5.2313
4300	25.1921	90361.3	104.1828	357624.7	91830.2	1607.2	-5.2292
4400	25.2199	92881.9	104.7623	368072.1	94350.8	1575.8	-5.2272
4500	25.2460	95405.2	105.3293	378576.7	96874.1	1536.6	-5.2253
4600	25.2704	97931.1	105.8845	389137.6	99399.9	1492.5	-5.2241
4700	25.2934	100459.3	106.4282	399753.2	101928.1	1440.7	-5.2227
4800	25.3150	102989.7	106.9610	410422.8	104458.6	1383.1	-5.2213
4900	25.3353	105522.2	107.4832	421145.2	106991.1	1319.6	-5.2200
5000	25.3545	108056.7	107.9952	431919.2	109525.6	1249.1	-5.2187
5100	25.3726	110593.1	108.4975	442743.9	112062.0	1170.5	-5.2177
5200	25.3897	113131.2	108.9903	453618.2	114600.1	1087.6	-5.2166
5300	25.4059	115671.1	109.4741	464541.7	117139.9	997.9	-5.2162
5400	25.4212	118212.4	109.9491	475512.9	119681.2	900.8	-5.2152
5500	25.4357	120755.2	110.4158	486531.1	122224.1	797.7	-5.2147
5600	25.4494	123299.5	110.8742	497595.7	124768.4	687.4	-5.2140
5700	25.4625	125845.1	111.3247	508705.7	127313.9	571.0	-5.2135
5800	25.4749	128392.0	111.7677	519860.6	129860.9	447.4	-5.2132
5900	25.4867	130940.1	112.2032	531058.9	132408.9	318.0	-5.2131
6000	25.4980	133489.3	112.6317	542300.7	134958.2	182.7	-5.2127

Table III
Ideal Gas Thermodynamic Properties of CH₂OH
 Formula Weight, 31.034.

T°K	C_p° cal/mole °K	$H_T^\circ - H_0^\circ$ cal/mole	S_T° cal/mole °K	$-(C_p^\circ - H_T^\circ)$ cal/mole	H_T° cal/mole	$(\Delta H_T^\circ)_f$ cal/mole	Log K_f
0	—	0	—	0	-6744.7	-2419.2	—
100	8.62	811.8	47.44	3932.2	-5932.9	-3106.9	4.5941
200	9.78	1737.4	53.81	9024.6	-5007.3	-3511.8	1.0403
298.15	10.80	2744.7	57.89	14515.2	-4000.0	-4000.0	-0.2988
300	10.83	2764.7	57.96	14623.3	-3980.0	-4010.0	-0.3159
400	12.15	3912.5	61.25	20587.5	-2832.2	-4504.7	-1.0882
500	13.48	5195.2	64.11	26859.8	-1549.5	-4955.0	-1.6029
600	14.68	6604.6	66.67	33397.4	-140.1	-5351.1	-1.9789
700	15.73	8126.5	69.02	40187.5	1381.8	-5696.2	-2.2652
800	16.66	9747.3	71.18	47196.7	3002.6	-5992.4	-2.4936
900	17.49	11456.0	73.19	54414.9	4711.3	-6245.7	-2.6795
1000	18.23	13242.7	75.07	61827.3	6498.0	-6455.5	-2.8341
1100	18.88	15098.7	75.84	69425.2	8354.0	-6631.0	-2.9636
1200	19.46	17016.3	78.51	77195.6	10271.6	-6774.4	-3.0745
1300	19.98	18988.6	80.09	85128.4	12243.9	-6895.6	-3.1697
1400	20.43	21009.4	81.59	93216.6	14264.7	-6993.8	-3.2528
1500	20.84	23073.3	83.01	101441.6	16328.6	-7078.4	-3.3270
1600	21.20	25004.1	84.36	109971.8	18259.4	-7323.1	-3.3693
1700	21.53	27312.1	85.66	118309.9	20567.4	-7210.6	-3.4497
1800	21.82	29479.9	86.90	126940.0	22735.2	-7261.8	-3.5010
1900	22.08	31675.2	88.09	135695.7	24930.5	-7305.0	-3.5470
2000	22.33	33895.8	89.23	144564.1	27151.1	-7341.9	-3.5888
2100	22.55	36139.4	90.32	153532.5	29394.7	-7373.8	-3.6283
2200	22.75	38404.2	91.37	162609.6	31659.5	-7404.0	-3.6638
2300	22.93	40688.3	92.39	171808.6	33943.6	-7428.4	-3.6950
2400	23.11	42990.4	93.37	181097.4	36245.7	-7452.8	-3.7248
2500	23.27	45309.8	94.32	190490.4	38564.6	-7476.4	-3.7505
2600	23.42	47643.8	95.23	199954.0	40899.1	-7496.9	-3.7772
2700	23.56	49992.7	96.12	209531.0	43248.0	-7517.5	-3.7997
2800	23.69	52355.5	96.98	219188.3	45610.8	-7536.7	-3.8212
2900	23.82	54731.0	97.81	228917.8	47986.3	-7556.2	-3.8426
3000	23.93	57118.7	98.62	238741.2	50374.0	-7576.0	-3.8613

Table III (contd.)

$T^{\circ}\text{K}$	C_p° cal/mole $^{\circ}\text{K}$	$H_T^{\circ} - H_0^{\circ}$ cal/mole	S_T° cal/mole $^{\circ}\text{K}$	$-(G_T^{\circ} - H_T^{\circ})$ cal/mole	H_T° cal/mole	$(\Delta H_T^{\circ})_f$ cal/mole	Log K_f
3100	24.05	59517.8	99.41	248653.1	52773.1	-7593.4	-3.8784
3200	24.15	61927.8	100.17	258615.9	55183.1	-7613.4	-3.8963
3300	24.25	64348.1	100.92	268687.7	57603.4	-7634.6	-3.9108
3400	24.35	66778.1	101.64	278797.6	60033.4	-7655.5	-3.9269
3500	24.44	69217.4	102.35	289007.4	62472.8	-7679.7	-3.9403
3600	24.52	71665.6	103.04	299278.1	64920.9	-7704.1	-3.9536
3700	24.60	74122.1	103.71	309604.7	67377.4	-7733.1	-3.9670
3800	24.68	76586.4	104.37	320019.1	69841.7	-7761.2	-3.9786
3900	24.76	79058.4	105.01	330480.1	72313.7	-7794.2	-3.9905
4000	24.83	81537.9	105.64	341021.8	74743.2	-7828.7	-4.0010
4100	24.90	84024.1	106.25	351600.4	77279.4	-7866.0	-4.0121
4200	24.96	86517.1	106.85	362252.6	79772.4	-7907.1	-4.0225
4300	25.02	89016.2	107.44	372975.3	82271.6	-7951.4	-4.0316
4400	25.08	91521.4	108.02	383766.3	84776.7	-7998.2	-4.0397
4500	25.14	94032.4	108.58	394577.2	87287.7	-8049.7	-4.0493
4600	25.19	96549.1	109.14	405494.7	89804.4	-8103.1	-4.0567
4700	25.24	99070.7	109.68	416424.9	92326.1	-8161.4	-4.0655
4800	25.29	101597.6	110.21	427410.0	94852.9	-8222.5	-4.0739
4900	25.34	104129.3	110.73	438447.4	97384.6	-8286.8	-4.0819
5000	25.38	106665.6	111.24	449534.0	99920.9	-8355.5	-4.0897
5100	25.43	109206.3	111.75	460718.4	102461.6	-8429.8	-4.0954
5200	25.47	111751.3	112.24	471896.3	105006.6	-8505.8	-4.1032
5300	25.51	114300.6	112.73	483168.2	107555.9	-8586.1	-4.1094
5400	25.55	116853.6	113.20	494426.2	110108.9	-8671.6	-4.1173
5500	25.59	119410.3	113.67	505774.2	112665.6	-8760.8	-4.1236
5600	25.62	121970.7	114.13	517156.9	115226.1	-8854.9	-4.1300
5700	25.65	124534.6	114.59	528627.9	117789.9	-8953.1	-4.1347
5800	25.69	127101.8	115.03	540071.8	120357.1	-9056.3	-4.1421
5900	25.72	129672.2	115.47	551600.4	122927.6	-9163.4	-4.1479
6000	25.75	132245.6	115.91	563214.2	125500.9	-9274.5	-4.1517

The CH_3O Radical

The moments of inertia for CH_3O were taken from FÖRGETEG and BÉRCES [2]. ΔH_{298}° for CH_3O was taken from BENSON's estimates [5]. The methanol vibrations used for CH_3O are listed in Table I.

The thermodynamic properties of the CH_3O radical were calculated by ENGLEMAN [6] from the JANAF [7] values for CH_3F , taking $\Delta H_{f298}^\circ = 3.0$ kcal. The calculated values of ENGLEMAN [6], FÖRGETEG [2] and BENSON and O'NEAL [5b] are compared with the present ones in Table IV. The differences can be attributed to the difference in the method. Being a more elegant method of calculation than that performed by ENGLEMAN it suggests that both are basically correct.

A second existing calculation of the CH_3O radical thermodynamic functions was presented by WALDMAN, WILSON and MALONEY [8]. This table was calculated according to the MECHREBLIAN, CRAWFORD and PARR Methods [9], and it is completely wrong. Besides having logical mistakes ($H^\circ - H_{298}^\circ$ is not 0.0 at 298°), it differs by as much as 5 to 25% from the values presented here and by ENGLEMAN [6].

The CH_2OH Radical

For the CH_2OH radical, the RRHO thermodynamic functions had to be corrected for the internal rotation. In order to account for this effect only 8 of the methanol vibrations could be used for the RRHO calculations, thus a reassignment of the vibrations was needed. BERNARDI *et al.* [10] have recently calculated energies and geometrical parameters for this radical. They have found interatomic distances and angles similar to those of methanol thus justifying the approach of using the methanol vibrations. They have found however that the C—O bond is shorter and the stretching force constant bigger: 6.72 and 5.73 mdyn/Å for CH_2OH and CH_3OH respectively. Therefore we have changed this vibration ($\nu = 8$ in methanol) accordingly ($\nu \propto \sqrt{k}$) from 1033 to 1119. From the rest of the methanol vibrations, those assigned purely to the CH_3 group were discarded while those related to the CH_2 group were retained (see Table I).

To find the correct moments of inertia and I_r we used BERNARDI's [10] values. To the RRHO calculation the internal rotation contributions were added using for rotational barrier $V_2 = 2$ kcal as given by BERNARDI. The internal rotation is complex involving two full rotations with two inversions. Therefore it was better represented by V_2 rather than the V_3 barrier used in methanol. The internal rotation contributions were calculated with LANNE's computer program [11]. ΔH_{f298}° was taken from BENSON's estimates [5b].

The thermodynamic properties for CH_2OH were previously calculated by BAHN [12] probably from graphical interpolation of similar homologues. However BAHN has chosen a completely unreasonable ΔH_{f298}° value of -14.0 kcal and low values of C_p at high temperatures. Also his compilation suffers from oscillations which make them unacceptable as a whole. Comparison with values of BENSON and O'NEAL [5b] and FÖRGETEG *et al.* [2] are presented in Table IV.

Table IV

Comparisons of the Calculated Thermodynamic Properties with Different Sources

 CH_2OH

	CH_2OH Pure RRHO	BENSON & O'NEAL	FÖRGETEG & BÉRCES	CH_2OH Internal rotation*	This calculation
C_{p298}	8.93	10.2	—	1.831	10.8
S_{298}	56.13	58.6	55.21	1.759	57.89

 CH_3O

	ENGLEMAN	BENSON & O'NEAL	FÖRGETEG & BÉRCES	This calculation
S_{298}	53.25	54.3	54.75	54.63
C_{p300}	—	9.1	—	9.09
C_{p500}	12.256	12.6	—	12.44
C_{p800}	—	16.8	—	16.62
C_{p1000}	18.44	18.9	—	18.60
$(H_T - H_{298})_{500}$	2131.	—	—	2166.
$(H_T - H_{298})_{1000}$	9975.	—	—	10096.
$(H_T - H_{298})_{2000}$	31275.	—	—	31514.
$(H_T - H_{298})_{4000}$	80056.	—	—	80386.

* See text.

The older vibrational assignment by IVASH, LI and PITZER [13] for methanol was also used for comparison purposes. The values for the CH_3O and CH_2OH radicals with these vibrations were within 0.25% of the values presented here, within the precision of the present calculation.

The present calculation is precise to within 1% of the values presented. Roughly it should be stated that for CH_3O table the last two digits in each column are insignificant and they are presented here so that smoother curve fitting polynomials may be generated.

A set of polynomial fits calculated with GORDON and MCBRIDE's program [4] are presented here for the range 300–5000 K. The polynomials are compatible with NASA's highly popular programs of shock and detonation properties [14], and kinetic calculations [15].

The polynomials given in Table V can generate the following thermodynamic properties

$$\frac{C_p}{R} = A_1 + A_2 T + A_3 T^2 + A_4 T^3 + A_5 T^4$$

$$\frac{H}{RT} = A_1 + \frac{A_2}{2} T + \frac{A_3}{3} T^2 + \frac{A_4}{4} T^3 + \frac{A_5}{5} T^4 + \frac{A_6}{6}$$

$$\frac{S}{R} = A_1 \ln T + A_2 T + \frac{A_3}{2} T^2 + \frac{A_4}{3} T^3 + \frac{A_5}{4} T^4 + A_7$$

$$\frac{G}{RT} = A_1(1 - \ln T) - \frac{A_2}{2} T - \frac{A_3}{6} T^2 - \frac{A_4}{12} T^3 - \frac{A_5}{20} T^4 + \frac{A_6}{T} - A_7$$

The first seven coefficients belong to the 1000–5000 K range, and the last seven coefficients to the 300–1000 K range.

Table V

Polynomial Coefficients of Thermodynamic Functions for CH₃O and CH₂OH in the range 300–5000°K to be used with NASA Programs

CH ₃ O G	U06/78C	1H	3O	1	0G	300.000	5000.000
0.37707996E+01	0.78714974E-02	0.26563839E-05	0.39444314E-09	0.21126164E-13			
0.12783252E+03	0.29295750E+01	0.21062040E+01	0.72165951E-02	0.53384720E-05			
-0.73776363E-08	0.20756105E-11	0.97860107E+03	0.13152177E+02				

CH₃O. curvefitting analysis

Function	Maximum error %	Average error %	
		at 300–1000° range %	at 1000–5000° range %
C_p/R	0.51% at 400° 0.87% at 1300°	0.2	0.43
$(H-H_0)/RT$	0.14% at 300° 0.35% at 1700°	0.04	0.15
S/R	0.018% at 300° 0.089% at 1800°	0.006	0.046
$(G-H_0)/RT$	0.004% at 300° 0.044% at 2600°	0.0015	0.033

H3CO G	H	3C	1O	1	0G	300.000	5000.000
0.47235041E+01	0.61020441E-02	-0.19132094E-05	0.27607427E-09	-0.14548367E-13			
-0.39329165E+04	-0.85243821E-01	0.33368406E+01	0.65881237E-02	0.29979328E-05			
-0.58719714E-08	0.21229572E-11	-0.33168267E+04	0.80668154E+01				

CH₃OH curvefitting analysis

Function	Maximum error %	Average error %	
		at 300—1000° range %	at 1000—5000° range %
C_p/R	0.26% at 400° 0.66% at 1300°	0.12	0.32
$(H-H_0)/RT$	0.05% at 500° 0.44% at 1600°	0.027	0.12
S/R	0.017% at 300° 0.07% at 1900°	0.008	0.033
$(G-H_0)/RT$	0.016% at 300° 0.16% at 1600°	0.009	0.037

*

Alexander BURCAT thanks Mr. D. L. MILLER for computational help.

REFERENCES

- [1] HAGEN, D. L.: Soc. Automotive Eng. Passenger Car Meeting, Paper 770792, September 1977
- [2] FÖRGETEG, S., BÉRCES, T.: Acta Chim. Acad. Sci. Hung., **51**, 205 (1967)
- [3] SHIMANOUCHI, T.: NSRDS—NBS, 39 (1972)
- [4] MCBRIDE, B., GORDON, S.: NASA TN D-4097 (1967) with corrections and adaptations
- [5] (a) BENSON, S. W.: "Thermochemical Kinetics", 2nd Edition, Wiley 1976
 (b) BENSON, S. W., O'NEAL, H. E.: NSRDS—NBS, 21 (1970), p. 588
 (c) O'NEAL, H. E., BENSON, S. W.: Thermochemistry of Free Radicals, Chapter 17 in "Free Radicals" edited by KOCHI, 1973
- [6] ENGLEMAN, V. S.: Environmental Protection Technology Series — EPA 600/2-76—003 (1976)
- [7] JANAF Thermodynamic Tables, NSRDS, NBS-37 (1972), D. R. STULL and H. PROFFET, ed.
- [8] WALDMAN, E. H., WILSON, R. P., MALONEY, K. L.: Report EPA 650/2-74-045, (1974)
- [9] REID, R. C., SHERWOOD, T. K.: "The Properties of Gases and Liquids Their Estimation and Correlation", McGraw-Hill, 2nd Edition (1966)
- [10] BERNARDI, F. *et al.*: J. Am. Chem. Soc., **98**, 469 (1976)
- [11] LEWIS, J. D., MALLOY, T. B., CHAO, T. H., LAMME, J.: J. Molec. Struct., **12**, 427 (1972)
- [12] BAHN, S.: Approximate Thermochemical Tables, NASA CR-2178 (1973)
- [13] IVASH, E. V., LI, J. C., PITZER, K. S.: J. Chem. Phys., **23**, 1814 (1955)
- [14] GORDON, S., MCBRIDE, B. S.: NASA SP-273 (1971)
- [15] BITTKER, D. A., SCULLIN, V. S.: NASA TN D-6586 (1972)

Alexander BURCAT Dept. of Aeronautical Engineering, Technion—Israel
Inst. of Tech., Haifa, Israel

Shanti KUDCHADKER Thermodynamic Res. Center, Texas A & M Univ.,
College Station, Texas 77843, USA

IR SPECTRA OF HYDROCARBONS CHEMISORBED ON TRANSITION METALS, I

THE INFRARED CELL AND CHEMISORPTION OF ETHYLENE ON
Ni/SiO₂ CATALYST

T. SZILÁGYI, A. SÁRKÁNY, J. MINK and P. TÉTÉNYI

(*Institute of Isotopes of the Hungarian Academy of Sciences, Budapest*)

Received March 14, 1978

Accepted for publication September 4, 1978

The present paper gives the description of an infrared cell used for recording the IR spectra of adsorbed ethylene. Ethylene was chemisorbed on silica-supported Ni at 55 and 150 °C. The chemisorbed species appear to be attached to the surface by σ bonds exclusively. The spectral features of chemisorbed C₂H₄ are discussed in terms of the reactivity of the surface species towards hydrogen.

Introduction

The investigation of the infrared spectra of adsorbed molecules has proved to be a valuable method in the study of chemisorption processes. Its increasing popularity may be attributed to the fact that the scientist can observe the surface of the catalyst directly, while the classical catalytic measurements (surface coverage, heat of adsorption, thermodesorption, etc.) offer information on the level of the system only, rather than on a molecular level. However, the amount and nature of information provided by infrared spectroscopy seems to be somewhat limited due to experimental difficulties. One of these problems is the energetics of the infrared spectrometer. Either the signal to noise ratio and the intensity of infrared bands are very low in the case of unsupported adsorbents (usually evaporated metal films) due to their small surface area and, consequently, the small number of light-absorbing molecules in the infrared beam, or, if metal catalysts finely dispersed on the surface of silica or alumina powders are used, a large proportion of the beam energy is lost owing to strong absorption by the support and the long-wave region the spectrum (below 1300 cm⁻¹) becomes unusable. For these reasons, the use of a spectrometer of high sensitivity is necessary. Another difficulty is the poor reproducibility of measurements. This problem may arise from difficulties of sample preparation or contamination of the surface of the adsorbent during experiments. As all the manipulations of preparation and also the infrared measurement must be performed in the same adsorption cell specially designed for the given purpose, the success strongly depends on the design of the cell and sample handling.

In the present publication a new type of adsorption cell for infrared measurements is described and some spectra of adsorbed ethylene on Ni/SiO_2 are reported. This study was performed as the first stage of a more detailed infrared investigation of hydrocarbons adsorbed on transition metals.

Apparatus and experimental methods

The adsorption cell (see Fig. 1) was made of Pyrex glass except for the part containing the heating wire, which was Rasotherm glass. An outer vessel, roughly of spherical shape, equipped with KBr windows had two side-tubes, for gas inlet and vacuum connection (the windows were sealed into the glass by Rhodorsil vacuum leak sealant produced by Rhone-Poulenc, Inc.). Its upper side forms a wide neck 65 mm in diameter and can be closed by a cap. Vacuum-tight sealing was achieved by a Viton O-ring situated between suitably worked and polished glass profiles. Glass-covered tungsten rods as electrical leads were soldered into the cap and the sample heater to the inner ends of rods at the height of the infrared beam. The heater is a double-walled cylinder with Kanthal heating wire between the glass walls. The space between the walls was evacuated and filled up with hydrogen to ensure a better thermal conductivity and a more uniform temperature distribution. The sample pellet was placed in a stainless steel sample holder, which slips into the inner cylinder of the heater. For the thermocouple inlet, a glass tube of small diameter is introduced through the cap to the heater.

Most of the cells described in the literature [1] are designed so that the furnace section is far from the infrared beam, requiring movability of the sample. Our arrangement has the following advantages:

- a) The fixed sample holder ensures the reproducible positioning of the sample;
- b) The design is simpler as the cell has no moving parts;
- c) It is possible to record spectra at elevated temperatures and also to monitor the reduction process.

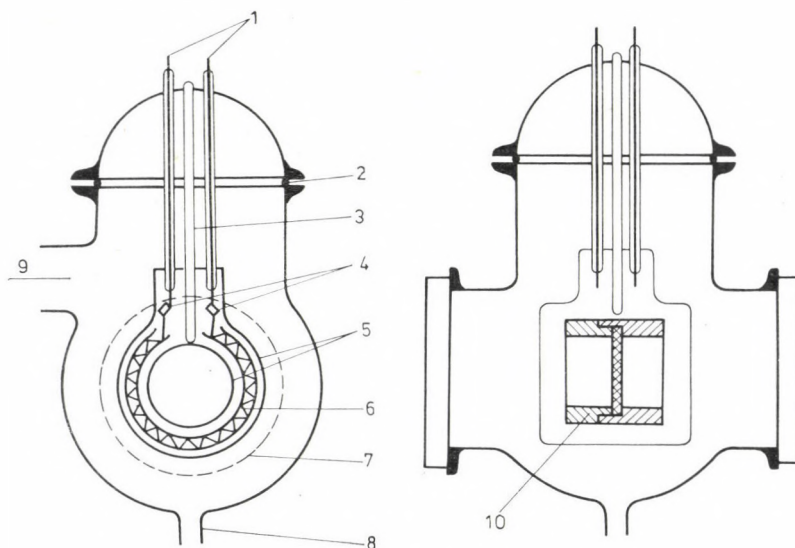


Fig. 1. Infrared cell. 1 — glass covered W rods; 2 — Viton O-ring; 3 — thermocouple; 4 — spot welding between Kanthal and tungsten; 5 — Rasotherm glass internal furnace; 6 — heating wire between mica foils; 7 — KBr windows; 8 — gas inlet; 9 — connection to the vacuum system; 10 — stainless steel sample holder positioned in the furnace

The cell was attached to a conventional all-glass vacuum system equipped with a mercury diffusion pump and a rotary pump. The ultimate pressure in the cell was 5×10^{-5} Torr measured by an ionization gauge. The gas pressure during adsorption was measured by an absolute manometer (Datametries Electronic Manometer). The cell was protected from contamination by liquid N_2 cooled traps. Greaseless Viton O-ring taps and connections were used everywhere in the system.

Samples were prepared by the usual impregnation technique. Cabosil HS5 grade silica was wetted with a solution of $Ni(NO_3)_2 \times 6H_2O$. The slurry was dried to ca. 30 wt. water content and pressed ($1-1.5$ tons/cm²) into self-supporting discs 25 mm in diameter, which weighed 60–100 mg. The disc was placed into the cell and it was reduced *in situ* at 400–450 °C for 6 hours in an atmospheric stream of hydrogen purified in a deoxo unit filled with BASF 11 contact. The water formed was trapped by molecular sieve previously evacuated at 300 °C and then cooled to liquid N_2 temperature.

After reduction the sample was allowed to cool in H_2 to the temperature of ethylene chemisorption. Hydrogen was then removed (residual pressure 10^{-5} Torr) and the background spectrum was recorded and stored. Then ethylene at a pressure of 30 Torr was admitted into the cell. After 5 min contact, the cell was evacuated for ca. 20 min in order to remove physically adsorbed hydrocarbons.

The infrared spectra were recorded at room temperature by means of a DIGILAB FTS-14 interferometer equipped with its own NOVA-1200 minicomputer. The computer has a 128K disc as mass storage memory for storing recorded spectra. Spectra were measured by collecting and signal-averaging 200 scans at an original resolution of 2 cm⁻¹ which was decreased by a factor of two in consequence of the subsequent smoothing procedure. This resulted in spectra with a reasonably high signal to noise ratio. All runs were performed in the single-beam mode and the computed spectra were stored on the disc.

The chemisorbed amount of ethylene was measured gravimetrically by means of a Sartorius electrobalance (Type 4102). (For further details, see Refs 2 and 17.) The removability of the chemisorbed species was investigated in hydrogen using static as well as flow conditions. The hydrodesorbed products were collected in a trap, filled with a small amount of silica gel, at liquid nitrogen temperature. Their composition was checked by gas chromatography. For chemisorption measurements a 0.274 g sample was used.

Results and discussion

1. Spectra of chemisorbed ethylene on an initially hydrogen-covered nickel

The spectrum of chemisorbed ethylene measured at 55 °C on a hydrogen-covered Ni/SiO₂ sample is shown in Fig. 2a. The recorded spectrum, similar to those reported by ERKELENS [3] and PRIMET [4], shows bands at 2963, 2932 and 2884 cm⁻¹. A weak shoulder appears also at ca. 2850 cm⁻¹. The three main bands have almost equal intensities. The band at 2884 cm⁻¹ is assigned to the CH_2 symmetric stretching vibration in associatively adsorbed ethylene with a configuration $NiCH_2-CH_2Ni$ [7, 18]. In addition to this band, part of the band at 2932 cm⁻¹ also belongs to this adsorbed species [8]. The relative intensity of the band at 2884 cm⁻¹ strongly depends on the experimental conditions, especially on the temperature of adsorption (see e.g. [3, 5–8, 18–20]).

The initial presence of a band at 2963 cm⁻¹ assigned to CH_3 groups indicates the presence of partially hydrogenated species with the possible configuration Ni_3C-CH_3 , Ni_2CH-CH_3 or $NiCH_2CH_3$.

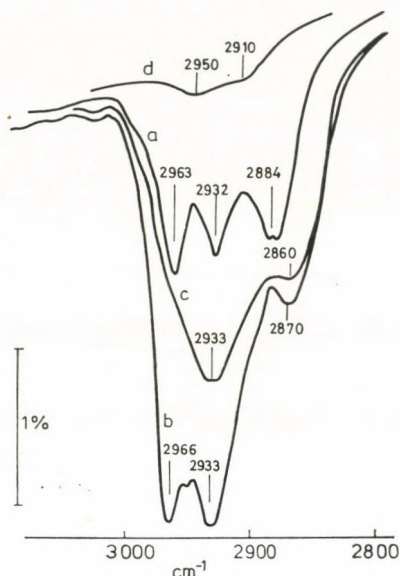


Fig. 2. a) Infrared spectrum of C_2H_4 on Ni/SiO_2 chemisorbed at 55 °C after evacuation of 30 Torr ethylene; b) After addition of hydrogen in the gas phase (25 Torr) at 35 °C; c) After hydrogenation at 180 °C for 5 min in a stream of atmospheric H_2 ; d) After 20 min of hydrogenation at 180 °C (Between c and d the sample was cooled rapidly to room temperature)

2. Spectra of adsorbed ethylene after hydrogenation

Hydrogen admission (Fig. 2b) — 25 Torr H_2 at 35 °C — increases the intensity of the 2963 and 2932 cm^{-1} bands by a factor of 2.4. Simultaneously, a broad band develops at 2870 cm^{-1} , whereas the 2884 cm^{-1} band is missing. At this temperature considerable part of the chemisorbed hydrocarbon can be removed after hydrogen admission (Table I). At 55 °C the desorbed product consists mainly of ethane. Only trace amount of CH_4 (0.1 mol%) and *n*-butane (ca. 0.15 mol%) can be detected. The observed spectrum (Fig. 2b) does not change very much during prolonged hydrogenation at room temperature. This observation is in agreement with chemisorption results, *i.e.* the chemisorbed species remaining on the surface can be only slowly removed with hydrogen (*c.f.* columns 3 and 4 in Table I).

The two strongest bands (Fig. 2b) at 2966 and 2933 cm^{-1} belong to the CH_3 and CH_2 groups, respectively, in the adsorbed layer [9].

The ratio of the absorbance of methyl and methylene bands (at 2966 and 2933 cm^{-1} , respectively) obtained for the hydrogenated species at 35 °C is about 1:1, which may be attributed to surface ethyl groups [4]. In this case, the medium broad band centered near 2873 cm^{-1} is assigned to the low frequency components of the CH stretching vibrations of methylene and methyl groups, *i.e.* to the symmetric CH_2 and CH_3 stretching modes. This interpreta-

Table I

Ethylene chemisorption on a nickel-silica catalyst (10 wt. % Ni/Cab—O—Sil HS 5)

Temp. (°C)	Amount of ethylene chemisorbed ($\mu\text{g mNi}^{-1}$) ^e			
	After evacuation (10 min, 10^{-6} Torr)	After hydrodesorption ($P_{\text{H}_2} = 30$ Torr, 10 min)	After 10 min H_2 flow ($P_{\text{H}_2} = 735$ Torr)	After hydrogenation for 15 min at 180 °C ($P_{\text{H}_2} = 735$ Torr)
25 ^a	220 ^d	120	110	0
25	210	160	160	15
55 ^a	247	165	143	27
58	255 ^b	215	205	55
145	605 ^c	—	—	233

a — H_2 evacuated at the temperature of chemisorption, otherwise at 350 °Cb — chemisorption is time-dependent, measurement after 20 min. Rate of carbon deposit formation $R = 1.1 \mu\text{g min}^{-1}$ c — chemisorption is time-dependent, measurement after 7.5 min ($R = 8 \mu\text{g min}^{-1}$)d — amount of CO chemisorbed irreversibly at room temperature is 365–380 μg , consequently, the surface coverage for C_2H_4 is $\Theta = 0.4\text{--}0.42$ e — all measurements were made in vacuum (10^{-6} Torr) in order to avoid boyancy effects

tion would contradict, however, the apparent large stability of the chemisorbed species.

We should take into account another interpretation as well. The spectrum of the chemisorbed species formed after hydrogenation of ethylene (Fig. 2b) on nickel at 35 °C is practically identical with the spectrum obtained for chemisorbed 1-butene at 20 °C [10]. Based on this spectroscopic similarity, it may well be suggested that in part the surface species have dimerized to C_4 species [11, 12]. In this case the C_4 surface species should have multiple carbon-metal bonds, which could give a CH_3/CH_2 intensity ratio similar to that in surface ethyl groups. [15]

We do not at this time wish to comment in detail on which interpretation is more reliable.

3. Spectra of adsorbed ethylene at high temperatures

Heating the sample at 180 °C for 5 min in an atmospheric stream of hydrogen decreases the intensity of the 2963 cm^{-1} band; it appears as a weak shoulder on a strong and broad band centered at 2933 cm^{-1} , which has a fairly prominent broad shoulder near 2860 cm^{-1} as shown in Fig. 2c. Desorption in hydrogen reveals the predominant formation of CH_4 . The "hydro-desorbed" product collected in the first 10 min contains 83 mol % CH_4 and 17 mol % C_2H_6 . The larger part of C_2H_6 is formed probably during the temperature rise to 180 °C, since further hydrogenation results in the formation of CH_4 exclusively.

The broad band at 2933 cm^{-1} is an interesting feature of the spectrum in Fig. 2c, which requires comment. Features of similar intensity and similar profile have not been reported in earlier works. The broad absorption band at 2933 cm^{-1} probably belongs to hydrogen-deficient species either in C_2 surface species of type $\text{Ni}_2\text{CH}-\text{CHNi}_2$ or more probably in C_4 or longer species with multiple carbon-metal bonds. Desorption of methane under the above conditions shows that C—C bonds are being broken. The absence of the 2966 cm^{-1} band might be peculiar to Ni, since on this metal C—C bond dissociation takes place exclusively at the end of the carbon chain [13, 14].

After a 20 min hydrogenation at 180°C , an extremely weak spectrum is obtained as shown in Fig. 2d. Overlapping broad bands around 2950 cm^{-1} and 2910 cm^{-1} are measured. In this spectrum the noise level is rather high for these weak bands.

4. Adsorption on a bare surface at high temperatures

The high temperature infrared spectra of a hydrogen-covered surface show some interesting features. For this reason we investigated the infrared spectrum of chemisorbed ethylene at 150°C in the absence of hydrogen. In the case of adsorption at 150°C (see Fig. 3a), a spectrum similar in intensity to Fig. 2a is observed, although, according to the gravimetric results, the surface coverage is considerably larger than at 55°C . A relatively sharp band appears at 2965 cm^{-1} and, beside this, a broad band at 2925 cm^{-1} and a weaker one at 2870 cm^{-1} can be discerned.

The spectrum in Fig. 3a seems to fall between those observed on a hydrogen-covered surface at 55°C (Fig. 2a) and on heated samples at 180°C after hydrogenation (Fig. 2c). This suggests that the species in the adsorbed layer formed on a bare surface could be characterized by $-\text{CH}_3$, CH_2 and $-\text{CH}$ groups, but, in accordance with the absence of the band near 2885 cm^{-1} , associatively adsorbed ethylene is not dominant. The hydrogen-deficient species $-\text{CHNi}_2$ or $>\text{CHNi}$ seem to be proved by the results on tritium exchange [16], since the tritium content of the ethane formed is greater than that expected on the basis of hydrogen addition.

Hydrogenation of this sample at 180°C for 7 min causes a greater increase in the intensity of the 2925 cm^{-1} band than in that of the 2965 cm^{-1} and the shoulder at about 2870 cm^{-1} persists (Fig. 3b). The chemisorbed species leaving the surface at 180°C in a stream of H_2 consists of 94.8 mol% methane and 5.2 mol% ethane.

Addition of hydrogen leads to the "hydrogenated" spectrum shown in Fig. 3b. The strongly overlapping spectrum profile makes it difficult to assign the spectrum in detail. The surface species may occur as an intermediate in the formation of various hydrogenated species.

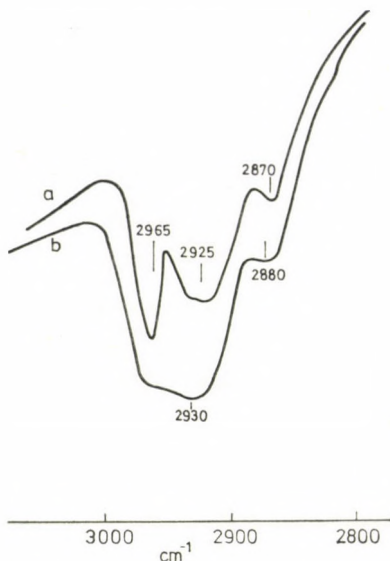


Fig. 3.a) Infrared spectra of C_2H_4 chemisorbed at $150^\circ C$ after evacuation of 30 Torr C_2H_4 ; b) After hydrogenation at $170^\circ C$ for 7 min ($p_{H_2} = 30$ Torr)

The CH stretching frequencies and assignments of the infrared bands are summarized in Table II.

It can be seen that the presence of the CH_3 groups can well be distinguished from the other surface species. It is more difficult, however, to distinguish between the CH_2 groups and the hydrogen-deficient CH surface species. A very characteristic band of the CH_2 symmetric stretching vibration of associatively adsorbed ethylene appears in the narrow range near 2880 cm^{-1} .

Table II

Experimental CH stretching frequencies and assignments of infrared bands of adsorbed ethylene

A	B	C	D	E	Assignment	Estimated surface species
2968 s	2966 vs	2965 sh	2965 s	2965 sh	$\nu_{as}CH_3$	$NiC-CH_3$
2932 s	2933 vs	2930 vvs, b	2925 s, b	2930 vvs, b	$\nu_{as}CH_2$, νCH	$NiCH_2^*$, $Ni-CH$
2885 s ^a					$\nu_s CH_2$	$NiCH_2-CH_2Ni$
	2873 m, s	2870 m, sh	2870 m	2875 sh	$\nu_s CH_3$, $\nu_s CH_2$, νCH	$Ni-C-CH_3$, $NiCH_2^*$, $Ni-CH$

A) Ethylene adsorbed on a hydrogen-covered nickel surface at $55^\circ C$; B) Hydrogen admitted at $35^\circ C$; C) Heated sample at $180^\circ C$ for 5 min in an atmospheric stream of hydrogen; D) Ethylene chemisorbed at $150^\circ C$ in the absence of hydrogen; E) Hydrogen admitted at $180^\circ C$;

a) Usually a doublet band centered at 2884 cm^{-1}

Notes: s — strong; m — medium; b — broad; sh — shoulder; v — very; ν_{as} — asymmetric CH stretching; ν_s — symmetric CH stretching

Our statements connected with the structure of the surface species formed under different conditions can be summarized as follows:

1. At low temperatures (under 60 °C) on an initially hydrogen-covered surface the presence of associative ethylene can be detected, but the appearance of the CH₃ species and the hydrogen-deficient ones is also considerable. On a bare surface the hydrogen-deficient species are more dominant, the associative ethylene being practically absent.

2. In the presence of hydrogen at 35 °C the intensities of bands both of the CH₃ and the CH₂ groups increase, which can be explained by the formation of C—H bonds at the expense of C—Ni ones. The change in the intensity ratio of CH₃ and CH₂ groups permits to suggest formation of C₄ — having multiple C—Ni bonds — or larger polymer species.

3. At higher temperatures (150—180 °C) the number of C—Ni bonds increases, because mainly bands characteristic of the CH and CH₂ groups are dominant.

Thus, upon increasing the temperature, the relative quantity of the CH₃ groups decreases.

4. Due to self-hydrogenation, the structure of surface species depends more strongly on the temperature of chemisorption than on the presence of hydrogen on the surface.

To identify more convincingly the estimated surface species, further work is necessary. Detailed results will be presented in a subsequent part of this series.

REFERENCES

- [1] LITTLE, L. H.: *Infrared Spectra of Adsorbed Species*, Academic Press, London 1966
- [2] SÁRKÁNY, A., TÉTÉNYI, P.: *Acta Chim. Acad. Sci. Hung.* (In press)
- [3] ERKELENS, J., LIEFKENS, T. H. J.: *J. Catal.*, **8**, 36 (1967)
- [4] PRIMET, M., SHEPPARD, N.: *J. Catal.*, **41**, 258 (1976)
- [5] PRENTICE, J. D., LESIUNAS, A., SHEPPARD, N.: *J. C. S. Chem. Comm.*, **76** (1976)
- [6] SHEPPARD, N., WARD, J. W.: *J. Catal.*, **15**, 50 (1969)
- [7] EISCHENS, R. P., PLISKIN, W. A.: *Adv. Catal.*, **10**, 2 (1958)
- [8] MORROW, B. A., SHEPPARD, N.: *J. Phys. Chem.*, **70**, 2406 (1966)
- [9] MORROW, B. A., SHEPPARD, N.: *Proc. Roy. Soc.*, **A311**, 391 (1969)
- [10] MORROW, B. A., SHEPPARD, N.: *Proc. Roy. Soc.*, **A311**, 415 (1969)
- [11] BELLAMY, L. J.: *Infrared spectra of complex molecules*, 2nd ed. Methuen, London 1958
- [12] KOKES, R. J., BARTEK, J. P.: *J. Catal.*, **12**, 72 (1968)
- [13] GUCZI, L., SÁRKÁNY, A., TÉTÉNYI, P.: *Proc. 5th Congr. Catalysis*, Vol. **2**, p. 1122
- [14] SÁRKÁNY, A., GUCZI, L., TÉTÉNYI, P.: *Acta Chim. Acad. Sci. Hung.*, **84**, 245 (1975)
- [15] MORROW, B. A.: *Can. J. Chem.*, **48**, 2192 (1972)
- [16] GUCZI, L., TÉTÉNYI, P.: *Z. Phys. Chem.*, **237**, 356 (1968)
- [17] SÁRKÁNY, A., MATUSEK, K., TÉTÉNYI, P.: *J. C. S. Faraday I*, **73**, 1699 (1977)
- [18] PLISKIN, W. A., EISCHENS, R. P.: *J. Chem. Phys.*, **24**, 482 (1956)
- [19] PERI, J. B.: *Disc. Faraday Soc.*, **41**, 121 (1966)
- [20] SHEPPARD, N.: *Disc. Faraday Soc.*, **41**, 177 (1966)

Tibor SZILÁGYI
Antal SÁRKÁNY
János MINK
Pál TÉTÉNYI

H-1525 Budapest, P.O. Box 77.

MODELLING OF THE THERMAL DECOMPOSITION OF HYDROCARBONS

V. ILLÉS and O. SZALAI

(Hungarian Oil and Gas Research Institute, Veszprém)

Received May 25, 1978

Accepted for publication September 4, 1978

On the basis of a generalized decomposition mechanism for normal paraffin hydrocarbons, a kinetic model of thermal decomposition is developed. For the construction of this model, it is supposed that hydrogen atoms, methyl and ethyl radicals participate in the hydrogen abstraction reactions and that decomposition is the only reaction of radicals larger than ethyl. Among secondary reactions, the inhibitory reactions of the propylene produced and the recombinations of methyl and ethyl radicals as chain termination steps are taken into account.

Pyrolysis experiments carried out with *n*-butane serve as examples for the actual application of this kinetic model. Experimental data satisfactorily agree in the entire conversions range with data derived from the theoretical model.

The kinetic law for the thermal decomposition reveals that the kinetic order of the term which describes the decomposition of the parent substance continuously decreases from 3/2 towards unity when the temperature is raised.

Introduction

Attempts at the construction of theoretical models of thermal decompositions have been made since decades on the basis of free-radical mechanisms consisting of the primary reaction steps and the kinetic parameters of these reactions. The first to develop such a model for the decomposition of hydrocarbons, e.g. ethane, were RICE and HERZFELD [1] in 1934.

It was in the 1960's that semi-empirical models based upon stoichiometric overall reaction equations (molecular reactions) and upon kinetic data found for these were applied. Among such efforts the best known are those of MYERS and WATSON [2], ANDREWS and POLLOCK [3], SNOW and SHUTT [4], SHAH [5], and FEIGIN *et al.* [6], which refer to the pyrolysis of light hydrocarbons, viz. to that of ethane and propane. A model also based upon the above principle was developed in recent years for the thermal decomposition of ethane, propane, butane and the mixtures of these, by FROMENT *et al.* [7, 8], further, for the description of the decomposition of propane, by ALBRIGHT *et al.* [9].

In the 1970's again the theoretical models based on primary reaction steps were discussed and then also the most important secondary reactions between chain-propagating radicals and olefinic products were considered. In this field the studies by ALLARA and EDELSON [10], SERES *et al.* [11],

ZALOTAI *et al.* [12] and the unpublished work of BENEDEK and VÁCI should be mentioned concerning models for the thermal decomposition process of hydrocarbon gases *via* multistep primary reaction systems. Based upon these models a description, in semi-quantitative agreement with empirical data for the range of low or medium conversions, has been the result. In past years, FEIGIN *et al.* [13, 14] developed a model, based upon a similar principle, for *n*-paraffins of greater molecular weight and for the mixture of these: this model, when applied to hydrocarbon gases, led to semi-quantitative agreement with the experimental data.

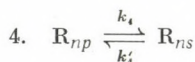
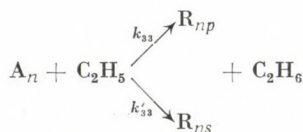
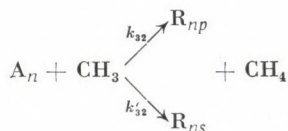
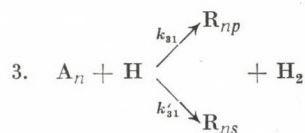
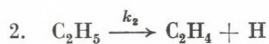
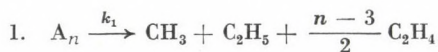
In this paper we discuss a theoretical kinetic model worked out on the basis of a general decomposition mechanism for normal paraffin hydrocarbons. The practical application of this model is exemplified by pyrolysis tests [15, 16] with *n*-butane.

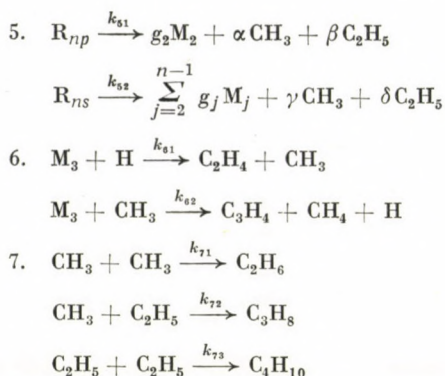
Kinetics model based on a decomposition mechanism

In order to facilitate the kinetic description, we write the decomposition of *n*-paraffin hydrocarbons in a generalized form that conforms to the reaction scheme shown in Table I.

Table I

Mechanism of the decomposition of normal paraffin hydrocarbons





where A_n is the parent paraffin hydrocarbon; n is the number of carbon atoms in molecule A_n , in primary radicals R_{np} , and in secondary radicals R_{ns} . M_3 is the symbol for C_3H_6 , the inhibitory olefin. α is zero, β is unity if n is an even number, $\gamma + \delta = 1$. $M_2, M_3 \dots M_j$ symbolize olefins; g_j is the weighting factor for the olefin yield.

According to the free-radical chain-theory propounded by RICE and HERZFELD [1], and KOSSIAKOFF and RICE [17], the most important reaction steps of the primary decomposition of paraffin hydrocarbons are the thermal dissociation of hydrocarbon molecules (reaction 1, in the reaction scheme), abstraction of hydrogen from parent molecules by chain-propagating radicals (reaction 3), isomerization of the alkyl radicals formed (reaction 4), and their decomposition (reactions 5), further the recombination of the radicals (reactions 7).

Besides the primary reaction steps just mentioned also the two most important inhibition processes (reactions 6) of the propylene (M_3) produced are included in the reaction scheme. According to the literature [19], when paraffin hydrocarbons are subjected to pyrolysis, propylene and *iso*-butylene exert the strongest inhibition effect, which consists of addition of propagating radicals H and CH_3 , to olefins. However, practically no *iso*-butylene is formed when normal paraffin hydrocarbons decompose.

In order to simplify the derivation, the radical decomposition reaction $R_{3s} \rightarrow M_3 + H$, characteristic of the pyrolysis of propane exclusively is left out of the generalized scheme thus making it valid for *n*-butane, and normal paraffins with more carbon atoms. The description of the decompositions of radicals in such a generalized form allows easier handling of the reaction system and is suitable, at the same time, for the description of the actual process of the decomposition of a given hydrocarbon, after the numerical values are inserted for factors α , β , γ , δ , and for g_j , the weighting factor for the olefin yields. The scheme can be extended to branched-chain hydrocarbons provided the hydrogen abstraction steps are complemented with the formation of the tertiary radicals R_{nt} , and the series of the decomposition of radicals is complemented with the decomposition reactions of these radicals, further

provided that also the inhibitory effect of *iso*-butylene, besides that of propylene, is taken into account. This is disregarded here because the treatment and the interpretation already of the kinetics according to the scheme given involves serious difficulties. A further simplification consists in that secondary reactions of olefins larger than propylene are not included into the scheme though also slight amounts of 1-butene and of heavier α -olefins are produced in the primary decomposition of *n*-pentane and heavier *n*-paraffins. However, the thermal decomposition of these is rapidly accomplished through the fission if the C—C bond in β -position weakened by the double bond.

It should be mentioned that the kinetic treatment of the reaction scheme generalized for normal hydrocarbons has been expounded by FEIGIN *et al.* [13]. In the hydrogen abstraction process these authors envisage the formation of radicals of the types R_1 , R_2 , and R_3 and, according to the definition given by them, radical R_1 decomposes *via* the cleavage of a hydrogen atom, R_2 *via* that of a methyl, and R_3 *via* that of an ethyl radical. (R_1 , R_2 and R_3 may belong equally to the group either of primary or of secondary radicals.) With regard to the diverse activation energies of the decomposition of the radicals just mentioned this grouping is quite logical but cannot be carried farther than up to pentane because secondary alkyl radicals produced by hydrogen abstractions decompose through the simultaneous cleavage of methyl and ethyl radicals. (FEIGIN *et al.* have applied the model actually to ethane, propane and *n*-butane, further to mixtures of these with propylene.) On the other hand, a grouping of radicals according to their having primary or secondary character is advantageous from a point of view focused on hydrogen abstraction reactions also because thus the activation energies differ by about 2 kcal mol⁻¹ (in the case of primary *vs.* tertiary radicals this difference is about 4 kcal mol⁻¹).

A further departure of our reaction scheme from the one given by FEIGIN *et al.* consists in that the latter did not reckon with the participation of ethyl radicals in the hydrogen abstraction reactions, thus did not reckon with the formation of ethane. It would seem that this simplification is not justifiable, even under the conditions (high temperature) of pyrolysis because of the significant amount of ethane produced.

Application of a steady-state treatment leads to the following balance equations for the concentrations of the radical to be written on the bases of the generalized reaction scheme proposed.

For hydrogen atom:

$$k_2[C_2H_5] + k_{62}[CH_3][M_3] - (k_{31} + k'_{31})[H][A_n] - k_{61}[H][M_3] = 0 \quad (1)$$

For CH_3 radicals:

$$k_1[A_n] + k_{51}\alpha[R_{np}] + k_{52}\gamma[R_{ns}] + k_{61}[H][M_3] - (k_{32} + k'_{32})[CH_3][A_n] - k_{62}[CH_3][M_3] - 2k_{71}[CH_3]^2 - k_{72}[CH_3][C_2H_5] = 0 \quad (2)$$

For C_2H_5 radicals:

$$k_1[A_n] + k_{51}\beta[R_{np}] + k_{52}\delta[R_{ns}] - k_2[C_2H_5] - (k_{33} + k'_{33})[C_2H_5][A_n] - k_{72}[CH_3][C_2H_5] - 2k_{73}[C_2H_5]^2 = 0. \quad (3)$$

For R_{np} radicals:

$$k_{31}[H][A_n] + k_{32}[CH_3][A_n] + k_{33}[C_2H_5][A_n] - k_{51}[R_{np}] = 0. \quad (4)$$

For R_{ns} radicals:

$$k'_{31}[H][A_n] + k'_{32}[CH_3][A_n] + k'_{33}[C_2H_5][A_n] - k_{52}[R_{ns}] = 0. \quad (5)$$

Further, the concentrations of chain-carrying radicals H , CH_3 , C_2H_5 will be expressed in terms of kinetic constants and concentrations of the initial substance A_n and that of propylene M_3 which exerts the inhibitory effect. For this purpose R_{np} and R_{ns} will be substituted from Eqs (4) and (5) into Eqs (1), (2) and (3). The first two equations thus obtained are then added together, this sum is then added to the corresponding Eq. (3) (with R_{np} and R_{ns} substituted), and the equality $k_{72} = 2\sqrt{k_{71}k_{73}}$ is utilized to give the equation

$$[CH_3] + \sqrt{\frac{k_{73}}{k_{71}}} [C_2H_5] = \sqrt{\frac{k_1[A_n]}{k_{71}}}. \quad (6)$$

Following this, the corresponding Eq. (3) is subtracted from the corresponding Eq. (2) (with R_{np} and R_{ns} substituted) and by utilizing Eq. (6) a new linear equation results. Thus the set of linear equations (6), (7) and (8) becomes available to replace with it the set of equations (1), (2) and (3), containing squared terms, *viz.*

$$[C_2H_5]k_2 + [CH_3]k_{62}[M_3] - [H] [(k_{31} + k'_{31})[A_n] + k_{61}[M_3]] = 0 \quad (7)$$

$$\begin{aligned} [C_2H_5] [k_2 + k_{33}(\alpha - \beta + 1)[A_n] + k'_{33}(\gamma - \delta + 1)[A_n]] - [CH_3] [k_{62}[M_3] + \\ + k_{32}(\beta - \alpha + 1)[A_n] + k'_{32}(\delta - \gamma + 1)[A_n] + 4\sqrt{k_1k_{71}}[A_n]] + \\ + [H] [k_{31}(\alpha - \beta)[A_n] + k'_{31}(\gamma - \delta)[A_n] + k_{61}[M_3]] = -2k_1[A_n] \end{aligned} \quad (8)$$

The coefficients can be written as

$$a_1 = \sqrt{\frac{k_{73}}{k_{71}}} \quad a_2 = k_2$$

$$\begin{aligned}
a_3 &= k_2 + k_{33}(\alpha - \beta + 1)[A_n] + k'_{33}(\gamma - \delta + 1)[A_n] \\
b_2 &= k_{62}[M_3] \\
b_3 &= -[k_{62}[M_3] + k_{32}(\beta - \alpha + 1)[A_n] + k'_{32}(\delta - \gamma + 1)[A_n] + \\
&\quad + 4\sqrt{k_1 k_{71}[A_n]}] \\
C_2 &= -(k_{31} + k'_{31})[A_n] - k_{61}[M_3] \\
C_3 &= k_{31}(\alpha - \beta)[A_n] + k'_{31}(\gamma - \delta)[A_n] + k_{61}[M_3] \\
d_1 &= \sqrt{\frac{k_1[A_n]}{k_{71}}} \quad d_3 = -2k_1[A_n].
\end{aligned}$$

With the new coefficients the set of linear equations (6), (7), and (8) will be

$$\begin{aligned}
[C_2H_5]a_1 + [CH_3] &= d_1 \\
[C_2H_5]a_2 + [CH_3]b_2 + [H]C_2 &= 0 \\
[C_2H_5]a_3 + [CH_3]b_3 + [H]C_3 &= d_3.
\end{aligned} \tag{9}$$

The solution of the set of equations (9) is the following

$$\begin{aligned}
[C_2H_5] &= \frac{-C_2d_3 - d_1(b_2C_3 - b_3C_2)}{a_2C_3 - a_3C_2 - a_1(b_2C_3 - b_3C_2)} \\
[CH_3] &= d_1 - a_1[C_2H_5] \\
[H] &= \frac{1}{C_2} [[C_2H_5](a_1b_2 - a_2) - b_2d_1].
\end{aligned} \tag{10}$$

Application of the kinetic model obtained on the basis of the decomposition mechanism to *n*-butane

Based on the general reaction scheme in Table I, and with the derivations and relationships applied to *n*-butane, and the numerical Runge—Kutta integration of the set of linear equations describing the change in time of the three components, calculations can be carried out concerning the change in time of the concentration of *n*-butane, ethylene and propylene involved in the secondary reaction, and concerning the changes of the yields of these as a function of the conversion. With these computations, the characteristics of the curves which represent the concentrations of the principal components and the yields, can be studied and also it can be examined whether the theoretically deduced model is appropriate to the experimental conditions obtaining here.

The program used computed the change in time of the concentrations of *n*-butane, ethylene and propylene, according to the following relationships

$$r_{A_n} = \frac{d[A_n]}{d\tau} = -k_1[A_n] - (k_{31} + k'_{31})[H][A_n] - (k_{32} + k'_{32})[CH_3][A_n] - (k_{33} + k'_{33})[C_2H_5][A_n] \quad (11)$$

$$\frac{d[M_2]}{d\tau} = \left(\frac{n-3}{2}\right) k_1[A_n] + k_2[C_2H_5] + g_2 k_{51}[R_{np}] + k_{61}[H][M_3] \quad (12)$$

$$\frac{d[M_3]}{d\tau} = g_3 k_{52}[R_{ns}] - k_{61}[H][M_3] - k_{62}[CH_3][M_3], \quad (13)$$

where

$$n = 4, g_2 = 1, g_3 = 1, \alpha = 0, \beta = 1, \gamma = 1, \delta = 0.$$

The kinetic parameters of the primary reactions referring to the pyrolysis of *n*-butane are collected in Table II.

R_{np} and R_{ns} , taken from Eqs (4) and (5), can be used for calculations in Eqs (12) and (13); in other respects the relationships (10), which refer to chain carrying radicals, are applicable. A type HP 9830 A computer was used.

The diagrams in Fig. 1 allow a comparison of conversion curves for *n*-butane as found at various temperatures with conversion curves computed on the basis of the kinetic model for the same temperatures. The pyrolysis of *n*-butane was carried out in a flow reactor under isothermal and isobaric

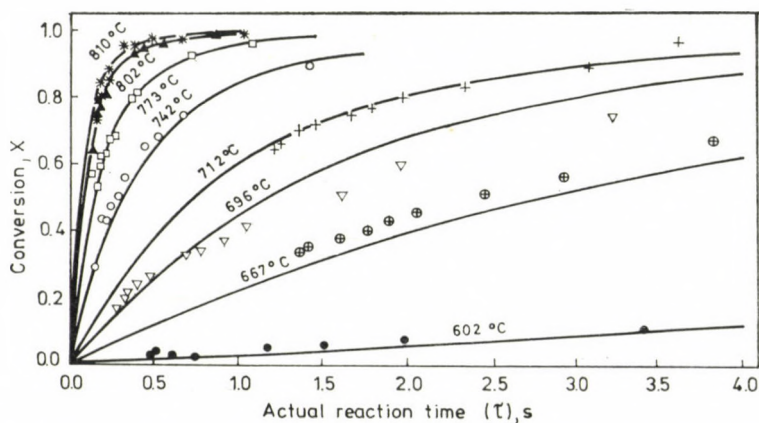


Fig. 1. Variation of the conversion as a function of the actual reaction time for the pyrolysis of *n*-butane
— curves calculated by means of the kinetic model

conditions at temperatures between 602 and 810 °C, and at a pressure of 1 atm without any diluent [15, 16]. As this Figure shows, the computed curves practically coincide with data found by experiment, with the exception of 667 and 696 °C, where empirical data lie above and below, respectively, the theoretical curve, *i.e.* are scattered in consequence of experimental errors. Thus the model given describes correctly the overall rate of decomposition of *n*-butane in the temperature and conversion range studied.

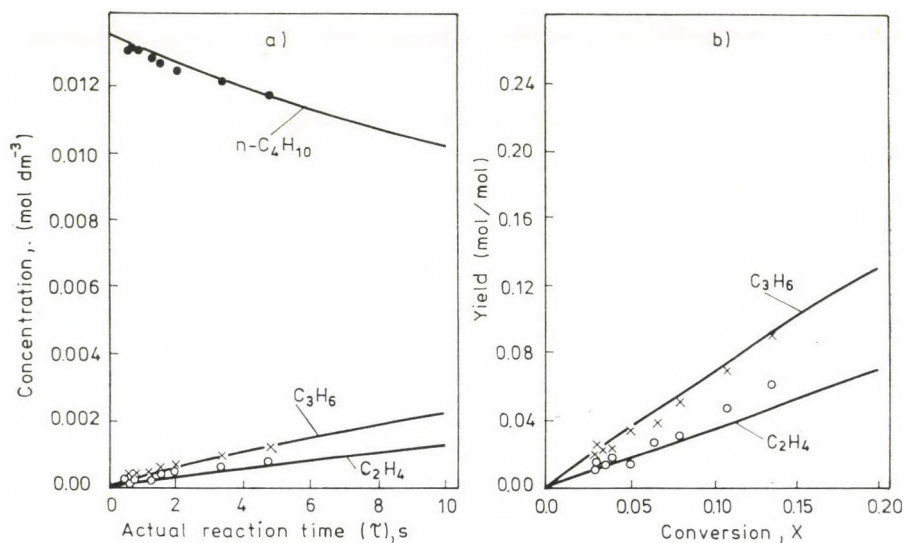


Fig. 2. Variation of the concentration of *n*-butane, ethylene and propylene as a function of the actual reaction time (a); variation of the yield of ethylene and propylene as a function of conversion (b) for the pyrolysis of *n*-butane, at 602 °C

Figures 2–5 show changes of concentration of *n*-butane, ethylene and propylene, found by experiment, and calculated from the model, as functions of the actual reaction times, and the curves representing the yields of ethylene and of propylene as a function of the conversion. An especially good agreement is to be seen for the experimental concentration *vs.* time curves with the corresponding theoretical data for *n*-butane; also in the cases of concentration and yield curves of ethylene and propylene this agreement is nearly quantitative. A slight systematic error is in evidence for ethylene: all the experimental values are higher than the calculated ones.

The concentration and yield curves for ethylene and propylene reveal characteristic differences. In the initial period of decomposition the concentration and the yield of propylene is greater than those of ethylene; however, as the decomposition proceeds, the concentration and yield of ethylene substan-

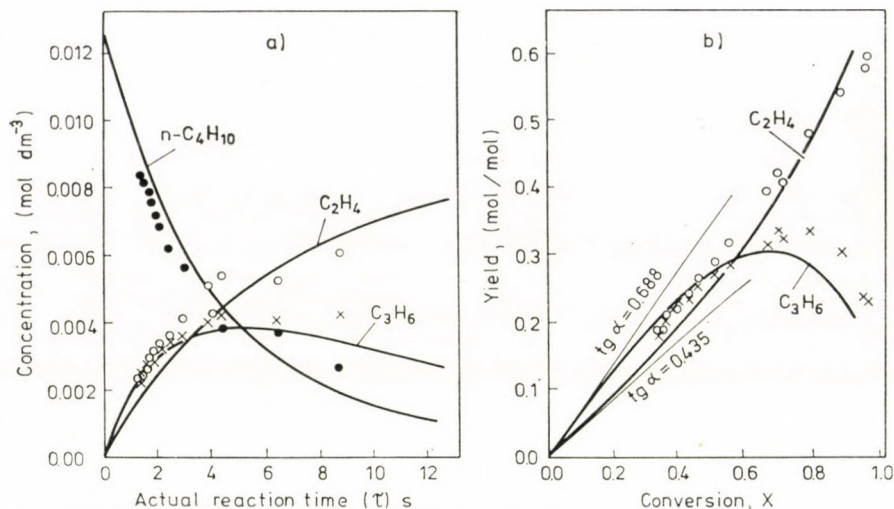


Fig. 3. Variation of the concentration of *n*-butane, ethylene and propylene as a function of the actual reaction time (a); variation of the yield of ethylene and propylene as a function of conversion (b) for the pyrolysis of *n*-butane at 667 °C
 — curves calculated by means of the kinetic model

tially exceed those of propylene. The concentration and yield curves of propylene show a maximum; the maximum of the concentration curve shifts to shorter reaction times as the temperature rises; the maximum of the yield curve appears in the conversion range from 0.7 to 0.8 practically regardless of the

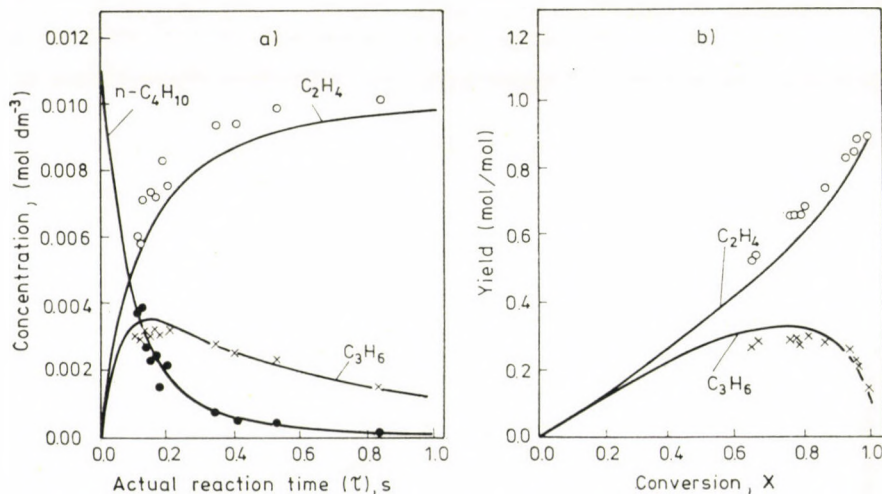


Fig. 4. Variation of the concentration of *n*-butane, ethylene and propylene as a function of the actual reaction time (a); variation of the yield of ethylene and propylene as a function of conversion (b) for the pyrolysis of *n*-butane at 742 °C
 — curves calculated by means of the kinetic model

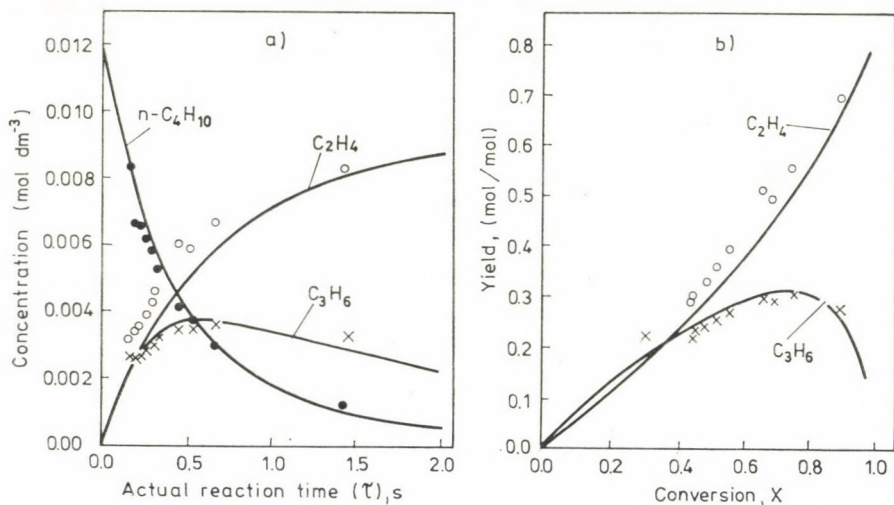


Fig. 5. Variation of the concentration of *n*-butane, ethylene and propylene as a function of the actual reaction time (a); variation of the yield of ethylene and propylene as a function of conversion (b) for the pyrolysis of *n*-butane at 802 °C
— curves calculated by means of the kinetic model

temperature. The secondary reactions explain the significant deviation of the concentration and yield curves for ethylene from those for propylene (the two target substances). The reaction $\text{C}_3\text{H}_6 + \text{H} \rightarrow \text{C}_2\text{H}_4 + \text{CH}_3$ is the most important among these secondary ones (cf. group 6 in the scheme of Table I); in it some of the propylene formed by primary decomposition of *n*-butane is converted into ethylene and methane. Due to this reaction, the relative amount of ethylene increases and that of propylene decreases, when the conversion becomes greater. This is very clearly shown in Fig. 3, where also the initial slopes of the yield curves are drawn. The ethylene yield curve deviates progressively upwards and the propylene yield curve downwards, from the respective initial slopes.

The calculated and found yield curves for ethylene (Fig. 6) and propylene (Fig. 7) are plotted against the conversion. The course of the curves, found and calculated, and the absolute values of yields are in good agreement for both of these compounds. A significant effect of temperature is put in evidence by the yield curves for ethylene; with propylene a similar effect, but in a lesser degree, is observable when the conversion is greater than 50%.

The production of ethyl radicals (reaction group 5 in the reaction scheme) in the reaction sequence of the primary decomposition of *n*-butane is the primary reason why the ethylene yields significantly increase with the temperature at a given level of conversion. According to reaction 2, ethyl radicals decompose to give ethylene and hydrogen atoms or are converted into ethane by hydrogen abstraction, according to reaction group 3. Since the activation energy (40 kcal

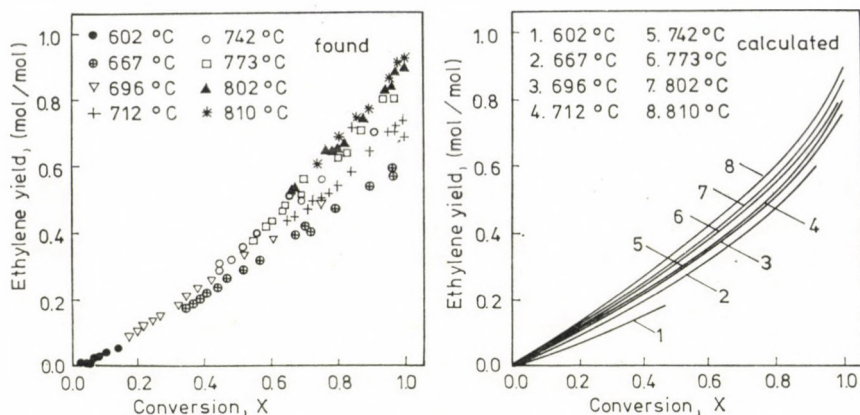


Fig. 6. Yield of ethylene (found and calculated) as a function of the conversion in the pyrolysis of *n*-butane at various temperatures

mol^{-1}) of the decomposition reactions of ethyl radicals is substantially greater the activation energies (10.4 and $12.6 \text{ kcal mol}^{-1}$) of hydrogen abstraction, higher temperatures increase the relative rate of decomposition and this in turn increases the yield of ethylene. Though to a far lesser degree, in the same sense are ethylene yields affected by the fact that the activation energy for H-abstraction from a primary carbon atom is greater by about 2 kcal mol^{-1} than that from a secondary one; thus the relative quantity of primary butyl radicals that decomposes with the formation of ethylene slightly increases when the temperature is raised.

With propylene, which is formed through the decomposition of secondary butyl radicals, consideration of this latter effect suggests a slight decrease of the yield when the temperature is raised. The yields found (Fig. 7) reflect this

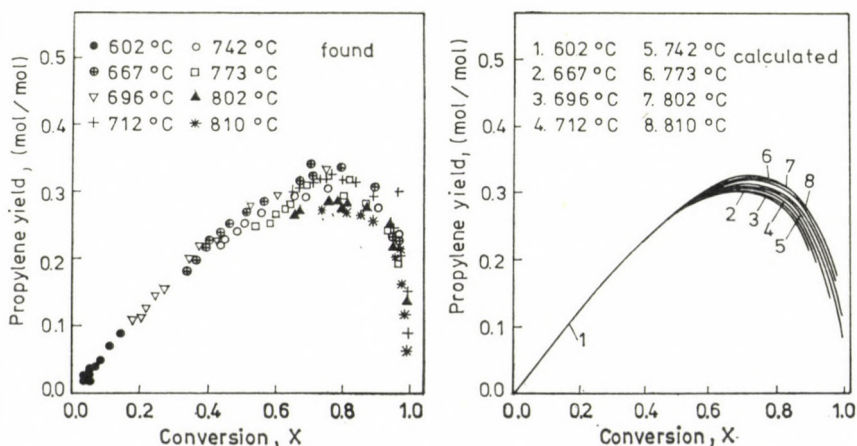


Fig. 7. Yields of propylene (found and calculated) as a function of conversion in the pyrolysis of *n*-butane at various temperatures

effect. In the case of calculated yield curves, the situation is the reverse: higher temperatures slightly enhance the propylene yields. This can be explained on the basis of the diverse activation energies of the primary reactions designed as the formation and the decomposition of propylene in the theoretical model. The reaction marked k_{52} , leading to the formation of propylene has an activation energy (according to Table II) of $31.9 \text{ kcal mol}^{-1}$, while the activation energies of processes k_{61} and k_{62} which describe the decomposition of propylene, are 2.9 and $7.4 \text{ kcal mol}^{-1}$, respectively.

The Figures shown permit the statement that the model developed on the basis of the simplified scheme of Table I, describes the experimental data even at high conversions with a satisfactory accuracy, provided that the kinetic parameters are appropriately selected from the literature.

With relationship (11) as a basis, we can study the effect of changes in the concentration of the parent hydrocarbon and that of rising temperature on the overall kinetic order of decomposition in the initial period, *viz.* when $[A_n^\circ] \approx 10^{-2} \text{ mol dm}^{-3}$, $[M_3] = 0$, and in the reaction affected by the propylene produced, *viz.* when $[A_n] = [M_3] \approx 3 \times 10^{-3}$.

The analysis of the overall kinetic relationship found for the rate of consumption of the initial A_n hydrocarbon suggests the following general statements.

Table II

Kinetic parameters of the primary reactions in Table I for the pyrolysis of n-butane [10, 18]

Rate constant	$\log A$	E (cal mol ⁻¹)	Reaction rate	
			$k_{873 \text{ K}}$	$k_{1073 \text{ K}}$
k_1	16.3	81 400	8.2×10^{-5}	0.52
k'_1	17.0	85 400	4.1×10^{-5}	0.40
k_2	13.0	40 000	9.6×10^{-2}	7.0×10^4
k_{31}	11.1	9 700	4.7×10^8	1.3×10^9
k'_{31}	11.3	8 400	1.5×10^9	3.8×10^9
k_{32}	9.1	11 600	1.5×10^6	5.4×10^6
k'_{32}	8.9	9 500	3.3×10^6	9.2×10^6
k_{33}	8.0	12 600	7.0×10^4	2.7×10^5
k'_{33}	8.0	10 400	2.4×10^5	7.6×10^5
k_{51}	12.2	28 000	1.5×10^5	3.1×10^6
k_{52}	13.4	31 900	2.6×10^5	7.9×10^6
k_{61}	10.0	2 900	1.9×10^9	2.5×10^9
k_{62}	8.5	7 400	4.4×10^6	9.8×10^6
k_{71}	10.4	0	2.5×10^{10}	2.5×10^{10}
k_{72}	9.8	0	6.3×10^9	6.3×10^9
k_{73}	8.6	0	3.9×10^8	3.9×10^8

a) In the temperature range from 600 to 700 °C, this being the initial temperature of industrial pyrolysis processes, the decomposition of the initial substance A_n can be approximately described by a kinetic equation of the order of 3/2.

b) With increasing the temperature besides the 3/2 order kinetic term, a first order kinetic term will progressively gain in importance in the complex decomposition process, thus the overall order of the reaction tends towards unity. A similar effect results from the dilution of the reaction mixture (*i.e.* of the initial concentration).

c) The statements in a) and b) unequivocally account for the fact that the overall order of the decomposition of the parent compound changes continuously with the changing conditions of the reaction, therefore, it is justifiable to write the equation for the overall decomposition rate as (a form used in a general form previously [15, 16, 20])

$$r_{A_n} = C_A^\circ \frac{dx}{d\omega} = k \left[\frac{C_A^\circ(1-x)}{1 + (E_v - 1)x} \right]^n \quad (15)$$

The results obtained [15, 16, 20] by means of this equation are in good agreement with conclusions a) and b) arrived at through derivations discussed before, namely a figure close to 3/2 is obtained for the decomposition of *n*-butane at about 700 °C (*cf.* Fig. 8); this value tends to decrease towards unity when the temperature is raised.

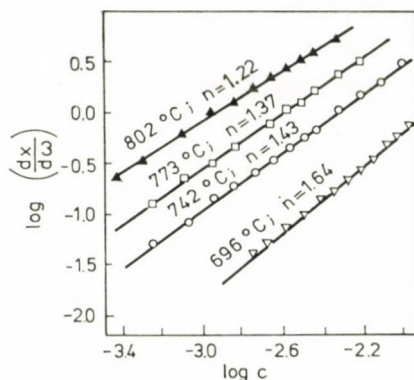


Fig. 8. Logarithm of the rate as a function of the logarithm of actual concentration in the pyrolysis of *n*-butane

*

The authors wish to thank Mr. Antal PUKLER, mathematician, for the programming of the kinetic model.

REFERENCES

- [1] RICE, F. O., HERZFELD, K. F.: J. Am. Chem. Soc., **56**, 284 (1934)
- [2] MYERS, P. S., WATSON, K. M.: National Petroleum News, **38**, 388, 439 (1946)
- [3] ANDREWS, A. J., POLLOCK, L. W.: Ind. Eng. Chem., **51**, 125 (1959)
- [4] SNOW, R. H., SHUTT, H. C.: Chem. Eng. Progr., **53**, 133 (1957)
- [5] SHAH, M. J.: Ind. Eng. Chem., **59**, 70 (1967)
- [6] FEIGIN, E. A., PLATONOV, V. M., MUKHINA, T. N., BARABANOV, N. L.: Neftekhimiya, **2**, 498 (1962)
- [7] SUNDAM, K. M., FROMENT, G. F.: Chem. Eng. Sci., **32**, 601 (1977)
- [8] SUNDAM, K. M., FROMENT, G. F.: Chem. Eng. Sci., **32**, 609 (1977)
- [9] HERRIOTT, G. E., ECKERT, R. E., ALBRIGHT, L. F.: AIChE Journal, **18**, 84 (1972)
- [10] ALLARA, D. L., EDELSON, D.: Internat. J. Chem. Kinet., **7**, 479 (1975)
- [11] SERES, L., BÉRCES, T., MÁRTA, F.: Kémiai Közl., **41**, 267 (1974)
- [12] ZALOTAI, L., BÉRCES, T., MÁRTA, F.: Kémiai Közl., **41**, 237 (1974)
- [13] FEIGIN, E. A., KALINENKO, R. A., BELOSTOTSKII, M. G.: Neftekhimiya, **14**, 866 (1974)
- [14] FEIGIN, E. A., BELOSTOTSKII, M. G., KALINENKO, R. A.: Neftekhimiya, **16**, 77 (1976)
- [15] ILLÉS, V.: Acta Chim. Acad. Sci. Hung., **59**, 35 (1969); Acta Chim. Acad. Sci. Hung., **59**, 299 (1969)
- [16] ILLÉS, V.: Erdöl u. Kohle-Erdgas-Petrochemie, **25**, 464, 542 (1972)
- [17] KOSSIAKOFF, A., RICE, F. O.: J. Am. Chem. Soc., **65**, 590 (1943)
- [18] ALLARA, D. L.: Compilation of Kinetic Parameters for the Thermal Degradation of *n*-Alkane Molecules, 1976
- [19] LAVROVSKII, K. P., KALINENKO, R. A., SEVELKOVA, L. V.: VIII. World Petroleum Congress, 1971 [PD 18(2)]
- [20] ILLÉS, V., WELTHER, K., PLESZKÁTS, I.: Acta Chim. Acad. Sci. Hung., **78**, 357 (1973)

Vendel ILLÉS }
 Ottó SZALAI }

H-8201 Veszprém 1. Pf. 92, MÁFKI

INVESTIGATION OF THE COMPLEX PROTEINS OF WHEAT

R. LÁSZTITY, F. BÉKÉS, J. NEDELKOVITS and J. VARGA

*(Department of Biochemistry and Food Technology, Technical University,
Budapest)*

Received July 28, 1978

Accepted for publication September 4, 1978

The petroleum ether soluble lipoprotein (lipopurothionin), the chloroform-methanol soluble glycolipoproteins and water soluble glycoproteins of wheat were studied.

The electrophoretic properties, amino acid composition and the nature of the lipid and carbohydrate components were determined. The character of the protein-lipid interaction was also investigated.

The results support the assumption that the complex is formed by electrostatic interactions between the numerous polar side chains of protein and polar phospho- or glycolipids. The effect of hydrophobic interactions may not be excluded.

Introduction

On the basis of the classical investigations of OSBORNE, five types of protein are distinguished in wheat flours: albumin, soluble in water; globulin, soluble in salt; gliadin, soluble in alcohol; glutenin, extractable with dilute alkali or acid; and finally a more closely not defined protein type material, called proteose.

The rapid development in the separation techniques of proteins, the widespread application of various extraction, chromatographic, electrophoretic and molecular sieve separation methods have brought some new results that claim for the extension or revision of the classification used so far. The data published in several reviews [1–9] lead to the conclusion that the classical wheat protein fractions are not at all homogeneous, and can be separated to several, possibly more than a hundred, further components. With regard to biological function and related chemical properties, differences can be found between the protein components of the germ, endosperm and aleurone layers. Furthermore, not only the embryo part, but also the endosperm contains many types of enzyme protein. As shown particularly by most recent investigations, wheat flour also contains many complex proteins which have been ignored in previous classifications.

Consequently, according to our present knowledge, the proteins of wheat can be classified as shown in Table I.

Table I
Classification of wheat proteins

On the basis of structure	On the basis of the function of the proteins	On the basis of protein chemistry
Germ proteins Aleurone proteins Endosperm proteins	Enzyme proteins (Amylases, Proteases, Oxydoreductases, etc.) Storage proteins (Gliadin, Glutelin) Membrane proteins Regulatory proteins, etc.	<i>Simple proteins</i> Histones Albumins Globulins Glutelins Enzyme proteins <i>Complex proteins</i> Nucleoproteins Lipoproteins Glycoproteins Enzyme proteins

A more detailed view about wheat proteins may be of interest for research workers and practical experts dealing with cereal processing. Of the new problems emerging, the question of complex proteins is extremely interesting from both the chemical and technological aspects, not only because very little research work has so far been devoted to the composite proteins of wheat flour, but also because according to the most recent investigations these proteins have a very important role in influencing the properties of gluten which are important in food technology.

Within the project of wheat protein chemistry in our institute, considerable stress has been laid in the last few years on complex proteins, particularly on lipo- and glycoproteins. Some of the results obtained are reviewed in this paper.

Lipoproteins and glycoproteins in wheat

An increasing amount of practical experience and experimental results indicate that wheat milling products and dough prepared there of contain lipoproteins, protein-lipid complexes, which affect both the technological properties of dough and the quality of bakery products.

The much different properties of the protein components of these complexes from other proteins of wheat, and the presence of many apoprotein fractions of biological activity detected so far, indicate that these substances play a unique role, from physiological aspects too, in the development of wheat plant.

It is commonly known that the majority of protein-lipid complexes detectable in dough, as first proved by McCaig and McCalla [10], are formed in the presence of phosphatides during the hydration of proteins. In addition to these complexes, which are most important owing to their influence on the quality of bakery products, various other "lipoproteins" have been isolated by BALLS [11, 12], CARTER [13], FISCHER and BROUGHTON [14], COOCKSON *et al.* [15], HOSENEY *et al.* [16], ROHRLICH *et al.* [17, 18], GARCIA-OLMEDO *et al.* [19]. These complexes have in common that they can be extracted from wheat flour by organic solvents, and even if the problem of artefact character may emerge in connection with them, it is clear on the basis of the large number of experiments that the protein components of the complexes show very great affinity towards lipids.

Our research group has been dealing for several years with the most widely studied wheat "lipoproteins", the purothionin-lipid complexes first isolated by BALLS.

Purothionin can be extracted from flour in the form of a lipid-protein complex by petroleum ether. Extraction methods using sodium chloride [19, 20], or dilute acids [21, 22] are also known.

Purothionin is a mixture of basic protein fractions, which, although in very small amounts, can be found in all wheat species, including diploid wheat, which can be regarded as primordial wheat. Purothionin differs in amino acid composition from other wheat proteins; it contains about 20% of cysteine, and more than 20% of basic amino acids (Arg + Lys), whereas histidine, methionine and tryptophane are absent, and the amounts of glutamic acid, aspartic acid and proline are also smaller in purothionin.

The most thoroughly investigated two purothionin fractions were the low molecular weight fractions called α and β purothionin on the basis of gel electrophoretic mobility. The fractions A—I and A—II obtained by the isolation method of OKADA [23] are identical with the α fraction and β fraction. The amino acid sequences of the above purothionin fractions are known: JONES and MAK [24] separated the α fraction into two subfractions and determined the sequence: in a second paper [25] they reported the sequence of the β -fraction. These sequences can be regarded to be the same as the primary structure given by OHTANI *et al.* [26].

The biological effect of purothionin has already been described by the first isolator, BALLS: the compound exhibits antimicrobial and uterus contracting properties. As to the toxicity of purothionin the extensive studies of GARCIA-OLMEDO *et al.* [19] and OKADA *et al.* [23] have revealed many facts. The most intensely studied field is its toxicity towards brewer's yeast, the mechanism of which is also known. Relatively little is known on the lipid binding ability of purothionin, and on the protein-lipid complexes. A method was described for the isolation of the complex by REDMAN and FISHER [27].

The lipids of the isolate proved to be mostly polar lipids, whereas triglycerides were absent.

The first studies on the purothionin content of wheat grown in Hungary were published by LÁSZTITY *et al.* [28]. The isolation method elaborated by BALLS was revised by BÉKÉS [29], SMIED and BÉKÉS [30] compared the properties of products isolated by extraction with petroleum ether and dilute sulfuric acid, respectively.

According to the results of BÉKÉS [31, 32, 33, 34], several fractions, similar in amino acid composition, can be found in addition to the two lower purothionin fractions, and purothionin can be regarded as a mixture of four proteins on the basis of molecular size, and of at least eight proteins on the basis of electrophoretic mobility.

Table II shows the main characteristics of these fractions.

Table II
Main characteristics of purothionin fractions

Characteristic	Fraction							
	A/1	A/2	B	C/1	C/2	D/1	D/2	E
N-terminal group	Arg	Asp	Lys	Glu	Arg	Lys	Ser	Ala
C-terminal group	Asp	Ala	Leu	Leu	Val	Lys	Arg	Gly
Molecular weight · 10 ⁻³	132	132	120	57.3	57.3	8.8	8.8	8.7

The primary aim of our investigations was to determine the types of lipids with which these protein fractions may form complexes and to determine the stoichiometry of complex formation. Therefore, the complex had to be prepared and then its protein and lipid components studied.

An other type of complex proteins was isolated from wheats by ROHR- LICH and NIEDERAUER [17, 18]. A chloroform-methanol (2:1) mixture was used for extraction. The protein part of the isolated complexes was similar to some gluten protein fractions. In the lipid part phospholipids and unsaturated triglycerides were found.

Many authors have successfully isolated carbohydrate-protein complexes from wheat. KÜNDIG and NEUKOM [37, 38] prepared an aqueous extract from ground wheat, from which the fractions containing carbohydrate were isolated after dialysis on DEAE cellulose column. In the carbohydrate unit of the glycopeptide part arabinose and galactose were found, and of the amino acids tyrosine and tryptophane were determined.

WRENCH [39] extracted glycoproteins, besides other proteins, from a commercial flour prepared from Australian wheat with 0.01 mole pyrophosphate solution. The fraction containing carbohydrate was separated on

Sephadex G-75 gel. The molecular weight was found to be around 40 000, and as it had no UV absorption in the 278 nm region, the presence of tyrosine, tryptophane and phenylalanine could be excluded.

The fraction was decomposed with pronase, and the peptide fractions were separated by ion exchange chromatography. In the peptides of carbohydrate content Leu, Val, Glu, Ser, Asp, and Ala were detected.

The carbohydrate part contained glucose, galactose and arabinose. The glucose-galactose ratio was found to be 4:1. Interesting by, the peptide part in the neighbourhood of the carbohydrate unit could not be decomposed enzymatically, probably owing to steric hindrance.

ROHRlich *et al.* [40, 41] investigated the properties and compositions of glycoproteins in commercial flour and in flours prepared from four thoroughbred wheats. The effect of proteins on the viscosity of the solutions and, by farinographic methods, the water absorption capacity, were also studied.

The glycoprotein fractions (I–II) were obtained from an aqueous extract, by separation on Dowex 50 X and DEAE Sephadex gel. The amino acid composition of the glycoprotein from the original aqueous extract was determined, and the quality and quantity of amino acids were found to be similar to those of gliadin.

Our investigations were concerned with the water soluble glycoproteins of Hungarian wheat species.

Experimental

Lipopurothionin

Isolation

Figure 1 shows the scheme of the investigations carried out.

Purothionin fractions were isolated from the petroleum ether extract in four ways,

- (i) by conventional hydrochloric acid cleavage,
- (ii) through the lipopurothionin isolation method elaborated by FISHER *et al.* [21] using methyl acetate, by cleaving the isolated complex,
- (iii) from the fractions obtained by the methyl acetate method and separated according to the molecular size, and
- (iv) directly from the petroleum ether extract, from the protein positive fractions separated on a Sephadex LH-20 column.

The petroleum ether extraction of wheat flour was performed in the following manner. 2000 g of wheat flour (Type 112) was shaken with 1600 ml of petroleum ether (b.p. 40–60 °C) for 2h. After 15 min of sedimentation the clear liquid phase was decanted, and then the solid was filtered off. Adding again 1600 ml of petroleum ether to the flour, shaking was repeated.

The petroleum ether solutions were evaporated in a rotating film vacuum still, and the residue was stored at –10 °C for 2 weeks. During this time the steroid components precipitated, and could be separated from the oil.

Purothionin was prepared by a modified version [13] of the dry hydrogen chloride method developed by BALLS [12]. The method consists in adding a sixfold amount of 1 N anhydrous alcoholic HCl solution to the extract dissolved in diethyl ether. The proteins precipitated upon this treatment are then purified with various solvents to prepare purothionin.

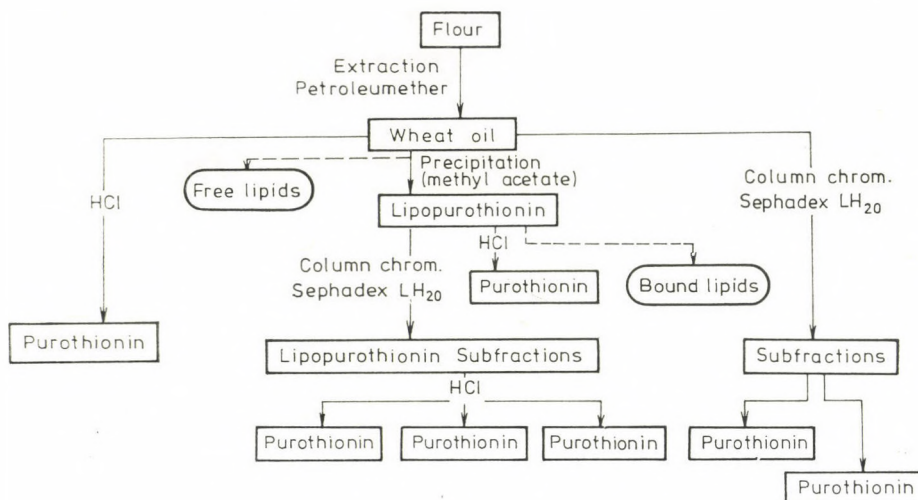


Fig. 1. Scheme of the investigations of lipopurothionin

Lipopurothionin was isolated by the methyl acetate method of REDMAN and FISHER [27]. Purothionin was separated from lipopurothionin by a semi-micro variant of the BALLS method. Bound lipids were separated by FOLCH washing.

Lipopurothionin and the petroleum ether extract were separated according to molecular size on a Sephadex LH-20 column with chloroform containing 5% of ethanol.

As can be seen in Fig. 1, these treatments enabled us to isolate the "free" lipids and those interacting with proteins. In addition the fractions prepared in four different ways give possibility to determine whether all purothionin fractions take part in the formation of the complex, and whether the complex contains any other protein in addition to the purothionin fractions.

Investigations on proteins

For a comparison of the protein preparations produced in different ways, the following investigations were carried out.

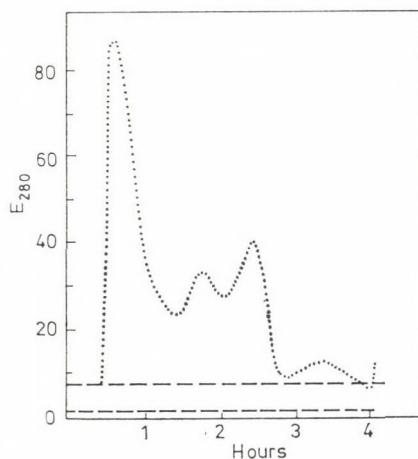


Fig. 2. Characteristic elution curve of purothionin on Sephadex G-75 column

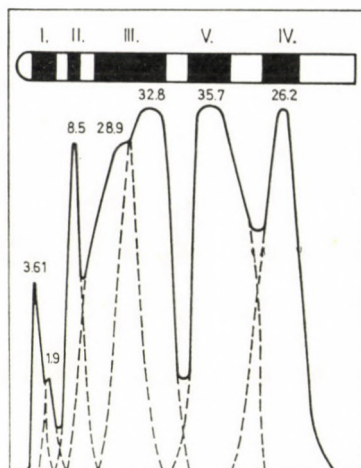


Fig. 3. The elphogram of purothionin obtained on PAG at pH = 3.1

- (i) Separation according to molecular size on a Sephadex G-75 column. The characteristic elution curve of purothionin is shown in Fig. 2.
 - (ii) Determination of the molecular weights of the fractions uniform in molecular size by means of an ultracentrifuge, with low-speed equilibrium measurements.
 - (iii) Gel electrophoretic investigation of the fractions. The elphogram of purothionin obtained on polyacrylamide gel at pH = 3.1 can be seen in Fig. 3.
 - (iv) Determination of the gross amino acid composition by means of an automatic amino acid analyser.
 - (v) Determination of terminal amino acid: *N*-terminal determination by the DNFB method, *C*-terminal investigations by carboxypeptidase digestion.
- All these investigations have been described in one of our previous papers [29].

Investigations on lipids

"Free" and "bonded" lipids were analyzed qualitatively and quantitatively by the following methods.

- (i) Group fraction on florisil column activated by acid treatment, with eluents of varying polarity.
- (ii) Further separation and quantitative analysis of group fractions by the TLC technique. The eluents and detecting agents applied are described in detail in another paper [34].
- (iii) Micro analysis for phosphorus in the group fractions [33].
- (iv) Determination of gross fatty acid compositions of the group fractions by gas chromatographic analysis [30].

Glycolipoproteins soluble in the system chloroform-methanol

Isolation

The technique described by ROHRlich and NIEDERAUER [17, 18] was applied, and after extraction with petroleum ether the appropriate complex proteins were extracted with a mixture of chloroform and methanol.

The preparation of the protein-lipid complex and the investigations carried out are shown schematically in Fig. 4.

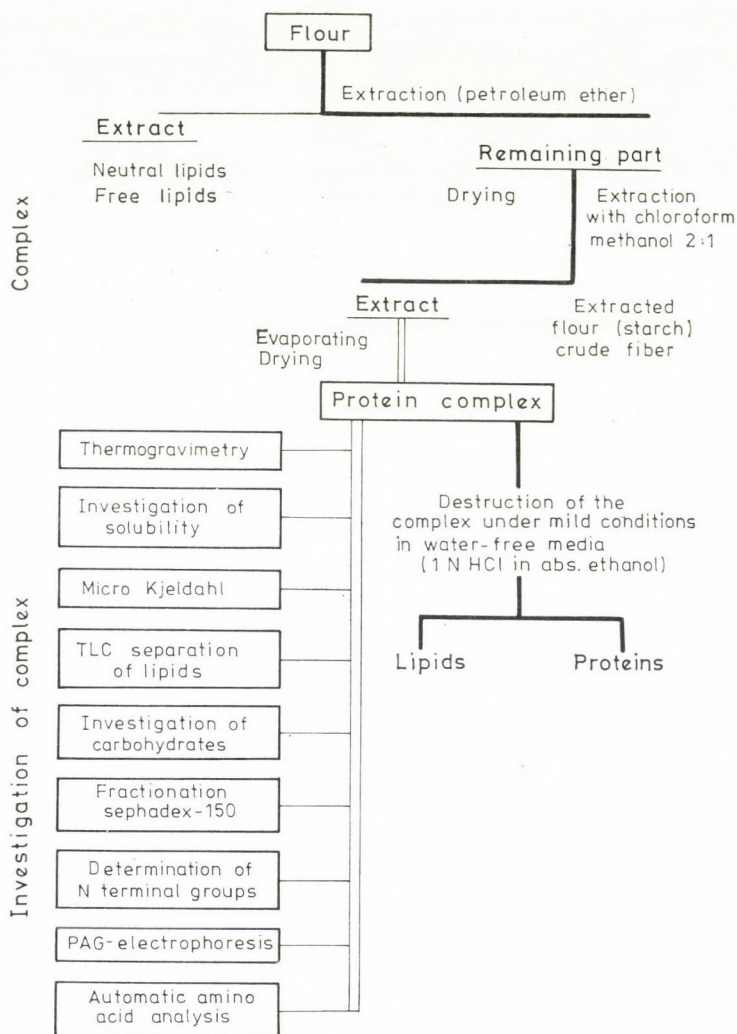


Fig. 4. Scheme of the preparation and investigation of wheat glycolipoprotein complexes

Investigation of the lipid components

The lipid components were investigated by TLC. The chromatograms were developed on Silica gel G layer with the solvent system acetone/benzene/water (91:30:10). The spots were detected by five methods.

1. 1% α -naphthol in 90% ethanol, containing 10% H_2SO_4 . At 100 °C glycolipids appear in red colour.

2. Phospholipids were visualized with DITTMER—LESTER [35] reagent on the basis of the molybdenum blue reaction.

A) 16 g of $(\text{NH}_4)_2\text{MoO}_4$ was dissolved in 120 ml of water.

B) 40 ml of conc. HCl + 10 ml of mercury were added to 80 ml of solution A), shaken for 30 min, and filtered on a G3 glass-filter.

200 ml of conc. H_2SO_4 and solution B) were added to the rest of solution A): the solution was cooled and filled up to 1 litre.

The plates sprayed with the reagent were heated at 110 °C in a drying oven. Lipids containing phosphorous gave blue colour.

3. Steroid glycosides can be detected by spraying the plates with a chloroform solution of antimony chloride. The spots are visible in UV light.

4. Amino groups and phosphatidyl choline were detected by 1% ninhydrine in acetone.

5. Elementary iodine is adsorbed by most of the fractions, thus it can be used to make visible all the spots in a nondestructive way.

Experimental conditions of TLC

System	acetone/water/benzene (91:10:30)
Temperature	25 °C
Time	40 min
Layer	Silica gel G (inactivated)

Determination of the carbohydrate components

For the determination of the carbohydrate content of the complex, the lipoprotein was hydrolyzed, and identified by paper chromatography.

Hydrolysis: 0.6 g of air dry material was placed into two hydrolyzing test tubes. The samples were hydrolyzed at 105 °C for 8 h with 10 ml each of 2*N* H₂SO₄. After hydrolysis, the solutions were washed into glass vessels, and sulfuric acid was neutralized by warming with solid Ba(OH)₂. The BaSO₄ precipitate was removed by filtration on a G3 glass filter. The pure, neutral filtrate was evaporated to a volume of 5 ml, and this solution was used in the subsequent experiments.

Chromatography: On the basis of preliminary experiments, from the samples 50 µl and from the standards 5 µl were applied on to the paper. Arabinose, galactose and ribose were used as standards in a concentration of 5 mg/ml.

Descending chromatograms were run in a cylindrical vessel of the usual size. Schleicher—Schüll 2043/B paper was used, from which strips of 10 × 45 cm were cut. The start line was at a distance of 10 cm from the edge of the plate, the mixture were placed in a Petri dish to the bottom of the solvents. After applying the sample, the paper strips were fastened into the boat by means of a glass rod so that the start line was at the same height as the bottom of the boat. This careful alignment before running the chromatogram is very important, since it ensures well discernible, parallel running spots, even after long runs. After these preparations the boat was filled with the mixture, the vessel was covered, and the chromatogram was run for 24 h. The spots of the chromatograms were detected with agents of different sensitivities (diphenylamine-aniline phosphoric acid and silver nitrate reagents).

Gel chromatography and electrophoresis

The complex was separated on Sephadex G-150 gel. The parameters of separation were the following:

Column height	40 cm
Internal diameter of column	20 mm
V_0	24 ml
V	125 ml
Flow rate	15–20 ml/h
Buffer	0.5% acetic + 7% Al lactate

Gel electrophoresis was performed on polyacrylamide gel at pH = 8.9 TRIS-glycine buffer of pH = 8.3 was used as the electrode buffer. The details of separation have been described in another paper [36].

Amino acid composition and N-terminal groups

The amino acid compositions of the fractions were determined by an automatic amino acid analyser (A 881 MIKROTECHNA PRAHA). The N-terminal groups of the fractions were determined with 1-dimethylaminonaphthalene-5-sulfonyl chloride reagent (dansylation).

Glycoproteins

The flour of "Besostaya-1" wheat species (ca. 70% extraction) was used for the investigations. The glycoproteins were extracted with distilled water at 20–25 °C. After centrifuging, the aqueous extract was purified by dialysis. The purified extract was further separated on Sephadex G-75 gel.

The carbohydrate content of the fractions was detected by means of the Molish reaction and resorcin test. Paper electrophoresis was carried out with the following parameters.

Paper	Whatmann 1
Buffer	Acetic acid-pyridine-water (pH = 5.6)
Voltage	220 V
Current	2 mA per strip
Time	6 h
Sample introduced	0.05 ml

After electrophoresis, the paper strips were dried at 105 °C, and a part of them was developed with a fuchsine solution in acetic acid. As differentiating solution a 10% acetic acid solution was used.

Another part of the paper strips was tested for carbohydrates, with a 4:1 mixture of 1% resorcin in alcohol and 2N phosphoric acid. Carbohydrates were separated by dialysis after hydrolysis, and investigated by paper chromatography. The method was identical to that described for glycolipoproteins.

The amino acid compositions were determined by an automatic amino acid analyser (A 881 MIKROTECHNA, PRAHA).

Results and Discussion

Lipopurothionin

In the complex coagulated with methyl acetate a protein-lipid ratio of 3:7 was found. After cleavage by hydrochloric acid, the protein part could be identified unambiguously with the purothionin fractions. The lipid part had a polar character and a high content of phospholipids (about 90%). A small amount of sterols was observed (Table III).

The main component of the lipid part was phosphatidyl ethanolamine.

Lipopurothionin coagulated with methyl acetate was separated according to molecular size on a Sephadex LH 20 column. As can be seen in Fig. 5, the elution curve indicates a very inhomogeneous fraction. The elution curves, as regards the fraction ratios, strongly vary with the age of the preparation; in the experiment shown in the Figure 5, separation was done immediately after isolation.

Examination of the eight main fractions isolated has shown that their protein and lipid compositions differ only in relative proportions, but all components can be found in every fraction.

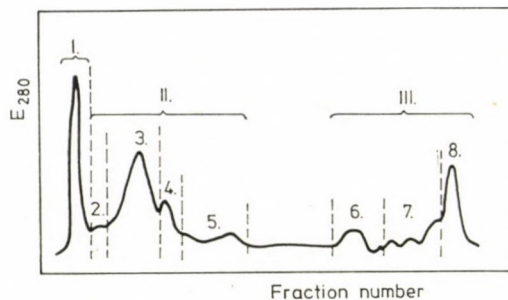


Fig. 5. Elution curve of the (chloroform extract) on Sephadex LH-20 column

Table III

Characteristics of lipopurothionin separated by precipitation with methylacetate

Characteristic	Lipopurothionin	Lipopurothionin		
		I.	II.	III.
Quantity of the fraction (%)	100	41.1	32.3	26.5
Protein content (%)	27.4	30.4	26.4	25.7
Gel electrophoretic subfractions of the protein part (%)				
Purothionin A	49.8	59.8	41.3	19.7
Purothionin B	17.3	28.7	43.6	46.5
Purothionin C	18.3	6.9	13.2	19.7
Purothionin D	14.6	4.6	1.9	14.1
Purothionin E	14.6	4.6	1.9	14.1
Lipid content (%)	72.6	69.6	73.6	74.3
Phosphorus content (mg/mg)	20.0	21.3	18.4	19.2
Lipid subfractions				
Phosphatidyl inosite	+	—	+	+
Phosphatidyl choline	+	+	+	+
Phosphatidyl ethanolamine	+	+	+	+
Lysophosphatidyl choline	+	+	—	—
Lysophosphatidyl ethanolamine	+	+	+	+
Monogalactosyl diglyceride	+	+	—	—
Sterol glycoside	+	+	+	—

These results seem to support the assumption that the complex is formed by electrostatic interactions between the numerous polar amino acid side chains in purothionin and the polar lipids. The instability of the system and the almost statistical composition of the lipopuroprotein fractions practically exclude the existence of a covalent bond between the proteins and lipids.

This schematic picture was enriched in several aspects by the results obtained in the direct fractionation of the petroleum ether extract.

Elution of the extract with chloroform on a Sephadex LH 20 column gives the elution curve shown in Fig. 6. Of the separated fractions, only the first two had a detectable protein content (Table IV). According to the results of more detailed investigations, this protein was undoubtedly purothionin. The lipid composition of the fractions containing protein was significantly

Table IV

Characteristics of the protein lipid complex isolated directly by fractionation of the petroleum ether extract

Characteristic	Fraction					
	I	II	III	IV	V	VI
Quantity of fraction(%)	11.7	53.3	11.7	15.0	3.3	5.0
Protein content (%)	14.9	10.6	—	—	—	—
Quantity of the protein subfractions (%)						
A	} 48.5	79.2	—	—	—	—
B						
C	43.6	19.7	—	—	—	
D	} 48.5	79.2	—	—	—	—
E						
Phosphorus content ($\mu\text{g}/\text{mg}$)	12.8	8.87	—	—	—	—
Lipid content (%)	85.1	89.4	100	100	100	100
Lipid subfractions(%)						
Polar lipids	46.5	32.2	19.2	16.1	17.4	13.7
Free sterols	—	—	8.8	10.1	8.8	8.7
1—2-diglycerides	—	—	11.4	13.0	14.9	6.0
1—3-diglycerides	—	—	14.8	12.6	10.3	6.2
Triglycerides	48.5	60.0	29.4	29.1	33.8	65.0
Sterol esters	4.8	7.8	16.4	19.1	15.4	5.4

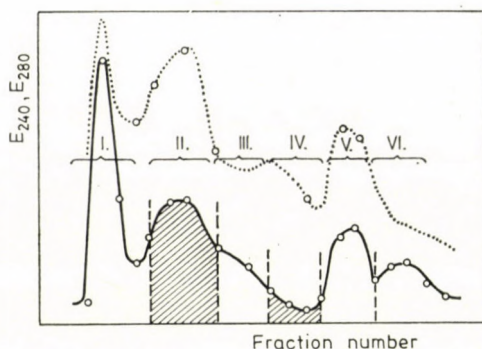


Fig. 6. Fractionation of wheat (petroleum ether) extract on Sephadex LH-20 column

different from that of the further four fractions: the proportion of polar lipids was higher in the former. The difference was also characteristic in the fatty acid composition; whereas with "free" lipids the main bulk consisted of linoleic and linolenic acids, in the two fractions of protein content the proportion of oleic acid markedly increased.

The composition of the protein-lipid complex prepared by this method had one significant difference as compared with the preparate ion isolated by methyl acetate coagulation: the former contained a substantial amount (more than 10%) of triglyceride. For the interpretation of this fact our hypothesis concerning the structure of lipopurothionin must be extended.

In addition to the *electrostatic* and perhaps *hydrogen bond* interactions between polar lipids and the basic amino acid side chains in purothionin, which occur very abundantly in wheat proteins, one must also assume the presence of *hydrophobic interactions* between the fatty acid side chain of phospholipids and triglycerides (lipid-lipid interactions). These interactions, being very weak, may already be eliminated by mild environmental effects, such as methyl acetate treatment.

Glycolipoproteins

The protein content of the complex was found to be 85.3%. Of the lipids, the following 10 components could be separated:

- phosphatidyl choline
- phosphatidyl ethanolamine
- phosphatidic acid
- sulfoglycolipid
- digalactosyl diglyceride
- polyglycerine phosphatide

monogalactosyl diglyceride
steroyl glycosides and neutral lipids.

One component could not be identified.

Of the carbohydrate constituents arabinose and galactose were identified unanimously in the hydrolysate.

The complex was separated into two fractions on Sephadex G-150 gel, of which the first fraction may presumably be decomposed into further fractions. This seems to be supported by the *N*-terminal amino acid analysis of the fractions, too. The first fraction was glycine, phenylalanine, and unidentified; the second fraction contained arginine as the *N*-terminal amino acid.

The *N*-terminal amino acids of the lipid-protein complex were also determined from the undecomposed complex. The *N*-terminal amino acids determined by means of 1-dimethylaminonaphthalene-5-sulfonyl chloride (DNS-Cl) were as follows:

arginine
glycine
phenylalanine
unidentified

The complexes could be decomposed into four fractions by PAG electrophoresis. Electrophoresis was carried out at four gel concentrations. The sample was dissolved in TRIS-glycine buffer of pH = 8.3, containing 0.1 g/ml of urea. The best separation was observed for a gel concentration of 3.75%.

N-terminal amino acid analysis and PAG electrophoresis both indicated the presence of four fractions. The investigations of the *N*-terminal amino acids of the complexe have also shown four amino acids, of which three could be identified qualitatively. The amino acid composition of lipoglycoprotein is given in Table V.

Glycoprotein

By separation on Sephadex G-75, one fraction containing carbohydrate could be isolated from the aqueous extract, with a molecular weight of *ca.* 16,000. This fraction could be separated further by electrophoresis into two fractions, one practically carbohydrate-free and one glycoprotein fraction. Of the carbohydrate components galactose, glucose and arabinose were identified, their ratio being 6:3:1.

The data on the amino acid composition (see Table VI) support the acidic character of the protein complex observed in the electrophoretic investigations.

Table V*The amino acid composition of the lipoglycoprotein complex*

Amino acid	g/100 g protein	Amino acid	g/100 g protein
Asp	1.17	Met	0.45
Thr	2.76	Pe	5.31
Ser	1.22	Leu	4.60
Glu	23.40	Tyr	1.60
Pro	22.20	Phe	4.71
Gly	1.55	Arg	2.20
Ala	1.65	Lys	2.35
Cys	8.20	His	1.22
Val	2.14	Ammonia	1.46

Table VI*Amino acid composition of the wheat glycoprotein*
(Acidic protein isolated from the wheat variety Besostaya-1)

Amino acid	g/100 g protein
Cys	3.82
Lys	5.82
Arg	4.57
Ser	8.91
His	1.40
Asp	11.81
Thr	3.00
Glu	11.81
Ala	7.91
Pro	7.14
Tyr	6.36
Met	1.81
Val	5.60
Phe	7.91
Leu	7.91
Ile	3.91

REFERENCES

- [1] LÁSZTITY, R.: Sütőipar, **12**, 57 (1966)
- [2] Society of Chemical Industry: Recent Advances in Processing Cereals. Monograph No. 16. London 1962
- [3] VAKAR, A. B., EL-MILIGI, A. K., TOLCSINSZKAJA, E. S., ZABRODINA, T. M.: Biochim. Zerna i Chlebopecsenyija, **7**, 3 (1964)
- [4] KACZKOWSKI, J.: Postep, Biochim., **13**, 326 (1965)
- [5] BLOKSMA, A. H.: Wallerstein Lab. Comm., **21**, 215 (1958)
- [6] LÁSZTITY, R.: Die Nahrung, **12**, 3 (1968)
- [7] LÁSZTITY, R.: A kémia újabb eredményei, 11. köt., Akadémia Kiadó, Budapest 1972
- [8] ELTON, G. A. H., EWART, E. A. D.: Baker's Digest, **41**, 36 (1967)
- [9] POMMERANZ, Y.: Adv. in Food Res., **16**, 335 (1968)
- [10] McCAIG, T., McCALLA, A. G.: Canadian J. Res., **19**, 163 (1941)
- [11] BALLS, A. K., HALE, W. S., HARRIS, T. H.: Cereal Chem., **17**, 243 (1940)
- [12] BALLS, A. K., HALE, W. S., HARRIS, T. H.: Cereal Chem., **19**, 279 (1942)
- [13] CARTER, H. E., McCLUER, R. H., SLIFER, E. D.: J. Am. Chem. Soc., **78**, 3755 (1956)
- [14] FISHER, N., BROUGHTON, M. E.: Chem. and Ind., **1963**, 869
- [15] COOKSON, M. A., RITCHIE, M. K., COPPOCK, J. B. M.: Sci. Fd. Agric., **8**, 105 (1957)
- [16] HOSENEY, R. C., POMERANZ, K. R.: Cereal Chem., **27**, 312 (1970)
- [17] ROHRlich, M., NIEDERAUER, H.: Fette, Seifen, Anstrichm., **69**, 226 (1967)
- [18] ROHRlich, M., NIEDERAUER, H.: Fette, Seifen, Anstrichm., **70**, 58 (1968)
- [19] GARCIA-OLMEDO, F., CARBONERO, P.: Experimentia, **25**, 1110 (1969)
- [20] NIMMO, C. C., O'SULLIVAN, M. T., BERNARDIN, J. E.: Cereal Chem., **45**, 28 (1968)
- [21] FISHER, N., REDMAN, D. G., ELTON, G. A. H.: J. Sci. Fd. Agric., **20**, 546 (1969)
- [22] KASARDA, D. P., BERNARDINI, J. E., NIMMO, C. C.: in "Advances in Cereal Science and Technology" (Ed. Y. POMERANZ), AACC. St. Paul 1976
- [23] OKADA, T., YOSHIZUMI, M., TERESHIHA, Y.: Agr. Biol. Chem., **34**, 1084 (1970) and **34**, 1089 (1970)
- [24] JONES, B. L., MAK, A. S.: Cereal Chem., **54**, 511 (1976)
- [25] MAK, A. S., JONES, B. L.: Can. J. Biochem., **22**, 835 (1976)
- [26] OHTANI, S., OKADA, T., KAGAMIYAMA, M., JOSHIZUMI, H.: Agr. Biol. Chem., **39**, 2269 (1975)
- [27] REDMAN, D. G., FISHER, N.: J. Sci. Fd. Agric., **19**, 652 (1968)
- [28] LÁSZTITY, R., MONORI, S., KOVÁCS, A.: Élelmiszervizsg. Közl., **15**, 257 (1969)
- [29] BÉKÉS, F.: Acta Alimentaria, **6**, 39 (1977)
- [30] SMIED, I., BÉKÉS, F.: In the press
- [31] BÉKÉS, F., MONORI, S.: Élelmiszervizsg. Közl., **21**, 163 (1975)
- [32] BÉKÉS, F.: Élelmiszervizsg. Közl., **22**, 135 (1976)
- [33] BÉKÉS, F., VÁRADI, Gy.: Élelmiszervizsg. Közl., **22**, 166 (1976)
- [34] BÉKÉS, F., SZITHA, E., SMIED, I.: In the press
- [35] DITTMER, J. C., LESTER, R. L.: J. Lipid Res., **5**, 126 (1964)
- [36] BATHÓ, Cs.: Diploma Work, Technical University, Budapest 1976
- [37] KÜNDIG, W., NEUKOM, H.: Helv. Chim. Acta, **46**, 1423 (1963)
- [38] KÜNDIG, W., NEUKOM, H., DENEL, H.: Helv. Chim. Acta, **44**, 823 (1961)
- [39] WRENCH, P.: J. Sci. Fd. Agric., **17**, 403 (1866)
- [40] ROHRlich, M., HERTEL, W., MÜLLER, V.: ZLUF, **143**, 401 (1970)
- [41] ROHRlich, M., ESSNER, W., LICHTENFELS, I.: ZLUF, **119**, 118 (1963)

Radomir LÁSZTITY
 Ferenc BÉKÉS
 János NEDELKOVITS
 János VARGA

H-1502, Budapest, P.O. Box 91.

RECENSIONES

János LISZI: *Nemelektrolit folyadékok dielektromos tulajdonságai*
(*Dielectric Properties of Non-electrolyte liquids*)

A kémia újabb eredményei
(*Advances in Chemistry*) Vol. 38

Akadémiai Kiadó, Budapest

1977, 262 pages (A/5), 70 figures, 38 tables

The book of J. LISZI reviews the theories of dielectric polarization and relaxation of dielectric liquids and relationships between the structure and dielectric properties of liquids containing no charge carriers. It also deals with some relationships between structures of molecules in. and dielectric properties of the liquid.

The second chapter (58 pp in length) discusses theories of the static relative permittivity of liquids; the third chapter (of about same length) is concerned with the theories of dielectric relaxation, i.e., the frequency dependence of dielectric properties.

The next two chapters discuss in more detail the relationships between the structure and dielectric properties, illustrated by data and relationships pertaining to individual substances. The fourth chapter (53 pp) is devoted to liquids in which the molecules are not associated, and the fifth chapter (73 pp) to "associative" liquids.

The sections dealing with theoretical, semi-empirical and empirical relationships between structure and dielectric properties are particularly valuable.

The presentation of basic theories creates the impression as if they had not been quite assimilated by the author. Some incomplete definitions (e.g. that of electric dipole, p. 15), inaccuracies (e.g. identification of random distribution with equal radial distribution, p. 16; or Equation 2.3.8, p. 20), and erroneous equations (e.g. Equation 2.5.6, p. 29 or Equation 2.5.14, p. 31) seem to confirm the above impression and suggest the lack of due care.

S. LENGYEL

Lecture Notes in Chemistry, Vol. 5.

Ramon CARBO, Joseph M. RIERA: *A General SCF Theory*

Springer-Verlag, Berlin—Heidelberg—New York, 1978, 210 pages

The subject of this book is the most important approximate method in modern quantum chemistry, the self-consistent field (SCF) method. The reviewer is not completely happy with this volume because the presentation is very heterogeneous. Strangely, the first part is the most demanding one; as one proceeds, the presentation becomes much simpler. It is hard to

see for whom the book was intended: the first part is simply too general and complicated for the beginner, while a reader with a good background in quantum chemistry will find much of the material already familiar.

After a brief historical introduction, the general SCF formalism, developed by HIRAO and by the authors, is described. Despite its occasionally poetical style, this is very hard reading, and the present reviewer found it necessary to consult the original papers. Unfortunately, the practical advantages of the general SCF theory are not stressed, and the examples treated can be calculated by conventional Hartree-Fock routines. Disproportionally much is written about the paired-excitation multiconfigurational SCF method which is little used nowadays. This is no wonder considering that, as a result in this book shows, a 56-configuration paired-excitation SCF wavefunction yields only about 4 per cent of the estimated correlation energy in water. SCF perturbation theory is well covered, as well as the multiconfigurational case for two and three electrons. The final part of the booklet describes various practical devices, e.g. basis sets, population analysis, etc., and contains a collection of fair-quality SCF calculations. The latter should be quite useful for the novice.

There is a serious error on p. 32, which deserves separate treatment here. From the fact that one can add to the Fock matrix an arbitrary projector which is diagonal in the SCF orbitals, the authors conclude that Koopmans' theorem has absolutely no significance, and orbital energies are completely arbitrary quantities. If this were true, the approximate correspondence between the observed ionization potentials and Hartree-Fock orbital energies would constitute a mystery. In reality, an orbital energy is equal to the difference in the energy expectation value of the ground-state determinant and a determinant in which the corresponding orbital has been deleted. An arbitrary level-shift operator cannot have any effect on this quantity. Thus, as far as orbital reorganization and correlation effects can be neglected, Koopmans' theorem remains valid.

P. PULAY

Heinrich NÖTH and Bernd WRACKMEYER: *Nuclear Magnetic Resonance Spectroscopy of Boron Compounds*,

NMR Basic Principles and Progress, Volume 14

(P. DIEHL, E. FLUCK, and R. KOSFELD, Eds).

Springer-Verlag, Berlin-Heidelberg-New York, 1978, 461 pages

Over the last decade, boron chemistry, especially the chemistry of higher boranes, has undergone major developments. To a fairly high extent, this has been due to the ever increasing applications of boron-11 nuclear magnetic resonance (^{11}B NMR) spectroscopic methods in the elucidation of composition, structure and dynamics of boron-containing molecules and systems. Since the proliferation in the early 70's of modern Fourier transform NMR equipment providing ^{11}B NMR data on moderate quantities of samples within relatively short periods of time, a considerable body of ^{11}B NMR information has been accumulated. This information however is widely scattered in the literature. The remarkable task of collecting these data had been undertaken by H. NÖTH and B. WRACKMEYER, well-known experts of this field, and resulted in this impressive volume 14 of the *NMR Basic Principles and Progress* series.

Data-oriented in the first place, the volume is built up around the collection of ^{11}B NMR data for more than 3000 compounds listed in well-organized tables that occupy some 300 of a total of 460 pages. The descriptive part is divided into 8 chapters. After the introductory remarks outlining the major scope of the volume (chapter 1), a brief summary of the NMR properties of boron is given (chapter 2) including the main empirical and semiempirical correlations of ^{11}B chemical shifts and one-bond coupling constants [$J(^{11}\text{B-X})$]. Chapter 3 surveys the few ^{11}B NMR data on two-coordinate boron to be followed by a detailed account on ^{11}B chemical shifts of three-coordinate boron (chapter 4) in a large variety of compounds with special emphasis on correlations of ^{11}B chemical shifts with substituent, anisotropy, σ and π bonding effects, the influence of ring size, steric hindrance. In this and subsequent chapters, the description of the major trends and characteristics of ^{11}B chemical shifts is care-

fully matched with the organization of the data collection. Chapter 5 deals with the available data on ^{11}B NMR of transition metal boron compounds, chapter 6 is devoted to ^{11}B NMR of diborane and derivatives while chapter 7 disserts on compounds with tetra-coordinate boron including, among others, metal borates, donor-acceptor complexes, boron adducts with various donors, etc. Spin-spin coupling constants involving ^{11}B [$n_J(^{11}\text{BX})$] are dealt with in chapter 8. Discussion of this parameter is extended over boron-boron and boron-other element coupling from the direct ($n = 1$) to long-range ($n \geq 4$) interactions.

The tables of ^{11}B NMR data (chapter 9) are organized as follows. At the head of each table structural symbols are provided. These symbols show the atoms to which the boron atom is directly bonded. In addition, the headlines of each table indicate the classes of compounds treated. The combination of classes of compounds with the structural symbol allow for an easy way of retrieving a specific compound. For this purpose, a compilation of compounds according to Chemical Abstract formula is provided. The volume is complete with formula and author index and references.

The book is a most valuable data collection for all those working in the field of borane and organoborane chemistry.

L. RADICS

J. ULBRICHT: *Grundlagen der Synthese von Polymeren*

Akademie-Verlag, Berlin, DDR, 1978

260 Seiten, 59 Abbildungen, 39 Tabellen

Die theoretischen und praktischen Kenntnisse der einzelnen Disziplinen sind in den mittlerweile erschienenen Handbüchern zusammengefasst. Über Entwicklungen während und seit ihrer Erscheinung berichten jedoch nur Fachzeitschriften, deren Studium viel Zeit und Mühe beansprucht.

Die wissenschaftliche Behandlung der Polymerisationsreaktionen hat in den letzten Jahrzehnten stark an Intensität gewonnen.

Verschiedene Fachrichtungen erfordern eingehendere Kenntnisse auf diesem Gebiet, die durch spezielle Vorlesungen, Übungen und Praktika ermittelt werden.

Um eine gezielte Reaktionssteuerung verwirklichen zu können, ist es erforderlich, mehr über den Ablauf der Elementarreaktionen der Polymerisation zu wissen.

Im vorliegenden Buch werden die folgenden Themenkreise erörtert: Einordnung des Verlaufes der Polymerisationsreaktionen, radikalische und ionische Elementarschritte, die Natur von Ionen und Ionenpaaren sowie deren Beeinflussung durch polare bzw. sterische Effekte bzw. durch Eigenschaften des Mediums. Das Buch behandelt die Kettenpolymerisation, die Gleichgewichtslage, Strukturprinzipien sowie Mechanismus und Kinetik der homogenen und heterogenen radikalischen, ionischen und koordinativen Kettenpolymerisation. Unter analogen Gesichtspunkten wird die Stufenpolymerisation und die Entstehung von Leiterpolymeren, Präpolymeren, Ionomeren und semiorganischen Polymeren besprochen. Des weiteren werden noch die Multipolymerisation, die Abmischung mit anderen Polymeren, polymeranaloge Reaktionen (darunter Pfropfungen) und die Modifikation der Polymere behandelt.

Das Buch behandelt das Thema logisch und konsequent. Ein großes Verdienst des Buches ist eine ausführliche Beschreibung der Grundprinzipien. Der Stil des Buches ist klar und knapp, die Tabellen sind übersichtlich, die Abbildungen und die sehr gut gewählten Beispiele erleichtern das Verständnis des Stoffes. Es liegt in der Natur des Buches, daß bei der Erörterung der einzelnen Begriffe auch auf deren praktische Anwendung großes Gewicht gelegt wird. Die Beispiele erleichtern die Aneignung des Wissensgebietes und fördern die sich auf die praktische Verwendbarkeit beziehenden Kenntnisse.

Um den Lesern den Zugang zur Originalliteratur der behandelten Gebiete zu erleichtern, sind den einzelnen Teilen Literaturhinweise angefügt. Ein ausführliches Sachverzeichnis am Ende des Buches erleichtert die Orientierung. Die Typographie und die Ausführung des reichen Tabellen- und Abbildungsmaterials ist recht gut.

Das Buch ist als Lehrbuch für die Ausbildung an Universitäten und Hochschulen der DDR anerkannt.

Als Leserkreis können fortgeschrittene Studenten, die sich bereits mit der makromolekularen Chemie vertraut gemacht haben, in Frage kommen. Praktiker in Forschungsinstituten

und in der Industrie, die über die Frage der Polymerisationsreaktionsmechanismen informiert sein möchten, ohne selbst als Spezialisten auf diesem Gebiet tätig zu sein, könnten dem Buch nützliche Anregungen entnehmen. Darüber hinaus wird auch der Praktiker die Möglichkeit eines Überblicks über sein Arbeitsgebiet wahrnehmen.

Auch die in der Lehre tätigen Leser werden in dem Buch viele geschickte pädagogische Gesichtspunkte und Ideen finden, die ihnen zur Verbesserung ihrer Vorlesungen verhelfen können.

Der Erfolg eines Fachbuches wird neben der guten Verwendbarkeit und dem hohen Niveau bei der Behandlung des Gegenstands durch einen leichtverständlichen Stil und eine klare und logische Ausführung des Stoffes bestimmt. All diese vorteilhaften Eigenschaften können bei dem vorliegenden Buch, dessen Verfasser auf diesem Gebiet der Wissenschaft ein allgemein anerkannter Wissenschaftler ist eindeutig festgestellt werden.

Der Autor bereicherte die Fachliteratur mit einem Buch, das sowohl den Fachleuten als auch den Lesern wertvolle und lehrreiche Kenntnisse vermittelt.

I. G ÉCZY

Structure and Bonding, Vol. 34

Novel Aspects

Springer-Verlag, Berlin—Heidelberg—New York, 1978

220 pages, figures 37, tables 39

This volume contains five compendious treatises which describe the present state of some rather diverse fields of chemistry: from quarkonium chemistry to lanthanide complexes.

S. HUBERT, M. HUSSONNOIS, and R. GUILLAUMONT are the authors of the first paper, entitled "Measurement of Complexing Constants by Radiochemical Methods". The equilibrium constants, determined by means of the classic extraction methods, and the formation constants, are significantly affected by the pH of the aqueous phase and by several parameters of the two-phase system: very often the accuracy, the reproducibility of experimental data leave much to be desired. However, the stability constant can be determined very accurately provided the radioactive isotope of the element in question is introduced into the system at a very low concentration, viz. at 10^{-6} M or lower. The citrato- and the theonyl-trifluoroacetato- (TTA)-complexes of the lanthanides and actinides serve as models on which to demonstrate the efficiency of this method. In the case of complexes of Me^{3+} ions with $n f^{3,4}$, $n f^7$, $n f^{10,11}$ ($n = 4, 5$) electron configurations the $\lg \beta$ vs. Z diagrams reveal the well-known "weak accidents": the phenomenon may be interpreted as a thermodynamic consequence of the nephelauxetic effect. Other methods which utilize radiating isotopes, e.g. radiopolarography or radiocoulometry, also furnish accurate thermodynamic data. 29 references to relevant literature are listed.

The second treatise, on "Predictable Quarkonium Chemistry", is authored by C. K. JØRGENSEN. By quoting 60 items of the literature, this author summarizes here quarkonium chemistry on 18 pages. The possibility of concentrating quarks, their properties, their adducts formed with atoms, ions, molecules are discussed. The fundamental differences between positive and negative quarks are explained. The properties of u-, d-, and s-quarks, also of the c-quarks introduced by some authors, are described. The analogy between neutrinos, muons, and other well known particles is dealt with; the principal features of the theories about quarkonium chemistry are presented.

"Chemistry of Plutonium and the Transuranics in the Biosphere", by R. A. BULMAN, is the third part, covering 30 pages. Here a very interesting and topical question is exposed. After a short review of the electron structure and chemical properties of the transuranics their occurrence in our biosphere, notably in the soil, the humic acids as lanthanide-bonding agents, their complexes, their incorporation by plant organisms can be read about. Further, their occurrence and distribution in water and their incorporation by animal organisms are mentioned. The possibility of removal of actinides from organisms by means of medication is reviewed in the last, short chapter. 193 references help to get acquainted with this very interesting topic.

J. W. BUCHLER, W. KOKISCH, and P. D. SMITH write about "Cis, Trans, and Metal Effects in Transitional Metal Porphyrins". Principal parts are: electron-effect in the case of

metal-porphyrins; *cis-trans* effect in the case of Os-, Co-, Fe-, and Ru-porphyrin systems. Three types of the spectra are dealt with, giving a detailed account of compounds which correspond, respectively, to a "normal type" spectrum, *i.e.* those of central metals with d and d^{10} electrons, to a "hypso type" spectrum, *i.e.* those with low spin d^5 - d^9 metal ions and to a "hyper type" spectrum, *i.e.* those with Cr(III), Mo(V), W(V), Mn(III), Re(V), Fe(III), Os(IV), and Os(VI). "Backbonding" plays an important role also in metal porphyrins. Chemical shift in H-NMR for the series of central metals follows the sequence $Fe > Mn > Cr$; for the series of axial ligands this sequence is $I > Br > Cl > N_3 > F > OPh$; the phenomenon is interpreted as a change of the π -interaction between metal and porphyrin, respectively, metal and ligand. A short survey of hemo-/hemi-chromic systems completes this chapter. 158 items from the literature are cited.

"Complexes of the Lanthanides with Neutral Oxygen Donor Ligands" is the title of the fifth article, by D. K. KOPPIKAR, P. V. SIVAPULLAIAH, L. RAMAKRISHNAN, and R. SOUNDARAJAN. The complexes are classified according to donor atoms, *viz.* C-O, N-O, P-O, As-O, S-O, Se-O. The method of preparation, the stoichiometry of the complexes, the possibilities of spatial arrangements follow. Among the techniques here applicable, vibrational spectra, *viz.* ligand-, anionic-, metal-oxygen vibrations, electron spectra, fluorescence emission spectra, H-NMR spectra and results of these are discussed, also data found by measurements of conductivity, determinations of molecular weight, and X-ray diffraction are reviewed. These complexes are formed with co-ordination numbers 6, 7, 8, 9, 10, and 12. Experimental results suggest that bonding in the complexes is chiefly electrostatic. 406 references close the article.

These five comprehensive papers offer a very good survey of the interesting topics they deal with: also this volume of the series "Structure and Bonding" is a valuable and useful addition to the scientific literature.

J. CSÁSZÁR

W. BARTKNECHT: *Explosionen — Ablauf und Schutzmaßnahmen*

Springer-Verlag, Berlin—Heidelberg—New York, 1978. 264 Seiten

Est ist schwierig die Gefahr von Explosionen für Menschen und Sachgüter einzuschätzen; die Gefahr ist um so grösser desto weniger Hinweise der eintretenden Explosion vorliegen. Zum Schutze des Lebens und materieller Güter ist es also von außerordentlicher Wichtigkeit, Explosionsgefahren dort, wo explosive Stoffe vorliegen und verarbeitet werden, erkennen, den Explosionsablauf unter Kontrolle zu halten und vor allem die Entstehung einer Explosion zu verhüten.

Das Buch "Explosionen — Ablauf und Schutzmaßnahmen" wurde mit der Absicht geschrieben, die Kenntnisse der Fachleute über das Gebiet der Sicherheitstechnik zu erweitern, und zwar nicht so sehr auf der theoretischen Ebene, als vielmehr in der alltäglichen Praxis. Der Verfasser — ein seit 25 Jahren auf diesem Gebiet tätiger Spezialist — stützt sich bei der gemeinverständlichen Beschreibung der Kennzeichen von Staubenexplosionen, auf die neuesten wissenschaftlichen Ergebnisse und technischen Erfahrungen.

Auf brennbare Gase und Dämpfe wird nur dort hingewiesen wo sich eine Gegenüberstellung, ein Vergleich als notwendig erweist. Der Verfasser tritt jedoch selbst hinsichtlich des bearbeiteten Gebietes nicht mit dem Anspruch auf Vollständigkeit auf, zumal zahlreiche Fragen noch auf ihre Klärung warten.

Einige solcher Probleme sind:

- Kennzeichen der Ausbreitung von großen entflammten Gaswolken,
- Ablauf der Explosion von brennbaren Gasen und Stäuben in mit Rohrleitungen untereinander verbundenen Behältern,
- Entwicklung eines Laboratoriumsverfahrens, das die Bestimmung von Kennwerten der Explosion von explosiblen Stäuben ermöglicht.

Das Buch ist in drei Teile gegliedert.

Im *Ersten Teil* behandelt der Verfasser die Vorbedingungen und den Ablauf von Explosionen in geschlossenen Behältern und in Rohrleitungen.

Die Heftigkeit des Ablaufs der Explosion in geschlossenen Behältern gegenwärtig für brennbare Gase und Staube mittels einer kubischen Gleichung mit hinreichender Genauigkeit annähernd bestimmt werden, falls

- a) die Art brennbaren Stoffes,
- b) der Rauminhalt des Behälters und sein Füllungsgrad mit dem explosiblen Gemisch,
- c) der Turbulenzgrad,
- d) der im Moment der Einwirkung der Zündquelle herrschende Druck sowie,
- e) die Art und Größe der Zündquelle bekannt sind.

Die berechneten Werte können auch im Laboratorium mittels kugel- oder würfelförmigen Versuchsgefäßen erhalten werden, wobei die Zündquelle im geometrischen Mittelpunkt angebracht wird. Der Rauminhalt dieser Gefäße darf bei brennbaren Gasen höchstens einen Liter betragen.

Für brennbare Staube sollen die Versuche in einer neuentwickelten Laboratoriumsanlage mit einem Rauminhalt von 1 m^3 durchgeführt werden, um wirklichkeitstreue Ergebnisse zu erhalten.

Sogenannte "Hybridgemische", bestehend aus Staub, Luft und Gas bzw. Dampf, müssen mit besonderer Aufmerksamkeit behandelt werden, selbst wenn ihre Gas- bzw. Dampfkonzentration tief unter der unteren Explosionsgrenze liegt. So kann z.B. ein nicht-explosibler Staub und ein nicht-explosibles Gas-Luftgemisch ein explosibles Hybridgemisch bilden.

Der Ablauf von Gas- und Staubexplosionen in am einen Ende geschlossenen Rohrleitungen ist stark davon abhängig, ob der Brand sich vom offenen Rohrende zum geschlossenen oder in entgegengesetzte Richtung bewegt. Der Ablauf wird außerdem durch die Art der Strömung (laminar oder turbulent), durch die Länge und den Durchmesser der Rohrleitung, durch die Verbrennungsgeschwindigkeit usw. beeinflusst.

Im zweiten Teil untersucht der Verfasser Möglichkeiten von Maßnahmen zur Verhinderung der Explosionen bzw. zur Abschwächung ihrer Auswirkungen.

Da der Leser im ersten Teil die Bedingungen der Entstehung und den Ablauf der Explosionen kennen gelernt hat, stehen nun die Daten zu Verfügung, aufgrund derer die entsprechenden Sicherheitsmaßnahmen für den Schutz der Behälter und Rohrleitungen und damit für den Schutz der gesamten Produktionsanlage ergriffen werden können.

Eine der aussichtsreichsten Methoden der Vorbeugung ist die Inertisierung. Zur Verhütung der Explosion sowohl von brennbaren Gasen als auch von brennbaren Stäuben können als Inhibitoren Stickstoff, Kohlendioxid, halogenierte Kohlenwasserstoffe, Löschpulver auf Ammoniumphosphat-Basis, in bestimmten Fällen auch Löschpulver auf Natriumhydrogencarbonat bzw. Kaliumhydrogencarbonat-Basis verwendet werden.

Ein unfachgemäßes Umgehen mit diesen Stoffen birgt jedoch die Möglichkeit einer Vergiftungsgefahr in sich.

Der Explosionsschutz von Behältern kann dadurch gewährleistet werden, daß sie aus einem Werkstoff hergestellt werden, der dem maximalen Explosionsdruck widersteht. Ist dies unmöglich, so muß irgendeine Vorrichtung zur Ableitung des bei der Explosion entstehenden Überdrucks gewählt werden. Für einmaligen Gebrauch werden zur Ableitung des Überdrucks Berstscheiben, für mehrmaligen Gebrauch Klappdeckel verwendet. Für denselben Zweck werden bei Gebäuden spaltöffnende Flächen ausgebildet.

Die verschiedenen Lösungen zum Ableiten des Überdrucks und die Methoden für ihre Dimensionierung werden im Buch ausführlich behandelt.

Vorrichtungen zum Ersticken der Explosion (im allgemeinen elektronische Vorrichtungen) sind anspruchsvoller in der Wartung, teurer und vielleicht gerade deswegen in der Industrie noch wenig verbreitet. Das Wesentliche dieser Vorrichtungen ist ein Ansprechsystem mit thermoelektrischen, optischen oder Druck-Fühler, das die Löschvorrichtungen automatisch in Betrieb setzt.

Bei Rohrleitungen und Armaturen werden ebenfalls verschiedentlich Sicherheitsvorrichtungen zur Verhinderung von Explosionen bzw. zur Abschwächung ihrer Auswirkungen angewendet, so unter anderem mechanische Feuerabschlüsse, automatische Auslösung des Löschvorgangs verschiedenartige druckableitende Ventile, Deckel usw.

Im dritten Teil des Buches werden Schutzmaßnahmen für Apparate und Anlagen behandelt. Auch hier hebt der Verfasser die sog. primären und sekundären Schutzmaßnahmen hervor, also jene, die sich auf die Vorbeugung, und jene, die sich auf die Abschwächung der Auswirkungen beziehen. Bei der Vorbeugung von Explosionen soll neben der Anwendung von Inhibitoren soweit als nur irgend möglich der Ausschluß von Zündquellen (menschliche Nachlässigkeit, Betriebs-Zündquellen wie Funken, Reibungswärme, elektrische Defekte, elektrostatische Aufladung usw.) beachtet werden.

Insofern Betriebszündquellen nicht auszuschließen sind, müssen sekundäre Schutzmaßnahmen getroffen werden: explosionssichere Konstruktionen, Vorrichtungen zum Ableiten des Explosionsüberdrucks bzw. zum Ersticken der Explosion oder eine Kombination von Feuerabschlüssen, Löschmittelauslösungen, Schnellabschlüssen, Sperren.

Die in der schemischen Industrie anzutreffenden möglichen Explosionsgefahren und die Methoden ihrer Bekämpfung erläutert der Verfasser anhand von üblichen Vorrichtungen, wie z.B. Sacköffner, Wirbelschicht-Trockner und — Mahlanlagen, Taubabtrenner-Filter usw.

Abschließend stellt der Verfasser fest, daß von absolut explosions sicheren Anlagen trotz aller Schutz — und sonstigen Maßnahmen keineswegs gesprochen werden kann. Es besteht stets ein Gefahrenrisiko dessen Größe zahlenmäßig kaum bestimmt werden kann. Inwiefern die bestehende Gefahr noch "erträglich" ist, hängt von den Erfahrungen und den Ergebnissen von systematischen experimentellen Untersuchungen ab. Keineswegs kann jedoch geduldet werden, daß Produktion und Wirtschaftlichkeit um jeden Preis über die Betriebssicherheit gestellt werden.

K. KITTRICH

Springer Series in Chemical Physics 3

Advances in Laser Chemistry

Ed. A. H. ZEWEIL, Springer-Verlag, Berlin—Heidelberg—New York, 1978

463 pages, 242 figures

The book contains the Proceedings of the Conference on Advances in Laser Chemistry held at the California Institute of Technology, Pasadena, March 20—22, 1978. Divided into five sections, it gives an account on the recent applications of lasers in chemistry.

The first chapter, "Laser Induced Chemistry" deals with chemical reactions induced or enhanced by laser radiation. The introductory plenary lecture by S. A. RICE summarizes our knowledge on the internal energy transfer in isolated molecules, which is of particular importance in interpreting the results of laser induced chemical reactions. Contributed papers report on laser synthetic chemistry, photogeneration of catalysts, isotope enrichment. Several speakers treated the questions outlined in the plenary lecture in detail, presenting data on the partitioning of electronic, vibrational, rotational and translational energies in unimolecular processes.

The second section of the book is devoted to picosecond processes and techniques. The plenary lecture by R. M. HOCHSTRASSER comprises several closely correlated topics, involving picosecond excitation and detection. The paper of ROBINSON *et al.* is a valuable summary of how a picosecond system should be set up. Picosecond phenomena are of particular importance in the following areas: early stages of bacterial photosynthesis, mechanism of vision (photo-reaction of rhodopsin), formation dynamics of charge transfer complexes and laser dye characteristics. Information about solvent structure is deduced from measurements of picosecond chromodynamics of electrons.

The third chapter, entitled "Non-Linear Optical Spectroscopy and Dephasing Processes", starts with the theory of optical dephasing in condensed phases, delivered by K. E. JONES and A. H. ZEWEIL. Relatively little experimental work is reported on dephasing processes. On the other hand a handful of novel spectroscopic methods is shown to yield valuable information. Coherent Anti-Stokes Raman Spectroscopy is utilized in many cases, and the thermal lensing or thermal blooming method is frequented also. These new techniques, with their exceptionally high resolving power in the visible part of the spectrum are growing in importance in order to obtain basic parameters of relatively simple molecules.

The next section deals with multiphoton excitation. Once again the fate of the absorbed energy, *i.e.* its partitioning between different states is a major problem of the field. The plenary lecture by R. A. MARCUS, D. W. NOID and M. L. KOSZYKOWSKI discusses the theoretical aspects of the problem. Multiphoton ionization spectroscopy, Doppler-free two photon spectroscopy, two photon spectroscopy combined with intracavity dye laser detection are the main areas which may be of interest to spectroscopists.

The last chapter is devoted to molecular dynamics by molecular beams. The plenary lecture by R. B. BERNSTEIN presents the possibilities of the utilization of lasers in molecular beam experiments. Attention is focused on the so-called van der Waals molecules (*e.g.* ArI₂). New and improved techniques are discussed for the study of fast desorption processes from metal surfaces.

Altogether the book is devoted to new techniques employing lasers, therefore, the most important application of lasers, *viz.* isotope enrichment does not receive special attention, because of its well-known utilization. The conference supports the opinion that lasers alone will not solve certain chemical problems of interest, but might prove to be a nearly ideal tool in studying them.

The book gives an excellent cross-section of the work done in the field on the western hemisphere — it is highly regrettable that the outstanding results of the Soviet and French scientists are missing.

Everyone who is interested in the developments of spectroscopic techniques and of reaction dynamics should read this book, because its fast publication assures the availability of up-to-date research ideas and results.

T. VIDÓCZY

Springer series in Chemical Physics 4

Picosecond Phenomena

Ed. C. V. SHANK, E. P. IPPEN, S. L. SHAPIRO

Springer-Verlag, Berlin—Heidelberg—New York, 1978

359 pages, 222 Figures

The book contains the Proceedings of the First International Conference on Picosecond Phenomena, held at Hilton Head, South Carolina, May 24–26, 1978. The conference was organized as a Topical Meeting of the Optical Society of America, and brought together scientists dealing with widely varying disciplines who shared a common interest in studying ultrafast processes.

The book is divided into nine sections — six of these are dedicated to special areas, two parts present poster sections and the last chapter is for the postdeadline papers.

The first section, "Interactions in Liquids and Molecules", and the following poster section might prove to be the most interesting to chemists. There are papers dealing with new techniques for measuring Raman dephasing dynamics and transient optical phenomena. A very active area is the study of the kinetics of light absorption and events taking place immediately afterwards. The techniques employed differ essentially and they are interesting in themselves.

In some cases experiment seems to be ahead of theory, *e.g.* two-pulse spectra (spectra taken with two simultaneous pulses of different wavelengths) are readily obtained, but the information contained them is not fully understood as yet. It is possible to capture clearly unrelaxed spectra of the excited states of aromatic molecules. Fluorescence spectroscopy on a subpicosecond time scale is reported, yielding data about short-lived upper states. K. B. EISENTHAL commented on the picosecond chemistry of two small elementary particles: the electron and the proton.

The third chapter gives an account on sources and techniques tunability being the most important feature of the sources discussed. Anti-Stokes emission can serve as a source of vacuum UV and even soft X-ray radiation.

Biological processes are discussed in the following chapter. As most of the papers deal with photosynthesis, it is evident that this part is as interesting for chemists as for biologists.

The following poster section seems to collect those papers which could not be put elsewhere — their subject ranges from ultrafast electrical switching to the design of a planar streak camera.

Coherent techniques are collected in the sixth section. Papers on widely different areas are included, *e.g.* electron localization in liquids, vibrational relaxation in SF_6 .

Solids are treated in the seventh chapter, mostly involving semiconductor materials.

The eight chapter is devoted to high power lasers and plasmas. Interesting considerations are reported for designing a master oscillator for laser fusion research, and fifth harmonic generation is considered as a source of extreme UV radiation. Plasma diagnostics with the aid of lasers are discussed.

From the postdeadline papers (last chapter) the work of S. L. SHAPIRO on excited states proton transfer reactions, the so-called laser pH jump technique should be mentioned.

The diversity of the themes is reflected in the poor dividing of the papers into chapters. It is impossible to give a full picture on the research involving ultrafast processes, nevertheless the effort of the organizers of the conference (Editors of the book) to include as many areas of interest as possible succeeded in a truly international and interdisciplinary conference.

The fast publication of the book, a credit to Springer-Verlag, ensures the availability of up-to-date information in the field. The book cannot be considered as a reference book, rather as an outstanding collection of ideas and techniques.

T. VIDÓCZY

Curt WENTRUP: *Reaktive Zwischenstufen I und II*

G. Thieme Verlag, Stuttgart, 1979

459 Seiten, Taschenbuch-Format

Dass organisch-chemische Reaktionen nicht unbedingt direkt zu den Produkten führen müssen, sondern auch über Zwischenstufen verlaufen können, weiss man schon lange (s. z.B. die Hughes-Ingold'schen Arbeiten über S_N1 - und $E1$ -Reaktionen, die Wheland'sche Lehre über die intermediären σ -Komplexe bei der S_E -Ar-Reaktion, die Franciscischen und Zelinski'schen Arbeiten über gemischte Additionen an Olefine, die Roberts-Kimballsche Lehre über cyclische Halonium-Ionen usw.). Eine wirklich stürmische Entwicklung unseres Wissens über die reaktiven Zwischenstufen der organischen Chemie setzte jedoch erst etwa Ende der sechziger Jahre ein. Sie wurde, paradoxerweise, u.a. durch die Formulierung des Begriffs der cyclischen Elektronverschiebungen und der konzertierten (dh. *nicht* über Zwischenstufen verlaufenden) pericyclischen Reaktionen und der Aufklärung ihrer Besonderheiten (Woodward-Hoffmann-Regeln) angeregt und durch die Entdeckung neuer Untersuchungsmethoden (NMR, ESR, CIDNP, spin trapping, ESCA usw.) ermöglicht. Diese stürmische Entwicklung schlug und schlägt sich notwendigerweise u.a. in einer ansehnlichen Reihe von Monographien und Handbüchern über reaktive Zwischenstufen nieder.

Das vorliegende Werk von C. WENTRUP — Band 8 und 9 der Serie A, "Theoretische und allgemeine Gebiete" des Taschenlehrbuches der organischen Chemie des Verlags G. Thieme — ist die neueste Erscheinung auf diesem Gebiet. Wenn kurz nach dem Erscheinen in verhältnismässig rascher Folge von $n-1$ Zusammenfassungen über ein bestimmtes Gebiet auch noch eine n -te erscheint, muss die Frage, ob dies tatsächlich notwendig war, unbedingt auftauchen. In Anbetracht einiger Besonderheiten des vorliegenden Werkes glaube ich, diese Frage mit ja beantworten zu dürfen.

Besonders wichtig in diesen Zusammenhang ist meines Erachtens, dass neun von den insgesamt zehn Kapiteln von ein und demselben Autor, einem Spezialisten dieses Gebietes, bekannt vor allem durch seine Arbeiten über Carbene und Nitrene, verfasst worden sind. (Das Kapitel über Carbokationen hat P. VOGEL geschrieben.) Dies ermöglichte unbedingt eine bessere Herausarbeitung der Zusammenhänge und Analogien sowie die Vermeidung von überflüssigen Wiederholungen. Sehr zu begrüßen ist weiterhin, dass der Autor sich der Mühe nicht gescheut hat, das Wesen und die Theorie der auf dem betrachteten Gebiet angewandten neueren Untersuchungsmethoden wie ESR und CIDNP kurz zu beschreiben. Und nicht zuletzt: der Preis der beiden Bände ist im Verhältnis dazu, was in ihnen geboten wird, angebracht.

Das Werk ist in erster Linie als Lehrbuch für fortgeschrittene Studenten, Doktoranden, aber auch für den Forschungsschemiker gedacht und besteht aus den folgenden 10 Kapiteln: 1. Allgemeine Prinzipien (14 Seiten), 2. Radikale (94 Seiten), 3. Biradikale (27 Seiten), 4. Carbene und Nitrene (67 Seiten), 5. Gespannte Ringe (23 Seiten), 6. Antiaromatische Systeme (11 Seiten), 7. Carbokationen (122 Seiten), 8. Carbanionen (28 Seiten), 9. Zwitterionen (14 Seiten) und 10. Schlussbemerkungen (10 Seiten). Zu jedem Kapitel gehört eine Liste von Literaturzitaten (insgesamt fast 500 Zitate; die Literatur wurde bis Ende 1976 berücksichtigt, einige wichtigere Arbeiten aus dem Jahr 1977 wurden ebenfalls zitiert). Das Buch schliesst mit einem ausführlichen Sachregister (39 Seiten).

Beschrieben werden in jedem Kapitel die Bildung, die Charakterisierung und die Reaktionen des betreffenden Typs der organischen Zwischenstufen sowie die benutzten Untersuchungs- und Charakterisierungsmethoden. Die wichtigeren physikalischen Daten sind insgesamt 28 Tabellen zusammengestellt. Am eingehendsten werden die Radikale, die Carbene und Nitrene sowie die Carbokationen besprochen, was der Bedeutung dieser Zwischenstufen auch entspricht. Die besonders in der Photochemie wichtigen Biradikale (warum eigentlich nicht Diradikale nach dem Muster Dikation und Dianion?), über welche unser Wissen in der letzten Zeit sich rasch bereichert, und die Carbanionen scheinen mir jedoch dabei etwas zu kurz zu kommen. Nitrenium- und die noch diskutierten Oxenium-Ionen werden überhaupt nicht erwähnt; die Radikalanionen, deren Bedeutung ständig zunimmt ($S_{RN}1$ -Reaktionen!), werden zwar verschiedentlich erwähnt, aber in einer Neuauflage sollte letzteren vielleicht ein eigenes Kapitel gewidmet werden.

Der Stoff ist gut verständlich dargestellt, Druck und Papier und überhaupt die Qualität der Ausstattung sind gut; leider ist jedoch die Anzahl der nicht ganz präzisen Formulierungen und der auch nach eigener Erfahrung gänzlich nicht vermeidbaren, aber in einem *Lehrbuch* ganz besonders störenden Druckfehler relativ hoch. Die folgende, sicherlich unvollständige Liste möge als Beleg für diese Behauptung dienen und die Überarbeitung des Textes für eine spätere Neuauflage — ich bin davon überzeugt, dass das Werk mehrere Auflagen erleben wird — erleichtern.

Auf S. 12., Zeile 1–3, wird ein hypothetisches Cyclohexatrien *ohne Resonanz*, jedoch trotzdem mit konjugativen Effekten zwischen den Doppelbindungen erwähnt — ist dies kein innerer Widerspruch? In Formel 5 auf S. 22 fehlen die p -ständigen t -Butyl-Substituenten der beiden Phenyl-Gruppen unten. In Fussnote b) auf S. 23 lautet der Name des dritten Autors NAUTA, nicht NANTA. Formel 23 auf S. 35 ist unrichtig: beide β -ständigen H-Atome befinden sich in Wirklichkeit hinter der Zeichenebene, das eine oberhalb, das andere unterhalb der Ebene der drei C-Atome. Die perspektivische Formel 37 auf S. 37 ist stark verzerrt wiedergegeben, wie auch die der Ausgangsverbindung im selben Formelschema. Als Elementensymbol für Jod wird bald J (S. 52, erstes Formelschema), bald I (S. 53, Tabelle 2.7) verwendet. In Gleichung (8) auf S. 58 handelt es sich um Acyloxy-, nicht um Acyl-Radikale, ebenso in Zeile 1, S. 59. Azo-Verbindungen werden öfters Diazo-Verbindungen genannt (S. 67, Zeile 3 und 6; S. 72, letzte Zeile; S. 116, Zeile 11 und letzte Zeile; S. 134, Zeile 2). Aus den in Tabelle 2.17 für die verschiedenen Stellungen des Pyrimidin-Radikalanions angegebenen Werten der Hyperfein-Kopplungskonstanten a_H folgt zwar (wie auf S. 103, oben, bemerkt), dass in der nucleophilen Substitution des Pyrimidin-Moleküls — in Übereinstimmung mit der Erfahrung — Stellung 4 gegenüber Stellung 2 bevorzugt sein sollte; doch würde man aufgrund der in der Tabelle angegebenen a_H -Werte des Pyridin-Radikalanions für das Pyridin-Molekül das gleiche erwarten, was aber — wenigstens für die Reaktion mit Amid-Anionen — der Erfahrung widerspricht. Ein Hinweis auf, geschweige denn eine Erklärung für diese Diskrepanz fehlen leider — oder sollten die angegebenen a_H -Werte unrichtig sein? In der gleichen Tabelle ist weiterhin der $a_H(3)$ -Wert des Pyridazin-Radikalanions in die falsche Spalte geraten. In Zeile 3 sowie im ersten Formelschema auf S. 132 wird das 1,2-Diazetin fälschlicherweise als 1,2-Diazet bezeichnet. Formel 46 auf S. 133 ist keine mesomere Grenzformel, während die darüber stehende Formel eine Grenzformel desselben Biradikals darstellt; das Zeichen der Mesomerie zwischen diesen beiden Formeln ist demnach nicht angebracht. Das Gleiche gilt für das Zeichen der Mesomerie zwischen Formel 53d auf S. 343 und der darunter stehenden Grenzformel; und auch die auf S. 397 unten links abgebildete Formel ist keine Grenzformel und steht daher mit den drei anderen Formeln im gleichen Formelschema *nicht* im Verhältnis der Mesomerie. Auf S. 157, oben, wird das Problem diskutiert, auf welche Weise man entscheiden kann, ob ein Produkt der Reaktion einer Diazoverbindung, welches sich im Prinzip über eine Carben-Zwischenstufe ableiten lässt, auch tatsächlich über eine solche entsteht; als Beispiel wird die Reaktion eines Azids angeführt. In der 2. Zeile unter dem Formelschema auf S. 190 fehlt das Subscript 2 in der Formel des Carbens: CF_2 . Auf S. 191 liest man über 1,3-Triplett-Radikale statt 1,3-Triplett-Biradikale. Aus dem Befund, dass die Photolyse von zwei verschiedenen *mono*-deutierten Ausgangsverbindungen zum gleichen Deuterocyclobutadien führte folgt — im Gegensatz dazu, was man auf S. 233 liest — nicht, dass die statische rechteckige Strukturalternative des Cyclobutadiens ausgeschlossen werden kann; dies folgt erst aus den (übrigens ebenfalls in der zitierten Arbeit beschriebenen) analogen Resultaten bei der Photolyse der entsprechenden *di*-deutierten Ausgangsverbindungen. In der Formel des *n*-Propyl-Radikals (zweites Formelschema, S. 250) fehlt das Subscript 2. Die Formel des Protoadamantyl-Produktes (zweites Formelschema, S. 277) enthält eine falsch eingezeichnete C—C-Bindung. In den beiden letzten Formeln auf S. 278 fehlt je ein R-Substituent. Im Formelschema auf S. 327 sollten in den beiden letzten Formeln die Symbole -Tos durch -OTos ersetzt werden. Die im Formelschema auf S. 340 besprochenen beiden Reaktionen können zwar über die gleiche

Zwischenstufe, nicht aber (wie unrichtigerweise dargestellt) über den gleichen, zu dieser Zwischenstufe führenden Übergangszustand verlaufen; die Formel in eckigen Klammern ist der Übergangszustand der Solvolyse des Cholesteryl-, nicht aber des Cyclocholestanyl-Derivates. Die Numerierung des Ringsystems in Formel 62 auf S. 341 ist falsch; daher ist der Ausdruck $\pi_{C-2,3}$ -Beteiligung im Formelschema unverständlich; in der 6. Zeile unter dem Formelschema sollte es C-2,3-statt C-1,2- π -Bindung heissen, ebenso zwei Zeilen später C-2,3-HOMO statt C-1,2-HOMO. In der folgenden Zeile wird die Stabilisierungsenergie mit ϵ , in dem entsprechenden MO-Diagramm (Fig. 7.12 S. 343) mit $\delta\epsilon$ bezeichnet. In der zweiten Formel oben auf S. 348 fehlt ein H-Atom. Die Mehrzahl der auf S. 363 und 364 aufgezählten Lösungsmittel ist nicht indifferent und kommt für die Darstellung von metallorganischen Verbindungen bzw. den entsprechenden Carbanionen nicht in Frage. Für die Deprotonierung des Malonesters ist die Wahl von Natriumhydroxid (S. 375, erstes Formelschema) weniger glücklich. In der Formel des Übergangszustandes der Reaktion von $HgBr_2$ mit der quecksilberorganischen Verbindung fehlt ein Brom-Atom (S. 381, zweites Formelschema); störend wirkt hier ausserdem, dass zur Symbolisierung einerseits der in Spaltung bzw. Bildung begriffenen, andererseits der hinter die Zeichenebene weisenden, durch die Reaktion nicht betroffenen Bindungen die gleichen gestrichelten Linien benutzt werden. Schlimmer ist, dass zudem aus dem angegebenen Beispiel streng genommen eigentlich gar keine Schlüsse über die Stereochemie der Substitution gezogen werden können! (100% Retention könnte auch dann beobachtet werden, wenn regio-selektive Spaltung der zur Isopropylgruppe führenden $Hg-C$ -Bindung stattfinden würde.) In der zitierten Arbeit wurde die Reaktion einer anderen Verbindung, nämlich des (–)-*sec*. Butyl-(+)-*sec*.butylquecksilbers mit $HgBr_2$ untersucht und aus den erhaltenen Resultaten konnte dann tatsächlich auf 100% Retention geschlossen werden. In Zeile 1, S. 389 liest man über eine "optisch aktive CR_3 -Gruppe" (*sic!*).

Schliesslich noch ein Vorschlag für die künftige Neuauflage: eine Liste der benutzten, meist thermochemische Symbole würde die Benutzung des Werkes sehr erleichtern.

K. LEMPert

INDEX

PHYSICAL AND INORGANIC CHEMISTRY

Electrochemical Behaviour of Ethylene Glycol and its Oxidation Products on a Platinum Electrode, V. Experimental Study of Electro-Oxidation and Oxidation Products of Glycolaldehyde and Glycolic Acid, Gy. INZELT, Gy. HORÁNYI	215
Electrochemical Behaviour of Ethylene Glycol and its Oxidation Derivatives on a Platinum Electrode, VI. Oxidation of Ethylene Glycol, Gy. INZELT, Gy. HORÁNYI ...	229
Investigations on the Association of Pentanol Isomers in Liquid Phase, F. RATKOVICS, T. SALAMON	241
Ideal Gas Thermodynamic Properties for $\text{CH}_3\text{O} \cdot$ and $\cdot\text{CH}_2\text{OH}$ Radicals, A. BURCAT, S. KUDCHADKER	249
IR Spectra of Hydrocarbons Chemisorbed on Transition Metals, I. The Infrared Cell and Chemisorption of Ethylene on Ni/SiO_2 Catalyst, T. SZILÁGYI, A. SÁRKÁNY, J. MINK, P. TÉTÉNYI	259
Modelling of the Thermal Decomposition of Hydrocarbons, V. ILLÉS, O. SZALAI	267

ORGANIC CHEMISTRY

Investigations of the Complex Proteins of Wheat, R. LÁSZTITY, F. BÉKÉS, J. NEDELKOVITS, J. VARGA	281
RECENSIONES	297

Printed in Hungary

A kiadásért felel az Akadémiai Kiadó igazgatója

Műszaki szerkesztő: Zacsik Annamária

A kézirat nyomdába érkezett: 1979. III. 6. — Terjedelem: 8,4 (A/5) ív, 32 ábra

79.6917 Akadémiai Nyomda, Budapest — Felelős vezető: Bernát György

РЕЗЮМЕ

Электрохимическое поведение этиленгликоля и его окисленных производных на платиновом электроде, V

Исследование электроокисления гликольальдегида и гликолевой кислоты, и продукты их окисления
ДЬ. ИНЗЕЛЪТ и ДЬ. ХОРАНИ

Электроокисление гликолевой кислоты и гликольальдегида было исследовано на электроде платинированной платины в 1М-ом растворе HClO_4 . На начальном участке стационарной потенциостатической поляризационной кривой наблюдалось две ступени. Это было свойственно и поляризационным кривым, полученным ранее в исследованиях с глиоксалем и глиоксальной кислотой. На основе аналогии и в данном случае полагаем, что появление ступеней объясняется, с одной стороны, ингибиционным влиянием вследствие хемосорбции, а с другой стороны, изменением глубины окисления. Опираясь на результаты различных аналитических методов, было установлено, что в случае гликольальдегида и при не слишком высоких потенциалах доминирует процесс с переходом два F на каждый моль. В результате этого, в большинстве образуется глиоксаль и лишь в меньшей степени глиоксальная кислота. С повышением потенциала в фазе раствора среди продуктов реакции все в большей степени была обнаружена щавелевая кислота, а при потенциалах, соответствующих второй ступени, конечным продуктом реакции является двуокись углерода.

В случае гликолевой кислоты в интервале потенциалов, соответствующий первой ступени, в растворе были найдены глиоксальная и щавелевая кислоты, а при потенциалах, соответствующих второй ступени, опять-таки образование двуокиси углерода становится доминирующим.

Электрохимическое поведение этиленгликоля и его окисленных производных на платиновом электроде, VI**Окисление этиленгликоля**

ДЬ. ИНЗЕЛЪТ и ДЬ. ХОРАНИ

Электроокисление этиленгликоля было исследовано в кислой среде на электроде платинированной платины. В противоположность более ранним литературным заключениям было установлено, что на первой ступени реакции окисления образуется гликольальдегид, и использование тока по отношению к гликольальдегиду, при не слишком высоких положительных потенциалах, может достигать 70—80%-ов. Дальнейшее окисление гликольальдегида приводит к образованию глиоксаля, глиоксальной кислоты и щавелевой кислоты. На основе этого следует изменить более ранние представления относительно механизма окисления этиленгликоля. Опираясь на более ранние результаты дальнейшего окисления окисленных продуктов этиленгликоля, ход потенциостатических поляризационных кривых объясняли тем, что реакция дегидрирования, приводящая к образованию гликольальдегида, не зависит от электродного потенциала, однако, покрытие хемисорбированными молекулами, образующимися в побочной реакции, т. е. размеры мест, доступных для реакции, зависят от электродного потенциала.

Исследование ассоциации изомеров пентанола в жидкой фазе

Ф. РАТКОВИЧ и Т. ШАЛАМОН

Вязкость семи изомеров пентанола была исследована в интервале температур 20—70°C. Была рассчитана энтальпия активация ламинарного течения, которая увеличивается с числом разветвлений: от *n*-пентанола (20,4 кдж/моль) до 2,2-диметилпропан-1-ола (30,3 кдж/моль). Исходя из исследований смесей 1-метилбутана и 1,1-диметилпропана с *n*-гексаном, можно заключить, что энтальпия активация ламинарного течения зависит от средней степени ассоциации спиртов (также и в случае изомеров) таким же образом, как это было найдено и для нормальных спиртов. Было найдено, что изомеры, содержащие больше разветвлений обладают более высокой общей степенью ассоциации. Это объясняется повышенным экранированием, вследствие разветвлений углеродной цепочки что стерически препятствует образованию циклических молекул, в результате чего образуются ассоциированные мультимеры с более длинными цепочками.

Термодинамические свойства радикалов $\text{CH}_3\text{O}\cdot$ и $\cdot\text{CH}_2\text{OH}$ как идеальных газов

А. БЁРКЭТ и Ш. КУДЧАДКЕР

Термодинамические свойства $\text{CH}_3\text{O}\cdot$ и $\cdot\text{CH}_2\text{OH}$ рассчитаны из относенных колебаний метанола. Полученные величины сравниваются с более ранними расчетами, произведенными другими методами.

ИК спектры углеводов, адсорбированных на переходных металлах, I

ИК камера и хемосорбция на катализаторе Ni/SiO_2

Т. СИЛАДИ, А. ШАРКАНЬ, Й. МИНК и П. ТЕТЕНИ

Описывается кювета, используемая для исследований ИК спектров адсорбированного этилена. Этилен был хемосорбирован при 55 и 150°C на никелевом катализаторе, нанесенном на SiO_2 . Согласно спектрам, на поверхности имеются соединения лишь с б-связью. Некоторые характерные свойства спектров адсорбированного этилена объяснялись на основе исследований реакционной способности поверхностных соединений с водородом.

Моделирование термического разложения углеводов

В. ИЛЛЕШ и О. САЛАИ

На основе обобщенного механизма разложения углеводов дряда нормальных парафинов, была составлена кинетическая модель, описывающая термическое разложение. При составлении модели полагали, что в реакции отрыва H принимают участие атомы водорода, метильные и этильные радикалы, а радикалы больные, чем этил, принимают участие исключительно в реакции разложения. Среди вторичных реакций принимали во внимание ингибирующие реакции пропилена, как продукта и в качестве обрыва цепи — рекомбинации метильных и этильных радикалов.

Конкретное применение кинетической модели демонстрируется на примере экспериментов пиролиза *n*-бутана. Согласие измеренных и рассчитанных из теоретической модели данных является удовлетворительным во всем интервале конверсий.

Рассматривая кинетическую зависимость, описывающую термическое разложение, можно видеть, что кинетический порядок выражения, описывающего разложение исходного вещества, с повышением температуры постепенно уменьшается от 3/2 до единицы.

Исследование комплексов белков пшена

Р. ЛАСТИТИ, Р. БЕКЕШ, Й. НЕДЕЛКОВИЧ и Й. ВАРГА

Были исследованы белки пшена: липопротейн (липопуротионин), растворимый в петролейном эфире, гликолипопротеины, растворимые в смеси хлороформа с метанолом, и гликопротеины, растворимые в воде.

Были определены электрофоретические свойства, содержание аминокислот иири-рода липоида, а также углеводные компоненты. Был также исследован характер взаимодействий белок-липоид.

Результаты подтверждают то заключение, что за счет электростатических взаимодействий, между многочисленными полярными боковыми цепями белков и полярными фосфо- или гликолипоидами образуется комплекс. Нельзя исключить и эффект гидрофобных взаимодействий.

Les Acta Chimica paraissent en français, allemand, anglais et russe et publient des mémoires du domaine des sciences chimiques.

Les Acta Chimica sont publiés sous forme de fascicules. Quatre fascicules seront réunis en un volume (4 volumes par an).

On est prié d'envoyer les manuscrits destinés à la rédaction à l'adresse suivante:

Acta Chimica
Budapest, P.O. Box 67, H-1450, Hongrie

Toute correspondance doit être envoyée à cette même adresse.

La rédaction ne rend pas de manuscrit.

Le prix de l'abonnement: \$ 36,00 par volume.

Abonnement en Hongrie à l'Akadémiái Kiadó (1363 Budapest, P. O. B. 24, C. C. B. 215 11488), à l'étranger à l'Entreprise du Commerce Extérieur «Kultura» (H-1389 Budapest 62, P. O. B. 149 Compte-courant No. 218 10990) ou chez représentants à l'étranger.

Die Acta Chimica veröffentlichen Abhandlungen aus dem Bereich der chemischen Wissenschaften in deutscher, englischer, französischer und russischer Sprache.

Die Acta Chimica erscheinen in Heften wechselnden Umfanges. Vier Hefte bilden einen Band. Jährlich erscheinen 4 Bände.

Die zur Veröffentlichung bestimmten Manuskripte sind an folgende Adresse zu senden

Acta Chimica
Budapest, Postfach 67, H-1450, Ungarn

An die gleiche Anschrift ist jede für die Redaktion bestimmte Korrespondenz zu richten. Manuskripte werden nicht zurückerstattet.

Abonnementspreis pro Band: \$ 36,00.

Bestellbar für das Inland bei Akadémiái Kiadó (1363 Budapest, Postfach 24, Bankkonto Nr. 215 11488), für das Ausland bei «Kultura» Außenhandelsunternehmen (H-1389 Budapest 62, P. O. B. 149. Bankkonto Nr. 218 10990) oder seinen Auslandsvertretungen.

«Acta Chimica» издают стихи по химии на русском, английском, французском и немецком языках.

«Acta Chimica» выходит отдельными выпусками разного объема, 4 выпуска составляют один том и за год выходят 4 тома.

Предназначенные для публикации рукописи следует направлять по адресу:

Acta Chimica
Budapest, P.O. Box 67, H-1450, BHP

Всякую корреспонденцию в редакцию направляйте по этому же адресу.

Редакция рукописей не возвращает.

Подписная цена — \$ 36,00 за том.

Отечественные подписчики направляйте свои заявки по адресу Издательства Академии Наук (1363 Budapest, P.O.B. 24, Текущий счет 215 11 188), а иностранные подписчики через организацию по внешней торговле «Kultura» (H-1389 Budapest 62, P.O.B. 149. Текущий счет 218 10990) или через ее заграничные представительства и уполномоченных.

Reviews of the Hungarian Academy of Sciences are obtainable
at the following addresses:

AUSTRALIA

C.B.D. LIBRARY AND SUBSCRIPTION SERVICE,
Box 4886, G.P.O., Sydney N.S.W. 2001
COSMOS BOOKSHOP, 145 Ackland Street, St.
Kilda (Melbourne), Victoria 3182

AUSTRIA

GLOBUS, Höchstädtplatz 3, 1200 Wien XX

BELGIUM

OFFICE INTERNATIONAL DE LIBRAIRIE, 30
Avenue Marnix, 1050 Bruxelles
LIBRAIRIE DU MONDE ENTIER, 162 Rue du
Midi, 1000 Bruxelles

BULGARIA

HEMUS, Bulvar Ruski 6, Sofia

CANADA

PANNONIA BOOKS, P.O. Box 1017, Postal Sta-
tion "B", Toronto, Ontario M5T 2T

CHINA

CNPICOR, Periodical Department, P.O. Box 50,
Peking

CZECHOSLOVAKIA

MAĎARSKÁ KULTURA, Národní třída 22,
115 66 Praha
PNS DOVOZ TISKU, Vinohradská 46, Praha 2
PNS DOVOZ TLAČE, Bratislava 2

DENMARK

EJNAR MUNKSGAARD, Norregade 6, 1165
Copenhagen

FINLAND

AKATEEMINEN KIRJAKAUPPA, P.O. Box 128,
SF-00101 Helsinki 10

FRANCE

EUROPERIODIQUES S.A., 31 Avenue de Ver-
sailles, 7 170 La Celle St.-Cloud
LIBRAIRIE LAVOISIER, 11 rue Lavoisier, 7500
Paris
OFFICE INTERNATIONAL DE DOCUMENTA-
TION ET LIBRAIRIE, 48 rue Gay-Lussac, 75240
Paris Cedex 65

GERMAN DEMOCRATIC REPUBLIC
HAUS DER UNGARISCHEN KULTUR, Karl-
Liebknecht-Strasse 9, DDR-102 Berlin
DEUTSCHE POST ZEITUNGSVERTRIEBSAMT,
Strasse der Pariser Kommune 3-4, DDR-104 Berlin

GERMAN FEDERAL REPUBLIC

KUNST UND WISSEN ERICH BIEBER, Postfach
46, 7000 Stuttgart 1

GREAT BRITAIN

BLACKWELL'S PERIODICALS DIVISION, Hythe
Bridge Street, Oxford OX1 2ET
BUMPUS, HALDANE AND MAXWELL LTD.,
Cowper Works, Olney, Bucks MK46 4BN
COLLET'S HOLDINGS LTD., Denington Estate,
Wellingborough, Northants NN 2QT
WM. DAWSON AND SONS LTD., Cannon House,
Folkestone, Kent CT19 5EE
H. K. LEWIS AND CO., 136 Gower Street, London
WC1E 6BS

GREECE

KOSTARAKIS BROTHERS, International Book-
sellers, 2 Hippokratous Street, Athens-143

HOLLAND

MEULENHOF-BRUNA B.V., Beulingstraat 2,
Amsterdam
MARTINUS NIJHOFF B.V., Lange Voorhout 9-11,
Den Haag

SWETS SUBSCRIPTION SERVICE, 347b Heere-
weg, Lisse

INDIA

ALLIED PUBLISHING PRIVATE LTD., 13/14
Asaf Ali Road, New Delhi 110001
150 B-6 Mount Road, Madras 600002
INTERNATIONAL BOOK HOUSE PVT. LTD.,
Madame Cama Road, Bombay 400039
THE STATE TRADING CORPORATION OF
INDIA LTD., Books Import Division, Chandralok,
36 Janpath, New Delhi 110001

ITALY

EUGENIO CARLUCCI, P.O. Box 252, 70100 Bari
INTERSCIENTIA, Via Mazzè 28, 10149 Torino
LIBRERIA COMMISSIONARIA SANSONI, Via
Lamarmora 45, 50121 Firenze
SANTO VANASIA, Via M. Macchi 58, 20124
Milano
D. E. A., Via Lima 28, 0019 Roma

JAPAN

KINOKUNIYA BOOK-STORE CO. LTD., 17-7
Shinjuku-ku 3 chome, Shinjuku-ku, Tokyo 160-91
MARUZEN COMPANY LTD., Book Department,
P.O. Box 5050 Tokyo International, Tokyo 100-31
NAUKA LTD. IMPORT DEPARTMENT, 2-30-19
Minami Ikebukuro, Toshima-ku, Tokyo 171

KOREA

CHULPANMUL, Phenjan

NORWAY

TANUM-CAMMERMEYER, Karl Johansgatan
41-43, 1000 Oslo

POLAND

WĘGIERSKI INSTYTUT KULTURY, Marszał-
kowska 80, Warszawa
CKP 1 W ul. Towarowa 28 00-95 Warszawa

ROUMANIA

D. E. P., Bucuresti
ROMLIBRI, Str. Biserica Amzei 7, Bucuresti

SOVIET UNION

SOJUZPETCHATJ - IMPORT, Moscow
and the post offices in each town
NEZHDUNARODNAYA KNIGA, Moscow G-200

SPAIN

DIAZ DE SANTOS, Lagasca 95, Madrid 6

SWEDEN

ALMQVIST AND WIKSELL, Gamla Brogatan 26,
S-101-20 Stockholm
GUMPERTS UNIVERSITETSBOKHANDEL AB,
Box 346, 401 25 Göteborg 1

SWITZERLAND

KARGER LIBRI AG, Petersgraben 31, 4071 Basel

USA

EBSCO SUBSCRIPTION SERVICES, P.O. Box
1943, Birmingham, Alabama 35201
F. W. FAXON COMPANY, INC., 15 Southwest
Park, Westwood, Mass. 02090
THE MOORE-COTTRELL SUBSCRIPTION
AGENCIES, North Cohocton, N.Y. 14 6
READ-MORE PUBLICATIONS, INC., 140 Cedar
Street, New York, N. Y. 10006
STECHELT-MACMILLAN, INC., 7250 Westfield
Avenue, Pennsauken N.J. 0 110

VIETNAM

XUNHASABA, 32, Hai Ba Trung, Hanoi

YUGOSLAVIA

JUGOSLAVENSKA KNJIGA, Terazije 27, Beograd
FORUM, Vojvode Mišića 1, 21000 Novi Sad

ACTA CHIMICA

ACADEMIAE SCIENTIARUM HUNGARICAE

ADIVVANTIBUS

M. T. BECK, R. BOGNÁR, V. BRUCKNER,
GY. HARDY, K. LEMPÉRT, F. MÁRTA,
K. POLINSZKY, E. PUNGOR,
G. SCHAY, Z. G. SZABÓ, P. TÉTÉNYI

REDIGUNT

B. LÉNGYEL, et GY. DEÁK

TOMUS 101

FASCICULUS 4



AKADÉMIAI KIADÓ, BUDAPEST

1979

ACTA CHIM. ACAD. SCI. HUNG.

ACASA2 101 (4) 309-419 (1979)

ACTA CHIMICA

A MAGYAR TUDOMÁNYOS AKADÉMIA
KÉMIAI TUDOMÁNYOK OSZTÁLYÁNAK
IDEGEN NYELVŰ KÖZLEMÉNYEI

FŐSZERKESZTŐ
LENGYEL BÉLA

SZERKESZTŐ
DEÁK GYULA

TECHNIKAI SZERKESZTŐ
HAZAI LÁSZLÓ

SZERKESZTŐ BIZOTTSÁG
BECK T. MIHÁLY, BOGNÁR REZSŐ, BRUCKNER GYŐZŐ,
HARDY GYULA, LEMPERT KÁROLY, MÁRTA FERENC,
POLINSZKY KÁROLY, PUNGOR ERNŐ, SCHAY GÉZA,
SZABÓ ZOLTÁN, TÉTÉNYI PÁL

Acta Chimica is a journal for the publication of papers on all aspects of chemistry in English, German, French and Russian.

Acta Chimica is published in 4 volumes per year. Each volume consists of 4 issues of varying size.

Manuscripts should be sent to

Acta Chimica
Budapest, P.O. Box 67, H-1450, Hungary

Correspondence with the editors should be sent to the same address. Manuscripts are not returned to the authors.

Subscription: \$36.00 per volume.

Hungarian subscribers should order from Akadémiai Kiadó, 1363 Budapest, P.O. Box 24. Account No. 215 11488.

Orders from other countries are to be sent to "Kultura" Foreign Trading Company (H-1389 Budapest 62, P.O. Box 149. Account No. 218 10990) or its representatives abroad.

SEPARATION AND DETERMINATION OF RADIOACTIVE IODINE ISOTOPES BASED ON ISOTOPE- AND ION-EXCHANGE

O. GIMESI and É. BÁNYAI

(Institute for General and Analytical Chemistry, Technical University Budapest)

Received June 26, 1978

Accepted for publication August 24, 1978

The authors elaborated methods of heterogeneous isotope- and ion-exchange for the determination of radioactive iodine. The optimum experimental conditions of reactions have been stated by step-by-step method (batch extraction), then a continuous measuring device based on the principle of Autoanalyzer was constructed.

In multicomponent systems the determination of radioactive iodine isotopes — first of all in biological samples — can generally be performed only after previous separation. The case is similar when examining the primary cooling water of reactors where, because of the presence of other radioactive components of considerable activity, previous separation should be applied.

Various processes have been developed for the selective separation of active iodine in different samples. JAWOROWSKI [1] determined iodine-131 in urine using asbestos mats. FAIRMAN and SEDLET [2] separated I-131 in milk on a silver chloride column. BROOKS, WALKER and REHNBERG [3, 4] stripped I-131 from anion-exchange resin with appropriate eluent, their methods have been elaborated for milk. BREVNOVA *et al.* [5] used satin scraps coated with silver iodide to retain the radioiodine. ECKHARDT, HERRMANN and SCHÜSSLER [6] utilized isotope or precipitate exchange reactions taking place in thin layers of adequate, preformed precipitates for the rapid isolation of short-lived radionuclides. Fission bromine and iodine activities were retained by silver chloride. SCHÜSSLER *et al.* [7] have developed an automatic equipment for increasing the speed of separation by means of which 90—99% of radioiodine in iodide form can be retained in 2—3 seconds on a silver chloride layer of 16 mg/cm² thickness. CSADA *et al.* [8] retained fission iodine isotopes from reactor water on silver iodide precipitate fixed in paper. In order to separate the fission iodine isotopes, LAVI [9] oxidized iodide ions to iodate, then they were reduced to iodine using hydroxylamine hydrochloride. Afterwards, the iodine was extracted with carbon tetrachloride. Following reduction and bringing the iodine back into aqueous phase, the activity was measured in the form of silver iodide. WARE, OLDHAM and BIBBY [10] oxidized iodide-131 to iodine with dichromate in fast reactor coolant systems. The iodine volatilized was collected on copper gauze which was subsequently checked for activity. BATE and DYER [11] elaborated a method for the determination of iodine-131 in

reactor dust particles collected on silver filters. LOVERIDGE and GORDON [12] developed an extraction method combined with oxidation and reduction for the determination of radioactive iodine in reactor effluent. JACOBS and LEHMANN [13] utilized isotope-exchange reaction taking place on silver iodide for the rapid isolation of radioactive iodine present in water. DOBOSZ [14] applied the following process for environmental samples: after mineralization he performs extraction, then the iodine is retained on a thin film of anion-exchange resin. The radioactivity is measured also in this form. ZADUBAN *et al.* [15] measured directly the iodine-131 content of the aqueous phase after isotope exchange with a liquid scintillator. PALÁGYI [16, 17, 18] thoroughly discussed the separation and concentration of radioiodine by isotope exchange in heterogeneous liquid systems. He also used a liquid anion exchanger for the rapid determination of iodine-131 in environmental waters.

For the separation of radioactive iodine isotope- and ion-exchange methods have been elaborated by us applying chloroform solution of tetrabutyl ammonium iodide (TBNi) and that of tetrabutyl ammonium bromide (TBNBr):



The optimum experimental conditions of separations have been stated by step-by-step method, then a continuously operated apparatus based on the principle of Autoanalyzer was constructed.

Step-by-step extraction experiments

Chemicals, solutions, apparatus

tetrabutyl ammonium bromide (TBNBr)

tetrabutyl ammonium iodide (TBNi)

potassium iodide

carrier-free, sterile Na^{131}I solution of 25 mCi/ml radioactive concentration

chloroform

For radiometric assay a nuclear spectrometer (type Nuclear Enterprise) and a well-type NaI(Tl) scintillator were used. The efficiency of exchange was determined so that the intensity of the same phase was measured before and after the exchange: $Q\% = \frac{I_1 - I_2}{I_1} \cdot 100$, where I_1 is the relative activity of solution before, and I_2 is the relative activity of solution after shaking. Activity values presented in Tables are mean values of 6 measurements corrected for the background values.

*Determination of radioactive iodine with
tetrabutyl ammonium iodide (TBNI)*

Table I contains the value of exchange yields *vs.* concentration of TBNI

Table I
Variation of exchange yield on TBNI concentration

TBNI <i>M</i>	<i>I</i> ₁ cpm	<i>I</i> ₂ cpm	<i>Q</i> %
10 ⁻³	71 526	41 466	42
10 ⁻²	70 530	19 746	72
10 ⁻¹	72 900	5 940	92

solution. In these experiments the aqueous phase was labelled with iodine-131 in the form of sodium iodide, its initial activity and the activity of the aqueous phase following extraction were measured, and on the basis of these values exchange yields were calculated. Performing the experiment with 0.1 *M* tetrabutyl ammonium iodide an exchange of 92% can be achieved, therefore later on TBNI solution of this concentration was employed.

The time of attaining exchange equilibrium was determined using carrier-free aqueous iodine-131 (Na¹³¹I), and applying mechanical shaking of different time periods. From Table II it can be seen that exchange equilibrium is instantaneously attained.

Table II
Dependence of exchange yield upon the shaking time

<i>t</i> s	<i>I</i> ₁ cpm	<i>I</i> ₂ cpm	<i>Q</i> %
10	71 140	5 827	92
90	72 041	6 141	91
300	72 974	5 587	92
600	71 626	5 902	92

Concerning the effect of the concentration of potassium iodide carrier, if it is higher than 10⁻² *M*, the activity of the organic phase starts significantly to decrease, while at a concentration of 10⁻¹ *M* the total activity is halved between the two phases. Similar curves are obtained in both cases, when either the aqueous phase or the organic phase is labelled with iodine-131 in the adequate form. In Fig. 1 a curve obtained by a series of experiments is demonstrated, when the chloroform solution of tetrabutyl ammonium iodide con-

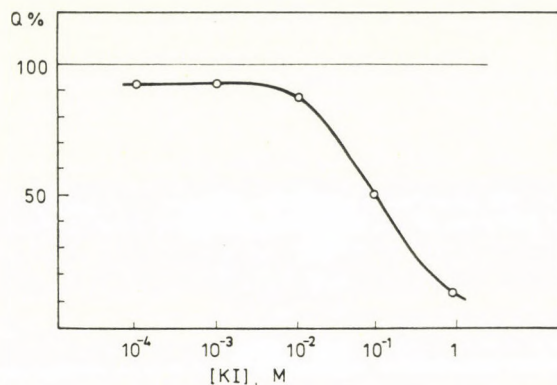


Fig. 1. Exchange yield as function of the carrier concentration; 0.1 M TBNi

taining radioactive iodide was shaken with inactive potassium iodide solutions of different concentrations.

*Determination of radioactive iodine with
tetrabutyl ammonium bromide (TBNBr)*

When labelled aqueous potassium iodide solution is shaken with a chloroform solution of tetrabutyl ammonium bromide, almost the whole activity is transferred into the organic phase. The activity of the aqueous phase can practically be decreased to the background value by two extractions. In Table III the exchange yield is to be seen as a function of TBNBr concentration.

Table III

Variation of exchange yield on TBNBr concentration

TBNBr M	I_1 cpm	I_2 cpm	$Q\%$
5×10^{-3}	80 844	14 609	82
1×10^{-2}	81 627	11 537	86
1.5×10^{-2}	82 114	7 452	91
3×10^{-2}	79 921	5 582	93
5×10^{-2}	79 897	4 892	94
1×10^{-1}	80 624	3 277	96
1.5×10^{-1}	81 014	1 720	98

According to the data, the extraction is expedient to be carried out with a reagent 10^{-1} M. The effect of the carrier concentration upon the exchange yield is presented in Table IV. If the potassium iodide concentration is 0.1 M

in the aqueous phase, the maximum of the total activity, according to equilibrium, is to be seen in the organic phase. As a matter of fact, in experiments

Table IV
Effect of carrier (KI) on exchange yield

C M	I_1 cpm	I_2 cpm	$Q\%$
1×10^{-4}	70 104	2 977	96
1×10^{-3}	68 814	3 336	95
1×10^{-2}	64 064	2 946	95
1×10^{-1}	69 868	2 924	96
2×10^{-1}	70 094	9 222	87
1×10^0	68 622	59 904	13

summarized in Tables III and IV, the aqueous phase was labelled with iodine-131.

It has been stated that the exchange yield is not influenced by the pH between pH 0 and 14 ($Q = 96\%$). Alkali-metal chlorides up to the concentration of 1 M , sulphate, nitrate and chloride ions added as potassium salts similarly up to 1 M concentration do not influence the high exchange yield.

Afterwards it has been examined by gamma-spectrometry whether some radionuclides — Na-24, Cr-51, Co-58, Fe-59 and Zn-65 — added to the aqueous phase as chlorides and sulphates, resp., will occur in the organic phase or not. It was found that the above radionuclides added to the aqueous phase do not occur in the organic phase, so in presence thereof the radioactive iodine isotopes can selectively be extracted from the aqueous phase.

Determination of fission iodine isotopes present in the primary cooling water of reactors

To a given volume of the fresh reactor water potassium iodide carrier, some diluted sulphuric acid and ascorbic acid are added, then the sample is shaken with 0.1 M chloroform solution of tetrabutyl ammonium iodide or bromide. Following the separation of phases, the gamma spectrum of the organic phase is recorded on a 1024-channel analyzer and Ge(Li) detector. In the spectrum only the photopeaks of the fission iodine isotopes (I-129, I-131, I-132, I-133, I-134 and I-135) appear, on the basis of which their quantity can be determined previously calibrating the detector and performing absolute activity measurements.

Development of an automatic analyzer

Because of the high radioactive concentration of samples to be analyzed, the plan of constructing an automatic analyzer has been realized. The apparatus constructed by us (see Fig. 2) consists of the following units:

- automatic sampler and feeder
- peristaltic pump
- spiral extractor with the separating vessel
- special measuring tube placed into a well-type scintillator of NaI(Tl) detector
- nuclear spectrometer with $x - t$ recorder and printer

The automatic sampler puts into the sampler tubes doses of 10 mls of each of the sample at atmospheric pressure and room temperature coming from the primary cooling water of nuclear reactors. Previously, to the sampler tubes some solid potassium iodide carrier (maintaining $10^{-3} M$ concentration of KI), some drops of dilute sulphuric acid and a few mgs of ascorbic acid were added. The sample is sucked from here by a peristaltic pump into the mixing tube and the extraction spiral, resp. where the extraction takes place with the chloroform solution of the reagent. The liquid stream is segmented by air addition. From the extractor the liquid gets into the separating vessel, where the phases separate. Underneath the chloroform phase is dropping out through a teflon

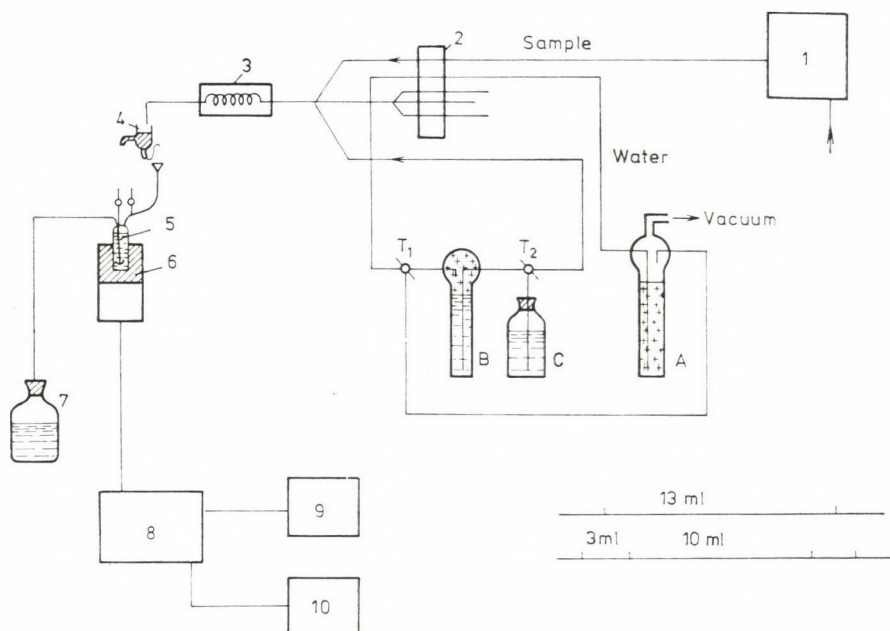


Fig. 2. Automatic Analyzer; 1 automatic sampler, 2 pump, 3 extractor, 4 separator, 5 measuring tube, 6 detector, 7 radioactive organic waste solution, 8 nuclear spectrometer, 9 printer, 10 $x - t$ recorder

siphon and then reaches through a funnelled pipe a special measuring tube placed in the detector. The volume of the tube is 13 mls. In operation the tube is slowly filled — in the meantime the detector signals are processed by the nuclear measuring device — then its content gets through a siphon into the radioactive organic phase reservoir and thus a new cycle is starting. Each 10 mls of the sample is followed by adding 3 mls of wash water (see in the right lower corner of Fig. 2).

The addition of the organic phase (reagent solution) is performed by the substitute vessel principle. From vessel A water is sucked by a peristaltic pump and pressed into the substitute vessel B, from where the organic reagent solution is pressed out. Vessel B is refilled in the following way: vessel A is evacuated, then by properly turning the three-way cocks T_1 and T_2 , the chloroform reagent solution is sucked from reagent vessel C into the substitute vessel B.

The development of a dosing apparatus was necessary since the chloroform solution cannot be pressed through the peristaltic pump at a constant volumetric rate, owing to the very short life-time of Solvaflex and Acidflex pump tubes which swell rapidly and consequently their transporting capacity is changing. However, the precondition of the good working of our device is that the same volume streams of the organic and aqueous phases should be ensured.

The faultless operation of the device was controlled in the way that inactive chloroform iodine solution was extracted by an aqueous solution of sodium thiosulphate. Working time was about 30 hours.

Afterwards an iodide solution — which was 10^{-3} M with respect to KI — of about 2000 cps/10 mls radioactive concentration was extracted by 10^{-1} M chloroform solution of tetrabutyl ammonium bromide. The radioactive iodine was applied in the form of I-131. (The nuclear spectrometer was adjusted in ratemeter print position with an integration time of 10 s, F.S.D. 10^4). The curves obtained by our measuring instrument are to be seen in Fig. 3. One

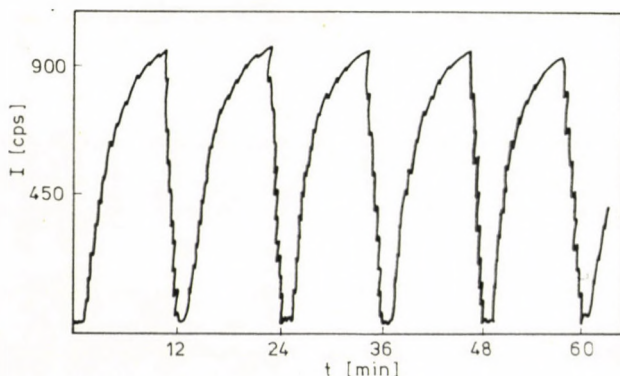


Fig. 3. Recorder curves for precision calculation

measuring cycle lasts for 12 mins, during which the isotope and ion-exchange equilibrium, resp., sets in. Reproducibility was determined on the basis of the data given by the printer and by planimetry the area of the curves (Fig. 3). Our experimental results are included in Table V. According to Table VI and Fig. 4, linear relationship was found between the two signals and the radio-

Table V

Reproducibility of examinations performed by the use of automatic analyzer

Counting rate cpm	Surface measurement with planimeter cm ²	Average of counting rate cpm	Average of planimetry cm ²	Maximal deviation from average value	
				Counting rate	Planimetry
3323	101.6	3326	103.1	$\pm 1.8\%$	$\pm 10.6\%$
3374	115.5				
3231	95.7				
3387	116.0				
3267	93.4				
3311	96.4				

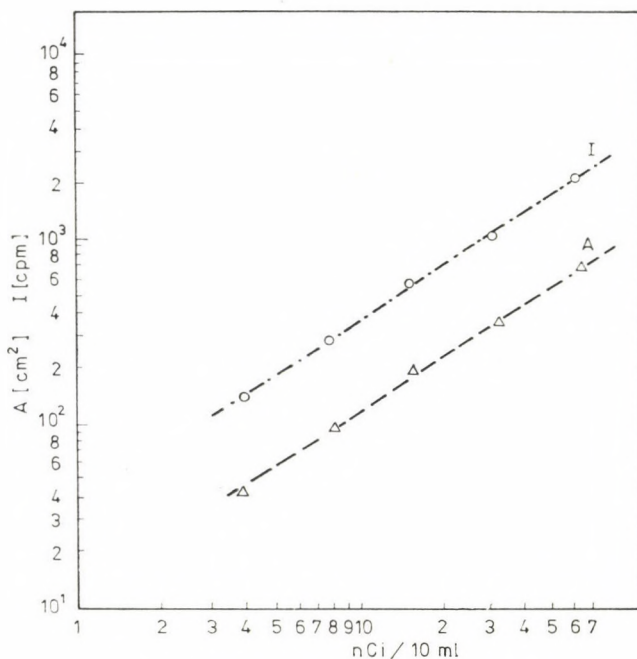


Fig. 4. Calibration curves

Table VI

Recording of calibration curve with automatic analyzer

I-131 nCi/10 ml	Counting rate cpm	Surface measurement with planimeter cm ²
62	2296	715.1
31	1140	355.0
15.5	571	180.6
7.8	283	92.2
3.9	140	42.2

active concentration. The detection limit was found to be about 1 nCi which is equal to a signal/noise ratio 2 : 1. Thus, our automatic analyzer is able to determine about 1 nCi radioactivity of I-131 contained in various samples after appropriate preparation of samples.

*

We express our thanks to Mr. Peter GRANDICS for his valuable contribution to this work.

REFERENCES

- [1] JAWOROWSKI, Z.: *Nukleonika*, **5**, 81 (1960)
- [2] FAIRMAN, W. D., SEDLET, J.: *Anal. Chem.*, **38**, 1171 (1966)
- [3] BROOKS, I. B., WALKER, J. P., REHNBERG, B. F.: *J. Dairy Science*, **51**, 1923 (1968)
- [4] WALKER, J. P., REHNBERG, B. F., BROOKS, I. B.: *ibid.*, **51**, 1373 (1968)
- [5] BREVNOVA, N. V. *et al.*: Symp. über das Wasserregime von Wasser—Wasser-Reaktoren, die Strahlenkontrolle der Wärmeträger und Methoden zur Verringerung der Strahlengefahr, DDR, Gera, 10—16 Nov. 1968
- [6] ECKHARDT, W., HERRMANN, G., SCHÜSSLER, H. D.: *Z. Anal. Chem.*, **226**, 71 (1967)
- [7] SCHÜSSLER, H. D. *et al.*: *Nucl. Inst. Methods*, **73**, 125 (1969)
- [8] CSADA, G. I., GIMESI, O., BÁNYAI, É., ÖRDÖGH, M.: *J. Radioanal. Chem.*, **21**, 427 (1974)
- [9] LAVI, N.: *J. Radioanal. Chem.*, **20**, 41 (1974)
- [10] WARE, A. R., OLDHAM, G. BIBBY, D. M.: *Talanta*, **17**, 339 (1970)
- [11] BATE, L. C., DYER, F. F.: *Radiochem. Radioanal. Lett.*, **16**, 59 (1974)
- [12] LOVERIDGE, B. A., GORDON, M. S.: AERE-R 5406, Harwell, Berkshire, 1967
- [13] JACOBS, H., LEHMANN, D.: *Jül.* — 410—51 Sept. 1977
- [14] DOBOSZ, E.: *Radiochem. Radioanal. Lett.*, **13**, 381 (1973)
- [15] ZADUBAN, M., STOLLÁROVÁ, N., PALÁGYI, Š.: *Radiochem. Radioanal. Lett.*, **3**, 129 (1970)
- [16] PALÁGYI, Š., ZADUBAN, M.: *Radiochem. Radioanal. Lett.*, **20**, 111 (1974)
- [17] PALÁGYI, Š.: *J. Radioanal. Chem.*, **30**, 299 (1976)
- [18] PALÁGYI, Š.: *J. Radioanal. Chem.*, **29**, 271 (1976)

Otto GIMESI
Éva BÁNYAI

} H-1521 Budapest, Gellért tér 4.

SYNTHESIS OF 6-AZA-B-HOMO-19-NORCHOLESTA-1,3,5(10)-TRIEN-7-ONE AND ITS 1-METHYL DERIVATIVE

SHAFIULLAH* and ISLAMUDDIN

(Department of Chemistry, Aligarh Muslim University, Aligarh-202001, India)

Received May 25, 1978

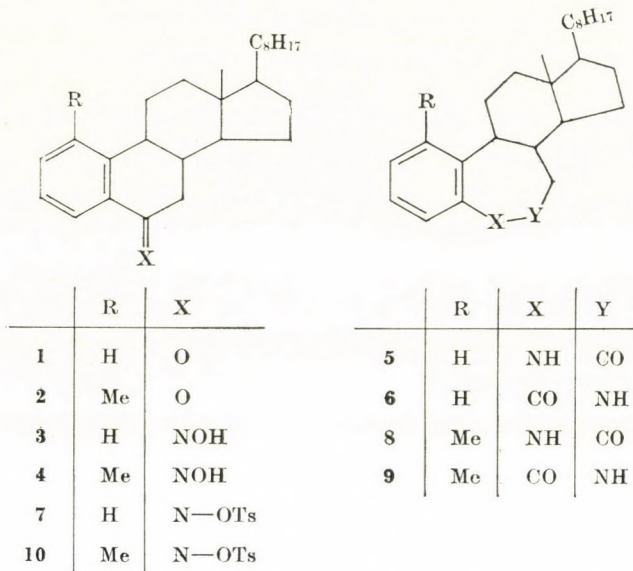
Accepted for publication September 4, 1978

The Schmidt reaction of 19-norcholesta-1,3,5(10)-trien-6-one (**1**) or Beckmann rearrangement of the corresponding oxime (**3**) gives 6-aza-B-homo-19-norcholesta-1,3,5(10)-trien-7-one(**5**). Similarly, 1-methyl-19-norcholesta-1,3,5(10)-trien-6-one (**2**) on Schmidt reaction, and its oxime (**4**) on Beckmann rearrangement, give 6-aza-B-homo-1-methyl-19-norcholesta-1,3,5(10)-trien-7-one (**8**). In view of the exclusive formation of the 6-aza-lactams **5** and **8** from the oximes **3** and **4**, the configuration of these oximes is assumed to be *anti* with respect to ring A.

In keeping with interest [1] in the synthesis of steroids containing nitrogen as part of the ring system, we felt inclined to undertake the syntheses of azasteroids from 19-norcholesta-1,3,5(10)-trien-6-one (**1**) and its 1-methyl analogue (**2**). Schmidt reaction of the ketones **1** and **2**, and Beckmann rearrangement of the corresponding oximes **3** and **4**, were employed to achieve the desired end.

The Schmidt reaction of **1** carried out with sodium azide and sulfuric acid in benzene gave a single lactam formulated as **5** on spectral evidence. The lactam was analyzed for $C_{26}H_{39}NO$. Its IR spectrum gave bands at 3280, 3150 (NH), 1670 (CONH), 1645 and 1580 cm^{-1} (aromatic C=C) [2]. These values are also compatible with the possible isomeric lactam **6**. A distinction between **5** and **6** was obtained by PMR spectroscopy which gave a singlet at δ 10.0 ppm for one proton; this signal disappeared on the addition of D_2O , implying that it was due to a proton on nitrogen. The four aromatic protons were observed at δ 7.11 ppm as a broad singlet. A multiplet at δ 2.2 ppm was ascribable to C7 α -methylene protons. These firmly support the structure **5**. On deuterium exchange, there was no appreciable change in any part of the spectrum, except for the disappearance of the signal at δ 10.0 ppm. The alternative structure **6** is expected to give a multiplet for $-CONH-CH_2$. Moreover, in **6** a signal for two protons should appear in the region around δ 3.5 ppm ($CONH-CH_2$) [3], which would be simplified on deuterium exchange.

Beckmann rearrangement of the oxime **3** obtained from **1** by the usual oxidation procedure, which was carried out by converting it to the oxime tosylate **7** by *p*-toluenesulfonylchloride-pyridine and then rearranging it on a column of alumina. This also provided **5** as the sole product. The formation of single



lactam (5) from the oxime (3) shows that the oximino hydroxyl group is away from ring A *i.e.* an *anti* oxime. Rearrangement of the *syn*-oxime (OH towards ring A) would have resulted in the formation of the isomeric lactam (6).

The Schmidt reaction of 1-methyl-19-norcholesta-1,3,5(10)-trien-6-one (2) was carried out exactly by the method described for 1. The single lactam (8) thus obtained was characterized on the basis of its spectral properties, which were analogous to those of 5. A strong structural resemblance is thus suggested between 5 and 8. By advancing the same arguments as in the case of 5, it may safely be concluded that also in the present case the PMR spectrum unambiguously supports structure 8, in preference to 9.

The ketone 2 was converted to its oxime 4 which, in turn, was transformed into the oxime tosylate (10). Beckmann rearrangement of 10 over alumina furnished only 8 and none of 9. This also requires 4 to be an *anti* oxime.

To the best of our knowledge, this study represents probably the first instance of the synthesis of azasteroids from substrates where the ketonic function is conjugated with the aromatic ring. A few reports [4—5] are available concerning the preparation of azasteroids from aromatic ketosteroids, but these are restricted to the estrone series.

Experimental

All m.p.'s are uncorrected. IR spectra were measured on Perkin-Elmer 621 grating infrared spectrophotometer and PMR spectra on a Varian A60D instrument with SiMe₄ as the internal standard. UV spectra were taken in ethanol on a Beckmann DK₂ spectrophotometer. Thin-layer chromatographic plates were coated with silica gel and sprayed with a 20% aqueous solution of Perchloric acid. Light petroleum refers to a fraction of b. p. 60—80 °C. Anhydrous sodium sulfate was used as the drying agent. (IR: s, strong; w, weak. PMR: s, singlet; d, doublet; m, multiplet).

6-Aza-B-homo-19-norcholesta-1,3,5(10)-trien-7-one (5)

A mixture of the ketone **1** (m.p. [8] 110 °C; 400 mg), dry benzene (5 ml) and *conc.* sulfuric acid (2 ml) was heated to a temperature of 50–60 °C and sodium azide (100 mg) was added slowly, with stirring. The reaction mixture was poured on to crushed ice. The benzene layer was separated and the aqueous layer extracted several times with chloroform. The chloroform solution was washed successively with water, sodium bicarbonate solution (5%) and water, and dried. Removal of the solvent left a semisolid material which was chromatographed over silica gel (10 g), collecting fractions of 15 ml. Elution with benzene chloroform (4 : 1) yielded the lactam **5**, which was recrystallized from light petroleum to obtain (250 mg) of the product, m.p. 88 °C.

$C_{26}H_{39}NO$. Calcd. C 81.87; H 10.21; N 3.67. Found C 81.71; H 10.01; N 3.43%.

IR: ν_{\max} 3280, 3150 (N—H), 1670 (CONH), 1645 and 1580 cm^{-1} (aromatic C=C).

PMR: δ 10.0 s ppm (disappeared on the addition of D_2O , CONH), 7.11 br, s (4H, aromatic, δ 2.2 m (C7a— H_2), 0.71 (C13— CH_3), 0.88 and 0.81 (remaining methyl signals).

UV: λ_{\max} 239 nm (ϵ , 6000),

MS: M^+ 381 ($C_{26}H_{39}NO$).

19-Norcholesta-1,3,5(10)-trien-6-one oxime (3)

The ketone **1** (400 mg), hydroxylamine hydrochloride (700 mg), sodium acetate trihydrate (800 mg) and ethanol (50 ml) were mixed together and heated under reflux for 1 h. The excess of the solvent was removed under reduced pressure and the residue diluted with cold water. The crude product thus obtained was recrystallized from light petroleum ether to give (300 mg) of **3**, m.p. 195 °C.

$C_{26}H_{39}NO$. Calcd. C 81.87; H 10.21; N 3.67. Found C 81.21; H 10.20; N 3.29%.

IR: ν_{\max} 3250 s (N—OH), 30.70 w (=C—H), 1620, 1600 cm^{-1} (aromatic C=C).

PMR: δ 8.26 ppm br (disappeared on the addition of D_2O , =N—OH), 7.5 br, s (4H, aromatic), 0.73 s (C13— CH_3), 1.0 and 0.86 (remaining methyls).

UV: λ_{\max} 255 nm (ϵ , 5500).

MS: M^+ 381 ($C_{26}H_{39}NO$).

19-Norcholesta-1,3,5(10)-trien-6-one oxime tosylate (7)

The oxime **3** (500 mg) was dissolved in pyridine (25 ml) and *p*-toluenesulfonyl chloride (500 mg) was added to the solution; the reaction mixture was kept at room temperature for 15 h. It was poured into ice-cooled water, extracted with ether and the ethereal extract was washed with water, dilute hydrochloric acid, sodium bicarbonate solution (5%) and water, and dried. Removal of the solvent provided an oil (450 mg) which was chromatographed over silica gel (15 g); fractions of 15 ml were taken. Elution with light petroleum benzene (4 : 1) gave the oxime tosylate (**7**), which was recrystallized from light petroleum ether to obtain (420 mg) of the product, m.p. 170 °C.

$C_{33}H_{45}NO_3S$. Calcd. C 74.01; H 8.41; N 2.60. Found C 73.98; H 8.22; N 2.41%.

IR: ν_{\max} 1600 cm^{-1} (aromatic C=C).

PMR: δ 8.15 and 7.5 ppm d each (4H, typical of *p*-disubstituted benzene; $J = 9$ Hz each), 7.48 (overlapping singlet, 4H, aromatic ring-A), 2.55 s (CH attached to benzene ring of the tosylate part), 2.2 m (C7— H_2), 0.71 s (C13— CH_3), 0.96 and 0.88 (remaining methyls).

Beckmann rearrangement of 7

The oxime tosylate **7** (400 mg) was dissolved in light petroleum and kept over a column of neutral alumina (25 g) for 10 h and then eluted in 15 ml portions. Elution with light petroleum benzene (5 : 1) gave the lactam, which was recrystallized from light petroleum to obtain (320 mg) of **5**, m.p. and mixed m.p. 88 °C.

6-Aza-B-homo-1-methyl-19-norcholesta-1,3,5(10)-trien-7-one (8)

To a solution of **2** (m.p. 140 °C [9]; 400 mg) in dry benzene (5 ml) and *conc.* sulfuric acid (1 ml) was added sodium azide (70 mg) with stirring at 55–56 °C on a water bath. A vigorous reaction ensued and after heating for 10 h, the reaction mixture was poured into

crushed ice. The benzene layer was separated and the aqueous layer extracted several times with chloroform. After the usual work-up of the organic extract, the solvent was removed under reduced pressure and the semisolid substance (300 mg) thus obtained chromatographed over silica gel (15 g). Fractions of 15 ml were collected. Elution with light petroleum chloroform (2 : 1) provided **8**; recrystallized from light petroleum ether: 160 mg, m.p. 170–71 °C.

$C_{27}H_{41}NO$. Calcd. C 82.02; H 10.37; N 3.54. Found C 81.89; H 10.16; N 3.43%.

IR: ν_{\max} 3190, 3130 (NH), 3030 w (=C–H), 1670 (CONH), 1645 and 1585 cm^{-1} (aromatic C=C).

PMR δ 10.15 ppm s (disappeared on the addition of D_2O , CONH), 6.95 m (3H, aromatic), 2.45 s ($Cl-CH_3$), 2.2 m ($C7a-H_2$), 0.91, 0.85 and 0.80 (remaining methyls).

UV: λ_{\max} 240 nm (ϵ 6200).

MS: M^+ 395 ($C_{27}H_{41}NO$).

1-Methyl-19-norcholesta-1,3,5(10)-trien-6-one oxime (4)

A mixture of the ketone **2** (600 mg), hydroxylamine hydrochloride (1.14 g), sodium acetate trihydrate (1.6 g) and ethanol (50 ml) was heated under reflux for 2 h. Most of the solvent has removed under reduced pressure and the residue thus obtained was recrystallized from light petroleum to give (500 mg) of **4**, m.p. 185 °C.

$C_{27}H_{41}NO$. Calcd. C 82.02; H 10.37; N 3.54. Found C 81.85; H 10.25; N 3.44%.

IR: ν_{\max} 3250 s (N–OH), 3070 w (=C–H) and 1660 cm^{-1} (aromatic C=C).

PMR: δ 9.45 ppm br, s (disappeared on the addition of D_2O , =N–OH), 7.85–7.16 br, s (3H, aromatic), 2.15 s ($Cl-CH_3$), 0.68 s ($Cl3-CH_3$), 0.93 and 0.83 (remaining methyl).

UV: λ_{\max} 255 nm (ϵ 5750).

MS: M^+ 395 ($C_{27}H_{41}NO$).

Beckmann rearrangement of 4

To a solution of the oxime **4** (580 mg) in pyridine (12 ml), *p*-toluenesulfonyl chloride (900 mg) was added and the reaction mixture allowed to stand at room temperature for 15 h. It was then poured into ice-cooled water and worked up in the usual manner. Removal of the solvent left an oil (450 mg). The crude material in light petroleum benzene was allowed to stand over a column of neutral alumina (15 g) for about 15 h and eluted in 15 ml portions. Elution with light petroleum chloroform (2 : 1) afforded the lactam, which was recrystallized from light petroleum ether to obtain (400 mg) of **8**, m.p. and mixed m.p. 170–171 °C.

*

We thank Prof. W. RAHMAN, Head, Department of Chemistry for the necessary facilities and Prof. M. S. AHMAD for a helpful discussion. Financial assistance from U.G.C. is gratefully acknowledged.

REFERENCES

- [1] AHMAD, M. S., SHAFIULLAH, ISLAMUDDIN: *Ind. J. Chem.*, **12**, 1323 (1974)
- [2] BELLAMY, L. J.: "The Infrared Spectra of Complex Molecule", 2nd ed., John Wiley, New York, 1958
- [3] BHACCA, N. S., WILLIAMS, D. H.: "Application of NMR Spectroscopy in Organic Chemistry". Holden-Day, San Francisco, 1964
- [4] MATKOVICS, B., GÖNDÖS, GY., TARÓDI, B.: *Acta. Chim., Acad. Sci. Hung.*, **57**, 119 (1968)
- [5] CARVANTES, A., CRABBE, P., JRIARTE, J., ROSENKRAN, G.: *J. Org. Chem.*, **33**, 4294 (1968)
- [6] FENSELAN, A. H., HAMAMVRA, E. H., MOFATT, J. G.: *J. Org. Chem.*, **35**, 3546 (1970)
- [7] MATKOVICS, B., TARÓDI, B., BALÁZSPIRI, L.: *Acta. Chim. Acad. Sci. Hung.*, **80**, 79 (1974)
- [8] HARA, J.: *Tetrahedron Letters*, **1968**, 3605
- [9] SHAFIULLAH, ISLAMUDDIN: *Bull. Chem. Soc. (Japan)*, (In press)

SHAFIULLAH	}	Department of Chemistry, A.M.U. Aligarh (202001),
ISLAMUDDIN		India

SYNTHESIS OF ^3H -LABELLED 2-DEOXY-D-RIBOSE AND ITS DERIVATIVES

(SHORT COMMUNICATION)

G. ZÓLYOMI, D. BÁNFI and J. KUSZMANN

(Institute for Drug Research, Budapest)

Received August 21, 1978

Accepted for publication September 4, 1978

The synthesis of 2-deoxy-(2- ^3H)-D-ribose (**5**), starting from 3,4-di-O-acetyl-D-ribal (**1**), as well as that of 2-deoxy-di-(2,2- ^3H)-D-ribose (**10**) by treating 2-deoxy-D-ribose under basic conditions with T_2O is described. The stability of the labelling of the different derivatives was investigated by repeated recrystallizations from ethanol.

The great biological importance of 2-deoxy-D-ribose justified the synthesis of the ^{14}C -labelled compound, which was first published in 1959 [1]. Another, independent synthesis has also been reported [2]. Interestingly, the corresponding ^3H -labelled analogues, which are much cheaper and also suitable for certain biological investigations, have not been synthesized so far. Here we describe the synthesis of 2-deoxy-2- ^3H - as well as 2,2-di- ^3H -D-ribose and its derivatives and our investigations concerning the stability of the labelling.

Mono-tritiated D-ribose was synthesized by applying the route described by VARGHA and KUSZMANN [3]. As starting material 3,4-di-O-acetyl-D-ribal [1] was used, which was converted by the addition of TiCl_4 [4, 5] into the 2- ^3H -labelled acetohalogen derivative **2**; this compound gave, on treatment with methanol in the presence of silver carbonate, the acetylated methyl-riboside **3**. The latter was deacetylated according to ZEMPLÉN to **4**, yielding on hydrolysis with benzoic acid 2-deoxy-2- ^3H -D-ribose [**5**] which was isolated as its crystalline *N*-phenyl riboside **6**.

For investigating the stability of the incorporated tritium, the anilide **6** was boiled in 20-fold ethanol for 1 h, and the activity of the compound obtained after crystallization was compared with that of the starting material. This procedure was repeated four times and the results (Table I, column A) proved that the incorporated tritium is stable under these conditions.

RADATUS *et al.* [6] obtained similar results when investigating the mono-2- ^3H -labelled anilide, and both the isotope proportion and the steric arrangement of the incorporated ^3H remained unchanged, even on hydrolyzing the anilide by acid [7].

In the next experiment we investigated whether any activity can be incorporated into the inactive anilide **7** by boiling it in T_2O containing ethanol. The resulting active material **9** was submitted to the same treatment as the

Table I

Change in the specific activity (cpm/mmmole · 10⁹) on recrystallizations

	A		B	
1	4.129	100.00%	6.438	100.00%
2	4.218	102.20%	1.287	19.90%
3	4.151	100.50%	0.098	1.52%
4	4.307	104.30%	0.028	0.43%
5	4.210	102.60%	0.007	0.11%

2-³H analogue, but in this case a sharp decrease of the incorporated activity was observed (Table I, column B), proving that only the protons reversibly bound to the hetero atoms had been exchanged. (The NH proton can be exchanged either directly, or *via* intermediate **8**.)

For obtaining 2-deoxy-2,2-di-³H-D-ribose (**11**), first the free sugar **10** was boiled in T₂O containing ethanol and the activity of the separated crystalline anilide was determined. In order to check the stability of the labelling, the compound was recrystallized four times from ethanol. The activity decreased rapidly during this procedure (Table II, column C), proving that no C—H proton had been exchanged to tritium, consequently, the structure of the labelled compound corresponds to **9**.

Table II

Change in the specific activity (opm/mmmole · 10⁹) on recrystallizations

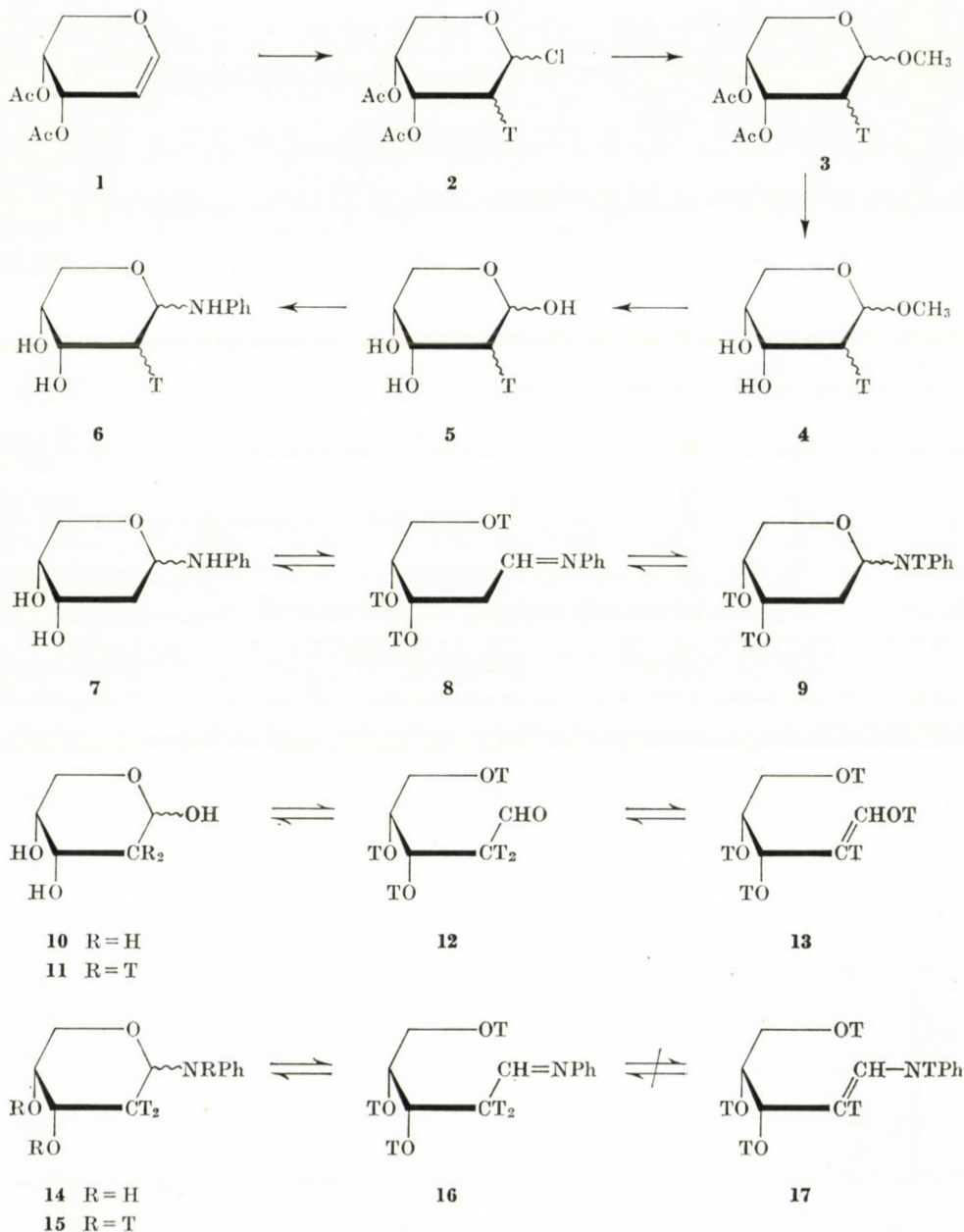
	C		D	
1	6.722	100.00%	7.533	100.00%
2	0.859	12.80%	4.196	55.70%
3	0.222	3.30%	3.071	40.76%
4	0.108	1.06%	3.019	40.08%
5	0.008	0.12%	3.078	40.86%

In our next experiment the free sugar **10** was treated in T₂O containing ethanol in the presence of NaOH (pH 7.8), as under basic conditions the protons at C-2 should be exchanged *via* the aldehyde **12** ⇌ enolate **13** equilibrium, according to the mechanism of the Lobry de Bruyn, van Ekenstein epimerization.*

The labelled sugar was again separated as its crystalline anilide **14** and this was submitted to the recrystallization process, as described before. This

* In the case of 2-deoxy-sugars C-2 is not an asymmetric carbon atom, therefore no epimerization takes place.

time the original activity decreased only by 60%, i.e. only 3/5 part of the incorporated tritium was bound exchangeably (Table II, column D). This is in full agreement with the *N*-glycoside **14** \rightleftharpoons aldimine **16** equilibrium, according to which three ³H atoms can be easily exchanged, leading to **15**. On the other



hand, the aldimine **16** does not undergo a tautomerization to **17**, which is the postulated intermediate of the Amadori rearrangement [8], as in this case the ^3H at C-2 should be exchanged too.

Experimental

M.p.'s were determined on a Boëtius hot stage and are uncorrected. Radioactivity was measured with a Packard-TRI-CARB liquid scintillation spectrometer. TLC was carried out on Silica Gel HF₂₅₄ and a Berthold TLC scanner was used for evaluation. All evaporations were carried out at diminished pressure.

N-Phenyl-2-deoxy-(2- ^3H)-D-riboside (**6**)

To benzoyl chloride (10 ml) T_2O (0.54 ml; 30 mmoles, 8 mCi/mmol) was added dropwise at 150 °C and the formed TCI was passed with a slow stream of nitrogen into an ice-cooled solution of diacetyl-D-arabinal [3] (2 g; 10 mmoles) in benzene (10 ml). The organic solution was then evaporated and the residue twice re-evaporated with benzene (2×10 ml). The yellow syrupy residue (2.45 g) was dissolved in methanol (15 ml) and boiled in the presence of silver carbonate (3 g) for 30 min. The pH of the cooled and filtered solution was adjusted with 1 M methanolic sodium methoxide to 9. After standing at room temperature overnight, the solution was evaporated, the residue was dissolved in water (30 ml) and 1 M hydrochloric acid was added to adjust pH 6. The solution was boiled after the addition of benzoic acid (1.5 g) for 45 min. Benzoic acid was filtered off from the cooled solution and the filtrate was extracted with ether (3×10 ml). The aqueous solution was evaporated and the residue treated with a solution of aniline (1.5 ml) in ethanol (15 ml). Next day the precipitated crystalline material was filtered off and was washed with ethanol (5 ml), to give the chemically and radiochemically pure compound **6** (1.5211 g; 73%); m.p. 171 °C (d.); R_F 0.78 (ethyl acetate-isopropanol 63 : 35). *Lit.* [3]m.p. 171–173° (d.).

N-Phenyl-2-deoxy-di-(2,2- ^3H)-D-riboside (**14**)

To a solution of 2-deoxy-D-ribose (1.34 g; 10 mmoles) in ethanol (15 ml) 0.1 M sodium hydroxide (1 ml) and T_2O (0.3 ml) was added. The solution was boiled for 1 h, cooled and then aniline (1.25 ml) was added. Next day the precipitated crystals were filtered off and washed with ethanol (1 ml) to give 1.3681 g of material. This was boiled in 20-fold ethanol for 1 h and the deposited crystals were filtered off next day. This treatment was repeated four times to yield 0.8348 g (4 mmoles) of the anilide **14**, m.p. 171–172 °C (d.); TLC: identical with compound **6**.

REFERENCES

- [1] BUTLER, G. C., MURRAY, D. H.: *Can. J. Chem.*, **37**, 1776 (1959)
- [2] SOUKOPUVA, V., VERES, K.: *J. Lab. Comp.*, **7**, 213 (1971)
- [3] VARGHA, L., KUSZMANN, J.: *Chem. Ber.*, **96**, 2016 (1963)
- [4] BROWN, H. C., GROOT, G.: *J. Am. Chem. Soc.*, **64**, 2223 (1942)
- [5] BENGSCH, E.: *J. Lab. Comp.*, **4**, 16 (1968)
- [6] RADATUS, B., YUNKER, M., FRASE-REID, B.: *J. Am. Chem. Soc.*, **93**, 3086 (1971)
- [7] RICHARDS, G. N.: *Methods Carbohydr. Chem.*, **1**, 180 (1962)
- [8] WEYGAND, F.: *Chem. Ber.*, **73**, 1259 (1940)

Gábor ZÓLYOMI	}	H-1045 Budapest, Szabadságharcosok útja 47.
Dezső BÁNFI		
János KUSZMANN		

SYNTHETIC LINEAR POLYMERS, XXXIV*

CHANGE OF SPECIFIC PROPERTIES OF DIMETHYLSILOXANE CO-OLIGOMERS AS A FUNCTION OF THE CHEMICAL COMPOSITION AND SIZE OF THE MOLECULE**

I. GÉCZY

(College of Commerce and Catering Trade, Chair for Knowledge of Goods, Budapest)

Received June 19, 1978

Accepted for publication September 11, 1978

The specific volume, parachor and — in one case — the refractive index of dimethylsiloxane (DMS) co-oligomers containing methylperfluoropropylbutyrosiloxane (MPFPBOS), cyclopenthylsiloxane (SCPS), methyl- β -cyanoethylsiloxane (MBCS) and methylchloromethylsiloxane (MCMS) groups have been investigated as a function of the chemical composition and the reciprocal molecular weight. These properties plotted against the reciprocal molecular weight — similarly to results obtained earlier for monoalkyl-, and *p*-alkylphenyl polyethylene-oxides — give a straight line, the intercept of which is characteristic of the repeating unit investigated, while its slope is proportional to the partial degree of polymerisation of the other repeating unit.

The values obtained for the change of the slope of the straight lines as a function of the chemical composition were compared with the values calculated on the basis of the relationship derived earlier; a good agreement was found. As indicated by the investigations, the specific properties can possess only values falling inside the triangle determined by the points $\varphi_{K'}$; $\varphi_{K''}$; φ_V .

It is illustrated by examples how the magnitude of hitherto unknown specific properties can be estimated on the basis of the results obtained, or how the accuracy of already available data can be checked.

It has been shown earlier [1] for linear polymer homologous oligomeric compounds, represented by the general formula



(where X and Y are identical or different end groups, M is the repeating unit, *n* the degree of polymerization) that a relationship of general validity — supported also by deduction — exists between the molecular weight and the specific properties derived from the additive ones:

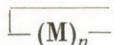
$$\varphi_{sp} = \frac{a}{M} + b, \quad (I)$$

where φ_{sp} is some specific property (e.g. specific refractivity, refractive index, specific parachor, specific volume, etc.), *M* is the molecular weight, *a* is a constant implicitly characteristic of the end groups, while *b* is a constant

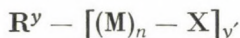
* Part XXXIII: Magyar Kém. Folyóirat, **81**, 177 (1975); Tenside, **14**, 64 (1977)

** Paper presented at the session of the Macromolecular Committee of the Hungarian Academy of Sciences, January 17, 1977

explicitly characteristic of the repeating units within the chain. It has been shown that the equation is also valid for cyclic polymer homologous oligomeric compounds represented by the general formula:



The value of the constant b is characteristic also in this case of the repeating unit, and its value is identical with that of the constant b referring to linear compounds of similar structure [2]. Moreover, it has been established that the equation is equally applicable to linear or branched polymer homologous oligomeric compounds represented by the following general formula:



where R is a hetero atom or atomic group of y valency. In this case, the constants of the equation are characteristic of the segment between the hetero atom or atomic group of the molecule and one of its end groups, and can be calculated therefrom [3].

In our further investigations the relationship has also been applied to non-ionic surfactants of the general formula:



i.e. essentially to such oligomeric molecules, in which the repeating units are built up from two different building elements in varying proportion, and where M' represents the hydrophobic part of the non-ionic surfactant, while M'' is the hydrophilic part (monoalkyl-polyethylene oxides [4]; *p*-alkylphenyl-polyethylene oxides [5]).

It has been shown that in this case Eq. (I) has the following form:

$$\varphi_{sp} = \frac{(mx'' + b')}{M} + \varphi'_k \quad (II)$$

where φ_k has the same meaning as earlier [constant b of Eq. (I)], the symbols' and'', respectively, refer to one (M') or the other (M'') repeating unit, x is the partial degree of polymerization of the repeating unit,

$$m = M''_k(\varphi'_k - \varphi''_k), \quad (III)$$

M_k being the molecular weight of the repeating unit,

$$b' = 2 M_v(\varphi_v - \varphi'_k), \quad (IV)$$

where M_v is the molecular weight of the end group (in the case of identical end groups); finally, indexes v and k refer to the end groups and to the repeating units, respectively.

On the basis of the equation (II), we studied the change of the refractive index, specific volume, specific refractivity and in the case of monoalkyl-polyethylene oxides also the specific reciprocal melting point, as a function of the molecular weight for the different surfactants. These properties were proportional to the reciprocal molecular weight, and the intercept of the straight lines obtained was characteristic of the repeating unit. It has been shown that the slope of the straight lines is proportional to the partial degree of polymerization of the other repeating unit.

The results permit to predict the expected value of specific properties for a given molecular weight, further the range of molecular weight within which a given specific property can be realized by changing the chemical composition. These results are valid for oligomers of any chemical composition and sequence, because deductions and conclusions show that the specific properties depend only on the relative ratio of the different repeating units.

Recent investigations

Non-ionic surfactants based on silicone were developed rather recently [6]. They reduce the surface tension of liquids, even in dilute solutions substantially more, than any of the conventional surfactants. The chemical structure of surfactants based on silicone is considerably different from that of conventional surface active agents due to the complete absence of a long hydrophobic hydrocarbon chain. Therefore, surfactants based on silicone require a revaluation of a series of theoretical concepts [7]. On the basis of these considerations, our aim was to investigate how far the relationships established earlier for non-ionic surfactants are applicable to non-ionic surfactants based on silicone, which are essentially siloxane co-oligomers.

It must be mentioned in advance that as yet there are relatively few data in the literature concerning the polymer-homologous members of these co-oligomers; these are known mainly from the recent Soviet literature [8, 9, 13, 14].

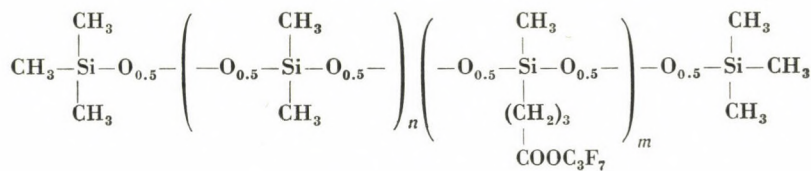
The dimethylsiloxane (DMS) co-oligomers investigated and their characteristic properties are given in Tables I, II, III and IV.* The specific properties calculated on the basis of these characteristics are summarized in Table V.

Differing from the earlier investigations, both end groups of these co-oligomers are identical $[(CH_3)_3Si-O]_n$. Owing to this, it was to be expected that the relationships established earlier can be further improved or will appear in a simpler form.

- * MPFPBOS: methylperfluoropropylbutyrosiloxane
- SCPS: silacyclopentylsiloxane
- MBCS: methyl- β -cyanoethylsiloxane
- MCMS: methylchloromethylsiloxane

Table I

Density, refractive index, and surface tension of
the co-oligomers (DMS-MPFPBOS) of the composition



as a function of n and m [8]

No.	n	m	d_4^{20}	n_D^{20}	γ^{20} (mN/m)
I	—	—	0.7640	1.3774*	15.48
II	1	—	0.8205*	1.3848*	16.96****
III	2	—	0.8536	1.3895*	17.60
IV	3	—	0.8780***	1.3925	18.10*
V	4	—	0.8910	1.3949	18.45
VI	5	—	0.9074***	1.3962	18.60*
VII	6	—	0.9130	1.3972	18.82
VIII	7	—	0.918***	1.3983	19.24
IX	8	—	0.925	1.3989	19.35
X	9	—	0.930***	1.3994	—
XI	15	—	0.9428	—	19.87
XII	23	—	0.9617	1.4042**	20.86
XIII	—	4	1.3260	—	21.43
XIV	—	6	1.3645	—	21.89
XV	—	8	1.3871	—	20.55
XVI	4	2	1.1453	—	20.82
XVII	3	3	1.2517	—	20.97
XVIII	2	6	1.3202	—	21.77

* see [10],

** see [9],

*** see [11],

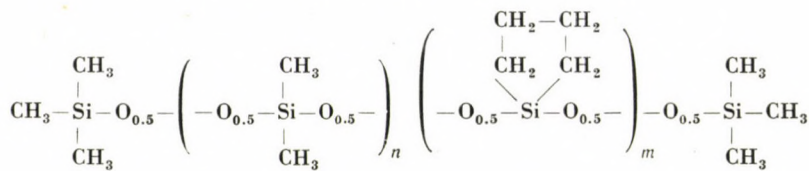
**** see [12].

Discussion

On the basis of the data contained in Table V, the specific volume, specific parachor, and where available, the refractive index have been plotted against the reciprocal molecular weight for the different oligomers of the polymer

Table II

Density refractive index, and surface tension of
the co-oligomers (DMS—SCPS) of the composition

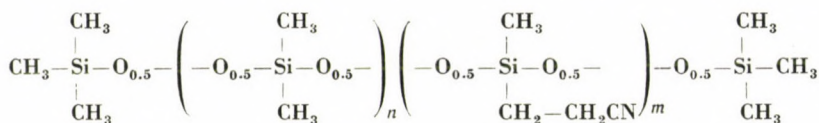


No.	n	m	d_4^{20}	n_D^{20}	γ_{20° (mN/m)
XIX	—	8	1.0760	—	21.69
XX	18	5	0.9881	1.4159	21.88
XXI	13	10	1.0322	1.4421	22.12
XXII	21	2	—	1.4121	—

* see [9]

Table III

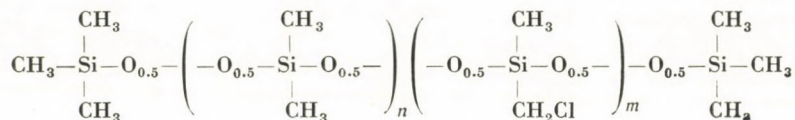
Density and surface tension of the co-oligomers (DMS—MBCS) of the composition



No.	n	m	d_4^{20}	γ_{20° (mN/m)
XXIII	24	—	0.9557	20.00
XXIV	23.5*	2.5*	0.9732	21.62
XXV	21	4	0.9821	22.13
XXVI	15	7	0.9980	22.91
XXVII	9	9	1.0497	25.31
XXVIII	—	20	1.1084	32.87

* Mean values (see [13])

Table IV

Density of the co-oligomers (DMS—MCMS) of the composition*as a function of n and m [14]*

No.	n	m	\bar{d}_4^{20}
XXIX	—	4	1.1739
XXX	—	8	1.2097
XXXI	—	13	1.2330
XXXII	—	18	1.2791
XXXIII	12	1	0.9987
XXXIV	11	2	1.0091
XXXV	10	3	1.0266
XXXVI	9	4	1.0590
XXXVII	8	5	1.0696
XXXVIII	6	7	1.1102
XXXIX	4	9	1.1554
XL	2	11	1.1974

homologous series investigated (Figs 1—8). It can be seen from the Figures that the corresponding points lie to a close approximation, along a straight line. The Figures also clearly show that, in accordance with our earlier results, the values of the intercepts are characteristic of the repeating units in the case of dimethylsiloxane oligomers being identical with the corresponding values found in our earlier investigations for homo-oligomers. In the other cases, no comparison can be made for lack of data on the homo-oligomers.

Further on, it has been investigated whether the relation deduced earlier for the slope of the straight line of Eq. (II) ($mx'' - b''$) is valid also in this case, *i.e.* how the slopes of the straight lines corresponding to various chemical compositions depend on the number of the other repeating unit. Our results are shown in Tables VI—VII and in Figs 9—14. The Figures also show the slopes and intercepts of the straight lines obtained from the points by the method of averages.

It must be mentioned that owing to the relatively few data available in part of the cases, the slopes of the straight lines corresponding to various chemi-

Table V

Reciprocal molecular weights of the compounds investigated and their specific properties calculated on the basis of Tables I, II, III and IV

No.	$1/M \cdot 10^4$	ν^{20°	$(\gamma^{1/4}/d) 20^\circ\text{C}$
I	61.65	1.309	2.596
II	42.32	1.219	2.459
III	32.22	1.171	2.398
IV	26.01	1.139	2.357
V	21.80	1.122	2.325
VI	18.74	1.102	2.289
VII	16.48	1.095	2.281
VIII	14.69	1.089	2.282
IX	13.25	1.081	2.267
X	12.06	1.075	—
XI	7.85	1.061	2.240
XII	5.36	1.040	2.222
XIII	7.05	0.7541	1.622
XIV	4.88	0.7328	1.585
XV	3.74	0.7209	1.535
XVI	9.20	0.8732	1.865
XVII	7.54	0.7990	1.710
XVIII	4.56	0.7575	1.636
XIX	10.38	0.9294	2.006
XX	5.01	1.012	2.189
XXI	4.70	0.9688	2.101
XXII	5.22	—	—
XXIII	5.13	1.046	2.213
XXIV	4.57	1.028	2.216
XXV	4.61	1.018	2.208
XXVI	4.84	1.002	2.192
XXVII	5.41	0.9527	2.137
XXVIII	4.12	0.9022	2.160
XXIX	17.76	0.8518	—
XXX	9.70	0.8266	—
XXXI	6.35	0.8110	—
XXXII	4.72	0.7818	—
XXXIII	8.62	1.0114	—
XXXIV	8.37	0.9910	—
XXXV	8.14	0.9741	—
XXXVI	7.92	0.9443	—
XXXVII	7.70	0.9350	—
XXXVIII	7.32	0.9007	—
XXXIX	6.96	0.8655	—
XL	6.66	0.8351	—

cal compositions in Figs 1—5, 8 have been calculated only from two points. In spite of this, it can be seen from Tables VI—VII and from Figs 9—14 that the slopes in Figs 1—5, 8 are linearly proportional to the number of one or the other repeating unit in the molecule, in accordance with our earlier results, and just as expected and predictable from Eq. (II). A somewhat larger scattering of certain points in Figs 9—14 can be attributed to the limited accuracy of the determination of the slopes of the straight lines in Figs 1—5, 8.

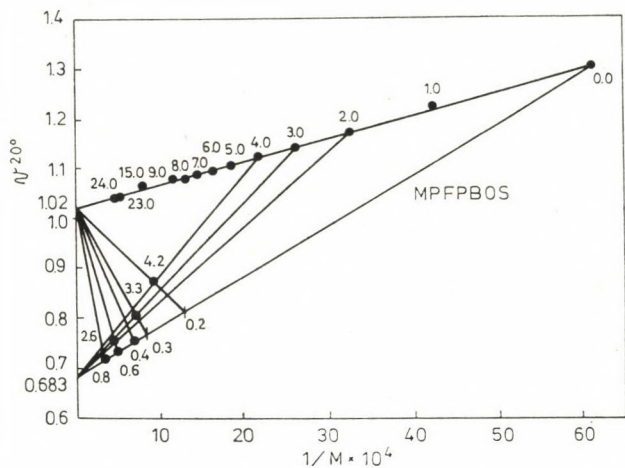


Fig. 1. Change of the specific volume of methylperfluoropropylbutyrosiloxane-dimethylsiloxane copolymers with the reciprocal molecular weight as a function of the chemical composition

It follows from the right- side term in parentheses of Eq. (III) that when the slope of the straight line obtained increases with increasing number of one of the repeating units, the slope of the straight line obtained with increasing number of the other repeating unit is decreasing, as can also be seen from Figs 9—14.

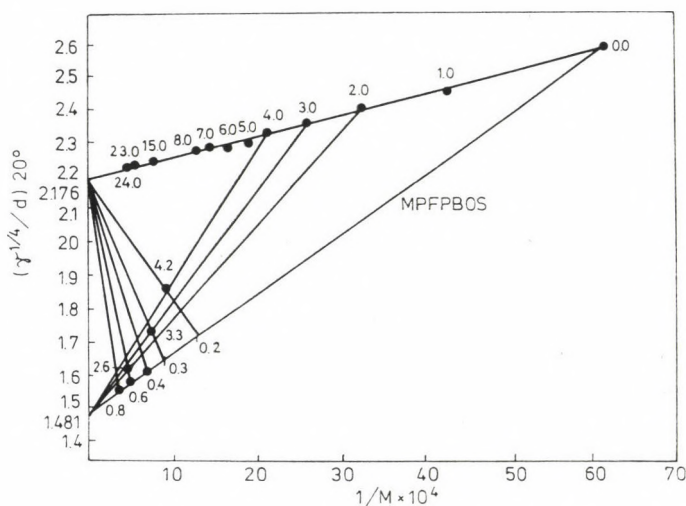


Fig. 2. Change of the specific parachor of methylperfluoropropylbutyrosilane-dimethylsiloxane copolymers with the reciprocal molecular weight as a function of the chemical composition

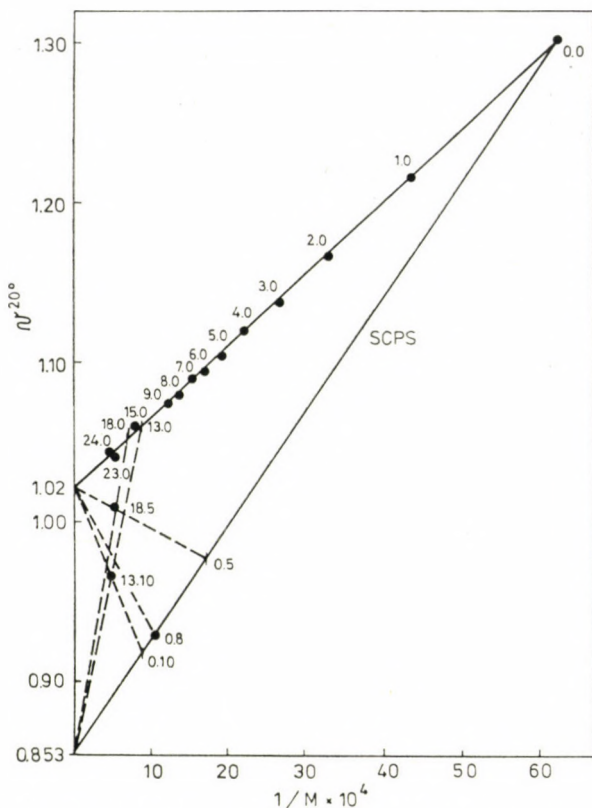


Fig. 3. Change of the specific volume of dimethylsilacyclopentylsiloxane copolymers with the reciprocal molecular weight as a function of the chemical composition

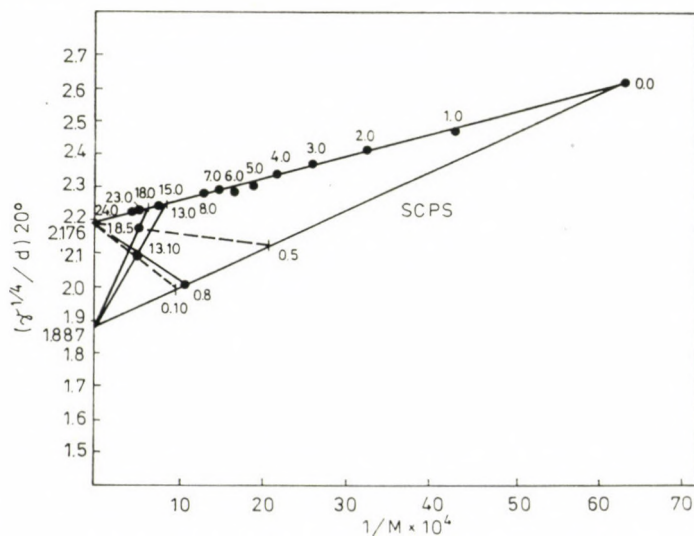


Fig. 4. Change of the specific parachor of dimethylsilacyclopentylsiloxane copolymers with the reciprocal molecular weight as a function of the chemical composition

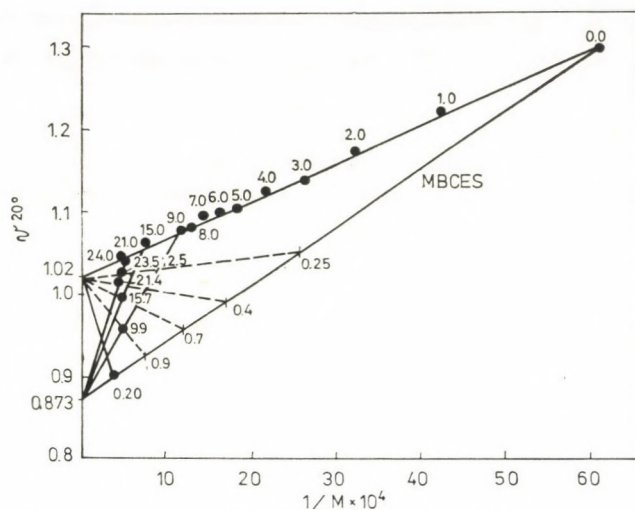


Fig. 5. Change of the specific volume of dimethylsiloxane-methyl-β-cyanoethylsiloxane copolymers with the reciprocal molecular weight as a function of the chemical composition

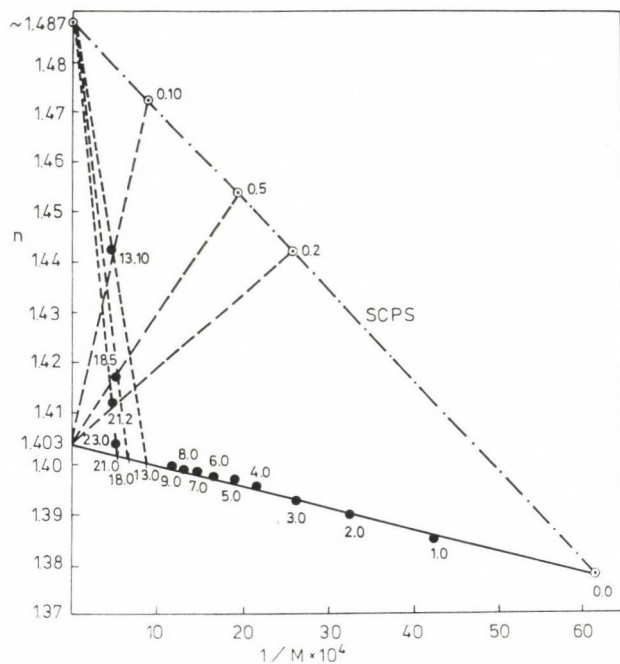


Fig. 6. Change of the refractive index of dimethylsilacyclopentylsiloxane copolymers with the reciprocal molecular weight as a function of the chemical composition

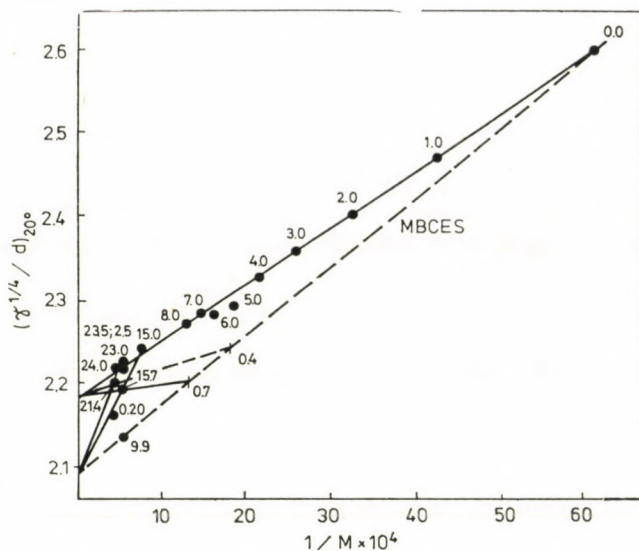


Fig. 7. Change of the specific parachor of dimethylsilacyclopentylsiloxane copolymers with the reciprocal molecular weight as a function of the chemical composition

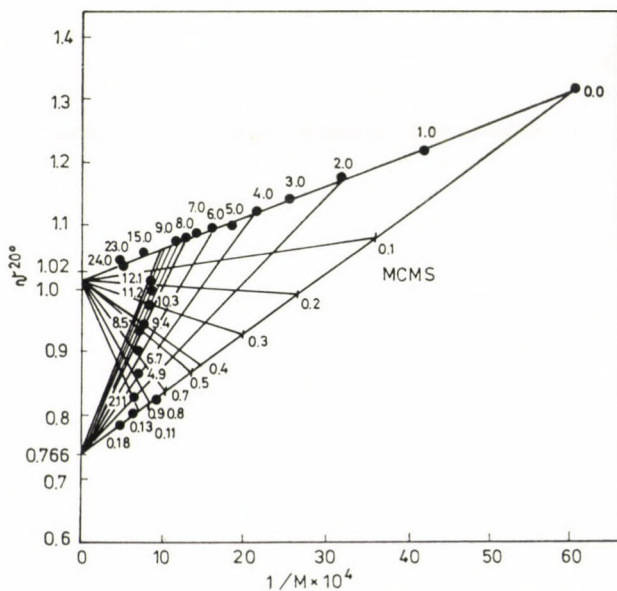


Fig. 8. Change of the specific volume of methylchloromethylsiloxane-dimethylsiloxane copolymers with the reciprocal molecular weight as a function of the chemical composition

Table VI

Changes of the slope of Equation (II) as a function of the number (x) of the dimethylsiloxane groups (DMS) in the case of co-oligomers of different composition

x	Methylperfluoropropylbutyrosiloxane (MPFPBOS)		Silacyclopentylsiloxane (SCPS)		Methyl- β -cyanoethylsiloxane (MBCES)	Methylchloromethylsiloxane (MCMS)
	In the case of the spec. volume on the basis of Fig. 1	In the case of the spec. parachor on the basis of Fig. 2	In the case of the spec. volume on the basis of Fig. 3	In the case of the spec. parachor on the basis of Fig. 4	In the case of the spec. volume on the basis of Fig. 5	In the case of the spec. volume on the basis of Fig. 8
0	101.4	182.8	74.0	115.1	70.7	55.6
2	149.5	272.5	—	—	—	131.4
3	184.2	350.3	—	—	—	—
4	197.5	365.1	—	—	—	172.8
6	—	—	—	—	—	212.1
8	—	—	—	—	—	263.1
9	—	—	—	—	183.9	315.7
10	—	—	—	—	—	255.6
11	—	—	—	—	—	266.8
12	—	—	—	—	—	284.7
13	—	—	246.4	455.3	—	—
15	—	—	—	—	196.0	—
18	—	—	317.4	602.8	—	—
21	—	—	—	—	321.0	—
23.5	—	—	—	—	345.7	—

Since the values of the terms in relations (III) and (IV) are known or can be calculated, this allowed a comparison of the values of the slopes and intercepts of the straight lines in Figs 9—14 with the values calculated on the basis of Eqs (III) and (IV). To facilitate their survey, the values used in the calculations have been summarized in Table VIII.

Values calculated in this way and those actually found are listed in Table IX.

It can be seen that there is a rather close agreement between the calculated and experimentally found values of the slopes. As concerns the intercepts, an agreement better than within an order of magnitude cannot be expected; yet the agreement is remarkably good also in this case, with the exception of three values.

Table VII

Changes of the slope of Equation (II) in the case of dimethylsiloxane co-oligomers as a function of the number (x) of the other group (co-monomer)

The other group

x	MPFPBOS		SCPS		MBCES	MCMS
	In the case of the spec. volume on the basis of Fig. 1	In the case of the spec. parachor on the basis of Fig. 2	In the case of the spec. volume on the basis of Fig. 3	In the case of the spec. parachor on the basis of Fig. 4	In the case of the spec. volume on the basis of Fig. 5	In the case of the spec. volume on the basis of Fig. 8
0	45.3	68.3	45.3	68.3	45.3	45.3
1	—	—	—	—	—	— 10.0
2	—159.6	—338.0	—	—	—	— 34.6
2.5	—	—	—	—	17.5	—
3	—293.1	—618.0	—	—	—	— 56.4
4	—377.2	—785.8	—	—	— 4.3	—104.6
5	—	—	— 16.0	26.0	—	—110.4
6	—588.5	—1593.8	—	—	—	—
7	—	—	—	—	— 37.2	—163.0
8	—799.7	—1713.9	— 87.3	—163.8	—	—
9	—	—	—	—	—124.4	—222.0
10	—	—	—108.9	—159.6	—	—
11	—	—	—	—	—	—277.6
20	—	—	—	—	—285.9	—

In view of the few data available at present, a closer agreement should not be required for the time being. These investigations have shown that our statements established earlier for monoalkyl and *p*-alkylphenyl polyethylene oxides hold also for dimethylsiloxane copolymers of various chemical composition, and the relations thus derived can also be extended to the specific parachor. Furthermore — over and above the earlier investigations — it is unambiguously evident from the present work that specific properties only can possess values which are inside the triangle determined by the points φ_K ; $\varphi_{K'}$; φ_v .

It follows from these results that the expected value of a specific property is predictable.

This method is of particular interest when data concerning the homopolymer or homo-oligomer of one of the repeating units are still missing, e.g. the value of n_D^{20} in the case of poly- and oligocyclopentylsiloxanes (see Table II and Fig. 6), i.e. one of the envelop lines is unknown, but the data for the co-oligomers are at once's disposal.

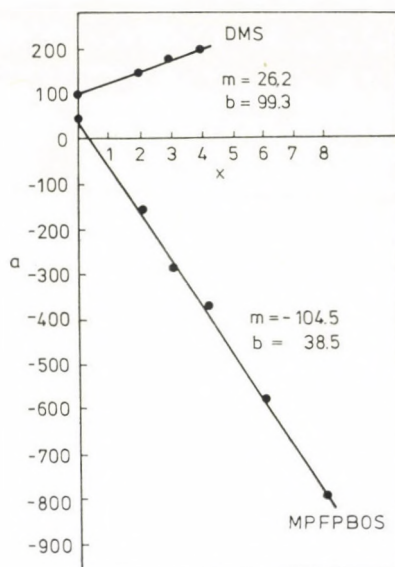


Fig. 9. Change of the slope (a) of Eq. (II) as a function of the number of the methylperfluoropropylbutyrosiloxane (MPFPBOS) and dimethylsiloxane (DMS) groups (x) in the case of the specific volume on the basis of Fig. 1.

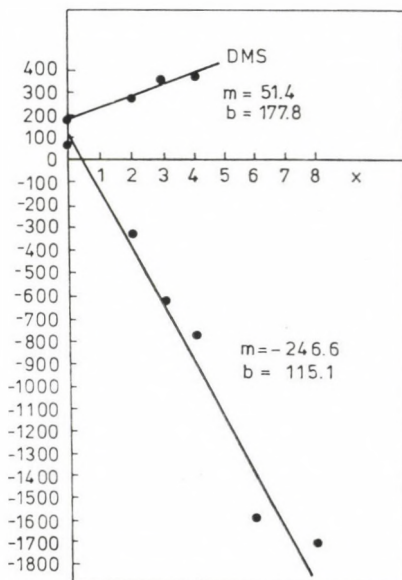


Fig. 10. Change of the slope (a) of Eq. (II) as a function of the number of the methylperfluoropropylbutyrosiloxane (MPFPBOS) and dimethylsiloxane (DMS) groups (x) in the case of the specific parachor on the basis of Fig. 2.

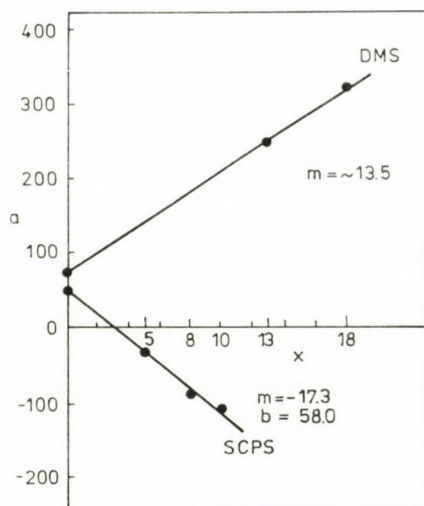


Fig. 11. Change of the slope (a) of Eq. (II) as a function of the number of silacyclopentyl (SCPS) and dimethylsiloxane (DMS) groups (x) in the case of the specific volume on the basis of Fig. 3.

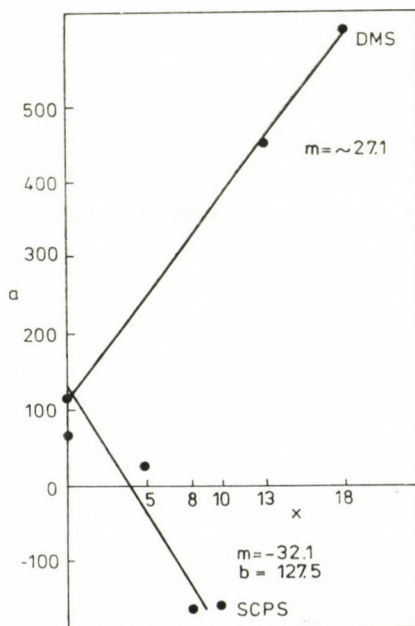


Fig. 12. Change of the slope (a) of Eq. (II) as a function of the number of silacyclopentyl (SCPS) and dimethylsiloxane (DMS) groups (x) in the case of the specific parachor on the basis of Fig. 4.

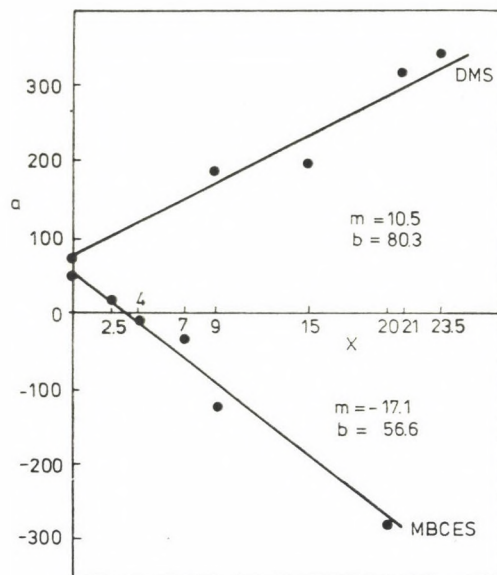


Fig. 13. Change of the slope (a) of Eq. (II) as a function of the number of methyl- β -cyanoethylsiloxane (MBCES) and dimethylsiloxane (DMS) groups (x) in the case of the specific volume on the basis of Fig. 5.

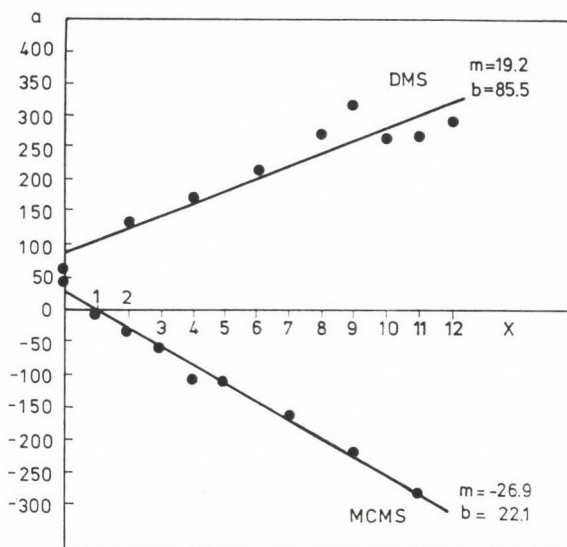


Fig. 14. Change of the slope (a) of Eq. (II) as a function of the number of methylchloromethylsiloxane (MCMS) and dimethylsiloxane (DMS) groups (x) in the case of the specific volume on the basis of Fig. 8.

Table VIII

Values required for calculations on the basis of Equations (III) and (IV)

Repeating unit	M_k	φ_k^*		Reciprocal molecular weights ($1/M \cdot 10^4$) belonging to the oligomers of the given degree (p) of polymerization	
		v	$\gamma^{1/4}/d$	p	$1/M \cdot 10^4$
$\begin{array}{c} \text{CH}_3 \\ \\ -\text{Si}-\text{O}- \\ \\ \text{CH}_3 \end{array}$	74.1	1.020	2.176	13 18 21 23.5	8.88 6.68 5.82 5.25
$\begin{array}{c} \text{CH}_3 \\ \\ -\text{Si}-\text{O}- \\ \\ (\text{CH}_2)_3-\text{COOC}_3\text{F}_7 \end{array}$	314.1	0.683	1.481	2 3	12.65 9.05
$\begin{array}{c} \text{CH}_2-\text{CH}_2 \\ \quad \\ \text{CH}_2 \quad \text{CH}_2 \\ \quad \\ -\text{Si}-\text{O}- \end{array}$	100.1	0.853	1.887	2 5 10	27.59 15.09 8.60
$\begin{array}{c} \text{CH}_3 \\ \\ -\text{Si}-\text{O}- \\ \\ \text{CH}_2\text{CH}_2\text{CN} \end{array}$	113.1	0.873	~ 2.09	2.5 4 7 9	22.47 16.27 10.48 8.47
$\begin{array}{c} \text{CH}_3 \\ \\ -\text{Si}-\text{O}- \\ \\ \text{CH}_2\text{Cl} \end{array}$	108.6	0.766	—	1 2 3 5 7 9 11	36.93 26.36 20.49 14.18 10.85 8.78 7.37
End group	M_v	φ_v^{**}			
$\begin{array}{c} \text{CH}_3 \\ \\ \text{CH}_3-\text{Si}-\text{O}- \\ \\ \text{CH}_{23} \end{array}$	81.1	1.309	2.596		

* see Figs 9–14

** from direct measurement (see values referring to substance No. I)

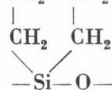
Table IX

Comparison of the values of the slopes and intercepts calculated on the basis of Equations (III) and (IV) with the corresponding values of the straight lines in Figs 9–14

φ	1/d		$\gamma^{1/4}/d$		1/d	
	DMS	MPFPBOS	DMS	MPFPBOS	DMS	SCPS
$m_{\text{calc.}}$	−105.8	25.0	−218.3	51.5	−16.7	12.4
m_{found}	−104.8	26.2	−246.6	51.4	−17.3	~13.5
$b_{\text{calc.}}$	46.9	101.6	68.2	180.9	46.9	—
b_{found}	38.5	99.3	115.1	177.8	58.0	—

φ	$\gamma^{1/4}/d$		1/d		1/d	
	DMS	SCPS	DMS	MBCES	DMS	MCMS
$m_{\text{calc.}}$	−28.9	21.4	−16.6	10.9	−27.6	18.8
m_{found}	−32.1	~27.1	−17.1	10.5	−26.9	19.2
$b_{\text{calc.}}$	68.2	—	46.9	74.0	46.9	88.1
b_{found}	127.4	—	56.6	80.3	22.1	85.5

In this case the intercepts of the straight lines obtained by connecting the available points and the points of the molecular weights corresponding to the homo-oligomers on the other envelop line — which are visibly converging approximately in the same point — will provide the value of the specific property of the repeating unit, in our case the refractive index ($n_D^{20} = 1.487$) of the repeating unit: $\text{CH}_2\text{—CH}_2$ of infinitely high molecular weight.



On the basis of the envelop line plotted in this way, the unknown specific property of the different homo-oligomers can be estimated.

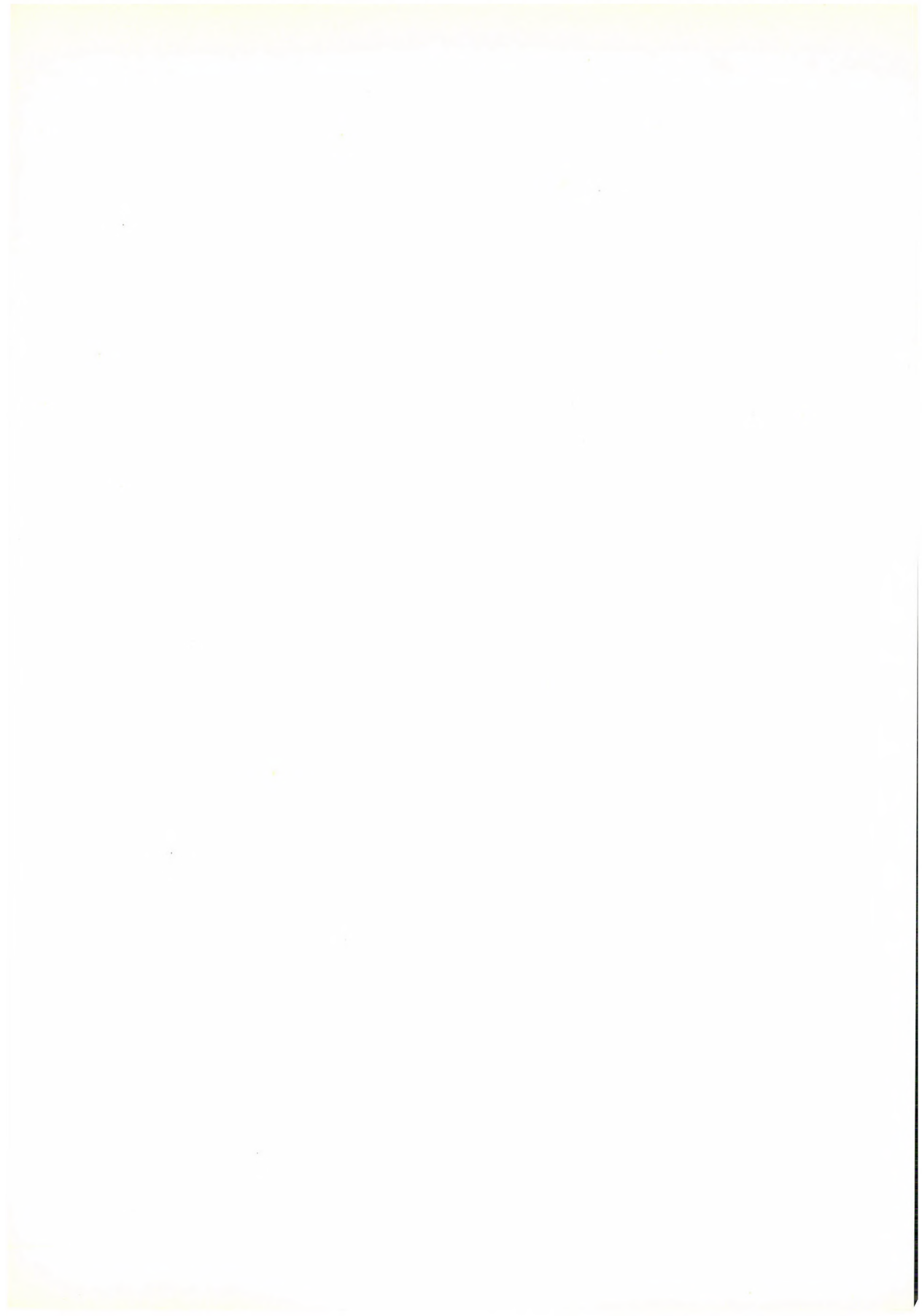
This method is also suitable for the estimation of the accuracy of data to be found in the literature; thus the reciprocal molecular weights of some homo-oligomers are also given in Table VIII.

One the basis of these values, it can be established that the individual straight lines in Figs 1–8 actually cut the appropriate envelop line at a point approximately corresponding to the molecular weight of the homo-oligomer. At the same time Fig. 7 shows that the values given for the surface tension of the co-oligomers of the chemical composition corresponding to Nos. XXVII and XXVIII are rather inaccurate; also inconsistent are the data in the original paper [13] on the chemical composition of compound XXVIII.

REFERENCES

- [1] See e.g.: GÉCZY, I.: *M. T. A. Kém. Tud. Oszt. Közl.*, **23**, 285 (1965), and references cited therein
- [2] GÉCZY, I.: *Magyar Kém. Folyóirat*, **71**, 551 (1965); *Polymer Previews*, **2**, 556 (1966); *J. Polym. Sci. (C)*, **16**, 2991 (1967)
- [3] GÉCZY, I.: *Magyar Kém. Folyóirat*, **74**, 339 (1968); *Acta Chim. Acad. Sci. Hung.*, **57**, 345 (1968)
- [4] GÉCZY, I.: *Kolorisztikai Értesítő*, **13**, 142 (1971); *Tenside*, **9**, 117 (1972)
- [5] GÉCZY, I.: *Kolorisztikai Értesítő*, **13**, 272 (1971); *Acta Chim. Acad. Sci. Hung.*, **79**, 133 (1973)
- [6] ROSSMY, G.: *Chemiker Ztg.*, **98**, 178 (1974)
- [7] DOLINA, T., DOBOZY, O.: *Magyar Kémikusok Lapja*, **31**, 42 (1976)
- [8] И. А. Лавыгин, И. И. Скороходов, М. В. Соболевский, Д. В. Назарова, М. Б. Лотарев, О. Н. Кудинова, Г. В. Боропаева: *Высокомол. Соед.*, **18**, (A) 90 (1976)
- [9] М. В. Соболевский, М. Б. Ломарев, Е. А. Чернышев, Н. Ф. Красновская: *Пласт. Массы*, [8] 9 (1972)
- [10] В. П. Давидова, З. С. Лебедева: *Высокомол. Соед.*, **10**, (Б) 401 (1968)
- [11] GÉCZY, I.: *Magyar Kém. Folyóirat*, **71**, 51 (1965); *Acta Chim. Acad. Sci. Hung.*, **43**, 129 (1965)
- [12] WARRICK, E. L.: *J. Am. Chem. Soc.*, **68**, 2455 (1946); HUNTER, M. J., WARRICK, E. L., HYDE, J. F., CURRIE, C. C.: *J. Am. Chem. Soc.*, **68**, 2284 (1946); *Исследования в области кремнийорганических соединений*, Сб. статей, Изд. Ак. Наук СССР Москва, 1962
- [13] И. А. Лавыгин, И. И. Скороходов, М. В. Соболевский, Д. В. Назарова, О. В. Лейман, Л. В. Коновалова, В. В. Стегалкина: *Высокомол. Соед.*, (Б) **18**, 749 (1976)
- [14] М. В. Соболевский, Т. В., Королева, Л. А. Голубчикова: *Пласт. Массы*, [2] 19 (1973);

István GÉCZY H-1363 Budapest, P.O.B. 21.



SPECTROCHEMICAL INVESTIGATION OF VOLATILE COMPONENTS RELEASED IN THERMOCHEMICAL PROCESSES, II

CADMIUM AND MERCURIC SALTS

E. GEGUS, J. KREITER, L. MÉRAY and J. INCZÉDY
(*Institute of Analytical Chemistry, University of Veszprém*)

Received August 4, 1978

Accepted for publication September 11, 1978

By means of the measurement technique described in part I, the thermal processes of cadmium salts (chloride, nitrate, sulphate and oxide) were investigated in detail up to 1200 °C in argon atmosphere, using platinum and graphite crucibles, and recording the cadmium signal of the vapour phase. Based on the characteristic conversion temperatures established with the knowledge of the time–temperature function, several processes (reduction, oxidation, thermal decomposition, evaporation, *etc.*) could be identified. The thermal properties of mercuric salts (chloride, nitrate, sulphate and oxide) were studied under lower heating rate up to 750 °C. Some results concerning other thermal processes (evaporation of BeCl_2 , release of volatile fluorine compounds) are mentioned.

Based on the experimental results, it was stated that essential differences exist between the processes taking place in platinum and graphite crucibles, respectively, and the surface quality and condition of graphite crucibles significantly affect the oxidation–reduction, decomposition and evaporation processes.

Introduction

Several thermochemical processes were investigated between 150 and 1350 °C, such as evaporation, and reactions of several salts of selected metals which volatilize in this range; tests were carried out by means of the resistance-heated microreactor, stabilized d.c. arc source, as well as radiation resolving and detecting system for recording the emission signal of the vapour phase, described in a previous publication [1]. Microcrucibles made of platinum and different graphite sorts were used, and the effect of several additives (acids, salts) and conditions on these systems was tested. Main results of this investigation, and the conclusions are given as follows.

Investigation of cadmium salts

Detection and determination of cadmium as a significant toxic element is of outstanding importance, and the behaviour of its compounds in the graphite cuvette used in atomic absorption spectrometry causes many difficulties.

To investigate thermal properties of these compounds, experimental conditions were selected so as to arrive at conclusions at the same time also on the processes occurring in the graphite cuvette.

For the tests, 25 μ l solutions of chloride, nitrate or sulphate stock solutions of 100 μ g Cd/ml concentration acidified with the corresponding acid (0.1 N), were weighed into the crucibles; thus each sample contained 2.5 μ g Cd. Beside solutions, experiments were carried out also with suitable solid salts but with greater, irregularly fluctuating amounts of the samples weighed-in,

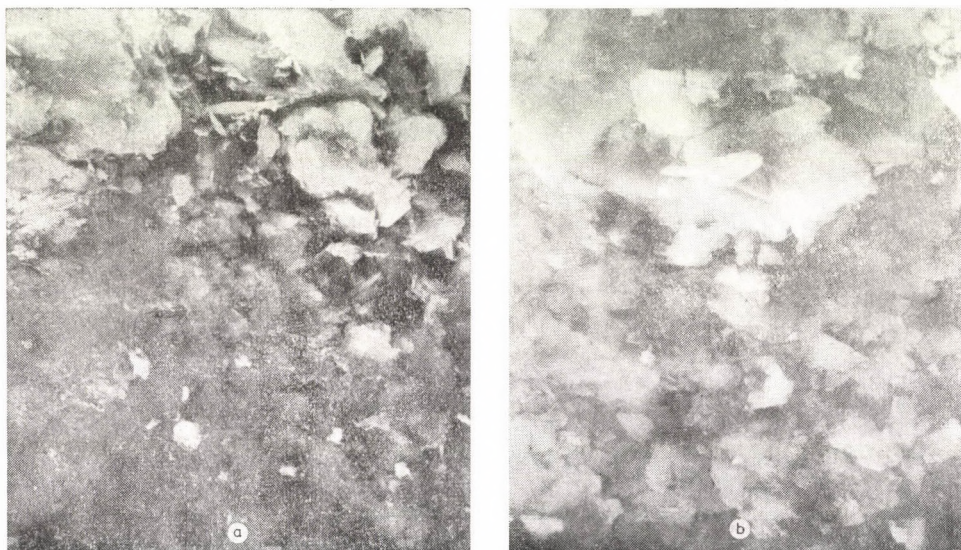


Fig. 1. Scanning electron micrographs of the inner surface of RW-crucibles (see text), $N = 1500\times$; a) unused crucible; b) three times heated crucible (with sample)

therefore the records are to be compared with the records of the solution samples only for estimation.

Beside the platinum crucible, two different sorts of graphite crucibles were adopted of spectral purity, with different degree of graphitization and porosity. The crucibles denoted RW were made of highly graphitized, dense (slightly porous) spectral graphite of RW I type supplied by "Ringsdorff-Werke GmbH" (G.F.R.), and the crucibles denoted Tč of less graphitized and more porous spectral graphite of SU type obtained from "Elektrokarbon, Kablo Topolčany" (Czechoslovakia). The original structure of the graphite crucibles after the heating cycles was significantly changed; microcrystalline grains and fragments, which were present on the freshly machined surface, disappeared or burned out, and the porosity of the graphite increased. The changes can be observed on the scanning electron micrographs of the surfaces (Figs 1 and 2, a and b); further informations are given with the changes of

emission signals, details of which will be dealt with at the discussion of the results. As a rule, it was observed that in crucibles used for the first time, cadmium evaporates earlier, *i.e.* the signal can be observed at lower temperatures than in the case of repeatedly used crucibles.

In agreement with our experiences, important statements have been made by STURGEON and CHAKRABARTI [2] in connection with the role of surface porosity of the graphite cuvette. They reported that, in contrast with a pyrolytic-graphite-coated surface of very low porosity, on an uncoated graphite

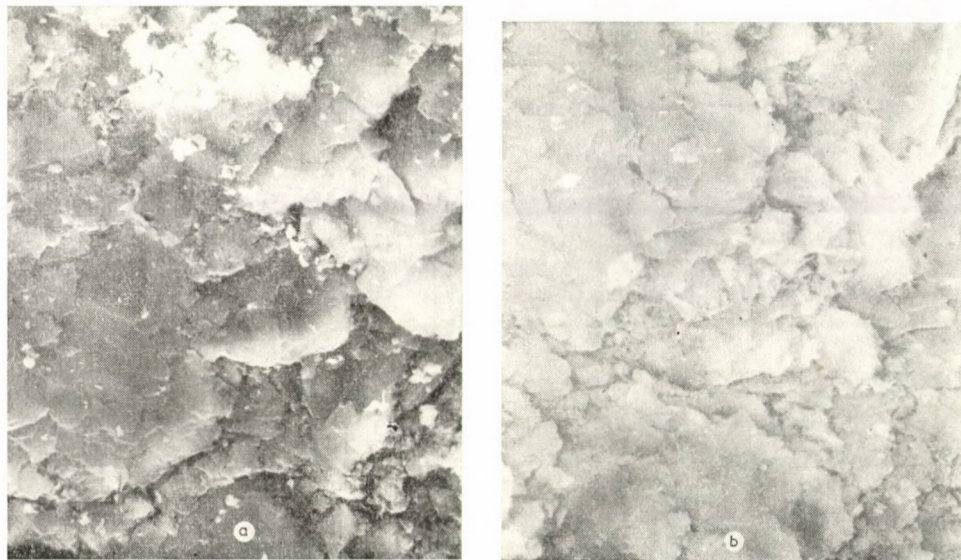


Fig. 2. Scanning electron micrographs of the inner surface of Tě-crucibles (see text), $N = 1500\times$; a) unused crucible; b) three times heated crucible (with sample)

surface the porosity rapidly increased under use, and the solute more and more penetrated into the pores, as a consequence of which the atomization process became more difficult, detection was smoothed, and "memory effects" took place.

At the discussion of results it is to be taken into account that under heating of the microreactor there is no thermodynamic equilibrium in the system. In spite of this fact, thermal decomposition and conversion processes, in general, can be characterized more or less by equilibria, and temperatures belonging to signal changes or maxima on the emission curves are characteristic and reproducible. Well-defined identification (or appearance) temperature is observed with the increase of the spectral line intensity at the appearance of cadmium in the gas phase, and the signal maximum shows decay of the process (*e.g.* loss of the compound or the metal). Peak intensities and integrated

intensities (areas below the curves), however, depend not only on the amount of the sample but also on the characteristics of the detector system (photo-multipliers).

For the sake of comparison, the records were normalized (Fig. 3). At the repeated testing of cadmium chloride solution sample in the same RW-crucible,

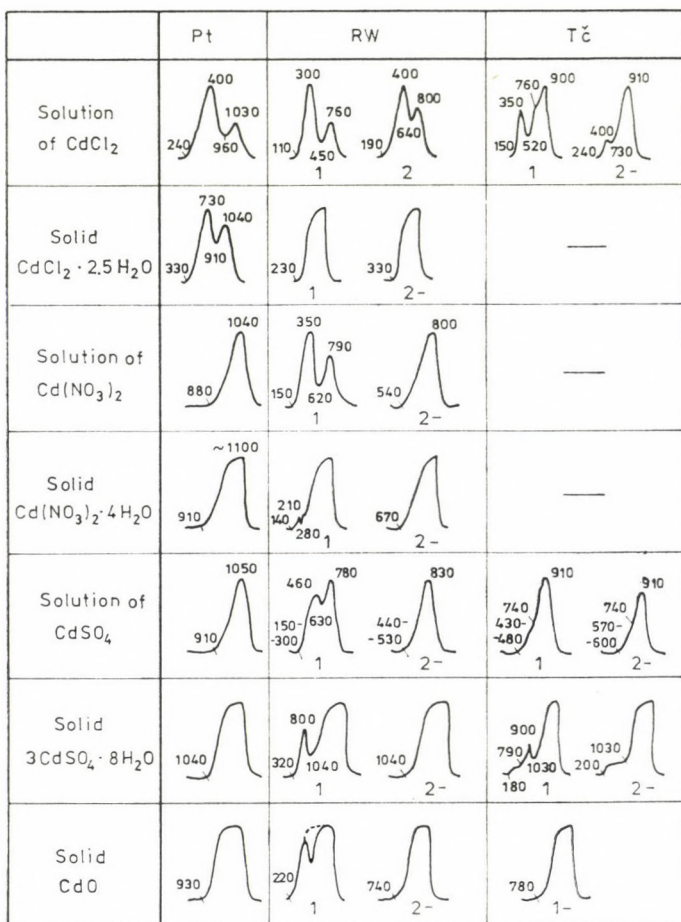


Fig. 3. Normalized intensity — time curves of cadmium salts, with characteristic temperatures. (The time — temperature axis on the diagrams is increasing left to right, in contrast with the original records.) Comments to 1, 2, 1-, 2- see Fig. 4

further changes were observed on the records of samples, as can be seen below (Fig. 4); in all other cases the character of the records has not been changed after the second heating. The test results are grouped and discussed according to the cadmium salt types as follows.

Cadmium chloride

It is striking on the records obtained using CdCl_2 sample solutions (Fig. 4) that in all cases two peaks appear, *i.e.* evaporation occurs in two steps. According to STURGEON *et al.* [3], CdCl_2 under similar conditions does not undergo thermal dissociation, so in our case, from a hydrochloric acid solution it partly evaporates in a molecular form (first peak), and partly it is converted into oxide by hydrolysis. Under heating in a platinum crucible (denoted as Pt in the Figs), cadmium oxide itself undergoes thermal decomposition causing a second peak at 1030 °C. On the other hand, in a graphite crucible (RW or Tč) CdO formed from CdCl_2 will be reduced to metal (second peak of lower temperature). Partial evaporation of CdCl_2 below its boiling point (960 °C) is in accordance with the observation that the volatility of materials in thin layers can be significantly enhanced (*e.g.* thin layer of cadmium metal begins to evaporate at an increasing rate above 450 °C, though its boiling point is 765 °C [4]). Similarly to the appearance and peak temperatures of the first peak, low CdCl_2 evaporation temperatures (300–450 °C) have been given by YASUDA and KAKIYAMA [5], as well as by FEGEŠ *et al.* [6] who observed a significant loss in chloride at 490 °C at the atomic absorption electrothermal atomization measurements.

On the serial tests performed by using RW-crucibles (Fig. 4, c) one can observe that the second peak obtained after the first heating cycle with the sample is of low intensity, *i.e.* only a small portion of CdCl_2 was converted into oxide (RW 1). When the surface of the crucible became more porous (RW 2, RW 5), the intensity ratio of the peaks changed so as the intensity associated with the second peak, *i.e.* the signal of cadmium originating from the reduction of oxide increased. Before the eighth cycle the crucible was heated on the open air for 1 min at 1100 °C; thus, after this cycle, under visually observable change of the upper graphite layer, the first peak almost completely disappeared. A similar effect could be observed in the serial tests performed with the originally more porous Tč-crucibles, where the surface layer had become loose much earlier. The rate of oxidation was determined by the rising amount of water bound on the surface layer formed.*

On the records of tests performed with solid samples of $\text{CdCl}_2 \cdot 2.5 \text{H}_2\text{O}$, double peaks could be identified only by using platinum crucible, where the second peak of higher temperature refers to the oxide formation. According to thermogravimetric tests, the water of crystallization of the chloride has resulted in oxide formation in the solid phase already at 600 °C [3]. Since water of crystallization evaporates early, and does not adhere to the surface, on the reducing graphite surfaces hydrolysis does not take place in the absence of water, and this is why only a single peak is observable.

* UBBELOHDE and LEWIS [7] called the layers obtained in the reaction of graphite and water as "lamellar compounds".

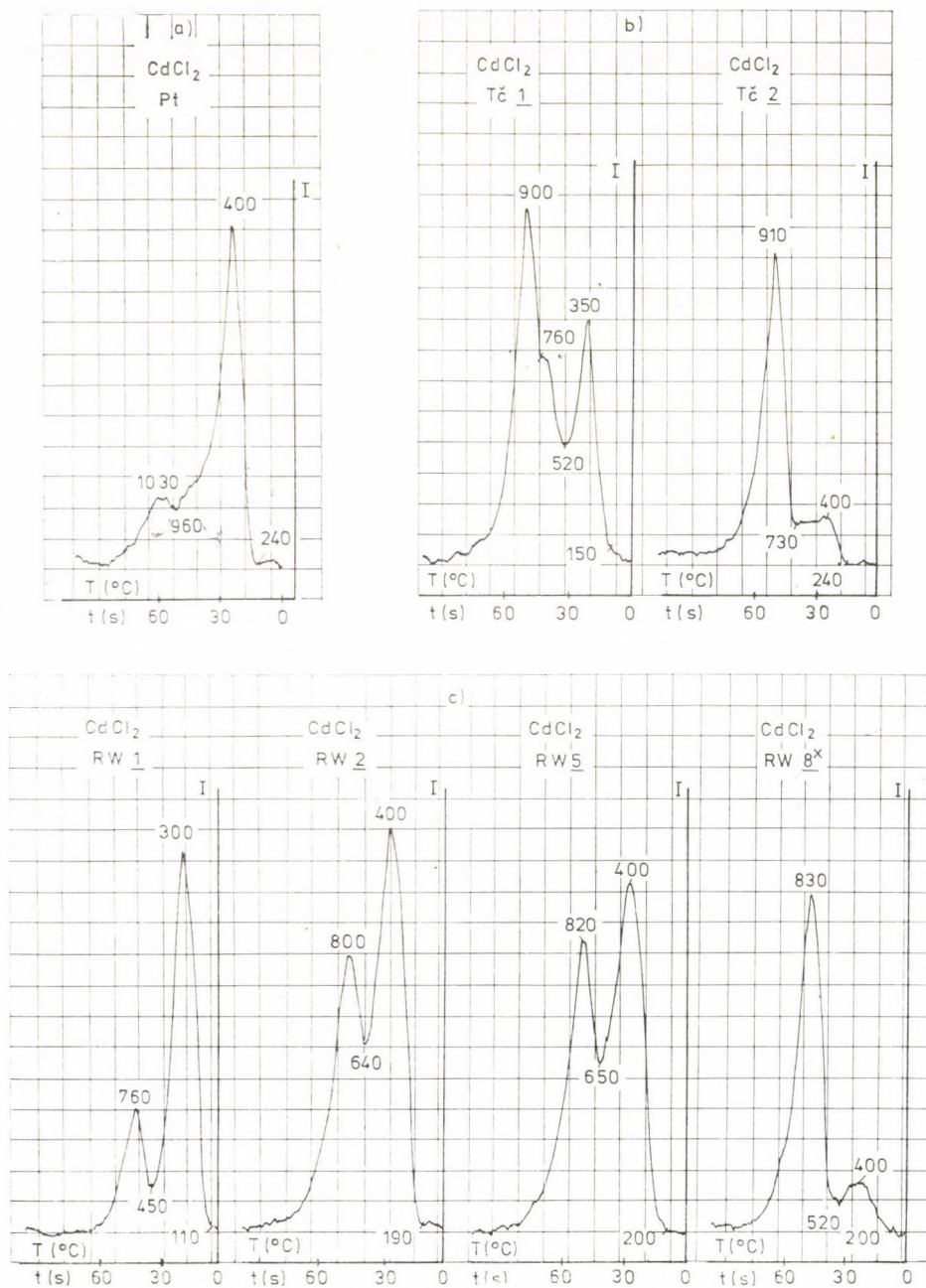


Fig. 4. Test results of cadmium chloride solution, a) in platinum crucible, b) in graphite Tč-crucible, c) in graphite RW-crucible; 1 for the first weighing-in, 2, 5, 8 at the second, fifth and eighth cycle, 1- or 2- unchanged at the further tests, ^x before this test the crucible was heated on the open air at 1100 °C for 1 min. (Original records, the time—temperature axis is increasing right to left.)

Cadmium nitrate

In platinum crucibles only a single peak was observable: the $\text{Cd}(\text{NO}_3)_2$ in the solid sample or a nitric acid solution completely decomposed to oxide, which underwent thermal dissociation above 900 °C. (A greater amount of solid sample weighed-in caused the rise of the area below the curve.) As in the case of chloride, especially for RW-crucibles (Fig. 4), the effect of the surface changes was detectable here as well; the low-temperature peak obtained in graphite crucibles on the first heating disappeared on the second heating (Fig. 3). According to the experiments of YASUDA and KAKIYAMA [5], with aqueous solutions of cadmium nitrate the signal of cadmium was obtained at 100—150 °C, and the signal of NO above 150 °C, *i.e.* a part of the nitrate decomposes already at a low temperature, especially on an active surface.

Cadmium sulphate

Introduced in solution into a platinum crucible, CdSO_4 resulted in a single peak starting above 900 °C, *i.e.* the evaporation and decomposition of the sulphate could not be resolved on the emission curve. The solid salt evaporated, presumably as an undecomposed molecule above its melting point (1000 °C), resulting from the greater amounts of the sample weighed-in. The effect of the active surface at the first heating was strongly expressed using RW-crucibles and less characteristic using Tč-crucibles, yielding peaks starting at low temperatures (Fig. 3). The decomposition of the sulphate was highly sensitive to surface quality; the curves at the first heating showed stronger variations than for other salts (Fig. 5, 1A, 1B, 1C). The peaks or breaking points visible on the curves at about 740—780 °C (as for the chloride — the oxide reduction) refer to the boiling point of the metal (765 °C). Authors cited [5] found in graphite cuvette tests of CdSO_4 solution a cadmium signal at 450 °C, and others [8] at 440 °C, these being comparable to our characteristic temperatures of about 400—500 °C.

Cadmium oxide

CdO weighed-in into a platinum crucible showed a cadmium signal only above its decomposing temperature. On the fresh surface of an RW-crucible was obtained a cadmium signal well below the decomposing temperature; in these cases the reduction of the oxide occurred in one or two steps (dotted line on Fig. 3). According to [9], the reduction of the oxide can take place already above 577 °C ($\Delta G^\circ < 0$), and others [4] claim that it is between 600 and 700 °C, and the extent of reduction depends on the rate of heating and the amount of the graphite (carbon).

Reduction of CdO , obtained from a small quantity of cadmium salts weighed-in as an aqueous solution and formed via hydrolysis or thermal decom-

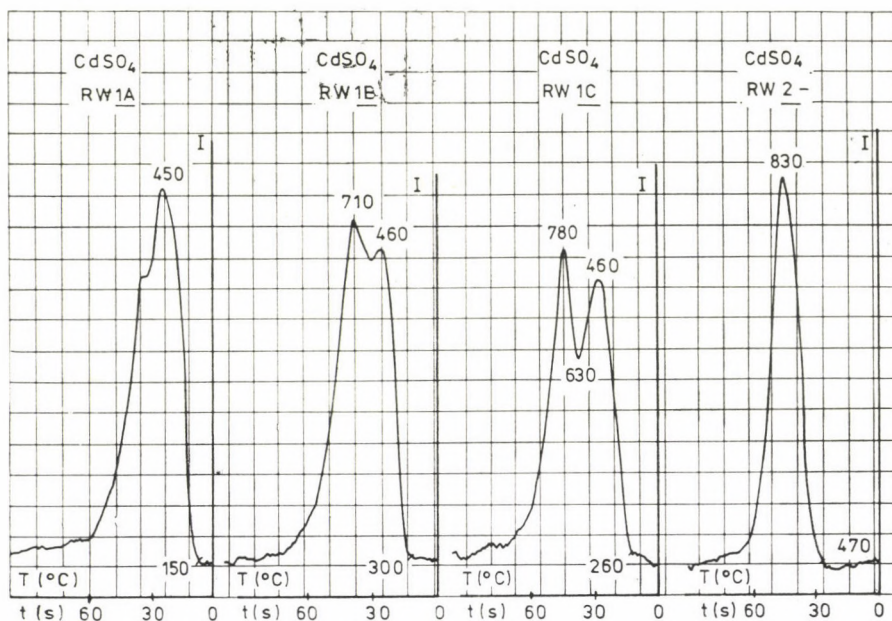


Fig. 5. Test results of cadmium sulphate solution weighed-in into RW-crucibles; 1A, 1B, 1C new crucibles at the first heating, 2- typical curve at the second and further cycles.

position, yields in the case of rapid heating a metal vapour, and therefore a signal can be observed below its boiling point (appearance temperatures of oxide peaks on the curves of chloride, nitrate and sulphate). Having a smaller contact surface area with the crucible wall, solid-phase CdO of greater quantity showed a slower reduction in which a metal of solid or liquid phase is obtained, and this is why a signal can be identified only above the boiling point of the metal.

It need to be mentioned that tests were carried out with Cd-115 isotope in chloride, nitrate and sulphate form, to check the amount of cadmium remained in the platinum and graphite microcrucibles, after heating up to 1150 °C. The amounts remaining in graphite crucibles after the first heating were as follows (average of 4 measurements): CdCl₂ 0.54%, Cd(NO₃)₂ 1.60% and CdSO₄ 3.98%. After the second and third cycles (weighing-in and heating), the retention increased, e.g. in the case of Cd(NO₃)₂ from 1.6% to 4.2 and 6.1%. In platinum crucibles the cadmium retention was slightly higher than in graphite crucibles. It means that during the heating period up to the temperature range used in all experiments the total amount of cadmium was practically volatilized.

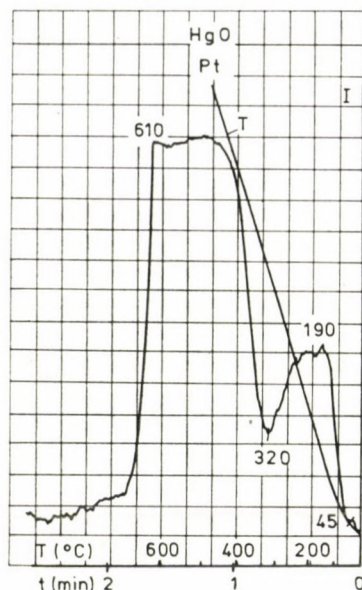


Fig. 6. Testing of mercuric oxide in platinum crucible at a rapid and smooth heating; intensity (*I*) and temperature (*T*) curves.

Investigation of mercuric salts

Conditions of investigations of mercuric salts were similar to those described above for the cadmium salts. However, the much higher volatility of the samples needed a slower heating-up, and to lower temperatures. As regards the HgO sample, a rapid heating of the microreactor gave a record (Fig. 6) which could be evaluated, but with other mercuric salts, owing to their higher volatility, the heating of the reactor was not switched on at the beginning of the test, *i.e.* the sample weighed-in into the crucible contacted at first only with the heat transferred from the arc plasma and the electrode by conduction. The heating rate was optimal at an arc current of 8 A. The signal of mercury was detectable also at the temperature of break-out of water and acid vapours, and therefore the stabilization of the d.c. arc by an external magnetic field had to be omitted (see the remark made on the experimental conditions in [1]). Before the thermal equilibrium was attained, the temperature of the microreactor was raised by a slow heating to 750 °C, so that the processes could be studied at a sufficient resolution; under these conditions, the characteristic temperatures remained essentially unchanged (Fig. 7). In graphite crucibles, in general, the first peak appeared at a lower temperature, obviously as a result of reduction, as can be seen in Fig. 8 representing the normalized curves of the mercuric salts tested.

The quality of the surface of the graphite crucibles, and its change during the repeated use with solution samples of chloride and nitrate failed to change the character of the curves, but in the case of solid samples of nitrate and oxide the surface effect was detectable. The changes of the mercury signal were studied in detail by using mercuric sulphate samples. Weighing in greater amounts of samples in platinum crucibles, the first peak increased, but the second one remained unchanged, along with the area below the curve, presumably because the excitation efficiency deteriorated with the rapid evapora-

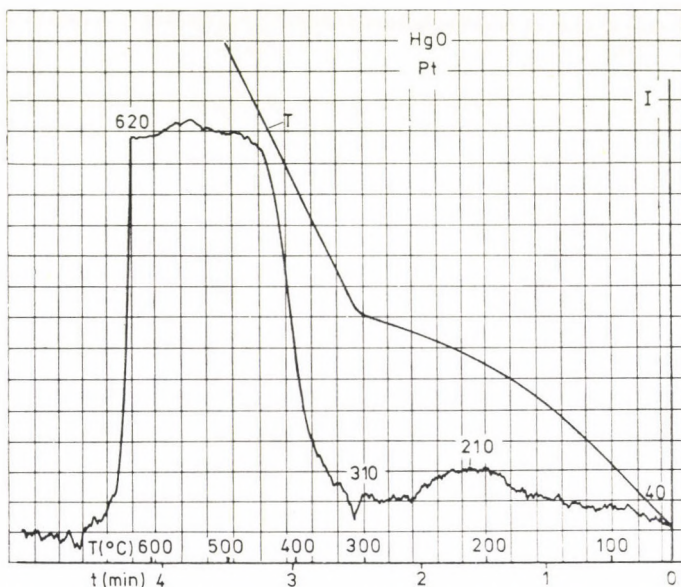


Fig. 7. Testing of mercuric oxide in platinum crucible at a reduced rate of heating: intensity (I) and temperature (T) curves.

tion of mercury, whereas the emission intensity did not increase. The effect of the active graphite surface on the decomposition process of the sulphate is clearly illustrated on the curves of Fig. 8.

For studying rapid thermal processes of mercuric salts at low temperatures, it seems to be practical to accomplish a programmable heating of the microreactor which could better approach equilibrium conditions in this system. The building of this device is planned later on.

Investigation of other compounds

Tentative tests were carried out to reveal the thermal behaviour of lead salts. However, lead vapour was bound on platinum surfaces forming alloy with it, and therefore the experimental system was not suitable for this investigation.

When operated under appropriate conditions, the device dealt with here was suitable for studying the volatility of beryllium chloride. In these tests, beryllium chloride tended to form oxide, and for this reason it distilled out only partly from a platinum crucible; the addition of graphite, or a greater

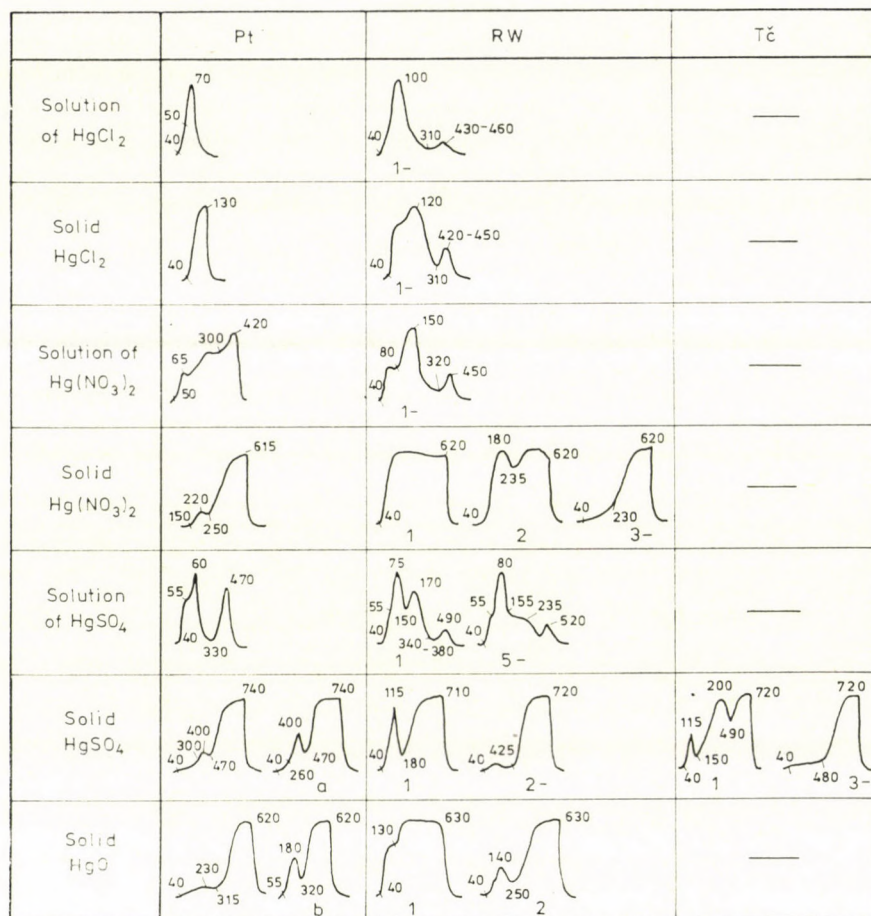


Fig. 8. Normalized intensity—time curves of mercuric salts, with characteristic temperatures; a) enhanced ($5\times$) amount of sample, b) faster heating

amount of chloride ions (NaCl , HCl), completed the evaporation process. Experimental results were similar as illustrated with cadmium salts.

The formation of volatile compounds of fluorine could be studied with thermal reactions carried out in the device described. Preliminary spectrographic investigations were performed on the decomposition of NaF , CaF_2 and AlF_3 by the addition of SiO_2 , and experiments were carried out with volatiliz-

ing additives $\text{Na}_2\text{W}_2\text{O}_7$, WO_3 , Na_3PO_4 and V_2O_5 . It was found that the application of a mixture of sample: SiO_2 : WO_3 in a ratio of 1 : 1 : 3 by weight for the release of SiF_4 yielded the optimal results. These investigations are dealt with in another work [10].

Conclusions

Investigation of thermal processes of cadmium salts in argon atmosphere in detail demonstrated that evaporation and conversion processes, as well as thermal reactions, were clearly identified with the cadmium signal in the experimental device elaborated; characteristic temperatures on the emission curves were reproducible ($\pm 20^\circ\text{C}$), and the occurrence of several processes was established. Investigation of thermal processes of mercuric salts underlined the statements.

The study of the correlation between the quality of the graphite surface and the course of the thermal reactions needs further investigations for its basic spectroscopic significance.

REFERENCES

- [1] GEGUS, E., KREITER, J., MÉRAY, L., INCZÉDY, J.: *Acta Chim. Acad. Sci. Hung.*, **100**,
- [2] STURGEON, R. E., CHAKRABARTI, C. L.: *Anal. Chem.*, **49**, 90 (1977)
- [3] SFURGEON, R. E., CHAKRABARTI, C. L., LANGFORD, C. H.: *Anal. Chem.*, **48**, 1792 (1976)
- [4] *Gmelins Handbuch der anorg. Chemie. Cadmium. Ergänzungsband 33.* Verl. Chemie GmbH, Weinheim, 1959
- [5] YASUDA, S., KAKIYAMA, H.: *Anal. Chim. Acta*, **89**, 369 (1977)
- [6] FEGEŠ, J., GOMIŠČEK, S., HUDNIK, V., ŠPAIN, M.: *Kém. Köz.*, **43**, 445 (1975)
- [7] UBBELOHDE, A. R., LEWIS, F. A.: *Graphite and its Crystal Compounds.* Oxford Press, London, 1960, p. 176
- [8] JOHNSON, D. J., SHARP, B. L., WEST, T. S.: *Anal. Chem.*, **47**, 1234 (1975)
- [9] CAMPBELL, W. C., OTTAWAY, J. M.: *Talanta*, **21**, 837 (1974)
- [10] KREITER, J.: *Dissertation. Veszprém*, 1977 (in Hung.)

Ernő GEGUS

József KREITER

László MÉRAY

János INCZÉDY

H-8201 Veszprém, P.O. Box 28.

INVESTIGATION OF THE MOLECULAR STRUCTURE OF PHENOL ETHERS BY QUANTUM CHEMICAL METHODS, I

EXPERIMENTAL DATA AND CALCULATION METHODS

P. HENCSEI and J. NAGY

(Department of Inorganic Chemistry, Technical University of Budapest)

Received May 5, 1978

Accepted for publication September 25, 1978

In the first part of our work the experimental physico-chemical data (ultraviolet spectra, dipole moments, ionization potentials, ^{13}C chemical shifts) of phenol ethers with general formula $\text{XC}_6\text{H}_4\text{OCH}_3$ (where $\text{X} = \text{H}, o-, m-, p\text{-CH}_3, \text{CH}_3\text{O}, \text{Cl}, \text{NO}_2, \text{F}, \text{NH}_2$) and the input parameters of calculation methods (DEL RE, iterative PPP, Extended Hückel) were published.

The molecular structures of phenol ethers have been investigated by several physico-chemical methods. This work is concerned with calculations by quantum-chemical approximations, with the interpretation of the physico-chemical properties of phenol ethers on the basis of these calculations, and with the effect of substituents. Molecules of the general formula $\text{XC}_6\text{H}_4\text{OCH}_3$ were studied, where $\text{X} = \text{H}, o-, m-, p\text{-CH}_3, \text{CH}_3\text{O}, \text{Cl}, \text{NO}_2, \text{F}$ or NH_2 .

Experimental data

Ultraviolet spectra

The uv spectroscopic data of the compounds were taken from the paper of DEARDEN and FORBES [1], and from two, slightly later publications of FORBES [2].

The spectra were recorded in cyclohexane solution. Table I shows the wavelengths of the maxima of α and ρ bands (λ_α and λ_ρ). For *m*-nitroanisole the maximum of the β band is also given.

According to the uv spectra of substituted anisoles, the maxima of α bands show in most cases a bathochromic displacement with respect to anisole. This shift is significant in the case of *p*-dimethoxybenzene, and in amino- and nitroanisoles. In the case of *o*- and *m*-fluoro derivatives hypsochromic displacements can be observed. In the maxima of ρ bands quite significant bathochromic effects can be seen with the amino and nitro derivatives, whereas from the maxima of the other compounds no unanimous conclusion can be drawn. The uv spectra of methyl and chloroanisoles are generally very similar to the

Table I
The experimental data of phenol ether of type
 $\text{CH}_3\text{OC}_6\text{H}_4\text{X}$

X	Ultraviolet maxima [1, 2]		Dipole moment [3, 4]			Ionization potential [5] I.P. (eV)
	λ_p (nm)	λ_α (nm)	μ (D)	solvent*	t (°C)	
H	220	275	1.25	average		8.39
2-CH ₃ O	225	275	1.32	B	25	
3-CH ₃ O	220	271.5	1.60	B	20	8.17
4-CH ₃ O	226	290	1.70	average		7.88
2-CH ₃	215.5	270	1.09	B	20	
3-CH ₃	217	277.2	1.25	B	20	8.35
4-CH ₃	222.5	276.5	1.24	B	20	8.33
2-Cl	219	283	2.44	B	20	
3-Cl	219	275	2.06	B	25	8.72
4-Cl	228	282	2.32	B	20	8.52
2-NO ₂	248.5	304	4.80	B	20	
3-NO ₂ **	260	313	4.0	B	20	9.09
4-NO ₂	—	291	4.98	B	20	9.04
2-F	219.5	271	2.31	B	25	
3-F	220	269.5	—			8.70
4-F	218.5	281.5	2.11	B	20	8.58
2-NH ₂	237	286	1.99	B		
3-NH ₂	233.5	283	1.72	B	25	7.76
4-NH ₂	236	303	1.80	B	25	7.60

*B: benzene, ** λ_p : 223 nm

spectrum of anisole itself, indicating that these substituents do not affect the electronic structure to a significant extent. Parasubstituted derivatives show the following sequence of bathochromic displacement:



Dipole moments

The experimental dipole moments of phenol ethers were taken from the comprehensive works of McCELLAN [3] and OSIPOV, MINKIN and GARNOVSKII [4]. Of the experimental data, if possible, the ones measured under the same experimental conditions (at 20 or 25 °C in benzene) were selected. For anisole and p- dimethoxybenzene, the mean values calculated from the most probable experimental results given in the work of McCELLAN [3] were selected as

experimental dipole moments. The data used are shown in Table I (1 Debye = $1/3 \cdot 10^{-29}$ Cm).

Ionization potentials

The experimental ionization potentials of phenol ethers were selected from the papers of BROWN [5]. The data used are also given in Table I.

^{13}C chemical shifts

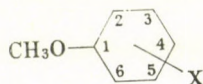
Several papers deal with the ^{13}C NMR spectra of phenol ethers [6–9]. The ^{13}C chemical shifts of the aromatic carbon atoms of substituted phenol ethers were selected from these papers. The data are shown in Table II. Some papers report chemical shifts with respect to carbon disulfide, they were converted into chemical shifts with respect to benzene by the conversion factor $\delta_{\text{C}}(\text{C}_6\text{H}_6/\text{CS}_2) = 65.0$ ppm.

Molecular geometry

Of the phenol ethers, the molecular geometry of *p*-dimethoxybenzene is known from the X-ray diffraction studies of GOODWIN *et al.* [10]. The other structural parameters necessary for the calculations were taken from the data of substituted benzene derivatives [11]. Bond lengths and angles used in the

Table II

The ^{13}C chemical shifts of the aromatic carbon atoms of phenol ethers (ppm, related to benzene) [6–9]



X	C-1	C-2	C-3	C-4	C-5	C-6
H	−30.2	14.7	− 0.9	8.1	− 0.9	14.7
2-CH ₃ O	−22.6	−22.6	15.5	6.9	6.9	15.5
3-CH ₃ O	−33.3	27.0	−33.3	21.7	− 2.2	21.7
4-CH ₃ O	−26.4	13.1	13.1	−26.4	13.1	13.1
2-CH ₃	−28.9	2.7	− 1.7	7.9	1.5	18.6
3-CH ₃	−30.9	14.1	−10.0	7.6	− 0.2	17.9
4-CH ₃	−29.7	14.5	− 1.7	− 0.9	− 1.7	14.5
4-Cl	−30.1	12.9	− 1.2	3.3	− 1.2	12.9
4-NO ₂	−37.1	13.3	2.1	−11.3	2.1	13.3
4-F	−27.1	13.2	13.2	−28.7	13.2	13.2

calculations are given in Table III (1 pm = 0.01 Å). The molecules were assumed to be planar, and therefore all substituents were placed in the plane of the ring, except of course the hydrogens of methyl and methoxy groups. In the calculation of dipole moments, a free rotation of methoxy groups was assumed.

Table III
Geometry data [10, 11]

Bond	Bond length (pm)	Note
C—C	139.7	aromatic-aromatic
	152	aromatic-aliphatic
C—H	108.4	aromatic
	109.3	aliphatic
C—O	136	
C—F	130.5	
C—Cl	170.6	
C—N	148	in nitro compounds
	142.6	in amino compounds
N—O	121	
N—H	101.4	

COC valence angle: 121°

Calculation methods

Del Re method

The σ electron system of compounds was studied by the approximation of DEL RE [12]. Of the original parameters, the value of inductive parameter γ_{CH} was modified, and the method was extended to more types of atoms and bonds [13]. The DEL RE parameters used in the calculations are given in Table IV.

Iterative Pariser–Parr–Pople method

The π electron system of compounds was studied by an iterative PPP method [14, 15]. During the calculation ionization energies were varied as a function of effective nuclear charge, whereas electron affinities and resonance integrals were constant. Ionization energies were determined by exponential functions of the Form $I_i = -a_i \exp(b_i Z_i^*)$, where Z_i^* is effective nuclear charge, and constants a_i and b_i were determined from the isoelectronic series of atoms and ions belonging to the same electronic state. Effective nuclear charge was calculated by the method of BURNS [16]. This method makes dis-

Table IV
Del Re parameters [12, 13]

$i-j$	ϵ_{ij}	γ_{ij}	γ_{ji}	δ_i^σ	δ_j^σ
C—C	1.00	0.1	0.1	0.07 (sp ³)	0.07 (sp ³)
				0.12 (sp ²)	0.12 (sp ²)
C—H	1.00	-0.2	0.4	0.07 (sp ³)	0
				0.12 (sp ²)	
C—O	0.95	0.1	0.1	0.07 (sp ³)	0.40
				0.12 (sp ²)	
C—N	1.00	0.1	0.1	0.12 (sp ²)	0.30 (sp ²)
C—F	0.85	0.1	0.1	0.12 (sp ²)	0.57
C—Cl	0.65	0.2	0.4	0.12 (sp ²)	0.35
N—O	1.00	0.1	0.1	0.30 (sp ²)	0.40
N—H	0.45	0.3	0.4	0.30 (sp ²)	0

tion between s and p orbitals, can also be used for d orbitals, and, in contrast with the Slater rules, it produces smaller overlap between the orbitals. Actual effective nuclear charges Z_i^* necessary for the iteration were calculated according to the equation

$$Z_i^* = Z_i^{*0} + 0.35(n_i + \delta_i^\sigma - q_i^\pi)$$

where Z_i^{*0} is the effective nuclear charge given by the BURNS method,
 n_i is the number of electrons supplied to the π electron system by the atom,
 δ_i^σ is partial σ charge from the DEL RE approximation, and
 q_i^π is π electron density.

On the basis of PARISER [17], the one-center electron interaction integrals γ_{ii} were taken as the difference between the valence state ionization energies I_i and electron affinities A_i :

$$\gamma_{ii} = I_i - A_i$$

The atoms which supply two electrons to the π electron system of the molecule (F, Cl, N, O) were accounted for with double electron interaction integrals γ_{ii}^+ :

$$\gamma_{ii}^+ = I_i^+ - I_i$$

where I_i^+ is the second ionization energy.

Valence state ionization energies and electron affinities were calculated by the empirical formula of MATAGA and NISHIMOTO [21] from the corresponding experimental ground state values [18—20]:

$$\gamma_{ij} = \frac{1}{a_{ij} + R_{ij}}; \quad a_{ij} = \frac{2}{\gamma_{ii} + \gamma_{jj}}$$

where R_{ij} is the interatomic distance.

Resonance integrals β_{ij}^0 were calculated by the WOLFSBERG—HELMHOLZ relationship [22]

$$\beta_{ij}^0 = \frac{1}{2} k(I_i + I_j) S_{ij}$$

where k is constant, and

S_{ij} is the overlap integral.

The value of k was determined from the resonance and overlap integrals of the C—C bond of benzene, to obtain $k = 0.6426$.

The most important parameters of IPPP calculations are given in Table V.

Table V
Parameters of iterative PPP calculations

i	a_i	b_i	γ_{ii} (eV)	i—j	$-\beta_{ij}^0$ (eV)
C	0.6133	1.0362	11.13	C—C	2.392—2.453
O ⁺	0.8660	0.8459	21.53	C—O	2.169—2.178
O	0.7093	0.8144	15.23	C—N _{nitro}	1.868—1.874
N ⁺	0.9702	0.8723	17.44	C—N _{amino}	2.057—2.065
F ⁺	0.7093	0.8144	21.713	N—O	2.550—2.551
Cl ⁺	0.4348	0.7417	12.949	C—F	1.850—1.856
				C—Cl	1.710—1.723

Extended Hückel method

Phenol ethers were also investigated by the Extended Hückel [EHT] all valence electron method [23, 24]. The ionization energies required for these calculations were taken from the work of HINZE [18] the orbital exponents ξ_i were determined on the basis of the rules of BURNS [16]. The ionization energy I_d of the 3d orbital of chlorine was taken from the paper of LEVISON and PERKINS [25]. The parameters of EHT calculations are given in Table VI.

The results of calculations, discussion and conclusions on molecular structure are the subject of Part II of this series.

Table VI
Parameters of Extended Hückel calculations

	I_s (eV)	ϵ_s	I_p (eV)	ϵ_p	I_d (eV)	ϵ_d
H	13.60	1.000	—	—	—	—
C	21.01	1.575	11.27	1.400	—	—
N	26.92	1.900	14.42	1.725	—	—
O	36.07	2.225	18.53	2.050	—	—
F	38.24	2.550	20.86	2.300	—	—
Cl	24.02	2.266	15.03	1.733	2.20	1.083

REFERENCES

- [1] DEARDEN, J. C., FORBES, W. F.: Can. J. Chem., **37**, 1305 (1959)
- [2] FORBES, W. F.: Can. J. Chem., **37**, 1977 (1959); **38**, 1104 (1960)
- [3] MCCCELLAN, A. L.: Tables of Experimental Dipole Moments. Vol. 1. FREEMAN and Co., London 1963; Vol. 2. Rahara Enterprises, El Cerrito 1974
- [4] OSIPOV, O. A., MINKIN, V. I., GARNOVSKII, A. D.: Spravochnik po dipolnim momentam. Visshaja Shkola, Moscow 1971
- [5] BROWN, P.: Org. Mass. Spectrom., **4**, 519, 533 (1970)
- [6] SPIESECKE, H., SCHNEIDER, W. G.: J. Chem. Phys., **35**, 731 (1961)
- [7] LAUTERBUR, P. C.: J. Am. Chem. Soc., **83**, 1846 (1961)
- [8] DHAMI, K. S., STOTHERS, J. B.: Can. J. Chem., **44**, 2855 (1966)
- [9] MACIEL, G. E., NATTERSTAD, J. J.: J. Chem. Phys., **42**, 2427 (1965)
- [10] GOODWIN, T. H., PRZYBYLSKA, M., ROBERTSON, J. M.: Acta Cryst., **3**, 279 (1950)
- [11] SUTTON, L. E.: Tables of Interatomic Distances and Configuration in Molecules and Ions. The Chemical Society, London 1958
- [12] DEL RE, G.: J. Chem. Soc., **1958**, 4031
- [13] NAGY, J., HENCSEI, P., RÉFFY, J.: Acta Chim. Acad. Sci. Hung., **65**, 51 (1970)
- [14] BROWN, R. D., HEFFERNAN, M. L.: Trans. Faraday Soc., **54**, 757 (1958)
- [15] BROWN, R. D., HEFFERNAN, M. L.: Aust. J. Chem., **12**, 319 (1959)
- [16] BURNS, G.: J. Chem. Phys., **41**, 1521 (1964)
- [17] PARISER, R.: J. Chem. Phys., **21**, 568 (1953)
- [18] HINZE, J.: Ph. D. Dissertation, University of Cincinnati 1962
- [19] HINZE, J., JAFFE, H. H.: J. Am. Chem. Soc., **84**, 540 (1962)
- [20] SANDERSON, R. T.: Chemical Periodicity, Reinhold Publ. Corp., New York 1960
- [21] MATAGA, N., NISHIMOTO, K.: Z. Phys. Chem. (Frankfurt), **13**, 140 (1957)
- [22] WOLFSBERG, M., HELMHOLZ, L.: J. Chem. Phys., **20**, 837 (1952)
- [23] HOFFMANN, R., LIPSCOMB, N. N.: J. Chem. Phys., **36**, 2179 (1962)
- [24] HOFFMANN, R.: J. Chem. Phys., **39**, 1397 (1963); **40**, 2474, 2480, 2745 (1964)
- [25] LEVISON, K. A., PERKINS, P. G.: Theor. Chim. Acta, **14**, 206 (1969)

Pál HENCSEI }
József NAGY } H-1521 Budapest, Gellért tér 4.

INVESTIGATION OF THE MOLECULAR STRUCTURE OF PHENOL ETHERS BY QUANTUM CHEMICAL METHODS, II

RESULTS AND DISCUSSION

P. HENCSEI,¹ G. PONGOR² and J. NAGY¹

⁽¹⁾*Department of Inorganic Chemistry, Technical University of Budapest,*

⁽²⁾*Chemical and Pharmaceutical Works, Ltd., Chinoin, Budapest)*

Received May 5, 1978

Accepted for publication September 25, 1978

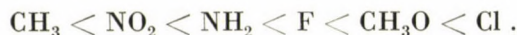
Experimental physico-chemical data (electronic transitions, dipole moments, ionizations energies and ¹³C chemical shifts) of phenol ether of the type XC₆H₄OCH₃ (X = *o*-, *m*-, *p*-CH₃, CH₃O, Cl, NO₂, F, NH₂) have been interpreted by means of quantum chemical calculations. Del Re, iterative PPP, and EHT approximations were used, the parameters of IPPP method were determined by new relationships. The calculations were performed on planar model, and a free rotation of methoxy groups was assumed. From the correlations between experimental and calculated data conclusions have been drawn on molecular structure.

Part I of our paper [1] was concerned with the physico-chemical data of substituted phenol ethers of the type XC₆H₄OCH₃ (X = *o*-, *m*-, *p*-CH₃, OCH₃, Cl, NO₂, F, NH₂), with the quantum chemical approximations, and the parameters used. This paper deals with the results of calculations, discussing the conclusions drawn on the structure of molecules.

Results

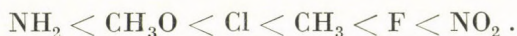
Charge distributions, partial charges, bond orders

The partial charges δ_σ obtained with the Del Re method show the following characteristics. The partial charge of oxygen atoms is nearly constant, $\delta_\sigma = -0.3020$, independently of the substituents. The partial charges of hydrogens increase in the sequence of methyl, methoxy, aromatic, amino. The partial charges of aromatic carbon atoms show already significant variation; the highest value can be found in *o*-fluoroanisole, on the carbon attached to the fluorine atom (+0.1799), and the lowest in *p*-methylanisole on the carbon attached to the methyl group (−0.0588). The δ_σ partial charges of aromatic carbons are characteristic of the inductive effect of the substituents. The substituent effect can be studied most advantageously in metasubstituted compounds. In metasubstituted phenol ethers δ_σ of the carbon atom between the two substituents increases in the sequence



This sequence is identical to that of the inductive effects of the above substituents.

The partial charges δ_π obtained with the IPPP method show the following features. The partial charge δ_π of the oxygen atom changes more strongly with the substituents than δ_σ ; it is the lowest in *o*-aminoanisole (+0.1173), and the highest in *o*-nitroanisole (+0.1482). Carbon atoms have generally negative δ_π values, positive charges can be found only in nitroanisoles. The δ_π charges of aromatic carbon atoms can be correlated with the mesomeric effects of substituents, in the following sequence (in metasubstituted phenol ethers):



The combined $\sigma\pi$ partial charges increase in the sequence



This sequence reflects the orientation effect of the substituents; amino, methoxy and methyl groups are first-order substituents, chlorine and fluorine are first-order deactivating groups, whereas the nitro group is a second-order substituent.

IPPP calculations produced the following π bond orders. The C—O bond order varies between 0.328 and 0.368, being only slightly modified by the substituents. The C—C bond order in the aromatic ring was found to vary between 0.603 and 0.683. The substituents have the following ranges of p_π .

C—Cl	0.176—0.186
C—F	0.153—0.161
C—N _{amino}	0.399—0.413
C—N _{nitro}	0.216—0.233
N—O	0.602—0.611

The partial charges given by the EHT method correspond to unreasonably strong shifts. For instance, the charge on the oxygen atom was found to be -1.06 , that of the nitro nitrogen varied around $+1.70$, and widely different charges were obtained for the carbon atoms: $+0.31$ in methoxy groups, -0.31 in methyl groups, and charges between -0.30 and $+0.82$ in the aromatic ring. The sequence of the hydrogen charges was also different from that obtained with the Del Re method: aromatic $<$ methoxy $<$ methyl $<$ amino. The results indicate that the partial charges given by EHT cannot be applied to draw conclusions on molecular structure.

Electronic transitions

The singlet electronic transition energies obtained from IPPP calculations were compared with the transition energies corresponding to the experimental uv absorption maxima. [In the calculations configuration interaction

Table I

Experimental and IPPP results of phenol ethers of type CH₃OC₆H₄X

X	$\Delta E_{\alpha}^{\text{exp}}$ (eV)	f_{exp} (eV)	${}^1E_{\text{CI}}^{\text{calc}}$ (eV)	f_{calc} (eV)	μ_{exp} (D)	μ_{calc} (D)	μ_{m} (D)	I.P. ^{exp} (eV)	I.P. ^{calc} (eV)
H	4.51	0.050	4.56	0.032	1.25	1.414	—	8.39	9.040
2-CH ₃ O	5.64	0.180	5.59	0.295	1.32	2.102	1.853	—	
	4.51	0.061	4.34	0.044					
3-CH ₃ O	5.51	0.171	5.20	0.212	1.60	1.790	1.766	8.17	8.665
	4.57	0.053	4.39	0.022					
4-CH ₃ O	5.64	0.175	5.42	0.115	1.70	1.579	1.722	7.88	8.313
	4.28	0.077	4.23	0.077					
2-CH ₃	5.49	0.233	5.27	0.490	1.09	1.474	1.386	—	
	4.59	0.048	4.56	0.031					
3-CH ₃	5.75	0.180	5.59	0.294	1.25	1.374	1.276	8.35	9.050
	4.47	0.046	4.57	0.032					
4-CH ₃	5.71	0.168	5.60	0.294	1.24	1.318	1.218	8.33	9.035
	4.48	0.053	4.56	0.035					
2-Cl	5.57	0.206	5.60	0.295	2.44	1.750	1.881	—	
	4.38	0.059	4.52	0.032					
3-Cl	5.66	0.180	5.51	0.236	2.06	2.385	2.190	8.72	9.022
	4.51	0.052	4.54	0.026					
4-Cl	5.66	0.175	5.57	0.238	2.32	2.646	2.329	8.52	8.904
	4.40	0.046	4.51	0.043					
2-NO ₂	5.44	0.281	5.52	0.362	4.80	3.920	4.016	—	
	4.08	0.060	3.14	0.105					
3-NO ₂	4.99	0.082	4.82	0.031	4.0	4.560	4.394	9.09	9.503
	3.96	0.058	3.44	0.036					
4-NO ₂	4.77	0.146	4.80	0.043	4.98	5.148	4.571	9.04	9.586
	5.56	0.312	5.70	0.616					
2-F	4.26	0.290	3.80	0.300	2.31	1.945	1.794	—	
	4.57	0.041	4.55	0.035					
3-F	5.65	0.170	5.57	0.273	—	2.641	2.093	8.70	9.085
	4.60	0.037	4.54	0.033					
4-F	5.64	0.180	5.58	0.269	2.11	2.937	2.228	8.58	9.070
	4.40	0.077	4.55	0.031					
2-NH ₂	5.67	0.129	5.55	0.322	1.99	2.263	2.093	—	
	4.33	0.083	4.09	0.067					
3-NH ₂	5.23	0.204	4.81	0.313	1.72	1.723	1.892	7.76	8.003
	4.38	0.054	4.16	0.034					
4-NH ₂	5.31	0.153	5.06	0.315	1.80	1.317	1.782	7.60	7.693
	4.09	0.064	3.92	0.085					
	5.25	0.218	4.92	0.594					

(CI) was taken into account.] The experimental and calculated transition energies are compared in Table I, and a plot of the experimental data *vs* calculated values is shown in Fig. 1.

As can be seen from the data, the agreement between experimental and calculated transition energies is satisfactory, the average differences being 0.186 eV for the α bands and 0.159 eV for the p bands. For the total data set the average difference is 0.173 eV (3.7%), and the correlation between the two quantities is 95%. Differences greater than average occur with nitroanisoles and *o*-bis-dimethoxybenzene. For these compounds the assumption of planarity is unjustified, and thus the results of IPPP calculations disagree with the

experimental data. Non-planarity is also indicated by the following facts. The differences between the uv maxima of anisole and phenol derivatives substituted in the same way are as follows [2, 3]:

<i>o</i> -nitro	38 nm (α) and 18.5 nm (p)
<i>m</i> -nitro	6 nm (α)
<i>p</i> -nitro	4 nm (α)
<i>o</i> -methoxy	9 nm (p)

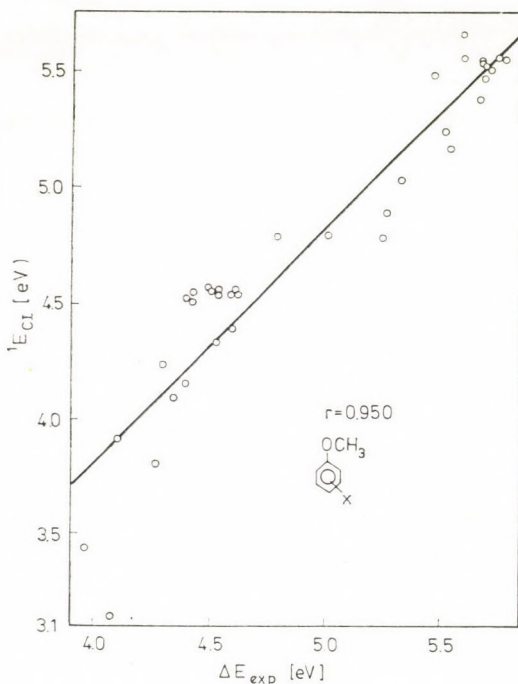


Fig. 1. Calculated ${}^1E_{Cl}$ values of phenol ethers as a function of experimental electronic transitions

These differences are readily interpreted if it is assumed that substituted anisoles are different in steric structure from the corresponding substituted phenol derivatives. It can also be seen from the data of the table that the calculated and experimental oscillator strengths of phenol ethers agree very well, with an average difference of 0.02 for α bands and 0.10 for p bands.

Dipole moments

The dipole moments of the molecules were calculated from the partial charges δ_o obtained from DelRe calculations and the partial charges δ_π obtained from IPPP calculations. It was assumed in the calculation of dipole moments

that the methoxy groups of phenol ethers may execute free rotation around the oxygen — aromatic carbon axis. The remainder of the molecule, including the other substituents, is fixed, and thus the total dipole moment consists of a constant vector and the rotating vectors of rotating groups (see Fig. 2).

The average dipole moment of a group executing free rotation can be determined by integration:

$$\bar{\mu}^2 = \frac{1}{2\pi} \int_0^{2\pi} [(a \cos \alpha \cos \varphi - x)^2 + (a \sin \alpha - y)^2 + (a \cos \alpha \sin \varphi)^2] d\varphi$$

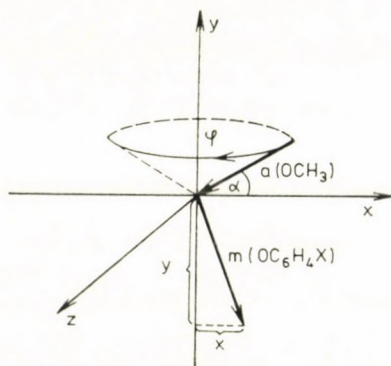


Fig. 2. Calculation of dipole moment with free rotation

During rotation, the charge distribution of the molecule was assumed to be invariant.

In addition to the charge distribution method, the dipole moments of the molecules were also determined by the method of group moments. The results can be found in column μ_m of Table I. According to the method, the molecular dipole moment is assumed to be the vector sum of the moments of atom groups. When a molecule contains two free rotating polar groups (see Fig. 3), the resulting dipole moment is given by the equation [4, 5]

$$\bar{\mu}^2 = \mu_1^2 + \mu_2^2 + 2\mu_1\mu_2 \cos \Theta_1 \cos \Theta_2 \cos \omega_{12}$$

where μ_1 and μ_2 are group moments,

Θ_1 and Θ_2 are the angles between the directions of rotation axes and the group moment vectors, and

ω_{12} is the angle between the axes (60° for *ortho*, 120° for *meta* and 180° for *para* substitution).

The values of μ_i and Θ_i used for the calculations and given in Table II were taken from the literature [6]. The calculated dipole moments are shown in Figs 4 and 5 as a function of the experimental values.

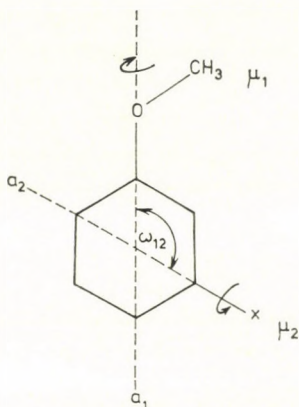


Fig. 3. Calculation of dipole moment from group moment

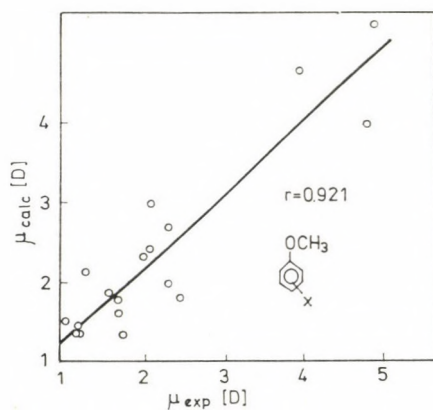


Fig. 4. Dipole moments of phenol ethers calculated from charge distributions, as a function of experimental values

Table II
Group moments [6]

C_6H_5-X	$\mu_i(D)$	θ_i
CH_3	0.37	0
CH_3O	1.28	72°
F	-1.47	0
Cl	-1.59	0
NH_2	1.53	48.5°
NO_2	-4.01	0

The data of Table I and the plots in Figs 4 and 5 permit the following conclusions to be drawn. The group moment method provides better results than the calculated charge distributions. In the former case the average difference between experimental and calculated data is 0.252 D (11.2%), whereas in the latter case it is 0.375 D (18.4%). With either method, the largest discrepancies were obtained for the orthosubstituted derivatives, indicating that in these molecules the rotation of the methoxy group is hindered. The better agreement obtained with the group moment method suggests that CH₃, Cl, F,

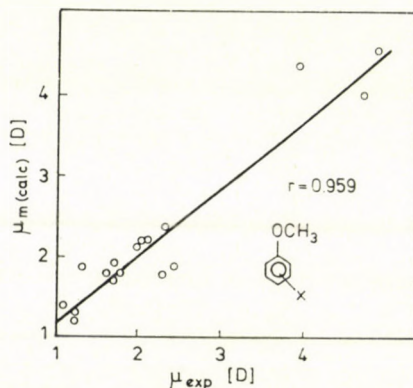


Fig. 5. Dipole moments of phenol ethers calculated from group moments, as a function of experimental values

CH₃O and NH₂ substituents have weak effect on the π bond system. The larger difference obtained for nitroanisoles can be explained by the strong $-M$ effect of the nitro group.

Ionization energies

As proposed by KOOPMANS [7], experimental ionization energies were compared to the energy of the highest occupied molecular orbital. Experimental and calculated data are given in Table I and Fig. 6. Calculated ionization energies are higher by 0.4–0.5 eV, in average, than experimental values, but the correlation between the two data sets is good, $r = 0.952$.

NMR correlations

The NMR chemical shifts of various nuclei (¹H, ¹³C, ¹⁹F, etc.) are usually correlated with calculated electron densities. Thus, e.g. according to KARLSSON and MARTENSSON [8], there is a simple proportionality between the NMR chemical shifts ¹H or ¹³C and the charges on the corresponding carbon atoms. It is most customary to correlate the total electron densities obtained from CNDO or EHT calculations with ¹³C chemical shifts, but the results of PPP

approximation can also be used for correlation. It is also possible to introduce a relative paramagnetic shielding factor σ_{rel}^* , and to use this quantity instead of a direct comparison with electron density. According to ENGELHARDT *et al.* [9], σ_{rel}^* of the carbon atoms of aromatic compounds is evaluated by the expression

$$\sigma_{\text{rel}}^* = \frac{2P_n}{3} \left(1 + \frac{0.35\delta}{Z^*} \right)^3$$

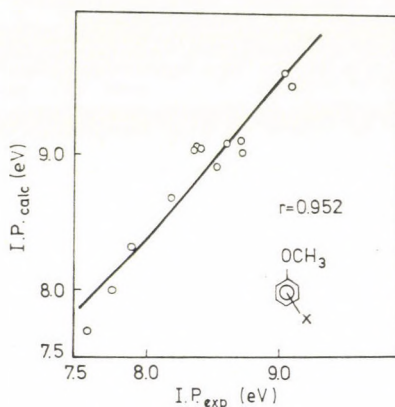


Fig. 6. Comparison of calculated and experimental ionization energies of phenol ethers

where P_n is a function of the hybridization and occupation of p orbitals, and can be evaluated from bond polarities,

δ is partial charge, and

Z^* is effective nuclear charge (2.80).

On the basis of this equation, σ_{rel}^* can be evaluated for all carbon atoms, and the results can be correlated with ^{13}C chemical shifts.

The partial charges obtained for phenol ethers by Del Re and IPPP methods are plotted against ^{13}C chemical shifts in Fig. 7. EHT partial charges are plotted against ^{13}C chemical shifts in Fig. 8. Finally, relative paramagnetic shielding factors σ_{rel}^* are plotted against ^{13}C chemical shifts in Fig. 9. The data used in NMR correlations are given in Table III.

As can be seen from Figs 7, 8 and 9, and from the data of Table III, there is a relatively good correlation in all the three cases between ^{13}C chemical shifts and the calculated quantities. The best correlation was obtained with EHT partial charges, for which the linear regression coefficient was $r = 0.953$, whereas for the other two quantities $r = 0.875$ and 0.881 , respectively. This shows that although the EHT approximation produces unreasonable charges for molecules containing hetero atoms, the tendencies of NMR chemical shifts are reproduced quite satisfactorily by the relative charges of aromatic carbon

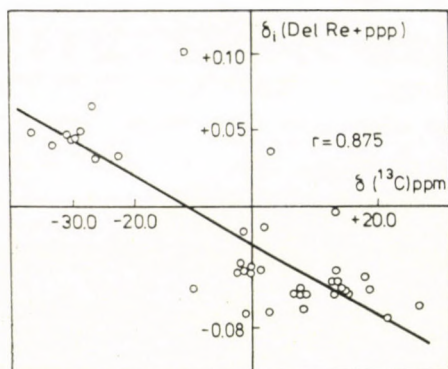


Fig. 7. Partial charges of the aromatic carbons of phenol ethers calculated by Del Re and IPPP methods, as a function of ^{13}C chemical shifts

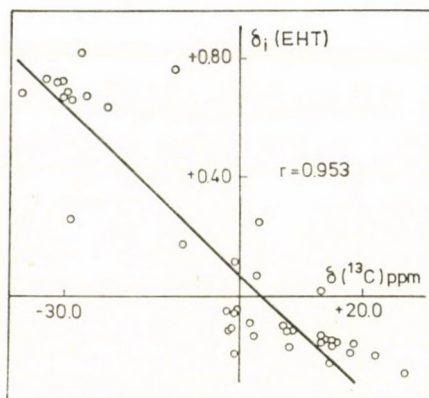


Fig. 8. Partial charges of the aromatic carbons of phenol ethers calculated by EHT method, as a function of ^{13}C chemical shifts

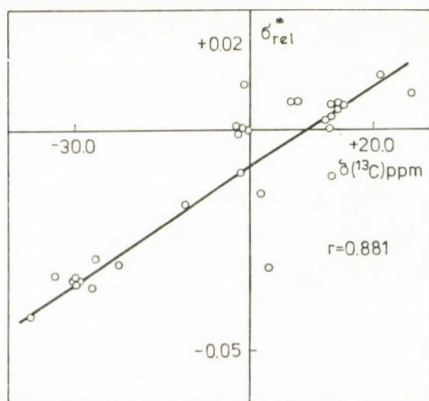


Fig. 9. The relative paramagnetic shielding factors of phenol ethers as a function of ^{13}C chemical shifts

Table III
NMR correlation results for phenol ethers of type CH₃OC₆H₄X

X	Atom	¹³ C (ppm)	δ _i (Del Re + PPP)	δ _i (EHT)	σ* _{rel}
H	1	-30.2	0.0469	0.7241	-0.0341
	2	14.7	-0.0574	-0.1570	0.0062
	3	- 0.9	-0.0420	-0.0521	0.0004
	4	8.1	-0.0597	-0.1141	0.0071
2-CH ₃ O	1	-22.6	0.0352	0.6419	-0.0302
	3	15.5	-0.0584	-0.1521	0.0065
	4	6.9	-0.0593	-0.1029	0.0069
3-CH ₃ O	1	-33.3	0.0435	0.7333	-0.0328
	2	27.0	-0.0661	-0.2529	0.0089
	4	21.7	-0.0754	-0.2063	0.0128
	5	- 2.2	-0.0430	-0.0415	0.0008
4-CH ₃ O	1	-26.4	0.0319	0.6759	-0.0287
	2	13.1	-0.0580	-0.1463	0.0063
2-CH ₃	1	-28.9	0.0504	0.6669	
	2	2.7	-0.0707	0.0738	
	3	- 1.7	-0.0387	-0.1188	
	4	7.9	-0.0580	-0.1112	
	5	1.5	-0.0428	-0.0930	
	6	18.6	-0.0563	-0.1569	
3-CH ₃	1	-30.9	0.0470	0.7255	
	2	14.1	-0.0554	-0.2222	
	3	-10.0	-0.0543	0.1722	
	4	7.6	-0.0567	-0.1753	
	5	- 0.2	-0.0433	-0.0495	
	6	17.9	-0.0477	-0.1968	
4-CH ₃	1	-29.7	0.0468	0.6858	-0.0340
	2	14.5	-0.0564	-0.1543	0.0057
	3	- 1.7	-0.0387	-0.1143	-0.0009
	4	- 0.9	-0.0715	0.1131	0.0115
4-Cl	1	-30.1	0.0458	0.6680	-0.0337
	2	12.9	-0.0504	-0.1524	0.0035
	3	- 1.2	-0.0167	-0.1953	-0.0093
	4	3.3	0.0365	0.2513	-0.0309
4-NO ₂	1	-37.1	0.0669	0.8200	-0.0414
	2	13.3	-0.0434	-0.1419	0.0009
	3	2.1	-0.0049	0.0084	-0.0136
	4	-11.3	-0.0004	0.2721	-0.0165
4-F	1	-27.1	0.0506	0.6819	-0.0355
	2	13.2	-0.0512	-0.1439	0.0038
	3	13.2	-0.0148	-0.1383	-0.0099
	4	-28.7	0.1036	0.7638	-0.0583
benzene		0.0	-0.0409		0.0

atoms. A comparison of Figs 7 and 9 shows that the relative paramagnetic shielding factors derived from the partial charges do not give better correlation than the $\sigma\pi$ partial charges themselves.

Discussion

Experimental physico-chemical properties of phenol ethers were compared to the results of quantum chemical calculations, and from the correlations conclusions were drawn on the structures of molecules. From the Del Re

partial charges δ_σ the inductive effects of substituents, from the IPPP partial charges δ_π the mesomeric effects, and from the gross $\sigma\pi$ partial charges the orientation effects of the substituents could be interpreted. Experimental and calculated transition energies were in good agreement. Discrepancies greater than average were found for *o*-bis-dimethoxybenzene and for nitroanisole derivatives, which could be explained by the non-planar structure of these molecules. Assuming the free rotation of methoxy groups, the dipole moments calculated from charges densities agreed satisfactorily with experimental dipole moments. The agreement was poorer for orthosubstituted derivatives, indicating that the rotation of methoxy groups is hindered in these compounds. The agreement of dipole moments calculated by the group moment method was better, suggesting that the substituents, except the NO_2 group, have only weak effect on the π electron system. The poorer agreement observed with nitroanisoles can be attributed to the strong $-M$ effect of the nitro group. An equally good correlation was found to exist between experimental and calculated ionization energies, as well as between the ^{13}C chemical shifts of aromatic carbon atoms and the partial charges and relative paramagnetic shielding factors, respectively. The satisfactory agreements prove the appropriateness of the methods used for the calculations (Del Re, iterative PPP), the correct choice of the basic quantities and relationships used for the calculation of the parameters, and the validity of the planar model.

Finally, it can be stated on the basis of the results that the majority of phenol ethers has planar structure, and the rotation of methoxy groups is free. With the exception of the nitro group, the effect of the substituents on the electron distribution of the molecules is insignificant. The rotation is hindered in orthosubstituted derivatives, and the structure of nitroanisoles is non-planar.

REFERENCES

- [1] HENCSEI, P., NAGY, J.: *Acta Chim. Acad. Sci. Hung.*, **101**, 365 (1979)
- [2] DEARDEN, J. C., FORBES, W. F.: *Can. J. Chem.*, **37**, 1294 (1959)
- [3] DEARDEN, J. C., FORBES, W. F.: *Can. J. Chem.*, **37**, 1305 (1959)
- [4] FUCHS, O.: *Z. Phys. Chem., B* **14**, 339 (1931)
- [5] TIGANIK, L.: *Z. Phys. Chem., B* **14**, 135 (1931)
- [6] MINKIN, V. I., OSIPOV, O. A., ZHDANOV, Y. A.: *Dipole Moments in Organic Chemistry*, Plenum Press, New York, 1970, p. 91
- [7] KOOPMANS, T.: *Physica*, **1**, 104 (1933)
- [8] KARLSSON, G., MARTENSSON, O.: *Theor. Chim. Acta*, **13**, 195 (1961)
- [9] ENGELHARDT, G., RADEGLIA, R., JANCKE, H., LIPPMAN, E., MAGI, M.: *Org. Magn. Resonance*, **5**, 561 (1973)

Pál HENCSEI	}	H-1521 Budapest, Gellért tér 4.
József NAGY		
Gábor PONGOR		
		H-1325 Budapest, P.O.B. 110

PHOTOCATALYTIC METHODS, II

PHOTO-OXIDATION OF SAFRANINE T IN THE PRESENCE OF IRON(III)

A. PÉTER and L. J. CSÁNYI

*(Reaction Kinetics Research Group of the Hungarian Academy of Sciences,
Institute of Inorganic and Analytical Chemistry, Attila József University, Szeged)*

Received July 12, 1978

Accepted for publication September 28, 1978

Photo-oxidation of Safranine T was observed during the UV irradiation of dye solutions containing iron(III) ions as sensitizer. The possible steps of photo-oxidation as well as the dependence of the fading on experimental conditions are discussed.

We have shown recently that the iron(III)-catalyzed photo-oxidation of Erioglaucin A is brought about by hydrolyzed iron(III) species [1], while the excited states of O_2 and the dye molecule play only subordinate roles. In this paper we present results obtained in connection with the catalyzed photo-oxidation of Safranine T (henceforth S-T). This dye was chosen because its γ -radiolysis was investigated thoroughly [2–5], and this allows some comparison between radiolysis and UV photolysis.

Experimental

Chemicals. Compounds employed in the measurements were of *p.a.* purity. S-Ts (Grübler preparation) was repeatedly recrystallized from aqueous alcoholic solution. Solutions were prepared with triply distilled water.

Measurements. The apparatus used for irradiation was described elsewhere [1]. Solutions of appropriate compositions were thermostated at 25 °C for 20–25 min during which they were saturated with oxygen, or flushed with nitrogen to remove dissolved oxygen. Then 3.0 cm³ of the solution handled as above was filled into a 1 cm quartz cell and irradiated for 10 min. During irradiation, the solutions were thermostated. After irradiation the change in the absorbance compared to the unphotolyzed solutions was determined at 530 nm.

Results

S-T (3,6-diamino-2,7-dimethyl-10-phenylphenazoniumchloride) is a redox indicator with a standard potential of $E^\circ = 0.235$ V. Under normal conditions S-T is present in the oxidized form, its aqueous acidic solution has an intensive bluish-violet colour, but is brown in basic media. Its reduced form is colourless. The oxidized form (R) has 3 peaks at 520, 275 and 247 nm in the pH range of 2–6 (Fig. 1, curve 1). In more acidic media ($pH < 1$) a new peak can be observed at 577 nm, which corresponds to the protonated form (RH^+) of the dye. The molar absorptivities of the oxidized forms are: $\epsilon_{(R)}^{520} = 43333$, $\epsilon_{(RH^+)}^{520} =$

$= 13880$, $\varepsilon_{(\text{RH}^+)}^{577} = 32330 \text{ dm}^3 \text{ mol}^{-1} \text{ cm}^{-1}$ [5]. Solutions acidified with perchloric acid, when the dye concentration exceeds 10^{-4} M , are not stable and a colloidal precipitate is formed in a relatively short time.

S-T weakly luminesces when it is excited by irradiation at its 520 nm absorption band. The maximum of the emission spectrum is at 590 nm (Fig. 1, curve 2).

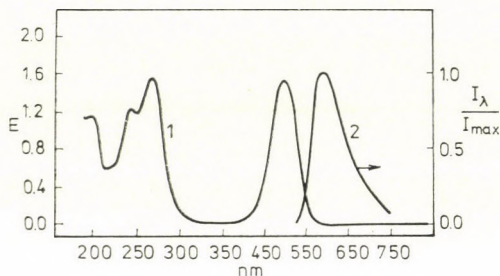


Fig. 1. Absorption and emission spectra of Safranine T. Curve 1: $3.5 \times 10^{-5} \text{ M}$ dye, absorption spectrum; curve 2: $3.5 \times 10^{-5} \text{ M}$ dye, emission spectrum excited at 520 nm

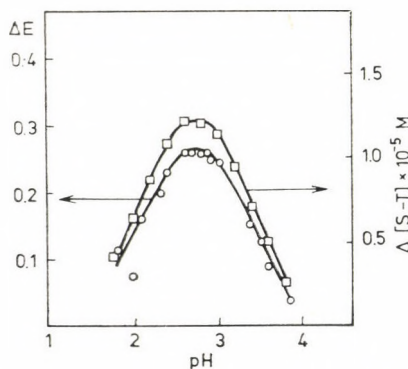


Fig. 2. pH dependence of the iron(III)-catalyzed photo-oxidation of Safranine T. Conditions: $8.0 \times 10^{-5} \text{ M}$ dye, $8.14 \times 10^{-5} \text{ M}$ $\text{Fe}(\text{ClO}_4)_3$, pH = 2.7, irradiation time 10 min

S-T is fairly photo-resistant, a decolourization of 2–4% can be observed only after longer (>20 min) irradiation. In the presence of iron(III), however, a fading of considerable extent can be observed while the concentration of iron(III) remains unchanged. It can be seen from Fig. 2 that in the presence of iron(III) the bleaching of S-T strongly depends on the pH. According to the ΔE_{520} vs. pH and the $\Delta[\text{dye}]$ vs. pH plots, the maximum of the fading is at pH 2.7, which does not depend on the concentration of the dye, iron(III) and dissolved oxygen either.

The photo-decolourization depends on the dye concentration (Fig. 3). The form of ΔE vs. $\Delta[\text{dye}]$ curve is determined by the cell thickness at which the absorbance is measured: in the case of a longer optical path a maximum,

while at short cell paths a saturation curve can be obtained. The dependence on the dye concentration does not alter on changing the concentration of iron(III).

The photo-oxidation strongly depends on the iron(III) concentration. Under the experimental conditions applied, the absorbance difference is pro-

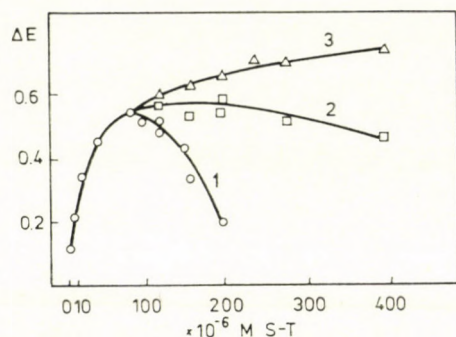


Fig. 3. Dependence of the photo-oxidation of Safranine T on the dye concentration. Conditions: $8.14 \times 10^{-5} M$ $Fe(ClO_4)_3$, pH = 2.7, irradiation time 10 min. Values measured at cell paths of 1 cm (1), 2 mm (2) and 1 mm (3), converted to 1 cm

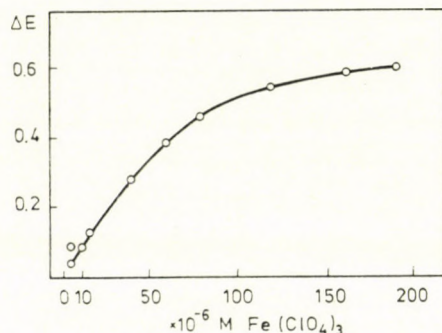


Fig. 4. Dependence of the photo-oxidation of Safranine T iron(III) concentration. Conditions: $4.0 \times 10^{-5} M$ dye, pH = 2.7 irradiation time 10 min

portional to the iron(III) concentration in the range of 0.056–5.0 γ Fe/cm³, while at higher catalyst concentrations the decolourization approaches a limiting value (Fig. 4).

The influence of foreign ions on the catalyzed photo-oxidation of S-T is shown in Table I. According to these data, chloride ions do not influence the photooxidation, while bromide, thiocyanate and nitrite ions exert strong inhibiting effects. Nitrate ions proved to be inert at low concentrations, but in the presence of a larger quantity ($>2 \times 10^{-3} M$) they promote the fading of the dye in the absence of iron(III) too. The effect of iodide and cerium(III)

Table I

Effect of various ions on the iron(III)-catalyzed photo-oxidation of Safranine T
 Experimental conditions: 8.0×10^{-5} M Safranine T, 8.14×10^{-5} M $\text{Fe}(\text{ClO}_4)_3$,
 pH = 2.7, 1.3×10^{15} photon s^{-1} , irradiation time 10 min

$c \times 10^5$ (M)	ΔE^{520}				
	Cl^-	Br^-	SCN^-	NO_2^-	NO_3^-
0	0.520	0.520	0.520	0.520	0.520
4	0.520	0.450	0.410	0.500	0.500
8	0.515	0.400	0.350	0.390	0.495
20	0.518	0.340	0.250	0.330	0.493
40	0.520	0.280	0.190	0.280	0.495
80	0.515	0.235	0.160	0.180	0.492
200	—	—	—	0.100	0.510
400	—	—	—	0.080	0.530

ions could not be investigated by an optical method because the dye is precipitated in the form of colloidal particles. The photo-oxidation can also be inhibited by copper (II) ions, especially when their concentration exceeds 10^{-3} M. In the presence of copper, iron(II) is also formed.

The photo-oxidation of S-T takes places in the absence of oxygen too when the solution contains iron(III). In such cases the decolourization of 1 mol S-T is accompanied by reduction of *ca.* 4 mol iron(III). In the presence of oxygen ferrous ions do not form, the photo-oxidation takes place at the expense of dissolved oxygen: the mole ratio of oxygen reduced to the dye oxidized is *ca.* 1.6—1.8. In the presence of oxygen the fading of the dye is 1.4—1.5 times greater than in its absence.

The photo-oxidation of S-T was also investigated in the presence of Methylene Blue and fluorescein both in aqueous and in 4 : 1 benzene-methanol solvent. In the absence of iron(III) these additives did not give rise to perceptible decolourization in an oxygen-saturated dye solution.

Attempts were made to establish the products of photo-oxidation by separating them on silica gel thin-layer plates (Merck Silikagel G) pre-treated in various ways and with running mixtures of chloroform or benzene-methanol in various proportions. In samples irradiated for 10—15 min the product(s) of photo-oxidation could not be distinguished by TLC from the original dye. At prolonged (exhaustive) photolysis, two main fractions were found: one consisting of fragments moving together with the solvent front and the other remaining near to the starting point.

In the difference spectra three bands were observed at 560, 450 and 290 nm (reference solution: unphotolyzed S-T solution diluted according to the actual fading). The ratios of band intensities are 5 : 6.2 : 12.5 (Fig. 5).

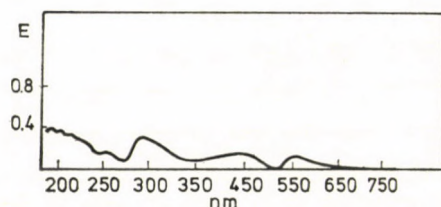
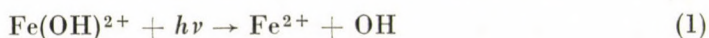


Fig. 5. Difference spectrum of the photolysis product of Safranin T. Conditions: $1.0 \times 10^{-4} M$ [dye, $8.14 \times 10^{-5} M$ $Fe(ClO_4)_3$, pH = 2.7, irradiation time 10 min

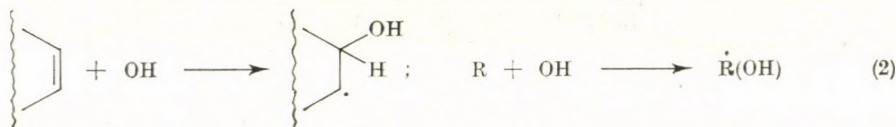
Discussion

For explaining the photo-oxidation of S-T, the direct photo-activation of the O_2 molecule cannot be assumed because at the wavelengths employed ($\lambda > 250$ nm) O_2 does not absorb to a perceptible extent. According to our experience, S-T exhibits a weak luminescence when excited at its 520 nm absorption band. The energy of emitted photons (maximum at 590 nm) would be high enough to excite the O_2 molecule, *i.e.* one could reckon with the activation of O_2 through excited dye molecule ($S \xrightarrow{h\nu} S^*$; $S^* + O_2 \rightarrow S + O_2^*$). In the absence of the iron(III) photo-catalyst, however, a fading of only 2–4% was observed even after prolonged irradiation, and the bleaching remained the same when the photolysis was carried out under exclusion of oxygen. Further, no change was found even in the extent of fading when irradiation was carried out either in aqueous and non-aqueous solution in the presence of fluorescein and Methylene Blue. These dyes are known, however, to be effective sensitizers for the production of singlet oxygen, particularly in non-aqueous media, where the life-time of excited oxygen is long enough to give rise to perceptible chemical reactions. Since even these sensitizers did not enhance the fading of S-T, it may be concluded that singlet oxygen does not participate or plays only a subordinate role in the photo-oxidation of S-T.

The iron(III)-catalyzed photo-oxidation of S-T exhibits a maximum at pH 2.7 at the same pH at which the iron(III)-catalyzed photo-oxidation of other dyes shows an optimum [1]. In this system the pH optimum does not shift if decolourization is measured at different wavelengths. This is obvious because the spectrum of S-T in this pH range is independent of the pH. A band shift and changes in the intensities can be observed only at pH < 1. In agreement with the iron(II)-catalyzed photo-oxidation of other dyes, the oxidative fading of S-T was observed only at wavelengths shorter than 350 nm. Based on this finding, we have to assume that in this system too hydrolyzed iron(III) species are responsible for the photo-oxidation:

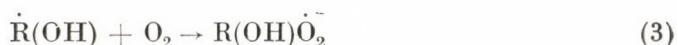


If the kinetic energy of OH radicals produced in reaction (1) is high enough to escape the solvent cage, the dye will be attacked. By analogy to the general reactions of aromatic compounds with OH radicals, it is assumed that S-T reacts similarly and substituted cyclohexadienyl radicals are formed:



The dye radical can be further oxidized at its amino or methyl group, leading to extended conjugation in comparison to the original molecule. This can be concluded from the appearance of the 560 nm band in the difference spectrum. In the absence of oxygen the fading of 1 mol dye is accompanied by the formation of about 4 mol of iron(II). According to this stoichiometry, 4 OH radicals are consumed by each S-T molecule.

In the presence of oxygen it is probable that dye radical reacts with O_2 very rapidly and a dye peroxide radical is formed:



Since iron(II) ions are not formed during the photolysis if sufficient oxygen is present, it must be assumed that the dye peroxide radical oxidizes the iron(II) back to iron(III). This is why we speak of photo-catalysis. Besides, dye peroxide radicals react with each other, giving stable product.

According to our experiments, only one oxidation product is formed up to 35–40% bleaching. This can be seen in Fig. 6: spectra taken after different irradiation times show 2 isosbestic points, at 572 and 442 nm. Only longer (exhaustive) irradiation results in the destruction of the primary product of photo-oxidation. In such cases the spectra no longer show isosbestic points.

If the yields of decolourization, both in the presence and absence of oxygen, are compared and it is assumed that the OH yield is the same in both cases, one has to conclude that O_2 exerts a multiplicative effect on the dye radicals formed in reaction (3). The enhancing factor amounts to 1.4–1.5. The data at hand are not sufficient to elucidate this multiplicative effect, however, it is conceivable that dye peroxide radicals play an important role, in analogy to autooxidation processes.

It should be mentioned that during the γ -radiolysis of S-T solutions containing O_2 , $G(-\text{Safranine T}) = 0.65$ was found at $\text{pH} = 3$ by MARKETOS and RAKINTZIS [3]. Having compared this value with the generally accepted $G_{\text{OH}} = 2.6$ ($\text{pH} = 3$) the conclusion was drawn that 4 OH radicals are consumed per dye molecule during the radiolytic oxidation. At lower doses only one oxidation product was found by the above authors but the isosbestic points

of the spectra were found at 558 and 445 nm. (In our γ -radiolysis study the isosbestic points were found at 556 and 450 nm). Upon γ -radiolysis at lower doses, the difference spectra show new bands at 558, 450 and 292, the ratios of the peaks being 5 : 7.2 : 17. The absorption bands of the γ -radiolysis product and the iron(III)-catalyzed photo-oxidation of S-T agree perfectly well but the intensity ratios are different. This latter and the fact that the isosbestic points are shifted from 556 to 572 and from 450 to 442 nm can be explained

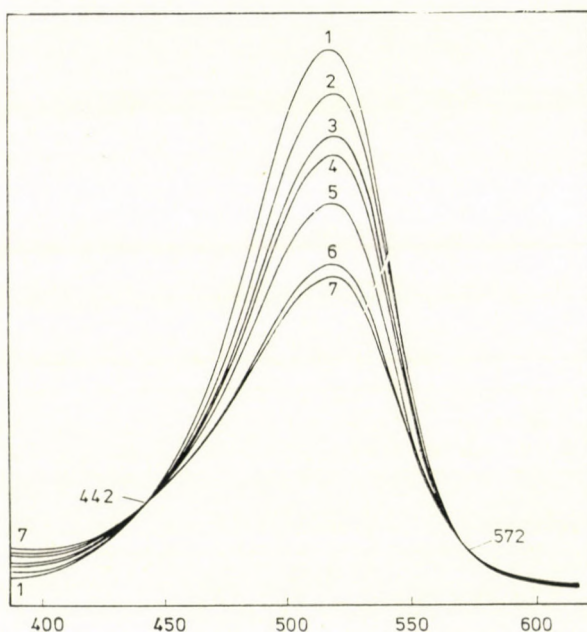


Fig. 6. Absorption spectra of Safranin T after different irradiation times. Curves 1 to 7 : 0, 1, 2, 4, 5, 16 and 33 min

by interaction between the dye and iron(III) ions. Another reason for the observed deviation may be that during the iron(III)-catalyzed photo-oxidation, only OH radicals are produced, while the γ -radiolysis of a dye solution saturated with oxygen results in both OH and HO_2 radicals. According to the literature [2–4], S-T is not attacked directly by HO_2 radicals, but the primary product of the reaction of OH radicals may react with HO_2 radicals present in the radiolyzed system. In our experiments, the addition of H_2O_2 causes strong decolourization of the dye during photolysis.

The results show that the decolourization varies according to a maximum or a saturation curve, depending on the dye concentration (Fig. 3). This can be explained, assuming that in more concentrated dye solutions polymeric species are present. These colloidal particles scatter the light and this apparent

absorbance may compensate the decrease in absorbance accompanying photo-oxidation.

The extent of photo-oxidation is proportional to the concentration of the photo-catalyst. The probable cause of saturation at higher catalyst concentrations (see Fig. 4) is that the solution becomes depleted in oxygen. A further cause may be a slight change in the stoichiometry of decolorization.

The photo-oxidation yield remains the same when chloride is added to the reaction mixture. This is in good agreement with the fact that the quantum yields of FeOH^{2+} and FeCl^{2+} ions are equal. Bromide, thiocyanate and nitrite ions act as inhibitors, possibly because they scavenge OH radicals rapidly, whereas their oxidized forms react more slowly with the dye molecule than do OH radicals.

The inhibiting effect of copper(II) ions is probably due to the faster reaction of the dye peroxide radical with copper(II) than with iron(II). In the course of this reaction copper(I) is formed, which reduces iron(III). This latter reaction may be responsible for the appearance of iron(II) in the system in spite of the presence of oxygen.

Analytical conclusions

The iron(III)-catalyzed photo-oxidation of S-T can be used to determine iron(III) on a micro scale ($0.05\text{--}5.0 \text{ } \gamma\text{Fe/cm}^3$) and in the presence of other transition metal ions. The procedure is similar to that described earlier [1] and has no special advantage over the Erioglaucin A method. The precision of the estimation depends primarily on the stability of the light emission source. In favorable cases, the reproducibility can be kept within $\pm 2\%$.

*

Luminescence spectra were taken by Gábor LACZKÓ (Institute of Biophysics, A. József University, Szeged) to whom the authors express their sincere thanks.

REFERENCES

- [1] PÉTER, A., CSÁNYI, L. J.: *Acta Chim. Acad. Sci. Hung.*, (In press)
- [2] RAKINTZIS, N., PAPACONSTANTINOU, E., SCHULTE-FROHLINDE, D.: *Z. phys. Chem. N. F.*, **44**, 257 (1965)
- [3] MARKETOS, D. G., RAKINTZIS, H. Th.: *Z. phys. Chem., N. F.*, **44**, 270 (1965)
- [4] MARKETOS, D. G., RAKINTZIS, N. Th., STEIN, G.: *Z. phys. Chem. N. F.*, **59**, 177 (1968)
- [5] MARKETOS, D. G.: *Z. phys. Chem. N. F.*, **65**, 306 (1969)

Antal PÉTER László J. CSÁNYI	}	H-6720 Szeged, Dóm tér 7.
---------------------------------	---	---------------------------

SYNTHESIS OF VINCA ALKALOIDS AND RELATED COMPOUNDS, XI*

ACRYLONITRILE ADDUCTS AS INTERMEDIATES

GY. KALAUS, L. SZABÓ, P. GYŐRY, É. SZENTIRMAY and Cs. SZÁNTAY

(*Institute for Organic Chemistry, Technical University, Budapest and
Central Research Institute for Chemistry, Hungarian Academy of Sciences, Budapest*)

Received April 19, 1978

In revised form August 14, 1978

Accepted for publication September 29, 1978

The reduction of the adduct obtained from the enamine of type **2a** and nitrile yielded the derivatives **4a** and **5a**, which undergo epimerization in methanolic sulfuric acid when converted into the ester. In alkaline media the conversions $\rightarrow \mathbf{4b} \rightarrow \mathbf{4c}$ and $\mathbf{5a} \rightarrow \mathbf{5b} \rightarrow \mathbf{5c}$ proceed with retention.

In our previous work, the intermediates of the synthesis of vinca alkaloids were adducts formed from the enamine **2a**, obtained from the salt **1a**, and from α -acetoxy-acrylic ester [2] or acrylic ester [3], and the reduction products of these adducts.

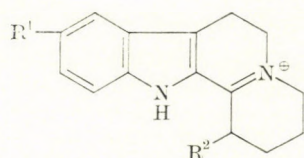
The possibility of application of acrylonitrile as the addition component has now been investigated.

The addition product of the enamine **2a** and acrylonitrile was isolated as the perchlorate (**3a**) in a satisfactory yield. Reduction of the adduct **3a** either catalytically or with sodium borohydride was achieved in about 80% yield, and two stereoisomers (**4a** and **5a**) could be isolated. The isomeric ratio (**4a** : **5a**) was 64 : 20 in the catalytic (Pd/C) reduction, and it varied between 77 : 15 and 43 : 29 when sodium borohydride was used, depending on the rate of adding the reagent. In order to confirm the steric structure and to convert the main product *trans*-**4a** into the well-known vincamine intermediate, **5c**, having *cis* configuration, the nitrile group was to be transformed into an ester group.

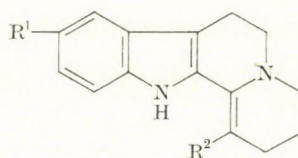
When compound **4a** was refluxed with methanolic sulfuric acid, a 3 : 2 mixture of the known **4c** and **5c** stereoisomeric esters [3] was obtained. The reaction thus gave no unambiguous evidence for the steric structure of **4a**.

The homogeneous esters **4c** and **5c** prepared earlier were then refluxed separately in methanolic sulfuric acid, whereupon the above mixture was again obtained; thus it corresponds to the thermodynamic equilibrium. It follows that under the given conditions the derivative **4c** carrying the annellation hydrogen and the ethyl group in *trans* position is the more stable isomer.

* For Part X, see Ref. [1]

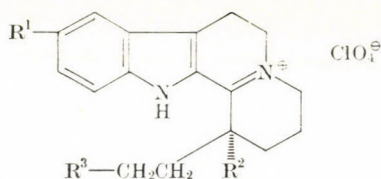


1a—c

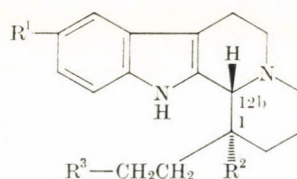


2a—c

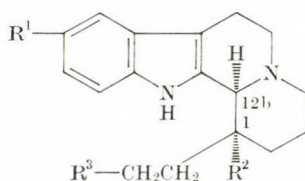
	R ¹	R ²
a	H	C ₂ H ₅
b	H	<i>n</i> -C ₄ H ₉
c	CH ₃ O	C ₂ H ₅



3a, f, h



4a—h



5a—c

	R ¹	R ²	R ³
3, 4, 5 a	H	C ₂ H ₅	CN
b	H	C ₂ H ₅	COOH
c	H	C ₂ H ₅	COOCH ₃
d	H	C ₂ H ₅	CH ₂ -NH ₂
e	H	C ₂ H ₅	CH ₂ -N(CH ₃) ₂
f	H	<i>n</i> -C ₄ H ₉	CN
g	H	<i>n</i> -C ₄ H ₉	CH ₂ NH ₂
h	CH ₃ O	C ₂ H ₅	CN

In acid media the epimerization takes place probably at the 12b annellation site, according to the mechanism studied by GASKEL and JOULE [4] in connection with the isomerization of reserpine.

Epimerization in sulfuric acid medium also rendered possible the isomerization of the undesired isomer **4c**, appearing in the synthesis of vincamine, into the desired **5c**, improving thereby the effectiveness of the procedure.

In order to establish an unambiguous correlation between the nitriles **4a** and **5a** and the esters of known structure, hydrolysis was then effected in alkaline medium, and the carboxylic acids **4b** and **5b**, obtained in satisfactory yields, were esterified with diazomethane. As a result of these reaction steps,

ester **4c** or **5c** was isolated exclusively, depending on the starting material; thus the steric structure of **4a** and **5a** can be regarded as confirmed.

The result is in accordance with our earlier observations, which indicated that the higher the space requirement of the substituent entering position 1 during the addition on the enamine **2a**, the greater is the extent of the formation of the ethyl \leftrightarrow 12bH *cis* compound during the reduction of the $>C=N-$ bond. Of the reactions examined so far, one extreme of the series is the reduction of the adducts formed with ethyl α -acetoxyacrylate or *t*-butyl acrylate, where the *cis* selectivity is 9 : 1; acrylonitrile is on the other extreme side giving **3a** which can be reduced with preponderant *trans* selectivity.

The addition and subsequent reduction were also effected starting with two other enamine derivatives, **2b** and **2c**. The reduction of adducts **3f** and **3h** yielded practically one single product in this case; their probable structures, **4f** and **4h**, are suggested on the analogy of the above results.

In order to prepare samples for pharmacological tests, the nitriles **4a** and **4f** were reduced to the amines **4d** and **4g** [7]. Amine **4d** can also be prepared by the direct, one-step reduction of adduct **3a** and it can be converted into the *N,N*-dimethylamino derivative (**4e**) by the Leuckart—Wallach reaction.

Experimental

The IR spectra were recorded in KBr pellets with a Spektromom 2000 instrument; the NMR spectra were obtained with a Perkin-Elmer R12 (60 MHz) spectrophotometer, the UV spectra were taken on a Unicam SP 800 spectrophotometer.

1-Ethyl-1-(2-cyanoethyl)-1,2,3,4,6,7-hexahydro-12H indolo[2,3-*a*]quinolizin-5-ium perchlorate (**3a**)

Compound **1a** (10 g; 28.4 mmoles) was suspended in dichloromethane (100 ml) and distilled water (75 ml) and 2*N* sodium hydroxide (20 ml) were added to it under continuous stirring in argon atmosphere. The reaction mixture was stirred for 10 min, the organic phase which separated was removed and dried over anhydrous potassium carbonate. The solution was filtered from the drying agent and mixed with freshly distilled acrylonitrile (10 ml; 149 mmoles) added slowly; the system was flushed with argon and allowed to stand at room temperature. After standing for 2 days (whereupon the colour of the solution strongly deepened and no starting material could be detected in it by chromatography) the solution was evaporated in vacuum and argon atmosphere (*max* 40–50 °C, water bath) to leave a dark red oil (9.6 g).

The oil was dissolved in hot methanol (180 ml), 70% aqueous perchloric acid was added dropwise in an amount equivalent to the base (the pH of the solution was 6–6.5). A yellow crystalline product separated on cooling (10.08 g; 87.5%), m.p. 210–212 °C. After recrystallization from methanol, the m.p. rose to 211–212 °C.

$C_{20}H_{24}ClN_3O_4$ (405.86). Calcd. C 59.18; H 5.96; N 10.35. Found C 59.08; H 5.71; N 10.43%.

IR(KBr): 3250 (indole NH), 2260 ($-C\equiv N$), 1596, 1612 cm^{-1} ($>C=N^{(+)}$).

UV(MeOH): λ_{max} log ϵ : 248 (3.8639); 253 (3.8041); 366 (4.2624).

1a-Ethyl-1 β -(2-cyanoethyl)-1,2,3,4,6,7,12,12b β -octahydroindolo[2,3-*a*]quinolizine (**4a**) and 1 α -ethyl-1 β -(2-cyanoethyl)-1,2,3,4,6,7,12,12b α -octahydroindolo[2,3-*a*]quinolizine (**5a**)

(a) 5% Pd/C catalyst (about 1 g) thoroughly washed with distilled water then with methanol was prehydrogenated in some methanol. After the absorption of hydrogen had stopped, a solution of **3a** (1.88 g; 4.64 mmoles) in methanol (150 ml) was slowly added to the cata-

lyst. Hydrogenation was effected at room temperature and atmospheric pressure. The calculated amount (115 ml) of hydrogen was absorbed in 15 min. At the end of the reaction the catalyst was filtered off and the solution concentrated in vacuum. Distilled water was added to it, then the pH of the solution was adjusted to 9–10 with saturated sodium carbonate solution. Dichloroethane was added, the solution was shaken, the organic phase was separated and dried (MgSO_4). The dichloroethane solution was filtered from the drying agent and evaporated solution was in vacuum to obtain a solid product (1.35 g).

Recrystallization from twenty parts of methanol gave **4a** as a white crystalline substance (0.92 g; 64.5%), m.p. 228–229 °C.

$\text{C}_{26}\text{H}_{25}\text{N}_3$ (307.42). Calcd. C 78.13; H 8.20; N 13.67. Found C 78.36; H 8.39; N 13.38%.

IR (KBr): 3370 (indole NH); 2248 cm^{-1} ($\text{C}\equiv\text{N}$).

NMR (CDCl_3): δ 7.91 (s, 1 H, indole NH); 7.62–7.09 (m, 4H, aromatic H); 3.42 (s, 1H, 12b β H); 0.87 (t, 3H, $-\text{CH}_2-\text{CH}_3$).

On concentration of the mother liquor, an additional amount of a crystalline product (**5a**) (0.28 g; 19.63%) was obtained, m.p. 160–164 °C.

$\text{C}_{26}\text{H}_{25}\text{N}_3$ (307.42). Calcd. C 78.13; H 8.20; N 13.67. Found C 78.33; H 8.04; N 14.07%.

IR (KBr): 3380 (indole NH); 2305 cm^{-1} ($\text{C}\equiv\text{N}$).

NMR (CDCl_3): δ 7.69 (s, 1H, indole NH); 7.60–6.94 (m, 4H, aromatic H); 3.29 (s, 1H, 12b α H); 1.12 (t, 3H, $-\text{CH}_2-\text{CH}_3$).

(b) Compound **3a** (1.88 g; 4.64 mmoles) was suspended in methanol (100 ml) and cooled to 0 °C. Sodium borohydride (1.00 g; 26.5 mmoles) was added to the suspension in small portions, with continuous stirring. The mixture was stirred for 1 h more after the end of addition and the reaction mixture was acidified with 5N HCl to pH 3. The acid solution was concentrated to 10 ml in vacuum, the residual suspension was mixed with distilled water (50 ml) and made alkaline with 40% NaOH solution to pH 9–10, with cooling; it was then extracted with dichloroethane (30, 20 and 10 ml). The organic phase was dried (MgSO_4) and evaporated to dryness in vacuum. The solid residue was crystallized from methanol to obtain 0.97 g (68.0%) of compound **4a**, m.p. 228–229 °C.

Concentration of the mother liquor yielded **5a** (0.25 g; 17.54%), m.p. 160–164 °C. The products were identical in all respect with those described under (a).

Conversion of **4a** and **5a** in methanolic sulfuric acid

Compound **4a** or **5a** (11.30 g; 36.9 mmoles) was suspended in anhydrous methanol (140 ml), conc. sulfuric acid (45 ml) was added dropwise and the solution was then refluxed for 11 h. The hot reaction mixture was poured onto ice and the pH was adjusted to 9–10 with conc. ammonium hydroxide solution.

It was then extracted with dichloroethane (80, 50 and 30 ml), and the organic phase was dried (MgSO_4). The solvent was evaporated in vacuum to leave an oil (11.80 g) which was rubbed with methanol (25 ml), whereupon it became crystalline. Filtration with suction gave a mixture of the esters **4c** and **5c** (8.60 g; 68.6%). Fractional crystallization from methanol yielded **4c** (3.15 g; 25.1%), m.p. 150–152 °C.

$\text{C}_{21}\text{H}_{28}\text{N}_2\text{O}_2$ (340.45). Calcd. C 74.08; H 8.29; N 8.23. Found C 74.18; H 8.37; N 8.16%.

IR (KBr): 3303 (indole NH); 1708 cm^{-1} ($>\text{C}=\text{O}$).

NMR (CDCl_3): δ 7.75 (s, 1H, indole NH); 7.60–6.87 (m, 4H, aromatic H); 3.52 (s, 3H, $-\text{OCH}_3$); 3.35 (s, 1H, 12b β H); 1.15 (t, 3H, $-\text{CH}_2-\text{CH}_3$).

When the mother liquor was concentrated to one-third volume, compound **5c** (2.00 g; 15.9%) separated, m.p. 139–141 °C.

$\text{C}_{21}\text{H}_{28}\text{N}_2\text{O}_2$ (340.45). Calcd. C 74.08; H 8.29; N 8.23. Found C 74.17; H 8.50; N 8.26%.

IR (KBr): 3400 (indole NH); 1730 cm^{-1} ($>\text{C}=\text{O}$).

NMR (CDCl_3): δ 8.83 (s, 1H, indole NH); 7.67–6.95 (m, 4H, aromatic H); 3.77 (s, 3H $-\text{OCH}_3$); 3.32 (s, 1H, 12b α H); 0.67 (t, 3H, $-\text{CH}_2-\text{CH}_3$).

Epimerization (**4c** \rightarrow **4c** + **5c** \leftarrow **5c**)

Compound **4c** or **5c** (0.35 g; 1.03 mmoles) was dissolved in a mixture of anhydrous methanol (4 ml) and conc. sulfuric acid (1.30 ml). The solution was refluxed for 12 h. The yellowish-brown solution was poured onto ice, then made alkaline (pH 10) with solid potassium carbonate. It was then extracted with dichloroethane (20, 15 and 10 ml) and the organic phase was dried (MgSO_4). The solution was evaporated to dryness in vacuum, and the residual oil

(0.32 g) was crystallized from methanol to obtain compound **4c** (0.18 g; 51.5%), m.p. 150–152 °C and compound **5c** (0.08 g; 22.7%), m.p. 139–141 °C.

The isomers were identical in all respect with the products described in the foregoing paragraph.

**1 α -Ethyl-1 β -[(2-methoxycarbonyl)ethyl]-1,2,3,4,6,7,12,12b β ,
-octahydroindolo[2,3-*a*]quinolizine (**4c**)**

Compound **4a** (1.00 g; 3.27 mmoles) was suspended in ethanol (30 ml) and a solution of sodium hydroxide (1.30 g; 32.6 mmoles) in distilled water (10 ml) was added to it. The reaction mixture was refluxed for 16 h, then the mixture was evaporated to dryness in vacuum. The residual paste was dissolved in distilled water and the pH of the solution was adjusted to 7 with 20% acetic acid. The separation of crystals started on scraping; this continued during standing at room temperature. After standing for a few hours, the white crystals were filtered off and washed with distilled water, to yield compound **4b** (1.00 g).

The crude **4b** was dissolved in dioxan (100 ml), and ethereal diazomethane solution was added to it (until the yellow colour of the solution persisted) and it was allowed to stand overnight. The excess diazomethane was decomposed with glacial acetic acid and the solution was evaporated in vacuum. The residual oil was suspended in distilled water, dichloroethane (50 ml) was added to the solution, and it was made alkaline with 40% NaOH solution to pH 9–10. The organic phase was separated and dried (MgSO₄). The solution was evaporated in vacuum and the residual oil crystallized from methanol to give **4c** as a crystalline powder (0.75 g; 67.2%), m.p. 150–152 °C.

The product was in all respects identical with that described above.

**1 α -Ethyl-1 β -[(2-methoxycarbonyl)ethyl]-1,2,3,4,6,7,12,12b α -
-octahydroindolo[2,3-*a*]quinolizine (**5c**)**

Compound **5a** (1.00 g; 3.27 mmoles) was dissolved in methanol (30 ml) and a solution of sodium hydroxide (1.30 g; 32.6 mmoles) in distilled water (10 ml) was added to it. The solution was refluxed for 16 h. The mixture was evaporated to dryness in vacuum, the residual mixture was dissolved in distilled water and the pH of the solution was adjusted to 7 with 20% acetic acid. Crystallization started on scraping. After standing for a few hours at room temperature, the crystalline product was filtered off and washed with distilled water to obtain **5b** (0.95 g).

The crude product **5b** was dissolved in dioxan (100 ml), the solution was filtered and a solution of diazomethane in ether was added to it. After standing overnight, the excess diazomethane was decomposed and the solution evaporated to dryness in vacuum. The residual oily material was suspended in distilled water, dichloroethane (50 ml) was added, and the pH was adjusted to 9–10 with 40% NaOH solution. The organic phase was separated and dried (MgSO₄). The solution was evaporated to dryness in vacuum, the residue was crystallized from methanol, to give **5c** (0.62 g; 55.7%) m.p. 138–141 °C.

The product was in all respect identical with that described above.

**1-*n*-Butyl-1-(2-cyanoethyl)-12,3,4,6,7-hexahydro-12H-
-indolo[2,3-*a*]quinolizine-5-ium perchlerate (**3f**)**

Compound **1b** [5] (5.00 g; 13.1 mmoles) was suspended in dichloromethane (50 ml), then distilled water (40 ml) and 2N NaOH solution (10 ml) were added to it under continuous stirring in argon atmosphere. The reaction mixture was stirred for 10 min, the organic phase was separated and dried over anhydrous potassium carbonate. After filtration, freshly distilled acrylonitrile (5 ml; 71 mmoles) was poured to the solution, the system was flushed with argon and allowed to stand at room temperature. After standing for 2 days, the solvent was evaporated in vacuum and in argon atmosphere, on a water bath of maximum 40–50 °C temperature. The residual oil was dissolved in hot methanol (80 ml), and an amount of 70% aqueous perchloric acid equivalent to the base was added to it dropwise (the pH of the solution was 6–6.5). On cooling, a yellow crystalline substance separated (3.70 g; 64.1%), m.p. 225–230 °C.

Recrystallization from methanol gave substance with m.p. 230–231 °C.

C₂₂H₂₈ClN₃O₄ (433.91). Calcd. C 60.87; H 6.50; N 9.68. Found C 60.60; H 6.29; N 9.82%.

IR(KBr): 3335 (indole NH); 2310 (–C \equiv N); 1629, 1609 cm^{–1} (>C=N⁽⁺⁾–).

**1 α -n-Butyl-1 β -(2-cyanoethyl)-1,2,3,4,6,7,12,12b β -
-octahydro-indolo[2,3-a]quinolizine (4f)**

Compound **3f** (5.60 g; 12.9 mmoles) was suspended in methanol (200 ml) and cooled to 0 °C. Sodium borohydride (2.80 g; 73.9 mmoles) was then added to the suspension in small portions under continuous stirring. Stirring was continued for 1 h more; the pH was then adjusted to 3 with 5N HCl solution. The acid solution was concentrated in vacuum, the residual suspension was mixed with distilled water (100 ml) and the solution was made alkaline with 2N NaOH (to pH 9–10), then it was extracted with dichloroethane (100, 70 and 50 ml). The organic phase was dried (MgSO₄) and evaporated to dryness in vacuum. The residual solid was crystallized from methanol to obtain a white crystalline substance (2.30 g; 53.1%), m.p. 190–192 °C.

C₂₂H₂₉N₃ (335.48). Calcd. C 78.76; H 8.71; N 12.53. Found C 78.98; H 8.72; N 12.34%.

IR(KBr): 3400 (indole NH); 2310 cm⁻¹ (—C≡N).

NMR(CDCl₃): δ 8.80 (s, 1H, indole NH); 7.60–6.64 (m, 4H, aromatic H); 0.82 (t, 3H, CH₃—).

**1-Ethyl-1-(2-cyanoethyl)-9-methoxy-1,2,3,4,6,7-hexahydro-12H-
indolo[2,3-a]quinolizin-5-ium perchlorate (3h)**

Compound **1e** [6] (3.00 g; 7.8 mmoles) was suspended in dichloromethane (30 ml), distilled water (22 ml) and 2N NaOH solution (6 ml) were added, and the mixture was shaken vigorously for 10 min. The organic phase was separated and the aqueous phase was extracted twice with dichloromethane (10 and 5 ml). The combined organic solution was dried (K₂CO₃), then acrylonitrile (6 ml; 90 mmoles) and *t*-butanol (1.2 ml) were added to it and the mixture was allowed to stand at room temperature for 2 days in argon atmosphere. The solution was evaporated to dryness in vacuum and in argon atmosphere on a water bath of maximum 40–50 °C temperature, the residual red oil was dissolved in some methanol, and the pH was adjusted to 6 with 70% aqueous perchloric acid. The crystals which separated on cooling were filtered off, and recrystallized from methanol. A yellow crystalline product was obtained (2.00 g; 58.0%), m.p. 201–202 °C.

C₂₁H₂₆ClN₃O₅ (435.90). Calcd. C 57.86; H 6.01; N 9.64. Found C 58.01; H 5.71; N 9.26%.

IR(KBr): 3230 (indole NH); 2280 (—C≡N); 1620 cm⁻¹ (>C=N⁽⁺⁾—).

**1 α -Ethyl-1 β -(2-cyanoethyl)-9-methoxy-1,2,3,4,6,7,12,12b β -
-octahydroindolo[2,3-a]quinolizine (4h)**

(a) 10% Palladium-on-carbon catalyst (about 1 g) was washed with water and methanol, and then prehydrogenated in methanol. A solution of the base (m.p. 172–174 °C) liberated from the salt **3f** (1.00 g; 2.84 mmoles) in methanol (150 ml) was added slowly to the catalyst and hydrogenation was effected at room temperature and atmospheric pressure. The calculated amount of hydrogen (68 ml) was absorbed in 20 min. At the end of the reaction the catalyst was filtered off, the solvent evaporated in vacuum and the residue crystallized from methanol, to give a white crystalline substance (0.70 g; 73.0%) m.p. 201–203 °C.

C₂₁H₂₇N₃O (337.47). Calcd. C 74.74; H 8.06; N 12.45. Found C 74.47; H 8.23; N 12.19%.

IR(KBr): 3370 (indole NH); 2800–2710 (Bohlmann bands); 2300 cm⁻¹ (—C≡N).

NMR(CDCl₃): δ 7.78 (s, 1H, indole NH); 7.40–6.75 (m, 3H, aromatic H); 3.88 (s, 3H, —OCH₃); 3.20 (s, 1H, 12b β H); 0.68 (t, 3H, —CH₂—CH₃).

(b) Salt **3f** (1.00 g; 2.84 mmoles) was suspended in methanol (50 ml), and sodium borohydride (0.60 g; 15.8 mmoles) was added to the suspension in small portions, with continuous stirring, at 0 °C temperature. After having completed the addition, the mixture was stirred further for 1 h at 0 °C, then the solution was acidified with 5N HCl to pH 3. The solvent was evaporated in vacuum, the residue was dissolved in a mixture of dichloromethane (30 ml) and distilled water (30 ml), the pH was adjusted to 10 with 2N NaOH solution and the organic phase was separated and dried over MgSO₄. The solution was evaporated to dryness and the residue crystallized from methanol to yield a white crystalline substance (0.60 g; 63.0%), m.p. 202–204 °C.

The compound was in all respects identical with that described under (a).

**1 α -Ethyl-1 β -(3-aminopropyl)-1,2,3,4,5,6,7,12,12b β -
-octahydroindolo[2,3-*a*]quinolizine (4d)**

Compound **4a** (3.10 g; 10.1 mmoles) was dissolved in methanol (250 ml) with gentle heating, then Raney nickel catalyst (2 g), which had been washed with distilled water then with methanol, was added to the solution under continuous stirring at 48–50 °C. A suspension of sodium borohydride (0.50 g; 16.3 mmoles) in 8*N* NaOH solution (2 ml) was poured to the mixture. Fizzing started immediately after the addition, and continued for about 30 min. Then more Raney nickel catalyst (2 g), prepared as above, was added together with a suspension of sodium borohydride (0.50 g; 16.3 mmoles) in 8*N* NaOH solution (2 ml). The reaction mixture was refluxed for 4 h, then the catalyst was removed by filtration, washed with methanol and the solvent was evaporated in vacuum. The residual oil was dissolved in some methanol and acidified to pH 4–5 with methanol saturated with hydrogen chloride gas. On the addition of ether, the product separated as the hydrochloride (3.50 g). Recrystallization from a mixture of methanol and ether gave the white dihydrochloride (3.20 g; 83.5%), m.p. 249–251 °C.

$C_{20}H_{29}N_3 \cdot 2 HCl$ (384.38). Calcd. C 62.48; H 8.12; N 10.93. Found C 62.22; H 7.90; N 10.71%.

IR(KBr): 3305 cm^{-1} (indole NH).

**1 α -*n*-Butyl-1 β -(3-aminopropyl)-1,2,3,4,6,7,12,12b β -
-octahydroindolo[2,3-*a*]quinolizine (4g)**

Compound **4f** (6.17 g; 18.4 mmoles) was suspended in methanol (500 ml), and Raney nickel catalyst (8 g), which had been washed with distilled water and methanol, was added.

The mixture was heated to 48–50 °C, a suspension of sodium borohydride (8.0 g; 210 mmoles) in 8*N* NaOH (32 ml) was added. After having maintained the above temperature for 3 h, a further amount of prepared Raney nickel catalyst (8 g) and sodium borohydride (8.0 g; 210 mmoles), suspended in 8*N* NaOH solution (32 ml), were added to the reaction mixture. It was refluxed for 3 h, then the catalyst was filtered off. The solution was concentrated to 50 ml in vacuum, distilled water (200 ml) was added, and the solution was extracted with dichloromethane (100, 70 and 50 ml). The organic phase was dried ($MgSO_4$), then evaporated to dryness in vacuum. The oily residue was crystallized from methanol to give a white crystalline powder (3.20 g; 51.0%), m.p. 161–164 °C.

$C_{22}H_{29}N_3$ (339.51). Calcd. C 77.82; H 9.80; N 12.38. Found C 77.78; H 9.83; N 12.14%.

IR(KBr): 3310 cm^{-1} (indole NH).

NMR($CDCl_3$): δ 7.72–6.98 (m, 5H, indole NH and aromatic H); 3.46 (s, 1H, 12b β H).

**1 α -Ethyl-1 β -(3-dimethylaminopropyl)-1,2,3,4,6,7,12,12b β -
-octahydroindolo[2,3-*a*]quinolizine (4e)**

Compound **3a** (2.00 g; 6.20 mmoles) was suspended in methanol (100 ml), and Raney nickel catalyst (2 g), which had been washed with water and methanol, was added to it. The solution was stirred and heated to 48–50 °C and a suspension of sodium borohydride (2.00 g; 53 mmoles) in 8*N* NaOH solution (8 ml) was added to it. The mixture was refluxed for 3 h. It was then cooled to 50 °C and Raney nickel catalyst (2 g; prepared as above) and a suspension of sodium borohydride (2.00 g; 53 mmoles) in 8*N* NaOH solution (8 ml) were added. Then mixture was refluxed for 3 h, and the catalyst was removed by filtration. The solution was evaporated to dryness in vacuum, the residual oil was dissolved in a small amount of methanol, and acidified to pH 4 with methanol saturated with hydrogen chloride. On the addition of ether a crystalline salt (2.20 g) separated. Recrystallization from a mixture of methanol and ether gave the white, crystalline dihydrochloride (**4d** · 2 HCl) (1.85 g; 77.8%), m.p. 248–251 °C.

Compound **4d** (6.95 g; 22.4 mmoles) liberated from the dihydrochloride salt was dissolved in 98% formic acid (14 ml; 368 mmoles), and 30% aqueous formaldehyde solution (6.30 ml; 63.2 mmoles) was added to the reaction mixture. It was refluxed for 4 h, the hot solution was poured onto ice and made alkaline (pH 10) with 40% NaOH solution. The solution was extracted with dichloroethane (70, 50 and 30 ml), the organic phase was dried ($MgSO_4$) and the solvent evaporated in vacuum. The residual oil was dissolved in anhydrous benzene (150 ml) and hydrogen chloride was passed into the solution, whereupon a pale yellow salt (7.85 g) separated. The pure dihydrochloride of **4e** (7.15 g; 78.1%) was obtained on recrystallization from a mixture of methanol and ether, m.p. 276–278 °C.

$C_{22}H_{33}N_3 \cdot 2 HCl$ (412.42). Calcd. C 64.06; H 8.55; N 10.19. Found 63.97; H 8.27; N 10.44%.
IR(KBr): 3385 cm^{-1} (indole NH).

REFERENCES

- [1] KALAUS, GY., SZABÓ, L., SZÁNTAY, CS., KÁRPÁTI, E., SZPORNY, L.: *Archiv der Pharm.* **312**, 312–319 (1979)
- [2] SZÁNTAY, CS., SZABÓ, L., KALAUS, GY.: *Tetrahedron*, **33**, 1803 (1977)
- [3] SZABÓ, L., KALAUS, GY., SZÁNTAY, CS.: Unpublished results
- [4] GASKEL, A. J., JOULE, J. A.: *Tetrahedron*, **23**, 4053 (1967)
- [5] KALAUS, GY., GYÖRY, P., SZABÓ, L., SZÁNTAY, CS.: *Acta Chim. Acad. Sci. Hung.*, **96** (4), 385–391 (1978)
- [6] KALAUS, GY., SZABÓ, L., HORVÁTH, J., SZÁNTAY, CS.: *Heterocycles*, **6**, 321 (1977)
- [7] EGLI, R. A.: *Helv. Chim. Acta*, **53**, 47 (1970)

György KALAUS	}	H-1521 Budapest, Gellért tér 4.
Lajos SZABÓ		
Péter GYÖRY		
Éva SZENTIRMAY		
Csaba SZÁNTAY		

PHOTOKATALYTISCHE SYSTEME, XVII*

SPIN-TRAPPING VON RADIKALEN BEI DER PHOTOLYSE VON CER(IV) IN ALKOHOLEN

D. REHOREK

(Sektion Chemie der Karl-Marx-Universität Leipzig, DDR)

Eingegangen am 8. Mai 1978

Zur Veröffentlichung angenommen am 11. Oktober 1978

Unter Verwendung von Nitrosodurol bzw. Phenyl-*N-tert.*-butylnitron als Spin-Traps wurden die bei der Photolyse von alkoholischen Cer(IV)-Lösungen entstehenden Radikale ESR-spektroskopisch nachgewiesen und identifiziert.

Bei Zimmertemperatur wurden neben Alkoxyradikalen sowohl Alkyl- als auch Hydroxyalkylradikale beobachtet, was auf Reaktionen der primär entstandenen Alkoxyradikale zurückgeführt wird.

I. Einleitung

Obwohl die Photooxidation von Alkoholen mittels Ce(IV) in den letzten Jahren sehr intensiv ESR-spektroskopisch sowohl in flüssiger [1] als auch in gefrorener Lösung [2] untersucht wurde, bestehen noch einige Unklarheiten bezüglich des Mechanismus dieser Reaktion.

So wurden in gefrorener Lösung hauptsächlich Hydroxyalkylradikale beobachtet, wogegen in flüssiger Lösung vor allem durch C—C-Bindungsspaltung entstandene Alkylradikale nachgewiesen werden konnten.

Diese Unterschiede wurden von GREATOREX *et al.* [1] mit der im Vergleich zur C—H-Spaltung größeren Aktivierungsenergie für die C—C-Bindungsspaltung erklärt.

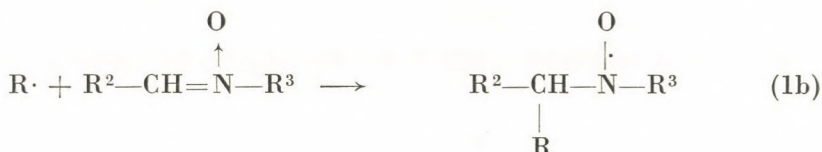
C—C-Bindungsspaltung sollte demnach vor allem bei höheren Temperaturen beobachtet werden. Allerdings kann damit das Fehlen von Hydroxyalkylradikalen nicht erklärt werden.

Wir vermuten vielmehr, daß die Hydroxyalkylradikale bei höheren Temperaturen unter den gegebenen Bedingungen für einen direkten ESR-Nachweis wegen ihrer geringen Stabilität in zu niedrigen Konzentrationen vorhanden sind.

Wir haben daher versucht, die Spin—Trapping-Methode [3, 4] für den Nachweis der Radikale zu verwenden.

* XVI. Mitteilung: REHOREK, D., SALVETTER, J., HANTSCHMANN, A., HENNIG, H.: J. prakt. Chem. **321**, 159 (1979).

Hierbei werden die bei der Reaktion entstehenden Radikale $R\cdot$ an die $N=O$ -Bindung einer Nitrosoverbindung bzw. an die $C=N$ -Bindung eines Aldonitrons zu stabilen Nitroxiden addiert (vgl. Gln. 1a und b).



In früheren Mitteilungen dieser Reihe [5—8] konnten wir zeigen, daß die von TERABE *et al.* [9] bzw. JANZEN und BLACKBURN [10] eingeführten Spin-Traps Nitrosodurol (2,3,5,6-Tetramethylnitrosobenzol, *ND*) und Phenyl-*N-tert.*-butylnitron (*PBN*) für die Untersuchung von photoinduzierten Redoxreaktionen von Metallkomplexen geeignet sind.

2. Experimenteller Teil

Es wurden Lösungen von $(NH_4)_2Ce(NO_3)_6$ (VEB Laborchemie Apolda) in verschiedenen, nach Standardmethoden [11] gereinigten Alkoholen untersucht. Diesen Lösungen wurde der in Methylenchlorid gelöste Spin-Trap zugesetzt, so daß die Gesamtkonzentration des Spin-Traps im Bereich von 0,005 *M* bis 0,1 *M* variierte. In einigen Fällen wurde anstelle von Methylenchlorid auch Chloroform als Lösungsmittel für den Spin-Trap verwendet.

Die für die Untersuchung günstigste Konzentration an Ce(IV) betrug etwa $5 \times 10^{-4} M$ bis $5 \times 10^{-3} M$. Bei höheren Konzentrationen an Ce(IV) ging die ESR-Signalintensität der erhaltenen Spin-Addukte stark zurück.

Als Spin-Traps wurden Nitrosodurol (*ND*) und Phenyl-*N-tert.*-butylnitron (*PBN*) verwendet. Die Darstellung der Spin-Traps erfolgte nach [12, 13].

Die Proben wurden mittels einer Quecksilberhochdrucklampe HBO-200 (VEB Narva Berlin) direkt im Resonator eines ESR-Spektrometers vom Typ JES-2BQ (Jeol, Japan) bestrahlt.

Alle Spektren wurden bei Raumtemperatur im X-Band aufgenommen.

Die Feldeichung erfolgte mittels Protonenresonanz.

Alle Lösungsmittel wurden direkt vor der Messung etwa 20 Minuten mit Stickstoff gespült.

3. Ergebnisse

Bei der Bestrahlung beobachteten wir die Bildung charakteristischer Spin-Addukte, deren ESR-Parameter in Tabelle I angegeben sind. Durch Vergleich mit früher nachgewiesenen Spin-Addukten [7—9, 14] konnten diese in den meisten Fällen auch identifiziert werden.

Tabelle I

ESR-Parameter der Spin-Addukte

Nr.	Alkohol	Addiertes Radikal	Spin-Trap	$a_N^a)$	$a_H^a)$
1	Methanol	$\cdot\text{CH}_2\text{OH}$	ND	$1,34 \pm 0,02$	$0,81 \pm 0,02$ (2H)
2	Methanol	$\cdot\text{CH}_2\text{C}_6\text{H}(\text{CH}_3)_2\text{NO}$	ND	$1,32 \pm 0,02$	$0,59 \pm 0,03$ (2H)
3	Ethanol	$\text{CH}_3\dot{\text{C}}\text{HOH}$	ND	$1,38 \pm 0,02$	$0,69 \pm 0,02$ (1H)
4	Ethanol	NO_2	ND	$1,43 \pm 0,02$	—
5	Ethanol	$\cdot\text{CH}_3$	ND	$1,43 \pm 0,03$	$1,31 \pm 0,03$ (3H)
6	n-Propanol	$\cdot\text{C}_2\text{H}_5$	ND	$1,42 \pm 0,02$	$1,19 \pm 0,02$ (2H)
7	n-Propanol	$\text{CH}_3\text{CH}_2\dot{\text{C}}\text{HOH}$	ND	$1,48 \pm 0,02$	$0,27 \pm 0,02$ (1H)
8	n-Propanol	NO_2	ND	$1,42 \pm 0,02$	—
9	iso-Propanol	$(\text{CH}_3)_2\dot{\text{C}}\text{OH}$	ND	$1,42 \pm 0,02$	—
10	iso-Propanol	$\cdot\text{CH}_3$	ND	$1,44 \pm 0,03$	$1,31 \pm 0,03$ (3H)
11	n-Butanol	$\text{CH}_3\text{CH}_2\text{CH}_2\dot{\text{C}}\text{HOH}$	ND	$1,39 \pm 0,02$	$0,69 \pm 0,02$ (1H)
12	n-Butanol	$\cdot\text{CH}_2\text{CH}_2\text{CH}_3$	ND	$1,42 \pm 0,02$	$1,16 \pm 0,02$ (2H)
13	sec.-Butanol	$\cdot\text{C}_2\text{H}_5$	ND	$1,43 \pm 0,02$	$1,18 \pm 0,02$ (2H)
14	sec.-Butanol	$\text{CH}_3\dot{\text{C}}(\text{C}_2\text{H}_5)\text{OH}$	ND	$1,43 \pm 0,02$	—
15	sec.-Butanol	$\text{CH}_3\text{CH}(\text{OH})\dot{\text{C}}\text{HCH}_3$	ND	$1,38 \pm 0,02$	$0,94 \pm 0,02$ (1H)
16	iso-Butanol	$\cdot\text{CH}(\text{CH}_3)_2$	ND	$1,42 \pm 0,02$	$0,91 \pm 0,02$ (1H)
17	iso-Butanol	$\cdot\text{C}(\text{CH}_3)_2\text{CH}_2\text{OH}$	ND	$1,42 \pm 0,02$	—
18	iso-Butanol	$(\text{CH}_3)_2\text{CHCH}_2\text{O}\cdot$	ND	$2,65 \pm 0,05$	—
19	tert.-Butanol	$(\text{CH}_3)_3\text{CO}\cdot$	ND	$2,77 \pm 0,03$	—
20	tert.-Butanol	$\cdot\text{CH}_3$	ND	$1,40 \pm 0,03$	$1,30 \pm 0,02$ (3H)
21	tert.-Butanol	$(\text{CH}_3)_3\text{C}\cdot$	ND	$1,40 \pm 0,02$	—
22	tert.-Butanol	$\cdot\text{CH}_2\text{C}(\text{CH}_3)_2\text{OH}$	ND	$1,41 \pm 0,03$	$0,33 \pm 0,02$ (2H)
23	Methanol ^{b)}	$\cdot\text{CCl}_3$	ND	$1,08 \pm 0,03$	$0,13 \pm 0,02$ (3Cl) ^{c)}
24	Methanol ^{b)}	$\cdot\text{COCl}$	ND	$0,81 \pm 0,01$	—
25	Methanol	$\text{CH}_3\text{O}\cdot$	PBN ^{d)}	$1,42 \pm 0,02$	$0,27 \pm 0,02$ (1H)
26	Ethanol	$\text{CH}_3\text{CH}_2\text{O}\cdot$	PBN ^{d)}	$1,44 \pm 0,02$	$0,26 \pm 0,02$ (1H)
27	n-Propanol	$\text{CH}_3\text{CH}_2\text{CH}_2\text{O}\cdot$	PBN ^{d)}	$1,43 \pm 0,02$	$0,25 \pm 0,02$ (1H)
28	iso-Propanol	$(\text{CH}_3)_2\text{CHO}\cdot$	PBN ^{d)}	$1,44 \pm 0,02$	$0,22 \pm 0,02$ (1H)
29	n-Butanol	$\text{CH}_3\text{CH}_2\text{CH}_2\text{CH}_2\text{O}\cdot$	PBN ^{d)}	$1,43 \pm 0,02$	$0,25 \pm 0,02$ (1H)
30	sec.-Butanol	$\text{C}_2\text{H}_5(\text{CH}_3)\text{CHO}\cdot$	PBN ^{d)}	$1,44 \pm 0,02$	$0,22 \pm 0,02$ (1H)
31	iso-Butanol	$(\text{CH}_3)_2\text{CHCH}_2\text{O}\cdot$	PBN ^{d)}	$1,44 \pm 0,02$	$0,23 \pm 0,02$ (1H)
32	tert.-Butanol	$(\text{CH}_3)_3\text{CO}\cdot$	PBN ^{d)}	$1,40 \pm 0,02$	$0,14 \pm 0,02$ (1H)

a) Angaben in mT; in Klammern: Anzahl der wechselwirkenden H-Atome

b) In anderen Alkoholen wurden dieselben Radikale beobachtet, vgl. Text

c) Cl-Hyperfeinaufspaltung

d) Zusätzlich zu den hier angegebenen Radikalen wurden noch Spin-Addukte von Alkyl- und Hydroxy-alkylradikalen beobachtet, die jedoch nicht identifiziert werden konnten.

3.1. Bestrahlung in Gegenwart von Nitrosodurol

Die folgenden Ergebnisse beziehen sich auf die Untersuchungen der Alkohol/Methylenchlorid-Gemische.

Bei der Photooxidation von *Methanol* konnten in Gegenwart hoher Spin-Trap-Konzentrationen (0,1 M) zwei Spin-Addukte beobachtet werden, von denen das eine als $\cdot\text{CH}_2\text{OH}$ -Addukt (1) identifiziert wurde. Bei dem zweiten Addukt handelt es sich ebenfalls um das Addukt eines $\cdot\text{CH}_2\text{R}$ -Radikals an ND. Da bei Verwendung von Chloroform als Lösungsmittel (siehe 3.2.) dieses Addukt ebenfalls beobachtet wurde, kann es sich hierbei nicht um das $\cdot\text{CH}_2\text{Cl}$ -Addukt handeln. Es ist denkbar, daß es sich bei dem Addukt (2) um das Spin-Addukt des durch H-Abstraktion aus Nitrosodurol entstandenen $\cdot\text{CH}_2\text{C}_6\text{H}(\text{CH}_3)_3\text{NO}$ -Radikals an ND handelt. Für diese Annahme spricht die Tatsache, daß 2 bei geringen ND-Konzentrationen nicht nachgewiesen werden konnte. Allerdings konnte die Bildung von 2 im Falle anderer Alkohole nicht beobachtet werden.

In *Ethanol* wurden bei Bestrahlung hauptsächlich das Addukt des $\text{CH}_3\dot{\text{C}}\text{HOH}$ -Radikals (3) sowie ein einfaches Triplett mit $a_N = (1,43 \pm 0,02)$ mT (4) beobachtet. Bei letzterem handelt es sich wahrscheinlich um das NO_2 -Addukt an ND (vergleiche [8]). Nach längeren Bestrahlungszeiten konnten zusätzlich $\cdot\text{CH}_3$ -Addukte (5) registriert werden.

Bei der Bestrahlung von Ce(IV) in *n-Propanol* werden Ethylradikale und 1-Hydroxypropylradikale ($\text{CH}_3\text{CH}_2\dot{\text{C}}\text{HOH}$) gebildet, die mittels ND abgefangen und als Spin-Addukte 6 bzw. 7 nachgewiesen werden konnten. Daneben wurde das Triplett des NO_2 -Addukts (8) beobachtet.

In *iso-Propanol* konnten $(\text{CH}_3)_2\dot{\text{C}}\text{OH}$ -Radikale (9) und Methylradikale (10) registriert werden.

In *n-Butanol* wurde neben der Bildung von 1-Hydroxybutylradikalen (11) das Entstehen von Propylradikalen (12) nachgewiesen.

Die Bestrahlung in *sec.-Butanol* lieferte dagegen in großer Ausbeute Ethylradikale (13) neben geringen Mengen $\text{CH}_3\dot{\text{C}}(\text{C}_2\text{H}_5)\text{OH}$ - und $\text{CH}_3\text{CH}(\text{OH})\dot{\text{C}}\text{HCH}_3$ -Radikalen (14 und 15, siehe Abbildung 1). Der Nachweis der $\text{CH}_3\dot{\text{C}}(\text{C}_2\text{H}_5)\text{OH}$ -Radikale war wegen der Überlagerung durch die ESR-Signale des Ethyl-Addukts erschwert. Die Untersuchung der Zeitabhängigkeit der ESR-Spektren ergab jedoch eindeutig, daß den Ethyl-Signalen ein einfaches Triplett geringer Stabilität überlagert ist.

In *iso-Butanol* wurde zunächst ein aus insgesamt sechs Linien bestehendes ESR-Signal (16) beobachtet, welches thermisch und photochemisch außerordentlich stabil ist. Hierbei handelt es sich um das *iso*-Propylradikal. Daneben wurde ein intensives Triplett registriert, das dem Addukt des $\cdot\text{C}(\text{CH}_3)\text{CH}_2\text{OH}$ -Radikals an Nitrosodurol (17) zugeordnet werden kann. Weitere Linien gerin-

ger Intensität, die an den Rändern des Spektrums auftraten, lassen sich dem iso-Butoxyl-Spin-Addukt (18) zuordnen.

Die Bestrahlung von Ce(IV) in *tert.*-Butanol lieferte folgende Radikale: $(\text{CH}_3)_3\text{CO}\cdot$ (19), $\cdot\text{CH}_3$ (20) und $(\text{CH}_3)_3\dot{\text{C}}$ (21) sowie bei geringeren ND-Konzentrationen das $\cdot\text{CH}_2\text{C}(\text{CH}_3)_2\text{OH}$ -Radikal (22).

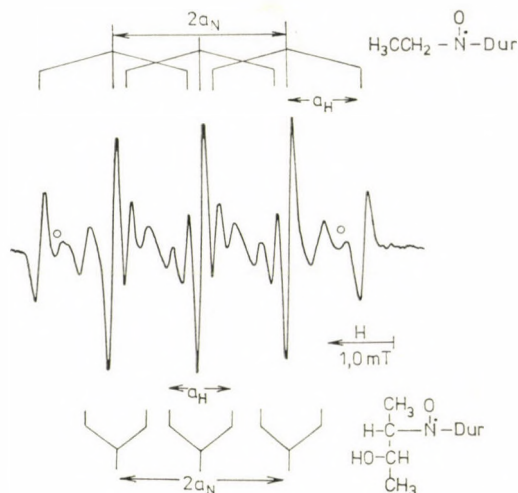


Abb. 1. ESR-Spektrum der Spin-Addukte, die bei der Bestrahlung von Ce(IV) in *sec.*-Butanol erhalten wurden. (0,05 M Nitrosodurol; o kennzeichnen die ESR-Linien eines nicht identifizierten Spin-Addukts)

3.2. Bestrahlung in Alkohol Chloroform-Gemischen in Gegenwart von Nitrosodurol

Die Bestrahlung der alkoholischen Ce(IV)-Lösungen ergab bei Zusatz von Chloroform-Lösungen des Spin-Traps Nitrosodurol neben den in Abschnitt 3.1. aufgeführten Radikalen zusätzlich das $\cdot\text{CCl}_3$ -Addukt (23), welches sich nach einigen Minuten in ein einfaches Triplett (24) mit $a_N = (0,81 \pm 0,01)$ mT umwandelte.

In Anlehnung an [15] nehmen wir an, daß es sich hierbei um das Addukt des $\cdot\text{COCl}$ -Radikals an Nitrosodurol handelt, welches durch Oxidation von 23 entsteht.

Auf Grund des Linienreichtums des Spin-Addukts 23 war die Auswertung der in Gegenwart von Chloroform erhaltenen ESR-Spektren außerordentlich erschwert. Chloroform muß deshalb als ungeeignetes Lösungsmittel für den Spin-Trap angesehen werden.

3.3. Bestrahlung in Gegenwart von Phenyl-*N*-*tert*.-butylnitron (*PBN*)

Bei Verwendung von *PBN* als Spin-Trap konnten in allen Fällen Alkoxyradikale (vgl. Tabelle I) nachgewiesen werden. Daneben wurden ESR-Signale mit etwas größerer β -H-Hyperfeinaufspaltung ($a_H \sim 0,4$ mT) beobachtet, bei denen es sich sowohl um Alkyl- als auch Hydroxyalkyl-Spin-Addukte handeln könnte [10, 14]. Eine genaue Identifizierung ist nur sehr schwer möglich und, da diese Radikale mit Hilfe von *ND* wesentlich besser identifiziert werden können, auch nicht unbedingt erforderlich.

Bereits nach 30 Sekunden Bestrahlungszeit wurde zusätzlich zu den oben erwähnten Spin-Addukten des ESR-Signal des Di-*tert*.-butylnitroxids [$a_N = (1,59 \pm 0,02)$ mT] beobachtet. Hierbei handelt es sich um ein Zerfallsprodukt des *PBN* [16].

Mit zunehmender Bestrahlungszeit wird das Signal des Di-*tert*.-butylnitroxids intensiver, so daß eine Auswertung der ESR-Spektren nur bei relativ kurzen Bestrahlungszeiten ($t \leq 30$ s) möglich ist.

4. Diskussion

Obwohl die bei der Bestrahlung von Ce(IV) in Alkoholen erhaltenen Spin-Addukte bedeutend instabiler sind als im Falle des kürzlich von uns untersuchten Uranyl-nitrats [8], konnten bei Zimmertemperatur auswertbare ESR-Spektren erhalten werden, die eine Reihe von Aussagen über den Mechanismus der photoinduzierten Alkoholorxidation gestatten. Verglichen mit direkten, d. h. ohne Verwendung von Spin-Traps durchgeführten ESR-Untersuchungen [1, 2] erfordert jedoch die Spin-Trapping-Methode einen wesentlich geringeren experimentellen Aufwand.

In Tabelle II sind die mit den einzelnen Methoden (Photolyse in flüssiger und gefrorener Lösung sowie Spin-Trapping) nachgewiesenen radikalischen Reaktionsprodukte der Alkohole zusammengefaßt.

Die Bildung des *tert*.-Butylradikals, das bei der Photolyse von Ce(IV) in *tert*.-Butanol beobachtet wurde, läßt sich auf den thermischen Zerfall des *tert*.-Butyldurylnitroxids zurückführen [17]. Die Bildung von NO_2 wurde auch bei der Photolyse in gefrorener Lösung beobachtet [2] und entsteht wahrscheinlich durch die Reaktion von Hydroxyalkylradikalen mit NO_3^- . In [8] konnten wir zeigen, daß die Bildung der Spin-Addukte des Typs 4 und 8 auf die Reaktion von *ND* mit freiem NO_2 zurückzuführen ist, wenn auch über die genaue Struktur des Spin-Addukts Unklarheiten bestehen.

Wie Tabelle II zeigt, konnten mit Hilfe der Spin-Trapping-Methode alle von GREATOREX und KEMP [2] in gefrorener Lösung gefundenen organischen Radikale nachgewiesen werden. Durch ESR-Messungen an flüssigen Lösungen konnten ohne Verwendung von Spin-Traps [1] lediglich die durch C—C-Bin-

Tabelle II

Vergleichende Übersicht über die bei der Photolyse von $Ce(IV)$ in Alkoholen zu beobachtenden Radikale

Alkohol	Spin-Trapping ^{a)}	Gefrorene Lösung ^{b)}	Flüssige Lösung ^{c)}
Methanol	$CH_3O\cdot$	—	keine Radikale
Methanol	$\cdot CH_2OH$	$\cdot CH_2OH$	
Ethanol	$CH_3CH_2O\cdot$	—	—
Ethanol	$CH_3\dot{C}HOH$	$CH_3\dot{C}HOH$	—
Ethanol	$\cdot CH_3$	$\cdot CH_3$	$\cdot CH_3$
<i>n</i> -Propanol	$CH_3CH_2CH_2O\cdot$	—	—
<i>n</i> -Propanol	$CH_3CH_2\dot{C}HOH$	$CH_3CH_2\dot{C}HOH$	—
<i>n</i> -Propanol	$\cdot CH_2CH_3$	$\cdot CH_2CH_3$	$\cdot CH_2CH_3$
<i>iso</i> -Propanol	$(CH_3)_2CHO\cdot$	—	—
<i>iso</i> -Propanol	$(CH_3)_2\dot{C}OH$	$(CH_3)_2\dot{C}OH$	—
<i>i: o</i> -Propanol	$\cdot CH_3$	$\cdot CH_3$	$\cdot CH_3$
<i>n</i> -Butanol	$CH_3CH_2CH_2CH_2O\cdot$	—	—
<i>n</i> -Butanol	$CH_3CH_2CH_2\dot{C}HOH$	$CH_3CH_2CH_2\dot{C}HOH$	—
<i>n</i> -Butanol	$\cdot CH_2CH_2CH_3$	—	$\cdot CH_2CH_2CH_3$
<i>iso</i> -Butanol	$(CH_3)_2CHCH_2O\cdot$	—	—
<i>iso</i> -Butanol	$(CH_3)_2\dot{C}H$	—	—
<i>iso</i> -Butanol	$\cdot C(CH_3)_2CH_2OH$	—	—
<i>iso</i> -Butanol	—	$(CH_3)_2CH\dot{C}HOH$	—
<i>sec.</i> -Butanol	$C_2H_5(CH_3)CHO\cdot$	—	—
<i>sec.</i> -Butanol	$CH_3\dot{C}(C_2H_5)OH$	—	—
<i>sec.</i> -Butanol	$CH_3CH(OH)\dot{C}HCH_3$	—	—
<i>sec.</i> -Butanol	$\cdot CH_2CH_3$	—	—
<i>sec.</i> -Butanol	—	$\cdot CH_3$	—
<i>tert.</i> -Butanol	$(CH_3)_3CO\cdot$	—	—
<i>tert.</i> -Butanol	$\cdot CH_3$	$\cdot CH_3$	—
<i>tert.</i> -Butanol	$\cdot CH_2C(CH_3)_2OH$	$\cdot CH_2C(CH_3)_2OH$	—

a) Diese Arbeit, Meßtemperatur ca. 300 K

b) GREATORIX und KEMP [2], Meßtemperatur 77 K

c) GREATORIX *et al.* [1], Meßtemperatur ca. 200 K, direkter ESR-Nachweis

dungsspaltung entstehenden Alkylradikale registriert werden, wobei die Meßtemperatur etwa 200 K betrug. Die Tatsache, daß wir bei wesentlich höheren Temperaturen (ca. 300 K) in den meisten Fällen sowohl Alkyl- als auch Hy-

droxyalkylradikale nachweisen konnten, spricht gegen einen merklich temperaturabhängigen Konkurrenzprozeß [Gl. (2)] bei der Bildung von Alkyl- und Hydroxyalkylradikalen.



Vielmehr nehmen wir auf Grund vorliegender Ergebnisse an, daß sowohl Alkyl- als auch Hydroxyalkylradikale Produkte von Sekundärprozessen sind.

Im ersten Schritt wird ein Elektron vom Alkohol zum Ce(IV) übertragen (vgl. Gl. 3a und 3b).

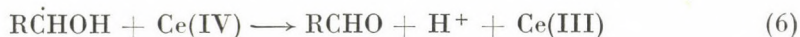


Das hierbei entstehende Alkoxyradikal, das auf direktem Wege ESR-spektroskopisch nur schwer nachgewiesen werden kann [18], wurde von uns mittels Spin-Trapping mit *PBN* und teilweise auch mit *ND* nachgewiesen (vgl. Tabelle I). Dieses Radikal kann fragmentieren (Gl. 4) oder unter H-Abstraktion mit dem Alkohol unter Bildung von Hydroxyalkylradikalen reagieren (Gl. 5).



Im Falle primärer Alkohole entstehen nach Gleichung 4 die um ein C-Atom kürzeren Alkylradikale. Bei unsymmetrisch substituierten sekundären Alkoholen, z. B. *sec.*-Butanol, ist dagegen die Bildung zweier verschiedener Radikale möglich. In Übereinstimmung mit den Ergebnissen von GILBERT *et al.* [19] und früheren Untersuchungen am Uranylinitrat [8] finden wir ausschließliche Bildung von Ethylradikalen. GREATOREX *et al.* [2] beobachteten dagegen Methylradikale. Wir können zur Zeit noch keine plausible Erklärung für diesen Widerspruch angeben.

Da die nach Gleichung 5 entstehenden Hydroxyalkylradikale starke Raduktionsmittel darstellen, ist eine thermische Folgereaktion (6) sehr wahrscheinlich. Diese Reaktion ist unserer Ansicht nach der wesentliche Grund dafür, daß in flüssiger Lösung Hydroxyalkylradikale nicht mehr auf direktem Wege ESR-spektroskopisch nachgewiesen werden konnten.



Durch Einfrieren der Lösung wird die Reaktion 6 unterdrückt und der ESR-Nachweis der Hydroxyalkylradikale möglich.

Die entsprechende Bildungsreaktion für die Hydroxyalkylradikale (Gl. 5) sollte durch das Einfrieren in weit geringerem Maße beeinflusst werden, da die Konzentration des Alkohols wesentlich größer ist als die des Ce(IV). Darüber hinaus sind auch Isomerisierungsreaktionen vom Typ (7) zu berücksichtigen [20].



Dafür, daß der Reaktion 6 größere Bedeutung zukommt, spricht auch die Tatsache, daß die Ausbeute an Hydroxyalkyl-Spin-Addukten mit zunehmender Ce(IV)-Konzentration bei konstanter Konzentration an Spin-Trap stark herabgesetzt wird. In diesem Fall konkurrieren Ce(IV) und Nitrosodurol um die Hydroxyalkylradikale. Zusätzlich ist auch eine Reaktion des Ce(IV) mit den Spin-Addukten in Betracht zu ziehen.

Die Oxidation der Alkylradikale wirkt sich dagegen erst bei Ce(IV)-Konzentrationen von größer als etwa 10^{-2} M merklich auf den ESR-Nachweis aus.

LITERATUR

- [1] GREATOREX, D., HILL, R. J., KEMP, T. J., STONE, T. J.: J. Chem. Soc. Faraday Trans. I, **70**, 216 (1974)
- [2] GREATOREX, D., KEMP, T. J.: Trans. Faraday Soc., **67**, 56 (1971)
- [3] JANZEN, E. G.: Acc. Chem. Res., **4**, 31 (1971)
- [4] LAGERCRANTZ, C.: J. Phys. Chem., **75**, 3466 (1971)
- [5] REHOREK, D.: Tetr. Lett., **1977**, 2611
- [6] REHOREK, D.: J. Signal AM **6**, 221 (1978)
- [7] REHOREK, D.: Z. Chem. **18**, 194 (1978)
- [8] REHOREK, D.: Z. anorg. allg. Chem. **443**, 255 (1978)
- [9] TERABE, S., KURUMA, K., KONAKA, R.: J. Chem. Soc. Perkin Trans. II, **1973**, 1252
- [10] JANZEN, E. G., BLACKBURN, B. J.: J. Amer. Chem. Soc., **90**, 5909 (1968)
- [11] Autorenkollektiv, Organikum, VEB Deutscher Verlag der Wissenschaften, Berlin 1974
- [12] SMITH, L. I., TAYLOR, F. L.: J. Amer. Chem. Soc., **35**, 2370, 2460 (1935)
- [13] RUNDEL, W.: Houben-Weyl, Methoden der organischen Chemie, Georg-Thieme-Verlag Stuttgart 1968, Bd. X/4
- [14] LEDWITH, A., RUSSELL, P. J., SUTCLIFFE, L. H.: Proc. Roy. Soc. London, A **332**, 151 (1973)
- [15] HARTGERINK, I. W., ENGBERTS, J. B. F. N., DE BOER, Th. J.: Tetr. Lett., **1971**, 2709
- [16] SOMMERMEYER, K., SEIFFERT, W., WILKE, W.: Tetr. Lett., **1974**, 1821
- [17] REHOREK, D.: Z. Chem. **19**, 65 (1979)
- [18] GILBERT, B. C., HOLMES, R. G. G., NORMAN, R. O. C.: J. Chem. Res. (S), **1977**, 1
- [19] ALIWI, S. M., BAMFORD, C. H.: J. Chem. Soc. Faraday Trans. I, **71**, 1733 (1975)

Detlef REHOREK DDR-701 Leipzig, Liebigstraße 18.

PENTA AND HEXA-COORDINATED COMPLEXES OF PLATINUM METALS OF POTENTIAL PENTADENTATE LIGANDS

V. B. RANA*, S. K. SAHNI and S. K. SANGAL

(Department of Chemistry, Meerut College, Meerut India)

Received February 12, 1977

In revised form August 31, 1978

Accepted for publication October 13, 1978

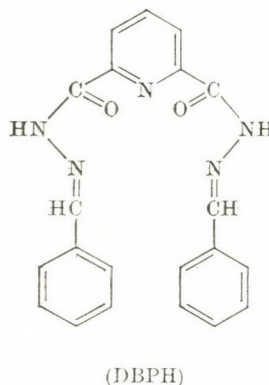
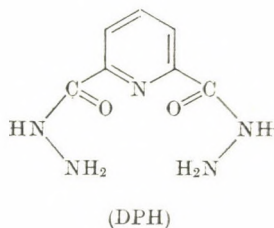
The complexes of ruthenium(III), rhodium(III), platinum(IV), palladium(II) and platinum(II) of two potential pentadentate ligands, 2,6-dipicolinic acid hydrazide (DPH) and *N,N'*-dibenzylidene dipicolinic acid hydrazide (DBPH) have been synthesized and characterized. The ruthenium(III), rhodium(III) and platinum(IV) complexes are found to be hexa-coordinated, while the bivalent palladium and platinum complexes are penta-coordinated, as revealed by their elemental analyses, magnetic susceptibility, ultraviolet-visible and infrared spectral measurements. In the far infrared region $\nu(\text{M-py})$, $\nu(\text{M-O})$ and $\nu(\text{M-N})$ vibrations have been assigned and an attempt has been made to assign the stereochemistry of the complexes on the basis of **6a** and **16b** vibrations of the pyridine ring.

Introduction

The penta-coordinated complexes of ruthenium(III), rhodium(III), palladium(II) and platinum(II) are known [1, 2], but the chemistry of such complexes of platinum metals has not received as much attention as the complexes of the metals of the first transition series [1, 3]. No systematic study has been made of the penta-coordinated complexes of these metals, except those of palladium(II) and platinum(II) with phosphines and arsines [4–7]. The lack of higher multidentate ligands complexed with platinum metals is noteworthy and a survey of literature reveals that no penta-coordinated complexes involving pentadentate ligands have been reported to date.

In this paper, we wish to report the synthesis and characterization of the complexes of ruthenium(III), rhodium(III), platinum(IV), palladium(II), and platinum(II) with two potential pentadentate ligands, 2,6-dipicolinic acid hydrazide (DPH) and *N,N'*-dibenzylidene dipicolinic acid hydrazide (DBPH), involving all "hard" donor atoms. The structures of the ligands, DPH and DBPH are given in the figure.

* For correspondence at 10 Shikshak Niwas, Meerut College, Meerut-250001 (India)



Experimental

Materials: Dimethyl ester of dipicolinic acid was procured from Midland Yorkshire Tar Distillers Ltd. Co., U.K. All other chemicals and solvent used were of reagent grade.

Synthesis of ligands: The ligands, 2,6-dipicolinic acid hydrazide (DPH) and *N,N'*-dibenzylidene dipicolinic acid hydrazide (DBPH) have been synthesized by the methods given in the literature [8]. The purity of the ligands has been confirmed by TLC and elemental analysis (Table I).

Preparation and isolation of the complexes

(a) *Monochloro monodipicolinic acid hydrazide ruthenium(III) dichloride*

DPH (0.3 g) dissolved in ethanol (95%) was added to 1% ethanolic solution of ruthenium trichloride (60 ml). A yellow colour deepens on refluxing the reaction mixture (pH \sim 2.5). The mixture was digested on a water bath for half an hour when the dark brown precipitate separated out. It was filtered and washed successively with hot water and ethanol and dried at 85 °C for three hours. Yield \sim 75%.

(b) *Monodipicolinic acid hydrazide rhodium(III) trichloride*

The solution of DPH (0.3 g) in hot ethanol (200 ml) was added to an ethanolic solution (1%) of rhodium chloride (60 ml) when a cherry-red colour developed. The mixture was refluxed on a water bath and concentrated to half of its volume (pH \sim 3.0). A yellow coloured mass which separates out was filtered, washed several times with distilled water and ethanol, and dried at 85 °C. Yield \sim 70%.

c) *Monochloro monodipicolinic acid hydrazide platinum(IV) trichloride*

The clear solution of chloroplatinic acid (0.2 g) in ethanol (100 ml) containing 1 ml hydrochloric acid was treated with a solution of DPH (0.2 g) in ethanol (50%), 100 ml) at pH \sim 2.5. Immediately, a golden yellow colour appeared. The reaction mixture was refluxed on a water bath for half an hour which, after evaporation, gave fawn precipitate. It was washed with hot water, ethanol, and dried at 85 °C. Yield \sim 70%.

(d) *Monodipicolinic acid hydrazide palladium(II) dichloride*

A solution of DPH (0.2 g) in distilled water was treated with a solution of palladium chloride (0.2 g) dissolved in water (25 ml) with a trace of concentrated hydrochloric acid at pH \sim 3.5. Immediately, the mixture became canary yellow which, on stirring, gave yellow precipitate. The mixture was digested on a water bath for one hour when the colour of the precipitate changed to brown. It was filtered, washed successively with distilled water and ethanol, and dried at 80 °C. Yield \sim 85%.

(e) *Monodipicolinic acid hydrazide palladium dichloride dihydrate*

By following the procedure outlined in (a), palladium(II) chloride gave a canary yellow precipitate which was filtered and washed thoroughly with hot water and ethanol. The complex was dried in an oven at 115 °C for five hours and weighed to a constant weight. It changed its colour to dark brown and was found to contain two molecules of water of crystallization. Yield ~80%.

(f) *[Monodipicolinic acid hydrazide platinum(II) dichloride]*

Platinum (II) chloride (5 mole) in aqueous ethanolic solution (50%, 25 ml)_g was added to ethanolic solution of the DPH (5 mmole) and the pH of the reaction mixture was brought down by adding dilute hydrochloric acid (pH ~3). The reaction mixture was refluxed for an hour, concentrated to a small volume to yield yellow precipitate. It was filtered, washed with hot water and ethanol, and dried. Yield ~70%.

Same procedures were adopted for the synthesis of DBPH complexes with different metals. All these preparations were carried out in absolute ethanol or acetone. The analytical results are given in Table I.

Methods of measurements and analysis

Magnetic susceptibility was determined by the Gouy's method, using copper sulphate pentahydrate as a calibrant. Diffuse reflectance spectra were recorded on a Beckman DK-2A spectrophotometer. Infrared spectra in potassium bromide pellets were recorded on a Perkin Elmer-621 (4000–650 cm⁻¹) and in Nujol mull (650–200 cm⁻¹) smeared on a polyethylene disc on a Beckman IR-12 spectrophotometer.

The metals were determined by the methods outlined in the literature [9]. The microanalysis of carbon, hydrogen and nitrogen was performed by Microanalytical Divisions of Central Drug Research Institute, Lucknow, and Department of Chemistry, Banaras Hindu University, Varanasi (India).

Results and Discussion

Elemental analysis indicates the 1 : 1 metal-to-ligand stoichiometry for all these complexes. The complexes of palladium(II) and platinum(II) have the formula of the type $[M(L)Cl_2]_nH_2O$, where L = DPH or DBPH and $n = 0$ or 2, while ruthenium(III), rhodium(III) and platinum(IV) may be represented by $[M(L)Cl]Cl_n$, where $n = 2$ or 3. The proposed formulations are supported by infrared spectra.

Infrared spectra

The infrared spectra of the ligands have not been reported, but studies on similar compounds are available [10]. The present assignments are based on these studies.

The ligands are 2,2'-disubstituted pyridine derivatives. The vibrations generally affected [11] on pyridine-nitrogen coordination to metal ions are the four $\nu(C=C)$, $\nu(C=N)$ bands observed between 1450 and 1610 cm⁻¹, the ring-breathing mode ~990 cm⁻¹, a skeletal mode around 740 cm⁻¹ and an out-of-plane C—C deformation vibration ~410 cm⁻¹.

Table I
Analytical data

Compound	Colour	Calculated %					Found %				
		C	H	N	Cl	M	C	H	N	Cl	M
$C_7H_9N_5O_2$		43.07	4.61	35.89	—	—	43.01	4.70	35.62	—	—
$C_{21}H_{17}N_5O_2$		67.92	4.58	18.86	—	—	68.05	4.70	18.78	—	—
$[Ru(C_7H_9N_5O_2)Cl]Cl_2$	Dark brown	20.86	2.23	17.38	26.45	25.10	21.12	2.42	17.50	27.09	25.32
$[Ru(C_{21}H_{17}N_5O_2)Cl]Cl_2$	Brown	43.53	2.93	12.09	18.40	17.47	43.40	2.95	12.01	18.38	17.50
$[Rh(C_7H_9N_5O_2)Cl]Cl_2$	Yellow	20.77	2.22	17.30	26.33	25.44	20.80	2.19	17.42	26.01	25.12
$[Rh(C_{21}H_{17}N_5O_2)Cl]Cl_2$	Pale yellow	43.41	2.92	12.06	18.34	17.73	43.37	2.95	12.01	18.40	17.70
$[Pt(C_7H_9N_5O_2)SI]Cl_3$	Fawn	16.91	1.81	14.09	21.44	39.28	16.70	2.02	14.21	21.12	39.71
$[Pt(C_{21}H_{17}N_5O_2)Cl]Cl_3$	Brown	35.58	2.40	9.88	20.05	27.55	35.65	2.42	9.91	20.01	27.48
$[Pd(C_7H_9N_5O_2)]Cl_2$	Brown	22.55	2.41	18.79	19.06	28.57	22.12	2.29	18.61	18.82	28.92
$[Pd(C_7H_9N_5O_2)]Cl_2 \cdot 2 H_2O$	Canary brown	20.56	3.18	17.14	17.38	26.05	21.02	2.30	17.32	17.72	27.01
$[Pd(C_{12}H_{17}N_5O_2)]Cl_2$	Brown	45.95	3.09	12.76	12.94	19.40	46.05	3.12	12.71	13.02	19.45
$[Pt(C_7H_9N_5O_2)]Cl_2$	Yellow	18.21	1.95	15.18	15.39	42.31	18.72	1.82	15.02	15.55	42.02
$[Pt(C_{21}H_{17}N_5O_2)]Cl_2$	Yellow	39.55	2.66	10.98	11.14	30.62	39.65	2.62	11.04	11.19	30.50

The four $\nu(\text{C}=\text{C})$, $\nu(\text{C}=\text{N})$ bands are found ~ 1580 , ~ 1560 , and 1440 cm^{-1} in the spectra of the ligands. The 1580 cm^{-1} band shows an upward shift ($10\text{--}15\text{ cm}^{-1}$) in the spectra of the complexes. The ring-breathing band $\sim 990\text{ cm}^{-1}$ is replaced by a new band $\sim 1020\text{ cm}^{-1}$. Two strong bands in the spectra of the ligands 790 and 730 cm^{-1} are assigned to $\nu(\text{C}-\text{H})$ and $\nu(\text{C}-\text{C})$ vibrational modes [12], respectively. On complexation, the later band splits into two components lying between 720 and 760 cm^{-1} , while the $\sim 790\text{ cm}^{-1}$ band appears as a broad band at $800\text{--}810\text{ cm}^{-1}$. The 415 cm^{-1} band also shifts towards higher frequencies ($\sim 430\text{ cm}^{-1}$). All these changes in the vibrations of the pyridine ring indicate coordination of pyridine-nitrogen to metal atom [11, 13]. The magnitudes of "shifts", though small, are meaningful. This small "shifts" may be interpreted in terms of weak interaction between pyridine nitrogen and metal atom [14].

Amide group vibrations: An amide group can coordinate either through nitrogen or oxygen atom, depending upon the experimental conditions. The vibrations of interest in an amide group include [15] amide I band (consisting mainly of $\nu\text{C}=\text{O}$) near 1680 cm^{-1} , amide II and III bands (arising from $\nu\text{CN} + \delta\text{N}-\text{H}$) around 1520 and 1240 cm^{-1} , respectively; amide IV and VI bands near 690 and 480 cm^{-1} (originating from $\text{C}=\text{O}$ out-of-plane and $\text{C}=\text{O}$ in-plane deformation vibration modes, respectively) [16]. In the spectra of complexes, amide I band shifts to lower frequencies ($1640\text{--}1650\text{ cm}^{-1}$), while amide II band increases in frequency ($1535\text{--}1540\text{ cm}^{-1}$) and amide III band splits into two components appearing between $1200\text{--}1210$ and $1380\text{--}1388\text{ cm}^{-1}$, respectively. The position of amide IV band remains unchanged, while the amide VI band shows an upward shift. These changes in the amide group vibrations reveal the coordination of the amide-oxygen to the metal ions [15]. The various changes occurring on amide-oxygen coordination may be explained by assuming the decrease of the double bond character of $\text{C}=\text{O}$ group and the subsequent increase of the $\text{C}=\text{N}$ double bond character [17].

Hydrazinic and azomethine group vibrations: The spectrum of DPH contains sharp bands between 3000 and 3210 cm^{-1} , while two bands of medium intensity at 3200 and 3030 cm^{-1} are observed in the spectrum of DBPH. These bands may be assigned to symmetric and asymmetric NH stretching vibrations, respectively. The bands appearing 980 cm^{-1} are attributable to $\nu(\text{NH})$ vibrational modes. In addition to these bands, another two bands at 1630 and 840 cm^{-1} (in the case of DPH only) appear which may be assigned to NH deformation coupled with OCN antisymmetric vibrations and NH out-of-plane bending modes [18], respectively. In the spectra of the complexes of DPH, the bands assigned to NH stretching vibrations exhibit a downward shift and appear as a broad band between 3200 and 3030 cm^{-1} , the band at 1630 cm^{-1} disappears altogether and the NH out-of-plane bending at 840 cm^{-1} diminishes appreciably in its intensity. All these changes show coordination

Table II
Important Infrared Spectral Bands (in cm^{-1}) with Assignments

Compound	Amide I	Amide II	Amide III	Amide IV	$\nu(\text{C}=\text{N})$	16b	16a	$\nu(\text{M}-\text{py})$	$\nu(\text{M}-\text{O})$	$\nu(\text{M}-\text{N})$
DPH	1688 s	1505 s	1240 s	484 m	—	405 m	610 m	—	—	—
DBPH	1680 s	1510 s	1234 s	480 m	1642 s 1630 sh	415 s	415 m	—	—	—
$[\text{Ru}(\text{DPH})\text{Cl}]\text{Cl}_2$	1642 m	1535 s	1205 m 1385 m	500 m	—	425 m	650 m	295 m	340 m	480 m
$[\text{Ru}(\text{DBPH})\text{Cl}]\text{Cl}_2$	1640 m	1535 s	1205 m 1382 m	502 m	1625 s	430 m	657 m	292 w	340 m	478 w
$[\text{Rh}(\text{DPH})\text{Cl}]\text{Cl}_2$	1640 m	1540 m	1210 m 1380 m	500 m	—	432 m	650 m	294 w	330 w	440 m
$[\text{Rh}(\text{DBPH})\text{Cl}]\text{Cl}_2$	1645 m	1535 m	1207 m 1385 m	500 m	1625 s	435 w	650 w	295 m	328 m	438 m
$[\text{Pt}^{\text{IV}}(\text{DPH})\text{Cl}]\text{Cl}_3$	1640 m	1535 m	1200 s 1380 m	495 m	—	425 m	645 m	290 w	345 w	480 m
$[\text{Pt}^{\text{IV}}(\text{DBPH})\text{Cl}]\text{Cl}_3$	1650 m	1540 s	1205 m	495 m	1620 m	435 m	650 m	295 m	345 m	480 w
$[\text{Pd}(\text{DPH})]\text{Cl}_2$	1640 m	1535 s	1210 m 1380 s	505 m	—	425 m	648 m	270 w	330 m	455 m
$[\text{Pd}(\text{DPH})]\text{Cl}_2 \cdot 2 \text{H}_2\text{O}$	1645 m	1537 m	1200 m 1382 m	490 m	—	432 w	650 m	280 m	330 m	450 m
$[\text{Pd}(\text{DBPH})]\text{Cl}_2$	1648 s	1540 s	1200 m 1385 m	505 m	1625 s	430 m	540 w	275 m	332 m	455 m
$[\text{Pt}(\text{DPH})]\text{Cl}_2$	1650 s	1540 m	1205 m 1385 m	500 m	—	425 m	640 m	292 w	355 m	460 w
$[\text{Pt}(\text{DBPH})]\text{Cl}_2$	1645 m	535 m	1205 m 1380 m	505 w	1620 s	435 w	645 w	290 m	355 w	460 w

of the hydrazinic nitrogen to the metal atom. The changes in the various NH vibrations are a consequence of drainage of electrons from nitrogen atom, resulting in the weakening of N—H bond [19].

The spectra of DBPH show one strong band 1640 cm^{-1} with a shoulder at 1630 cm^{-1} . These two vibrations may be assigned to symmetric and asymmetric stretching vibration modes of the azomethine linkage [20] by comparing its spectra with that of the hydrazide. In the spectra of the complexes of DBPH, the 1640 cm^{-1} band shifts to lower range by $15\text{--}20\text{ cm}^{-1}$. This lowering may be taken as an indication that the azomethine nitrogen is coordinated to the metal atom. The "shifts" are small, but it is expected in view of the stronger force present in the (C=N) bond [21].

The presence of broad bands $3600\text{--}3450\text{ cm}^{-1}$ in the spectra of $[\text{Pd}(\text{DPH})\text{Cl}_2] \cdot 2\text{H}_2\text{O}$ indicate the presence of water of crystallization [21].

Far infrared spectra ($650\text{--}200\text{ cm}^{-1}$)

In the infrared region, the bands appearing at 610, 550, 415 and 280 cm^{-1} may be assigned to in-plane ring deformation, NH_2 -rocking, C—C out-of-plane deformation and C—C torsional mode [18], respectively. Some unassigned bands occur around 495, 360, 235 and 204 cm^{-1} .

New bands are observed in the far infrared spectra of the complexes. These bands appear in three regions: $270\text{--}295$, $325\text{--}345$ and $440\text{--}480\text{ cm}^{-1}$. The bands appearing at 295, 290, 275, and 290 cm^{-1} may be assigned $\nu(\text{Ru-py})$, $\nu(\text{Rh-py})$, $\nu(\text{Pt}^{\text{IV}}\text{-py})$, $\nu(\text{Pd-py})$ and $\nu(\text{Pt}^{\text{II}}\text{-py})$ vibrations [22], respectively. The bands around 340, 328, 345, 332, 335 cm^{-1} are tentatively assigned to $\nu(\text{Ru-O})$, $\nu(\text{Rh-O})$, $\nu(\text{Pt}^{\text{IV}}\text{-O})$, $\nu(\text{Pd-O})$ and $\nu(\text{Pt-O})$ vibrations, respectively. Similarly, the new bands appearing 478, 438, 480, 455 and 460 cm^{-1} may be assigned to $\nu(\text{Ru-N})$, $\nu(\text{Rh-N})$, $\nu(\text{Pt}^{\text{IV}}\text{-N})$, $\nu(\text{Pd-N})$ and $\nu(\text{Pt-N})$ vibrations, respectively. The intensity of these bands vary from medium to weak and the assignments are comparable to those reported earlier [22–24].

The values of these various metal-oxygen and metal-nitrogen stretching frequencies observed for Pd and Pt complexes are different from 4-or-6-coordinated complexes of these metal ions and are in between these two geometries. These values indicate that the complexes are penta-coordinated.

Various metal chlorine stretching frequencies are observed 302 and 315, 325 and 355, 345 and 358 cm^{-1} may be assigned to $\nu(\text{Ru-Cl})$, $\nu(\text{Rh-Cl})$ and $\nu(\text{Pt-Cl})$ frequencies.

The changes observed in the i.r. spectra of the complexes indicate that DPH and DBPH are pentadentate ligands. The coordination sites are the pyridine nitrogen, amide-oxygens and hydrazinic or azomethine nitrogen. Both the side chains are symmetrical.

Stereochemistry and far infrared spectra

GILL *et al.* [25] and CLARK *et al.* [22] have shown that the 6a (an in-plane pyridine ring deformation) and the 16b (an out-of-plane ring deformation) vibrations suffer significant shifts towards higher frequencies on coordination of pyridine to a metal atom. The magnitude of the shifts depends on the stereochemistry of the complexes and on the metal atoms, but are virtually independent of coordinated halogen atoms. Accordingly, the stereochemistry of a large number of tetra- and hexa-coordinated complexes of the first, second and third row transition metals has been established on the basis of 6a and 16b vibrations. But no such attempt appears to have been made in the case of five-coordinate complexes.

In the spectra of the ligands 6a and 16b bands appear 610 and 415 cm^{-1} , respectively. The bands observed in the spectra of the complexes are noted against each metal: ruthenium(III) (650, 425 cm^{-1}), rhodium(III) (650, 432 cm^{-1}), platinum(IV) (645, 425 cm^{-1}), palladium(II) (648, 425 cm^{-1}) and platinum(II) (640, 425 cm^{-1}). The shifts observed for 6a and 16b vibrations are comparatively small on account of weak interactions between metal atoms and pyridine nitrogen. Thus, these values are of little diagnostic value for assigning the stereochemistry of the present complexes.

Magnetic and electronic spectral studies

It has been found that, owing to the greater oxidizing power of the metal ions of the fourth and fifth transition series, the charge-transfer bands in complexes appear at much lower wave numbers [26]. In addition, the extinction coefficient of the bands in the spectra of IV and V transition series metal ions are large. Thus, it becomes difficult to make definite assignments to the bands which appear as shoulders [27].

Ruthenium(III) complexes

The magnetic moments of ruthenium complexes lie in the range 1.98—2.02 BM at room temperature (300 °K). These values are close to the spin-only value of 2.10 BM (calculated, using a value of -1180 cm^{-1} for the free ion at 300 °K) normally observed for hexa-coordinated ruthenium complexes [27]. Spin-orbit coupling plays an important role in describing the magnetic behaviour of $4d^5$ (configuration of ruthenium) complexes. The value of spin-orbit coupling constant can be calculated by the following equation [26]

$$\mu_{\text{eff.}}^2 = 3 \left(1 - \frac{2K}{10Dq} + \frac{8K^2kT}{Dq} \right)$$

Table III
Electronic spectral and magnetic data

1	Electronic spectra					Mangetic data	
	Observed bands (cm ⁻¹)	Assignment	10 <i>Dq</i> cm ⁻¹	Racah parameters (cm ⁻¹)		μ_{eff} BM	λ cm ⁻¹
				5	6		
2	3	4	5	6	7	8	
[Ru(DPH)Cl]Cl ₂	17 200 21 700 25 900 32 800	² T _{2i} → ² A _{2g} → ² E _g → ² A _{1g} π → t _{2g} (π*)	32 993	<i>B</i> = 643 <i>C</i> = 2154	0.00	1.98	−1230
[Ru(DBPH)Cl]Cl ₂	17 000, 21 500, 25 500 & 32 500	−Do−	32 946	<i>B</i> = 646 <i>C</i> = 2108		2.02	−1460
[Rh(DPH)Cl]Cl ₂	12 500 17 480 20 500 27 000 33 000	¹ A _{1g} → ³ T _{1g} → ³ T _{2g} → ¹ T _{1g} → ¹ T _{2g} Charge-transfer	24 500	<i>B</i> = 406 <i>C</i> = 4000	0.56	Diamag.	—
[Rh(DBPH)]Cl ₂	12 500, 18 200, 20 450, 26 800,, & 33 550	−Do−	24 425	<i>B</i> = 397 <i>C</i> = 3975	0.55	Diamag.	—
[Pt ^{IV} (DPH)Cl]Cl ₃	20 000 27 000 36 500 40 200	¹ A _{1i} → ³ T _{1g} → ¹ T _{1g} → ¹ T _{2g} Charge-Transfer	31 250	<i>B</i> = 563 <i>C</i> = 3750	0.78	Diamag.	—
[Pt(DBPH)Cl]Cl ₃	20 700, 28 000, 36 700 & 40 000	−Do−	31 610	<i>B</i> = 544 <i>C</i> = 3650	0.75	Diamag.	—
[Pd(DPH)]Cl ₂	17 200 26 300 27 700 3 4400 40 300	¹ A ₁ → ¹ B ₁ → ¹ E ₁ → ¹ A ₂ Charge-transfer	—	—	—	Diamag.	—
[Pd(DPH)Cl ₂ · 2 H ₂ O]	20 500, 26 000, 27 900, 35 000, & 41 000	−Do−	—	—	—	Diamag.	—
[Pd(DBPH)]Cl ₂	21 000, 26 200, 27 000, 34 500 & 40 000	−Do−	—	—	—	Diamag.	—
[Pt(DPH)]Cl ₂	24 000 28 200 30 500 34 000 39 500	¹ A ₁ → ¹ B ₁ → ¹ E ₁ → ¹ A ₂ Charge-transfer	—	—	—	Diamag.	—
[Pt(DBPH)]Cl ₂	24 000, 28 500, 30 500, 34 500, & 39 500	−Do−	—	—	—	Diamag.	—

as applicable for ${}^2T_{2g}$ term for the low-symmetry molecules and neglecting the last term $\frac{8K^2kT}{Dq}$. The values of spin-orbit coupling constant are in the range suggested [27] for pseudo-octahedral ruthenium(III) complexes and suggest distortion along one of the axes of the octahedron [26].

Four well defined bands are observed in the electronic spectra of these complexes. The bands are observed in the regions 17 000, 21 700, 25 900 and 32 500 cm^{-1} , and may be assigned to ${}^2T_{2g} \rightarrow {}^2A_{2g}$, ${}^2T_{2g} \rightarrow {}^2E_g$, ${}^2T_{2g} \rightarrow {}^2A_{1g}$ and $\pi \rightarrow t_{2g}(\pi^*)$, respectively, in an octahedral field [28]. The hexa-coordinated nature of the ruthenium complexes is revealed by the far infrared spectra which show characteristic band [28] of $\nu(\text{Ru-Cl})$ around 315 cm^{-1} . The values of ligand field and Racah interelectronic parameters have been calculated by methods suggested in the literature [30,31] and are given in Table III.

Platinum(IV) complexes

The platinum(IV) complexes are hexa-coordinated. The hexa-coordinated nature of platinum(IV) complexes is revealed by far infrared spectra which contain band at 345 cm^{-1} assignable to $\nu(\text{Pt}^{\text{IV}}\text{-Cl})$ vibrations. The complexes are diamagnetic as expected.

The platinum(IV) complexes show bands 20 000, 27 500, 36 500 and 40 200 cm^{-1} . The first three bands may be assigned [28] to ${}^1A_{1g} \rightarrow {}^3T_{1g}$, ${}^1A_{1g} \rightarrow {}^1T_{1g}$ and ${}^1A_{1g} \rightarrow {}^1T_{2g}$, in the order of increasing energy. The band $\sim 40\,200\text{ cm}^{-1}$ appears to have its origin in charge-transfer phenomenon [27].

The values of ligand field splitting energy ($10Dq$) and Racah interelectronic repulsion parameters have been evaluated, using the equations [30], applicable to low-spin complexes of d^6 systems. The values of $10Dq$, B and C are given in Table III and they are consistent [31] with the pseudooctahedral geometry of the platinum(IV) complexes.

Rhodium(III) complexes

The magnetic measurements of the rhodium complexes at room temperature show that they are diamagnetic. The rhodium complexes are hexa-coordinated. The five donors are provided by the ligands DPH and DBPH and the sixth ligand is Cl as revealed by far infrared spectra which contain a band 325 cm^{-1} assignable to $\nu(\text{Rh-Cl})$ vibrations [24].

Rhodium(III) is a d^6 system like cobalt(III). However, relative to cobalt(III) the crystal field bands of rhodium(III) move to higher energies, whilst the ligand-to-metal charge-transfer bands move to lower energies [30]. In the spectra of rhodium complexes five bands are observed in the regions 12 500, 20 000, 27 000 and 33 000 cm^{-1} . The bands are very distinct, and first

two bands appear as shoulders. The first four bands may be assigned [30] to ${}^1A_{1g} \rightarrow {}^1T_{1g}$, ${}^1A_{1g} \rightarrow {}^3T_{2g}$, ${}^1A_{1g} \rightarrow {}^1T_{1g}$ and ${}^1A_{1g} \rightarrow {}^1T_{2g}$ in the order of increasing energy. The 33 000 band is probably due to ligand-to-metal charge-transfer [27].

The values of various ligand field and nephelauxtic parameters have been calculated, using the equations suggested by LEVER [30] for d^6 spin-paired systems. The values of these parameters are given in Table III.

Palladium(II) and platinum(II) complexes

The magnetic measurements of palladium and platinum complexes reveal the diamagnetic nature of the complexes. These two metal ions have d^8 electronic configuration, but unlike nickel(II), they form diamagnetic complexes both with "hard" and "soft" donor atoms. Thus, the magnetic properties of these metal ions do not help in the assignments of the stereochemistry of their complexes and to ascertain their coordination number.

The electronic spectra have been of specific use in establishing the stereochemistry of such complexes. The electronic spectra of palladium complexes contain bands in the regions 20 500, 26 300, 27 700, 34 400 and 40 300 cm^{-1} . These bands resemble those of tetra-coordinated square planar complexes of palladium(II). But the presence of a well defined band 20 500 cm^{-1} is puzzling. Penta-coordinated palladium(II) complexes show [5] a characteristic band around 20 500 cm^{-1} . Similarly, platinum complexes show bands 24 000, 28 000, 31 000, 34 000 and 39 500 cm^{-1} . The 24 000 band is characteristic of penta-coordinated platinum(II) complexes [6]. Thus, it appears that palladium and platinum complexes are penta-coordinated.

The molecular models of the complexes were constructed which showed that the square-pyramidal structure is the most likely structure to result when the two amide-oxygens and two hydrazinic-nitrogens form the basal plane, with pyridine-nitrogen being present on the Z-axis. Thus, a square pyramidal geometry may be assumed for these complexes. The electronic absorption and circular dichroism spectra of square-pyramidal complexes have been reported [32] and various assignments can be made, assuming the energy level sequence as $d_{xy} < d_{x^2}, d_{y^2} < d_{z^2} < d_{x^2-y^2}$. Accordingly, various assignments can be made as ${}^1A_1 \rightarrow {}^1B_1$ (20 500, 24 000 cm^{-1}), ($d_{z^2} \rightarrow d_{x^2-y^2}$), ${}^1A_1 \rightarrow {}^1E$ (26 300, 28 000 cm^{-1}), ($d_x, d_{y^2} \rightarrow d_{x^2-y^2}$) and ${}^1A_1 \rightarrow {}^1A_2$ (27 700, 31 000 cm^{-1}), ($d_{xy} \rightarrow d_{x^2-y^2}$) for palladium and platinum complexes, respectively assuming the effective symmetry to be C_{4v} . The calculation of ligand field parameters can not be attempted in the absence of energy level equation.

*

The authors are thankful to CSIR and UGC, New Delhi, for financial assistance. Thanks are due to RSIC, IIT, Madras, for spectral measurements. The gift sample of dimethylester of dipicolinic acid by Midland Yorkshire Tar Distiller Ltd., U.K. is gratefully acknowledged.

REFERENCES

- [1] WOOD, J. S.: *Progr. Inorg. Chem.*, **16**, 227 (1972)
- [2] MUETTERTIES, E. L., SCHUNN, R. A.: *Quart. Revs. (London)*, **20**, 245 (1976)
- [3] FURLANI, C.: *Coord. Chem. Revs.*, **3**, 141 (1968); MORASSI, R., BERTINI, I., SACCONI, L.: *Coord. Chem. Revs.*, **11**, 351 (1973)
- [4] VENANZI, L. M.: *Angew. Chem.*, **76** 621 (1964); *Angew. Chem., Internat. Edn.*, **3**, 453 (1964)
- [5] DYER, G., VENANZI, L. M.: *J. Chem. Soc.*, **1965**, 2771
- [6] HEADLEY, O. St. C., NYHOLM, R. S., McAULIFFE, C. A., SINDELLAN, L., TOBE, M. L., VENANZI, L. M.: *Inorg. Chim. Acta*, **4** 93 (1970)
- [7] GRAY, H. B., PREER, J. R.: *J. Am. Chem. Soc.*, **92**, 7306 (1970)
- [8] EFIMOVSKY, O., RUMPF, P.: *C. A.*, **48**, 10 746b (1954); TERONOBUE, U., TOKUHIKO, S., HONDE, I.: *C. A.*, **72**, 121985V (1970)
- [9] BEAMISH, F. E.: "The Analytical Chemistry of the Noble Metals", Vol. **24**, Pergamon Press, Oxford, 1966, 252, 269
- [10] NONOYAMA, N., TOMOMOTO, Y., YAMASAKI, K.: *Nippon Kagaku Zasshi*, **93**, 562 (1972)
- [11] BALDWIN, D. A., LEVER, A. B. P., PARISH, R. V.: *Inorg. Chem.*, **8**, 107 (1969)
- [12] GREEN, J. H. S., KYNASTAN, W., PAISELY, H. M.: *Spectrochim. Acta*, **19**, 549 (1963); SINHA, S. P.: *Spectrochim. Acta*, **20**, 879 (1964)
- [13] GILL, N. S., KINGDOM, H. J.: *Aust. J. Chem.*, **19**, 2197 (1966)
- [14] KEETON, M., LEVER, A. B. P.: *Inorg. Chem.*, **10**, 47 (1971); KEETON, M., LEVER, A. B. P., RAMASWAMY, B. S.: *Can. J. Chem.*, **48**, 3185 (1970)
- [15] NONOYAMA, M., YAMASAKI, K.: *Inorg. Chim. Acta*, **3**, 385 (1969); MYAZAWA, T., SHIMANOUCHI, T., MIZUSHIMA, S.: *J. Chem. Phys.*, **29**, 611 (1958)
- [16] NONOYAMA, M., TOMITA, S., YAMASAKI, K.: *Inorg. Chim. Acta*, **12**, 33 (1975); JAIN, S. C., GILL, M. S., RAO, G. S.: *J. Indian Chem. Soc.*, **53**, 537 (1976)
- [17] DRAGO, R. S.: "Physical Methods in Inorganic Chemistry", (East-West Affiliated Press, New Delhi) 230 (1968) 30
- [18] SEKIZAKI, M., YAMASAKI, K.: *Spectrochim. Acta*, **25A** 475 (1969)
- [19] SVATOS, G. F., CURRAN, C., QUAGLIANO, J. V.: *J. Am. Chem. Soc.*, **77**, 6159 (1955)
- [20] SPENCER, C. T., TAYLOR, L. T.: *Inorg. Chem.*, **10**, 2407 (1970)
- [21] SHARMA, B. D., BAILAR, J. C., Jr.: *J. Am. Chem. Soc.*, **77**, 5476 (1955)
- [22] CLARK, R. J. H., WILLIAMS, C. S.: *Inorg. Chem.*, **4**, 350 (1965)
- [23] MIKAMI, M., NAKAGAWA, I., SHIMANOUCHI, T.: *Spectrochim. Acta*, **23A**, 1037 (1967)
- [24] ADAMS, D. M.: "Metal-ligand and Related Vibrations" (E. Arnold, London), 1967
- [24b] NAKAMOTO, K.: *Infrared Spectra of Inorganic and Coordination Compounds*, Wiley-Interscience, New York, 216 (1970)
- [25] GILL, N. S., NUTTALL, R. H., SCAIFE, D. F., SHARP, D. W. A.: *J. Inorg. Nucl. Chem.*, **18**, 79 (1961)
- [26] FIGGIS, B. N.: "Introduction to Ligand Field Theory" (Interscience Publishers Inc., New York, 1966)
- [27] DWIVEDI, J. S., AGARWALA, U.: *Indian J. Chem.*, **10**, 657 (1972)
- [28] KEY, D. L., LARKWORTHY, L. F., SALMON, J. E.: *J. Chem. Soc.*, (A), **1971**, 371, 2583
- [29] SWIHART, D. L., MASON, W. R.: *Inorg. Chem.*, **9**, 1749 (1970)
- [30] LEVER, A. B. P.: "Inorganic Electronic Spectroscopy", Elsevier (Amsterdam) 303 (1968)
- [31] RASTOGI, D. K., SRIVASTAVA, A. K., JAIN, P. C., AGARWAL, B. R.: *J. Less-Common Metals*, **24**, 383 (1971)
- [32] BOSNICH, B., JACKSON, W. G., LO, S. J. D.: *Inorg. Chem.*, **14**, 2998 (1975)

V. B. RANA

S. K. SAHNI

S. K. SANGAL

Chemistry Department Meerut-College, Meerut-250001, India

RECENSIONES

Lecture Notes in Chemistry, Vol. 8

E. E. NIKITIN and L. ZÜLICHE: *Theory of Chemical Elementary Processes*

Springer-Verlag, Berlin, Heidelberg, New York (175 pp)

During the last decade quantum chemistry has made an impressive progress in the quantitative interpretation of the electronic structures of atoms, molecules and ions. The quantitative treatment of these stationary systems is, however, much less problematic than to apply quantum chemistry to processes in which electronic structure and nuclear motions rapidly change in time. Reaction kinetics, discussed in this volume, belongs to the latter group. Nevertheless, despite the difficulties emerging, several research groups deal with the rigorous theoretical interpretation of chemical reactions. Fortunately enough, a number of experimental methods, primarily the method of Molecular Beam Spectroscopy, may be of help in understanding reaction mechanisms and testing theoretical results.

NIKITIN and ZÜLICHE are concerned with the theory of gas phase reactions. In the first chapter of the volume the authors discuss classical and quantum chemical models with such eloquence that even for those unfamiliar with the authors' activities and reputation it becomes clear that the knowledge of the authors is far beyond the level of the present treatment. The chapters discussing approximate methods are somewhat more difficult to read. It is also stressed by the authors that for the full understanding of these chapters the original papers given in the references should be consulted.

In accord with the title of the volume, but perhaps not quite properly, the experimental methods do not receive an attention deserved by their great importance.

In my opinion, the book is hard to understand for those completely unfamiliar with the fundamentals of quantum chemistry and the theory of vibrational and rotational spectra. Those, however, with sufficient theoretical background, receive a very clearly compiled review of the present state of reaction theory.

F. TÖRÖK

Dynamic NMR Spectroscopy: Alois STEIGEL, Mechanistic Studies of Rearrangements and Exchange Reactions by Dynamic NMR Spectroscopy; Hans Wolfgang SPIESS, Rotation of Molecules and Nuclear Spin Relaxation

NMR Basic Principles and Progress, Vol. 15

(P. DIEHL, E. FLUCK and R. KOSFELD, Eds)

Springer-Verlag, Berlin, Heidelberg, New York, 1978, 214 pp.

Historically, dynamic NMR (DNMR) spectroscopy encompasses two major fields of research activity: chemical studies based on NMR band shape phenomena in liquids under steady state conditions and physical studies of the motion of spins in liquids and solids through measurements of the nuclear relaxation times. Recent developments of NMR instrumentation and theories, however, have rendered such a clear distinction between the two groups of studies somewhat arbitrary. Theories now allow for the extraction of detailed relaxation information from band shapes of multispin NMR spectra, while Fourier transform NMR relaxation spectroscopy may provide detailed motional description of fairly complex molecules including the dynamical parameters for internal motions of individual groups.

In the present volume, two specific topics of DNMR are dealt with. The first part (56 pp.), written by A. STEIGEL, is devoted to the uses of modern band shape analyses to obtain mechanistic informations on rearrangements and dynamical exchange processes. After introductory remarks (chapter 1), the author outlines the basic experimental requirements and general mathematical procedures (chapter 2). The formulation of the exchange problem in terms of a kinetic exchange matrix (chapter 3) is illustrated by two classical DNMR studies (chapter 4) to show that dissimilar kinetic matrices are a necessary but not sufficient precondition for a clear-cut difference in DNMR behaviour. Another classical DNMR approach, the use of prochiral CH_2Y -groups as mechanistic probes is dealt with in chapter 5 and illustrated by examples taken from recent literature. Permutational approach to polytopal rearrangements (i.e. rearrangements proceeding *via* intermediates whose spatial arrangements can be described in forms of idealized polyhedra) is presented in chapter 6 and comparison of the known methods of analysis for NMR-differentiable permutational isomerization reactions is made on the basis of literature examples. Description of the chemical-shift-based band shape analysis is completed with a brief account on split modes of rearrangement (chapter 7) using examples from spirocyclic phosphoranes. Mechanistic analyses of exchanging systems in which spin-spin couplings are used as a tool are dealt with in chapters 8 (first-order spin systems) and 9 (non-first-order-spin systems) to be followed by a brief outline of the mechanistic analysis of intermolecular exchange reactions (chapter 10). The presentation of the entire material is extremely clear and well-balanced and the reader interested in mechanistic studies will certainly find a number of stimulating new ideas for his own research. The bibliography contains 76 references and includes citations of earlier review articles and monographs.

The second part of this volume (150 pp.), compiled by H. W. SPIESS, presents the theoretical background necessary to obtain information about the types and rates of molecular rotations in solids and nonviscous liquids through analysis of the NMR line shapes in solids and nuclear spin relaxation times in solids and liquids. Introduction (chapter 1) and formulation of nuclear spin Hamilton operators (chapter 2) are followed by calculations of the NMR spectra of solids (chapter 3) for the cases of various types of interactions: chemical shift anisotropy, spin-rotation, quadrupole, dipolar and scalar couplings. Attention is focussed on the anisotropic part of the spin Hamiltonian providing dynamic informations about molecular motions. Chapter 4 is of particular interest. Here a detailed description is given of how to calculate NMR line shapes for slow rotational jump motions in solids, and a uniform derivation of the spin relaxation rates in liquids for all the internuclear couplings, and completely anisotropic rotation of the molecules in liquids using irreducible tensor calculus. The derivation of relaxation rates closely follows Abragam's treatment for, as the author points out, it provides explicit formulas directly applicable to the analyses of relaxation data. For such analyses, the coupling constants of the respective relaxation mechanisms have to be known. The theory and experimental determinations of the various coupling tensors are discussed in chapter 5, with particular emphasis on anisotropic couplings derivable from solid state measurements. Representative experimental examples illustrating the applications of the theory given in preceding chapters are discussed in chapter 6, which is followed by a series of appendices (chapter 7) devoted to some of the fundamental mathematical relationships. The references contain some 300 citations covering the fundamental works, monographs as well as original papers up to mid-1976.

Among the merits of this report one should point out the uniformness of presentation, the highly practical approach of the author in discussing the interrelations between theory and experiments. This work may be recommended both as a good introduction to the field of nuclear relaxations and as a comprehensive reference book for readers interested in molecular motions.

L. RADICS

Topics in Current Chemistry, Volume 76

(Managing Editor: F. L. BOSCHKE)

Aspects of Molybdenum and Related Compounds

by G. A. TSIGDINOS and G. MOH

Springer-Verlag, Berlin, Heidelberg, New York, 1978 159 pp with 71 figures

The book consists of three nearly independent reviews:

- 1) G. A. TSIGDINOS: "Heteropoly Compounds of Molybdenum and Tungsten" (pages 1—64; with 275 references)

2) G. A. TSIGDINOS: "Inorganic Sulfur Compounds of Molybdenum and Tungsten (Their Preparation, Structure and Properties)" (pages 66—105; with 228 references)

3) G. MON: "High-Temperature Metal Sulfide Chemistry" (pages 107—159; with 261 references).

In spite of the titles, the most important and sometimes the only element discussed is molybdenum.

The three reviews are good examples how different such summaries could be: the first one is a general, well understandable, "professional" work (with its mistakes, too); the second one deals with a more special field but deeper; the third one is a survey about the results of a very special technique on a very special field.

The more detailed references about the book are as follows.

The first part entitled as "Heteropoly compounds of molybdenum and tungsten" summarizes the classification and nomenclature principles, typical properties of heteropoly anions; gives a short survey on preparations and structures in solid and solution phases. (All of these take only 18 pages but the most important — not always the newest — informations are given.)

The short reviews about preparations, structures chemical and physical properties of different polyanions, as those of the 12- (both series A and B), 11-, 10-, 9-, 6- (again both series) and dimeric 9- and other (sometimes mixed) heteropoly anions are collected in the next chapters of this part, which closes with some rather short summaries on general properties of heteropoly compound. This part is not complete at all excepting the last chapter about uses in practice.

It is easy to read and understand this review — but several mistakes and misprints can be found. As an example: the most disturbing mistake is made about $R_2AsMo_4O_4(OH)^{2-}$, which is a 1 : 4 heteropoly anion in reality, in the original paper and on p. 52, but in an incorrect form the representative of 1 : 1 heteroanions in Table 2 (and in the legend of Fig. 25).

The second review deals with the inorganic sulfur compounds of molybdenum and tungsten, but very typical is that *e.g.* the first main chapter on sulfides (altogether 15.5 pages: nearly 40% of the whole part) contains 10 pages about MoS_2 and only six lines about the sulfides of tungsten. The other topics are: oxysulfides, thiohalides, thiomolybdates, reaction products of molybdenum compounds with H_2S/H_2 , thiomolybdates and thiotungstates.

This review differs from the first one by its style, too: more recent data are summarized for a definite aim. So it is understandable that the MoS_2 , its lubricating and catalytic properties as well as the catalytic effects of other Mo—S compounds in hydrodesulfurization processes are emphasized.

In the third part which has a very general title: "High-temperature metal sulfide chemistry", the most important chapter is a very short one about the experimental procedures, as all results summarized in the next chapters could only be reached by a special, new and very effective method, by the so-called "tube-in-tube-in-tube" procedure.

In a chapter binary systems, the Cr—S, Mo—S and W—S systems are discussed; in that about ternary systems the systems containing Fe or Cu beside the three mentioned metals (and sulfur); and in the third one about the quaternary systems, the Fe—Cu—Mo—S, Fe—Cu—W—S systems and Zn—Mo—W—S phase equilibria (some of them even up to 2000 °C).

The author tries to refer to all recent results of this very special field with the highest expertness and precision.

The 76th Volume of "Topics in Current Chemistry" ("Aspects of Molybdenum and Related Chemistry") contains three review papers of very different styles but on rather high level corresponding to their own objects.

The first part summarizes data of nearly general interest for inorganic chemistry; the second part is less general but interesting for several specialists;

the third summary is very special but could be extremely interesting for a few people, first of all for researchers in geochemistry.

L. BARCZA

INDEX

ANALYTICAL CHEMISTRY

Separation and Determination of Radioactive Iodine Isotopes Based on Isotope- and Ion-Exchange, O. GIMESI, É. BÁNYAI	309
Spectrochemical Investigation of Volatile Components Released in Thermochemical Processes, II. Cadmium and Mercuric Salts, E. GEGUS, J. KREITER, L. MÉRAY, J. INCZÉDY	347

PHYSICAL AND INORGANIC CHEMISTRY

Synthetic Linear Polymers, XXXIV. Change of Specific Properties of Dimethylsiloxane Co-Oligomers as a Function of the Chemical Composition and Size of the Molecule, I. GÉCZY	327
Investigation of the Molecular Structure of Phenol Ethers by Quantum Chemical Methods, I. Experimental Data and Calculation Method, P. HENCSEI, J. NAGY	359
Investigation of the Molecular Structure of Phenol Ethers by Quantum Chemical Methods, II. Results and Discussion, P. HENCSEI, G. PONGOR, J. NAGY	367
Photocatalytic Methods, II. Photo-Oxidation of Safranin T in the Presence of Iron(III), A. PÉTER, L. J. CSÁNYI	379
Photocatalytic Systems, XVII. Spin-trapping of Radicals in the Photolysis of Cer(IV) in Alcohols, D. REHOREK (in German)	395
Penta and Hexa-coordinated Complexes of Platinum Metals of Potential Pentadentate Ligands, V. B. RANA, S. K. SAHNI, S. K. SANGAL	405

ORGANIC CHEMISTRY

Synthesis of 6-Aza-B-homo-19-norcholesta-1,3,5 (10)-trien-7-one and its 1-Methyl Derivative, SHAFIULLAH, ISLAMUDDIN	319
Synthesis of ³ H-Labelled 2-Deoxy-D-ribose and its Derivatives (Short Communication) G. ZÓLYOMI, D. BÁNFI, J. KUSZMANN	323
Synthesis of Vinca Alkaloids and Related Compounds, XI. Acrylonitrile Adducts as Intermediates, GY. KALAUS, L. SZABÓ, P. GYÓRY, É. SZENTIRMAY, Cs. SZÁNTAY	387
RECENSIONES	417

Printed in Hungary

A kiadásért felel az Akadémiai Kiadó igazgatója.

Műszaki szerkesztő: Zacsik Annamária

A kézirat nyomdába érkezett: 1979. III. 19. — Terjedelem: 10,15 (A/5) ív, 51 ábra

79.6977 Akadémiai Nyomda, Budapest — Felelős vezető: Bernát György

Kremmer, Tibor — Boross, László:

GEL CHROMATOGRAPHY

The authors give a general and detailed description on the origin, character and utilization of gels. The book is divided into three parts: 1) Theory; 2) Methods and Techniques; 3) Applications of Gel Chromatography. A detailed subject index and a bibliography complete the work. The diagrams, tables and connexion schemes given may be of great help in numerical calculations and in the everyday work of specialists.

In English — Approx. 290 pages — 338 figures — Cloth — ISBN 963 05 1738 8

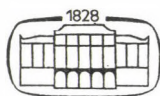
AKADÉMIAI KIADÓ, Budapest JOHN WILEY AND SONS LTD, Chichester

Gánti, Tibor:

A THEORY OF BIOCHEMICAL SUPER-SYSTEMS. Its application to problems of natural and artificial biogenesis

The *chemoton theory* represents a conceptionally new approach to the deduction of the simplest physical—chemical, macromolecular super-systems satisfying those criteria of life which have been reformulated by the author almost axiomatically, in a more exact presentation than commonly known from the literature. The prospects of the further development of the theory are promising, because the principles of the chemoton model are simple and clear, making the deduction of many basic biological phenomena possible already in its present form, and offering a feasible explanation for the origin of living systems from which the outlines of the strategy for the artificial synthesis of living systems also emerge.

In English — Approx. 80 pages — 17×25 cm — ISBN 963 05 1719 1 — Cloth



AKADÉMIAI KIADÓ, Budapest
Publishing House of the Hungarian Academy of Sciences

РЕЗЮМЕ

Изотопное и Ионо-обменное разделение и определение радиоактивных изотопов иода

О. ГИМЕШИ и Е. БАНЬАИ

Был разработан метод изотопного и ионо-обменного определения радиоактивного иода, используя технику экстракции. Оптимальные экспериментальные условия были определены с помощью ступенчатого метода (порционная экстракция), на основе которых был сконструирован аппарат непрерывного измерения по принципу Автоанализатора.

Синтез 6-аза-В-гомо-19-норхолеста-1,3,5(10)-триен-7-она и его 1-метильных производных

ШАФИУЛАХ и ИСЛАМУДДИН

Реакция Шмидта для 19-норхолеста-1,3,5(10)-триен-6-она (1) или бэкмановская перегруппировка соответствующего оксима (3) дают 6-аза-В-гомо-19-норхолеста-1,3,5(10)-триен-7-он (5). Подобным образом 1-метил-19-норхолеста-1,3,5(10)-триен-6-он (2) в реакции Шмидта и его оксим (4) в бэкмановской перегруппировке дают 6-аза-В-гомо-1-метил-10-норхолеста-1,3,5(10)-триен-7-он (8). В соответствии с исключительным образованием 6-аза-лактамов 5 и 8 из оксимов 3 и 4, полагается, что конформация в этих оксимах является *анти* по отношению к кольцу А

Синтез 2-деокси-Д-рибозы и ее производных, меченных H^3

Г. ЗОЙОМИ, Д. БАНФИ и Й. КУСМАН

Описывается синтез 2-деокси-(2- H^3)-Д-рибозы (5), исходя из 3,4-ди-О-ацетил-Д-рибала (1), а также синтез 2-деокси-ди-(2,2- H^3)-Д-рибозы (10) обработкой 2-деокси-Д-рибозы T_2O в щелочных условиях. Стабильность меченности различных производных была исследована повторной перекристаллизацией из этанола.

Синтетические линейные полимеры, XXXIV

Изменение удельных свойств сополимеров диметилсилоксана в зависимости от состава и размера молекул

Й. ГЕЦИ

Удельный объем, удельный паракор и — в одном случае — коэффициент рефракции сополимеров диметилсилоксана, содержащих группы метилперфторопропилбутиросилоксана, циклопентилсилоксана и метил- β -цианэтилсилоксана, были исследованы в зависимости от состава, а также обратной величины молекулярного веса. Эти свойства, изобра-

женные в зависимости от обратной величины молекулярного веса, — подобно ранее полученным результатам с моноалкил- и *n*-алкилфенилполи(этиленоксидом) — дают прямую, отрезок на оси ординат которой является характерным для повторяющегося звена, а наклон пропорционален парциальной степени полимеризации другого повторяющегося звена.

Сравнивались величины, полученные из изменения наклонов в зависимости от изменения состава, с величинами, рассчитанными на основе ранее выведенных уравнений. Из исследований видно, что удельные свойства могут приобретать лишь значения, находящиеся в треугольнике, ограниченном точками φ_k , φ_k , φ_v . На примерах демонстрируется, как может быть оценен на основе полученных результатов порядок удельных данных, отсутствующих на данном этапе, а также как может быть проверена точность уже имеющихся данных.

Спектрохимическое исследование летучих компонентов в термохимических процессах, II

Экспериментальные результаты некоторых систем и их обсуждение

Е. ГЕГУШ, Й. КРЕЙТЕР, Л. МЕРЕИ и Й. ИНЦЕДИ

С помощью установки, описанной в первой части цикла сообщений, были подробно исследованы термические процессы солей кадмия (хлорида, нитрата, сульфата и оксида) вплоть до температуры 1200°C, записывая сигнал кадмия в паровой фазе. Исходя из характеристических температур превращений, определенных при знании функций время-температура, можно делать заключения относительно хода некоторых процессов (восстановления, окисления, терморазложения, испарения и т. д.). Термическое поведение ртутных солей (хлорида, ниграта, сульфата и оксида) было исследовано при медленном нагреве вплоть до температуры 750°C. Упоминаются также опыты других термических процессов (испарение BeCl_2 , выделение летучих соединений фтора).

Основываясь на результатах экспериментов, утверждали, что значительные расхождения имеют место между процессами, протекающими в платиновых и графитных тиглях соответственно, и качество поверхности и условия графитных тиглей значительно влияют на процессы окисления-восстановления, разложения и испарения. Разработанная установка пригодна для детального исследования дальнейших термохимических процессов.

Исследование молекулярной структуры фенольных эфиров с помощью квантово-химических методов, I

Экспериментальные данные и методы расчета

П. ХЕНЧЕИ и Й. НАДЬ

Приводятся экспериментальные физико-химические данные (УФ спектры, дипольные моменты, потенциалы ионизации, химические сдвиги ^{13}C) фенольных эфиров с основной формулой $\text{XC}_6\text{H}_4\text{OCH}_3$ (где $\text{X} = \text{H}$, *o*-, *m*-, *p*- CH_3 , CH_3O , Cl , NO_2 , F , NH_2) и исходные параметры для различных методов расчета (Дэль Рэ, итерационного ППП, расширенного Хюккеля).

Исследование молекулярного строения эфиров фенолов с помощью квантово-химических методов, II

Результаты и их обсуждение

П. ХЕНЧЕИ, Г. ПОНГОР и Й. НАДЬ

Экспериментальные физико-химические данные — электронные переходы, дипольные моменты, энергии ионизации, химические сигналы C^{13} — эфиров фенолов и общей формулой $\text{XC}_6\text{H}_4\text{OCH}_3$ (где $\text{X} = \text{H}$, *o*-, *m*-, *p*- CH_3 , CH_3O , Cl , NO_2 , F , NH_2) были интерпретированы с

помощью квантово-химических расчетов. Для расчетов были использованы методы Дель Рэ, итеративный ППП и ЭХТ. Для определения параметров ИШШ были разработаны новые зависимости. Расчеты проводились на плоской модели и полагались на плоской модели и полагалось свободное вращение метоксигруппы. Исходя из корреляций между экспериментальными и расчетными данными делались заключения относительно молекулярного строения.

Фотокаталитические методы, II

Фотоокисление сафранина Т в присутствии железа(III)

А. ПЕТЕР и Л. Й. ЧАНИ

Наблюдалось фотоокисление сафранина Т при УФ облучении раствора красителя, содержащего ионы сенсибилизатора железа(III). Обсуждаются вероятные ступени окисления, а также зависимость обесцвечивания от экспериментальных условий.

Синтез алкалоидов Винка и их аналогов, XI

Аддукты акрилонитрила как промежуточные продукты

Д. КАЛАУШ, Л. САБО, П. ДЬЁРИ, Е. СЕНТИРМАИ и Ч. САНТАИ

Восстановление аддукта, образующегося между энамином типа 2а и акрилонитрилом, дает производные 4а и 5а, которые в сернокислом растворе метанола, наряду с превращением в эфир, претерпевают эполимеризацию. В щелочной среде превращения протекают по пути 4а → 4б → 4с и 5а → 5б → 5с.

Фотокаталитические системы, XVII

Спиновые ловушки радикалов при фотолизе Се(IV) в спиртах

Д. РЕХОРЕК

Применяя нитрозодурол и фенил-N-трет.-бутилнитрон в качестве спиновых ловушек, были детектированы и идентифицированы радикалы, образующиеся при фотолиз Се(IV) в спиртах. При комнатной температуре наблюдались как алкоксильные, так и алкильные и гидроксильные радикалы, что указывает на реакции первичных алкоксильных радикалов.

Пяти- и шестикоординированные комплексы платиновых металлов потенциальными пентадентатными лигандами

В. Б. РАНА, С. К. САХНИ и ШАНГАЛ

Были синтезированы и охарактеризованы комплексы рутения(III), родия(III), платины(IV), палладия(II) и платины(II) с двумя потенциальными пентадентатными лигандами: гидразидом 2,6-дипикколиновой кислоты и гидразидом N, N'-добензилиден-дипикколиновой кислоты. Комплексы рутения(III), родия(III) и платины(IV) имеют координационное число, равное 6, а комплексы двухвалентных палладия и платины являются пятикоординированными, что было найдено, исходя из данных их элементного анализа, измерений магнитной восприимчивости, УФ-видимых и ИК (обычных и далеких ИК) спектров. Характерные параметры лигандного поля были определены там, где это возможно. В далекой ИК области были отнесены колебания $\nu_{(M-ру)}$, $\nu_{(M-O)}$ и $\nu_{(M-N)}$, а также были сделаны попытки определения стереохимии комплексов на основе колебаний 6а и 16б пиридинового кольца.



Les Acta Chimica paraissent en français, allemand, anglais et russe et publient des mémoires du domaine des sciences chimiques.

Les Acta Chimica sont publiés sous forme de fascicules. Quatre fascicules seront réunis en un volume (4 volumes par an).

On est prié d'envoyer les manuscrits destinés à la rédaction à l'adresse suivante:

Acta Chimica

Budapest, P.O. Box 67, H-1450, Hongrie

Toute correspondance doit être envoyée à cette même adresse.

La rédaction ne rend pas de manuscrit.

Le prix de l'abonnement: \$36,00 par volume.

Abonnement en Hongrie à l'Akadémiai Kiadó (1363 Budapest, P.O.B. 24, C. C. B. 215 11488), à l'étranger à l'Entreprise du Commerce Extérieur « Kultura » (H-1389 Budapest 62, P.O.B. 149 Compte-courant No. 218 10990) ou chez représentants à l'étranger.

Die Acta Chimica veröffentlichen Abhandlungen aus dem Bereich der chemischen Wissenschaften in deutscher, englischer, französischer und russischer Sprache.

Die Acta Chimica erscheinen in Heften wechselnden Umfangs. Vier Hefte bilden einen Band. Jährlich erscheinen 4 Bände.

Die zur Veröffentlichung bestimmten Manuskripte sind an folgende Adresse zu senden:

Acta Chimica

Budapest, Postfach 67, H-1450, Ungarn

An die gleiche Anschrift ist jede für die Redaktion bestimmte Korrespondenz zu richten. Manuskripte werden nicht zurückerstattet.

Abonnementspreis pro Band: \$36,00.

Bestellbar für das Inland bei Akadémiai Kiadó (1363 Budapest, Postfach 24, Bankkonto Nr. 215 11488), für das Ausland bei »Kultura« Außenhandelsunternehmen (H-1389 Budapest 62, P.O.B. 149. Bankkonto Nr. 218 10990) oder seinen Auslandsvertretungen.

«Acta Chimica» издают статьи по химии на русском, английском, французском и немецком языках.

«Acta Chimica» выходит отдельными выпусками разного объема, 4 выпуска составляют один том и за год выходят 4 тома.

Предназначенные для публикации рукописи следует направлять по адресу:

Acta Chimica

Budapest, P.O. Box 67, H-1450, ВНР

Всякую корреспонденцию в редакцию направляйте по этому же адресу.

Редакция рукописей не возвращает.

Подписная цена — \$36,00 за том.

Отечественные подписчики направляйте свои заявки по адресу Издательства Академии Наук (1363 Budapest, P.O.B. 24, Текущий счет 215 11488), а иностранные подписчики через организацию по внешней торговле «Kultura» (H-1389 Budapest 62, P.O.B. 149. Текущий счет 218 10990) или через ее заграничные представительства и уполномоченных.

Reviews of the Hungarian Academy of Sciences are obtainable
at the following addresses:

AUSTRALIA

C.B.D. LIBRARY AND SUBSCRIPTION SERVICE,
Box 4886, G.P.O., Sydney N.S.W. 2001
COSMOS BOOKSHOP, 145 Ackland Street, St,
Kilda (Melbourne), Victoria 3182

AUSTRIA

GLOBUS, Höchstädtplatz 3, 1200 Wien XX

BELGIUM

OFFICE INTERNATIONAL DE LIBRAIRIE, 30
Avenue Marnix, 1050 Bruxelles
LIBRAIRIE DU MONDE ENTIER, 162 Rue du
Midi, 1000 Bruxelles

BULGARIA

HEMUS, Bulvar Ruski 6, Sofia

CANADA

PANNONIA BOOKS, P.O. Box 1017, Postal Sta-
tion "B", Toronto, Ontario M5T 2T8

CHINA

CNPICOR, Periodical Department, P.O. Box 50,
Peking

CZECHOSLOVAKIA

MAD'ARSKÁ KULTURA, Národní třída 22,
115 66 Praha

PNS DOVOZ TISKU, Vinohradská 46, Praha 2

PNS DOVOZ TLACE, Bratislava 2

DENMARK

EJNAR MUNKSGAARD, Norregade 6, 1165
Copenhagen

FINLAND

AKATEEMINEN KIRJAKAUPPA, P.O. Box 128,
SF-00101 Helsinki 10

FRANCE

EUROPERIODIQUES S.A., 31 Avenue de Ver-
sailles, 78170 La Celle St-Cloud

LIBRAIRIE LAVOISIER, 11 rue Lavoisier, 75008
Paris

OFFICE INTERNATIONAL DE DOCUMENTA-
TION ET LIBRAIRIE, 48 rue Gay-Lussac, 75240
Paris Cedex 05

GERMAN DEMOCRATIC REPUBLIC

HAUS DER UNGARISCHEN KULTUR, Karl-
Liebknecht-Strasse 9, DDR-102 Berlin

DEUTSCHE POST ZEITUNGSVERTRIEBSAMT,
Strasse der Pariser Kommüne 3-4, DDR-104 Berlin

GERMAN FEDERAL REPUBLIC

KUNST UND WISSEN ERICH BIEBER, Postfach
46, 7000 Stuttgart 1

GREAT BRITAIN

BLACKWELL'S PERIODICALS DIVISION, Hythe
Bridge Street, Oxford OX1 2ET

BUMPUS, HALDANE AND MAXWELL LTD.,
Cowper Works, Olney, Bucks MK46 4BN

COLLET'S HOLDINGS LTD., Denington Estate,
Wellingborough, Northants NN 2QT

WM. DAWSON AND SONS LTD., Cannon House,
Folkestone, Kent CT19 5EE

H. K. LEWIS AND CO., 136 Gower Street, London
WC1E 6BS

GREECE

KOSTARAKIS BROTHERS, International Book-
sellers, 2 Hippokratous Street, Athens-143

HOLLAND

MEULENHOF-BrUNA B.V., Beulingstraat 2,
Amsterdam

MARTINUS NIJHOFF B.V., Lange Voorhout
9-11, Den Haag

SWETS SUBSCRIPTION SERVICE, 347b Heere-
weg, Lisse

INDIA

ALLIED PUBLISHING PRIVATE LTD., 13/14
Asaf Ali Road, New Delhi 110001

150 B-6 Mount Road, Madras 600002

INTERNATIONAL BOOK HOUSE PVT. LTD.,
Madame Cama Road, Bombay 400039

THE STATE TRADING CORPORATION OF
INDIA LTD., Books Import Division, Chandralok,
36 Janpath, New Delhi 110001

ITALY

EUGENIO CARLUCCI, P.O. Box 252, 70100 Bari
INTERSCIENTIA, Via Mazzè 28, 10149 Torino

LIBRERIA COMMISSIONARIA SANSONI, Via
Lamarmora 45, 50121 Firenze

SANTO VANASIA, Via M. Macchi 58, 20124
Milano

D. E. A., Via Lima 28, 00198 Roma

JAPAN

KINOKUNIYA BOOK-STORE CO. LTD., 17-7
Shinjuku-ku 3 chome, Shinjuku-ku, Tokyo 160-91

MARUZEN COMPANY LTD., Book Department,
P.O. Box 5050 Tokyo International, Tokyo 100-31

NAUKA LTD. IMPORT DEPARTMENT, 2-30-19
Minami Ikebukuro, Toshima-ku, Tokyo 171

KOREA

CHULPANMUL, Phenjan

NORWAY

TANUM-CAMMERMEYER, Karl Johansgatan
41-43, 1000 Oslo

POLAND

WĘGIERSKI INSTYTUT KULTURY, Marszał-
kowska 80, Warszawa

CKP 1 W ul. Towarowa 28 00-958 Warszawa

ROUMANIA

D. E. P., Bucuresti

ROMLIBRI, Str. Biserica Amzei 7, Bucuresti

SOVIET UNION

SOJUZPETCHATJ - IMPORT, Moscow

and the post offices in each town

MEZHDUNARODNAYA KNIGA, Moscow G-200

SPAIN

DIAZ DE SANTOS, Lagasca 95, Madrid 6

SWEDEN

ALMQVIST AND WIKSELL, Gamla Brogatan 26,
S-101-20 Stockholm

GUMPERTS UNIVERSITETSBOKHANDEL AB,
Box 346, 401 25 Göteborg 1

SWITZERLAND

KARGER LIBRI AG, Petersgraben 31, 4071 Basel

USA

EBSCO SUBSCRIPTION SERVICES, P.O. Box
1943, Birmingham, Alabama 35201

F. W. FAXON COMPANY, INC., 15 Southwest
Park, Westwood, Mass. 02090

THE MOORE-COTTRELL SUBSCRIPTION

AGENCIES, North Cohocton, N.Y. 14 6

READ-MORE PUBLICATIONS, INC., 140 Cedar
Street, New York, N. Y. 10006

STECHELT-MACMILLAN, INC., 7250 Westfield
Avenue, Pennsauken N.J. 0 110

VIETNAM

XUNHASABA, 32, Hai Ba Trung, Hanoi

YUGOSLAVIA

JUGOSLAVENSKA KNJIGA, Terazije 27, Beograd
FORUM, Vojvode Mišića 1, 21000 Novi Sad